Trinity College Dublin
Coláiste na Tríonóide, Baile Átha Cliath
The University of Dublin

# Exploring the influence of obesity, fatty acids, and current treatment modalities on the immune-metabolic profiles of adipose tissue in oesophageal cancer.

**Fiona O'Connell**
Student No. 11361651

Ph.D. Thesis
Submitted to Trinity College Dublin for the degree of Doctor of Philosophy

August 2023

Department of Surgery, Trinity Translational Medicine Institute, Trinity College Dublin

Thesis Supervisors:
Prof. Jacintha O'Sullivan[1] (Primary Supervisor)
Prof. Helen M. Roche[2,3] (Secondary Supervisor)

1. Department of Surgery, Trinity St. James's Cancer Institute and Trinity Translational Medicine Institute, St. James's Hospital and Trinity College Dublin, Dublin 8, Ireland

2. Nutrigenomics Research Group, UCD Conway Institute, School of Public Health, Physiotherapy and Sports Science, University College Dublin, Dublin 4, Ireland.

3. Institute for Global Food Security, School of Biological Sciences, Queens University Belfast, Belfast, Ireland.

**Declaration**

I declare that this thesis has not been submitted as an exercise for a degree at this or any other university and it is entirely my own work. I agree to deposit this thesis in the University's open access institutional repository or allow the library to do so on my behalf, subject to Irish Copyright Legislation and Trinity College Library conditions of use and acknowledgement.

I consent to the examiner retaining a copy of the thesis beyond the examining period, should they so wish (EU GDPR May 2018).

_____ _____

**Fiona O'Connell** **Date**

**Thesis Abstract**

Oesophageal adenocarcinoma (OAC) is a poor prognosis cancer with limited response rates to current standard of care treatments including chemotherapy and chemoradiotherapy. OAC has one of the strongest associations with obesity, its anatomical location is surrounded by the visceral adipose depot has been postulated to intensify this association. Adipose tissue is a regulatory organ with many downstream functions that are not fully understood, including its response to chemotherapy and radiotherapy. To better elucidate the role of visceral adiposity in this disease state, a full metabolic profile combined with analysis of secreted pro-inflammatory cytokines, metabolites, and lipid profiles were assessed using human ex-vivo adipose tissue explants from obese and non-obese OAC patients. These data were correlated to extensive clinical data including obesity status, metabolic dysfunction, previous treatment exposure, and tumour regression grades. In this thesis, we identified that visceral fat from obese OAC patients had significantly elevated oxidative phosphorylation metabolism profiles, increased secretion of mediators of immune cell recruitment and Th17 immunity, in addition to altered secretions of glutamine associated metabolites. Adipose explants from patients with metabolic dysfunction also demonstrated increased oxidative phosphorylation metabolism, and increased secretion of pro-inflammatory associated mediators and triacylglycerides. Adipose explants generated from patients who had previously received neo-adjuvant chemotherapy showed elevated secretions of pro-inflammatory mediators and a decreased expression of triacylglycerides compared with patients who received no neo-adjuvant treatment or chemoradiotherapy regimen. For those patients who showed the poorest response to currently available treatments, their adipose tissue was associated with higher glycolytic metabolism compared to patients who had good treatment responses.

Dietary fatty acids have been strongly linked with metabolic heath, particularly oleic acid (OA) and palmitic acid (PA) which are differentially expressed with increasing obesity, in the circulation and at an adipose tissue level. We assessed whether these fatty acids would differentially affect the adipose tissue of non-cancer and OAC patients with respect to metabolic and secreted profiles and the role of the adipose secretome on immune cell function. We observed that exogenous PA induced differential effects on adipose tissue metabolism, significantly decreasing metabolic profiles of adipose tissue of OAC patients, an effect that was not observed in non-cancer patients. PA treatment elicited an immunosuppressive effect on the adipose secretome, most apparent in OAC patients. PA treatment in the adipose secretome also led to the observation of paradoxical effects on DC maturation and Mϕ polarisation between OAC and non-cancer patients.

To further interrogate the action of these fatty acids on the adipose tissue, we assessed we examined the action of these fatty when used in combination with irradiation. We observed that the immunosuppressive effects induced by PA were augmented by increasing irradiation and increasing visceral adiposity within OAC patients. PA treatment induced differential responses in adipose tissue metabolism and secretome of non-obese and obese OAC patients, which were more pronounced following exposure to increasing radiation. Adipose tissue from obese patients displayed higher reliance on oxidative phosphorylation in the unirradiated and decreased reliance on glycolysis following high dose radiation compared with adipose tissue from non-obese patients. However, this diminished reliance on glycolysis in adipose tissue from obese patients was reinvigorated by OA treatment. Interestingly, macrophages cultured with the PA treated adipose secretome with and without increasing irradiation demonstrated conflicting polarisation responses

depending on patient obesity status. In the unirradiated setting, the adipose secretome of non-obese patients treated with PA decreased expression of markers associated with M1 phenotypes and increased markers associated with M2 phenotypes. In contrast, PA treated adipose secretome of obese patients differentially effected expression of these markers, increasing M1 markers and decreasing M2 markers. However, following exposure to the PA treated adipose secretome exposed to increasing irradiation, opposing results were observed.

Next, we explored the downstream effects this irradiated and fatty acid treated adipose secretome could have on cancer cell metabolism and invasive capacity, by utilising a OAC cancer cell line FLO-1 and matched liver derived metastatic cell line FLO-LM. We identified that these cells employ different metabolic mechanisms with FLO-1 cells being more reliant on glycolysis, while metastatic FLO-LM cells utilise oxidative phosphorylation associated mechanisms as well as being acutely affected by inhibition of fatty acid oxidation. Further to this, we observed elevated secreted levels of sCD147, a factor known to drive metastasis, in the PA treated adipose secretome exposed to increasing radiation, which was most apparent in the obese adipose secretome. Inhibition of fatty acid oxidation, a mechanism known to support metastasis, was seen to have differential response in enhancing invasion of primary and metastatic towards the PA enriched adipose secretome, an effect that was further amplified by patient obesity status and increasing radiation treatment.

The role of adipose tissue and the influence of obesity on cancer treatment response has been contentiously reported. We examined the influence chemotherapy and chemoradiotherapy regimens on adipose tissue metabolism and its secretome. We observed that chemotherapy and chemoradiotherapy differentially alter adipose tissue metabolism and secreted factors, with chemoradiotherapy significantly increasing pro-inflammatory associated mediators. Exogenous fatty acids differentially altered the adipose secretome in response to these treatments. However, both treatments combined with exogenous fatty acids showed significant increases in mediators of Th17 immune responses. The chemotherapy treated adipose secretome enhanced mitochondrial dysfunction in cancer cells, increasing their reliance on glycolysis. Whilst the chemotherapy treated adipose secretome significantly increased dendritic cell maturation markers, it also promoted anti-inflammatory macrophage phenotypes. The chemoradiotherapy treated adipose secretome in combination with fatty acids induced opposing effects on macrophage polarisation. In combination with OA, it decreased M1 primed expression of pro-inflammatory markers, whilst in combination with PA, it decreased M2 primed expression of anti-inflammatory markers.

Overall, the body of research in this thesis has elucidated that adipose tissue has the potential to act as an influential mediator of cancer progression and treatment resistance. The adipose secretome is enriched with a series of factors that impact inflammatory and immune responses which are heavily influenced by patient's demographics. Further to this, addition of external stresses such as exogenous fatty acids, increasing radiation or cytotoxic drugs can differentially affect the adipose secretome and its complex microenvironment, priming it to repress anti-tumour immunity and conferring cancer cells with enhanced metabolic and invasive capacity. Most significantly, this thesis identifies that obesity is a fundamental cause of the aberrant adipose tissue biology seen in these OAC patients. The obese adipose secretome contributes to a wider tumour microenvironment primed to support cancer progression and the establishment of metastasis highlighting the critical need to further address the cancer-obesity link and if this can be exploited to improve treatment responses and overall patient outcome.

**Acknowledgments**

The first thanks of this PhD must be to my amazing supervisor Professor Jacintha O'Sullivan. I don't think I fully appreciated when I first emailed you that I had struck gold, but at the end of this PhD I most certainly do! You have been a constant source of encouragement, support, and kindness throughout this PhD. You have given me so many opportunities during this PhD, allowing me to grow not only as a collaborative and independent scientist but as an outreach enthusiast as well! I feel blessed to have had a supervisor who is as equally enthusiastic about science and outreach as me. Every meeting with you led to more questions being asked and more experiments excitedly being planned, which led to this project evolving into so much more than I thought possible or could fit in one thesis. I don't believe that I could have accomplished half as much as I have throughout this PhD without you. I hope that wherever I end up in the future, I'll still be able to come back and collaborate with you because you truly are the most inspirational mentor and scientist that I have ever met.

A special thanks to my co-supervisor Professor Helen Roche. Thank you for being a such a calming force when the data didn't turn out as expected and for taking the time to trouble shoot and guide me in understanding the outcomes of this project. Your expertise and guidance have been so very much appreciated throughout this PhD!

To Breakthrough Cancer and Musgraves for funding this PhD, I will always be grateful that you supported this project and gave me the opportunity to do all of this work! A special thanks to Orla Dolan, Eoghan O'Sullivan, Frances Drummond, Linda O'Neill, Mary Morrish, Nora Lieggi, and all the amazing team at Breakthrough Cancer Research. Thank you for celebrating every achievement big or small with me, including me in so many of your amazing charity events and for the endless support throughout this PhD. You've made me feel like one of the family and I'm just so thankful for having had the opportunity to work with a charity that is as amazing as Breakthrough Cancer Research!

A special thank you to all the clinical staff in St James's Hospital, especially Prof. Reynolds, Prof Ravi and Dr. Donohoe for consenting and procuring samples for this study. To the patients who have donated to this study, this kind of translational research would not be possible without your contribution. Thank you so much for taking part in this research during your most trying of times, your contribution will always be so very much appreciated.

Thank you to all the PIs in the Department of Surgery Dr. Joanne Lysaght, Dr. Stephen Maher, Dr. Niamh Lynam-Lennon and Dr. Graham Pidgeon for your input in this project. Your invaluable advice, expertise, and lab meeting questions have greatly helped to evolve this project and prepare me for the world of academia. A special thank you to Dr. Margaret Dunne and Dr. Melissa Conroy, you are the living proof that even when an amazing mentor leaves the building they can't get away from the questions! Thank you both for your insights, training and experimental knowledge. Your constant question answering, support and guidance has helped me so much throughout this PhD and in life! A special thanks to Dr. Simone Marcone, you have been such a positive encouraging force through this PhD and it's been so much appreciated! A massive thank you to Dr. Martin Barr, you really are the problem-solving master, thank you for always having the time to deal with any issue and all the chats that brightened up this PhD!

I want to say a massive thanks to the past and present members of Department of Surgery and the wider TTMI/UCD family, Dr. Aoife Cannon, Dr. James Phelan, Dr. Mia Morrissey, Dr. Aisling Heeran, Dr. Aisling Ui Mhaonaigh, Dr. Aoife Kilgallon, Dr.Ashanty Melo, Dr. Susan Kennedy, Dr.

Viviana Salvatore, Dr. Padraic McDonagh, Dr. Tim Nugent, Dr. Fiona Crotty, Dr. Jim O'Connell, Dr. Cliona Lorton, Niamh Clarke, Maitiú Ó Murchú, Lorraine Smith, Cathy McShane, Kirstan Murphy, Jason McGrath, Rebecca O'Brien, Croi Buckley, Andrew Sheppard, Christina Cahill, Greg Melotte, Rebecca Lyons, Dr. Brendan Moran, Caroline Marion, David Hackett, Kathleen Mitchelson, Marzia Pendino, Dr. Kathy Gately, Dr. Melissa Tutty, Dr. Anna Bogdanska, Sarah Holmes, and Gabriele Vella. Thank you for all the coffee breaks, the conference catch ups, the practicals fun and most importantly all the interesting science chats! It has been a pleasure working with you all and wish you all the best for the future! This kind of work doesn't happen without the incredible support of biobank managers, Christine, Anshul, Niamh, and Meghana thank you for doing a job that is not easy! Thank you procuring so many samples and collecting so much data for this project your help is greatly appreciated! A special thank you to Dr Marina Zaki and Dr. Roisin Corcoran for being such incredible people to work with, I'm very lucky to have you as friends! A massive thank you to Dr. Noel Donlon for the endless VFA calculations, clinical data requests, organising sample collections, and the list goes on… your help has been so greatly appreciated throughout this project! A huge thanks to Dr. Maria Davern, you truly are the most amazing scientist (no friend goggles!). I'm so grateful you were always ready to chat science and help trouble shoot any problems. Also thank you for all the cat pictures they immensely improved the writing process! A massive thanks to my lab wife Klaudia! We started our journey in research together in the dark room of BSB and it has grown into the most amazing friendship! From our constant shenanigans to late night westerns, your humour always made science more fun than it probably should be!

A humongous thank you to my other half of the hypoxia hood Eimear Mylod! I think I will be forever conditioned to only use half of the hood waiting for you to hop in! Your constant support, humour, and sass have brightened the darkest days of this PhD! I'm so lucky to have had the opportunity to work with you so closely even if it was staining samples at 10 o clock a night, only to find out the Canto was broken down again, you are an absolute Superstar "resilient" Scientist! (Also, I don't think anyone else would have listened to the 72 pieces song without killing me!).

A massive thank you to the best travel buddy I could ever have Laura Kane, I wouldn't trade our travel experiences for the world! You are one of the most magical and kindest people I know! No matter what goes wrong, you always find a way to laugh about it, even in a different country with absolutely no luggage and conference to go to! I'm so grateful to have had you on this PhD journey to share my coding ramblings with, from the glitches to the importance of a good colour scheme, we've just always been in tune!

An enormous thank you to Laura Edgerton for all her support and positive encouragement throughout this PhD! You are an amazing hype woman! I'm so lucky to have worked with you throughout this PhD our shared love of seahorse and metabolism started an amazing friendship that I'm sure our shared sense of humour will keep alive for the rest of our lives, even when you plate an exorbitant amount of 6 well plates instead of a couple of t-75s!

I will always be grateful for this PhD experience, because I have met three of the most amazing scientists and incredible human beings that I have no doubt are going to do amazing things in the future! You are the most incredible friends anyone doing a PhD could ask for, you have been there for me through thick and thin and I'm just so lucky to have been blessed with you all!

To my amazing friends Breda, Anthony, Nicola, Bríd, Siobhan, Patrick, Helena, Ciara, Liam, Niamh, Dinny, Margaret, Ashley and Sinead thank you for putting up with my recent disappearing act! You have all been such an amazing support throughout this PhD, constantly encouraging and rooting for me! I'm so lucky to have all you guys in my life!! A massive thanks to the amazing

roommates I've had throughout this PhD. Rachel, Orla, Christine, Izzy, Tracy, Bridin and Aislinn, thank you for the constant support, the listening ears, making sure that I've eaten, and that the fridge was stocked with the goods!!! I've no doubt that ye are nearly as much of an expert on seahorses as I am at this stage!

The extended family Mommy N, Pat, Sean, Mark, Michelle, Nora, Shannon, Lilly, Mary C, Mary F, Jo, Lucy, Eddie, Mary, Larry and Rita, thank you for all your support and kindness throughout this PhD, ye really are the best bunch! To my amazing aunties Betty and Joan, and my wonderful cousins Jean, Tracey, and Liz thank you for always being there for me and supporting me along this journey! Ye made me laugh, lifted my spirit and were always there rooting me on, I'm so lucky to always have ye in my corner!

Thank you to my amazing sister Orla, particularly for making sure I was fed and caffeinated on a Sunday afternoon during this fabulous writing period! You have always been such a support and encouragement, I'm so lucky to have you taking care of me in my life!

An incredible thank you to my amazing Mom, thank you for always encouraging me to chase my dreams and reminding me what's for you won't past you by! I've no doubt that if it wasn't for your support and encouragement my life would look very different. I definitely wouldn't have been brave enough to give up teaching and go back to college, but you always believed in me, supported me and I just know I would not have accomplished any of this without you so thank you for every single little thing you do for me!

To my uncle Mossie, Nana, Nan, Anna, Noreen, John-Joe, Mickey, Ciara, Gogga, and Grandad thank you for being my guiding stars.

This thesis is very much in dedication of my Dad who lost his battle to oesophageal cancer far too quickly. I'm sure if you were still alive you would be so proud of this accomplishment but then I'm equally sure my career trajectory would have been very different. You will always be behind my motivation for pursuing a career in cancer research and the amount of dedication and work I put into this field. Thank you for being my hero and making sure I knew I could accomplish anything I put my mind to.

**Ph.D. Outputs**
**Publications:**

*First Author:*

**O'Connell F,** Mylod E, Donlon NE, Heeran AB, Butler C, Bhardwaj A, Ramjit S, Durand M, Lambe G, Tansey P, Welartne I, Sheahan KP, Yin X, Donohoe CL, Ravi N, Dunne MR, Brennan L, Reynolds JV, Roche HM, O'Sullivan J. Energy Metabolism, Metabolite, and Inflammatory Profiles in Human Ex Vivo Adipose Tissue Are Influenced by Obesity Status, Metabolic Dysfunction, and Treatment Regimes in Patients with Oesophageal Adenocarcinoma. Cancers. 2023; 15(6):1681**.**

**O'Connell F**, O'Sullivan J. Help or hindrance: The obesity paradox in cancer treatment response. Cancer Lett 2021; 522:269–80.

*Co-author:*

A. M. Malebari, D Fayne, S. M. Nathwani, **F O'Connell**, S Noorani, B Twamley, N. M. O'Boyle, J O'Sullivan, D. M. Zisterer, M. J. Meegan. Beta-lactams with antiproliferative and antiapoptotic activity in breast and chemoresistant colon cancer cells, European Journal of Medicinal Chemistry, 189, 2020, p112050.

S.A. Kennedy, M.E. Morrissey, M.R. Dunne, **F. O'Connell**, C.T. Butler, M.C. Cathcart, A.M. Buckley, B.J. Mehigan, J.O. Larkin, P. McCormick, B.N. Kennedy, J. O'Sullivan. Combining 1,4-dihydroxy quininib with Bevacizumab/FOLFOX alters angiogenic and inflammatory secretions in ex vivo colorectal tumors, BMC Cancer. 20 (2020) 1–14.

Slater, K., Heeran, A.B., Garcia-Mulero, S., Kalirai, H., Sanz-Pamplona, R., Rahman, A., Al-Attar, N., Helmi, M., **O'Connell, F**., Bosch, R., Portela, A., Villanueva, A., Gallagher, W.M., Jensen, L.D., Piulats, J.M., Coupland, S.E., O'Sullivan, J., Kennedy, B.N. High Cysteinyl Leukotriene Receptor 1 Expression Correlates with Poor Survival of Uveal Melanoma Patients and Cognate Antagonist Drugs Modulate the Growth, Cancer Secretome, and Metabolism of Uveal Melanoma Cells. Cancers 2020, 12, 2950.

Donlon, N.E., Sheppard, A., Davern, M., **O'Connell, F.,** Phelan, J.J., Power, R., Nugent, T., Dinneen, K., Aird, J., Greene, J., Nevins Selvadurai, P., Bhardwaj, A., Foley, E.K., Ravi, N., Donohoe, C.L., Reynolds, J.V., Lysaght, J., O'Sullivan, J., Dunne, M.R. Linking Circulating Serum Proteins with Clinical Outcomes in Esophageal Adenocarcinoma—An Emerging Role for Chemokines. Cancers 2020, 12, 3356.

C. Cahill, **F. O'Connell**, K.M. Gogan, D.J. Cox, S.A. Basdeo, J. O'Sullivan, S. V. Gordon, J. Keane, J.J. Phelan, The Iron Chelator Desferrioxamine Increases the Efficacy of Bedaquiline in Primary Human Macrophages Infected with BCG, Int. J. Mol. Sci. 2021, Vol. 22, Page 2938. 22 (2021) 2938.

N.E. Donlon, M. Davern, A. Sheppard, R. Power, **F. O'Connell**, A.B. Heeran, R. King, C. Hayes, A. Bhardwaj, J.J. Phelan, M.R. Dunne, N. Ravi, C.L. Donohoe, J. O'Sullivan, J. V. Reynolds, J. Lysaght, The Prognostic Value of the Lymph Node in Oesophageal Adenocarcinoma, Incorporating Clinicopathological and Immunological Profiling, Cancers 2021, Vol. 13, Page 4005. 13 (2021) 4005.

M. Davern, N.E. Donlon, A. Sheppard, **F.O. Connell**, C. Hayes, A. Bhardwaj, E. Foley, D.O. Toole, N. Lynam-Lennon, N. Ravi, J. V. Reynolds, S.G. Maher, J. Lysaght, Chemotherapy regimens induce inhibitory immune checkpoint protein expression on stem-like and senescent-like oesophageal adenocarcinoma cells, Transl. Oncol. 14 (2021) 101062.

N. Essa, **F. O'Connell,** A. Prina-Mello, J. O'Sullivan, S. Marcone, Gold nanoparticles and obese adipose tissue microenvironment in cancer treatment, Cancer Lett. 525 (2022) 1–8.

C. Cahill, D.J. Cox, **F. O'Connell,** S.A. Basdeo, K.M. Gogan, C. Ó'maoldomhnaigh, J. O'sullivan, J. Keane, J.J. Phelan, The Effect of Tuberculosis Antimicrobials on the Immunometabolic Profiles of Primary Human Macrophages Stimulated with Mycobacterium tuberculosis, Int. J. Mol. Sci. 2021, Vol. 22, Page 12189. 22 (2021) 12189.

E. Mylod, **F. O'Connell**, N.E. Donlon, C. Butler, J. V. Reynolds, J. Lysaght, M.J. Conroy, The Omentum in Obesity-Associated Cancer: A Hindrance to Effective Natural Killer Cell Migration towards Tumour Which Can Be Overcome by CX3CR1 Antagonism, Cancers 2022, Vol. 14, Page 64. 14 (2021) 64.

N.E. Donlon, M. Davern, A.D. Sheppard, **F. O'Connell**, M.R. Dunne, C. Hayes, E. Mylod, S. Ramjit, H. Temperley, M. Mac Lean, G. Cotter, A. Bhardwaj, C. Butler, M.J. Conroy, J. O'Sullivan, N. Ravi, C.L. Donohoe, J. V. Reynolds, J. Lysaght, The Impact of Esophageal Oncological Surgery on Perioperative Immune Function, Implications for Adjuvant Immune Checkpoint Inhibition, Front. Immunol. 13 (2022) 114.

R.M. Corcoran, P. MacDonagh, **F. O'Connell**, M.E. Morrissey, M.R. Dunne, R. Argue, J. O'Sullivan, D. Kevans, Association Between Ex Vivo Human Ulcerative Colitis Explant Protein Secretion Profiles and Disease Behaviour, Dig. Dis. Sci. 67 (2022) 5540–5550.

M. Davern, M.C. Fitzgerald, C.E. Buckley, A.B. Heeran, N.E. Donlon, J. McGrath, **F. O' Connell**, M.R. Deshpande, C. Hayes, J. MacDonald, A.D. Sheppard, J. V. Reynolds, S.G. Maher, N. Lynam-Lennon, B. Murphy, J. Lysaght, PD-1 and TIGIT blockade differentially affect tumour cell survival under hypoxia and glucose deprived conditions in oesophageal adenocarcinoma, implications for overcoming resistance to PD-1 blockade in hypoxic tumours, Transl. Oncol. 19 (2022) 101381.

M. Davern, D. Bracken-Clarke, N.E. Donlon, A.D. Sheppard, **F. O' Connell**, A.B. Heeran, K.D. Majcher, E. Mylod, M.J. Conroy, C. Butler, C. Donohoe, D O'Donnell, M Lowry, A. Bhardwaj, N. Ravi, J. O'Sullivan, J. V. Reynolds, J. Lysaght Visceral adipose tissue secretome from early and late-stage oesophageal cancer patients differentially affects effector and regulatory T cells., (2022).

M. Davern, N.E. Donlon, **F. O' Connell**, A.D. Sheppard, C. Hayes, R. King, H. Temperley, C. Butler, A. Bhardwaj, J. Moore, D. Bracken-Clarke, C. Donohoe, N. Ravi, J. V. Reynolds, S.G. Maher, M.J. Conroy, J. Lysaght, Cooperation between chemotherapy and immune checkpoint blockade to enhance anti-tumour T cell immunity in oesophageal adenocarcinoma, Transl. Oncol. 20 (2022) 101406.

N.E. Donlon, M. Davern, **F. O'Connell**, A. Sheppard, A. Heeran, A. Bhardwaj, C. Butler, R. Narayanasamy, C. Donohoe, J.J. Phelan, N. Lynam-Lennon, M.R. Dunne, S. Maher, J. O'Sullivan, J. V. Reynolds, J. Lysaght, Impact of radiotherapy on the immune landscape in oesophageal adenocarcinoma, World J. Gastroenterol. 28 (2022) 2302–2319.

M. Davern, N.E. Donlon, A.S. Sheppard, K.D. Majcher, **F.O. Connell**, A.B. Heeran, M. Grant, R.A. Farrell, C. Hayes, D. Bracken-Clarke, M.J. Conroy, E. Foley, D.O. Toole, A. Bhardwaj, N. Ravi, J. V. Reynolds, S.G. Maher, J.O. Sullivan, J. Lysaght, FLOT and CROSS chemotherapy regimens alter the frequency of CD27+ and CD69+ T cells in oesophagogastric adenocarcinomas: implications for combination with immunotherapy, J. Cancer Res. Clin. Oncol. (2022).

L.E. Kane, G.S. Mellotte, E. Mylod, R.M. O'Brien, **F. O'Connell**, C.E. Buckley, J. Arlow, K. Nguyen, D. Mockler, A.D. Meade, B.M. Ryan, S.G. Maher, Diagnostic Accuracy of Blood-based Biomarkers for Pancreatic Cancer: A Systematic Review and Meta-analysis, Cancer Res. Commun. 2 (2022) 1229–1243.

Davern, M., Donlon, N.E., **O'Connell, F**., Gaughan, C., O'Donovan, C., McGrath, J., Sheppard, A.D., Hayes, C., King, R., Temperley, H., et al. Nutrient Deprivation and Hypoxia Alter T Cell Immune Checkpoint Expression: Potential Impact for Immunotherapy. J. Cancer Res. Clin. Oncol. 2022, 1–19.

Davern, M., Donlon, N.E., **O'Connell, F**., Gaughan, C., O'Donovan, C., Habash, M., Sheppard, A.D., MacLean, M., Dunne, M.R., Moore, J., et al. Acidosis Significantly Alters Immune Checkpoint Expression Profiles of T Cells from Oesophageal Adenocarcinoma Patients. Cancer Immunol. Immunotherapy. 2023, 72, 55–71.

Slater, K., Bosch, R., Smith, K.F., Jahangir, C.A., Garcia-Mulero, S., Rahman, A., **O'Connell, F**., Piulats, J.M., O'Neill, V., Horgan, N., et al. 1,4-Dihydroxy Quininib Modulates the Secretome of Uveal Melanoma Tumour Explants and a Marker of Oxidative Phosphorylation in a Metastatic Xenograft Model. Front. Med. 2023, 9.

**Under preparation**

Palmitic acid diminishes metabolism in adipose tissue from oesophageal adenocarcinoma patients and augments an immunosuppressive secretome in both cancer and non-cancer patients.

**Fiona O'Connell,** Eimear Mylod, Noel E. Donlon, Kathleen A. Mitchelson, Martina Wallace, Maria Davern, Christine Butler, Niamh O'Connor, Tim Nugent, Jessie Elliot, Claire L. Donohoe, Narayanasamy Ravi, Derek Doherty, Margaret R. Dunne, John V. Reynolds, Helen M. Roche, Jacintha O'Sullivan.

(Target Journal - Journal of Lipid Research)

The differential influences of oleic and palmitic acid on the metabolism and secretome of adipose tissue explants of patients with oesophageal adenocarcinoma is augmented by increasing radiation.

**Fiona O'Connell,** Eimear Mylod, Noel E. Donlon, Maria Davern, Christine Butler, Niamh O'Connor, Tim Nugent, Jessie Elliot, Claire L. Donohoe, Narayanasamy Ravi, Derek Doherty, Margaret R. Dunne, John V. Reynolds, Helen M. Roche, Jacintha O'Sullivan.

(Target Journal - Journal of Lipid Research)

The secretome of adipose explants from oesophageal adenocarcinoma patients is differentially altered by chemotherapy FLOT and chemoradiotherapy CROSS regimens, an effect which is augmented by fatty acid treatment.

**Fiona O'Connell,** Eimear Mylod, Noel E. Donlon, Maria Davern, Christine Butler, Niamh O'Connor, Claire L. Donohoe, Narayanasamy Ravi, Joanne Lysaght, Derek Doherty, Margaret R. Dunne, John V. Reynolds, Helen M. Roche, Jacintha O'Sullivan.

(Target Journal - European Journal of Cancer)

Palmitic acid differentially alters the adipose secretome of oesophageal adenocarcinoma patients leading to contrasting metabolic and invasive capacity in primary and metastatic oesophageal cancer cell lines.

**Fiona O'Connell,** Eimear Mylod, Laura E. Kane, Noel E. Donlon, Christine Butler, Niamh O'Connor, Claire L. Donohoe, Narayanasamy Ravi, Margaret R. Dunne, John V. Reynolds, Helen M. Roche, Jacintha O'Sullivan.

(Target Journal - Cancer Letters)

Increasing radiation augments a pro-tumorigenic adipose secretome that differentially effects the metabolism of primary and metastatic oesophageal cancer cell lines.

**Fiona O'Connell**, Eimear Mylod, Laura E. Kane, Noel E. Donlon, Christine Butler, Niamh O'Connor, Claire L. Donohoe, Narayanasamy Ravi, Stephen G. Maher, Margaret R. Dunne, John V. Reynolds, Helen M. Roche, Jacintha O'Sullivan.

(Target Journal – Translational oncology)

High dose radiation on the adipose secretome promotes anti-tumour immunity by diminishing dendritic cell maturation and polarising anti-inflammatory macrophages

**Fiona O'Connell**, Eimear Mylod, Laura E. Kane, Noel E. Donlon, Christine Butler, Niamh O'Connor, Claire L. Donohoe, Narayanasamy Ravi, Margaret R. Dunne, John V. Reynolds, Helen M. Roche, Jacintha O'Sullivan.

(Target Journal – Immunology Letters)

The tumour and adipose microenvironment augmented by hypoxia leads to metabolic and phenotypic dysfunction in macrophages.

**Fiona O'Connell**, Klaudia D. Majcher, Bahram Khan, Eimear Mylod, Noel E. Donlon, Christine Butler, Anshul Bhardwaj, Claire Donohoe, Narayanasamy Ravi, Stephen G. Maher, John V. Reynolds, Margaret R. Dunne, Helen Roche, Jacintha O'Sullivan.

(Target Journal – Immunology Letters)

Obesity in oesophageal adenocarcinoma patients alters the frequency of myeloid subsets in adipose tissue and its secretome enhances myeloid cells metabolic requirements.

**Fiona O'Connell,** Eimear Mylod, Noel E. Donlon, Christine Butler, Anshul Bhardwaj, Niamh O'Connor, Claire L. Donohoe, Narayanasamy Ravi, Margaret R. Dunne, John V. Reynolds, Helen M. Roche, Jacintha O'Sullivan.

(Target Journal – Immunology Letters)

Profiling the inflammatory alterations and immunomodulatory effects of Q8 on ex-vivo oesophageal adenocarcinoma tumour explants.

**Fiona O'Connell,** Klaudia D. Majcher, Eimear Mylod, Noel E. Donlon, Lauren Devitt, Anshul Bhardwaj, Narayanasamy Ravi, John V. Reynolds, Derek Doherty, Margaret R. Dunne, Breandáin N Kennedy, Jacintha O'Sullivan.

(Target Journal - Cancer Letters)

Assessing the influence of Pyrazinib in combination with increasing irradiation on the metabolic and secreted profiles of ex-vivo adipose tissue explants from oesophageal adenocarcinoma patients.

**Fiona O'Connell,** Eimear Mylod, Noel E. Donlon, Christine Butler, Niamh O'Connor, Claire L. Donohoe, Narayanasamy Ravi, Margaret R. Dunne, John V. Reynolds, Breandáin N Kennedy, Helen M. Roche, Jacintha O'Sullivan.

(Target Journal – Translational Oncology)

**Oral Presentations**

*National*

**IRRS Annual Scientific Meeting 2021, Virtual event, 6-7 September 2021**

Title: The influence of increasing radiation on immune-metabolic regulation in adipose tissue explants.

Fiona O'Connell, Aisling B. Heeran, Eimear Mylod, Margaret R. Dunne, Noel E. Donlon, Christine Butler, Anshul Bhardwaj, Narayanasamy Ravi, John V. Reynolds, Helen Roche, Jacintha O'Sullivan.

**Annual Irish Association for Cancer Research Conference, 2023, 24th-26th March 2023**

Title: Examining the influence of obesity on the pro-inflammatory landscape of adipose tissue and what effects this holds for macrophage and cancer cell metabolism

Fiona O'Connell, Eimear Mylod, Noel E. Donlon, Maria Davern, Aisling B. Heeran, Christine Butler, Anshul Bhardwaj, Sinead Ramjit, Micheal Durand, Gerard Lambe, Paul Tansey, Ivan Welartne, Kevin P. Sheahan, Xiaofei Yin, Claire L. Donohoe, Narayanasamy Ravi, Derek Doherty, Margaret R. Dunne, Lorraine Brennan, John V. Reynolds, Helen M. Roche, Jacintha O'Sullivan.

**Poster Presentation**

*International*

**Defence is the Best Attack: Immuno-Oncology Breakthroughs, Virtual event, 16 - 17 February 2021**

Title: The influence of radiation on immune-metabolic activity in human ex-vivo adipose tissue explants. Fiona O'Connell, Klaudia D. Majcher, Aisling B. Heeran, Margaret R. Dunne, Anshul Bhardwaj, Narayanasamy Ravi, John V. Reynolds, Helen Roche, Jacintha N. O'Sullivan.

**4th Annual Conference of The European Macrophage and Dendritic Cell Society, Virtual event, 24-25 June 2021**

Title: The influence of radiation on immune-metabolic activity of human ex-vivo adipose tissue explants from oesophageal cancer patients. Fiona O'Connell, Aisling B. Heeran, Eimear Mylod, Margaret R. Dunne, Noel E. Donlon, Christine Butler, Anshul Bhardwaj, Narayanasamy Ravi, John V. Reynolds, Helen Roche, Jacintha O'Sullivan.

**27$^{th}$ congress of the European Association for Cancer Research, Virtual event, 24-25 June 2021**

Title: The influence of radiation on metabolic activity and cytokine expression in adipose tissue explants. Fiona O'Connell, Aisling B. Heeran, Eimear Mylod, Margaret R. Dunne, Noel E. Donlon, Christine Butler, Anshul Bhardwaj, Narayanasamy Ravi, John V. Reynolds, Helen Roche, Jacintha O'Sullivan.

**6th European Congress of Immunology, Virtual event, 1 - 4 September 2021**

Title: Obesity alters adipose tissue energy metabolism profiles and inflammatory secretions: their influence on Dendritic Cell maturation. Fiona O'Connell, Aisling B. Heeran, Eimear Mylod, Margaret R. Dunne, Noel E. Donlon, Christine Butler, Anshul Bhardwaj, Narayanasamy Ravi, John V. Reynolds, Helen Roche, Jacintha O'Sullivan.

**Cancer metabolism showcase, Virtual event, 2021**

Title: Exploring adipose tissue metabolism and the influence of the adipose secretome on myeloid cell metabolism in oesophageal adenocarcinoma. Fiona O'Connell, Eimear Mylod, Noel E. Donlon, Christine Butler, Anshul Bhardwaj, Aisling B. Heeran, Claire Donohoe, Narayanasamy Ravi, John V. Reynolds, Margaret R. Dunne, Helen Roche, Jacintha O'Sullivan

**AACR Annual meeting 2022, New Orleans, USA, 8-13 April 2022**

Title: Exploring the immune-metabolic mechanisms of adipose tissue in oesophageal adenocarcinoma. Fiona O'Connell, Eimear Mylod, Noel E. Donlon, Christine Butler, Anshul Bhardwaj, Aisling B. Heeran, Claire Donohoe, Narayanasamy Ravi, John V. Reynolds, Margaret R. Dunne, Helen Roche, Jacintha O'Sullivan.

**28th congress of the European Association for Cancer Research, EACR, Seville, Spain, 20-23 June 2022**

Title: Examining the influence of adipose tissue metabolism and secretome in oesophageal adenocarcinoma. Fiona O'Connell, Eimear Mylod, Noel E. Donlon, Christine Butler, Anshul Bhardwaj, Aisling B. Heeran, Claire Donohoe, Narayanasamy Ravi, John V. Reynolds, Margaret R. Dunne, Helen Roche, Jacintha O'Sullivan.

*National*

**Annual Irish Association for Cancer Research Conference, Galway, Ireland, 26th-28th February 2020**

Title: The influence of radiation on metabolic activity in human ex-vivo adipose tissue explants from oesophageal cancer patients. Fiona O'Connell, Klaudia D. Majcher, Aisling B. Heeran, Margaret R. Dunne, Anshul Bhardwaj, Narayanasamy Ravi, John V. Reynolds, Helen Roche, Jacintha N. O'Sullivan.

**Annual Irish Association for Cancer Research Conference, Cork, Ireland, 30th March-1st April 2022**

Title: The influence of radiation on metabolic activity and cytokine expression in adipose tissue explants. Fiona O'Connell, Eimear Mylod, Aisling B. Heeran, Margaret R. Dunne, Anshul Bhardwaj, C. Butler, N. E. Donlon, Narayanasamy Ravi, John V. Reynolds, Helen Roche, Jacintha N. O'Sullivan.

**Annual Irish Association for Cancer Research Conference, Cork, Ireland, 30th March-1st April 2022**

Title: Exploring the metabolism and pro-inflammatory secretions of adipose tissue in oesophageal adenocarcinoma. Fiona O'Connell, Eimear Mylod, Noel E. Donlon, Christine Butler, Anshul Bhardwaj, Aisling B. Heeran, Claire Donohoe, Narayanasamy Ravi, John V. Reynolds, Margaret R. Dunne, Helen Roche, Jacintha O'Sullivan.

**Annual Irish Association for Cancer Research Conference, Cork, Ireland, 30th March-1st April 2022**

Title: Exploring the influence of the adipose secretome on myeloid cell metabolism and function. Fiona O'Connell, Eimear Mylod, Noel E. Donlon, Christine Butler, Anshul Bhardwaj, Maria Davern, Claire Donohoe, Narayanasamy Ravi, John V. Reynolds, Margaret R. Dunne, Helen Roche, Jacintha O'Sullivan.

**The Irish Society for Immunology Annual Meeting, Maynooth, Ireland, 1st – 2nd September 2022**

Title: Exploring the influence of the adipose secretome on dendritic cell and macrophage phenotype and metabolism. Fiona O'Connell, Eimear Mylod, Noel E. Donlon, Christine Butler, Anshul Bhardwaj, Maria Davern, Claire Donohoe, Narayanasamy Ravi, John V. Reynolds, Margaret R. Dunne, Helen Roche, Jacintha O'Sullivan.

**Trinity St James's Cancer Institute, 12th International Cancer Conference, Dublin, Ireland, 13-14th October 2022**

Title: Exploring the influence of the adipose and tumour microenvironment on myeloid cell metabolism and function. Fiona O'Connell, Eimear Mylod, Noel E. Donlon, Christine Butler, Anshul Bhardwaj, Maria Davern, Claire Donohoe, Narayanasamy Ravi, John V. Reynolds, Margaret R. Dunne, Helen Roche, Jacintha O'Sullivan.

**Trinity St James's Cancer Institute, 12th International Cancer Conference, Dublin, Ireland, 13-14th October 2022**

Title: exploring the relationship of adipose tissue metabolism and secretome with clinical parameters of patients with oesophageal adenocarcinoma. Fiona O'Connell, Eimear Mylod, Noel E. Donlon, Christine Butler, Anshul Bhardwaj, Aisling B. Heeran, Claire Donohoe, Narayanasamy Ravi, John V. Reynolds, Margaret R. Dunne, Helen Roche, Jacintha O'Sullivan.

**Awards**

- GESINAS-ImmunoTools-Award for Social commitment 2021.
- IACR AOIFA Conference Award 2020.
- The Musgraves - Breakthrough Cancer Research PhD Scholarship, 2019.

**Outreach**

- Science Week 2022 – Experimental lead for school visit "STEM"
- Transition Year Programme – Introductory talk and feedback session 2022
- Transition Year Programme – Organized and gave talk and Experimental lab Proteins in Cancer from Biomarkers to Treatment
- Science Week 2020 – Experimental lead for online video resource for schools entitled "A day in the life of a cancer researcher in the Trinity St. James's Cancer Institute"
- Science Week 2019 – Experimental lead for school visit "STEM"
- TTMI TAP Day - Acids and Bases Station – 2019
- Transition Year Programme – Introductory talk and feedback session 2019

**Teaching**

- Assisted in the delivery of "Cell Culture" and "ELISA" practical for MSc in Translational Oncology 2021.
- Assisted in the delivery of "Practical Course in Molecular Biology Techniques" week for MSc in Molecular Medicine 2022.
- Assisted in the delivery of "Cell Culture" and "ELISA" practical for MSc in Translational Oncology 2022.
- Assisted in the delivery of "Practical Course in Molecular Biology Techniques" week for MSc in Molecular Medicine 2021.
- Supervisor of a medical student on a Dr. Henry Cooke Drury Research Fellowship 2020.

Project Title: Assessing the effects of 1,4-dihydroxy quininib on macrophage phenotype and polarisation.

- Co-supervisor on MSc project Translational Oncology 2021.

Project Title: Evaluation of the effects of a novel dual radiosensitiser drug with gold nanoparticles on obese microenvironment in oesophageal adenocarcinoma.

- Co-supervisor on MSc project Molecular Medicine 2022.

Project Title: Assessing the influence of fatty acid metabolism on macrophage phenotype and function in oesophageal adenocarcinoma.

**Table of contents**

**List of Figures**

**List of Tables**

**Abbreviations**

| | |
|---|---|
| 5-FU | 5-fluorouracil |
| ACM | Adipose conditioned media |
| AJCC | American Joint Committee on Cancer |
| AKT | Protein kinase B |
| AMPK | AMP activated protein kinase |
| ANOVA | Analysis of variance |
| APC | Allophycocyanin |
| ASCO | American Society of Clinical Oncology |
| ATCC | American Type Culture Collection |
| ATP | Adenosine triphosphate |
| Bax | Bcl-2 associated X protein |
| BCA | Bicinchoninic acid |
| Bcl-2 | B cell lymphoma 2 |
| Bcl-xl | B-cell lymphoma-extra large |
| bFGF | Fibroblast growth factor (basic) |
| Bid | BH3 interacting-domain |
| BMI | Body mass index |
| BO | Barrett's oesophagus |
| BSA | Bovine serum albumin |
| CAA | Cancer-associated adipocytes |
| CAF | Cancer-associated fibroblast |
| cAMP | Cyclic adenosine monophosphate |
| CCL | Chemokine ligand |
| CCR | Chemokine receptor |
| CD | Cluster of differentiation |
| CM | Conditioned media |
| CRM | Circumferential resected margin |
| CRP | C-reactive protein |
| CRT | Chemoradiation |
| CSF | Colony stimulating factor |
| CT | Computed tomography |
| DC | Dendritic cell |
| DMEM | Dulbecco's Modified Eagle Medium |
| DMSO | Dimethyl sulfoxide |
| DSB | Double strand break |
| ECAR | Extracellular acidification rate |
| EDTA | Ethylenediaminetetraacetic acid |

| | |
|---|---|
| ELISA | Enzyme-linked immunosorbent assay |
| EUS | Endoscopic ultrasound |
| FASN | Fatty acid synthesis |
| FAO | Fatty acid oxidation |
| FACS | Fluorescent activated cell sorting |
| FBS | Foetal bovine serum |
| FCCP | Carbonyl cyanide-p-trifluoromethoxyphenylhydrazone |
| FDG-PET | Fluorodeoxyglucose positron emission tomography |
| Flt-1 | Fms related receptor tyrosine kinase 1 |
| GDF-15 | Growth/differentiation factor 15 |
| GORD | Gastroesophageal reflux disease |
| GI | Gastrointestinal |
| GM-CSF | Granulocyte-macrophage colony-stimulating factor |
| Gy | Gray |
| H+ | Leak Proton leak |
| HIF | Hypoxia inducible factor |
| HLA-DR | Human leukocyte antigen – DR isotype |
| ICAM | Intercellular adhesion molecule |
| ICCM | Irradiated cell conditioned media |
| IFN | Interferon |
| IL | Interleukin |
| IP-10 | Interferon gamma induced protein 10 |
| JAK | Janus kinase |
| LPS | Lipopolysaccharide |
| M-CSF | Macrophage colony-stimulating factor |
| MCP | Monocyte chemoattractant protein |
| MDC | Macrophage derived chemokine |
| MDSC | Myeloid-derived suppressor cell |
| MDT | Multidisciplinary team |
| MEK | Mitogen activated protein kinase |
| MIP | Macrophage inflammatory protein |
| MMP | Matrix metalloproteinase |
| MRI | Magnetic resonance imaging |
| NADH | Nicotinamide adenine dinucleotide + hydrogen |
| NF-κB | Nuclear factor kappa B |
| NK | cells Natural killer cells |
| NKT | cells Natural killer T cells |
| OA | Oleic acid |
| OAC | Oesophageal adenocarcinoma |

| | |
|---|---|
| OCR | Oxygen consumption rate |
| OGJ | Oesophagogastric junction |
| OS | Overall survival |
| OXPHOS | Oxidative phosphorylation |
| PA | Palmitic acid |
| PARP1 | Poly[ADP-Ribose] polymerase 1 |
| PBS | Phosphate buffered saline |
| PD-1 | Programmed cell death protein 1 |
| PDGF | Platelet derived growth factor |
| PD-L1 | Programmed death-ligand 1 |
| PET | Positron emission tomography |
| PET-CT | Positron emission tomography computed tomography |
| PlGF | Placental growth factor |
| ROS | Reactive oxygen species |
| RPM | Revolutions per minute |
| RPMI | 1640 Roswell Park Memorial Institute 1640 |
| SAA | Serum amyloid A |
| SAT | Subcutaneous adipose tissue |
| SCC | Squamous cell carcinoma |
| SEM | Standard error of the mean |
| sICAM | Soluble intercellular adhesion molecule |
| STAT-3 | Signal transducer and activator or transcription 3 |
| sVCAM | soluble vascular cell adhesion molecule |
| TAM | Tumour associated macrophage |
| TARC | Thymus and activation regulated chemokine |
| TCA | Tricarboxylic acid |
| TCM | Tumour conditioned media |
| TGF-β | Transforming growth factor beta |
| TLR | Toll like receptor |
| TNF | Tumour necrosis factor |
| TRG | Tumour regression grade |
| TSLP | Thymic stromal lymphopoietin |
| US | Ultrasound |
| VAT | Visceral adipose tissue |
| VEGF | Vascular epidermal growth factor |
| VFA | Visceral fat area |

# *Chapter 1*

## *Introduction*

## 1.1 Oesophageal cancer

### 1.1.1 *Epidemiology and incidence*

Oesophageal cancer is the seventh most common oncological malignancy globally and the sixth leading cause of cancer mortality [1]. Oesophageal cancer is classified into two histologically distinct subtypes, squamous cell carcinoma (SCC) and oesophageal adenocarcinoma (OAC), the OAC subtype also includes oesophagogastric junctional adenocarcinomas (OGJ). SCC are predominantly identified in the middle and upper third of the oesophagus, whilst OAC is usually identified in the distal third of the oesophagus. OGJ occur between the distal end of the oesophagus, the oesophageal gastric junction and within the cardia and subcardia of the stomach (**Figure 1.1.1**). OGJ are further categorised using the Siewart classification, into type I, type II and type III depending on the tumour epicentre location. Generally according to Siewarts classification, type I is where the epicentre lies 1-5 cm above the oesophageal gastric junction, type II the epicentre lies within 1 cm above to 2 cm below the oesophageal gastric junction and type III is where the epicentre lies 2-5 cm below the 1 cm above to 2 cm below the oesophageal gastric junction (**Figure 1.2.2**).

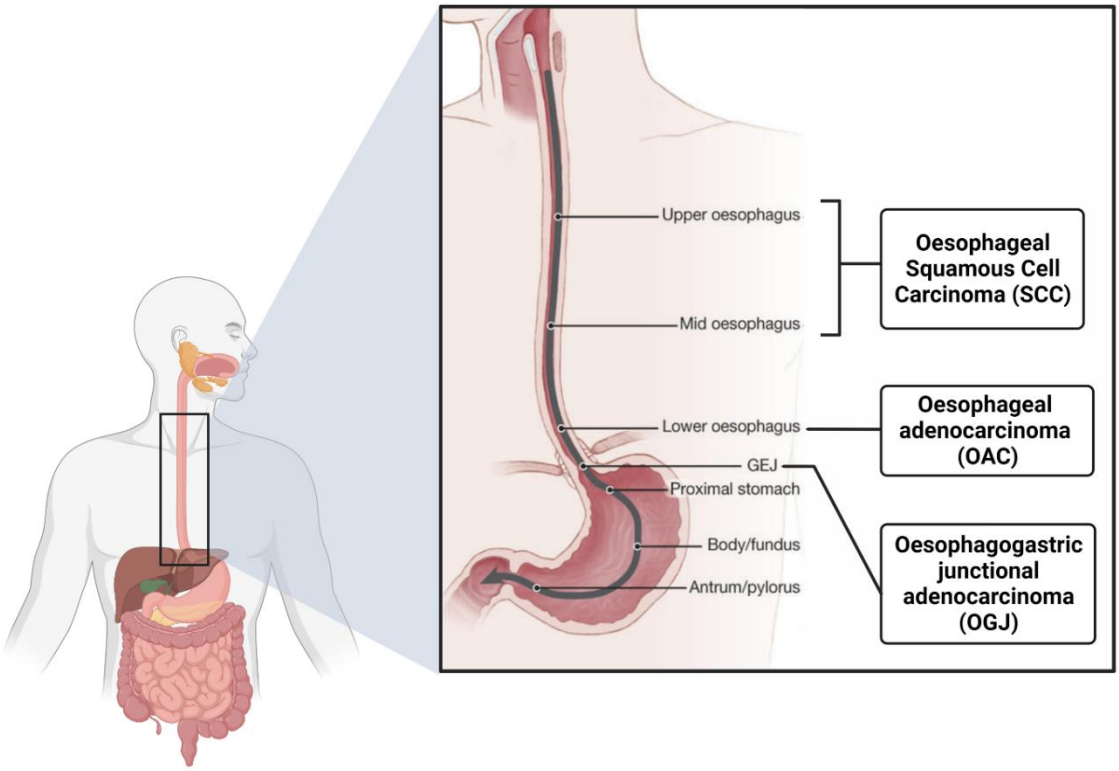


**Figure 1.1.1 Location of SCC, OAC, and OGJ tumours**

This figure depicts the anatomical locations that cancers of the oesophagus develop. SCC tumours predominantly develop in the mid to upper third of the oesophagus. OAC tumours are typically located in the distal third of the oesophagus. Whilst oesophagogastric junctional adenocarcinomas occur between the distal end of the oesophagus, the oesophageal gastric junction and within the cardia and subcardia of the stomach. Adapted from [2]

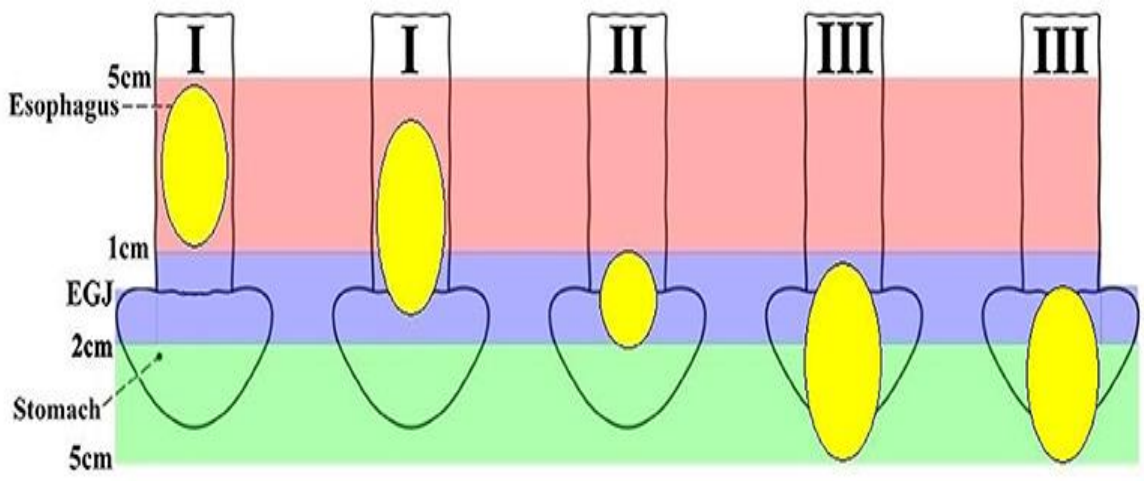


**Figure 1.1.2 Depiction of the Siewert classification criteria for OGJ.**
Definition OGJ (oesophageal gastric junction) cancer is defined and classified according to the location of its epicenter by Siewert's classification, which defines three types of OGJ cancers.

- Type I tumors (lower oesophageal adenocarcinoma) are located 1–5 cm above the OGJ, irrespective of oesophageal gastric junction involvement.
- Type II tumors (cardia adenocarcinoma) are located 1 cm above to 2 cm below the oesophageal gastric junction.
- Type III tumors (subcardial gastric adenocarcinoma) are located 2–5 cm below the oesophageal gastric junction with involvement of the oesophageal gastric junction and distal esophagus. Adapted from [3]

The incidence of oesophageal cancer is variable across different countries. However, typically oesophageal cancer cases are more prevalent in the western world, Asia, and southeast African countries. Ireland in particular falls in the highest percentile with greater than 4.6% prevalence of oesophageal cancer in 2020 [1,4]. SCC is the predominant pathological type of oesophageal globally, however, most of these SCC cases are reported in China, Japan, and southeast Africa countries. OAC is more prevalent in the United States, Australia, and the northwest of Europe (**Figure 1.1.2, OAC in green and SCC in yellow global map**) [1,4]. Smoking and heavy alcohol consumption are identified as risk factors for SCC development, whilst, the rising prevalence of OAC particularly in high-income countries is strongly linked to the paralleled surge observed in increased body weight and GORD [5,6].

The incidence of OAC is reported to have increased by 48% over the past 15 years [7]. The incidence of oesophageal cancer mirrors the pattern of prevalence, with the highest incidences being reported in the western world, Asia, and southeast African countries (**Figure 1.1.2, blue global map**) [1,4].

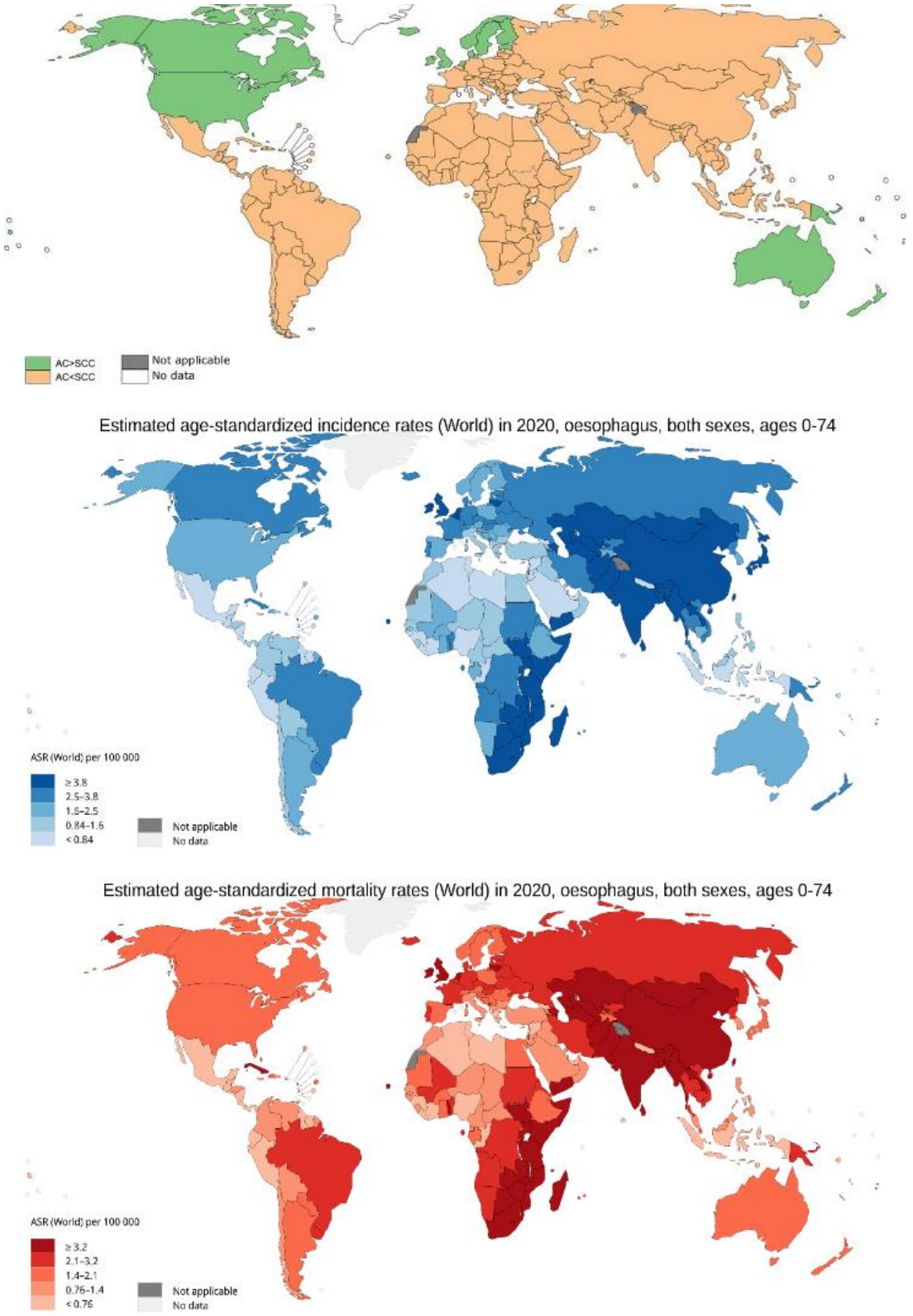


**Figure 1.1.3 Global illustration of the prevalence, incidence and mortality rates associated with oesophageal cancer.**

Prevalence of OAC over SCC is indicated by the green shading in the top global map (2018), incidence is indicated within the blue middle global map (2020), whilst the associated mortality is illustrated within the red middle global map (2020) [1,4].

Ireland again falls into the highest percentile globally reporting over 3.8% of oesophageal cancer cases [1,4]. A cumulative incidence of 515 oesophageal cancer cases were reported in ireland from 2018-2020, of these reported cancers 66% of the cases were reported to be males [8].

OAC has been identified as a poor prognosis cancer, with a survival rate of approximately 20% when diagnosed at an early stage. The mortality rates associated with oesophageal cancer again reflects the pattern of prevalence and incidence, with the highest mortality being reported in the western world, Asia, and southeast African countries [1,4]. Ireland again falls in the highest percentile with greater than 3.2% mortality rates being reported due to oesophageal cancer in 2020 [1,4]. The cumulative mortaility attributed to this disease in ireland from 2018-2020 was 438 cases with 66 % of these being male [8]. Between the period of 2018 to 20202 deaths from cancers of the oesophagus in males ranked the 5th most common and comprised 5.7% of all cancer deaths in males [8]. It was further reported that mortality rankings for this high fatality cancer were actually higher than their incidence ranking [8].

In Ireland the predicted incidence and mortality rates associated with oesophageal cancer are bleak and predicted to increase by 67% by 2040 in both male and females combined. Unfortunately, increases in mortality rates are predicted to rise to equal the level of incidence of oesophageal cancer in males in Ireland by 2040 [4].

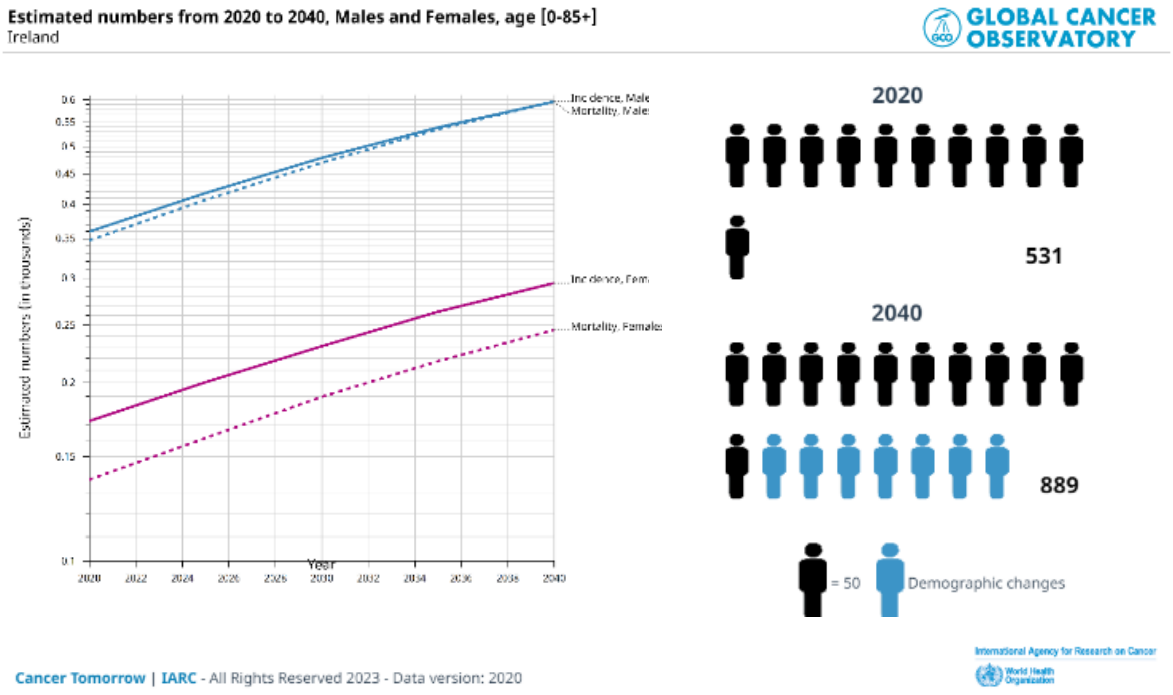


**Figure 1.1.4 Schematic of the predicted trends in oesophageal cancer until 2040**

The incidence and mortality rates associated with oesophageal cancer are predicted to increase by 67% by 2040 in both male and females combined. With the mortality rate predicted to matching the level of incidence of oesophageal cancer in males by 2040 [4].

### 1.1.2 *Diagnosis and Staging*

OAC is typically diagnosed at a locally advanced stage, this is largely due to its asymptomatic nature. Patients usually present with unexplained weight loss, dysphagia, and acid reflux. A multi-modality approach is usually taken for the diagnosis of OAC, consisting of endoscopic ultrasound, a computed tomographic (CT) scan and positron-emission tomography (PET) scan [9].

Endoscopy is predominantly used to determine the classification of tumour growth (T classification) and preliminarily identify whether there is any nodal involvement (N classification). CT scans further aid in the classification by defining the local extent of tumour growth, identifying enlarged nodes which may indicate lymph node involvement as well as assessing the local environment for metastasis (M classification). Whole body molecular imaging with fludeoxyglucose (18F-FDG) using PET scan is typically utilised in the initial staging of tumours to assess nodal involvement and distant metastasis [10]. This technique also aids in monitoring tumour response to therapy, long-term cancer surveillance especially in patients with locally advanced disease. These classifications are then combined to create a TNM classification that accounts for the extent of tumour invasion, nodal involvement as well as local and distant metastasis (**Figure 1.1.5**). This classification is further informed using histological grading of tumour biopsies, identifying whether a cancer is undifferentiated, poorly, moderately, or well differentiated [11]. The criteria for each of these subclassifications is outlined in **Table 1.1.1** [12,13].

Clinical staging of OAC is carried out using the TNM (spell out here even though I know you individually said what each one is above)system which was developed and routinely updated by the American Joint Committee on Cancer (AJCC) [11]. The correct utilisation of this staging system is critically important as its combined outputs inform the subsequent treatment decisions. Appropriate treatment actions and regimens are chosen depending on patient TNM classification as outlined in **Table 1.1.2** to better optimise OAC patient outcomes.

Following completion of neo-adjuvant therapy, patients are restaged in a similar manner to diagnosis. This is a critical step in individualizing therapy, as it allows for initial guidance on treatment response but also can detect potentially emerged distant metastasis which may influence a patients treatment regimen plan and care [14].

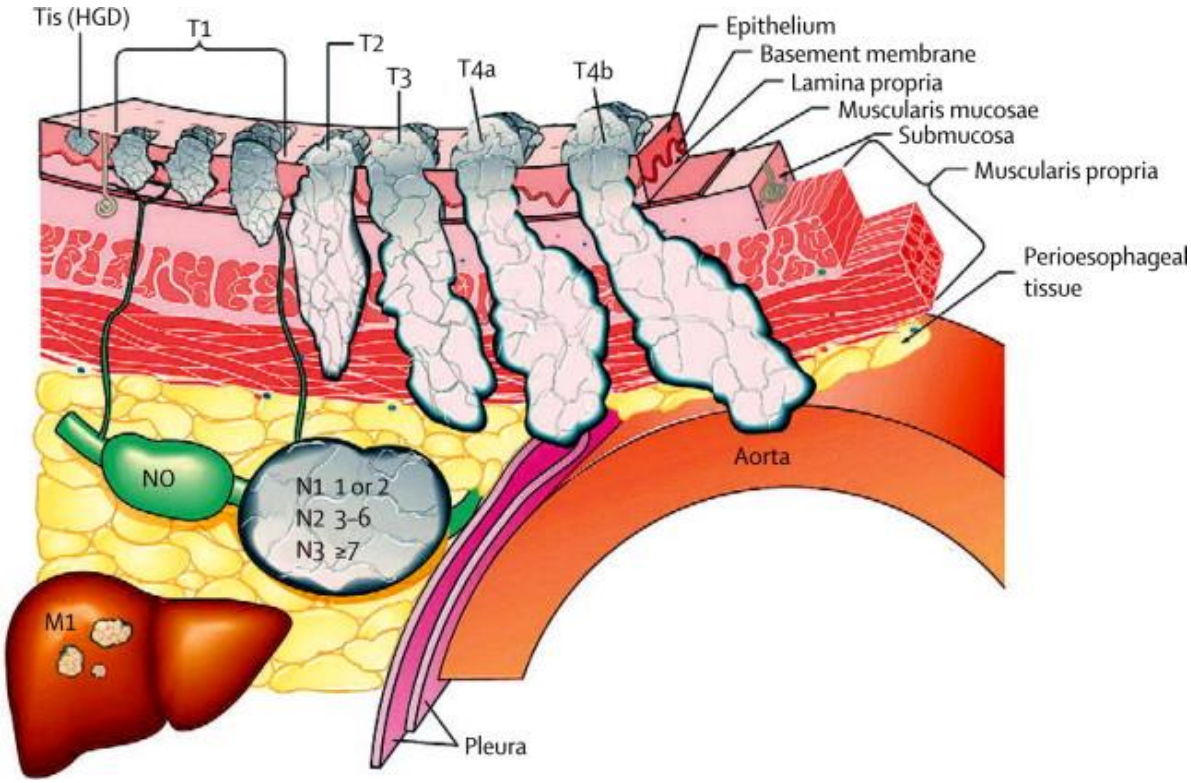


**Figure 1.1.5 Illustration of TNM Classification and histological grading for OAC**
Depiction of the latest version of the TNM classification system for OAC grading, indicating the level of tumour invasion (T classification), nodal involvement (N classification) and presence of metastasis (M classification). Taken from [15].

**Table 1.1.1 TNM Classification and histological grading for OAC adapted from [12,13].**

| Classification | | Criteria |
|---|---|---|
| **T** | TX | Tumour cannot be assessed |
| | T0 | No evidence of primary tumour |
| | Tis | High grade dysplasia |
| | T1 | Tumour invades lamina propria, or muscularis mucosa, or submucosa |
| | (T1a) | Tumour invades lamina propria, or muscularis mucosa |
| | (T1b) | Tumour invades submucosa |
| | T2 | Tumour invades muscularis propria |
| | T3 | Tumour invades adventitia |
| | T4 | Tumour invades adjacent structures |
| | (T4a) | Tumour invades pleura, pericardium, azygos vein, diaphragm, peritoneum |
| | (T4b) | Tumour invades adjacent structures, the aorta, vertebral body, trachea |
| **N** | N0 | No regional lymph node metastasis |
| | N1 | 1 to 2 positive lymph node metastasis |
| | N2 | 3 to 6 positive lymph node metastasis |
| | N3 | ≥7 positive lymph node metastasis |
| **M** | M0 | No distant metastasis |
| | M1 | Distant metastasis |
| **Histo - logical Grade** | G1 | Well differentiated |
| | G2 | Moderately differentiated |
| | G3 | Poorly differentiated |
| | G4 | Undifferentiated |

**Table 1.1.2 OAC tumour stage classification based on TNM and therapeutic options [16].**

| Stage | T Classification | N Classification | M Classification | Therapeutic options |
|---|---|---|---|---|
| **0** | Tis | N0 | M0 | Local ablative therapy (EMR) |
| **I** | T1 | N0 | M0 | Surgery |
| **IIA** | T2 | N0 | M0 | Surgery |
| | T3 | N0 | M0 | |
| **IIB** | T1 | N1 | M0 | Neo-adjuvant therapy with or without surgery |
| | T2 | N1 | M0 | |
| **III** | T3 | N1 | M0 | Neo-adjuvant therapy with or without surgery |
| | T4 | Any N | M0 | |
| **IVA** | Any T | Any N | M1a | Chemotherapy/Radiation therapy with/without surgery |
| **IVB** | Any T | Any N | M1b | Palliative treatment |

### 1.1.3 *Treatment options for OAC patients*

If tumours are identified early at stage 0, (which can typically be identified as part of the routine screening for Barrett's patients), these can be treated endoscopically with local ablation therapy. Additionally, if OAC is identified at the earlier stages of I-IIB, these patients can be sent directly for surgical resection. However, unfortunately the most common occurrence is the diagnosis of OAC at the later stages IIB-IVA. Therapy is then required to debulk the tumour prior to surgical resection. Consequently, a multi-modality approach is used to treat this disease at later stages which involves perioperative chemotherapy regimens (treatment before and after surgery) or neoadjuvant treatment combination chemoradiotherapy (treatment prior to surgery) for locally advanced tumours followed by surgical resection. Patients identified at the final stage of IVB are typically referred for palliative treatment. The recommended treatment for each patient is highly dependent on multiple factors including tumour stage, tumour location, and the patients' medical fitness for receiving a particular therapeutic modality.

In Ireland, currently the standard of care for OAC is surgery alone, perioperative chemotherapy including **FLOT regimen** or neo-adjuvant chemoradiotherapy including **CROSS regimen** with or without surgery [17,18] **(example of treatment flow in Figure 1.1.6)**. Cancer Trials Ireland sponsored the Neo-AEGIS randomised, phase III clinical trial. It has recently reported no evidence that peri-operative chemotherapy regimen FLOT was unacceptably inferior to multimodal neo-adjuvant chemoradiotherapy regimen CROSS therapy. However, results did identify a slight enhancement in local tumour response in the chemoradiotherapy CROSS regimen arm compared with peri-operative chemotherapy regimen FLOT [19]. Unfortunately, approximately 70% of patients do not show a complete pathological response to these therapies which is accompanied with an increased risk of recurrence [20].

With this knowledge, research has recently turned to assessing the efficacy of adjuvant immunotherapy in OAC and OGJ. The CheckMate577 phase-3 clinical trial which examined the efficacy of using PD-1 checkpoint inhibitor nivolumab as an adjuvant treatment combined with neoadjuvant chemoradiotherapy and surgery, saw significant increases in disease free survival in the nivolumab group [21]. Recently, increased expression of circulating soluble checkpoints PD-1, PD-L2, TIGIT and LAG-3 were observed in OAC and OGJ patients up to 6 weeks after surgery, an occurrence that was correlated with the development of metastatic disease in early postoperative course [22]. Taken as a whole, immunotherapy in the adjuvant setting particularly directly after surgery could hold the potential to aid cancer regression and prevent recurrence by invoking an anti-tumour immune response.

Further to this, research has also highlighted that increased PD-L1 expression is associated with deficient mismatch repair in HER2 positive breast cancer, indicating that MMR screening may aid in the personalisation and efficacy of anti-PD-L1 immunotherapy [23]. However, research in the setting upper gastrointestinal cancers, reports that PD-L1 expression in tumour cells was associated with poorer outcomes, whilst PD-L1 expression on tumour associated immune cells was associated with more favourable outcomes [24]. These observed effects were HER2 independent, but further research is required to assess if dual inhibition of HER2 and PD-L1 improves patient survival.

Whilst there are several classification systems for grading tumour response to neo-adjuvant treatment, the most widely used is the Mandard scoring system, which categorises tumour regression grades (TRG) into 5 scores 1-5 (**Figure 1.1.7**) [25]. TRG 1 is representative of a complete pathological response with an absence of viable residual tumour cells and fibrosis extending through the tumour margin. TRG 2 is characterised by the presence of residual isolated tumour cells scattered through the fibrosis. TRG 3 is described as an increase in residual viable tumour cells but is still predominated by fibrosis. TRG 4 is characterised by residual viable tumour cells outgrowing the fibrosis. The final score of TRG 5 represents an absence of any regressive changes. Within the Mandard scoring system, a TRG of 1-3 was significantly associated with disease-free survival, when compared to TRG 4-5 [25].

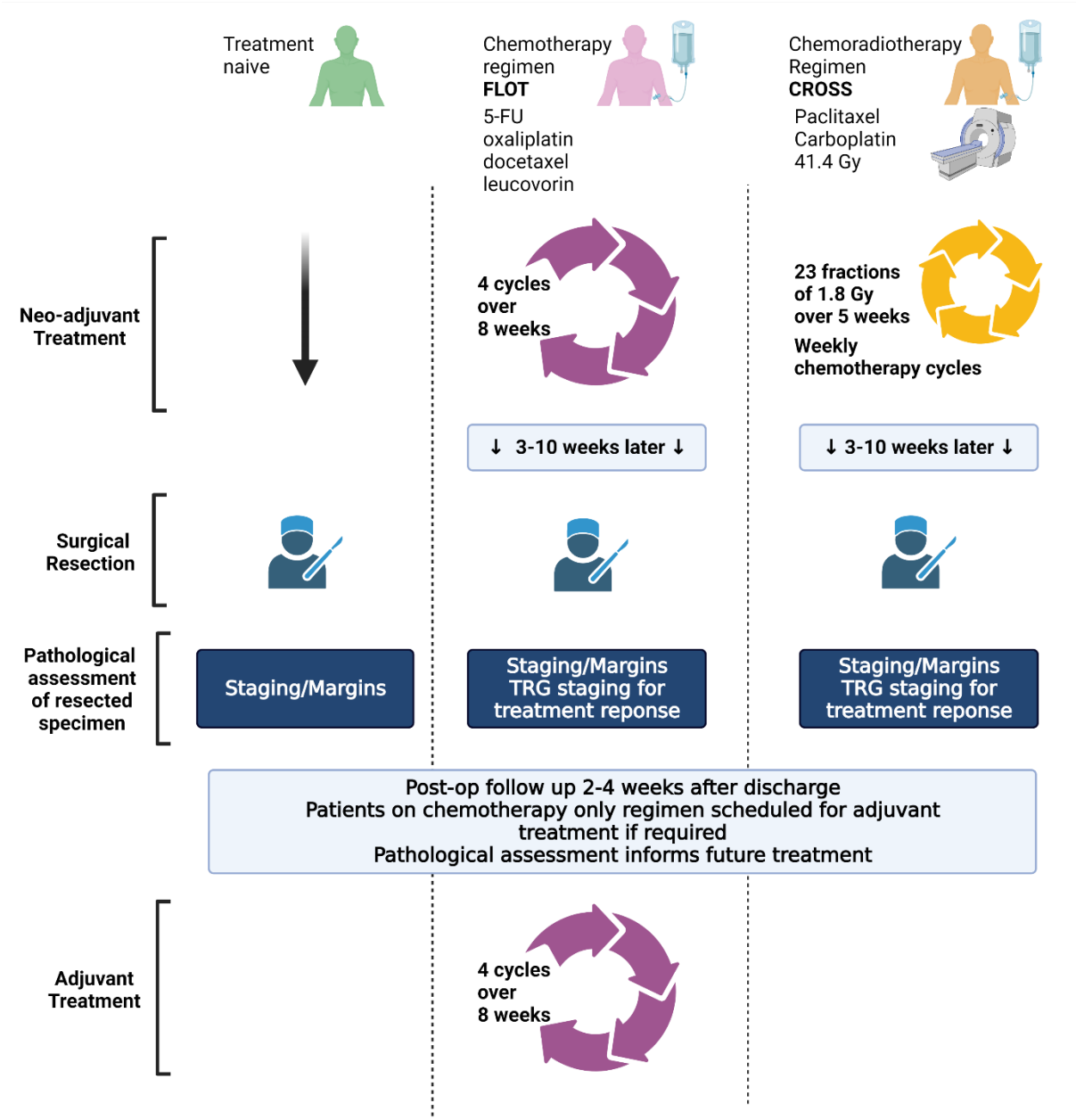


**Figure 1.1.6 Flow diagram indicating the current treatment options in Ireland for OAC**
Details of treatment options for OAC patients, treatment naïve patients go straight to surgery, patients who perioperatively receive chemotherapy regimen FLOT and patients who receive neo-adjuvant chemo radiotherapy regimen CROSS. Illustrated from the information in *Reynolds et al* [26].

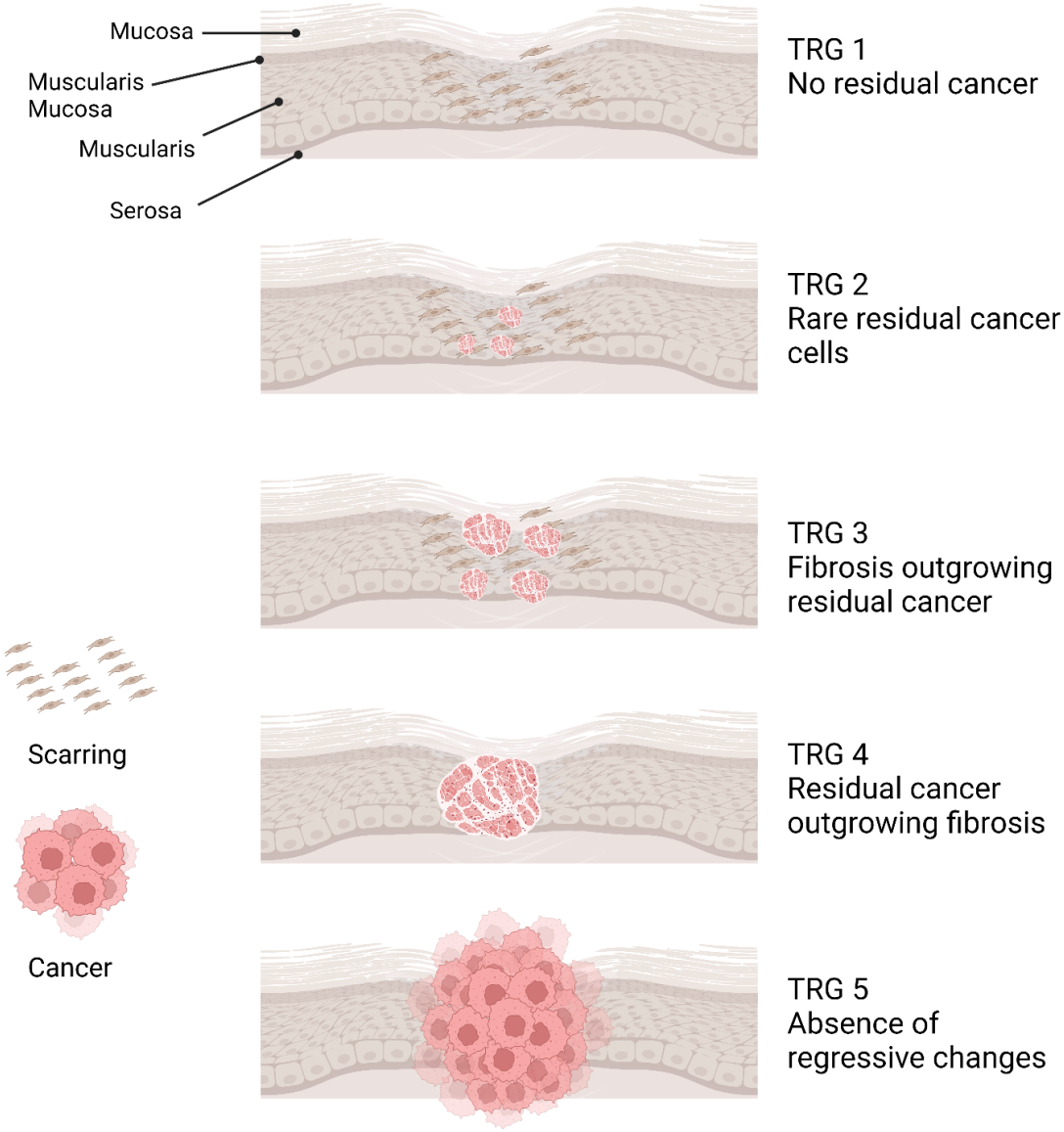


**Figure 1.1.7 Pathological response grading using Mandard grading for oesophageal cancer**
Mandard grading characterises complete response as histologic fibrosis but with no viable residual tumour cells (TRG 1). Subtotal response (TRG 2) as the presence of rare residual cancer cells scattered through the fibrosis. Partial response (TRG 3) was inferred from an increased number of residual cancer cells, but still predominated by fibrosis. Minimal remission (TRG 4) showed residual cancer outgrowing fibrosis. Whilst no response was indicated by absence of any regressive changes (TRG 5). Adapted from [25]

### 1.1.4 *Risk factors for the development of OAC*

Three of the strongest risk factors associated with the development of OAC include gastro-oesophageal reflux disorder (GORD), precursory condition Barrett's oesophagus and increased visceral obesity [27].

**GORD**

GORD is a common clinical condition, that allows the abnormal reflux of the gastric contents and acid from the stomach back into the oesophagus, due to a weakness or relaxation of the lower oesophageal sphincter (**Figure 1.1.8**). Symptomatic GORD increases the risk of malignant transformation due to the continued exposure of the lower oesophagus to repeated inflammation and oxidative stress. The use of proton pump inhibitors is the common treatment for GORD. However, up to 40% of patients remain symptomatic on this standard therapy, with a further 15% of patients that suffer from erosive esophagitis failing to achieve complete healing after the common 8 weeks of treatment [28,29]. Chronic oesophageal exposure to gastric acid overtime is linked to the development of ulcers, peptic strictures, or Barrett's oesophagus(BO) [30]. However, only approximately 10% of patients with GORD have been reported to progress to BO [31] .

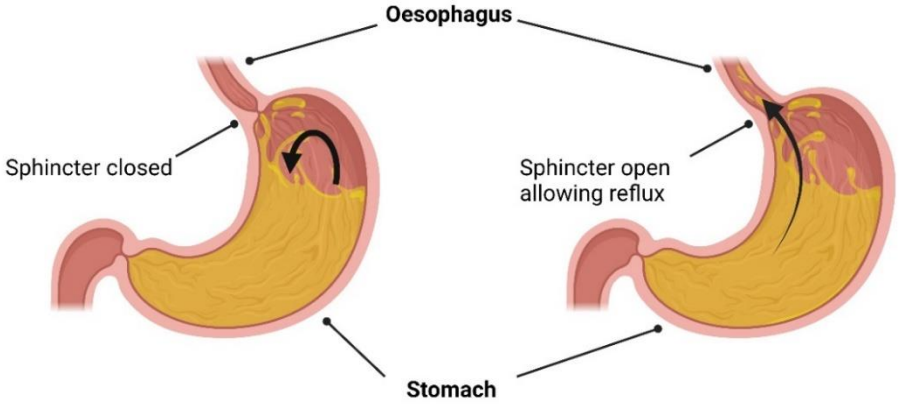


**Figure 1.1.8 Schematic of gastroesophageal reflux disorder**
GORD is the reflux of gastric contents and acid from the stomach back into the oesophagus due to an untypical weakening or relaxation in the lower oesophageal sphincter which can be observed on the right, the typical closure is depicted on the left of the figure.

**Barrett's Oesophagus**

BO is a premalignant condition associated with the development of OAC. BO is defined as a change in the normal stratified normal squamous epithelium of the oesophagus into mucin secreting columnar epithelium, as a result of exposure to chronic inflammation. The transition of BO goes from non-dysplastic Barrett's oesophagus to low grade dysplasia, followed by high grade dysplasia that has been linked to the development of OAC [32] (**Figure 1.1.9**). Previous work from our group has identified positive correlations in BO tissue between pro-inflammatory mediator IL-1β and GAPDH, a surrogate of glycolytic metabolism [33]. Further to this, p53 expression which has been linked to increased risk of neoplastic progression in BO patients, was observed to be positively correlated with oxidative phosphorylation associated ATP5B and

negatively associated with GAPDH [33]. Interestingly, previous work in our group has also identified that OAC biopsies utilise higher levels of oxidative phosphorylation than glycolysis, strengthening the postulation that cancer cells utilise metabolic plasticity to aid in their progression and proliferation.

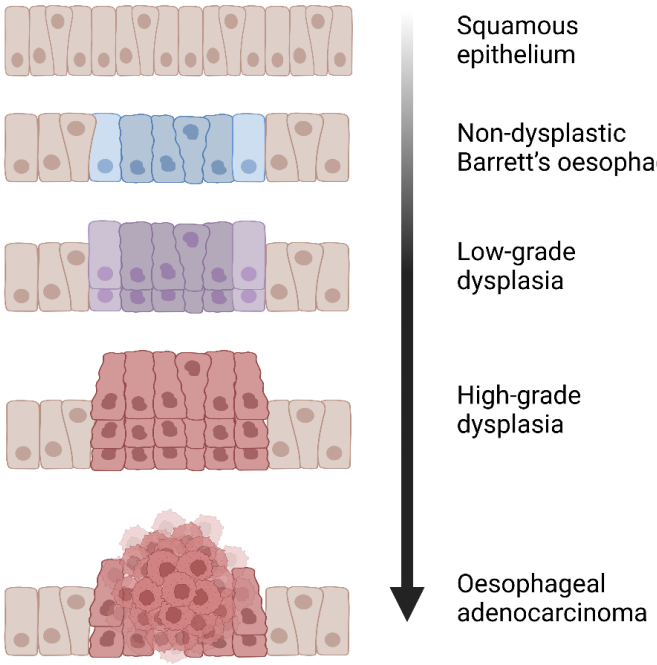


**Figure 1.1.9 Histopathological progression of Barrett's oesophagus**
Progression from squamous epithelia to non-dysplastic Barrett's oesophagus, low-grade dysplasia, high-grade dysplasia, and finally oesophageal adenocarcinoma.

Previously research has linked the development of BO with long-standing GORD, familial history of the disease, and obesity. It has also been identified to be more prevalent in men [34]. Previous work from our lab also identified that GAPDH was positively correlated not only with pro-inflammatory IL-1β, but also with length of BO segment and waist circumference a key identifier of visceral obesity [33]. Whilst BO has been identified as a precursory condition to OAC, approximately 0.22% of patients per year are identified to have progressed from BO to OAC. However, the incidence of these reports varied depending on whether there was evidence of dysplasia (1.4%) or no dysplasia (0.07%) [35]. Previously, a meta-analysis has shown that surveillance of patients with non-dysplastic BO increases early detection of neoplastic lesions and improves patient survival [36]. Given these findings, identifying stratification criteria to inform which patients with BO will progress to OAC and does who will not is a critical field of research. Whilst no clinical criteria is currently available for this, work is ongoing with current reports identifying a promising multi-biomarker panel [37]. These types of panels have been reported to outperform single markers in early detection of oncological diseases [38] and may prove a promising stratification tool to identify BO patients before they progress to OAC.

**Obesity**

Obesity is defined as the accumulation of excess fat tissue and overwhelming evidence from the literature identifies its association with the development and progression of certain cancers [39,40]. Obesity is a rising global epidemic, one in need of crucial insight to elucidate how it confers increased risk for numerous diseases. The World Health Organisation has established that a Body Mass Index (BMI) greater than 25 is overweight and a BMI greater than 30 is obese [41] and numerous chronic health conditions are directly caused or deleteriously effected by obesity. Diabetes mellitus, cardiovascular disease, hypertension and several types of cancer are highly associated with elevated BMI [42]. The American Society of Clinical Oncology (ASCO) has stated that if current obesity trends continue, in the next twenty years obesity will surpass smoking as the leading preventable cause of cancer [43]. Therefore, with an ever-rising obesity level throughout the global population, research and further understanding into the implications of obesity particularly in relation cancer development, progression and treatment response is imperative. The most recent assessment of the global burden of cancer attributable to high body-mass index was conducted in 2012 by the WHO. It stated that 75% of the reported cases of OAC were situated in America and Europe combined (**Figure 1.1.9**). The number of OAC cases that are attributable to excess body mass index are most prevalent in the western world (**Figure 1.1.10**).

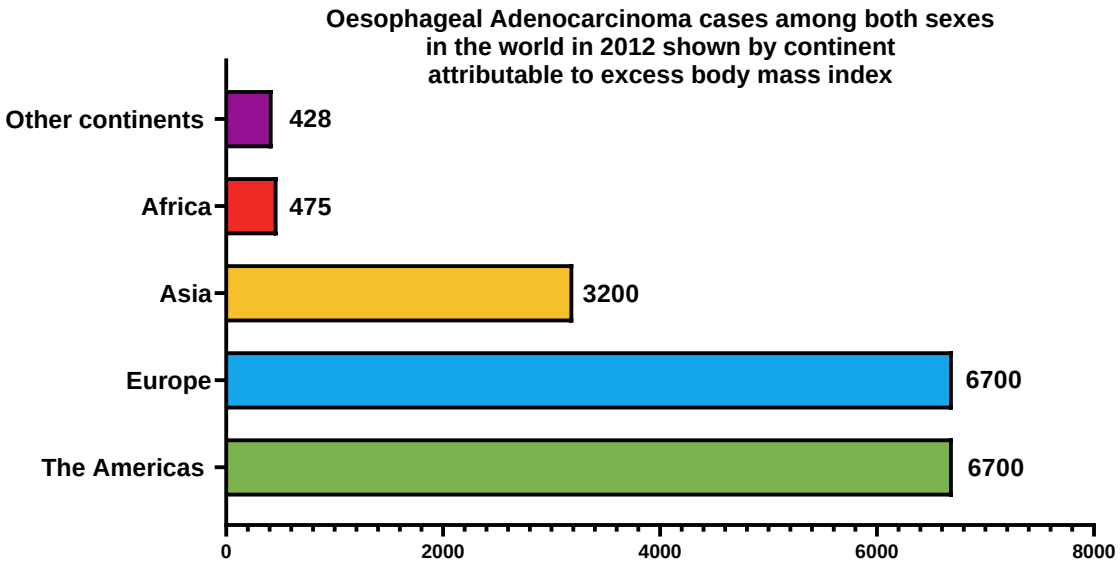


**Figure 1.1. 10 Prevalence of obesity associated OAC cases by continent.**
Prevalence of OAC cases that were attributable to excess body mass index in 2012 per each continent, 75% of the cases of obesity associated OAC reported were in America and Europe combined. Illustrated from [44].

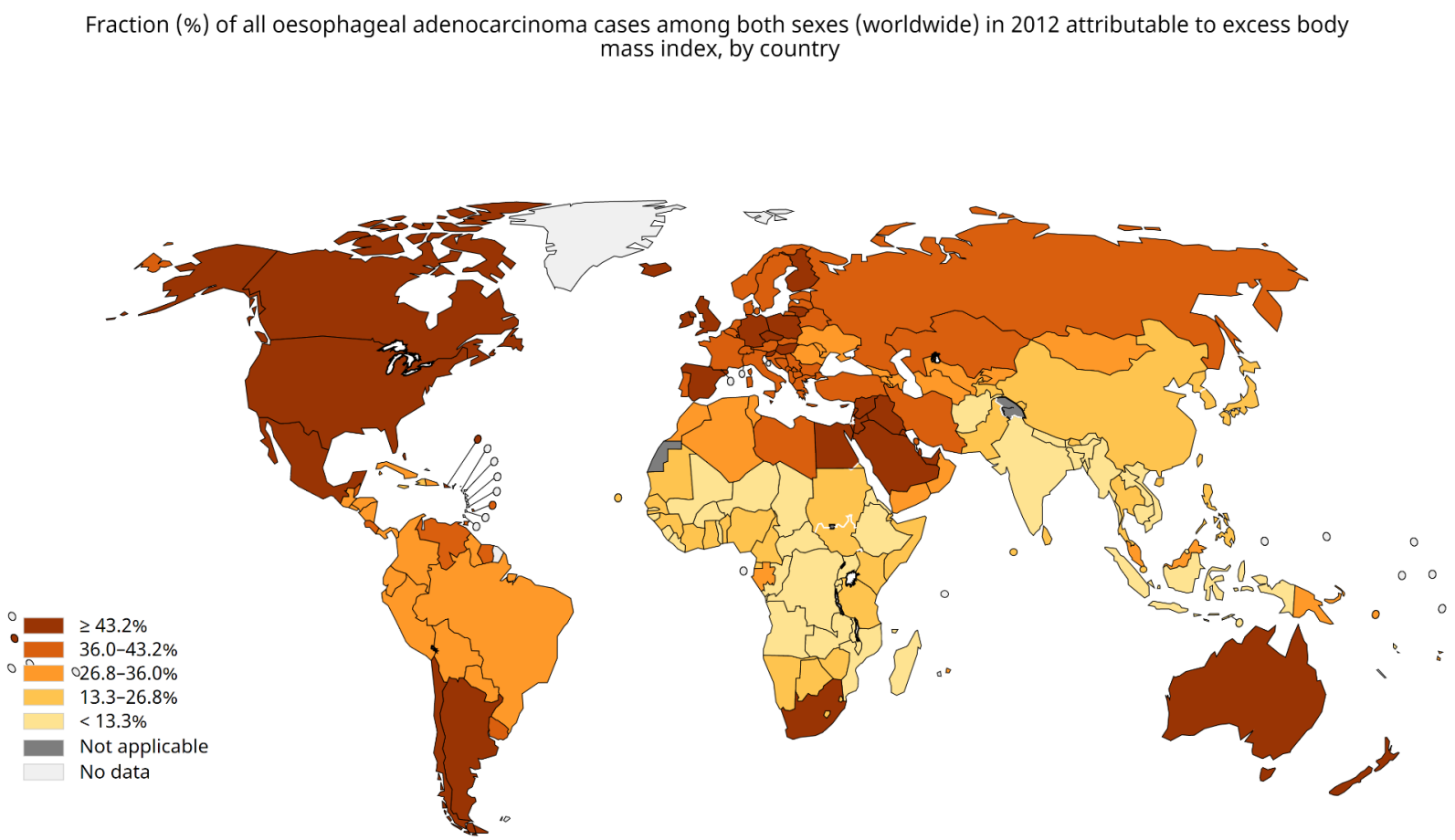


**Figure 1.1. 11 Global prevalence of obesity associated OAC cases.**

Global prevalence of OAC cases reported that were attributable to excess body mass index in 2012, countries highlighted in a darker brown indicate the percentage of OAC cases reported in this country that were attributable to obesity were greater or equal to 43.2% of all reported OAC cases. Taken from [44].

Large-scale epidemiological studies demonstrate a consistent and compelling association between the risk of cancer development/progression and elevated body mass index (BMI) for many gastrointestinal cancers including OAC. OAC, is one of the most strongly associated cancer types with the rising level obesity levels [45–49], making it an ***exemplar model for studying the influence of obesity in cancer particularly due to its proximity to visceral adipose depots***.

One of the significant factors of obesity that affects cancer progression and resistance to current therapies is the development of a hypertrophic dysfunction adipose tissue biology and its secretome. Adipose tissue has been linked to the secretion of a series of pro-inflammatory factors, this leads to a local environment that is primed to aid tumour development and progression [50]. Obese adipose tissue has been implicated in potentiating the efficacy of therapies as well as aiding in metastasis due to its anatomical distribution. Adipose tissue surrounds tumours that establish in the abdominal cavity providing them with an enriched pro-tumorigenic nutrient environment that can aid their tumour growth and transition.

However, research has now begun to infer that obese individuals may possess an added advantage in treatment response known as the "***the obesity paradox***". This is the conception that whilst obesity may negatively impact in the initiation and progression of cancer, it may aid in treatment efficacy and decreased toxicities [51]. However, issues have previously been reported in the administration of chemotherapy at full body weight dosing [52], particularly in morbidly obese cancer patients, which may offer another explanation for some of these diminished toxicities. We and others have shown that many different cellular processes in the tumour microenvironment of OAC tumours that can confer cancer cells with added survival advantages and aid in their resistance to current modalities of treatment [53–55].

## 1.2 Adipose tissue

### 1.2.1 *Adipose tissue biology*

Adipose tissue is a regulatory tissue with many endocrine and metabolic functions. It comprises of two main types of adipocytes, white and brown, which have an inverse contribution to energy production and storage. Brown adipose tissue consumes energy reserves and produces heat. Brown adipocytes have a large abundance of mitochondria that confers a larger capacity for substrate oxidation. The mitochondria in brown adipocytes utilise uncoupling protein 1 (UCP1), to induce proton leak that uncouples oxygen consumption from ATP production, to facilitate macronutrient catabolism including oxidation of fatty acids [56]. Adipocytes in white adipose tissue possess a large unilocular lipid droplet and can store excess energy as fat. The visceral adipose depot is one of the largest sites of white adipose tissue. Visceral adipose tissue surrounds and protects organs in the abdominal cavity. Visceral adipose depots are an enriched nutrient environment that has the potential to secrete numerous inflammatory mediators into circulation when it undergoes hypertrophy.

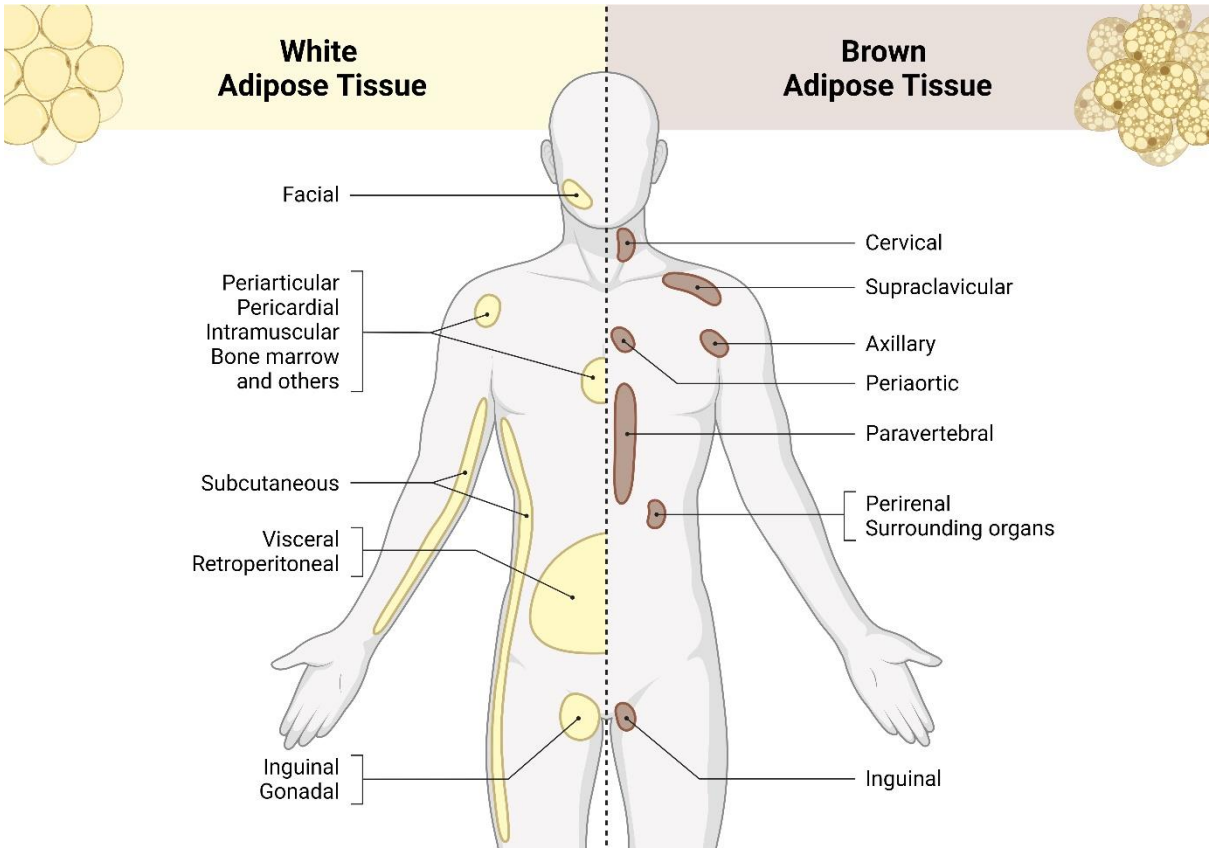


**Figure 1.2.1 The anatomical distribution of white and brown adipose depots**.
White adipose tissue which stores excess energy and nutrients is mainly located in visceral and subcutaneous depots with other minor depots around the body. Depots of brown adipose tissue which participates in catabolic reactions are more typically located in the upper back, above the clavicles, around the vertebrae, and in the mediastinum. Image adapted from Biorender template.

Obesity is one of the key drivers of hypertrophic adipose tissue, leading to the establishment of a chronic low-grade inflammatory state, that deleteriously alters many processes in metabolic diseases. Numerous biological processes have been linked with amplifying the aberrant biological function of obese adipose tissue and its complex microenvironment. Factors such as inflammation, angiogenesis, fibrosis and the altered secretions and recruitment of immune cells have all been implicated in propagating the hypertrophic obese adipose microenvironment that leads to the development of cancer [57,58] (**Figure 1.2.2**).

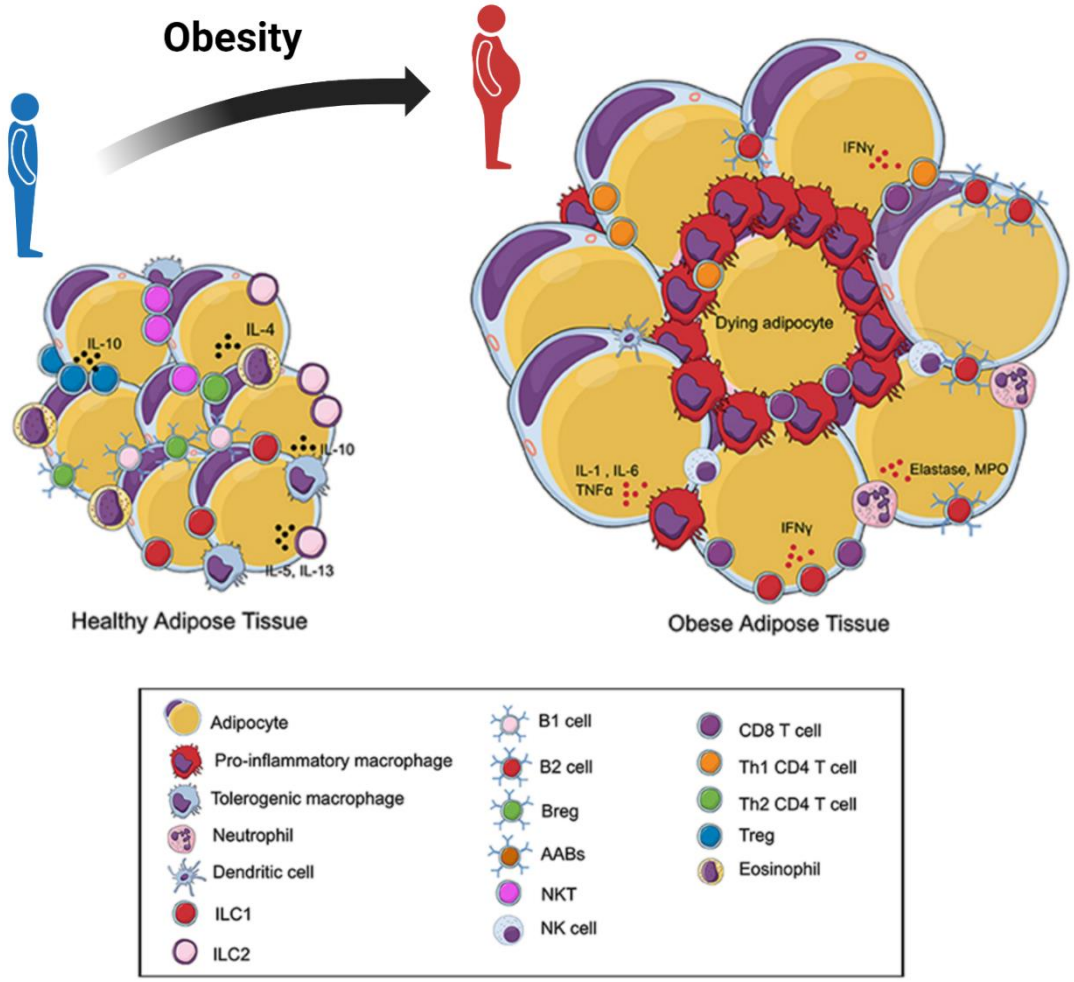


**Figure 1.2.2 Adipose tissue biology and its changes from healthy to obese.**
Adipose tissue is composed of a series of components including adipocytes and a series of immune cell. In healthy adipose tissue the recruitment, activation and secretome of the adipose tissue immune cell infiltrate appears to be regulated. However as adipose tissue expands and becomes hypertrophic due to obesity, there is a change within the immune cell infiltrate and adipose secretome. Immune cells including M1 macrophages, Neutrophils, CD8+ T cells and Th1 associated mediators become more highly expressed and result in elevated secreted levels of pro-inflammatory mediators including IFN-γ IL-1, IL-6 and TNF-α which aid in propagating the low-grade inflammatory state associated with obese adipose tissue. Adapted from [59]

Interestingly, previous work from our department has shown that visceral adipose tissue explants from OAC patients have a higher reliance on oxidative phosphorylation associated metabolism compared with explants derived from subcutaneous adipose depots [60]. This study also identified increased secreted levels of key mediators of inflammation, angiogenesis and immune cell recruitment from visceral adipose tissue, with these levels being the highest in the most viscerally obese of OAC patients [60].

### 1.2.2 *Fatty acids*

Dietary fatty acids are generally categorised into three main subsets, saturated fatty acids, mono-unsaturated fatty acids, and polyunsaturated fatty acids. Saturated fatty acids only possess single carbon bonding and do not have any double bonds within their structure. **Palmitic acid** is composed of a 16-carbon backbone all with single bonds (C16:0) (**Figure 1.2.3, B**). Mono-unsaturated fatty acids have one single carbon bond with their structure and the rest of their carbon bonds are single. **Oleic acid** is composed of an 18-carbon backbone with double bon at Carbon 9 and all remaining carbons having single bonds (C18:1) (**Figure 1.2.3, A**). Poly-unsaturated fatty acids have more than one double bond within their carbon structure.

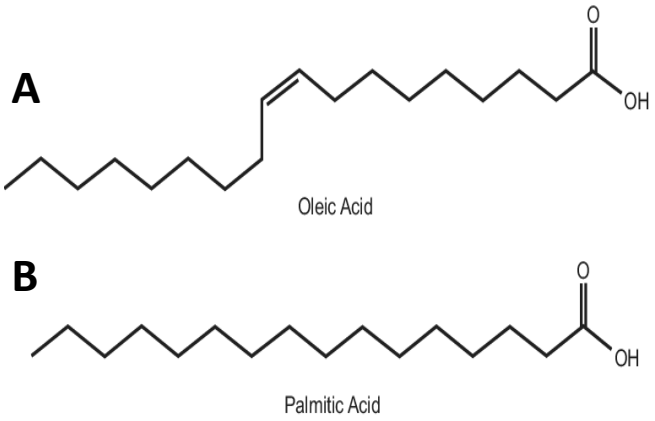


**Figure 1.2.3 Skeletal depiction of the chemical structure of oleic acid and palmitic acid.**
Oleic acid is composed of 18 carbons with a single double bond at Carbon9, palmitic acid is composed of 16 carbons all with single bonding and both fatty acids have the familial identifier of carboxyl group at the end of their structure. Taken from [61]

Saturated fats have been widely reported to have negative effects on heath, increasing obesity, worsening insulin sensitivity and diminishing cardiovascular health [62]. Mono-unsaturated and particularly poly-unsaturated fatty acids have been reported to have widespread health benefits and even postulated to have anti-cancer effects [63,64]. **Oleic (OA) and palmitic acid (PA)** are two of the most common fatty acids found in the human diet. Saturated fatty acids such as palmitic acid have been linked with pro-inflammatory response [65] whilst unsaturated fatty acids including oleic acid have been reported to act in anti-inflammatory manner [66] as well as ameliorating the pro-inflammatory effect of saturated fatty acids [67].

Further to this, fatty acid levels in circulation and within adipose tissue have also been reported to be abrogated by obesity. One of the most common saturated fatty acids found in the human body is PA, which has been observed to be increased in circulation in obese patients [68], however its expression at tissue level is tightly regulated. In contrast, OA one of the most commonly found monounsaturated fatty acid in the human body has previously been reported to be increased in adipose tissue of obese mouse models [69]. This increase was paired with a corresponding increase in Δ 9 desaturated lipids [69], Stearoyl-CoA desaturase (SCD1) is responsible for catalysing the synthesis of monounsaturated fatty acids supported by ELOLV6, with OA being its main product [70,71] (**Figure 1.2**).

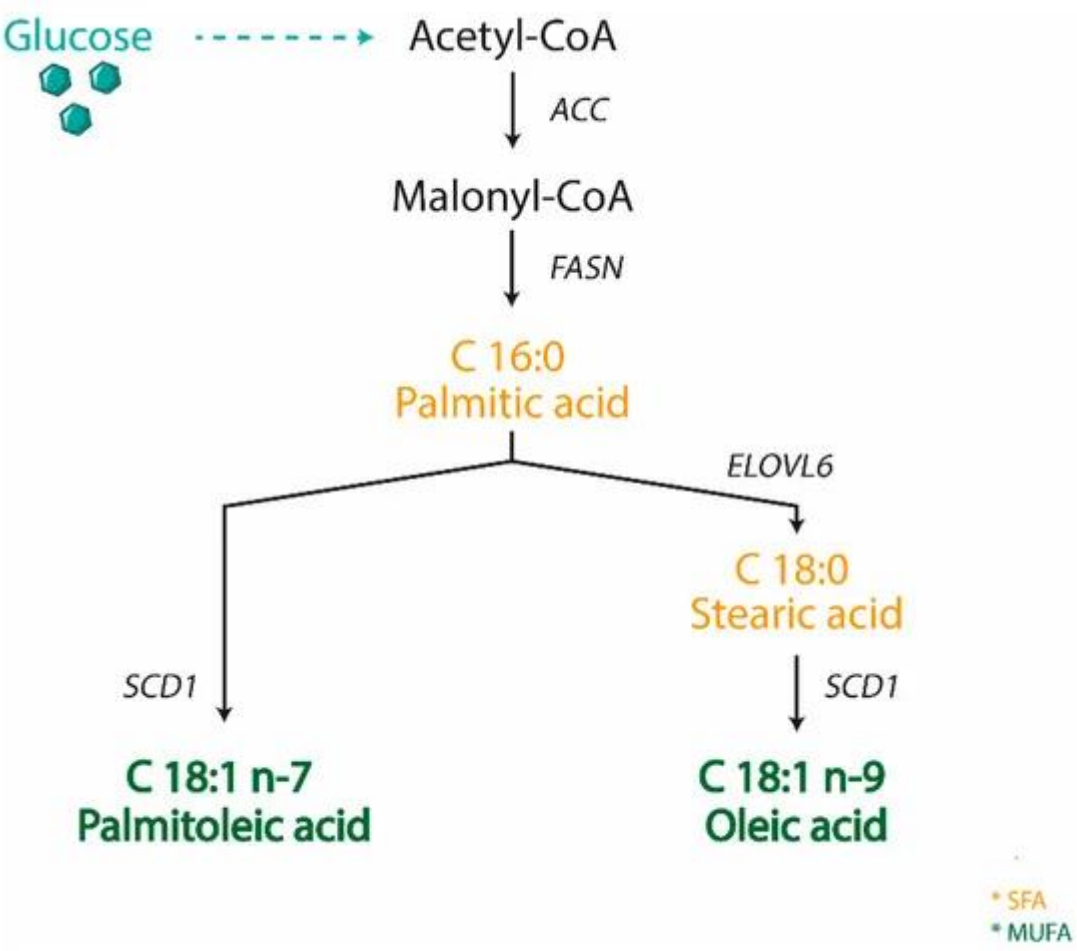


**Figure 1.2.4 Schematic figure representing the biosynthesis of mono-unsaturated fatty acids within the body.**

Glucose that has been catalysed to acetyl-CoA is acted upon by acetyl-CoA c which carboxylates acetyl-CoA to form malonyl-CoA. Malonyl-CoA then undergoes fatty acid synthesis to form palmitic acid. From here palmitic acid is catalysed by Stearoyl CoA Desaturase 1 (SCD1) into palmitoleic acid or is elongated by ELOVL fatty acid elongase 6 (ELOVL6) to stearic acid and then catalysed by SCD1 to form oleic acid. Illustrated from [72]

### 1.2.3 *The obese tumour microenvironment*

Obesity is a major clinical challenge that confers increased risk for numerous diseases as well as potentiating the efficacy of current cancer treatment regimens. The influence of obesity in cancer progression and treatment response is a critical question, as the obesity epidemic is predicted to increase exponentially.

The dysfunctional and hypertrophic biology of adipose tissue in obese individuals, is primed to support a chronic low-grade inflammatory state that has been linked to augmenting metabolic disease and cancer development [73,74]. Inflammation, its signalling pathways, and downstream effectors, play a central role in tumour response to chemotherapy and radiation therapy. Obesity has been reported to maintain this state of low-grade inflammation through the induction of a series of pro-inflammatory mediators including IFN-γ, IL-1, IL-6, IL-8 and TNF-α. Cancer associated adipocytes (CAAs) have been implicated to the increase in secreted level of pro-inflammatory mediators. CAAs have also been reported to have increased secreted levels of Leptin [75], which is increased in obesity [76]. Leptin signalling has been suggested to possess a role in promoting hypoxia, with downstream effects in angiogenesis, aiding cancer cell growth and upregulation of invasion matrix metalloproteinases as well as promoting survival of cancer stem cells [77].

Further to this, chemotherapy and chemoradiotherapy have been reported to augment the secretion of factors from adipose tissue to aid cancer metastasis and survival from cytotoxic interventions [78]. It is postulated that the adipose secretome is a potential attractive therapeutic target to potentiate tumour progression and enhance treatment efficacy [79]. Obesity further supports the tumour microenvironment by recruiting immune cells into adipose tissue, perturbing anti-tumour immunity. Previously we have demonstrated an increase in secreted levels of mediators of immune cell recruitment [80], whilst others studies have shown that obesity status can have detrimental effects the functionality of immune cells [81–85].

The obese adipose milieu leads to deleterious changes in angiogenesis, fibrosis, increased pro-tumorigenic secretions as well as the recruitment and death of immune cells. These alterations in the obese tumour microenvironment confer cancer cells with an added survival advantage allowing them to alter the efficacy of current modalities of therapy [57,58] (**Figure 1.2.5**).

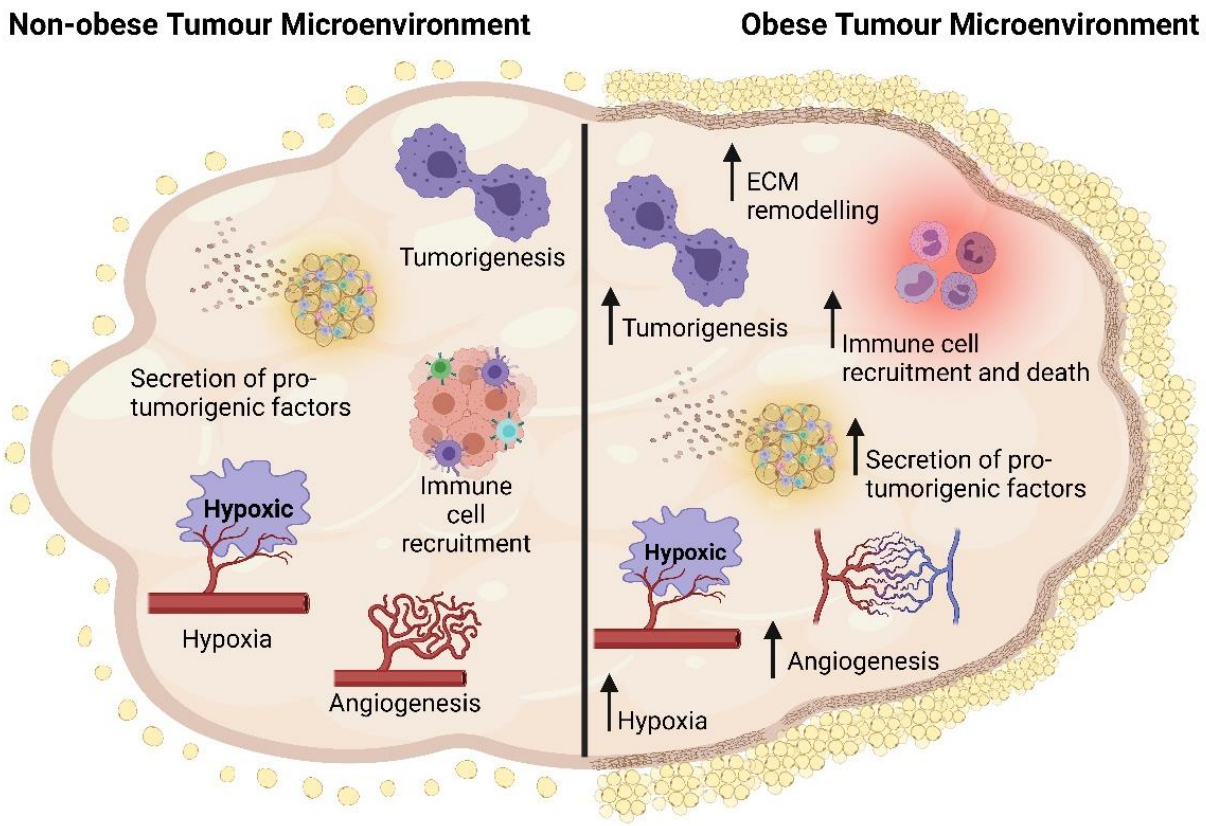


**Figure 1.2.5 The obese tumour microenvironment is primed to aid cancer progression and treatment resistance.**
The tumour microenvironment is composed of tumour cells, immune cells, blood vessels, fibroblasts, extracellular matrix (ECM) and signalling molecules. This pro-tumorigenic milieu is propagated by a series of aberrant processes including angiogenesis, hypoxia, ECM remodelling. Secretion of pro-tumorigenic factors and tumorigenesis. Obesity leads to an accumulation of adipose tissue surrounding the tumour which leads to an environment primed to enhance the cancer cell growth, proliferation, and invasion by inducing augmented levels of angiogenesis, hypoxia, pro-tumorigenic secreted factors, immune cell recruitment and death, and increasing tumorigenesis. The obese tumour microenvironment plays a critical role in protecting cancer cells by altering the delivery of anticancer therapy to the tumour tissue, reducing treatment efficacy, and developing treatment resistant cancer cells. Adapted from [86]

## 1.3 Obesity in chemotherapy treatment response

Chemotherapy has held a central long-standing role in the treatment of cancer [87]. Modern regimens are now more aggressive currently delivered as either primary or combination therapies to treat a series of cancer subsets [88–90]. However, emerging evidence has suggested that factors associated with obesity may contribute to chemoresistance in numerous cancers [91]. With the global incidence of obesity rising, the question surfaces if current chemotherapy regimens still function for all modern society.

### Mechanisms implicated in chemoresistance

#### 1.3.1 *Pharmacokinetics issues*

Obesity has in recent years been linked in certain cancers with a decrease in pathological complete response [92]. Previous research in breast cancer identified obesity and a higher BMI (body mass index) as a negative prognostic factor with worse overall survival neo-adjuvant chemotherapy [93]. Adjuvant chemotherapy regimens investigated in breast cancer were also less efficacious. Obese patients cohorts were identified to have higher associations with distant metastasis and death as a result of breast cancer and other obesity associated comorbidities [94]. Dosing and treatment related toxicities have proved challenging for most cancers but particularly in the obesity setting [95]. This concerns haematological malignancies particularly due to the intensive chemotherapy regimens required for complete pathological response [96]. Obesity had significant impact on decreased overall survival in one “favourable” chemosensitive subgroup of acute myeloid leukaemia (AML) [96]. The “favourable” chemosensitive cohort was designated in accordance with European Leukaemia Network (ELN) guidelines which is used to stratify risk of resistance on the basis of cytogenetics [97]. Studies have reported possible causes for these pharmacokinetics issues may arise from the interactions between adipocytes and lipophilic chemotherapies. Research has shown acute lymphoblastic leukaemia cells co-cultured with adipocytes induced an oxidative stress response in adipocytes which in turn protected cancer cells from daunorubicin [98]. Furthermore, in murine studies, adipocytes have been shown to sequester and metabolise daunorubicin to its inactive form daunorubicinol reducing its cytotoxic effects [99]. However, obesity has also been indicated in the alteration of individuals pharmacokinetics for many drugs including chemotherapy agents [100]. This combined with the highly cytotoxic nature of treatment regimens previously led to chemotherapy dose reduction in obese patient cohorts [101]. However, obese patients receiving chemotherapy are now recommended full weight dosing [52] for rectal, colon, lung cancer and AML did not develop increased therapy related toxicities compared to their non-obese counterparts [102–105]. Studies

conducted in breast, oesophageal and colon cancer have reported decreased treatment related toxicities with regards leukopenia, neutropenia and overall toxicity in obese patients when compared with the non-obese cohort [103,106,107].

### 1.3.2 *Adipocytes producing tumour promoting factors*

Adipocytes play a central role through their interaction with cancer cells at the invasive tumour front which leads to a cascade of events that alter the tumour microenvironment and aid in chemoresistance [108]. Adipocytes are responsible for the secretion of a series of bioactive molecules, including factors commonly denoted as adipokines. Adipokines consist of essential hormones such as adiponectin, resistin and leptin which work in in parallel with proteases, cytokines and growth factors to promote tumorigenesis [109]. It has been widely reported that expression of these adipocyte secreted hormones is deregulated in obesity, metabolic syndrome as well as tumorigenesis and cancer progression [110–112]. This dysregulation leads to serious implications regarding both hormone response and effects on downstream target genes that aid in tumour growth and invasion [112]. Leptin, an adipokine whose secretion is increased in the obese setting [113], has been widely researched for its role in tumorigenesis and treatment response. Leptin signalling have been associated with cancer progression in a series of cancers and have been implicated in contributing to chemoresistance[30–32].

**Leptin**

Leptin has been shown to contribute to taxol chemoresistance in epithelial ovarian cancer cell lines [117]. Previous studies in mouse models have shown that disruption in leptin signalling led to reduced tumour burden compared to mice with normal leptin signalling and extended survival times more significantly than cisplatin or Tamoxifen controls [118,119]. Leptin signalling has been suggested to possess a role in promoting hypoxia, with downstream effects in angiogenesis, aiding cancer cell growth and upregulation of invasion matrix metalloproteinases as well as promoting survival of cancer stem cells in breast cancer [77]. Leptin treatment aided in the survival of vinblastine-resistant triple negative breast cancer cells treated with paclitaxel or cisplatin. Whilst inhibition of Leptin's receptor OBR showed resensitization of these cells to both paclitaxel and cisplatin [120]. This has led to suggestions that combination of leptin antagonists and leptin receptor inhibition with current chemotherapy regimens may present an alternative more efficacious therapeutic strategy [121].

**Adiponectin**

Studies conducted in one such adipokine, adiponectin, have shown negative correlations between circulating adiponectin and mortality in obese cancer patients [122]. Decreased adiponectin has also been strongly associated with an increased risk of colorectal adenoma and early cancer development [123]. Lower levels of serum adiponectin and high tumour tissue adiponectin levels have been reported in breast cancer, cervical, ovarian and endometrial [124]. Adiponectin has also been illustrated to stimulate sensitivity of peripheral tissue to insulin uptake, therefore decreased adiponectin levels leads to increased insulin serum levels with a knock on effect of increased insulin resistance leading to high blood glucose levels [125]. High blood sugar levels have been associated with enhanced oxaliplatin chemoresistance in colorectal cancer, inhibition of which significantly decreased cell proliferation. Similar findings were noted in patients with high blood glucose having significantly poorer disease free survival than their low blood glucose counterparts at a two year end point [126]. Studies have indicated that adiponectin may have a role in signalling directly to cancer cells reducing angiogenesis and apoptosis. In a mouse angiogenesis model, adiponectin significantly inhibited FGF-2 induced neovascularization and induced apoptosis in a thyroid cancer mouse model [127].

**Resistin**

Resistin is an adipokine that increases with obesity and has been shown to be upregulated in various cancers including colorectal, prostate and endometrial [128]. Resistin has been associated with poorer disease free and overall survival in breast cancer as well as being positively correlated with tumour stage, size and lymph node metastasis [129]. Research in breast cancer cell lines have indicated that upregulated levels of resistin attenuates Doxorubicin induced apoptosis through the induction of autophagy [130]. Cancer cell chemo-sensitivity has been shown to be significantly diminished in hepatocellular carcinoma cells through Galectin-1 induced autophagy limiting the effect of cisplatin [131]. Resistin has also been identified to confer multidrug resistance in multiple myeloma. A study conducted in multiple myeloma cell lines and primary myeloma cells, showed that resistin significantly decreased melphalan induced apoptosis [132].

### 1.3.3 *Free fatty acid uptake*

Recent studies indicate that adipocytes induce elevated expression of fatty acid receptor CD36 in cancer cells which leads to increase free fatty acid uptake and drives cell proliferation and epithelial mesenchymal transition [133,134]. Higher CD36 expression in patients with pancreatic ductal adenocarcinoma has been significantly correlated with microinvasion. Furthermore,

patients in this study who had a higher expression of CD36 had significantly lower overall survival and recurrence free survival compared with patients with low expression of CD36 following gemcitabine adjuvant chemotherapy. Higher expression CD36 was also identified in gemcitabine resistant pancreatic ductal adenocarcinoma cell lines compared with parent cell lines suggesting it may be more influential influence in chemotherapy resistant cancers [135]. Additionally, doxorubicin treatment has also been reported to dysregulate adipose tissue and adipocytes, leading to disruption in lipid storage and elevated free fatty acid levels which may aid in cancer cell metabolism and proliferation [136].

### 1.3.4 *Hypoxia*

Adipose tissue in obese individuals is linked to low-grade hypoxia. This largely results from decreased blood flow in the obese adipose tissue, enlarged adipocytes, increased lipid droplet and the decreased spread of micro-vessels leading to inhibition of oxygen diffusion [137].Hypoxia leads to the activation of HIF-1a which can target adipose stromal cells gene transcription of downstream effector proteins [138]. Hypoxia increases phosphorylation of STAT3 in ovarian cancer cell lines, with cisplatin and taxol showing diminished efficacy in cells in this hypoxic state and resensitization upon return to a normoxic state [139]. HIF-1a holds a significant role in regulation of pro-angiogenic genes including VEGF, Ang-1, Ang-2, bFGF and PDGF [140]. This leads to increased neovascularity allowing increased blood flow and nutrient influx to tumour cells aiding chemoresistance [141]. Chemoresistance in prostate cancer has been highly correlated with intratumoral hypoxia, prostate cancer cells have been shown to have enhanced resistance to doxorubicin, epirubicin and cisplatin under hypoxic conditions [142]. Similar findings have been reported in gastric cancer cell lines, where all cell lines demonstrated an hypoxic acquisition of drug resistance to five common drugs used to treat gastric cancer, including 5-fluorouracil, Adriamycin (doxorubicin), cisplatin, vincristine and etoposide [143]. Hypoxia has also been reported to possess a role in the suppression of adiponectin secretion which as previously mentioned is downregulated in obesity as well [144].

### 1.3.5 *Growth factors lead to angiogenesis and cancer cell survival*

Obesity has been widely associated with hyperinsulinism, insulin resistance and higher secretion levels of IGF-1 in breast, colon, lung and prostate cancers [145]. Increased circulating levels have been observed in OAC patients compared with SCC patients, and interestingly within the OAC patient cohort, IGF-1 was observed to be increased in obese patients [146]. IGF-1R has also been

implicated in chemoresistance in colorectal cells through upregulation of multidrug resistance associated protein 2 (MRP-2) which inhibits drug delivery to tumour cells by reducing intracellular concentrations of cytotoxic chemotherapies [147]. Inhibition of IGF-1R has also demonstrated increased sensitivity in colorectal cancer cell lines to 5-Fluorouracil, Mitomycin C, Oxaliplatin, and Vincristine through the suppression of the MRP-2 promotor [148]. Tumour cells have been shown to survive chemotherapy regimens through the secretion of pro-angiogenic factors such as VEGF, contributed to by the upregulation of HIF-1a in obese patients [140]. Studies in colorectal cancer cell lines have shown that deletion of VEGF expression decreased cell growth, increased spontaneous apoptosis and increased chemosensitivity to 5-fluorouracil [149]. However, another study conducted in ovarian cancer cell line has indicated that taxotere and cisplatin resistant cell lines exhibited decreased expression of VEGF and VEGF receptors compared to chemosensitive cell lines. However this may indicate decreased angiogenesis and as such may effect drug delivery at the tumour site aiding in chemoresistance [150]. Indicating the role of VEGF in chemoresistance may be multifactorial.

### 1.3.6 *Adipose Stromal Cells and Fibrosis*

Adipose Stromal Cells are a central source of the extracellular matrix that drives tumour desmoplasia which not only stimulates vascularization which enhances chemoresistance [151]. One mechanism suggested to be used in prostate cancer to resist chemotherapy, is adipose stromal cells ability to increase nitric oxide synthesis [91]. It has been postulated that adipose stromal cells may possess some of the same immunosuppressive capabilities as mesenchymal stromal cells [152]. Mesenchymal stromal cells have also been implicated in stimulating epithelial mesenchymal transition (EMT) which is intricately linked with chemoresistance [153]. A study conducted in a breast cancer cell line SKBR3 suggests that adipose stromal cells may be manipulated to increase chemosensitivity to doxorubin treatment [154]. Research in prostate cancer has also indicated targeting adipose stromal cells enhances inhibition of cancer cell migration and resistance to docetaxel, cabazitaxel, and cisplatin [155]. In pancreatic ductal adenocarcinoma (PDAC), obesity has been suggested to enhance a pro-fibrotic state leading to a complex stroma desmoplastic reaction which is central in PDAC development [156]. This pancreatic desmoplasia state has been reported to confer increased resistance to chemotherapeutic agents as fibrosis crosstalk diminishes drug delivery [157,158].

**Table 1.3.1 The influence of obesity on the efficacy of chemotherapy in obesity associated cancers.**

| Obesity associated cancer type | Positive or Negative Association | Supporting literature |
|---|---|---|
| Oesophageal Adenocarcinoma | Negative Association | [159] |
| Gastric Cardia | Negative Association | [160] |
| Colon and rectum | Negative Association | [161] |
| Pancreas | Negative Association | [162] |
| Breast: postmenopausal | Negative Association | [136] |
| Endometrial | Negative Association | [163] |
| Ovary | Negative Association | [164] |
| Multiple myeloma | Negative Association | [165] |
| Prostate | Negative Association | [155] |

Whilst obesity has been linked to decrease chemotherapy associated toxicities this is far outnumbered by factors alleviating chemotherapy efficacy. Obesity holds a significant role in enhancing tumour microenvironment to aid chemoresistance through altered adipocyte secretions, enhanced free fatty acid uptake, increased hypoxic conditions and up regulation of associated genes. Indicating that obesity holds a relatively substantial role in enabling cancer cells to develop chemoresistance to enhance growth and evade cell death.

## 1.4 Obesity in radiotherapy treatment response

Radiotherapy, the use of targeted ionizing radiation for the treatment of cancer has been in use since the late 19$^{th}$ century. Modern day treatment has evolved with developments in fractionating doses, x-ray production and delivery technologies, imaging and computerized treatment planning and an evolving understanding of how cancers behave [166]. However, radioresistance and poorer survival rates has been more highly associated with obese patient cohorts than their non-obese counterparts [167].

### Mechanisms implicated in resistance

#### 1.4.1 *Treatment delivery challenges and combination therapies*

Radioresistance and poorer survival rates has been more highly associated with obese patient cohorts than their non-obese counterparts [167]. Studies conducted in endometrial cancer patients, showed that BMI was positively correlated with daily shifts and margin requirements in adjuvant intensity-modulated radiotherapy (IMRT). However it was reported that Image guided Radiotherapy (IGRT), a form of external beam radiotherapy (EBRT), led to a reduction in set up error and resultant margin requirement when compared to no IGRT [168]. The use of cone

beam computed tomography (CBCT) has been reported to improve safety and treatment accuracy by verifying tumour position in endometrial cancer[169].Research conducted in localised prostate cancer has shown similarly that increasing BMI on IMRT was significantly associated with biochemical failure, distant metastasis, cause specific mortality and overall mortality. These significant outcomes have been proposed again to strongly correlate with tumour shifts in obese men which leads to increased error margins [170]. It has also been reported in rectal cancer patients that at three year follow up, obese patients after receiving combined radiotherapy and surgery, showed significantly lower local control than their non-obese counterparts. This could be contributed to set up uncertainties increasing error margins or lack of surgical visibility limiting resection [171].

However, studies conducted in head and neck cancer, a non-obese associated cancer, showed contrasting results. Higher BMI was more positively associated with improved overall survival, recurrence free survival and distant metastasis recurrence free survival compared with non-obese patients [172]. It has also been reported in oesophageal adenocarcinoma, an exemplar model of obesity associated cancer, that overweight and obese patients have an enhanced tumour regression response to neo-adjuvant chemoradiotherapy in comparison to their normal weight counterparts [55]. This calls to question the influence of obesity on the efficacy of radiotherapy or whether combination therapy in obesity associated cancers may enhance tumour regression grade, however further research is required to interrogate this.

### 1.4.2 *Radiotherapy related treatment toxicities*

An issue that has been widely researched in regards radiation therapy regimens is the implications of radiation associated toxicities. In contrast to chemotherapy related toxicities, where obesity has been suggested to improves drug related toxicities, research has indicated that obese patients may develop more radiation related toxicities when compared to normal weight cancer patient cohorts. Research conducted in oesophageal cancer patients receiving chemo-radiation therapy has indicated that higher BMI was correlated with reduced high-grade oesophagitis, oesophageal stricture and high-grade hematologic toxicity common side effects associated with IMRT [106]. Studies in endometrial cancer patients identified that increasing BMI was associated with increased cutaneous radiation toxicities and more gynaecological related toxicities. Multivariate analysis also indicated that gynaecological toxicities were especially increased in the young morbidly obese cohort [173]. In breast cancer similar findings have been reported with higher BMI being correlated with acute skin toxicities such as dry desquamation and moist skin desquamation when compared to normal BMI cohorts [174]. Additionally a BMI

over 30 has been widely cited as a risk factor for radiotherapy-induced cardiotoxicity in breast cancer patients [175]. Similar findings in oesophageal cancer patients were identified, where higher exposure to radiation correlated with greater occurrence of cardiac events [176]. Current research in modernizing combination therapies such as chemo-radiotherapy or radiosensitizers could prove an important avenue of research to allow reduced radiation doses to decrease treatment related toxicities particularly in obese patients.

### 1.4.3 *Adipocytes (Adipocytokines)*

On a cellular level many of the factors suggested to enhance radioresistance are linked with adipocytes. The adipocyte secretome which is altered in obesity, has been suggested to aid cancer cell survival by enabling protective mechanisms to allow cells to evade the toxicity of radiotherapy. Research conducted in melanoma cancer cells has shown that treatment with adipocyte conditioned media protected cancer cells from radiation therapy. Following radiation, adipocyte conditioned media treated cells possessed increased metabolic activity and cellular viability compared to untreated irradiated cells. With the inference, the adipocyte secretome conferred malignant melanocytes an enhanced survival advantage against radiation induced oxidation stress [177]. In contrast, research has shown that exogenous adiponectin and adipocyte conditioned media can protect fibroblasts from radiation-induced senescence, a common side effect of radiotherapy. Adiponectin alone not only diminished prostate and colorectal cancer cells growth but also did not protect cancer cells from radiation induced damage [178].

Senescence is a common feature of obesity supporting a low-grade inflammatory state with defective adipocytokine production and adipogenesis [179]. While it has been postulated that adipocyte senescence could influence the local environment, spreading out the stress response through senescence-associated secretory phenotype (SASP), more research is required to fully elucidate the role of adipocyte senescence in radioresistance [180]. One effect of the adipocyte secretome that is highly evoked in cancer cells, is adipocytes ability to secrete factors that can alter the pro-inflammatory landscape of the tumour environment [181]. The role of inflammation in cancer progression and treatment response is a well-versed topic, with its influence in radioresistance no different. Inflammation, its signalling pathways, and downstream effectors, play a central role in tumour response to radiation therapy.

A central action identified in adipocytes, is their potential to elevate tumour cells IL-6 secretions [182]. Breast cancer cells co-cultured with adipocytes prior to irradiation showed higher secretion of IL-6 from cancer cells alone. Further investigation revealed that incubation with recombinant

IL-6 following irradiation, also led to increased levels of phosphorylation in Chk-1 inhibitors and greater radioresistance in cancer cells. This reiterates the same effect observed by adipocyte co-culture on tumour cell secretions [78]. Research conducted in colorectal cancer cell lines indicated that constitutive levels of NF-kB activity is positively associated with the amount of radiation induced NF-kB activity. With the arising concept that the level of constitutive NF-kB activity may be predictive of the efficacy of radiotherapy in patients allowing for more individualized therapy [183]. Research conducted *in-vitro* and *in-vivo* in colorectal cancer cells illustrated that proteasome inhibitors, such as bortezomib, enhanced radiotherapy efficacy and augment radiation induced apoptosis through NF-kB inhibition.

Research has well established the influence of STAT3 in radioresistance. Persistent activation of STAT3 has been shown to aid in tumour promoting inflammation including pathways such as NF-kB and IL-6-Jak. Stat-3 has been highly researched as a therapeutic target due to its role in inflammation mediated radio-resistance [184]. It has also been in established in the obese setting that increased circulating levels of leptin has led to chronic activation of the JAK-STAT3 pathway, which may also contribute to radioresistance in obese cancer patients [185]. Adipocyte secreted factors have also been suggested to play a role in activating Chk-1 mediated pathway, potentially leading to deregulated DNA damage response and cell recovery from cytotoxic stress. Research *in-vivo* and *in-vitro* in HNSCC has shown that CHK1/2 inhibitors enhance the cytotoxic effect of radiation therapy and showed significant anti-tumour effects [186]. Similar results were observed in breast cancer cells which were co-cultured with adipocytes, adipocyte secretions lead to higher expression of Chk-1 and an more resistant phenotypes [78]. Research conducted in breast cancer cell lines showed that after radiation treatment cancer cells expressed higher levels of IGF-1R and could recruit adipose derived mesenchymal stem cells, which produce IGF-1. It was also illustrated that inhibition of IGF-1R, decreased radioresistance caused by IGF-1 expressed by adipose derived mesenchymal stem cells [187].

### 1.4.4 *Hypoxia*

As previously mentioned, hypoxia is upregulated in in obesity and has been widely reported to aid chemoresistance in cancer cells. It has also been implicated in possessing a role in aiding tumour cell evasion from radiotherapy through the oxygen effect [188]. The availability of oxygen is integral to how efficacious radiotherapy is, as it exerts its cytotoxic effect via generation of reactive oxygen species. Obesity has been widely confirmed to be a state of chronic low-grade inflammation and leads to increased tissue and tumour hypoxia. HIF-1 which is upregulated in hypoxic conditions has been reported to promote radioresistance, however research has

indicated that unsuitable timing of HIF-1 inhibition can suppress radiotherapy mediated killing rather than aid it. An *in-vivo* mouse model of cervical cancer cells treated with HIF-1 inhibitor prior to radiation treatment showed increased tumour hypoxia suppressing the efficacy of radiation therapy. However post radiation treatment with a HIF-1 inhibitor was shown to greatly enhance the efficacy of radiotherapy and delay tumour growth [189].

### 1.4.5 *Metabolism*

Metabolic changes have been reported to induce radioresistance in cancer cells. In particular glucose and mitochondrial pathways have been highlighted to affect the efficacy of radiotherapy [190]. Resistance was suggested to be conferred in tumour cells through abrogated AKT signalling, as inhibition of AKT decreased Glut1 expression and lactate production [191]. Reprograming of lipid metabolism with increased uptake of exogenous lipids and interchange from polyunsaturated fatty acids to saturated fatty acids. This has been suggested to confer tumour cells with protection from lipid peroxidation hence decreasing efficacy of radiation treatment [192]. Further to this, our group has previously shown in an isogenic cell line model of radioresistant OAC, mitochondrial function, morphology and energy metabolism were altered in radioresistant cells. Moreover, radioresistant cells were also reported to demonstrate enhanced metabolic plasticity, effectively switching between oxidative phosphorylation and glycolytic energy metabolism pathways which was associated with enhanced clonogenic survival [53].

### 1.4.6 *Genetic Instability*

Obesity has been reported to elevate genomic instability and SAC gene expression in oesophageal cancer cell lines. Parental radiosensitive cancer cells treated with adipose tissue conditioned media (ACM) generated from obese individuals, showed enhanced radioresistant profiles [193].

**Table 1.4.1 The influence of obesity on the efficacy of radiotherapy in obesity associated cancers.**

| Obesity associated cancer type | Positive or Negative Association | Supporting literature |
|---|---|---|
| **Oesophageal Adenocarcinoma** | Positive association | [194] |
| **Colon and rectum** | Negative association | [171] |
| **Pancreas** | Positive association | [195] |
| **Breast: postmenopausal** | Negative association | [78] |
| **Endometrial** | Negative association | [196] |
| **Thyroid** | No significant association reported | [197] |
| **Prostate** | Negative association | [170] |

Whilst obesity has been linked to decreased genetic instability and improved response rates to chemoradiation therapy in certain cancers this is far outnumbered by factors alleviating radiotherapy efficacy. Obesity holds a key role in the treatment delivery challenges, which requires significant planning to minimise error margins which are greater in obese individuals. Radioresistance is also aided through altered adipocyte secretions, increased hypoxic conditions and up regulation of associated genes. Research currently suggests that obesity enables cancer cells to develop radioresistance increasing their ability to survive and avoid cell death.

## 1.5 Obesity in combination cancer therapies

It is becoming more common place to treat cancer patients with combination therapies. These therapies can combine two or more drugs or different types of therapy such as immunotherapy, chemotherapy, and radiotherapy along with inhibitors of aberrant biological processes that are known to be perturbed in the cancer setting [198].

### Mechanisms implicated in treatment efficacy or resistance

#### 1.5.1 *Targeted monoclonal antibodies*

Studies conducted in mouse models indicated that anti-CD40 and IL-2 systemic immunotherapy in aging mice with increased visceral adiposity developed reduced anti-tumour efficacy and overall survival rates compared with their lean counterparts. It was shown in obese mice the above therapy induced cytokine storm, enhanced adipose M1 macrophage polarization and increased secretion of pro-inflammatory factors IL-6 and TNF-a culminating in lethality [199]. Research conducted in metastatic colorectal cancer patients has also reported that bevacizumab, a VEGF targeted monoclonal antibody, combination therapy may be less efficacious in obese patients, with progression free survival and overall survival [200]. It was also reported in breast cancer patients, that bevacizumab lack of efficacy could be contributed to obesity. It was reported that breast cancer patients with a higher BMI were found to have higher levels of systemic IL-6 and FGF-2 with a downstream effect of their tumour vasculature being less sensitive to bevacizumab [201].

A clinical issue established in HER2 positive breast cancer is the development of acquired resistance to trastuzumab, a monoclonal antibody targeting the HER2 receptor. An increased BMI in patients receiving this treatment has also been correlated with decreased overall survival. PI3-K signalling pathway activated by adipocyte secreted factors such as GDF15 has been implicated in HER2 positive cell lines decreased response to trastuzumab [202]. Elevated circulating levels of GDF-15 have been associated with obesity [203]. Further research is required

to interrogate the potential use of this correlation of patients with higher BMI developing acquired resistance to trastuzumab and have poorer outcomes.

### 1.5.2 *Hormone therapy*

Research conducted in Breast cancer cell lines have shown that obesity inhibits the efficacy of tamoxifen treatment. Adipocytes and their secretome derived from adipose stem cells from obese women counteracted the anti-proliferative effect of tamoxifen treatment whereas adipocytes from normal weight women did stimulate the same effect. Furthermore, the addition of leptin, IL-6 and TNF-a at concentrations corresponding to plasma levels in obese patients also inhibited the anti-proliferative effect of 4-hydroxytamoxifen [204]. In prostate cancer, obese patients treated with radiotherapy and androgen deprivation therapy (ADT) had a greater association with prostate cancer related mortality [205]. This may be contributed to by ADT side effects which has been correlated with the development of an enhanced pro-inflammatory and obesity like adipose tissue microenvironment [206]. However, in metastatic castration-recurrent prostate cancer a higher BMI has been suggested to have protective effect against overall and cancer related mortality [207].

### 1.5.3 *Protease inhibitors*

As previously discussed, proteasome inhibitors have been shown to enhance the efficacy of radiotherapy in colorectal cancer cells. However, it has been indicated that bortezomib as first line treatment has decreased efficacy in early diagnosed symptomatic multiple myeloma patients with excess visceral adipose tissue [208].

### 1.5.4 *CD36 inhibitors*

As previously addressed, CD36 has been suggested to confer chemoresistance to cancer cells through enhancing stemness and free fatty acid levels. Research in breast cancer cell lines have shown that inhibition of stearoyl-CoA desaturase 1 (SCD1), induces apoptosis, cell cycle arrest and prevents migration, however, exogenous monounsaturated fatty acid (oleic acid) reverses these anti-tumour effects. Conversely, exogenous oleic acid could not reverse SCD1 inhibition in CD36 knockdown cells indicating that lipid availability outside of the cancer cell may have influence on cancer cell lipid metabolism as well as de novo lipogenesis. Highlighting that fatty acid uptake and transporters like CD36 may prove attractive as future therapeutic targets [209]. Studies have also indicated that CD36 enhances cell growth, migration, and expression of anti-apoptosis genes in breast cancer cells. CD36 was reported to attenuate tamoxifen inhibited cell

growth which was restored upon inhibition of CD36 by siRNA [210]. Additionally, in diet induced obese mouse models CD36 inhibition by salvionolic acid B reduced visceral fat accumulation and insulin resistance [211]. This may indicate CD36 inhibition as a potential strategy to improve metabolic dysfunction in obesity which may hold benefit for attenuating cancer cell progression via CD36.

**Table 1.5.1 The influence of obesity on the efficacy of combination therapy in obesity associated cancers.**

| Obesity associated cancer type | Positive or Negative Association | Supporting literature |
|---|---|---|
| **Colon and rectum** | Negative association | [200] |
| **Breast: postmenopausal** | Negative association | [201,202] |
| **Kidney: renal cell** | Negative association | [212] |
| **Multiple myeloma** | Negative association | [208] |
| **Prostate** | Positive and negative associations | [205,207] |

## 1.6 Obesity in immunotherapy treatment response

With breakthrough developments and an evolving interest in research in immunotherapies, it is quickly being regarded the fourth arm of cancer treatment. Whilst these therapies do not directly kill cancer cells, they play an important role in aiding the restoration of immune responses in the tumour microenvironment [213]. As obesity has been widely regarded as a chronic low-grade state of inflammation, it follows that it is associated with a pro-inflammatory driven state and the impairment of immune responses [214]

### Mechanisms implicated in treatment efficacy or resistance

#### 1.6.1 *Adipocyte Secretome Leptin signalling*

The role of leptin signalling particularly in the obesity setting has been shown to have a significant impact on chemotherapy and radiotherapy resistance. Research reported in a renal adenocarcinoma cell line *in-vivo* mouse model, indicated CTLA-4 monoclonal antibody or TRAIL encoding adenovirus, provided no survival benefit in diet induced obese mice whilst being efficacious in their non-obese counterparts. Leptin deficient obese mice were also shown to respond to treatment and the reduction of leptin systemically with a soluble leptin receptor did restore treatment response [212]. Research into the role of leptin in immunotherapies still requires further investigation to fully extract its influence in immunotherapy treatment response.

### 1.6.2 *Inflammation and Toxicities in Adoptive Cell therapy*

Chimeric antigen receptor (CAR) T cells have proven effective in the treatment of haematological cancers [215,216]. Conditions like obesity, where a pre-existing low-grade inflammation is already established, have been postulated to increase immunotherapies toxicities [213]. However, two significant side effects associated with this treatment, cytokine release syndrome and macrophage activation syndrome require further research to fully understand the effects of the toxicity associated with this treatment and whether they are associated with increasing BMI [217].Research is ever evolving in the field of immunotherapies, with further Investigation and clinical trials in other adoptive cell therapies ongoing in Tumour-Infiltrating Lymphocyte (TIL) Therapy, T-cell Receptor (TCR) engineered T-cell Therapy and Natural Killer (NK) Cell Therapy [218–220]. However, no links have been established in the current literature on whether obesity aids in the efficacy or resistance of these therapies.

### 1.6.3 *Immune modulation via checkpoint inhibitors*

Obesity has been identified as a potential positive prognostic factor for checkpoint blockade in cancer [221], however, the influence of obesity on recently developed immune checkpoint inhibitors is currently ongoing.

**PD-1/PD-L1**

It was reported in a multicentre study that overweight patients on anti-PD1/PD-L1 inhibitors in melanoma, non-small cell lung cancer and renal cell carcinoma had more favourable outcomes. With overweight patients experiencing a significant increase in progression free survival, time to treatment failure and overall survival compared with their non-obese counterparts [222].

A study conducted across a series of *in-vivo* mouse models, including breast, lung, and melanoma cancer cell lines, has indicated that obesity associated PD-1 mediated T-cell dysfunction led to increased tumour response to checkpoint blockade. This further correlates with improved outcomes for obese cancer patients in response to immune checkpoint inhibition [223]. In contrast, research conducted in breast cancer *in-vivo* mouse models, has shown that PD-L1 secreted in adipose tissue alters the efficacy of PD-1/PD-L1 checkpoint inhibition. Adipocyte secreted PD-L1 was reported to prevent PD-L1 targeted antibodies from activating essential anti-tumour functions of CD8+ T-cells. Inhibition of adipogenesis was also shown to reduce PD-L1 expression levels in adipose tissue and adipocytes which enhanced the efficacy of PD-L1/PD-1 checkpoint inhibition in mouse models [224].

Further research in a metastatic breast cancer patient cohort treated with avelumab, a PD-L1 inhibitor, has indicated that PD-L1 expression in tumour associated immune cells, could be associated with an enhanced clinical response to avelumab [225]. Continued research is required to fully understand the influence of systemic PD-L1 expression and whether in influences the efficacy of checkpoint blockade in metastatic breast cancer.

It has also been reported in melanoma cancer patients, that overweight and obese individuals did not have improved survival rates compared with normal weight counterparts. However, in cohorts receiving combination therapy, a significant survival advantage was observed in obese patients as opposed to normal weight patients. This may be attributed to the many factors, such as, the postulated obesity immunotherapy link or decreased toxicities in obese patients following chemotherapy. Nevertheless, the suggested correlation between obesity and improved outcomes following PD-1/PD-L1 inhibitor treatment still requires further interrogation as comprehensive reproducibility in these studies has yet to be achieved [226].

**CTLA-4**

Research conducted in metastatic melanoma patients treated with ipilimumab a monoclonal antibody checkpoint inhibitor that blocks the CTLA-4 pathway, has shown that obesity correlates with more favourable outcomes. Patients with above normal BMI showed significantly higher response rates, decreased levels of metastasis to the brain and a trend towards increased overall survival when compared to normal BMI patients [227].

In mouse models, CTLA-4-Ig treatment in obese mice has also been shown to decrease body weight, reduce adipose tissue inflammation and alleviate insulin resistance. This was linked with increased adiponectin expression in adipose tissue which as previously mentioned possess a role in in cancer cell proliferation. Induction of pro-inflammatory M1 to anti-inflammatory M2 macrophage polarization which was attributed to improved insulin resistance [228]. This may contribute to enhanced efficacy of combination therapies with checkpoint inhibitors in obese cancer patients.

### 1.6.4 *Emerging immunotherapies*

Oncolytic Virotherapy, in the form of Talimogene laherparepvec (T-VEC), has also shown promise in the field of immunotherapies, with clinical trials reporting surprising results in the treatment of melanoma [229]. Interest is still ongoing with dendritic cell (DC) vaccines with clinical trials in cancers such as glioblastomas giving promising results [230]. Both these therapies seem to possess less side effects and treatment associated toxicities compared with checkpoint inhibitors, however, research has yet to identify if obesity influences efficacy of these therapies.

**Table 1.6. 1 The influence of obesity on the efficacy of immunotherapy in obesity associated cancers.**

| Obesity associated cancer type | Positive or Negative Association | Supporting literature |
|---|---|---|
| **Breast: postmenopausal** | Positive and negative association | [224,225] |
| **Kidney: renal cell** | Positive and negative association | [212,222] |
| **Lung: non-small cell** | Positive association | [222] |
| **Skin cancer: Melanoma** | Positive association | [222] |

Obesity has been linked to enhanced checkpoint inhibition in certain cancers adding fuel to the flame of the "the obesity paradox", however this field is still emerging with very little focus on the effect of obesity on immunotherapies currently reported. However, obesity and its association with chronic low-grade inflammation, have been postulated as a possible factor that alleviates immunotherapy efficacy. Altered adipocyte secretions have also been implicated decrease effectiveness in immunotherapies, leptin has been shown to diminish the effect of certain immunotherapy treatments in an obese setting, which was not observed in normal weight comparisons. Research currently suggests that obesity is associated with improved outcomes in checkpoint blockade, however, the obese state has also been suggested to be more associated with immunotherapy-induced immune-related adverse events. Accordingly, further research is required into the effects of obesity in immunotherapy efficacy, before an adverse or positive correlation can be established.

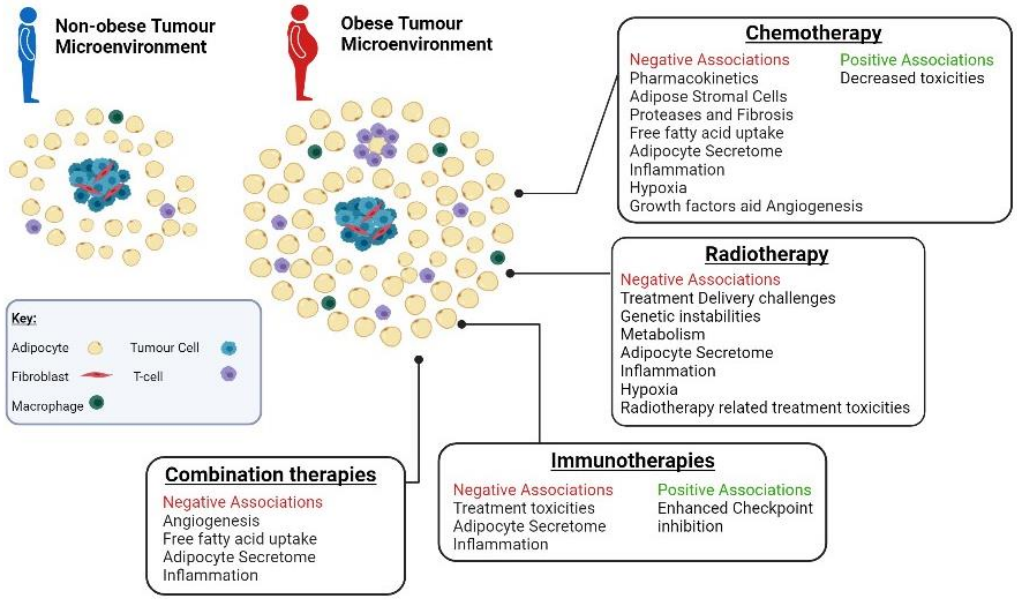


**Figure 1.6.1 The altered landscape of the obese tumour microenvironment has been reported to diminish and enhance treatment response in patients**

Obesity has been reported to modulate the efficacy of current treatment modalities through an altered adipocyte secretome, angiogenesis, hypoxia, fibrosis, free fatty acid uptake as well as a modulated immune landscape. Obesity has been demonstrated to have positive associations that benefit patients receiving Chemotherapy and Immunotherapy. However, negative associations have been more commonly identified between obese patients and their response to current treatments. Illustrated from [231]

## 1.7 Anti-tumour immunity

Previous research has indicated that a series of pro-inflammatory mediators in circulation and expressed at the tissue level have been linked to clinical outcomes, particularly factors that are involved in the recruitment and activation of innate immune cells [232]. Key inflammatory mediators including Eotaxin-3, IL-10, IL-13, MIP-1α, and MIP-1β are involved in the recruitment, activation and inhibition of immune cells are perturbed by obesity [233–235]. Many of these factors directly affect the antigen presenting abilities and polarisation of cells like Dendritic Cells (DCs) and Macrophages (Mϕ) [236]. The tumour microenvironment has been shown to induce immunosuppressive landscape. It induces this pro-tumour immunity by diminishing immunosurveillance and immuno-editing. The tumour microenvironment promotes the infiltration of immune cells such as M2-macrophages, MDSC, NKT2, Treg, Th2, NK2, ILC2, and N2 cells. These cells secrete a series of factors that act in an anti-inflammatory and regulatory manner that reduce the induction of an immune response that would lead to tumour killing. Further to this the tumour microenvironment also decreases the infiltration of immune cells know to evoke tumour killing including M1-macrophages, Th1, NKT, NK1, ILC1, DC, and N1 (**Figure 1.7.1**) [237].

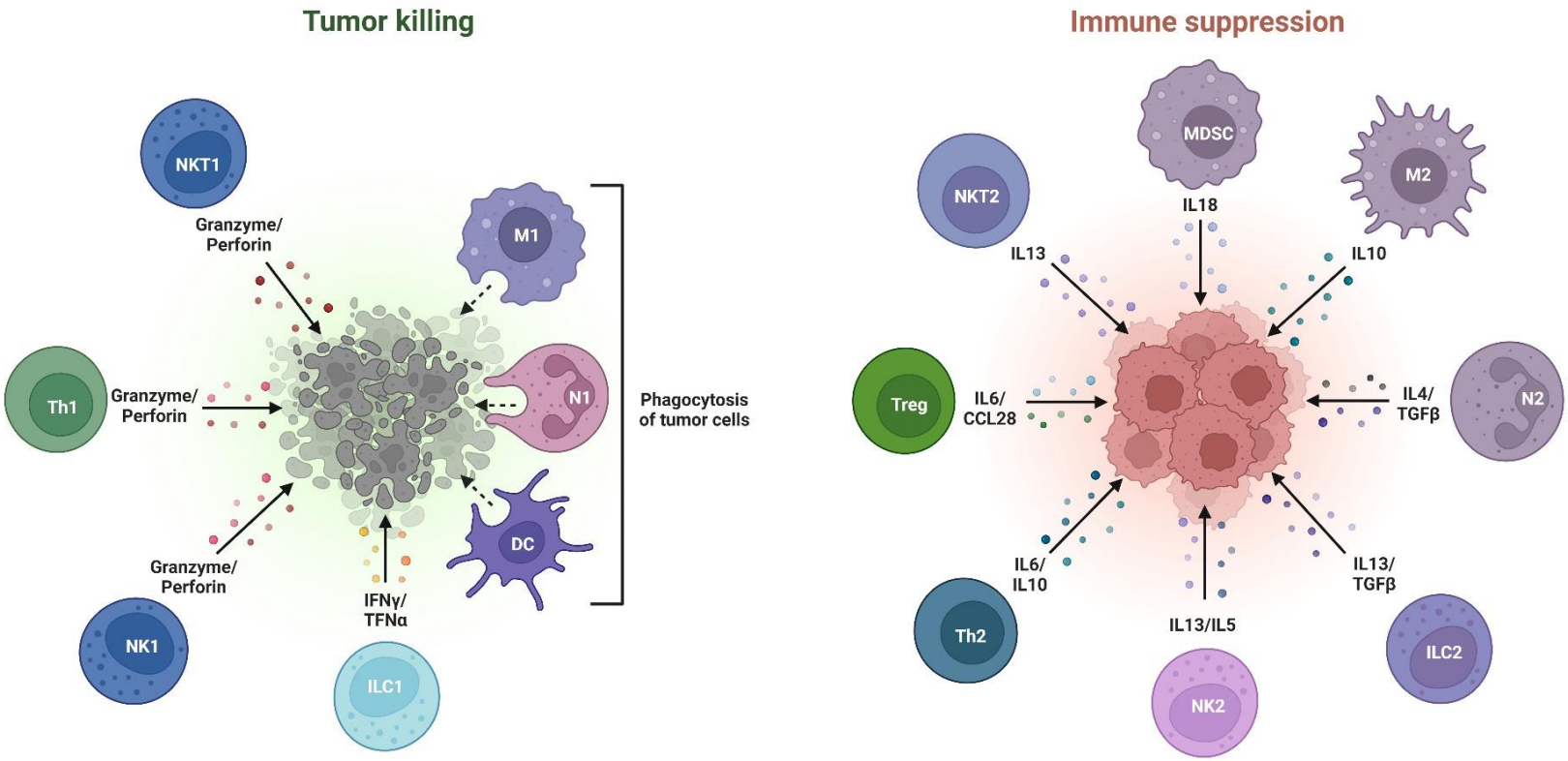


**1.7.1 The differential immune responses that support tumour killing and immune suppression in the tumour microenvironment.**
Tumour killing is enhanced by the infiltration of immune cells know to evoke anti-tumour immunity including M1-macrophages, Th1, NKT, NK1, ILC1, DC, and N1, which increase the secretion of pro-inflammatory and pro-apoptotic mediators IFN-γ, TNF-α, Granzyme and Perforin. The tumour microenvironment promotes the infiltration of immune cells such as M2-macrophages, MDSC, NKT2, Treg, Th2, NK2, ILC2, and N2 cells, which augment anti-inflammatory effects to hinder immunosurveillance and immuno-editing. They further this through the secretion of cytokines including IL-4, IL-5, IL-10, IL-13, and TGF-β that promote regulatory and tolerogenic immune cell phenotypes. Image adapted from Biorender template.

### 1.7.1 *Dendritic Cells*

DCs play a pivotal role in antigen presentation and initialising the anti-tumour immune response. Typically, as DCs mature they upregulate expression of co-stimulatory complex CD80 and CD86, which allows them to cross present with naïve CD4 T cells and activate immune responses. DCs that release IL-12 and IFN-γ induce Th1 immune responses leading to the production of IFN-γ and TNF-α, which aids anti-tumour immunity and tumour killing. DCs secreting IL-2 and IL-4 lead to the activation of TH2 immunity, with increased secretion of IL-4, IL-5, IL-9 and IL-13, cytokines that aid pro-tumour immunity [238].

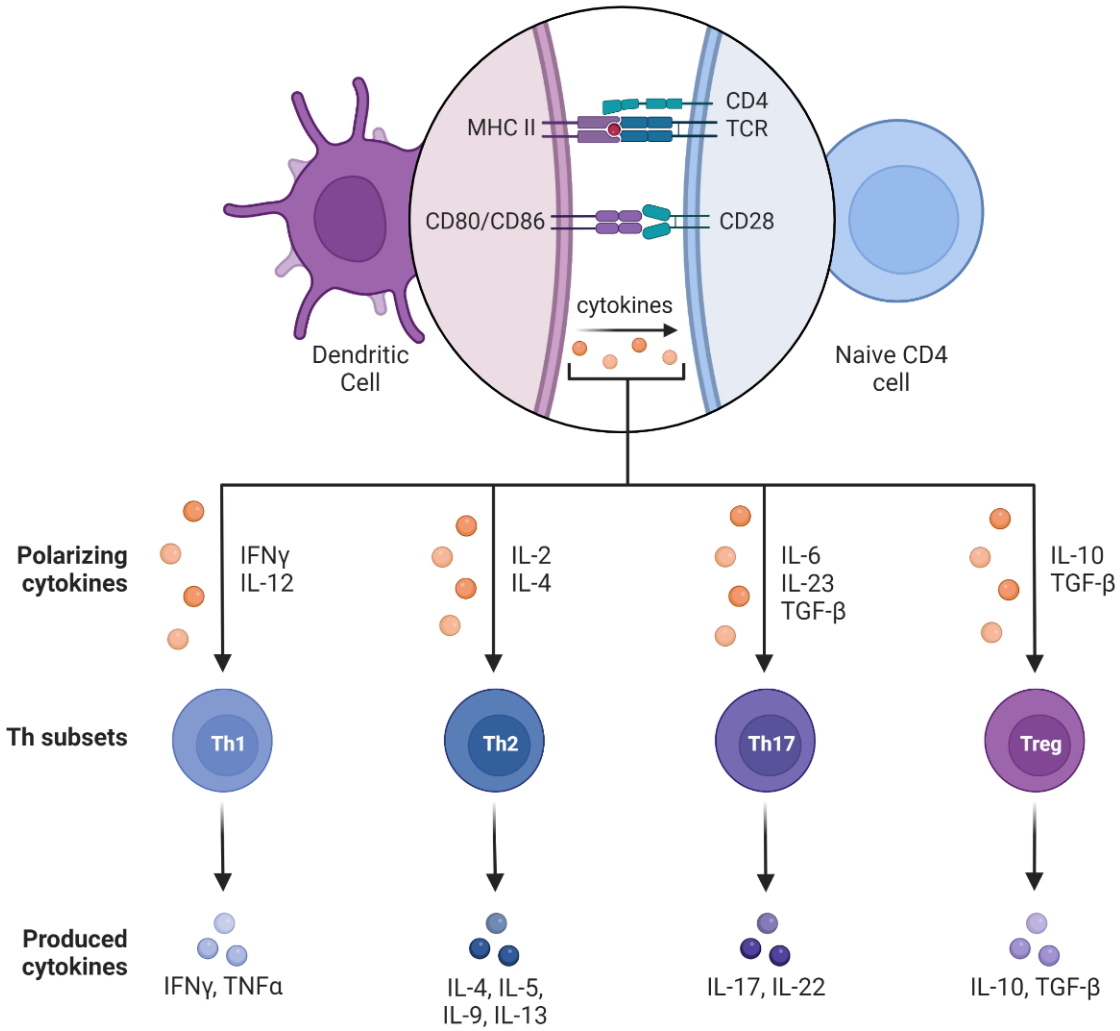


**1.7. 2 DC antigen cross presentation leads to T cell activation and initiates immune responses.**

DCs cross present antigens to Naïve CD4 T cells, resulting in the induction of Th1, Th2, Th17 or regulatory immune responses.

DCs secreting IL-6, IL-23 and TGF-β lead to the induction of Th17 immunity, leading to an increase in secreted levels of IL-17 and IL-22 [239]. Th17 immunity has a complex and opposing effect in anti-cancer immunity, as these cells can promote and supress cancer growth [240]. Finally, production of IL-10 and TGF-β lead to a tolerogenic DC phenotype, that stimulates the induction of regulatory T cells, that suppress excessive immune responses and can diminish the efficacy of anti-tumour immunity [241].

Chemotherapy has previously been reported to increase DC antigen presentation [242], however induction of DC response following radiotherapy was shown to be dependent on an active immune infiltrate already being present [243].

### 1.7.2 *Macrophages*

Macrophages are an essential part of the innate immune system and play a pivotal role in both pro-inflammatory and anti-inflammatory responses. Polarisation of macrophages towards a pro-inflammatory phenotype can contribute to tumour destruction or facilitate tumour growth and metastasis, depending on their phenotype.

M0 macrophages can be polarised towards an M1 pro-inflammatory phenotype by LPS, IFN-γ, or TNF-α, or towards a M2 anti-inflammatory phenotype by IL-4, IL-10, IL-13 or TGF-β. M1-macrophages have been denoted as a key effector cell in propagating inflammation in adipose tissue microenvironment, particularly in obesity[244]. Macrophages in both their pro-inflammatory and anti-inflammatory phenotypes play a central role in cancer progression and treatment resistance.

Anti-inflammatory or TAMs have reported to be induced by chemotherapy [245] as well as mediating chemoresistance [246]. Pro-inflammatory macrophages have been reported to play a vital role in radiation induced inflammation, inducing an anti-tumour immunity through the generation of an inflammatory response [247].

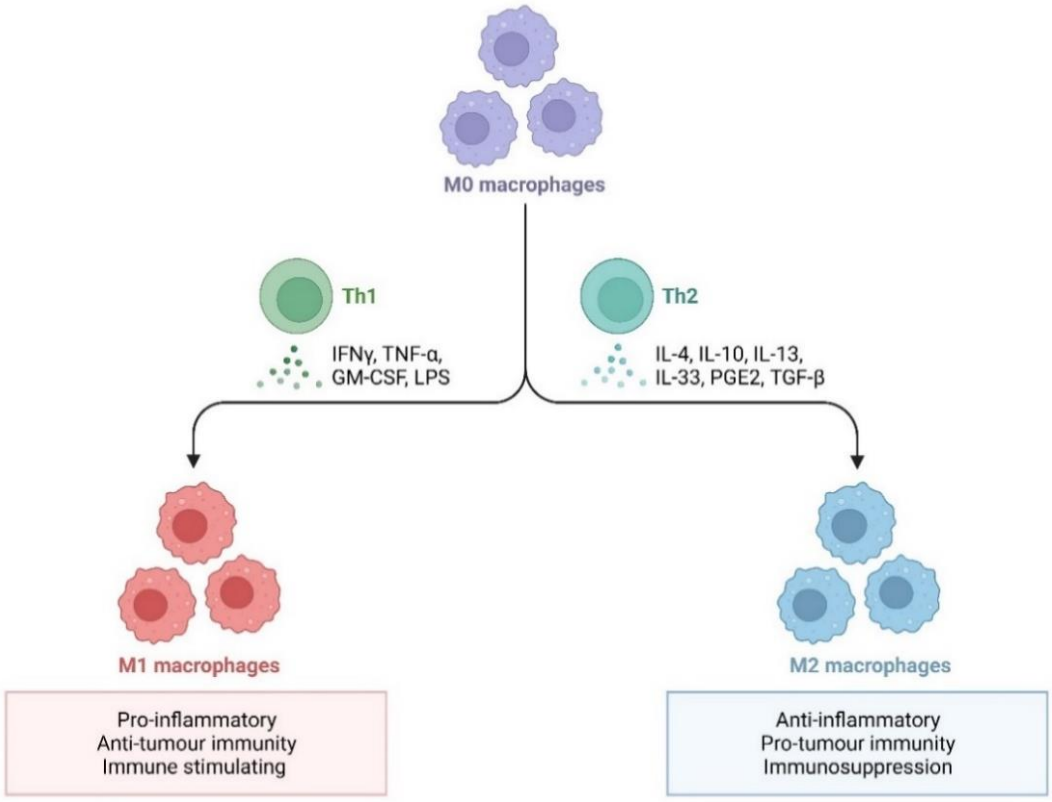


**1.7.3 Macrophage polarisation to M1 and M2 phenotypes.**
M0 macrophages can be polarised towards an M1 pro-inflammatory phenotype by LPS, IFN-γ, TNF-α, or GM-CSF, or towards a M2 anti-inflammatory phenotype by IL-4, IL-10, IL-13, IL-33, PGE or TGF-β. Image adapted from Biorender template.

### 1.7.3 *Myeloid derived suppressor cells (MDSC)*

MDSC are a population of immature myeloid cells which arise from the bone marrow and migrate towards the tumour site, where they inhibit anti-tumour immunity. MDSCs illicit this suppressive effect by inhibiting T cell activation, NK cell cytotoxicity and driving M2 TAM-like macrophage polarisation [248]. MDSCs have been observed to be increased with obesity both in mice models and obese humans, in circulation and at an adipose tissue level [249,250]. Interestingly, lipid accumulation in the tumour site has been linked with metabolic plasticity in MDSCs driving them from a glycolytic phenotype towards increased utilisation of fatty acid oxidation and oxidative phosphorylation. This shift in metabolic preference has been reported to confer MDSCs with enhanced immunosuppressive properties which in turn augments the diminishing effect on anti-tumour immunity [251].

### 1.7.4 *Innate lymphoid cells (ILCs)*

ILCs are a subset of innate immune cells which lack antigen-specific receptors commonly expressed on T and B lymphocytes. ILCs have recently been reported to play a crucial role in metabolic homeostasis, tissue inflammation and metabolic diseases [252]. ILCs have been shown to be increased at an adipose tissue level in obese type 2 diabetes patients, an elevation that was positively associated with increasing glycaemic parameters. Elevated ILCs infiltrate in adipose tissue in mouse models were further shown to promote adipose fibrogenesis and activation of $CD11c^{+}$ macrophages [253]. Indicating that ILCs may be a significant contributor to the low-grade inflammation associated with the obese adipose tissue microenvironment. ILC2s, have been shown to be enriched with fatty acid metabolism gene sets and have been shown to increase uptake and utilisation of fatty acids under infection or malnutrition to maintain IL-13 production [254,255]. ILCs production of IL-13, a cytokine renowned for its anti-inflammatory properties, may act as a diminishing force on anti-tumour immune responses by supporting TH2 immunity [256].

### 1.7.5 *Neutrophils*

Neutrophils are a subset of immune cells within the innate immune system, which possess regulatory effects on the adaptive immune system [257]. Increased frequencies of low-density neutrophils which are commonly associated with inflammatory disorders have been reported to be increased with in morbidly obese humans [258]. Comparably, increased frequencies of neutrophils have also been observed in the visceral adipose depots of diet induced obese mice models [259]. This elevated infiltration of neutrophils could act as a contributing factor maintaining the low-grade chronic inflammation observed in adipose tissue in patients with obesity. Interestingly, within a glucose limited milieu such as the tumour microenvironment, neutrophils have been reported to utilize fatty acid oxidation to fuel ROS production and suppression of T cells [260]. Whilst this metabolic plasticity has previously been implicated in aiding cancer growth and metastasis as well as recurrence[261], making research into these cells an attractive strategy mitigating the tumour immunosuppressive environment.

### 1.7.6 *Natural Killer (NK) Cells*

NK cells are a member of the innate immune system, capable of producing a potent cytotoxic response making them a vital player in cancer immunosurveillance [262]. Interestingly, NK cells resident in adipose tissue have been shown to regulate adipose tissue resident macrophages which in turn promoted adipose tissue inflammation and insulin resistance in obesity induced

mouse models [263]. Further to this, obese humans have been shown to have decreased NK cell frequencies with diminished cytotoxicity which could lead to impaired immune responses [264]. However it is of further note, that research currently indicates that increased lipid metabolism impairs NK cell functionality which occurs upon exposure to a fatty acid enriched microenvironment [265], supporting the concept that obesity may have detrimental effects on NK cell functionality. In particular, NK cells from cancer patients with obesity have been shown to be recruited to adipose tissue where they become irreparably dysregulated leading to cell death. In OAC patients, higher frequencies of NK cells have been reported within the visceral adipose tissue whilst reduced expression was observed within tumour tissue [84,266].

### 1.7.7 *T cells*

T cells form the most well-known subset of the adaptive immune response with two major subtypes including cytotoxic T cells and helper T cells. Cytotoxic T cells, or $CD8^+$ T cells play a critical role in the adaptive immune defence against intracellular pathogens and cancer cells [267]. Helper T cells or $CD4^+$ T cells execute their function through the secretion of cytokines largely through four alternative responses including Th1, Th2, Th17 and regulatory T cells (Tregs) [268] as previously discussed in section 1.7.1 *Dendritic Cells*. Metabolic plasticity has been implicated as a key regulator of these T cell responses, with regulatory T cells demonstrating increased utilisation of fatty acid oxidation, whilst effector cells have been reported to preferably use glycolysis [269]. Interestingly, adipose tissue derived from viscerally obese patients has been reported to possess increased secreted levels of mediators associated with TH17 immune responses. This increase in secreted IL-17 could contribute to the maintenance of obesity associated inflammation thus aiding cancer progression by stimulating the infiltration of myeloid cells such as macrophages and neutrophils [270,271].

### 1.7.8 *Natural Killer T cells (NKT cells)*

NKT cells are a specific subset of T cells which become rapidly activated in response to excess lipids bound through the antigen-presenting molecule CD1d which is expressed by DCs or Mϕ [272]. Interestingly, previous research indicates that $CD1d^+$ cells are highly expressed in the omentum. However, frequencies of these cells have been shown to be depleted in the omentum of morbidly obese patients and cancer patients [273]. Due to NKT cells close interplay with lipid antigens, it is perhaps unsurprising that alterations in the lipid profile of tumour microenvironment would alter their immuno-modulatory effects. Increased levels of lactic acid

in the tumour microenvironment have been implicated in reducing PPARγ on intratumoral NKT diminishing their cholesterol synthesis and IFN-γ production, thus diminishing the efficacy of their anti-tumour immunity. However, the introduction of a PPARγ agonist combatted these effects and restored IFN-γ production [274]. Indicating the importance of the lipid profile of the tumour microenvironment to stimulate an effective anti-tumour immune response.

### 1.7.9 *Mucosal-associated invariant (MAIT cells)*

MAIT cells are a subset of T cells which display innate, effector-like properties with highly variable TCRs capable of targeting a large array of foreign peptide epitopes [275]. MAIT cells have been implicated in the development of a series of metabolic disorders including obesity. Elevated frequencies of IL-17 producing MAIT cells were observed in children with obesity which was also correlated with increased insulin resistance [276]. In mouse models, MAIT cells were also implicated in promoting inflammation in adipose tissue through the induction of M1 Mϕ, which was also associated with insulin resistance, impaired glucose metabolism and lipid metabolism [277]. Interestingly, $CD127^{+}$ MAIT cells have been shown to have an energetic mitochondrial metabolic phenotype that was critical for IL-17A production, a mechanism that was largely supported by fatty acid uptake [278]. MAIT cells have garnered great interest in the field of cancer research, due to their MR1-dependant manner of recruiting pro-inflammatory macrophages or through their ability to regulate NK cell activation particularly within the tumour microenvironment [277,279]. However, their role in the tumour microenvironment is a still in contention as they have also been implicated in cancer development as well as in tumour growth and metastasis [280].

### 1.7.10 *The influence of adipose secretome on anti-tumour immunity*

The adipose tissue secretome has also been reported to evoke detrimental effects on immune cells. Dendritic cells, Macrophages, T-cells, and natural killer cells have all been reported to be deleteriously affected by obesity, with many changing to further perpetuate the chronic low-grade inflammation that is prevalently associated with obesity. Dendritic cells in adipose tissue have been reported to originally upregulate PPARγ and β-catenin pathways to enhance a tolerogenic phenotype which suppresses activation and initially supports an anti-inflammatory response delaying the onset of inflammation from visceral adipose secretions. However, after increased exposure to over-nutrition, visceral adipose mediators have been reported to inhibit DC activation of PPARγ and β-cantenin pathways and thus enhance and perpetuate the chronic

low-grade inflammation associated in obesity [281]. Previous research has shown that DCs from cancer patients have higher amounts of triglycerides than non-cancer patients, which negatively impacted DCs antigen presenting and T-cell stimulating capabilities [282]. Further to this, free fatty acids have also been shown to lead to lipid -loaden DCs with diminished antigen presenting capabilities and reduced capacity to effectively stimulate T cells [282]. Increased free fatty acids, which have been reported in obesity, have been shown to enhance Mϕ polarisation towards M1-like phenotype [283]. In particular, Palmitic Acid (PA) has been reported to elevate pro-inflammatory response signals [65,284]. In contrast, Oleic Acid (OA) has been identified to have anti-inflammatory effects through inhibiting pro-inflammatory responses driven by other fatty acids [67] as well as promoting M2-like polarisation in macrophages [285].

## 1.8 Metabolic flexibility in cancer cells in the tumour microenvironment

The role of metabolism in tumour development and progression has been widely reported. However, the metabolism of adipose tissue and the influence of its secretome on cancer cell metabolism is a research field still in its infancy. Mitochondrial dysfunction is commonly induced by cancer cells to aid tumour progression [286]. Aberrant cellular metabolism has been implicated as an essential survival advantage induced by cancer in order to evade the cytotoxic effects of chemotherapy and chemoradiotherapy [191,287]. Particularly, lipid metabolism and fatty acid oxidation (FAO) has recently been reported to enhance cancer cell resistance to current cancer treatments [288]. Exploitation of FAO and lipid metabolism has been reported to be heavily evoked by metastatic cancer cells, M2 macrophages, memory CD8 T cells as well as tissue resident regulatory T cells particularly in visceral adipose tissue [289–292]

.

### 1.8.1 *Glucose Metabolism*

The Warburg effect was first coined in the 1950's, when cancers cell elevated production of Lactate was linked with a higher utilisation of glucose metabolism [293]. Reprogramming of glucose metabolism is an intrinsic adaption in cancer cells, it increases the availability of pyruvate in the mitochondria of cancer cells conferring them with enhanced survival advantage [294]. Cancer cells have been reported to induce glycolytic metabolism in response to oxidative stress caused by radiotherapy, to enhance DNA damage repair and decrease cytogenetic damage [295]. Glucose is transported into the mitochondria of cancer cells through glucose transporters such as GLUT1, here it typically undergoes aerobic respiration leading to the

production of pyruvate which is further converted into acetyl-CoA. Acetyl-CoA is then utilised in a series of metabolic processes through the cell including the TCA cycle (**Figure 1.8.1**).

### 1.8.2 *Lipid metabolism in cancer*

The tricarboxylic acid (TCA) cycle, which is also known as Krebs cycle, is the main source of energy for cells and is an important process contributing to overall cellular aerobic respiration. The TCA cycle metabolises acetyl-CoA in a cyclical process through to citrate, iso-citrate, α-ketoglutarate, succinyl-CoA, succinate, fumarate, malate and finally oxaloacetate (**Figure 1.8.1**). Citrate acts as a precursor to the process of de novo lipogenesis, citrate is derived from both the TCA cycle and from glutamine oxidation within the cell. The conversion of acetyl-CoA to malonyl-CoA then catalyses the production of palmitate within the cell. From here palmitic acid is catalysed by SCD1 into palmitoleic acid or is elongated by ELOVL6 to stearic acid and then catalysed by SCD1 to form oleic acid. These fatty acids are then stored in lipid droplets to provide for energy needs during times of cellular stress [296]. Interestingly, FASN has been shown to be decreased in obesity [297,298], whilst FAO is increased [299], indicating that obesity may promote a metabolic shift leading to enhanced utilisation of lipid metabolism and FAO.

### 1.8.3 *Glutamine metabolism*

Alterations in cancer metabolism have been reported to render tumour cells addicted to glutamine. Metabolism of glutamine has been shown to be upregulated by MYC and KRAS driven tumours miking the combination of targeted inhibitors of these oncogenic drivers with inhibition of glutamine metabolism an attractive therapeutic target. Glutamine metabolism has been linked to fuelling the TCA cycle as well as providing α-ketoglutarate for citrate production which leads into FASN (**Figure 1.8.1**). Previously we have reported that glutamine and its metabolised product glutamate are differentially expressed in the adipose secretome of obese and non-obese OAC patients [80].

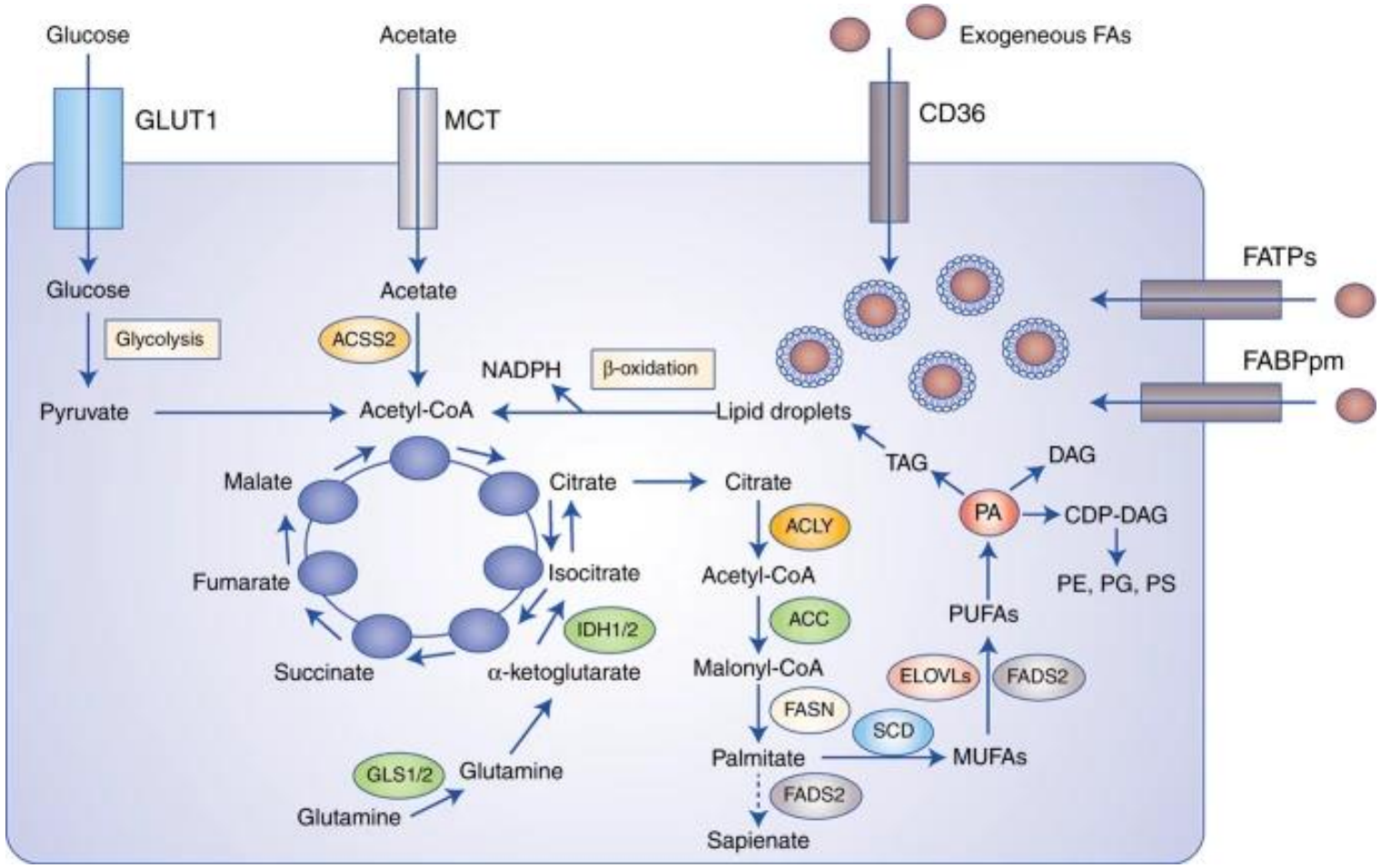


**1.8.1 The TCA cycle and its interactions with FASN and FAO**

Lipid droplet formation and lipid metabolism are both increased in obesity, an alteration that is utilised by cancer cells to aid their proliferation and progression. To support this metabolic shift, exogenous fatty acids are taken up through transporters including CD36, FATPs and FABPpm or synthesised by de novo lipogenesis using FASN. These stored lipids can then be utilised for energy needs at a later stage through fatty acid oxidation (FAO, β-oxidation), particularly under situations of stress. Citrate acts as a precursor to the products of de novo lipogenesis, citrate is derived from both the TCA cycle and from glutamine oxidation within the cell. Illustrated from [296]

## 1.9 The role of adipose tissue in cancer metastasis

Approximately half of OAC patients are initially diagnosed with late-stage disease with metastasis. Metastatic OAC has a 5-year survival rate of less than 5% [300] . Research is focused into the role of obesity and how it contributes to the metabolic changes and epithelial to mesenchymal transition that support cancer cells migratory capacity to develop distant metastasis. Metastasis involves a series of transformative changes in cancer cells including their plasticity, metabolic preferences as well as their changes in their surrounding stroma, which can be induced in response to cancer treatments. The stages involved in colonization of distant metastasis include, local invasion, intravasation, circulation of cancer cells, extravasation and finally the colonization of local and distant metastasis [301] (**Figure 1.9.1**).

### 1.9.1 *Metabolic flexibility supports cancer cells invasive capacity*

Primary cancer cells have been reported to heavily rely on glycolytic metabolism in order to grow and survive, even inducing this metabolic reliance in the face of oxidative stress evoked by radiation induced inflammation order to aid DNA damage repair [295]. Metastatic cancer cells however have been shown to rely more so on oxidative phosphorylation associated metabolism and fatty acid oxidation [302,303]. Flexibility in energy metabolism has been reported to be critical in aiding cancer cell's ability to undergo epithelial to mesenchymal transition and migration to facilitate distant metastasis [304]. PA has previously been reported to be increased in circulation in obese patients has also been linked to enhanced uptake of fatty acids [305]. It has also been implicated in the upregulation of lipid metabolism genes that has been reported to aid in the initiation of metastasis [306], making it an attractive target to diminish cancer cells ability to resist treatment and establish distant metastasis.

### 1.9.2 *Pre-metastatic niches in adipose tissue*

Recently evidence is rising linking obesity and the development of metastatic cancer, particularly in cancers that are surrounded by the visceral adipose depot and whose development is strongly linked with obesity to begin with [307]. The influence of obesity on adipose tissue has been demonstrated to increase lipid droplet formation and secretion of pro-tumorigenic factors in adipocytes, alter immune cell recruitment, promote angiogenesis, remodel the extracellular matrix and enhance lipid metabolism and the release of free fatty acids [231]. These developments prime obese adipose tissue as a highly amenable site to support the development of pre-metastatic niches.

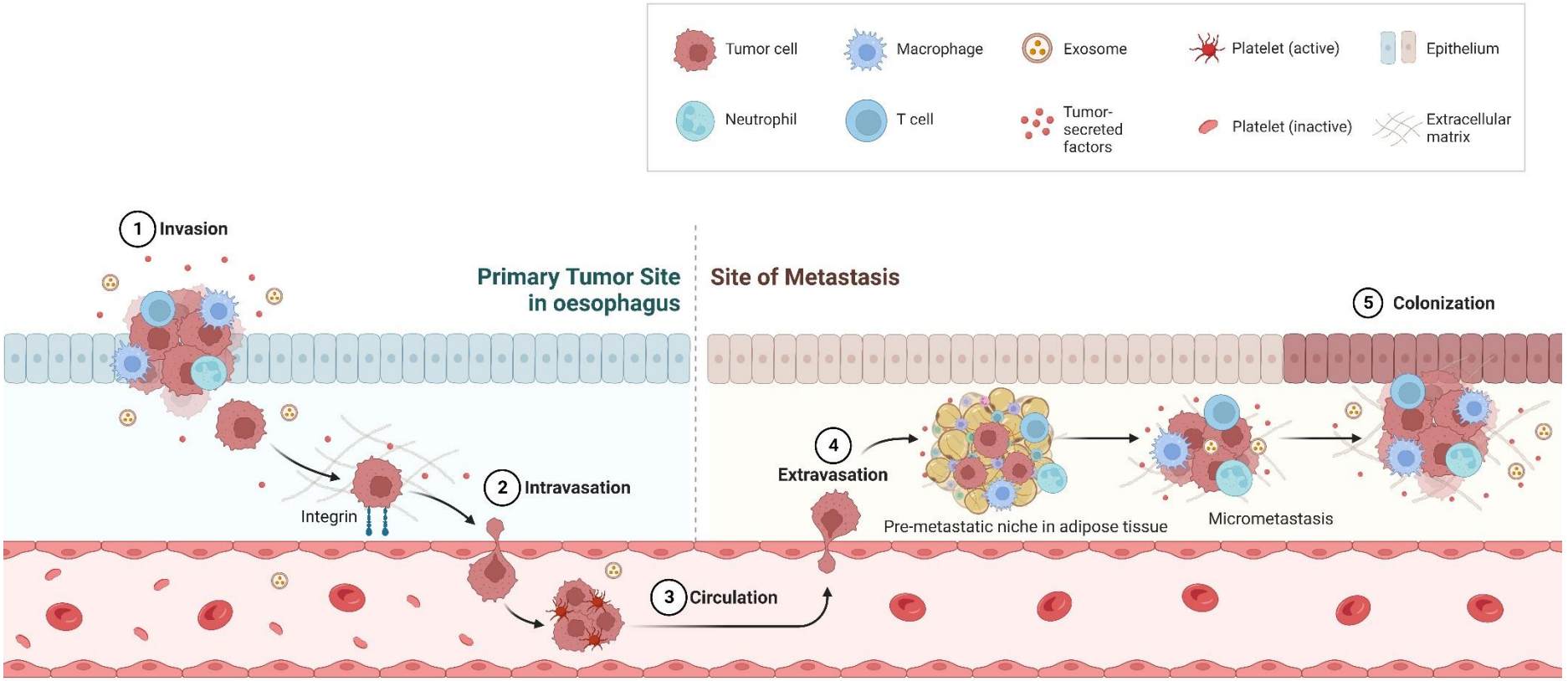


**1.9.1 The process of metastatic invasion to distant colonisation sites.**

The pre-colonization phase of metastasis includes a series of stages where cancer cells under transformative changes in plasticity, surrounding stroma and metabolism. These stages include (1) local invasion of cancer cells in the primary tumour mediated by integrins (2) intravasation into the tumour vasculature, (3) circulation of cancer cells within the vasculature (4) extravasation into the visceral adipose depot in a pre-metastatic niche (5) Colonization into local and distant metastasis. Image adapted from Biorender template.

## 1.10 Thesis hypothesis and specific aim

### 1.10.1 *Overall hypothesis*

Obesity alters the immune metabolic profiles of adipose tissue explants, that would lead to suppression of DC maturation, increased M1-polarisation in Mϕ, and enhance cancer metabolism and invasion. The introduction of saturated fatty acid PA should increase adipose pro-inflammatory responses whilst OA decreases them, an effect that would be augmented by the introduction of chemotherapy and radiotherapy.

### 1.10.2 *Overall aim*

The overall aim of this thesis was to assess the metabolic and secreted profiles of adipose tissue explants from OAC patients and whether these factors were influenced by exposure to different exogenous fatty acids, increasing irradiation or cytotoxic drugs and what downstream effects this would have on cancer and immune cell metabolism and function.

Specific aims of thesis (representing the five results chapters)

1. Assess whether patient demographics including obesity, metabolic dysfunction, previous exposure, and response to treatment affects adipose tissue metabolism and its secreted pro-inflammatory, lipidomic and metabolomic profiles.

2. Examine the influence of exogenous fatty acid treatment on adipose tissue metabolism and secreted profiles in non-cancer and OAC patients and examine the downstream effects on immune cell function, and the influence of obesity on these responses in the cancer setting.

3. Investigate if increasing irradiation augments the influence of exogenous fatty acid treatment on adipose tissue metabolism and secreted profiles in non-obese and obese OAC patients and what downstream effects this has on immune cell function.

4. Assess the influence of the adipose secretome of non-obese and obese OAC patients treated with exogenous fatty acids and increasing irradiation on primary and metastatic OAC cancer cells metabolism and invasive capacity.

5. Investigate if chemotherapy or chemoradiotherapy would differentially affect the influence of exogenous fatty acid treatment on adipose tissue metabolism and its secreted profiles in non-obese and obese OAC patients and the downstream effects on cancer and immune cell function.

*Chapter 2*

# *Energy metabolism, metabolite, and inflammatory profiles in human ex-vivo adipose tissue are influenced by obesity status, metabolic dysfunction, and treatment regimes in patients with oesophageal adenocarcinoma*

## 2.1 Objective and specific aims:

**Objective**:

The overall objective of this chapter was to assess the immuno-metabolic profiles of adipose explant derived from oesophageal cancer patients using real-time metabolic profiles, multiplex ELISA, metabolomics and lipidomics. As well as determining whether these immuno-metabolic profiles were associated with key patient clinical factors and how these profiles correlated with extensive patient clinical demographics.

**Specific Aims**

- To assess metabolic profiles including oxidative phosphorylation and glycolysis of adipose explants in real time, as well as their metabolic preference.
- To assess the secreted profiles of these adipose explants for mediators of inflammation, metabolism, angiogenesis, and immune response.
- To determine whether obesity, metabolic dysfunction, previous treatment exposure or response to treatment was associated with alterations in adipose tissue metabolism and secreted factors.
- To evaluate whether these immune-metabolic profiles correlated with extensive patient clinical demographics.

## 2.2 Introduction

Oesophageal adenocarcinoma (OAC) is an aggressive disease associated with a poor prognosis and a five-year survival rate of approximately 20% [7], with current projections indicating that the incidence of this disease is increasing [308]. Currently, the standard of care for treatment involves neo-adjuvant treatment (treatment prior to surgery) with either chemotherapy alone including the FLOT regimen (consisting of 5FU, Folinic acid, Oxaliplatin, Docetaxel) or combination chemo-radiotherapy such as the CROSS regimen (consisting of Carboplatin, paclitaxel with concurrent 41.4 Gy radiation), for locally advanced tumours [19]. Unfortunately, only approximately 30% of patients show a complete response to these current treatment modalities, leaving a large proportion of patients with no therapeutic gain and a possible delay to surgery [309,310]. Furthermore, large-scale epidemiological studies demonstrate a consistent and compelling association between the risk of cancer development/progression and elevated body mass index (BMI) for many gastrointestinal cancers including OAC, with this cancer having one of the strongest associations with obesity [47,48,311]. This makes it an exemplary model for studying the influence of obesity on cancer and the role of the adipose tissue microenvironment in this setting.

Numerous factors are associated with the obese adipose tissue microenvironment such as chronic low-grade inflammation, angiogenesis, fibrosis, and the altered secretions of cells, all implicated in the progression and recurrence of cancer [57,58]. One of the significant effects of the obese adipocyte secretome is the release of a series of pro-inflammatory factors, leading to a local environment that is primed to aid tumour development and progression [50]. The altered milieu of the obese tumour environment has been extensively shown to have detrimental effects on the anti-tumour response, diminishing immune cell function and treatment efficacy [83,85,312]. It has been previously shown that adipose-conditioned media from oesophageal cancer patients increases radiosensitivity [55], and this could be linked to the differential expression of leptin receptors and its associated biology in driving inflammation in the adipose tissue microenvironment [313].

Currently, discrepancies are reported in the literature on whether obesity diminishes [314] or ameliorates [55] treatment resistance and whether obese individuals possess an enhanced survival benefit compared with their non-obese counterparts [167], which highlights the importance of identifying the underlying biological mechanisms which play a role in this setting in the complex adipose tissue microenvironment. Previous work has observed elevated oxidative phosphorylation in visceral adipose tissue compared with subcutaneous adipose tissue [313], and adipocytes derived from metabolically unhealthy obese individuals show

elevated mitochondrial response profiles [315]. Whilst the role of tumour explant energy metabolism in OAC treatment response has been reported [316], the energy metabolism profiles of visceral adipose tissue between obese and non-obese OAC patients and the influence of its secretome on the cancer cell and immune cell function is still largely unknown.

For the first time, this study aims to better characterise the adipose tissue microenvironment using real-time energy metabolism profiles, profiling the secreted inflammatory environment, and assessing altered metabolites and lipid profiles of human ex vivo adipose explants. These profiles were examined based on obesity status, metabolic dysfunction, previous treatment exposure, and treatment responses in OAC patients. Overall, the profiling data and clinical correlations described in this study suggest the adipose microenvironment as well as potentiating a pro-tumorigenic milieu may also be linked with the efficacy of current standard-of-care cancer treatments. With the knowledge that the obesity epidemic is projected to increase, with 50% of the Western world population being obese by 2030[317], this research endeavours to address an exigent question: what influence might the adipose microenvironment possess in the cancer–obesity link?

## 2.3 Materials and Methods

### 2.3.1 *Ethics Statement and Patient Recruitment*

Ethical approval was granted by the St James's Hospital/AMNCH ethical review board (Ethics number: REC_2019-07 List 25(27)), and written informed consent was collected from all patients in this study. Thirty-two patients were recruited within the period between 1 December 2019 and 30 January 2022, and the patient demographics are listed in Table 1. All fresh adipose tissues were taken at the start of the surgical tumour resection procedure from OAC or OGJ (oesophagogastric junctional adenocarcinoma) patients being treated with curative intent.

**Table 2.3.1 Clinical demographics of patient cohort.**

| **Patient Clinical Parameters** | |
|---|---|
| **Diagnosis** | OAC = 13<br>OGJ = 19 |
| **Sex** | Male = 21<br>Female =11 |
| **Obesity Status via Visceral Fat Area** | Obese = 16<br>Non-obese =16 |
| **Age at diagnosis** | 51-83 (Mean = 67.83) |
| **Post-treatment BMI** | 22.34-43 (Mean = 32.391)<br>22.34–43 (Mean = 32.391)<br>**Non-obese** Mean = 28.4, **Obese** Mean = 30.025<br>**Male** Mean = 40.282, **Female** Mean = 29.822 |
| **Weight** | 57.2–176 kg (Mean = 86.697)<br>**Non-obese** Mean = 82.865, **Obese** Mean = 94.093<br>**Male** Mean = 94.72, **Female** Mean = 76.79 |
| **Mean VFA** | 22.9–485.2 (Mean = 139.404)<br>**Non-obese** Mean = 115.192, **Obese** Mean = 167.1<br>**Male** Mean = 148.436, **Female** Mean = 122.872 |
| **Metabolic Dysfunction** | *n* = 15 |
| **High cholesterol or intervention for high cholesterol** | *n* = 21 |
| **High blood pressure or intervention for high blood pressure** | *n* = 20 |
| **High Triglycerides or intervention for high Triglycerides** | *n* = 4 |
| **Diabetes** | *n* = 10 |
| **Barrett's oesophagus** | *n* = 17 |
| **ASA grade (risk-stratifying system to help predict preoperative risks)** | Grade 1 *n* = 3<br>Grade 2 *n* = 15<br>Grade 3 *n* = 10 |
| **Clavien-Dindo classification (grading for adverse events which occur as a result of surgical procedures)** | Classification 0 *n* = 5<br>Classification 1 *n* = 4<br>Classification 2 *n* = 7<br>Classification 3 *n* = 7<br>Classification 4 *n* = 5 |

| | |
|---|---|
| **Treatment** | Naïve *n* = 10<br>FLOT *n* = 14<br>CROSS *n* = 8 |
| **Tumour Regression Grading (TRG)** | TRG 1 *n* = 3 (CROSS *n* = 2, FLOT *n* = 1)<br>TRG 2 *n* = 3 (CROSS *n* = 1, FLOT *n* = 2)<br>TRG 3 *n* = 8 (CROSS *n* = 3, FLOT *n* = 5)<br>TRG 4 *n* = 3 (CROSS *n* = 2, FLOT *n* = 1)<br>TRG 5 *n* = 3 (CROSS *n* = 0, FLOT *n* = 3) |
| **Clinical Stage (T)** | T1 *n* = 10<br>T2 *n* = 3<br>T3 *n* = 19 |
| **Clinical Stage (N)** | N0 *n* = 17<br>N1 *n* = 8<br>N2 *n* = 7 |
| **Path stage (T)** | T0 *n* = 3<br>T1 *n* = 9<br>T2 *n* = 4<br>T3 *n* = 13<br>T4 *n* = 3 |
| **Path Stage (N)** | N0 *n* = 17<br>N1 *n* = 6<br>N2 *n* = 6<br>N3 *n* = 3 |
| **Perineural Invasion** | *n* = 9 |
| **Lymph Involvement** | *n* = 17 |
| **Vascular Involvement** | *n* = 11 |
| **Evidence of Disease** | *n* = 10 |

### 2.3.2 *Clinical Data Collation and Assessment*

Obesity was defined using visceral fat area (VFA) measurements with a cut-off value for VFA of 163.8 $cm^2$ for males and 80.1 $cm^2$ for females as previously categorised [318]. Metabolic dysfunction was defined if a patient had 3 or more of the following criteria: visceral obesity (as assessed with the VFA cut-offs mentioned above), previously diagnosed type 2 diabetes or impaired fasting glucose, triglycerides ≥1.7 mmol/L or interventional treatment for high triglycerides; high-density lipoprotein cholesterol or interventional treatment for low HDL, systolic blood pressure ≥130 mmHg and/or diastolic blood pressure ≥85 mmHg or treatment for hypertension [318,319]. Previous treatment was classified as a patient receiving either neo-adjuvant chemotherapy only (FLOT regimen) or chemo-radiotherapy (CROSS regimen), patients who received no neo-adjuvant treatment prior to surgery were classified as treatment naïve. Histological assessment of resected tumours was conducted by a pathologist, using the Mandard tumour regression grade to assess patient's response to neo-adjuvant treatment; therefore, no TRG scoring is available for treatment naïve patients who did not receive chemotherapy or chemo-radiotherapy. The clinical data summary is listed in Table 1

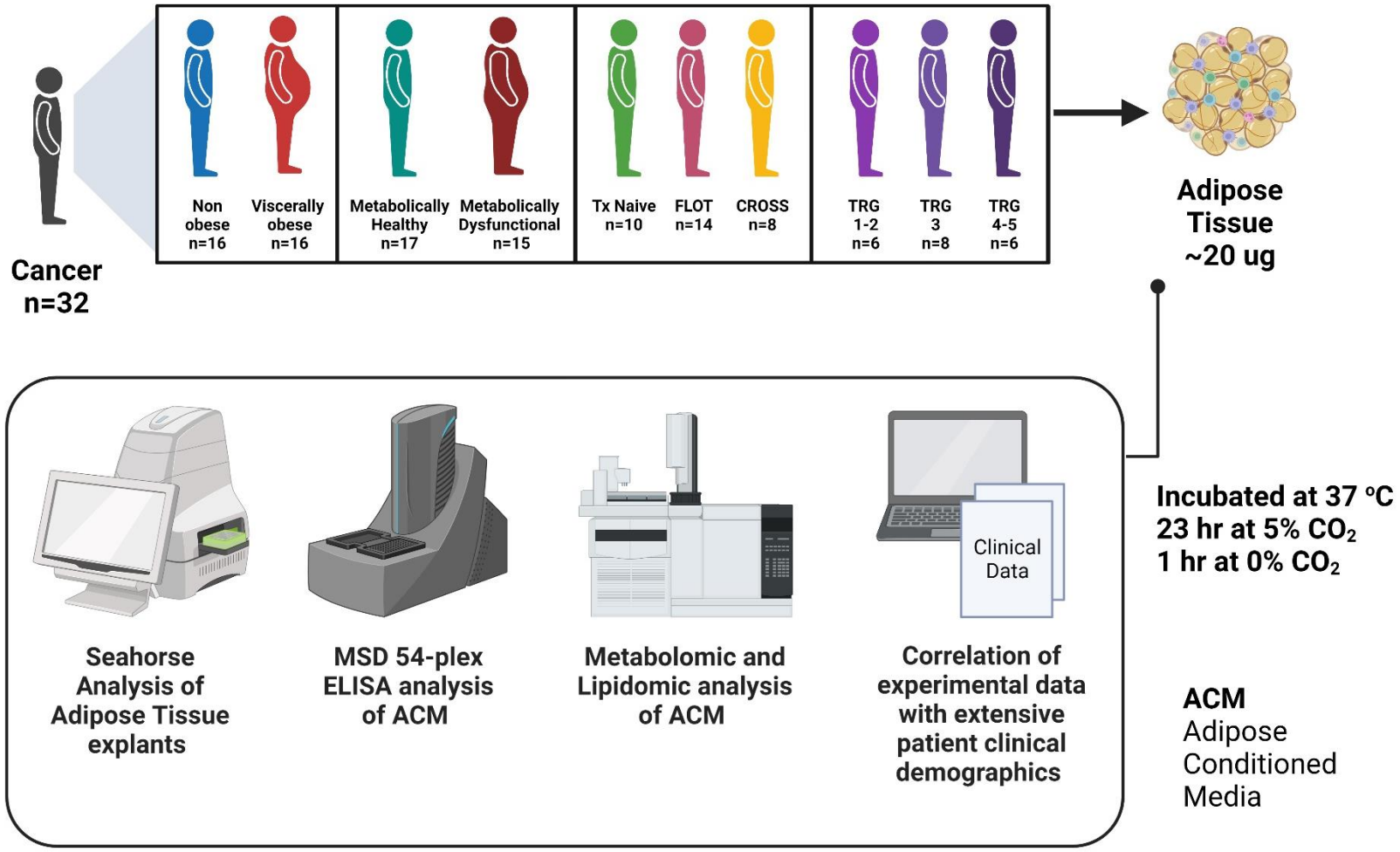


**Figure 2.3.1 Schematic of experimental methodology workflow associated with Chapter 2**

Real time metabolic and secreted profiles of adipose explants from OAC or OGJ cancer patients were assessed by Agilent seahorse, MSD multiplex ELISA or metabolomic and lipidomic analysis conducted by LC-MS/MS.

### 2.3.3 *Seahorse Analysis of Metabolic Profiles from Adipose Tissue Explants and Generation of Adipose Conditioned Media (ACM)*

Fresh omental tissue was collected from theatre and processed within 30 min by dissecting it into pieces weighing approximately 20 mg. Tissue was plated in triplicates in 1 mL of M199 (Gibco, Thermofisher, Waltham, Massachusetts, USA) supplemented with 0.1% gentamicin (Lonza, Switzerland), in a 24-well plate (Sarstedt, Nümbrecht, Germany). Adipose explants were cultured for 24 h at 37 °C and 5% carbon dioxide in a humidified incubator (Thermofisher, MA, USA). In the last hour of culture, adipose tissue and ACM were transferred to an islet capture microplate with capture screens (Agilent Technologies, Santa Clara, California, USA) and incubated in a non-CO2 incubator at 37 °C (Whitley, West Yorkshire, UK) prior to analysis. Seahorse Xfe24 analyser was used to assess metabolic profiles in adipose explants (Agilent Technologies, CA, USA). Following a 12 min equilibrate step, three basal measurements of OCR (Oxygen Consumption Rate) and ECAR (Extracellular Acidification Rate) were taken over 24 min consisting of three repeats of the following sequence "mix (3 min)/wait (2 min)/measurement (3 min)" to establish basal respiration. Adipose Conditioned Media (ACM) was extracted in a sterile environment and tissue was weighed using a benchtop analytical balance (Radwag, Radom, Poland) and snap frozen. All samples were then stored at −80 °C for further processing.

### 2.3.4 *Multiplex ELISA*

The collected Adipose Conditioned Media (ACM) was processed according to MSD (Meso Scale Discovery, Rockville, Maryland, USA) multiplex protocol. To assess angiogenic, vascular injury, pro-inflammatory, and cytokine and chemokine secretions from ACM, a 54-plex ELISA kit separated across seven plates was used (Meso Scale Discovery, Rockville, Maryland, USA). The multiplex kit was used to quantify the secretions of CRP, Eotaxin, Eotaxin-3, FGF(basic), Flt-1, GM-CSF, ICAM-1, IFN-γ, IL-10, IL-12/IL-23p40, IL-12p70, IL-13, IL-15, IL-16, IL-17A, IL-17A/F, IL-17B, IL-17C, IL-17D, IL-1RA, IL-1α, IL-1β, IL-2, IL-21, IL-22, IL-23, IL-27, IL-3, IL-31, IL-4, IL-5, IL-6, IL-7, IL-8, IL-8 (HA), IL-9, IP-10, MCP-1, MCP-4, MDC, MIP-1α, MIP-1β, MIP-3α, PlGF, SAA, TARC, Tie-2, TNF-α, TNF-β, TSLP, VCAM-1, VEGF-A, VEGF-C, and VEGF-D from ACM. All assays were run as per the manufacturer's recommendation, and an overnight supernatant incubation protocol was used for all assays except Angiogenesis Panel 1 and Vascular Injury Panel 2, which were run according to the same-day protocol. ACM was run undiluted for all assays except Vascular Injury Panel 2, where a one-in-four dilution was used, as per previous optimization experiments. Assays were run on a MESO QuickPlex SQ 120, and all analyte concentrations were calculated using Discovery Workbench software (version 4.0). Secretion data for all factors were normalized to adipose post-incubation weight and expressed as pg/mL per gram of adipose tissue.

### 2.3.5 *Metabolomic and Lipidomic Screening*

10 µl of ACM was analysed using a targeted metabolomic platform and was prepared according to the MxP® Quant 500 assay manual (Biocrates Life Sciences, Innsbruck, Austria). Samples were dried and derivatised using derivatization solution (5% phenyl isothiocyanate in ethanol/water/pyridine (volume ratio 1/1/1)) and incubated for 1 h at room temperature and then dried under nitrogen for 1 h. After the addition of 300 µL of 5 mM ammonium acetate in methanol, the plate was shaken for 30 min and then centrifuged at 500 g for 2 min, and then 150 µL of high-performance liquid chromatography (HPLC)-grade water was added for liquid chromatography-tandem mass spectrometry (LC-MS/MS) analysis. Additionally, 10 µL of the eluate was diluted with 490 µL of methanol running solvent for flow injection analysis tandem mass spectrometry (FIA-MS/MS) analysis. Samples were analysed using the Sciex ExionLC series UHPLC system coupled to a Sciex QTRAP 6500+ mass spectrometer. UHPLC columns were installed, and mobile phases A and B were 100% water and 95% acetonitrile (both added 0.2% formic acid), respectively. In the LC-MS/MS analysis, amino acids (*n* = 20) and amino acid-related (*n* = 30), bile acids (*n* = 14), biogenic amines (*n* = 9), carboxylic acids (7), hormones and related (*n* = 4), indoles and derivatives (*n* = 4), nucleobases and related (*n* = 2), fatty acids (*n* = 12), trigonelline, trimethylamine N-oxide, p-Cresol sulphate, and choline were quantified. Lipid classes such as lysophosphatidylcholines (*n* = 14), phosphatidylcholines (*n* = 76), sphingomyelins (*n* = 15), ceramides (*n* = 28), dihydroceramides (*n* = 8), hexosylceramides (*n* = 19), dihexosylceramides (*n* = 9), trihexosylceramides (*n* = 6), cholesteryl esters (*n* = 22), diglycerides (*n* = 44), and triglycerides (*n* = 242) were quantified using the FIA-MS/MS analysis. Furthermore, acylcarnitines (*n* = 40) and the sum of hexose were also quantified using the FIA-MS/MS analysis. The multiple reaction monitoring (MRM) method, which was optimized by Biocrates Life Sciences, was applied to identify, and quantify all metabolites. (Experimental work carried out by Dr. Xiaofei Yin and Prof. Lorraine Brennan, UCD)

### 2.3.6 *Statistical Analysis*

All statistics were conducted using GraphPad Prism 9.0 (GraphPad Software, San Diego, California, USA). The Mann–Whitney test was used for the continual non-parametric dependent variable analysis of data with two groups. For more than two groups, Kruskal–Wallis testing with Dunn's correction was used. Details of specific statistical tests are given in each corresponding figure legend. To determine if protein expression levels identified via 54-plex ELISA correlated with patient clinical factors, spearman correlations were carried out using R software version 3.6.2 [320]. Correlations were generated using R package 'Hmisc' version 4.4-0 [321]. Graphical representations of correlations were generated with the R package 'corrplot' version 0.84 [322].

All correlations with an associated *p*-value < 0.05 were considered statistically significant. The Holm–Bonferroni post hoc correction was used to control for multiple comparison testing.

## 2.4 Results

### 2.4.1 *Increased oxidative phosphorylation metabolism and elevated secreted pro-inflammatory mediators were observed in adipose tissue explants from viscerally obese patients*

To assess whether obesity determined using visceral fat area alters metabolic and secreted profiles of visceral omental ex vivo explants from obese OAC patients (*n* = 16) and non-obese patients (*n* = 16), the Agilent Seahorse Xfe24 analyser was used to assess real-time metabolic parameters. To further assess the influence of these clinical parameters on this explant model, the matched ACM secretome was evaluated using MSD 54 plex ELISA and metabolomic and lipidomic profiling.

Significant increases were observed in OCR and ECAR profiles in visceral adipose explants derived from obese oesophageal cancer patients compared with non-obese patients **(Figure 2.4.1)**. Increased secretions of cytokines Eotaxin-3, IL-17A, IL-17D, IL-3, MCP-1, and MDC and a decrease in the secretion of VEGF-D were observed in adipose explants from obese patients compared with their non-obese counterparts **(Figure 2.4.2)**. An elevated expression of metabolites GABA, Glutamic acid, TG (16:0_35:3), TG(18:2_38:4), and TG(22:5_34:3) was observed in the adipose secretome from obese patients whilst Aspartic acid, Glutamine, and PC aa C42:6 were observed to be decreased in the adipose secretome of obese patients compared with non-obese patients **(Figure 2.4.3)**. Significant correlations observed between the experimental data and visceral fat area were visualised using corrplot **(Figure 2.4.4)**, and the associated R numbers and *p*-values are detailed in Table 2.4.1. (* $p < 0.05$, ** $p < 0.01$, *** $p < 0.001$.)

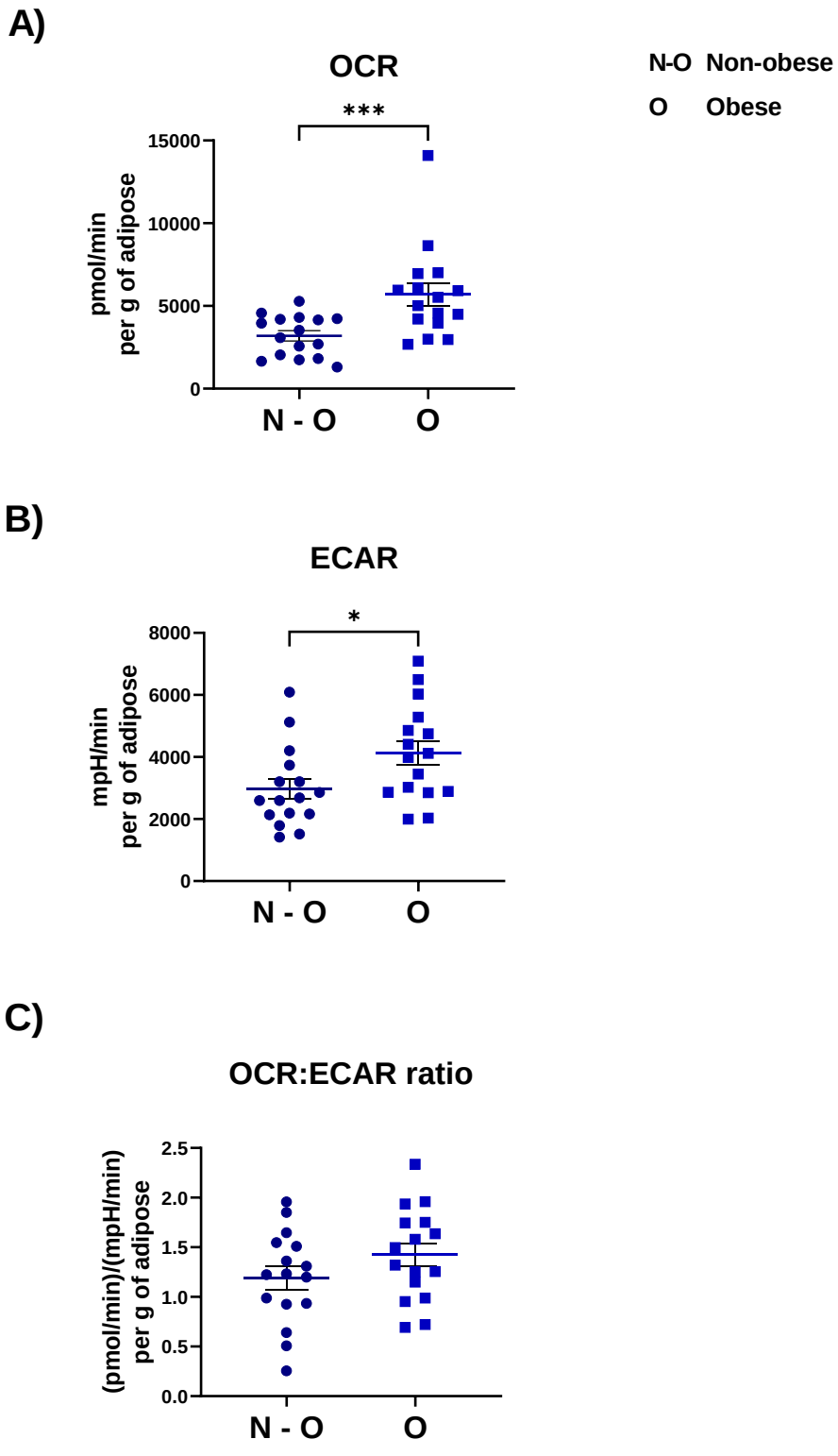


**Figure 2.4.1 Altered OCR, ECAR, pro-inflammatory cytokines, and metabolites in adipose explants from obese OAC patients compared with non-obese patients.**
(A-C) OCR, ECAR, and OCR:ECAR ratio (Mann–Whitney test). All data expressed as mean ± SEM, obese n = 16, non-obese n = 16, * $p < 0.05$, *** $p < 0.001$.

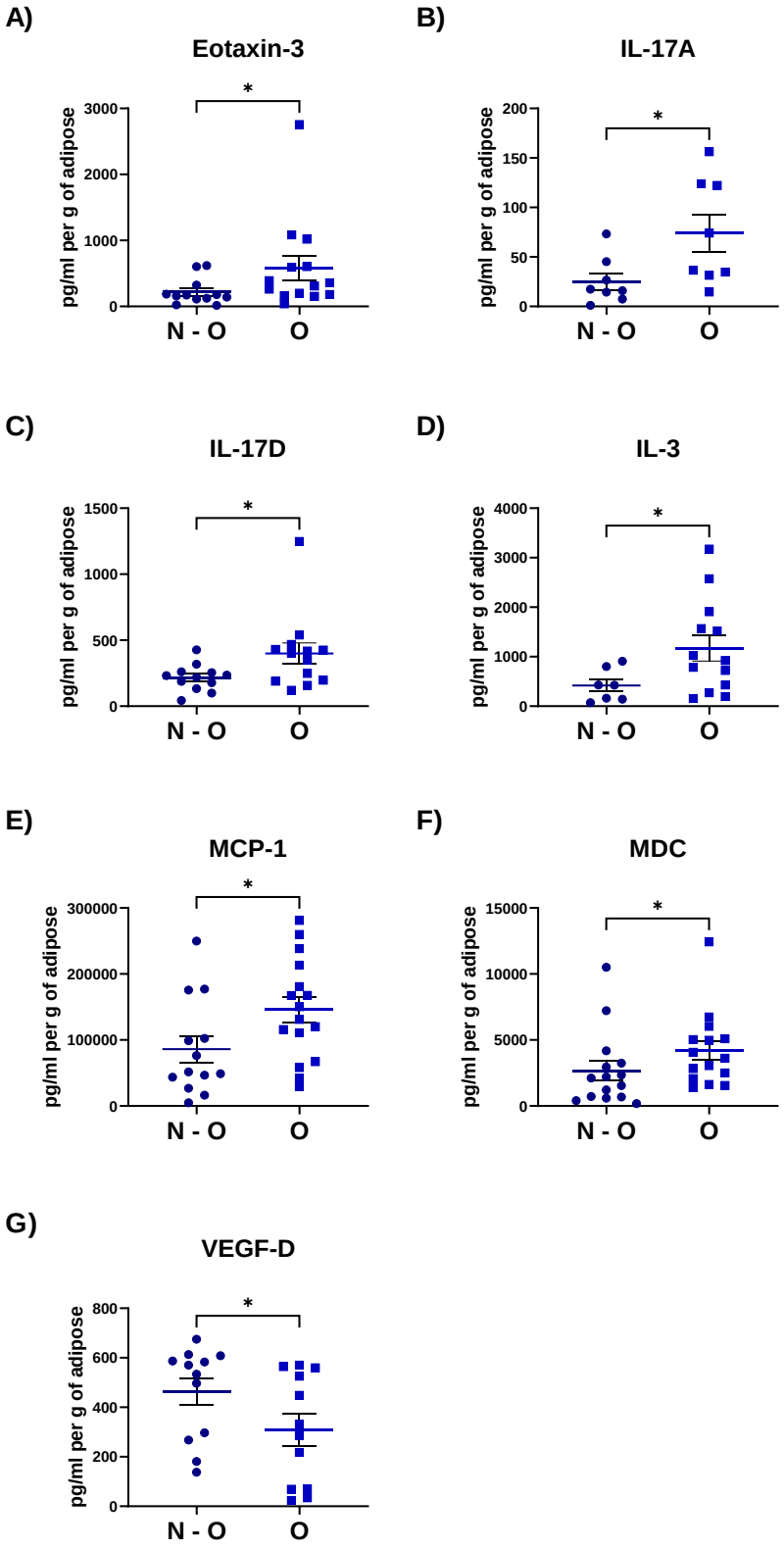


**Figure 2.4.2 Obesity increases secreted levels of mediators associated with immune recruitment and Th17 response.**

Eotaxin-3, IL-17A, IL-17D, IL-3, MCP-1, MDC, and VEGF-D (Mann–Whitney test). All data expressed as mean ± SEM, obese n = 16, non-obese n = 16, * $p < 0.05$.

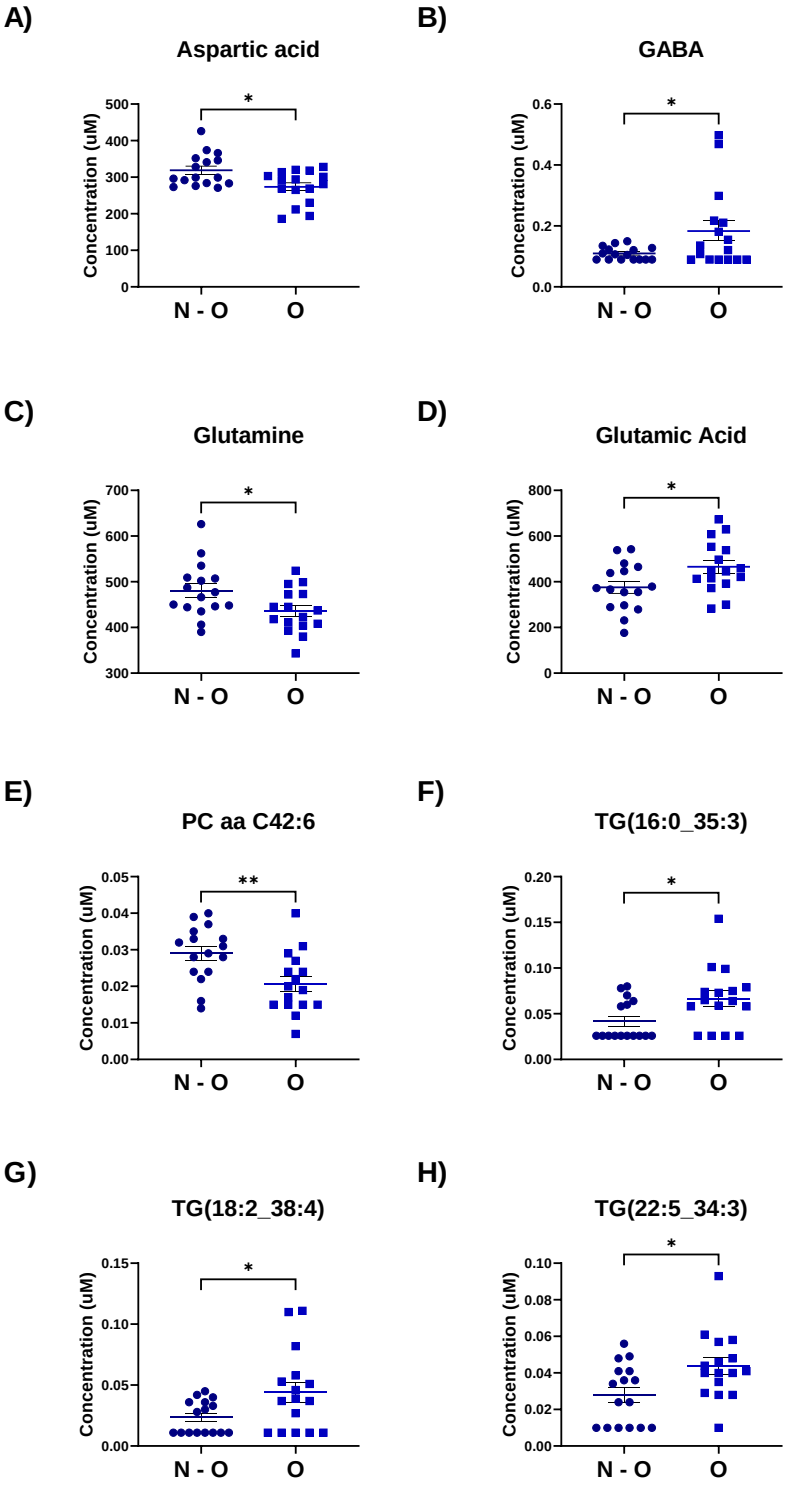


**Figure 2.4.3 Obesity differential alters key metabolites associated with glutamine metabolism.**

A series of metabolites and triacylglycerides were observed to be differentially altered in obese adipose tissue from OAC patients including (A-H) Aspartic acid, GABA, Glutamine, Glutaric acid, and PC aa C42:6, TG(16:0_35:3), TG(18:2_38:4), and TG(22:5_34:3) (Mann–Whitney test). All data expressed as mean ± SEM, obese n = 16, non-obese n = 16, * $p < 0.05$, ** $p < 0.01$.

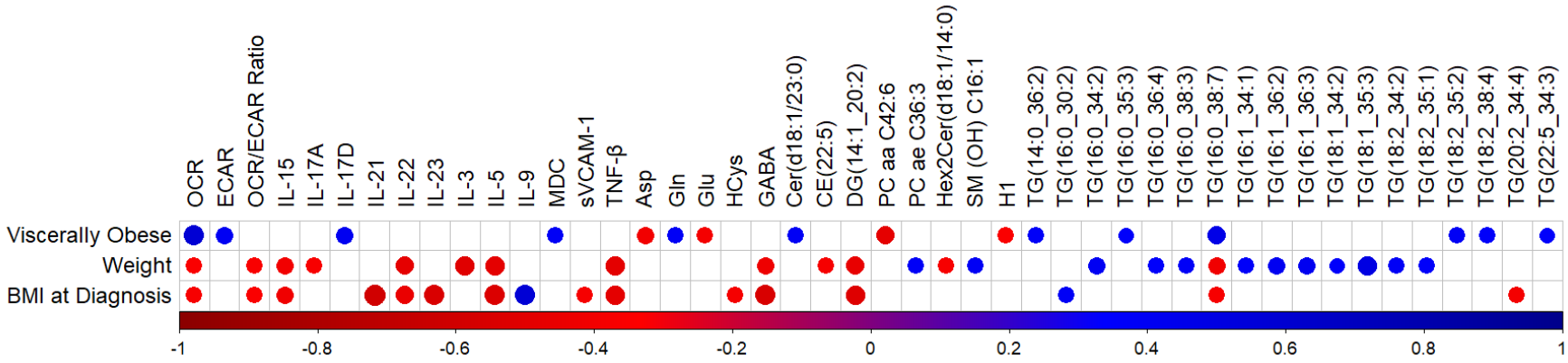


**Figure 2.4.4 Obesity classified by increased visceral fat area correlates differentially with experimental data compared with BMI and weight**
Correlation plot showing only significant correlations ($p < 0.05$) between experimental data and visceral obesity (Spearman correlation, blue indicates positive correlations and red indicates inverse negative correlations). Holm–Bonferroni post hoc correction was used to control for multiple comparison testing. obese $n = 16$, non-obese $n = 16$, circle symbol present $p < 0.05$.

**Table 2.4.1 Significant correlations associated with visceral obesity and metabolic profiles, pro-inflammatory mediators, metabolites, and lipid analysis as illustrated in Figure 2.4.4.**

| | Viscerally Obese | Weight | BMI at Diagnosis |
|---|---|---|---|
| **Factors** | **R number (p value)** | | |
| **OCR** | 0.575 (0.001) | -0.361 (0.042) | -0.376 (0.034) |
| **ECAR** | 0.399 (0.024) | | |
| **OCR/ECAR Ratio** | | -0.362 (0.042) | -0.359 (0.044) |
| **IL-15** | | -0.406 (0.023) | -0.418 (0.019) |
| **IL-17A** | | -0.370 (0.044) | |
| **IL-17D** | 0.411 (0.041) | | |
| **IL-21** | | | -0.598 (0.011) |
| **IL-22** | | -0.478 (0.013) | -0.450 (0.021) |
| **IL-23** | | | -0.547 (0.043) |
| **IL-3** | | -0.508 (0.019) | |
| **IL-5** | | -0.486 (0.022) | -0.539 (0.010) |
| **IL-9** | | | 0.574 (0.032) |
| **MDC** | 0.381 (0.038) | | |
| **sVCAM-1** | | | -0.385 (0.033) |
| **TNF-β** | | -0.487 (0.029) | -0.486 (0.030) |
| **Asp** | -0.403 (0.022) | | |
| **Gln** | 0.379 (0.032) | | |
| **Glu** | -0.393 (0.026) | | |
| **HCys** | | | -0.388 (0.028) |
| **GABA** | | -0.431 (0.014) | -0.552 (0.001) |
| **Cer(d18:1/23:0)** | 0.391 (0.027) | | |
| **CE(22:5)** | | -0.383 (0.030) | |
| **DG(14:1_20:2)** | | -0.461 (0.008) | -0.519 (0.002) |
| **PC aa C42:6** | -0.482 (0.005) | | |
| **PC ae C36:3** | | 0.378 (0.033) | |
| **Hex2Cer(d18:1/14:0)** | | -0.378 (0.033) | |
| **SM (OH) C16:1** | | 0.389 (0.028) | |
| **H1** | -0.359 (0.044) | | |
| **TG(14:0_36:2)** | 0.370 (0.037) | | |
| **TG(16:0_30:2)** | | | 0.383 (0.031) |
| **TG(16:0_34:2)** | | 0.398 (0.024) | |
| **TG(16:0_35:3)** | 0.350 (0.049) | | |
| **TG(16:0_36:4)** | | 0.356 (0.046) | |
| **TG(16:0_38:3)** | | 0.375 (0.034) | |
| **TG(16:0_38:7)** | 0.467 (0.007) | -0.409 (0.020) | -0.374 (0.035) |
| **TG(16:1_34:1)** | | 0.362 (0.042) | |
| **TG(16:1_36:2)** | | 0.412 (0.019) | |
| **TG(16:1_36:3)** | | 0.415 (0.018) | |
| **TG(18:1_34:2)** | | 0.351 (0.049) | |
| **TG(18:1_35:3)** | | 0.494 (0.004) | |
| **TG(18:2_34:2)** | | 0.383 (0.030) | |
| **TG(18:2_35:1)** | | 0.357 (0.045) | |
| **TG(18:2_35:2)** | 0.389 (0.028) | | |
| **TG(18:2_38:4)** | 0.357 (0.045) | | |
| **TG(20:2_34:4)** | | | -0.392 (0.027) |
| **TG(22:5_34:3)** | 0.352 (0.048) | | |

### 2.4.2 *Adipose Explants Derived from OAC Patients with Metabolic Dysfunction Show Increased Oxidative Phosphorylation Associated Metabolism and Secreted Pro-inflammatory Mediators*

Aberrant biological mechanisms such as obesity, diabetes, high triacylglycerides, high cholesterol, and high blood pressure have all been identified as contributors to the development of metabolic syndrome, a pro-inflammatory condition that aids cancer progression[27]. In this study, to assess the influence of metabolic dysfunction, on visceral adipose explants from metabolically healthy (*n* = 17) and metabolically dysfunctional (*n* = 15) OAC patients, four profiling assays looking at metabolism, secreted pro-inflammatory mediators, and lipid/metabolite profiles were used.

In adipose explants derived from patients with clinically annotated metabolic dysfunction, significant increases in OCR ($p = 0.0486$) and the OCR/ECAR ratio were identified in metabolic profiles compared with metabolically healthy patients **(Figure 2.4.5)**. Furthermore, significant increases in secreted cytokines including IL-5, IL-7, SAA, and VEGF-C were detected in metabolically unhealthy patients compared with metabolically healthy patients **(Figure 2.4.6)**. The following metabolites were also identified to be significantly elevated in the adipose secretome of patients with metabolic dysfunction: C0, Glycine, Histidine, Phenylalanine, Tryptophan, Asymmetric dimethylarginine, Homocysteine, Hypoxanthine, Taurine, beta-Ala, CE(22:5), and PC aa C38:4 (Figure 2.4.7). Following the lipidomic analysis, triglycerides including TG(16:0_35:3), TG(18:0_34:3), TG(18:1_33:3), TG(18:2_38:4), TG(20:2_36:5), TG(20:4_33:2), TG(20:4_34:0), and TG(20:4_36:5) were also seen to be elevated in the adipose secretome of OAC patients with metabolic dysfunction compared with patients who were metabolically healthy **(Figure 2.4.7-8)**. Significant correlations were also observed between the experimental data with metabolic dysfunction, Barrett's oesophagus, smoking history, the ASA grade, and the Clavien–Dindo grade, which were visualised using corrplot **(Figure 2.4.9)**, and the associated R numbers and *p*-values are detailed in Table 2.4.2. (* $p < 0.05$, ** $p < 0.01$, *** $p < 0.001$.)

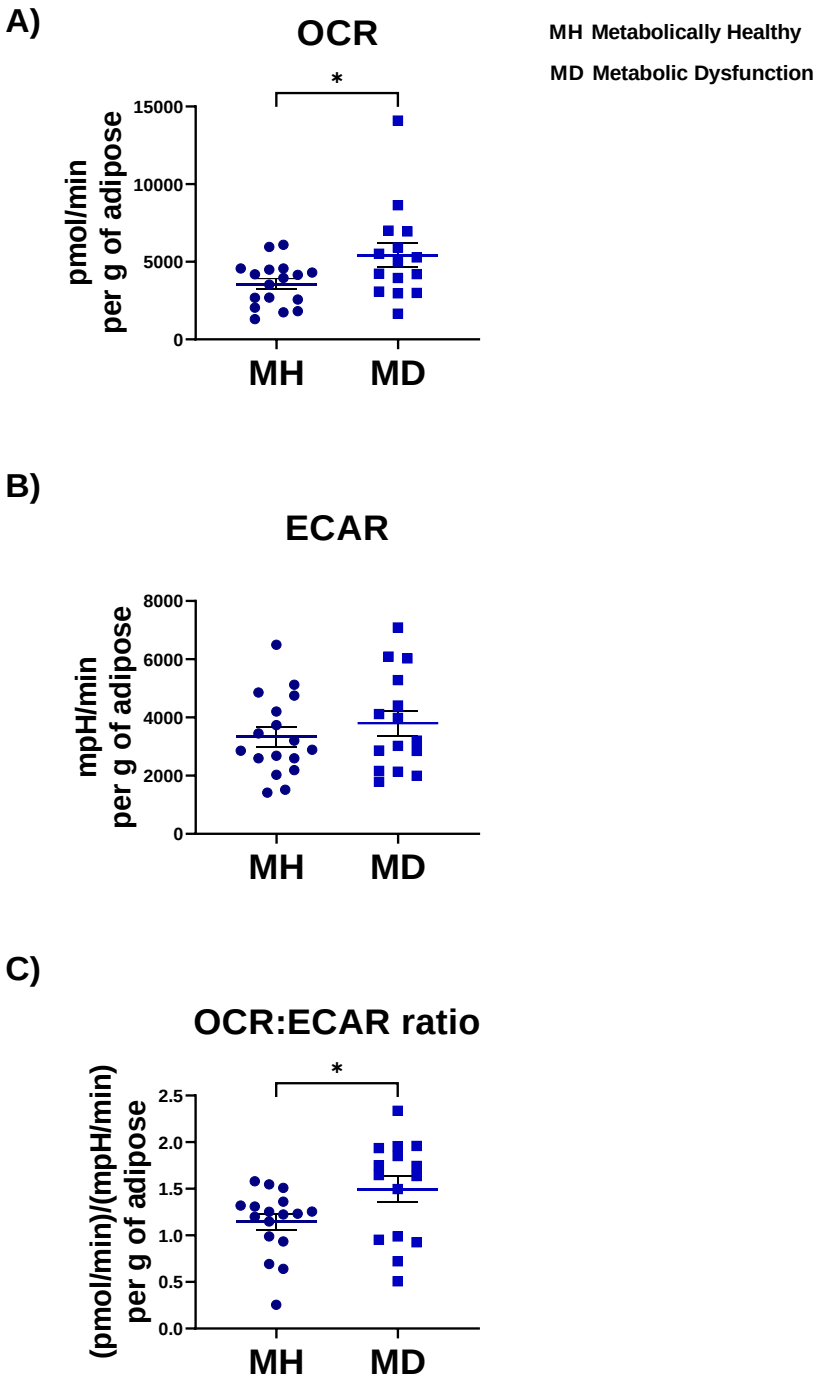


**Figure 2.4.5 Adipose explants from OAC patients with metabolic dysfunction show increased OCR profiles and enhanced reliance on oxidative phosphorylation over glycolysis**

(**A-C**) OCR, ECAR, and OCR:ECAR ratio profiles of adipose tissue explants from metabolically dysfunctional (MD) and metabolically healthy (MH) OAC patients (Mann–Whitney test). All data expressed as mean ± SEM, metabolic dysfunction $n = 15$, metabolically healthy $n = 17$, * $p < 0.05$.

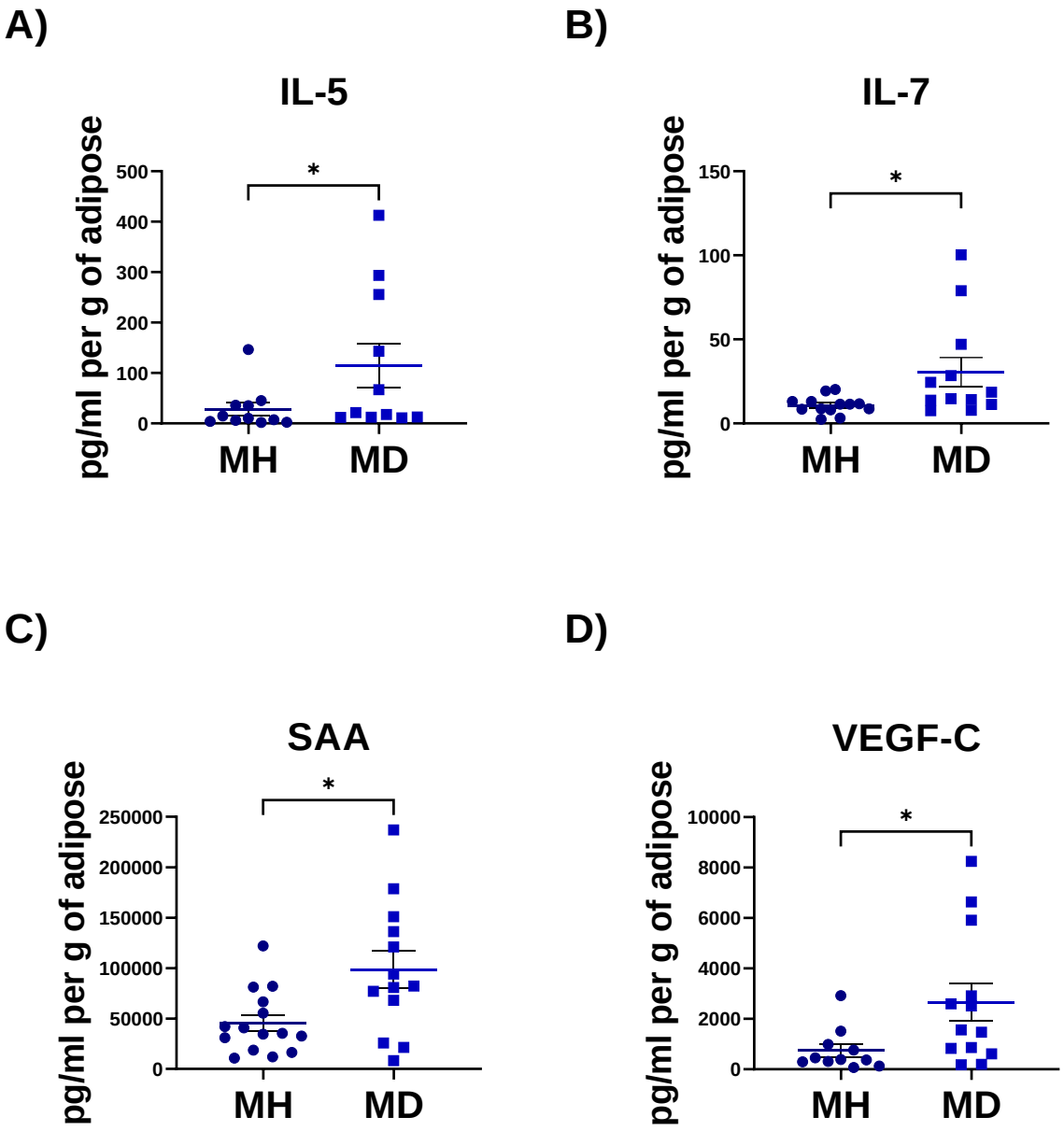


**Figure 2.4.6 Increased secreted levels of IL-7 a contributor to glucose and insulin resistance is observed in OAC patients with metabolic dysfunction**

**(A-D)** Secreted levels of IL-5, IL-7, SAA, and VEGF-C in the adipose secretome of metabolically dysfunctional (MD) and metabolically healthy (MH) OAC patients (Mann–Whitney test). (All data expressed as mean ± SEM, metabolic syndrome $n = 15$, metabolically healthy $n = 17$, * $p < 0.05$.

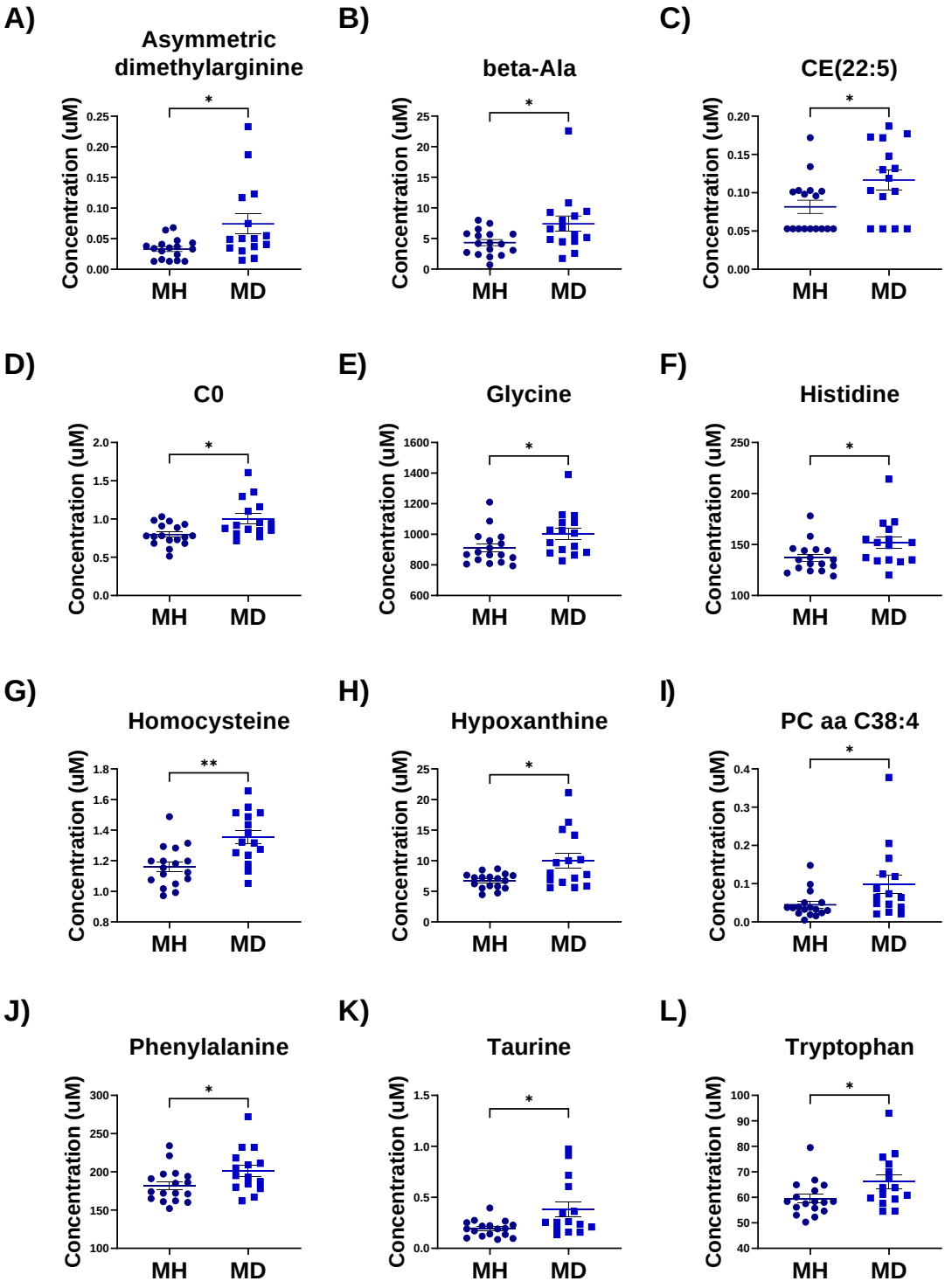


**Figure 2.4.7 Adipose explants from OAC patients with metabolic dysfunction have increased secreted levels of metabolites associated with a series of metabolic diseases**

**(A-L)** Secreted levels of Asymmetric dimethylarginine, beta-Ala, CE(22:5), C0, Glycine, Histidine, Homocysteine, Hypoxanthine, PC aa C38:4, Phenylalanine, Taurine, and Tryptophan in the adipose secretome of metabolically dysfunctional (MD) and metabolically healthy (MH) OAC patients (Mann–Whitney test). All data expressed as mean ± SEM, metabolic syndrome *n* = 15, metabolically healthy *n* = 17, * $p < 0.05$, ** $p < 0.01$.

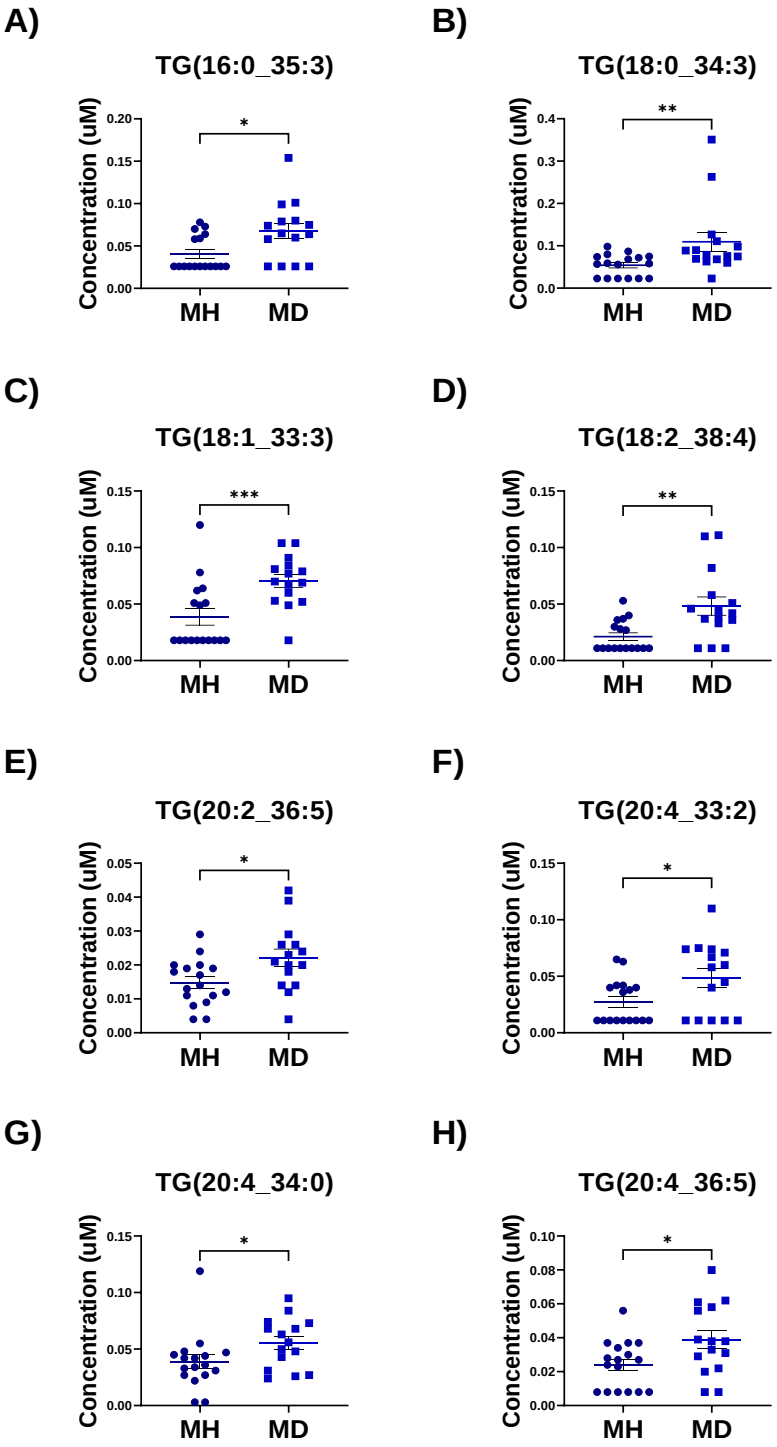


**Figure 2.4.8 Adipose explants from OAC patients with metabolic dysfunction have increased secreted levels of triacylglycerides**

Secreted levels of TG(16:0_35:3), TG(18:0_34:3), TG(18:1_33:3), TG(18:2_38:4), TG(20:2_36:5), TG(20:4_33:2), TG(20:4_34:0), and TG(20:4_36:5) in the adipose secretome of metabolically dysfunctional (MD) and metabolically healthy (MH) OAC patients (Mann–Whitney test). All data expressed as mean ± SEM, metabolic syndrome $n = 15$, metabolically healthy $n = 17$, * $p < 0.05$, ** $p < 0.01$, *** $p < 0.001$.

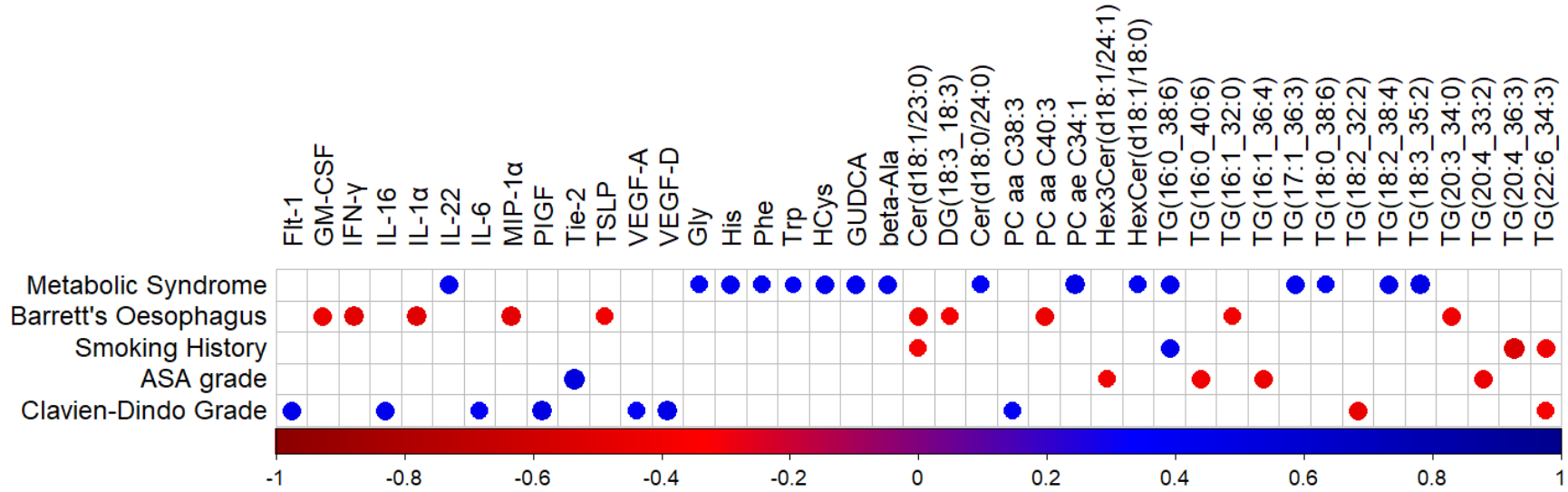


**Figure 2.4.9 Metabolic dysfunction positively correlates with a series of metabolites whilst the previous history of Barrett's oesophagus correlated with decreased inflammatory proteins and mediators of immune cell recruitment.**

Correlation plot showing only significant correlations ($p < 0.05$) between experimental data and metabolic syndrome, Barrett's oesophagus, smoking history, ASA grade, and Clavien–Dindo grade (Spearman correlation, blue indicates positive correlations and red indicates inverse negative correlations). The Holm–Bonferroni post hoc correction was used to control for multiple comparison testing. All data expressed as mean ± SEM, metabolic syndrome n = 15, metabolically healthy n = 17, circle present $p < 0.05$.

**Table 2.4.2 Significant correlations associated with Figure 2.4.9 between experimental data and factors associated with metabolic dysfunction and systemic disease.**

| | Metabolic Dysfunction | Barrett's Oesophagus | Smoking History | ASA grade | Clavien-Dindo Grade |
|---|---|---|---|---|---|
| **Factors** | R number (p value) | | | | |
| **Flt-1** | | | | | 0.448 (0.019) |
| **GM-CSF** | | -0.44 (0.028) | | | |
| **IFN-γ** | | -0.5 (0.025) | | | |
| **IL-16** | | | | | 0.436 (0.023) |
| **IL-1α** | | -0.506 (0.016) | | | |
| **IL-22** | 0.436 (0.026) | | | | |
| **IL-6** | | | | | 0.394 (0.042) |
| **MIP-1α** | | -0.485 (0.022) | | | |
| **PIGF** | | | | | 0.501 (0.008) |
| **Tie-2** | | | | 0.525 (0.037) | |
| **TSLP** | | -0.404 (0.045) | | | |
| **VEGF-A** | | | | | 0.382 (0.049) |
| **VEGF-D** | | | | | 0.475 (0.022) |
| **Gly** | 0.383 (0.03) | | | | |
| **His** | 0.414 (0.018) | | | | |
| **Phe** | 0.4 (0.023) | | | | |
| **Trp** | 0.363 (0.041) | | | | |
| **HCys** | 0.424 (0.016) | | | | |
| **GUDCA** | 0.418 (0.017) | | | | |
| **beta-Ala** | 0.421 (0.017) | | | | |
| **Cer(d18:1/23:0)** | | -0.422 (0.032) | -0.376 (0.037) | | |
| **DG(18:3_18:3)** | | -0.39 (0.049) | | | |
| **Cer(d18:0/24:0)** | 0.379 (0.032) | | | | |
| **PC aa C38:3** | | | | | 0.4 (0.035) |
| **PC aa C40:3** | | -0.434 (0.027) | | | |
| **PC ae C34:1** | 0.469 (0.007) | | | | |
| **Hex3Cer(d18:1/24:1)** | | | | -0.409 (0.038) | |
| **HexCer(d18:1/ 18:0)** | 0.392 (0.026) | | | | |
| **TG(16:0_38:6)** | 0.434 (0.013) | | 0.433 (0.015) | | |
| **TG(16:0_40:6)** | | | | -0.418 (0.034) | |
| **TG(16:1_32:0)** | | -0.4 (0.043) | | | |
| **TG(16:1_36:4)** | | | | -0.434 (0.027) | |
| **TG(17:1_36:3)** | 0.429 (0.014) | | | | |
| **TG(18:0_38:6)** | 0.382 (0.031) | | | | |
| **TG(18:2_32:2)** | | | | | -0.46 (0.014) |
| **TG(18:2_38:4)** | 0.46 (0.008) | | | | |
| **TG(18:3_35:2)** | 0.481 (0.005) | | | | |
| **TG(20:3_34:0)** | | -0.418 (0.034) | | | |
| **TG(20:4_33:2)** | | | | -0.45 (0.021) | |
| **TG(20:4_36:3)** | | | -0.545 (0.002) | | |
| **TG(22:6_34:3)** | | | -0.419 (0.019) | | -0.377 (0.048) |

### 2.4.3 *Adipose Explants from Patients Receiving the FLOT Chemotherapy Regimen Showed Increased Oxidative Phosphorylation and Pro-inflammatory Mediators and Decreased Triacylglycerides*

Patients were classified as treatment naïve if they had received no treatment prior to surgical intervention (*n* = 10), FLOT if they had received neo-adjuvant chemotherapy only regimen FLOT (*n* = 14), or CROSS if they received neo-adjuvant chemo-radiotherapy regimen CROSS (=8). The four experimental assays looking at metabolism, secreted pro-inflammatory mediators, and lipid/metabolite profiles were utilised to identify whether any associations were observed between previous treatment exposure and adipose tissue functionality.

Increased OCR metabolic profiles were observed in adipose explants derived from patients who had previously been treated with the FLOT chemotherapy regimen compared with patients who did not have neo-adjuvant treatment **(Figure 2.4.10)**. Increased secretion of cytokines IL-12p40, IL-1α, IL-22, and TNF-β were observed in the adipose secretome of patients previously treated with FLOT compared with patients who were treatment-naïve. Decreased secretion of cytokines IL-7 and VEGF-C were observed in the adipose explants from patients who had received neo-adjuvant chemo-radiotherapy regimen CROSS compared with FLOT **(Figure 2.4.11)**.

Metabolites including Cer(d16:1/22:0), SM (OH) C22:1, TG(16:0_34:3), TG(16:0_40:6), TG(16:1_34:1), TG(16:1_36:4), and TG(18:0_36:3) were significantly decreased in the secretome of the adipose explants derived from patients who had previously been treated with the FLOT regimen compared with treatment-naïve patients. Significant decreases were observed in metabolites p-Cresol-SO4, Hex3Cer(d18:1/24:1), and TG(20:2_34:4) whilst metabolite TG(16:1_36:5) was significantly increased in the adipose secretome of patients who had previously received the CROSS regimen compared with patients who were treatment-naïve.

Metabolites GUDCA, Hex2Cer(d18:1/14:0), and TG(20:2_34:4) were all observed to be decreased and metabolites DCA, TG(14:0_36:2), TG(16:0_33:2), TG(16:0_30:2), TG(18:0_36:3), and TG(18:2_35:2), TG(18:3_32:1) were observed as increased in the adipose secretome of patients who received the chemo-radiotherapy CROSS regimen compared with patients who received the chemotherapy only FLOT regimen. In particular, the metabolite TG(18:0_36:3) was decreased in the adipose secretome of patients receiving the FLOT regimen compared with both the treatment-naïve patients and patients receiving the CROSS regimen whilst metabolite TG(20:2_34:4) was decreased in the adipose secretome of patients receiving the CROSS regimen compared with both treatment-naïve patients and patients receiving the FLOT regimen **(Figure 2.4.11-12)**.

Significant correlations observed between the experimental data with neo-adjuvant treatment, chemotherapy only, chemoradiotherapy, tumour differentiation, lymph involvement, venous involvement, and perineural involvement were visualised using corrplot **(Figure 2.4.13)**, and the associated R numbers and *p*-values are detailed in Table 2.4.3 and Table 2.4.4.

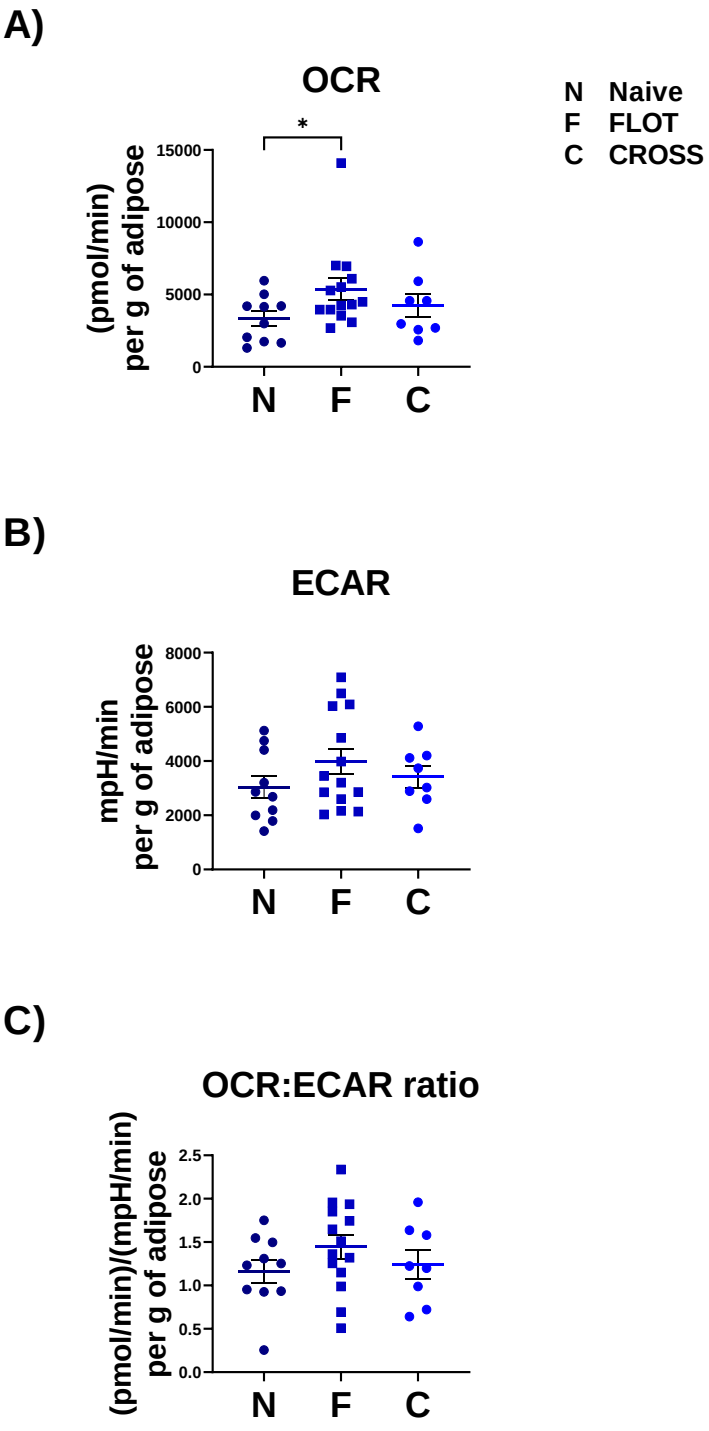


**Figure 2.4.10 Adipose explants from OAC patients who had received chemotherapy regimen FLOT showed increased OCR profiles compared with treatment naïve patients.**
(A-C) OCR, ECAR, and OCR:ECAR ratio profiles of adipose tissue explants from OAC patients who were treatment naïve (N), received chemotherapy regimen FLOT (F), or chemoradiotherapy regimen CROSS (C) (Kruskal–Wallis with Dunn's correction). All data expressed as mean ± SEM, Naïve n = 10, FLOT n = 14, CROSS n = 8, * $p < 0.05$.

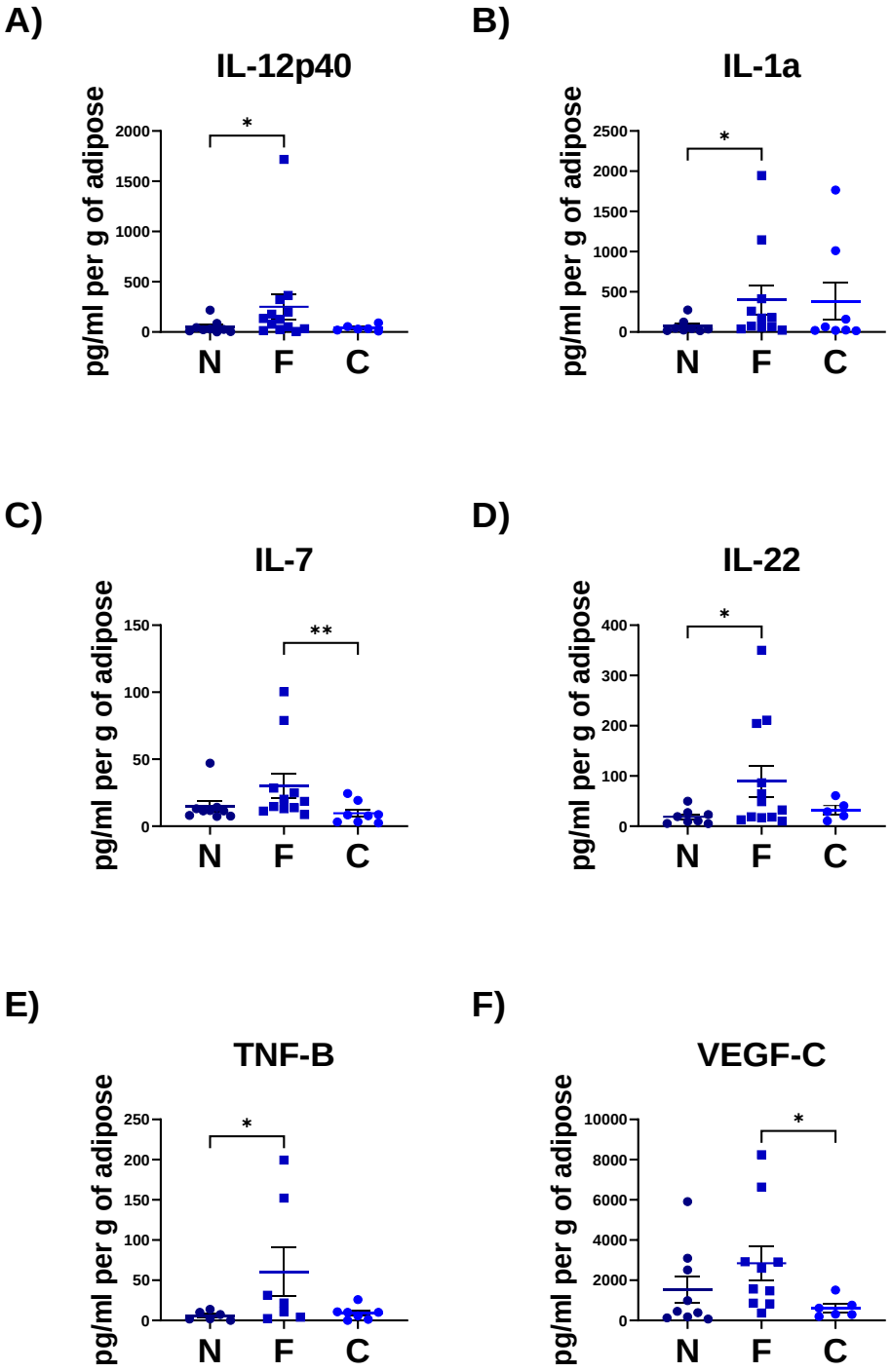


**Figure 2.4.11 Increased secreted levels of pro-inflammatory and pro-angiogenic mediators are observed in the adipose secretome of patients who received FLOT chemotherapy.**
(A-F) Secreted levels of IL-12p40, IL-1α, IL-7, IL-22, TNF-β, and VEGF-C from the secretome of adipose tissue explants from OAC patients who were treatment naïve (N), received chemotherapy regimen FLOT (F), or chemoradiotherapy regimen CROSS (C) (Kruskal–Wallis with Dunn's correction). (B) (Kruskal–Wallis with Dunn's correction). All data expressed as mean ± SEM, Naïve n = 10, FLOT n = 14, CROSS *n* = 8, * $p < 0.05$, ** $p < 0.001$.

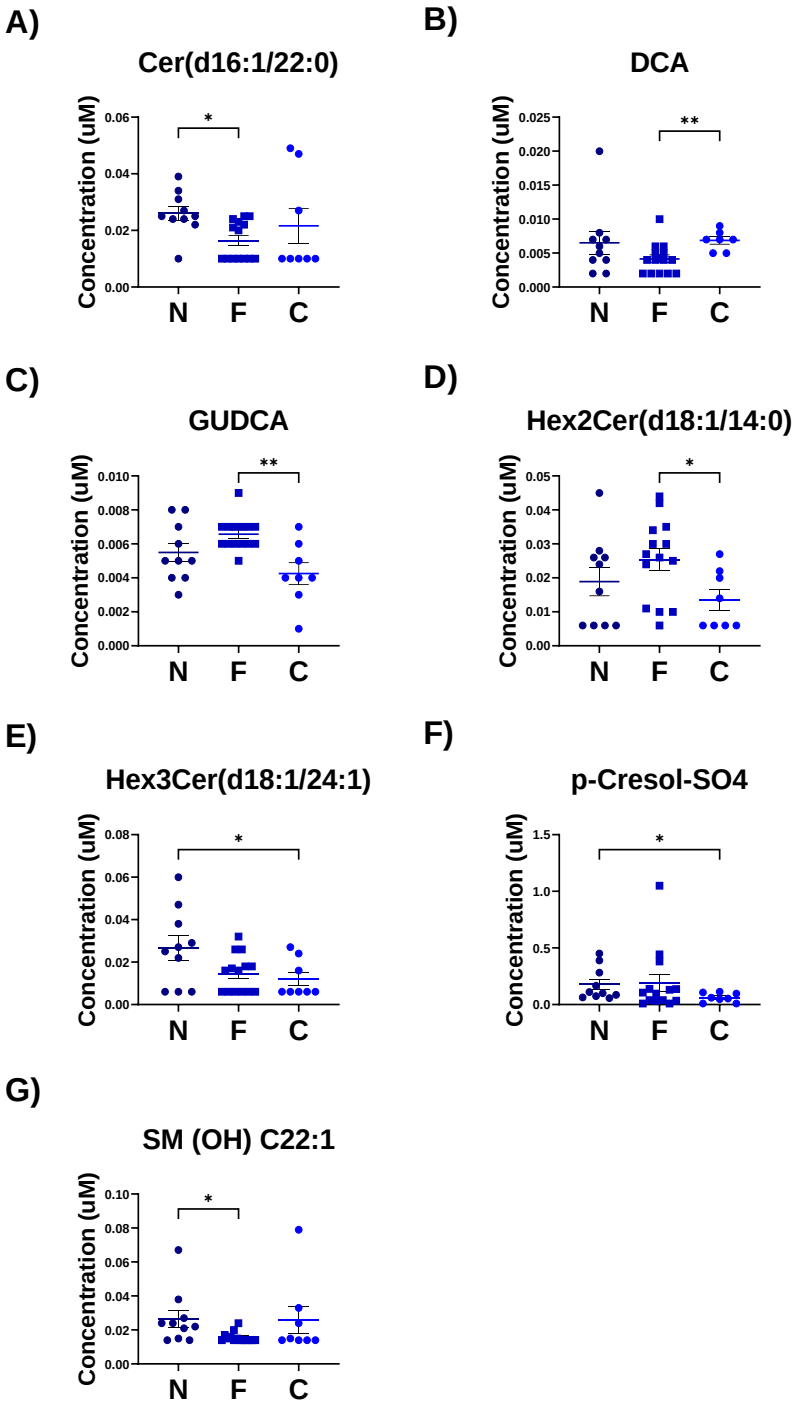


**Figure 2.4.12 Decreased levels of hexosylceramides were observed in the adipose secretome of OAC patients who had received CROSS chemoradiotherapy.**

(A-G) Secreted levels of Cer(d16:1/22:0), DCA, GUDCA, Hex2Cer(d18:1/14:0), Hex3Cer(d18:1/24:1, p-Cresol-SO4, and SM (OH) C22:1 from the secretome of adipose tissue explants from OAC patients who were treatment naïve (N), received chemotherapy regimen FLOT (F), or chemoradiotherapy regimen CROSS (C) (Kruskal–Wallis with Dunn's correction). All data expressed as mean ± SEM, Naïve n = 10, FLOT n = 14, CROSS n = 8, * $p < 0.05$, ** $p < 0.001$.

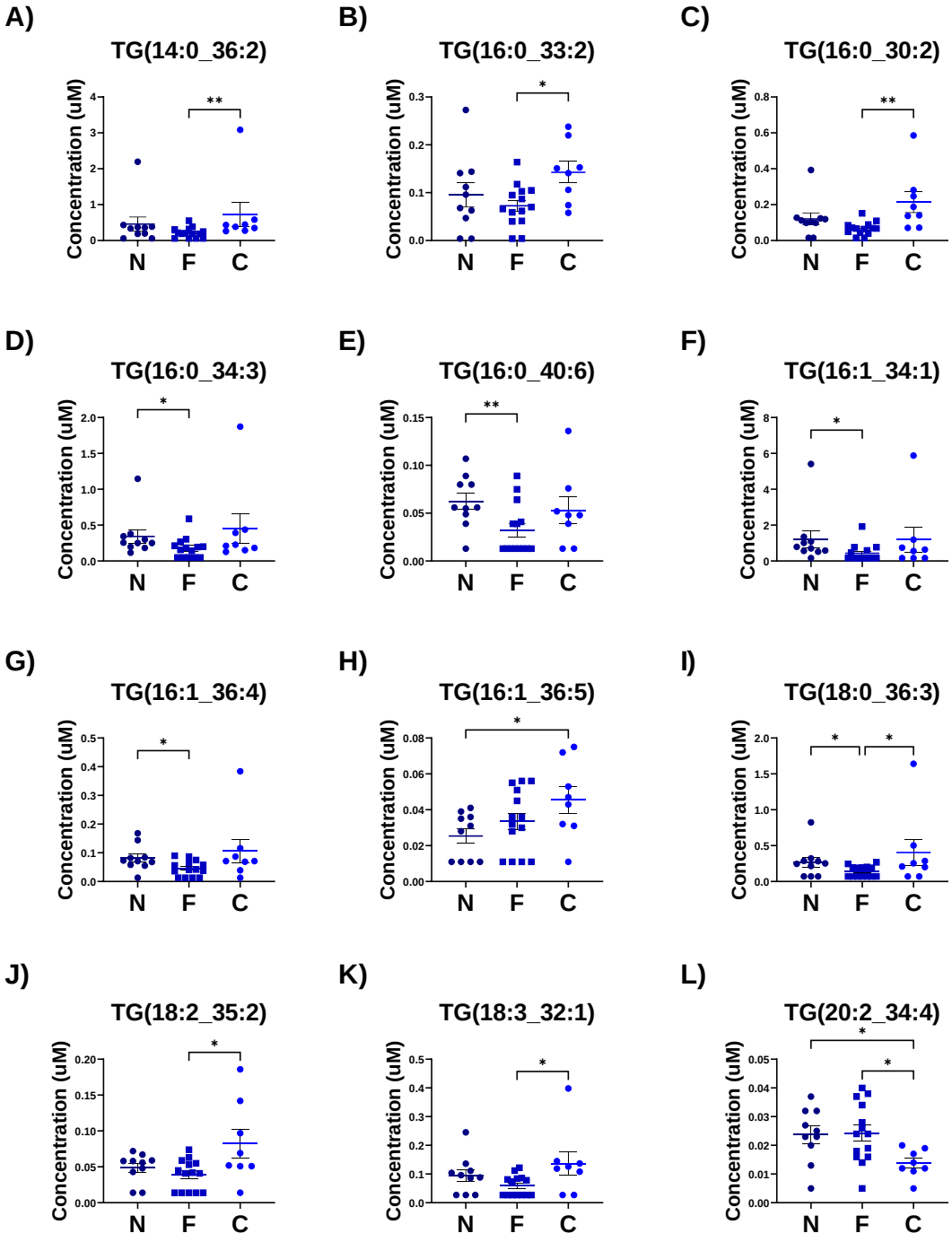


**Figure 2.4.13 Increased levels of short chain triacylglycerides were observed in the adipose secretome of OAC patients who had received CROSS chemoradiotherapy.**

(A-L) Secreted levels of TG(14:0_36:2), and TG(16:0_33:2), TG(16:0_30:2) ), TG(16:0_34:3), TG(16:0_40:6), TG(16:1_34:1), TG(16:1_36:4), TG(16:1_36:5), TG(18:0_36:3), TG(18:2_35:2), TG(18:3_32:1), and TG(20:2_34:4 from the secretome of adipose tissue explants from OAC patients who were treatment naïve (N), received chemotherapy regimen FLOT (F), or chemoradiotherapy regimen CROSS (C) (Kruskal–Wallis with Dunn's correction). All data expressed as mean ± SEM, Naïve n = 10, FLOT n = 14, CROSS n = 8, * $p < 0.05$, ** $p < 0.001$.

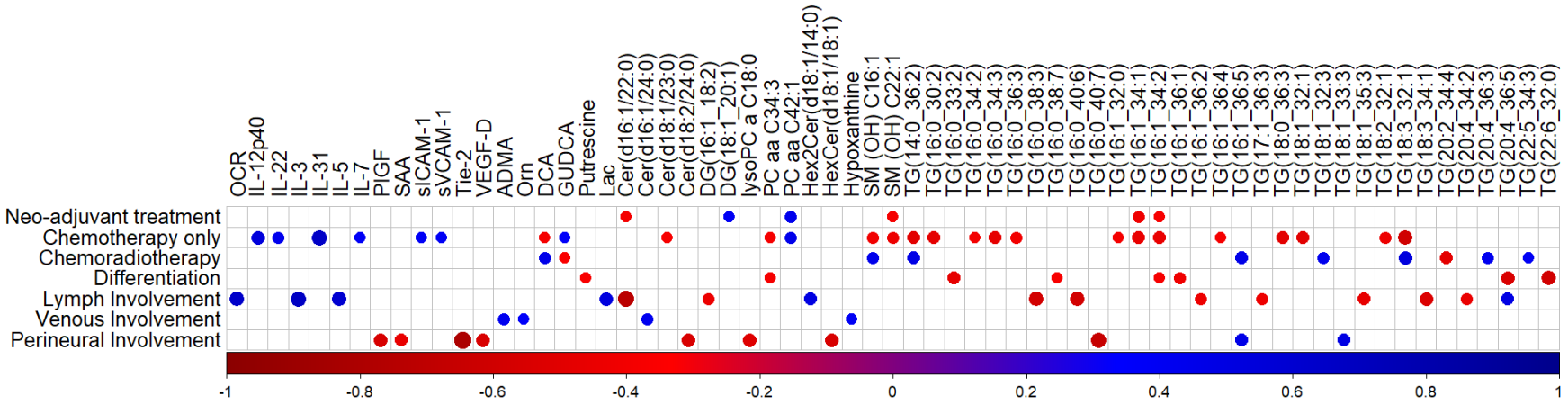


**Figure 2.4.14 Therapy regimen differentially correlates with bile acid levels in the adipose secretome, and increased lactate correlates with increased lymphatic invasion.**

Correlation plot showing only significant correlations ($p < 0.05$) between experimental data and with neo-adjuvant treatment, chemotherapy only, chemo-radiotherapy differentiation, lymph involvement, venous involvement, and perineural involvement (Spearman correlation, blue indicates positive correlations and red indicates inverse negative correlations). The Holm–Bonferroni post hoc correction was used to control for multiple comparison testing. All data expressed as mean ± SEM, Naïve n = 10, FLOT n = 14, CROSS = 8, circle present p < 0.05.

**Table 2.4.3 Significant correlations associated with Figure 2.4.15 between experimental data and factors associated with metabolic dysfunction and systemic disease.**

| | Neo-adjuvant treatment | Chemotherapy only | Chemoradiotherapy |
|---|---|---|---|
| **Factors** | | **R number (p value)** | |
| **IL-12p40** | | 0.536 (0.006) | |
| **IL-22** | | 0.433 (0.034) | |
| **IL-31** | | 0.659 (0.004) | |
| **IL-7** | | 0.383 (0.049) | |
| **sICAM-1** | | 0.381 (0.041) | |
| **sVCAM-1** | | 0.39 (0.037) | |
| **DCA** | | -0.387 (0.034) | 0.455 (0.012) |
| **GUDCA** | | 0.366 (0.047) | -0.364 (0.048) |
| **Cer(d16:1/22:0)** | -0.391 (0.033) | | |
| **Cer(d18:1/23:0)** | | -0.376 (0.04) | |
| **DG(18:1_20:1)** | 0.393 (0.032) | | |
| **PC aa C34:3** | | -0.387 (0.035) | |
| **PC aa C42:1** | 0.437 (0.016) | 0.453 (0.012) | |
| **SM (OH) C16:1** | | -0.412 (0.024) | 0.446 (0.013) |
| **SM (OH) C22:1** | -0.386 (0.035) | -0.432 (0.017) | |
| **TG(14:0_36:2)** | | -0.499 (0.005) | 0.48 (0.007) |
| **TG(16:0_30:2)** | | -0.483 (0.007) | |
| **TG(16:0_34:2)** | | -0.397 (0.03) | |
| **TG(16:0_34:3)** | | -0.472 (0.008) | |
| **TG(16:0_36:3)** | | -0.403 (0.027) | |
| **TG(16:1_32:0)** | | -0.395 (0.031) | |
| **TG(16:1_34:1)** | -0.423 (0.02) | -0.459 (0.011) | |
| **TG(16:1_34:2)** | -0.375 (0.041) | -0.459 (0.011) | |
| **TG(16:1_36:4)** | | -0.388 (0.034) | |
| **TG(16:1_36:5)** | | | 0.465 (0.01) |
| **TG(18:0_36:3)** | | -0.491 (0.006) | |
| **TG(18:1_32:1)** | | -0.494 (0.006) | |
| **TG(18:1_32:3)** | | | 0.432 (0.017) |
| **TG(18:2_32:1)** | | -0.432 (0.017) | |
| **TG(18:3_32:1)** | | -0.606 (0.0003) | 0.527 (0.003) |
| **TG(20:2_34:4)** | | | -0.484 (0.007) |
| **TG(20:4_36:3)** | | | 0.423 (0.02) |
| **TG(22:5_34:3)** | | | 0.395 (0.031) |

**Table 2.4.4 Significant correlations associated with Figure 2.4.15 for clinical correlations with differentiation, lymph involvement, venous involvement and perineural involvement.**

| | Differentiation | Lymph Involvement | Venous Involvement | Perineural Involvement |
|---|---|---|---|---|
| **Factors** | | **R number (p value)** | | |
| **OCR** | | 0.641 (0.001) | | |
| **IL-3** | | 0.677 (0.004) | | |
| **IL-5** | | 0.598 (0.011) | | |
| **PIGF** | | | | -0.558 (0.013) |
| **SAA** | | | | -0.462 (0.047) |
| **Tie-2** | | | | -0.806 (0.0001) |
| **VEGF-D** | | | | -0.553 (0.021) |
| **ADMA** | | | 0.422 (0.018) | |
| **Orn** | | | 0.366 (0.043) | |
| **Putrescine** | -0.371 (0.047) | | | |
| **Lac** | | 0.521 (0.013) | | |
| **Cer(d16:1/22:0)** | | -0.728 (0.0001) | | |
| **Cer(d16:1/24:0)** | | | 0.422 (0.018) | |
| **Cer(d18:2/24:0)** | | | | -0.551 (0.014) |
| **DG(16:1_18:2)** | | -0.44 (0.04) | | |
| **lysoPC a C18:0** | | | | -0.521 (0.022) |
| **PC aa C34:3** | -0.391 (0.036) | | | |
| **Hex2Cer(d18:1/14:0)** | | 0.501 (0.018) | | |
| **HexCer(d18:1/18:1)** | | | | -0.562 (0.012) |
| **Hypoxanthine** | | | 0.392 (0.029) | |
| **TG(16:0_33:2)** | -0.473 (0.01) | | | |
| **TG(16:0_38:3)** | | -0.592 (0.004) | | |
| **TG(16:0_38:7)** | -0.374 (0.046) | | | |
| **TG(16:0_40:6)** | | -0.588 (0.004) | | |
| **TG(16:0_40:7)** | | | | -0.66 (0.002) |
| **TG(16:1_34:2)** | -0.38 (0.042) | | | |
| **TG(16:1_36:1)** | -0.425 (0.022) | | | |
| **TG(16:1_36:2)** | | -0.436 (0.043) | | |
| **TG(16:1_36:5)** | | | | 0.47 (0.042) |
| **TG(17:1_36:3)** | | -0.431 (0.045) | | |
| **TG(18:1_33:3)** | | | | 0.489 (0.034) |
| **TG(18:1_35:3)** | | -0.47 (0.027) | | |
| **TG(18:3_34:1)** | | -0.535 (0.01) | | |
| **TG(20:4_34:2)** | | -0.452 (0.035) | | |
| **TG(20:4_36:5)** | -0.55 (0.002) | 0.49 (0.02) | | |
| **TG(22:6_32:0)** | -0.592 (0.001) | | | |

### 2.4.4 *Increased ECAR and Altered Metabolites Are Observed in Adipose Explants from OAC Patients with Increasing Tumour Regression Grades*

Tumour regression grading was used to assess patients' response to treatment received; therefore, experimental data within this section only relates to patients who received neo-adjuvant treatment prior to surgery, and patients who did not receive treatment prior to surgery were excluded from this analysis. TRG 1–2 ($n$ = 6) indicates patients who had a complete or good response to therapy, patients with TRG 3 ($n$ = 8) showed an intermediate response, and patients with TRG 4–5 ($n$ = 6) had a poor response. The association of this staging with adipose explant metabolism and secretome was assessed using the four profiling assays looking at metabolism, secreted pro-inflammatory mediators, and lipid/metabolite profiles.

Significantly increased ECAR profiles were observed in the secretome of adipose explants derived from patients with TRG scoring of 4–5 compared with patients with TRG scorings of 1–2 **(Figure 2.4.16)**. A decreased expression of metabolites Cer(d18:1/23:0), PC aa C36:1, PC aa C40:3, PC ae C34:2, HexCer(d18:1/18:0), TG(17:1_36:3), and TG(18:1_33:3) and an increased expression of DG(18:1_20:1) ($p$ = 0.0393) were observed in the adipose secretome from patients with a TRG of 3 compared with patients with TRG scorings of 1–2. A decreased expression of metabolites Cer(d18:1/23:0), TG(17:0_36:4), and TG(22:6_34:3) and an increased expression of TG(18:0_38:6) were observed in the secretome of adipose explants derived from patients with a TRG of 4–5 compared with patients with TRG scorings of 1–2. A significant decrease was observed in metabolites Cer(d16:1/23:0), PC aa C36:1, PC aa C40:3, PC ae C40:2, PC ae C44:5, Hex2Cer(d18:1/22:0), TG(17:1_36:3), TG(18:0_38:6), TG(20:3_34:3), and TG(20:4_36:5) and a significant increase in triglyceride TG(20:4_36:3) were observed in the adipose secretome of patients with a TRG of 3 compared with patients with a TRG of 4–5. It is of note, metabolite Cer(d18:1/23:0) was decreased in the adipose secretome of patients with a TRG score of 3 and TRG of 4–5 compared with patients who had a TRG of 1–2. A decreased expression was also observed in TG(18:0_38:6) in the secretome of adipose explants derived from patients with a TRG of 1–2 and a TRG of 3 compared with patients who possessed a TRG score of 4–5. It was also identified that metabolites including PC aa C36:1, PC aa C40:3 and TG(17:1_36:3) had increased expression in the adipose secretome of patients with TRGs of 1–2 and 4–5, respectively, compared with patients with a TRG scoring of 3 **(Figure 2.4.17-18)**. Significant correlations observed between experimental data with tumour regression grade, clinical tumour stage, clinical nodal stage, pathological tumour stage, pathological nodal stage, and no evidence of disease were visualised using corrplot **(Figure 2.4.19)**, and the associated R numbers and $p$-values are detailed in Tables 2.4.5 and 2.4.6.

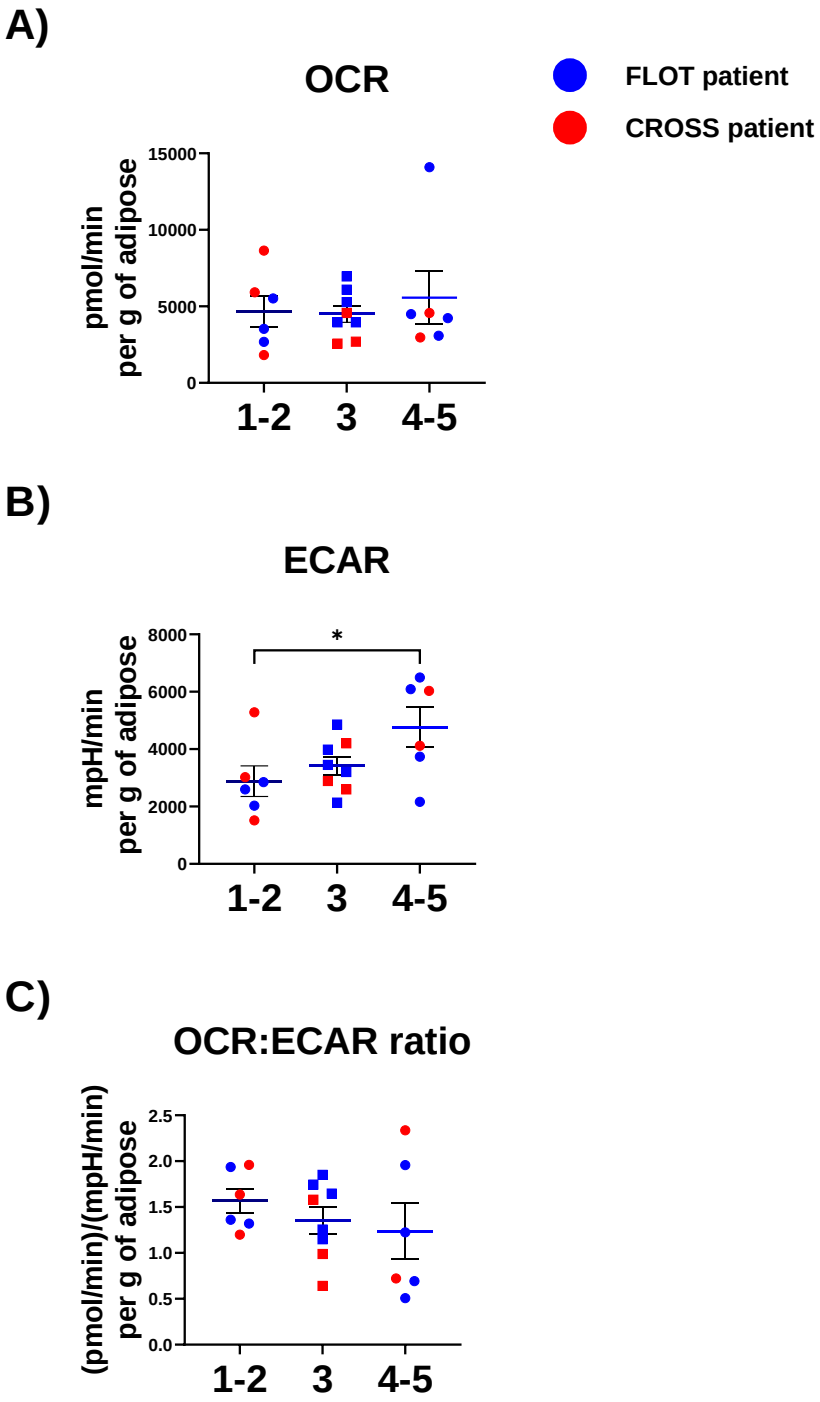


**Figure 2.4.15 Increased ECAR profiles are observed in adipose explants from OAC patients with increasing tumour regression grades**

(**A-C**) OCR, ECAR, and OCR:ECAR ratio profiles of adipose explants from OAC patients who showed TRG 1-2 (good response), TRG 3, (partial response) and TRG 4-5 (poor response) to chemotherapy regimen FLOT or chemoradiotherapy regimen CROSS (Kruskal–Wallis with Dunn's correction). All data expressed as mean ± SEM, TRG 1–2 $n$ = 6, TRG 3 $n$ = 8, TRG 4–5 $n$ = 6, * $p < 0.05$. Blue symbols identify patients who received neo-adjuvant chemotherapy (FLOT) and red symbols identify patients who received neo-adjuvant chemo-radiotherapy (CROSS).

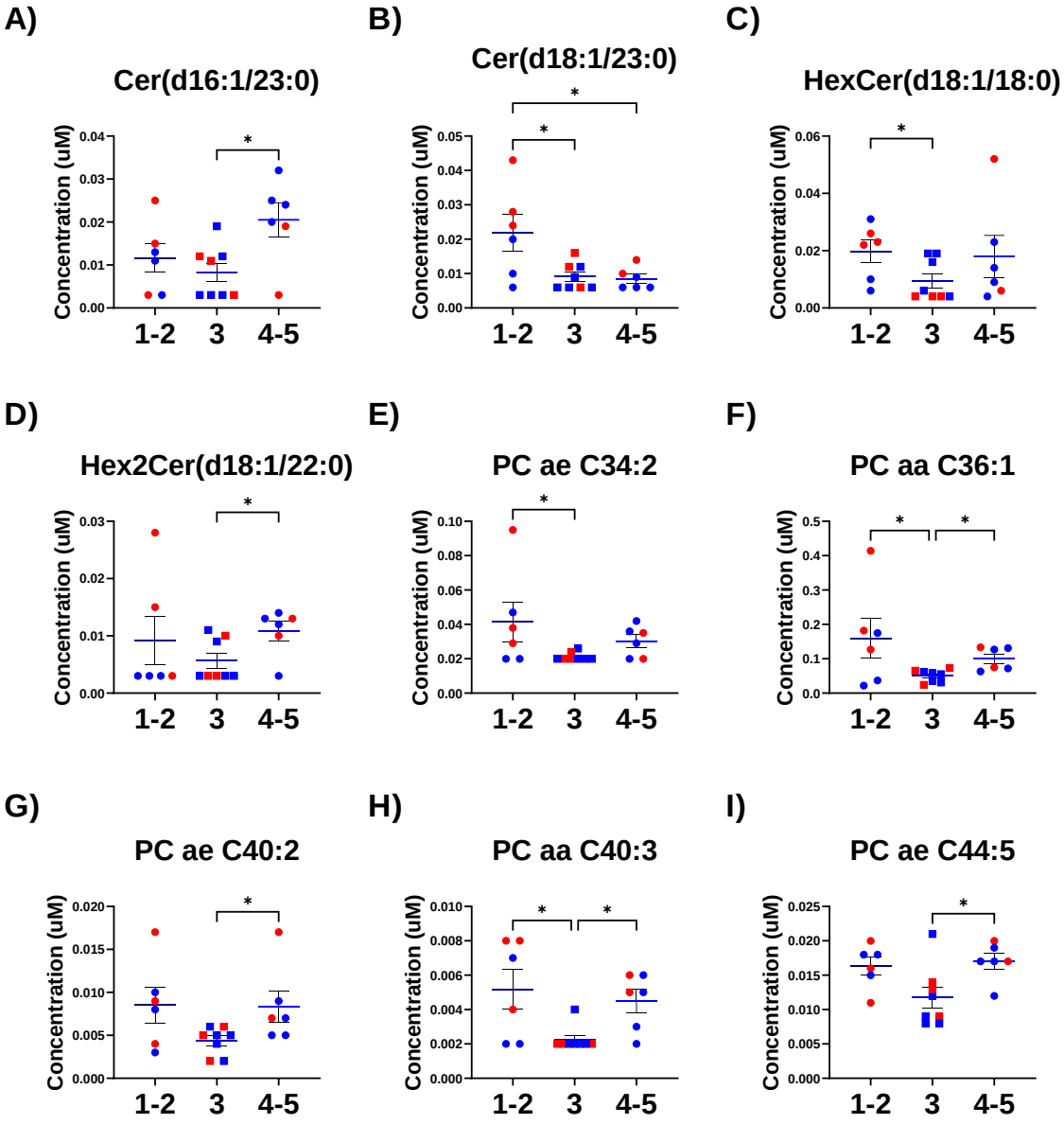


**Figure 2.4.16 The adipose secretome of patients with partial response neo-adjuvant therapies exhibited decreased secreted levels of ceramide and phosphatidylcholine metabolites**

(A-I) Secreted levels of metabolites including Cer(d16:1/23:0), Cer(d18:1/23:0), Hex2Cer(d18:1/22:0), HexCer(d18:1/18:0), PC ae C34:2, PC aa C36:1, PC ae C40:2, PC aa C40:3, and PC ae C44:5 were differentially altered in the adipose explants of OAC patients who with TRG 1-2 (good response), TRG 3, (partial response) and TRG 4-5 (poor response) to chemotherapy regimen FLOT or chemoradiotherapy regimen CROSS (Kruskal–Wallis with Dunn's correction). All data expressed as mean ± SEM, TRG 1–2 n = 6, TRG 3 n = 8, TRG 4–5 n = 6, * $p < 0.05$. Blue symbols identify patients who received neo-adjuvant chemotherapy (FLOT) and red symbols identify patients who received neo-adjuvant chemo-radiotherapy (CROSS).

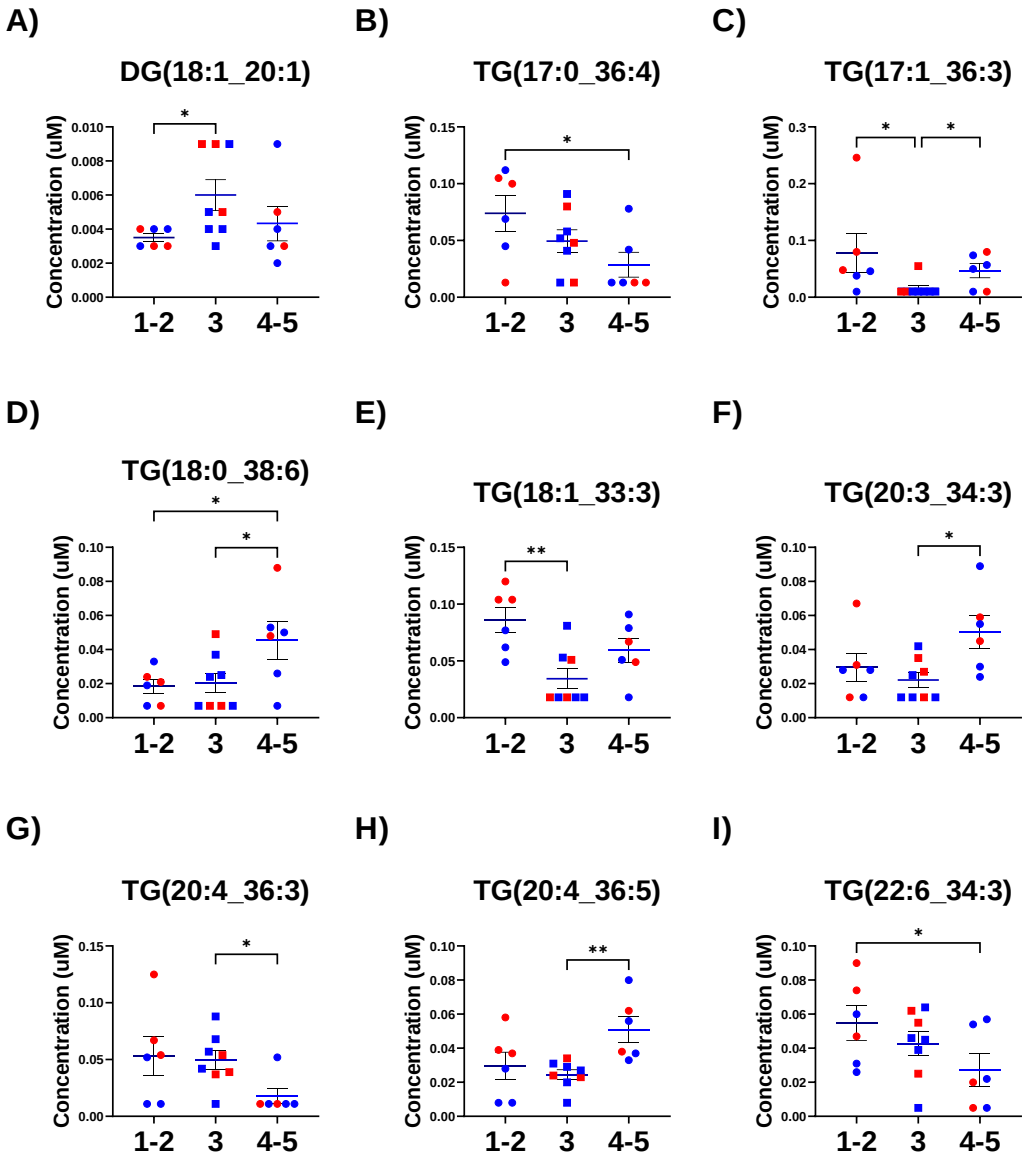


**Figure 2.4.17 The adipose secretome of patients with good and poor response to neo-adjuvant therapies exhibited differential secreted levels of triacylglycerides**

(**A-I**) Secreted levels of triacylglycerides including DG(18:1_20:1), TG(17:0_36:4), TG(17:1_36:3), TG(18:0_38:6), TG(18:1_33:3), TG(20:3_34:3), TG(20:4_36:3), TG(20:4_36:5), and TG(22:6_34:3) were differentially altered in the adipose explants of OAC patients who with TRG 1-2 (good response), TRG 3, (partial response) and TRG 4-5 (poor response) to chemotherapy regimen FLOT or chemoradiotherapy regimen CROSS (Kruskal–Wallis with Dunn's correction). All data expressed as mean ± SEM, TRG 1–2 $n$ = 6, TRG 3 $n$ = 8, TRG 4–5 $n$ = 6, * $p < 0.05$, ** $p < 0.01$. Blue symbols identify patients who received neo-adjuvant chemotherapy (FLOT) and red symbols identify patients who received neo-adjuvant chemo-radiotherapy (CROSS).

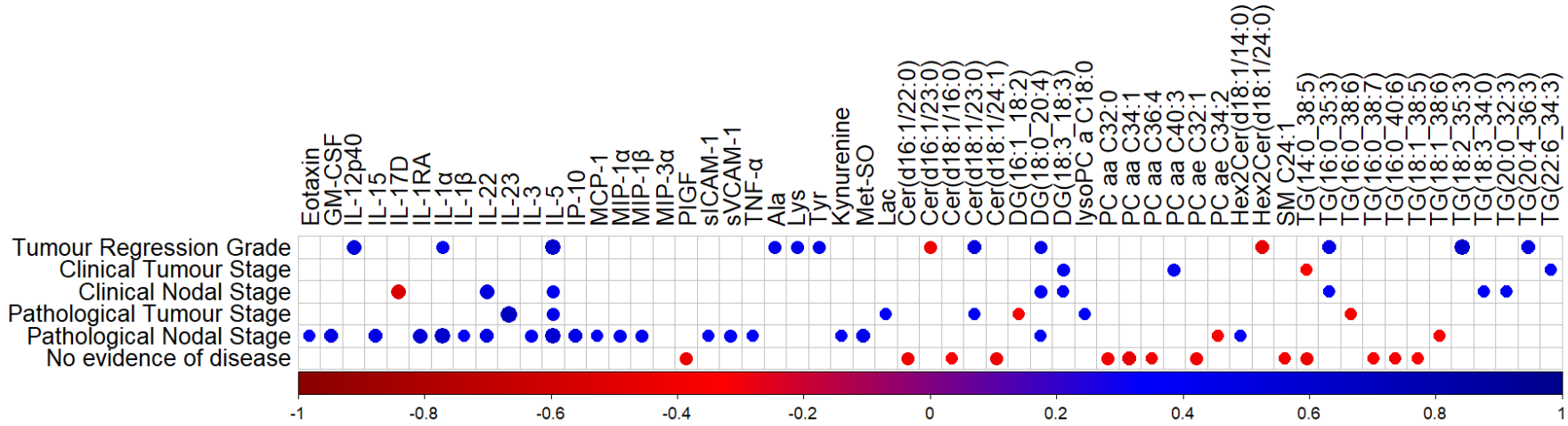


**Figure 2.4.18 Increased secreted levels of pro-inflammatory mediators in the adipose secretome correlated with increased evidence of pathological nodal invasion**

Correlation plot showing only significant correlations ($p < 0.05$) between experimental data and tumour regression grade, clinical tumour stage, clinical nodal stage, pathological tumour stage, pathological nodal stage, and no evidence of disease (Spearman correlation, blue indicates positive correlations and red indicates inverse negative correlations). The Holm–Bonferroni post hoc correction was used to control for multiple comparison testing. All data expressed as mean ± SEM, TRG 1–2 $n = 6$, TRG 3 $n = 8$, TRG 4–5 $n = 6$, circle present $p < 0.05$. Blue symbols identify patients who received neo-adjuvant chemotherapy (FLOT) and red symbols identify patients who received neo-adjuvant chemo-radiotherapy (CROSS).

**Table 2.4.5 Significant correlations associated with Figure 2.4.18 for clinical correlations with tumour regression grade, clinical tumour stage and clinical nodal stage**

| | Tumour Regression Grade | Clinical Tumour Stage | Clinical Nodal Stage |
|---|---|---|---|
| **Factors** | | **R number (p value)** | |
| **IL-12p40** | 0.544 (0.02) | | |
| **IL-17D** | | | -0.548 (0.004) |
| **IL-1α** | 0.435 (0.049) | | |
| **IL-22** | | | 0.521 (0.006) |
| **IL-5** | 0.639 (0.006) | | 0.434 (0.043) |
| **Ala** | 0.417 (0.048) | | |
| **Lys** | 0.436 (0.037) | | |
| **Tyr** | 0.452 (0.03) | | |
| **Cer(d16:1/23:0)** | -0.439 (0.036) | | |
| **Cer(d18:1/23:0)** | 0.516 (0.012) | | |
| **DG(18:0_20:4)** | 0.455 (0.029) | | 0.403 (0.022) |
| **DG(18:3_18:3)** | | 0.411 (0.02) | 0.37 (0.037) |
| **PC aa C40:3** | | 0.424 (0.016) | |
| **Hex2Cer(d18:1/24:0)** | -0.491 (0.017) | | |
| **TG(14:0_38:5)** | | -0.353 (0.047) | |
| **TG(16:0_35:3)** | 0.496 (0.016) | | 0.371 (0.037) |
| **TG(18:2_35:3)** | 0.617 (0.002) | | |
| **TG(18:3_34:0)** | | | 0.37 (0.037) |
| **TG(20:0_32:3)** | | | 0.396 (0.025) |
| **TG(20:4_36:3)** | 0.511 (0.013) | | |
| **TG(22:6_34:3)** | | 0.351 (0.049) | |

**Table 2.4.6 Significant correlations associated with Figure 2.4.18 for clinical correlations with pathological tumour stage, pathological nodal stage, and no evidence of disease.**

| | Pathological Tumour Stage | | Pathological Nodal Stage | | No evidence of disease | |
|---|---|---|---|---|---|---|
| **Factors** | **R number (p value)** | | | | | |
| **Eotaxin** | | | 0.37 | (0.04) | | |
| **GM-CSF** | | | 0.491 | (0.005) | | |
| **IL-15** | | | 0.476 | (0.007) | | |
| **IL-1RA** | | | 0.578 | (0.001) | | |
| **IL-1α** | | | 0.64 | (0.0003) | | |
| **IL-1β** | | | 0.364 | (0.044) | | |
| **IL-22** | | | 0.482 | (0.013) | | |
| **IL-23** | 0.695 | (0.006) | | | | |
| **IL-3** | | | 0.425 | (0.049) | | |
| **IL-5** | 0.449 | (0.036) | 0.605 | (0.003) | | |
| **IP-10** | | | 0.486 | (0.006) | | |
| **MCP-1** | | | 0.384 | (0.033) | | |
| **MIP-1α** | | | 0.423 | (0.025) | | |
| **MIP-1β** | | | 0.42 | (0.019) | | |
| **PIGF** | | | | | -0.447 | (0.012) |
| **sICAM-1** | | | 0.381 | (0.035) | | |
| **sVCAM-1** | | | 0.4 | (0.026) | | |
| **TNF-α** | | | 0.382 | (0.034) | | |
| **Kynurenine** | | | 0.376 | (0.034) | | |
| **Met-SO** | | | 0.46 | (0.008) | | |
| **Lac** | 0.358 | (0.045) | | | | |
| **Cer(d16:1/22:0)** | | | | | -0.409 | (0.02) |
| **Cer(d18:1/16:0)** | | | | | -0.371 | (0.037) |
| **Cer(d18:1/23:0)** | 0.372 | (0.036) | | | | |
| **Cer(d18:1/24:1)** | | | | | -0.436 | (0.013) |
| **DG(16:1_18:2)** | -0.372 | (0.036) | | | | |
| **DG(18:0_20:4)** | | | 0.384 | (0.03) | | |
| **lysoPC a C18:0** | 0.365 | (0.04) | | | | |
| **PC aa C32:0** | | | | | -0.402 | (0.023) |
| **PC aa C34:1** | | | | | -0.467 | (0.007) |
| **PC aa C36:4** | | | | | -0.398 | (0.024) |
| **PC ae C32:1** | | | | | -0.405 | (0.022) |
| **PC ae C34:2** | | | -0.351 | (0.049) | | |
| **Hex2Cer(d18:1/14:0)** | | | 0.362 | (0.042) | | |
| **SM C24:1** | | | | | -0.385 | (0.029) |
| **TG(14:0_38:5)** | | | | | -0.438 | (0.012) |
| **TG(16:0_38:6)** | -0.378 | (0.033) | | | | |
| **TG(16:0_38:7)** | | | | | -0.359 | (0.044) |
| **TG(16:0_40:6)** | | | | | -0.388 | (0.028) |
| **TG(18:1_38:5)** | | | | | -0.354 | (0.047) |
| **TG(18:1_38:6)** | | | -0.368 | (0.038) | | |

## 2.5 Summary of main findings

- Visceral adipose explants from obese OAC patients had significantly elevated oxidative phosphorylation metabolism profiles and an increase in Eotaxin-3, IL-17A, IL-17D, IL-3, MCP-1, and MDC and altered secretions of glutamine associated metabolites compared to visceral fat from non-obese patients.

- Adipose explants from patients with metabolic dysfunction correlated with increased oxidative phosphorylation metabolism, and increases in IL-5, IL-7, SAA, VEGF-C, triacylglycerides, and metabolites compared with metabolically healthy patients.

- Adipose explants generated from patients who had previously received neo-adjuvant chemotherapy showed elevated secretions of pro-inflammatory mediators, IL-12p40, IL-1α, IL-22, and TNF-β and a decreased expression of triacylglycerides. Furthermore, decreased secreted levels of triacylglycerides were also observed in the adipose secretome of patients who received the chemotherapy-only regimen FLOT compared with patients who received no neo-adjuvant treatment or chemo-radiotherapy regimen CROSS.

- For those patients who showed the poorest response to currently available treatments, their adipose tissue was associated with higher glycolytic metabolism compared to patients who had good treatment responses.

## 2.6 Discussion

This study for the first time has conducted a detailed assessment of adipose tissue metabolism, as well as adipose secreted pro-inflammatory, metabolite and lipid profiles and determined whether these profiles correlate with significant clinical parameters in OAC patients including obesity, metabolic dysfunction, previous treatment exposure and tumour regression grades. Recent literature has identified an elevated reliance of certain subtypes of cancers on oxidative phosphorylation rather than glycolysis [320]. Previous research from our group has shown an increased reliance on oxidative phosphorylation correlating with enhanced radioresistance in oesophageal cancer cells [53]. In this study, elevated OCR and ECAR metabolic profiles have been observed in adipose explants from obese OAC patients compared with their non-obese counterparts, indicating higher metabolic rates with increasing visceral adiposity. Previous work conducted in mouse models, has shown that diminished oxidative phosphorylation function ameliorated obesity in mice on high-fat diets disrupting weight gain and improving glucose tolerance [321]. This study further shows that elevated OCR and OCR/ECAR ratio profiles were observed in patients classified with metabolic dysfunction compared with metabolically healthy patients. Previously, increased mitochondrial respiration was observed in adipocytes of metabolically unhealthy patients compared with metabolically healthy patients [315]. This shift towards utilisation of oxidative phosphorylation pathways within adipose tissue of obese and metabolically unhealthy individuals may provide insight into aberrant mitochondrial functioning that promotes pro-tumorigenic signalling. In addition to this, an elevated utilisation of oxidative phosphorylation pathways was also observed in adipose tissue from our patients who received FLOT chemotherapy treatment compared with treatment naïve patients Previous research has shown that treatment with 5-FU and oxaliplatin upregulated genes associated with oxidative phosphorylation in mouse models [322]. This may be further augmented by elevated oxidative phosphorylation in adipose tissue sequestering chemotherapy within adipose tissue [99], which may hinder chemotherapy efficacy. Additionally, increased reliance on glycolysis was observed in adipose explants of our patients with increasing TRGs (poor response), Research has previously indicated that cancer cells co-cultured with adipose stromal cells upregulate glycolysis and mediated chemoresistance, which may indicate why elevated ECAR is observed only in adipose explants of patients who had the poorest response to chemotherapy [163].

The secretome of adipose tissue comprises many pro-tumorigenic cytokines that are primed to aid cancer cell growth and survival [231]. Pro-inflammatory cytokines and metabolism are interlinked and essential in regulating adipocyte function and lipid metabolism particularly in metabolic diseases [323]. Eotaxin-3, an adipose associated cytokine was observed as being elevated with obesity in this study. Eotaxin-3 has been correlated with increased BMI [324] and

as being highly expressed in circulation of OAC patients with longer survival rates [232]. However, Eotaxin-3 had also been reported to be highly expressed in tumour tissue in aggressive disease [325] and is linked with increased macrophage infiltration [325]. Coupling this knowledge with the observed increased secretion of MDC and MCP-1 in this study, both macrophage associated cytokines [326,327], the adipose secretome of obese individuals could aid the recruitment of macrophages and other immune cells to the adipose tissue leading to a diminished immune response in the local tumour microenvironment. The secretion of IL-17 A and IL-17 D were also increased in the adipose secretome of obese patients. Studies have linked elevated IL-17 in adipose tissue to increases in infiltrating immune cells [328,329] and poor prognosis [330] and disruption of this pathway diminishes metastasis and enhances treatment response [331–333]. This cytokine may be a potential target for future investigation particularly in the obese tumour microenvironment. This study has also shown a decreased secretion of VEGF-D in the adipose secretome of obese OAC patients. Previous work has seen that while VEGF-A, VEGF-B and VEGF-C showed increased circulating levels in obese individuals, levels of VEGF-D were significantly diminished [334]. VEGF-D in particular has been linked with metastatic disease and this diminished secretion may be amelioratory [335].

Increased expression of IL-5 in the adipose secretome of patients with metabolic dysfunction was identified. Previous studies in mouse models with suppressed IL-5/CD300f expression have showed decreased diet induced weight gain and insulin resistance [336]. IL-5 facilitates lung metastasis [337], and targeting of the IL-5 axis could ameliorate some symptoms associated with metabolic dysfunction. Previous findings have identified elevated circulating SAA in patients with metabolic syndrome, as was observed in the adipose secretome of metabolically unhealthy patients in this cohort [338]. SAA is connected with the inflammatory processes, which plays pivotal roles in both obesity, metabolic syndrome [339]. Elevated levels of IL-7 were observed in this study in the adipose secretome of metabolically unhealthy patients and in patients who received FLOT chemotherapy compared with CROSS chemo-radiotherapy. Previous work has shown that IL-7 overexpression in mouse models is associated with glucose and insulin resistance [340]. However elevated IL-7 could prove beneficial in the context of FLOT chemotherapy as IL-7 can aid in T cell growth [341]. Recent studies have indicated that IL-7 could potentially re-sensitize tumours to cisplatin [342]. As previously mentioned, obese individuals have elevated circulating levels of VEGF-C and overexpression of VEGF-C in mouse models has been linked to increased weight gain and insulin resistance [334,343], consequently this elevated secretion in the adipose secretome could potentiate metabolic disorder and prime the local tumour microenvironment for cancer cell survival. Elevated VEGF-C has also been linked to

chemoresistance [344] and the increased secretion of VEGF-C observed within the adipose secretome of FLOT chemotherapy treated patients compared to CROSS treated patients may indicate a more systemic effect as this VEGF-C enriched adipose secretome could potentiate VEGF-C mediated metastasis [345].

Increased secretion of IL-22 and TNF-β was observed in the adipose secretome of patients who received FLOT chemotherapy compared with patients who received no neo-adjuvant therapy. IL-22, whilst possessing both pro- and anti-inflammatory effects, has been shown to promote cancer cell growth and enhance chemoresistance [346], allowing infiltration of M2-like macrophages in adipose tissue, helping to drive a systemic anti-tumour effect [347]. TNF-β promotes proliferation and invasion in cancer cell models [348], however the influence of chemotherapies on the functional role of TNF-β in adipose tissue is unknown. This study reports elevated levels of pro-inflammatory cytokines IL-12p40 and IL-1α in the adipose secretome of patients who received FLOT chemotherapy compared with treatment naïve patients. Expression of IL-1 α in tumour tissue of gastric cancers has been shown to correlate with a more aggressive disease state and metastasis [349], however these cytokines can also act in immune cell recruitment [350].

Recent research has supported the utility of the metabolome in many diseases [351]. This study observed altered secretions of key metabolites involved in the glutamate/GABA-glutamine cycle. Increased secretion of GABA and glutamic acid (ionic form glutamate) and decreased secretion of glutamine was observed in the adipose secretome of obese patients compared with their non-obese counterparts. Previous research has also observed decreased glutamine and increased glutamate in circulation in obese individuals [352,353]. Glutamine is effective in polarisation of anti-inflammatory M2 like macrophages which may act as a potential therapeutic target to resolve the low-grade inflammation associated with obesity [353]. Aspartic acid was also decreased in the adipose secretome of obese patients compared with non-obese patients, which emulates previous research where decreased N-acetylaspartate was observed in patients with higher BMIs [354]. A combination of aspartic acid and glutaric acid may be capable of inducing tumour cell death [355]. Interestingly, both of these amino acids were decreased in the obese setting in our study. Elevated secreted levels of triacylglycerides TG(16:0_35:3), TG(18:2_38:4) and TG(22:5_34:3) were also detected in adipose tissue from obese OAC patients compared with non-obese. Accumulation of triacylglycerides has previously been reported in obese adipose tissue [356] and in cancers [357,358]. Elevated levels of asymmetric dimethylarginine, homocysteine and hypoxanthine have been reported in individuals with metabolic syndrome [359–361]. This study also identified increased secretion of these amino acids in the adipose tissue

of OAC patients that have metabolic dysfunction compared with metabolically healthy patients. Previous research has identified increased circulating levels of both homocysteine and hypoxanthine in cancer patients, however, the role they play in tumorigeneses or cancer cell survival is not fully understood [362,363]. However, reports of elevated asymmetric dimethylarginine in cancer have suggested it may attenuate apoptosis in response to stress and chemotherapy [364]. This study has also identified elevated levels of glycine and taurine in the adipose secretome of metabolically unhealthy versus metabolically healthy OAC patients. Elevated circulating levels of these amino acids should ameliorate the pro-inflammatory effects of metabolic syndrome and attenuate cancer cell proliferation as well as enhancing the efficacy of chemotherapy [365,366]. One of the classification criteria for metabolic syndrome is elevated triglycerides [367] and within this study increased expression of a series of triglycerides including TG(16:0_35:3), TG(18:0_34:3), TG(18:1_33:3), TG(18:2_38:4), TG(20:2_36:5), TG(20:4_33:2), TG(20:4_34:0) and TG(20:4_36:5) were detected in the adipose secretome of OAC patients with metabolic dysfunction. Previous research has indicated that elevated serum triglycerides in individuals with metabolic syndrome was associated with significant risk of certain cancers [368], however further research is required to fully assess the significance of this finding.

Furthermore *p*-Cresyl sulfate was decreased in the adipose secretome of patients who received CROSS regimen compared with patients who received no neo-adjuvant therapy. Recent studies have linked *p*-Cresyl sulfate to potentiating the malignancy of cancers by aiding in cancer cell migration and epithelial-mesenchymal transition [369,370] and this diminished secretion in the adipose secretome of CROSS treated patients could possess beneficial effects. In this study DCA was observed to be increased in the adipose secretome of CROSS regimen treated patients compared with FLOT treated patients whilst GUDCA (glycoursodeoxycholic acid) was observed to be decreased. DCA (dichloroacetate) has previously been reported to decrease cell proliferation and migration in mouse models [371]. A series of triglycerides were also identified to be decreased in the adipose secretome of FLOT regimen receiving patients compared with treatment naïve patients. Only TG(20:2_34:4) was found to be decreased in the adipose secretome of patients receiving CROSS compared with treatment naïve and FLOT receiving patients. In particular, the metabolite TG(18:0_36:3) was decreased in the adipose secretome of patients receiving FLOT regimen compared with both patients' treatment naïve and patients receiving CROSS regimen, whilst metabolite TG(20:2_34:4) was decreased in the adipose secretome of patients receiving CROSS regimen compared with both treatment naïve patients and patients receiving FLOT regimen. Previous research has identified an increase in circulating triglycerides during neo-adjuvant chemotherapy which gradually decrease to normal levels [372].

Decreased secretion of triglycerides in the adipose secretome of patients only receiving chemotherapy raises the question, whether this decreased expression correlates with increased circulating levels and potentially can this be utilised to enhance current therapies. Diminished levels of ceramides, glycosylceramides and sphingomyelins were also observed in the adipose secretome of treated patients compared with treatment naïve patients. Ceramide metabolism has previously been reported to induce cancer cell death through induction of cellular stress [373] and the diminished presence of ceramide and associated molecules following cancer treatment exposure could prove interesting as a therapeutic target.

Metabolite Cer(d18:1/23:0) was observed to be decreased in the adipose secretome of patients with a TRG 3 and TRG 4-5 compared with patients who had a TRG 1-2. Diminished levels of ceramides could prevent ceramide metabolism, which induces cancer cell death through induction of cellular stress [373]. The diminished presence of ceramide in the adipose secretome of patients with more aggressive cancers could indicate that anti-cancer ceramide analogs may aid poor responding tumours [374]. Decreased expression was observed in TG(18:0_38:6) in the secretome of adipose explants derived from patients with a TRG of 1-2 and a TRG of 3 compared with patients who had a TRG 4-5. Higher levels of TG(18:0_38:6) were observed in the adipose secretome of patients with a TRG 4-5 compared with a TRG 1-2, in addition to increased expression of TG(17:1_36:3), TG(18:0_38:6), TG(20:3_34:3), TG(20:4_36:5) in TRG 4-5 patients compared with TRG 1-2. Higher expression of triglycerides has been linked with more aggressive cancers as well as decreased disease free survival and overall survival [375]. Metabolites including PC aa C36:1, PC aa C40:3 had increased expression in in the adipose secretome of patients with TRGs of 1-2 and 4-5 compared with patients with a TRG 3. Phosphatidylcholine metabolism has previously been linked to both cellular proliferation and cell death [376]. The decreased expression found in this study in the adipose secretome of patients with a TRG of 3 compared with patients with more regressive TRG 1-2 and more aggressive cancers with TRG scoring of 4-5 pose an interesting question on whether the adipose secretome and phosphatidylcholine metabolism may attenuate or potentiate cancer cells response to current treatment modalities.

Throughout this study a series of significant correlations were observed between clinical factors and experimental data. It is of interest that elevated levels of OCR and ECAR in adipose tissue correlate with increasing viscerally obesity in OAC patients but negatively correlate with BMI and weight, as it is well-documented that viscerally obesity is a significant risk factor for the development of OAC [377], and the use of BMI and weight have in more recent times been deemed a substandard measurement of obesity [378]. The metabolic role adipose tissue plays in cancer development and whether it aids tumour progression and treatment resistance requires

further study to fully understand whether this relationship can be altered and utilised for therapeutic benefit. Furthermore this study reports a negative correlation between increasing weight and BMI and decreased secretion of a series of powerful pro-inflammatory cytokines including IL-15, IL-17, IL-21, IL-22, IL-23, IL-3 and IL-5 [379–384] which would not be expected in the context of obesity, which is known to be a setting of chronic low-grade inflammation, however this effect is not observed when obesity is classified by visceral fat area. However, a series of triglycerides were observed as positively correlating with increased weight and visceral fat area in this patient cohort as previously mentioned increased triglycerides have been observed both in the setting of obesity and cancer but the influence they play in adipose tissue or what aid they may provide tumorigenesis in the obese tumour microenvironment is an unresearched field. Previous studies have linked triglycerides to key roles in cellular processes in immune cell and dysregulated triglycerides expression may have deleterious effects on immune cell function [385,386], but within the context of cancer these correlations require more study to identify if they can be a beneficial therapeutic target.

Additionally, elevated Clavien-Dindo grade, a classification of post operative complications was positively correlated with a series of adipose secreted cytokines associated with pro-inflammatory response and angiogenesis including IL-6, IL-16, FLt-1, PlGF, VEGF-A and VEGF-D. It has been previously reported that increased expression of circulating IL-6 following major abdominal surgery was associated with increased risk of complications [387]. Furthermore, previously elevated circulating levels of VEGF have been reported following major abdominal surgery [388] and associated with poor cancer specific survival [389]. The elevation of these cytokines in the adipose secretome could potentiate post-op complications in these patients and may act as a future therapeutic target to ameliorate the locally based and circulating effects of these cytokines. Within this study positive correlations were observed between increasing secretion of IL-3, IL-5, and lactic acid in the adipose secretome, and patients with increasing nodal invasion. Previous research has indicated that tumour associated leukocytes from patients with metastatic lymph nodes secreted higher levels of IL-3 and IL-5 [390]. Additionally, elevated levels of circulating lactate were previously identified in OAC patients whose tumour had metastasised to the lymph nodes compared with patients with no lymph node metastasis [391]. The potential of the adipose secretome to augment these analytes in circulation and whether this plays a pivotal role in aiding tumour metastasis to the lymph node requires further investigation to see if this associations could be utilised for therapeutic benefit. Furthermore, within this study decreased levels of PlGF and lactic acid in the adipose secretome were correlated with patients who showed no evidence of disease following treatment and resection.

As previously mentioned elevated lactate levels have been associated with nodal metastasis [391], it has also been reported to be generated by cancer cells and holds critical roles in cancer cell proliferation, promoting angiogenesis and acting as a key immunosuppressive analyte [392]. This decreased expression of lactate in the adipose secretome in patients whose tumours have regressed is of interest, as it raises questions on how adipose tissue plays a role in sequestering or releasing lactate and whether this could potentiate the tumour microenvironment to aid nodal invasion or recede to support cancer regression. Additionally decreasing levels of PlGF was observed in the adipose secretome of patients whose cancers had regressed. PlGF has been reported to promote tumour desmoplasia in pancreatic mouse models with PlGF blockade enhancing the efficacy of chemotherapy [393]. It is unknown if PlGF reduction could enhance tumour regression.

Adipose tissue is a regulatory organ with many downstream effects which are still not understood. This study has endeavoured to evaluate the metabolic profile of adipose tissue explants and its secreted factors as well as investigating how clinical factors associated with OAC patients correlate with these findings. Within this study, increases in OCR, pro-inflammatory cytokines and metabolites associated with aiding tumorigenesis have been identified in the most viscerally obese of OAC patients and in patients with metabolic syndrome. This now draws the question on whether abrogated signalling within adipose tissue aids priming the tumour milieu and whether targeting particularly this pro-inflammatory obese tumour microenvironment could aid current cancer treatments, which so far have proved disappointedly ineffective in OAC. Furthermore, elevated levels of OCR, anti-inflammatory cytokines and lactic acid have also been identified to corelate in the adipose tissue and secretome of patients who have received neo-adjuvant therapy and with patients whose tumours show poorer regression following these treatments. Whether the adipose secretome can be modulated to aid in the efficacy of these therapies in patients who show poor responses, is a field of research that could hold immense therapeutic benefit. Adipose tissue is fast being recognised as a significant factor that potentiates cancer initiation, progression, and metastasis, diminishes treatment efficacy, and has deleterious effects on immune cell function, with these effects only augmented in the obese cancer setting. With obesity levels steadily increasing, understanding of the complex nature of adipose tissue and whether its effects can be harnessed for therapeutic gain is research field that critically requires development.

*Chapter 3*

# *Palmitic acid alters metabolism in adipose tissue from oesophageal adenocarcinoma patients and augments an immunosuppressive adipose secretome in both cancer and non-cancer patients.*

## 3.1 Objective and specific aims:

**Objective:**

The overall objective of this chapter was to assess the influence of exogenous fatty acids on immuno-metabolic profiles of adipose explant derived from both non-cancer patients and oesophageal cancer patients using real-time metabolic profiles and multiplex ELISA. As well as determining whether these altered immuno-metabolic profiles were associated with increased visceral adiposity in cancer patients. This chapter further looks to assess how these alterations in these treated adipose secretome effect immune cell function.

**Specific Aims**

- To assess metabolic profiles including oxidative phosphorylation and glycolysis of adipose explants derived from non-cancer and cancer patients in real time following culture with dietary fats Oleic Acid and Palmitic acid (PA).
- To assess the secreted profiles of these adipose explants for mediators of inflammation, metabolism, angiogenesis, and immune response and whether they are influenced by OA and PA.
- To determine whether obesity differentially effects the metabolic and secreted profiles of adipose explants derived from cancer patients in response to OA and PA treatment.
- To evaluate whether the adipose secretome of non-cancer and cancer patients treated with OA and PA influence dendritic cell (DC) expression of maturation markers, and whether this is altered by obesity in the cancer setting.
- To evaluate whether the adipose secretome of non-cancer and cancer patients treated with OA and PA influence macrophage (Mϕ) polarisation towards a pro-inflammatory (M1-like) or anti-inflammatory (M2-like) phenotype, and whether this is altered by obesity in the cancer setting.

## 3.2 Introduction

Adipose tissue is a regulatory organ with many downstream effects [397], many of which are not fully understood. However, it has been widely reported that adipose tissue becomes dysregulated with obesity leading to a chronic low-grade inflammatory state [398], primed to support cancer development and progression [399]. Oesophageal adenocarcinoma (OAC) is a poor prognosis cancer and one of the most closely associated cancers with obesity [311], making it an exemplar model to study the effects of cancer progression on visceral adipose tissue.

Previously we have reported that obesity and metabolic dysfunction in OAC patients have differential effects on adipose tissue metabolism and secreted factors including pro-inflammatory mediators and triacylglycerides [80]. Both obesity and metabolic dysfunction have been linked to increased circulating levels of free fatty acids, which propagate inflammation [399]. Fatty acids are an essential biomolecule component known to fuel metabolic processes and are a vital structural component of biological membranes [400]. They have also been linked to regulating intracellular signalling pathways transcription factor activity and gene expression [62]. Dietary fats are commonly categorised into three subsets, saturated, monounsaturated, and polyunsaturated. Saturated fatty acids are molecules that are linked with single carbon bonds, monounsaturated fatty acids possess one double carbon bond in their structure with the rest being single carbon bonds, and poly-unsaturated fatty acids contain more than one double carbon bond in their structure [401].

Saturated fatty acids such as palmitic acid have been linked with pro-inflammatory response [65] whilst unsaturated fatty acids including oleic acid have been reported to act in anti-inflammatory manner [66] as well as ameliorating the pro-inflammatory effect of saturated fatty acids [67]. Further to this fatty acid levels in circulation and within adipose tissue have also been reported to be abrogated by obesity. One of the most common saturated fatty acids found in the human body is PA, which has been observed to be increased in circulation in obese patients [68], however its expression at tissue level is tightly regulated. In contrast OA one of the most commonly found monounsaturated fatty acid in the human body has previously been reported to be increased in adipose tissue of obese mouse models [69]. This increase was paired with a corresponding increase in Δ 9 desaturated lipids [69], Stearoyl-CoA desaturase (SCD1) is responsible for catalysing the synthesis of monounsaturated fatty acids supported by ELOLV6, with OA being its main product [70,71].

Adipose tissue has been reported to recruit immune cells whilst having deleterious effects on their function which can potentiate anti-tumour immunity [81–85]. Previous research has indicated

that a series of pro-inflammatory mediators in circulation and expressed at the tissue level have been linked to clinical outcomes, particularly factors that are involved in the recruitment and activation of innate immune cells [232]. Key inflammatory mediators including Eotaxin-3, IL-10, IL-13, MIP-1α, and MIP-1β are involved in the recruitment, activation and inhibition of immune cells are perturbed by obesity [233–235]. Many of these factors directly affect the antigen presenting abilities and polarisation of cells like Dendritic Cells (DCs) and Macrophages (Mϕ) [236].

Increased free fatty acids, which have been reported in obesity, have been shown to enhance Mϕ polarisation towards M1-like phenotype [283]. In particular, Palmitic Acid (PA) has been reported to elevate pro-inflammatory response signals [65,284]. In contrast, Oleic Acid (OA) has been identified to have anti-inflammatory effects through inhibiting pro-inflammatory responses driven by other fatty acids [67] as well as promoting M2-like polarisation in macrophages [285]. Further to this, free fatty acids have also been shown to lead to lipid -loaden DCs with diminished antigen presenting capabilities and reduced capacity to effectively stimulate T cells [282].

This study for the first time examined if adipose tissue from non-cancer and OAC patients have differential metabolic and secreted inflammatory profiles and the effects of exogenous fatty acids including PA and OA on this adipose tissue microenvironment. Within the cancer cohort, we also assessed whether obesity as defined by visceral adiposity influences the metabolic and secreted profiles of adipose tissue following fatty acid treatment. Furthermore, this study assessed how this adipose secretome affected dendritic cells (DCs) maturation and macrophage (Mϕ) polarisation, and whether this was influenced by obesity in the cancer setting.

## 3.3 Materials and Methods

### 3.3.1 *Ethics Statement and Patient Recruitment*

Ethical approval was granted by the St James's Hospital/AMNCH ethical review board (Ethics number: REC_2019-07 List 25(27)) and written informed consent was collected from all patients in this study. 12 cancer patients and 6 non-cancer patients were recruited within the period between 3rd of April 2021 and 14th of January 2023. Patient demographics are listed in Table 3.3.1. Fresh adipose tissues were taken from all patients at the start of the surgical procedure. All OAC patients were being treated with curative intent and non-cancer patients were undergoing surgery for benign conditions. For the cancer cohort, obesity was defined via visceral fat area (VFA) measurements with cut-off value for VFA of 163.8 $cm^2$ in males and 80.1 $cm^2$ for females as previously categorised[318]. Here adipose tissue was collected form 6 obese and 6 non-obese patients.

**Table 3.3.1 Clinical demographics associated with OAC patients**

| **Patient Clinical Parameters** | |
|---|---|
| **Diagnosis** | OAC = 6<br>OGJ = 6 |
| **Sex** | Male = 8<br>Female = 4 |
| **Obesity Status via Visceral Fat Area** | Obese = 6<br>Non-obese = 6 |
| **Age at diagnosis** | 55-81 (Mean = 68.5) |
| **Post-treatment BMI** | 22.34-34.29 (Mean = 27.56) |
| **Weight** | 58.4–113 kg (Mean = 77.85) |
| **Mean VFA** | 71.86–303 (Mean = 138.1) |
| **Treatment** | Naïve *n* = 5<br>FLOT *n* = 5<br>CROSS *n* = 2 |
| **Tumour Regression Grading (TRG)** | TRG 1 *n* = 3 (CROSS *n* = 2, FLOT *n* = 1)<br>TRG 2 *n* = 3 (CROSS *n* = 1, FLOT *n* = 2)<br>TRG 3 *n* = 8 (CROSS *n* = 3, FLOT *n* = 5)<br>TRG 4 *n* = 3 (CROSS *n* = 2, FLOT *n* = 1)<br>TRG 5 *n* = 3 (CROSS *n* = 0, FLOT *n* = 3) |
| **Clinical Stage (T)** | T1 *n* = 5<br>T2 *n* = 0<br>T3 *n* = 7 |
| **Clinical Stage (N)** | N0 *n* = 7<br>N1 *n* = 1<br>N2 *n* = 4 |
| **Path stage (T)** | T0 *n* = 1<br>T1 *n* = 5<br>T2 *n* = 0<br>T3 *n* = 6<br>T4 *n* = 0 |
| **Path Stage (N)** | N0 *n* = 5<br>N1 *n* = 2<br>N2 *n* = 3<br>N3 *n* = 2 |

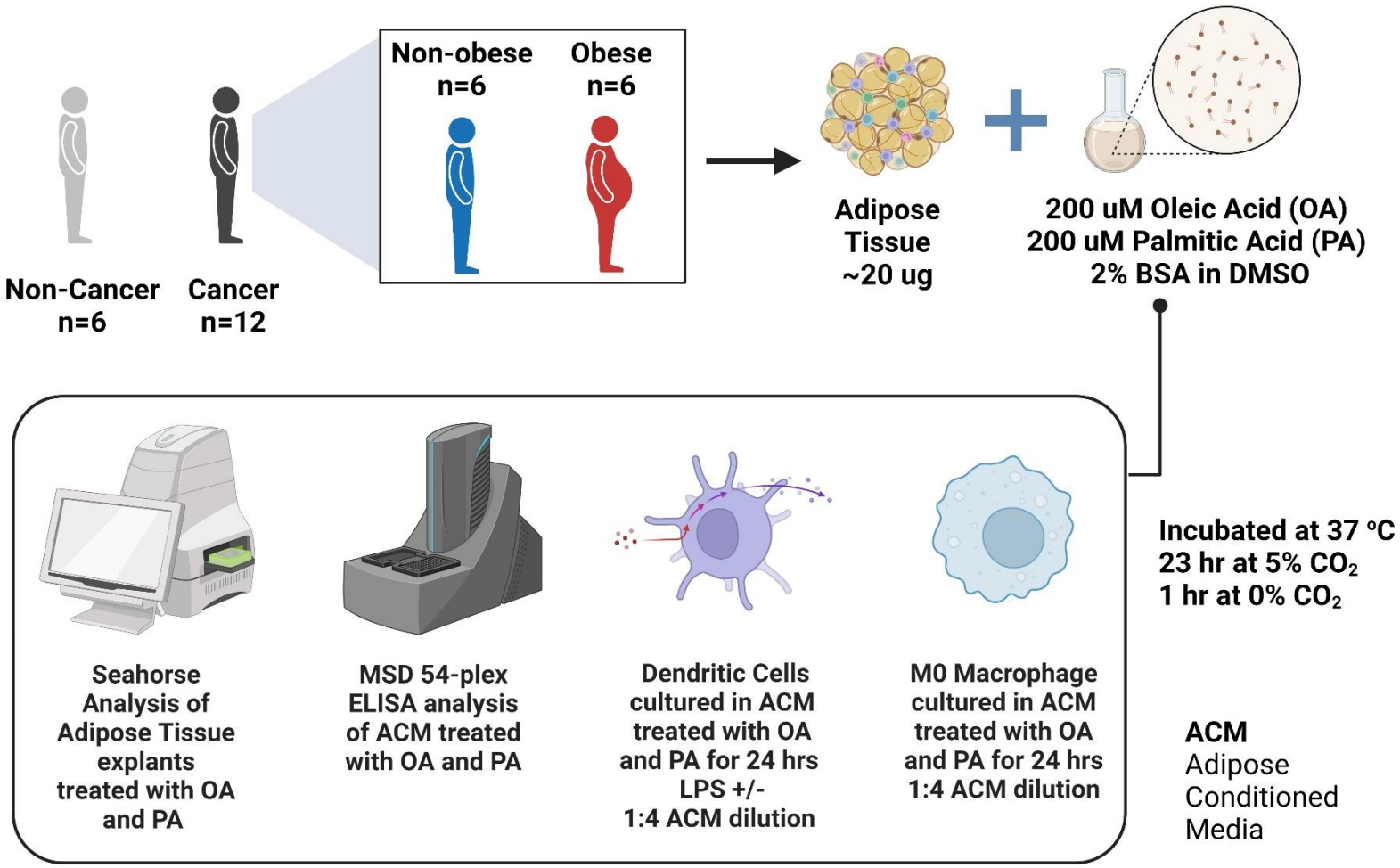


**Figure 3.3.1 Schematic of experimental methodology workflow associated with Chapter 3**

Real time metabolic and secreted profiles of adipose explants from non-cancer patients and OAC or OGJ cancer patients were assessed by Agilent seahorse, MSD multiplex ELISA following exogenous fatty acid treatment with OA And PA. The influence of these treated adipose secretome on dendritic cell maturation and macrophage polarisation were then assessed via flow cytometry.

### 3.3.2 *Lipid Treatment*

For stock solutions OA and PA (Sigma Aldrich, California, USA) were dissolved in DMSO (Sigma Aldrich, California, USA) at a concentration of 2M and heated at 60 $^{o}$C for 15 minutes to ensure solution is fully dissolved. 10 µl of this stock solution or equivalent DMSO for control was then conjugated with 2% fatty acid and endotoxin free BSA dissolved in 1 ml of M199 (Gibco, Thermofisher, Massachusetts, USA). This solution was heated again at 40 $^{o}$C for 30 minutes to ensure fatty acids were fully dissolved to give a working stock solution of 20mM, which was aliquoted and stored at -20 $^{o}$C for further use.

### 3.3.3 *Seahorse Analysis of metabolic profiles from adipose tissue explants and generation of Adipose Conditioned Media (ACM)*

Fresh omental tissue was collected from theatre and processed within 30 minutes by dissecting into pieces weighing approximately 20 µg. Tissue was plated in triplicates in 1 ml of M199 (supplemented with 0.1% gentamicin (Lonza, Switzerland), in a 24 well plate (Sarstedt, Germany). Adipose explants were then treated with 0.01% DMSO 2% BSA control or 200 µM OA or PA in 0.01% DMSO 2% BSA in M199. Adipose explants were cultured for 24 hours at 37ºC at 5% Carbon Dioxide in a humidified incubator (Thermofisher, Massachusetts, USA). In the last hour of culture, adipose tissue and ACM was transferred to islet capture microplate with capture screens (Agilent Technologies, California, USA) and incubated in a non-CO2 incubator at 37$^{o}$C (Whitley, United Kingdom) prior to analysis. Seahorse Xfe24 analyser was used to assess metabolic profiles in adipose explants, (Agilent Technologies, California, USA) following a 12 minute equilibrate step, three basal measurements of OCR and ECAR were taken over 24 minutes consisting of three repeats of the following sequence “mix (3 min) / wait (2 min) / measurement (3 min)” to establish basal respiration. Adipose Conditioned Media (ACM) was extracted in a sterile environment and tissue weighed using a benchtop analytical balance (Radwag, Poland) and snap frozen. All samples were then stored at -80$^{o}$C for further processing.

### 3.3.4 *Multiplex ELISA*

Methodology carried out as per section *2.3.4 Multiplex ELISA*

### 3.3.5 *Isolation of monocytes*

Peripheral blood mononuclear cells (PBMCs) obtained from buffy coats (National Blood Centre, St. James’s Hospital, Dublin, Ireland). Buffy coats were supplemented with 0.5 mM EDTA and diluted 1:4 with PBS and separated by density gradient centrifugation (Lymphoprep, Thermo

Fischer Scientific, Massachusetts, USA) at 400xg for 20 minutes with the brake off. Monocytes were then isolated via column separation by positive selection using anti-CD14 magnetic microbeads as per manufacturers protocol (Miltenyi, Germany).

### 3.3.6 *Dendritic Cell Culture and Stimulation*

Human monocyte-derived immature DC (moDC) were seeded at a density of $1\times10^6$ cells/mL in 6-well plates in 3 mL of RPMI-1640 medium containing 10% defined low-endotoxin HyClone FBS (Thermo Fischer Scientific, Massachusetts, USA), 1% penicillin-streptomycin (Lonza, Switzerland), 1% Fungizone (Sigma Aldrich, California, USA) , human granulocyte macrophage colony-stimulating factor (50 ng/mL) (Immunotools, Germany) and human IL-4 (70 ng/mL) (Immunotools, Germany). moDC were incubated in a humidified atmosphere with 5% CO2 at 37°C. Cells were fed at day 3 with a half medium change supplemented with fresh cytokines. At day 6, moDCs were assessed for immaturity, with CD11c+ cells exhibiting an immature DC phenotype capable of upregulating maturation markers activation. Freshly generated moDCs were plated in 96-well plates at $2 \times 10^5$ cells in 150 µl RPMI 1640 media supplemented with 10% defined low-endotoxin HyClone FBS (Fisher Scientific, Massachusetts, USA) and stimulated with treated ACM, or matched background media controls, for 6 hours before exposure to 10 µg/mL of ultrapure TLR4 agonist Escherichia coli lipopolysaccharide (LPS-EB; Invivogen, California, USA) overnight for the LPS positive cohort, the LPS negative cohort was not treated with LPS. Supernatants were harvested and stored at -80$^{o}$C for further processing, and cells were assessed for expression of surface markers as described below.

### 3.3.7 *Macrophage Culture and Stimulation*

Human monocyte-derived immature Macrophages (moMϕ) were seeded at a density of $1\times10^6$ cells/mL in 6-well plates in 3 mL of RPMI-1640 medium containing 10% FBS (Thermo Fischer Scientific, Massachusetts, USA), 1% penicillin-streptomycin (Lonza, Switzerland), human macrophage colony-stimulating factor (50 ng/mL) (Immunotools, Germany). moMϕ were incubated in a humidified atmosphere with 5% CO2 at 37°C. Cells were fed at day 3 with a half medium change supplemented with fresh cytokines. At day 6, moMϕ were assessed for immaturity, with CD68+ cells exhibiting an immature Mϕ phenotype capable of upregulating markers of polarisation following stimulation. Freshly generated moMϕ were plated in 96-well plates at $2 \times 10^5$ cells in 150 µl and stimulated with treated ACM, or matched background media controls, for 6 hours before exposure to 100 ng/mL of ultrapure TLR4 agonist Escherichia coli lipopolysaccharide (LPS-EB; Invivogen, California, USA) or 100ng/ml of IL-4 (Immunotools,

Germany) overnight for the M0 naïve (untreated) cohort, M1-like LPS stimulated, M2-like IL-4 stimulated. Supernatants were harvested and stored at -80$^{o}$C for further processing, and cells were assessed for expression of surface markers as described below.

### 3.3.8 *Flow cytometry*

Zombie viability dye (Biolegend, California, USA) was resuspended in 100 µl of DMSO and then further diluted to 1000x in PBS. All cells were washed with PBS and stained with 80 µl zombie UV viability dye for 15 mins at room temperature in the dark. 20 µl of antibody master mix was then added, cells resuspended and incubated for an additional 15 mins at room temperature in the dark. Antibodies used for DC staining included CD40, CD11c, CD80, CD83, CD86, HLA-DR, CD54, TIM-3 and PD-L1. Antibodies used for Mϕ staining included CD68, CD11b, CD11c, CD80, CD86, CD163, CD206, HLA-DR, and TIM-3. Details and concentrations of antibodies used for DC maturation check, DC analysis and Mϕ analysis are listed in table 3.3.2, 3.3.3, and 3.3.4 respectively.

Cells were then centrifuged at 120xg (Thermo Scientific Megafuge 40R Centrifuge, Thermofisher, Waltham, Massachusetts, USA), supernatants removed and washed with 200 µl of FACS buffer (2% FBS (Gibco, Thermofisher, Waltham, Massachusetts, USA), 0.01% sodium azide (Sigma Aldrich, USA) in PBS (Gibco, Thermofisher, Waltham, Massachusetts, USA)). Cells were then centrifuged at 120xg again and FACS wash removed. Cells were then fixed with 100 µl 4% PFA (ChemCruz, California, USA) and allowed to incubate for 15 mins at room temperature in the dark. Cells were then centrifuged at 120xg, PFA removed and washed with 200 µl of FACS buffer. Cells were then centrifuged at 120xg again and FACS wash removed. Cells were then resuspended in 150 µl of FACs buffer on 96 well plates. Samples were acquired on Amnis cell stream flow cytometer (Luminex, Austin, Texas, USA) with compensation performed with positive and negative compensation beads (Miltenyi, Bergisch Gladbach, Germany, BD Biosciences, Wokingham, UK). Gating on and analysis of single cells, Zombie UV Live/Dead negative cells (Biolegend, California, USA) and either CD11c+ for DC or CD68+ for Mϕ cells was performed using Cell Stream software (Lumines, Austin, Texas, USA).

**Table 3.3.2 Antibodies used to assess DC maturation check**

| Marker | Fluorochrome | Clone | Company | Volume (20x) |
|---|---|---|---|---|
| **CD14** | Vio-Green | REA599 | Miltenyi, Germany | 2 µl |
| **Lineage Marker** | FITC | MϕP9, NCAM16.2, 3G8, SK7, L27, SJ25C1 | BD Biosciences, UK | 5 µl |
| **CD209** | APC | REA | Miltenyi, Germany | 2 µl |
| **CD11c** | Vio-Blue | REA618 | Miltenyi, Germany | 2 µl |
| **HLA-DR** | PE-Vio615 | REA805 | Miltenyi, Germany | 1 µl |
| **CD80** | PE | REA661 | Miltenyi, Germany | 2.8 µl |
| **CD83** | APC-Vio770 | REA714 | Miltenyi, Germany | 2.8 µl |
| **CD86** | PerCp-Vio700 | REA968 | Miltenyi, Germany | 2.8 µl |
| **CD40** | BV510 | 5C3 | BD Biosciences, UK | 8 µl |
| **PD-L1** | PE-Vio | REA1197 | Miltenyi, Germany | 5.6 µl |

**Table 3.3.3 Antibodies used to assess DC expression of phenotypic, maturation and immunoinhibitory markers**

| Marker | Fluorochrome | Clone | Company | Volume (100x) |
|---|---|---|---|---|
| **Zombie** | UV | N/A | Biolegend, USA | 8 ml |
| **HLA-DR** | PE-Vio615 | REA805 | Miltenyi, Germany | 5 µl |
| **CD11c** | Vio-Blue | REA618 | Miltenyi, Germany | 5 µl |
| **CD80** | PE | REA661 | Miltenyi, Germany | 14 µl |
| **CD83** | APC-Vio770 | REA714 | Miltenyi, Germany | 14 µl |
| **CD86** | PerCp-Vio700 | REA968 | Miltenyi, Germany | 14 µl |
| **CD40** | BV510 | 5C3 | BD Biosciences, UK | 40 µl |
| **CD54** | APC | REA266 | Miltenyi, Germany | 5 µl |
| **PD-L1** | PE-Vio-770 | REA1197 | Miltenyi, Germany | 28 µl |
| **TIM-3** | FITC | REA635 | Miltenyi, Germany | 28 µl |

**Table 3.3.4 Antibodies used to assess Mϕ expression of phenotypic, pro-inflammatory and anti-inflammatory markers**

| Marker | Fluorochrome | Clone | Company | Volume (100x) |
|---|---|---|---|---|
| **Zombie** | UV | N/A | Biolegend, USA | 8 ml |
| **CD68** | PE-Vio-770 | REA886 | Miltenyi, Germany | 10 µl |
| **HLA-DR** | Vio-green | REA805 | Miltenyi, Germany | 10 µl |
| **CD11c** | Vio-Blue | REA618 | Miltenyi, Germany | 10 µl |
| **CD11b** | FITC | REA713 | Miltenyi, Germany | 10 µl |
| **CD80** | PE | REA661 | Miltenyi, Germany | 15 µl |
| **CD86** | PerCp-Vio700 | REA968 | Miltenyi, Germany | 15 µl |
| **CD163** | PE-Vio-615 | REA812 | Miltenyi, Germany | 15 µl |
| **CD206** | APC-Vio-770 | DCN228 | Miltenyi, Germany | 75 µl |
| **TIM-3** | APC | 5D12 | BD Biosciences, UK | 30 µl |

### 3.3.9 *Statistical Analysis*

All statistics were conducted using GraphPad Prism 9.5 (GraphPad Software, California, USA). A significance level of $p<0.05$ was used in all analysis and all p-values reported were two-tailed. Friedman testing with Dunn's post hoc correction, was employed for non-parametric testing between paired cohorts (Control vs. OA vs. PA within the non-cancer cohort and Control vs. OA vs. PA within the cancer cohort). For statistical testing between unpaired non-parametric cohorts, Kruskal Wallis test with Dunn's correction was used (Control/OA/PA non-cancer vs Control/OA/PA cancer. and between fatty acids treatments in non-obese and obese cancer cohorts). Details of specific statistical tests are stated in each figure legend.

## 3.4 Results

### 3.4.1 *Palmitic acid significantly decreases the OCR metabolic profiles of adipose tissue derived from cancer patients but not in adipose tissue from non-cancer patients.*

Human *ex-vivo* adipose tissue explants derived from non-cancer and OAC patients were assessed via Agilent Seahorse Xfe24 analyser to examine the influence of OA and PA treatments on their metabolic profiles. Within the cancer cohort the influence of obesity, classified by Visceral Fat Area (VFA), on adipose tissue metabolic response to these fatty acids was also assessed.

In adipose tissue explants derived from non-cancer patients, OA and not PA treatment significantly increased OCR compared to control (untreated) adipose tissue. In contrast, PA treatment in adipose explants from cancer patients significantly decreased OCR compared to untreated control (**Figure 3.4.1 A**). Adipose tissue derived from non-cancer patients treated with OA significantly increased ECAR compared to untreated adipose tissue, an effect not observed in cancer patients (**Figure 3.4.1 B**). PA treatment in adipose tissue explants from cancer patients also significantly decreased ECAR compared with PA treatment in adipose from non-cancer patients and OA treated adipose tissue from cancer patients (**Figure 3.4.1 B**). No differential effects were observed in OCR:ECAR ratio in adipose tissue explants of non-cancer and cancer patients or in response to exogenous fatty acids (**Figure 3.4.1 C**)

Within the cancer cohort control adipose tissue from obese patients showed significantly higher OCR profiles compared with adipose tissue from non-obese cancer patients. Also, within the cancer cohort PA treatment significantly decreased OCR in adipose tissue explants from non-obese cancer patients compared with OA treatment. Whilst in obese OAC patients PA treatment significantly decreased adipose tissue OCR profiles compared with control adipose tissue (**Figure 3.4.2. A**). No differential effects were observed in ECAR or OCR:ECAR ratio in adipose tissue explants of non-obese and obese cancer patients or in response to exogenous fatty acids (**Figure 3.4.1 B-C**)

(* $p < 0.05$, ** $p < 0.01$, *** $p < 0.001$.)

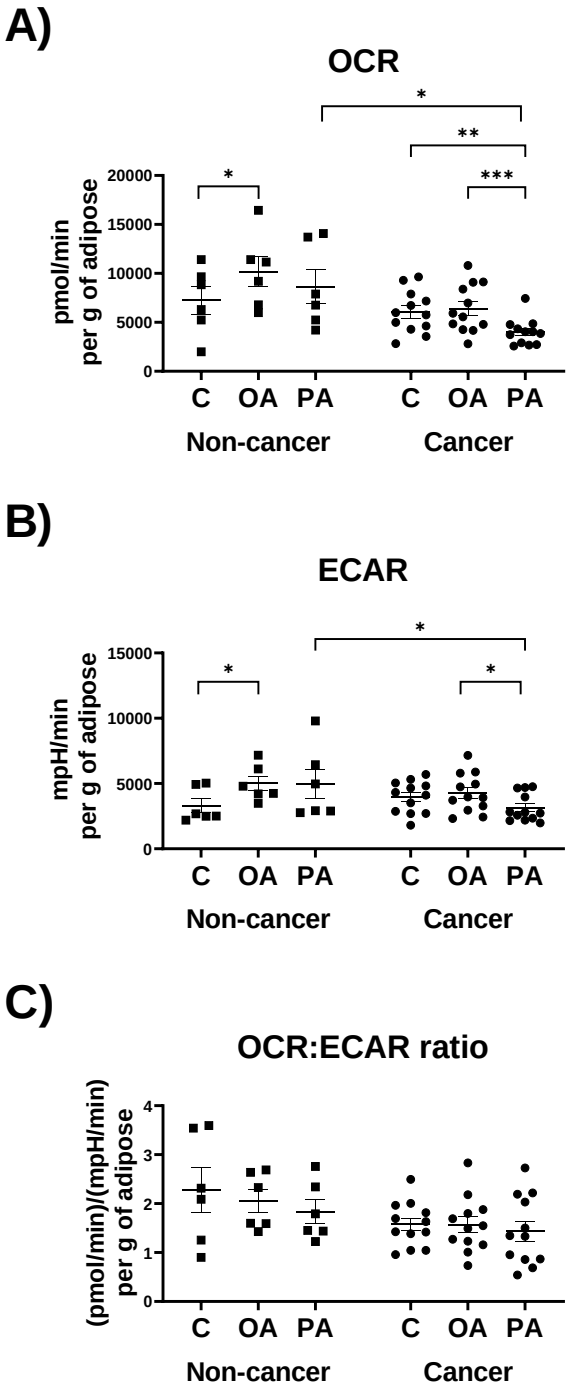


**Figure 3.4.1 Palmitic acid differentially effects OCR metabolism in adipose tissue from cancer and non-cancer patients**

A-C) OCR, ECAR and OCR:ECAR ratio profiles of adipose tissue derived from non-cancer and OAC cancer patients treated with BSA Control (C), Oleic Acid (OA) or Palmitic Acid (PA).

(To assess fatty acid treatment in non-cancer and cancer cohorts Friedman test with Dunn's correction was used, to assess the difference between non-cancer compared with cancer cohorts Kruskal Wallis test with Dunn's correction was used) All data expressed as mean ± SEM, non-cancer $n = 6$, cancer $n = 12$, * $p < 0.05$, ** $p < 0.01$, *** $p < 0.001$.

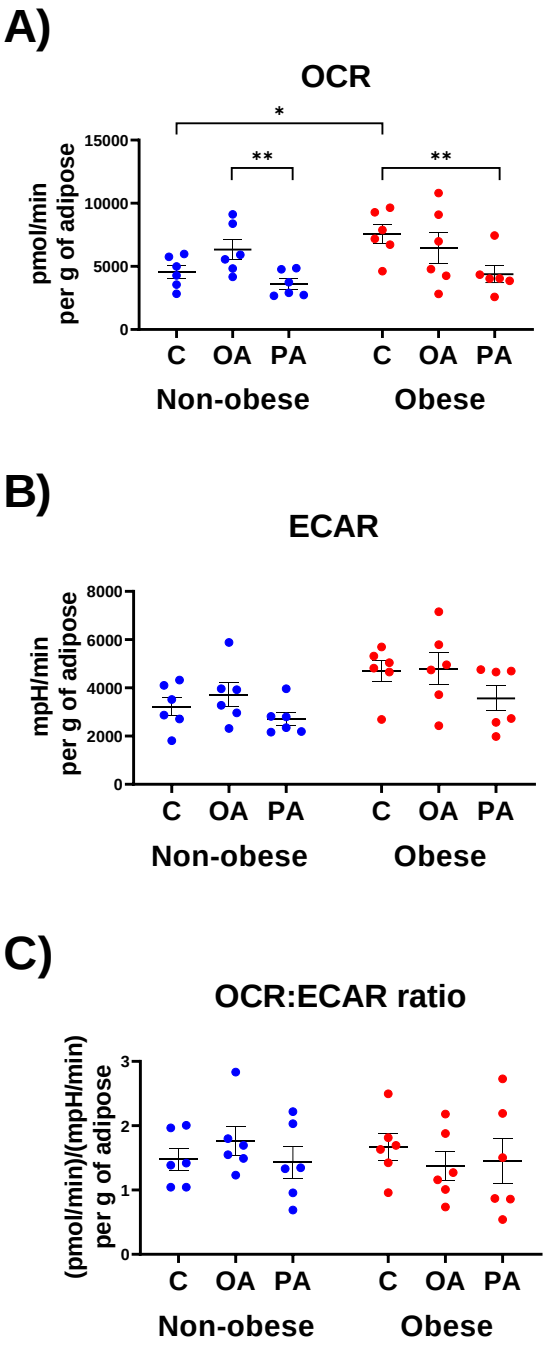


**Figure 3.4.2 Exogenous fatty acid treatment differentially effects OCR metabolism in adipose tissue from non-obese and obese cancer patients**

A-C) OCR, ECAR and OCR:ECAR ratio profiles of adipose tissue derived from non-obese and obese OAC cancer patients treated with BSA Control (C), Oleic Acid (OA) or Palmitic Acid (PA).

To assess fatty acid treatment in non-obese cancer and obese cancer cohorts Friedman test with Dunn's correction was used, to assess the difference between non-obese cancer compared with obese cancer cohorts Kruskal Wallis test with Dunn's correction was used. All data expressed as mean ± SEM, non-obese cancer $n = 6$, obese cancer $n = 6$, * $p < 0.05$, ** $p < 0.01$.

● symbols = non-obese OAC patients, ● symbols = obese OAC patients.

### 3.4.2 *Palmitic acid augments an immunosuppressive secretome in adipose tissue from both non-cancer and cancer patients.*

The presence of PA and OA in circulation have been reported to play a role in augmenting or suppressing inflammatory mediators. To determine whether OA and PA treatments influenced the adipose secretome of non-cancer and cancer patients a 54-analyte multiplex was used to assess the profiles of inflammatory mediators, with and without the different fatty acids.

Cancer vs. Non-Cancer

Control ACM from non-cancer patients showed higher secreted levels of Eotaxin-3, IL-2, and IL-17A and decreased secretion of IL-10, IL-13, MCP-4, and TNF-α compared with control ACM derived from cancer patients (**Figure 3.4.3- 3.4.6**).

OA treated ACM from non-cancer patients showed higher secreted levels of Eotaxin-3, IL-2, IL-8, and IL-17A and decreased secretion of IL-1β, IL-10 IL-13 MCP-4, and TNF-α compared with OA treated ACM derived from cancer patients (**Figure 3.4.3- 3.4.6**).

PA treated ACM from non-cancer patients showed higher secreted levels of Eotaxin-3, IL-2, IL-17A, MIP-1α, MIP-1β, MIP-3α, and TLSP and decreased secretion of IL-13 compared with PA treated ACM derived from cancer patients (**Figure 3.4.3, 3.4.4, 3.4.6**).

Non-cancer

The OA treated ACM derived from non-cancer patients showed decreased IL-1β and IL-10 compared with matched control (**Figure 3.4.5- 3.4.6**).

OA treated ACM also showed decreased IL-1β compared with PA treated ACM from non-cancer patients (**Figure 3.4.5**).

PA treated ACM from non-cancer patients also showed decreased secreted levels of IL-6, IL-13, IL-17A, MCP-1 and MCP-4 compared with matched control ACM (**Figure 3.4.3, 3.4.5, 3.4.6**).

PA treated ACM from non-cancer patients showed decreased secreted levels of Eotaxin, Eotaxin-3, IL-4, IL-8, and MDC compared with OA treated ACM from non-cancer patients (**Figure 3.4.3, 3.4.5, 3.4.6**).

Cancer

PA treated ACM from cancer patients also showed decreased secreted levels of Eotaxin, Eotaxin-3, GM-CSF, IFN-γ, IL-1α, IL-1β, IL-1Ra, IL-2 IL-4, IL-6, IL-10, IL-13, IP-10, MCP-1, MDC, MIP-1α, MIP-1β, MIP-3α, TNF-α, and TSLP compared with matched control ACM (**Figure 3.4.3-3.4.6**).

PA treated ACM from cancer patients also showed decreased secreted levels of GM-CSF, IFN-γ, IL-1α, IL-1β, IL-1Ra, IL-2, IL-4, IL-6, IL-10, IL-12p70, IL-13, IP-10, MCP-1, MDC, MIP-1β, MIP-3α, TNF-α, TSLP compared with OA treated ACM from cancer patients (**Figure 3.4.3- 3.4.6**).

(* $p < 0.05$, ** $p < 0.01$, *** $p < 0.001$, **** $p < 0.0001$.)

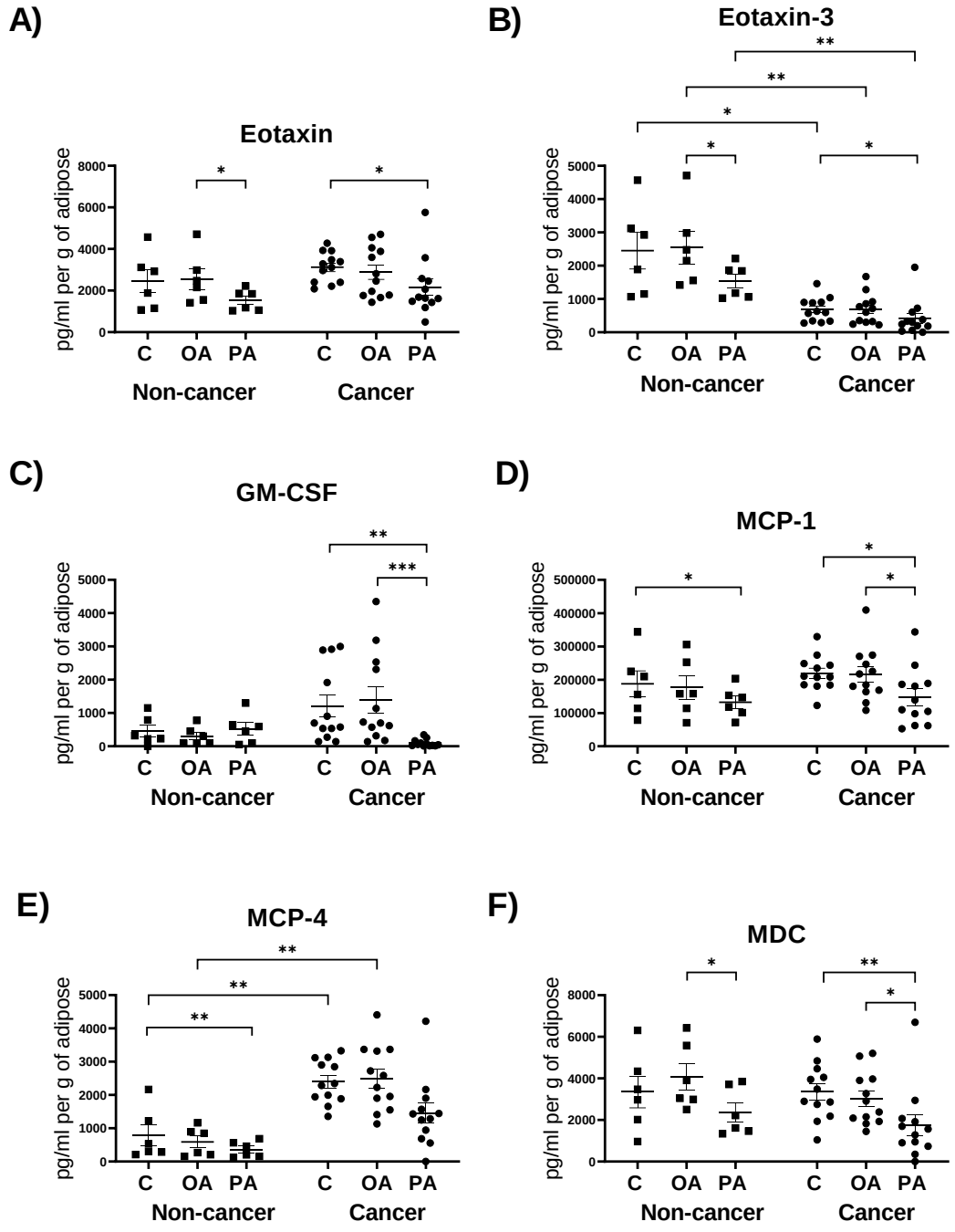


**Figure 3.4.3 Palmitic acid decreases secreted levels of mediators associated with immune cell recruitment in the adipose secretome of non-cancer and cancer patients**

A-F) Secreted levels of Eotaxin, Eotaxin-3, GM-CSF, MCP-1, MCP-4, and MDC from adipose tissue derived from non-cancer and OAC cancer patients treated with BSA Control (C), Oleic Acid (OA) or Palmitic Acid (PA).

(To assess fatty acid treatment in non-cancer and cancer cohorts Friedman test with Dunn's correction was used, to assess the difference between non-cancer compared with cancer cohorts Kruskal Wallis test with Dunn's correction was used) All data expressed as mean ± SEM, non-cancer $n = 6$, cancer $n = 12$, * $p < 0.05$, ** $p < 0.01$, *** $p < 0.001$.

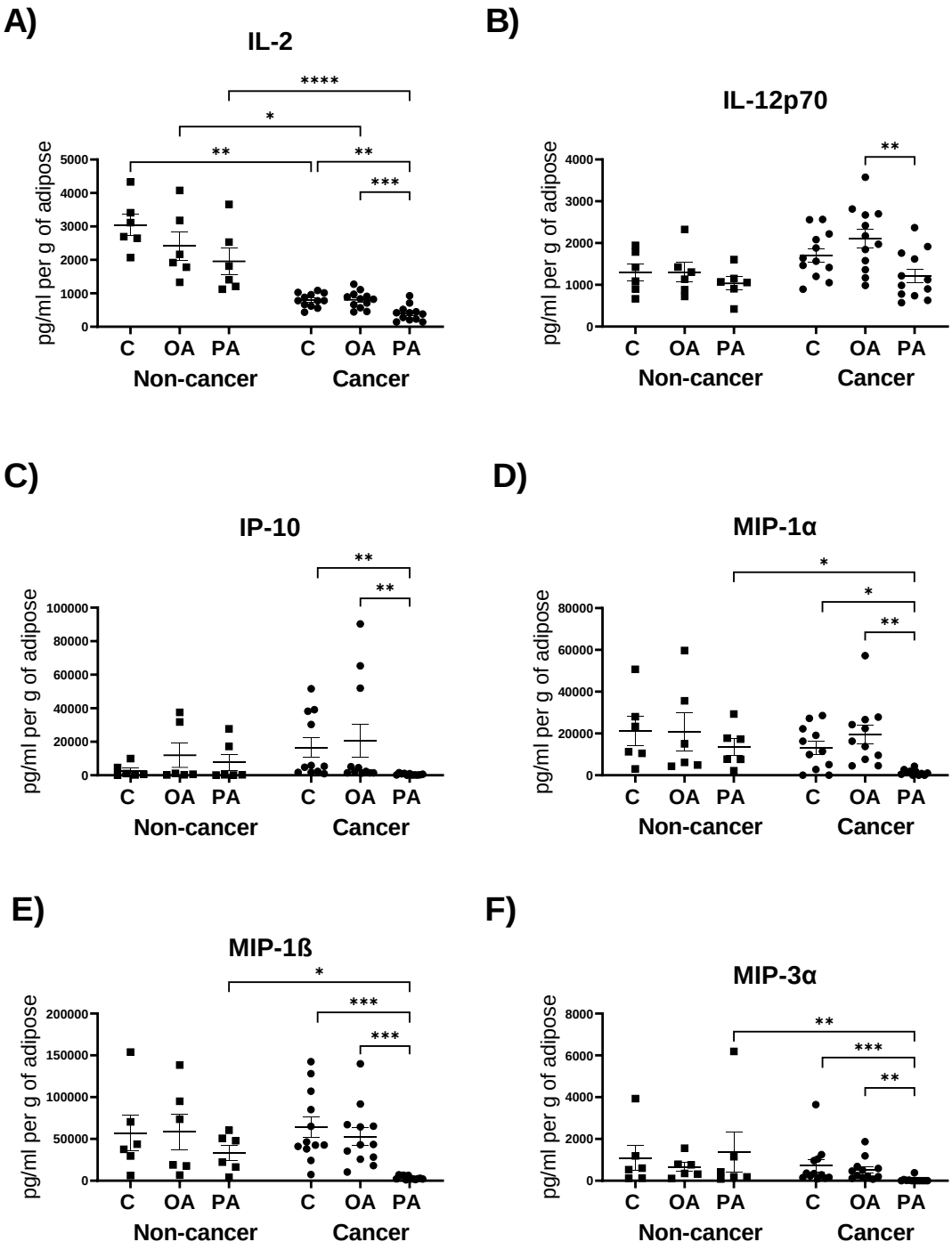


**Figure 3.4.4 Palmitic acid significantly decreases secreted levels of mediators associated with immune cell activation in the adipose secretome of cancer patients**

A-F) Secreted levels of IL-2, IL-12p70, IP-10, MIP-1α, MIP-1β, and MIP-3α from adipose tissue derived from non-cancer and OAC cancer patients treated with BSA Control (C), Oleic Acid (OA) or Palmitic Acid (PA).

(To assess fatty acid treatment in non-cancer and cancer cohorts Friedman test with Dunn's correction was used, to assess the difference between non-cancer compared with cancer cohorts Kruskal Wallis test with Dunn's correction was used) All data expressed as mean ± SEM, non-cancer $n = 6$, cancer $n = 12$, * $p < 0.05$, ** $p < 0.01$, *** $p < 0.001$, **** $p < 0.0001$.

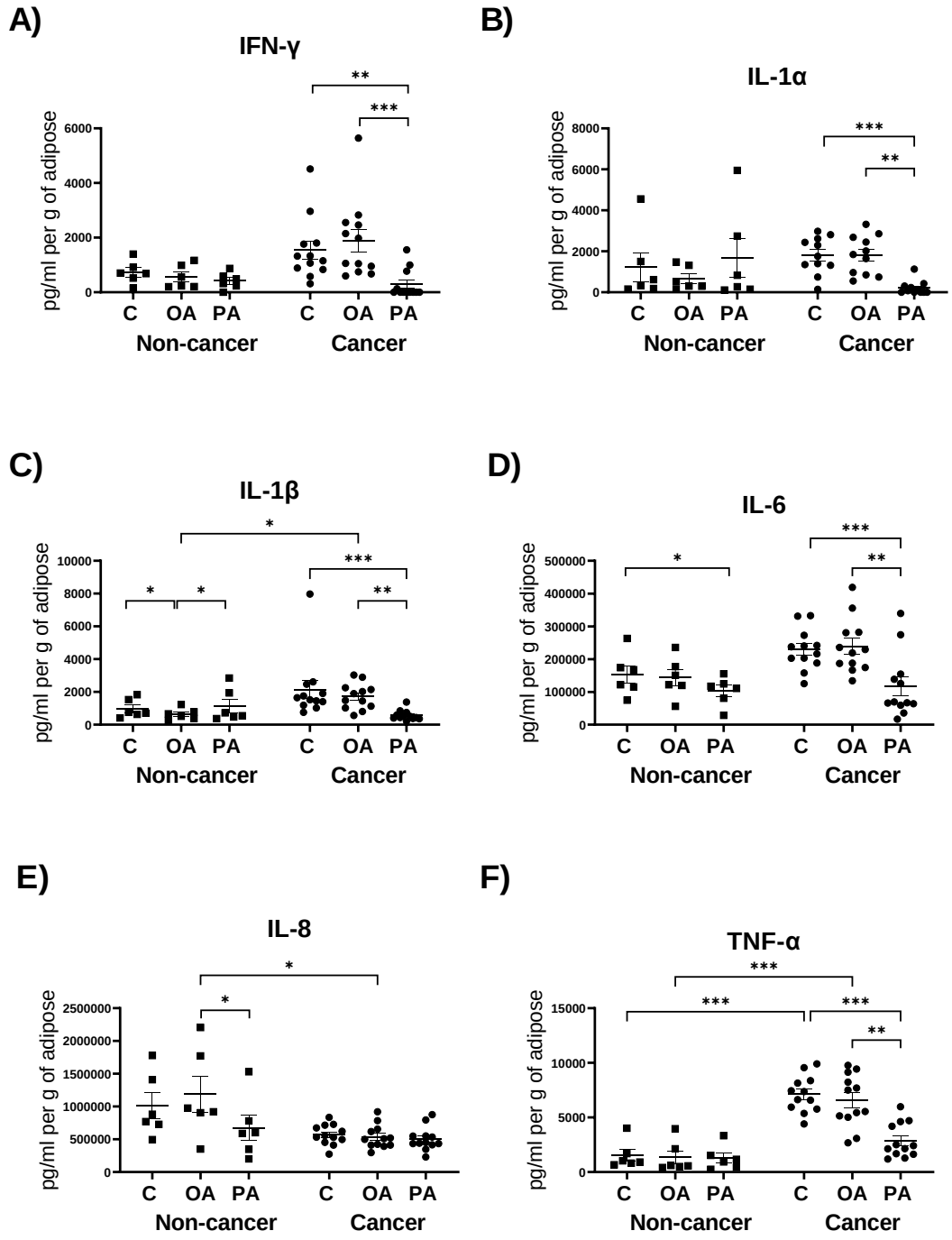


**Figure 3.4.5 Palmitic and Oleic Acid have differential responses on the secreted levels of pro-inflammatory mediators in the adipose secretome of non-cancer and cancer patients**

A-F) Secreted levels of IFN-γ, IL-1α, IL-1β, IL-6, IL-8, and TNF-α from adipose tissue derived from non-cancer and OAC cancer patients treated with BSA Control (C), Oleic Acid (OA) or Palmitic Acid (PA).

(To assess fatty acid treatment in non-cancer and cancer cohorts Friedman test with Dunn's correction was used, to assess the difference between non-cancer compared with cancer cohorts Kruskal Wallis test with Dunn's correction was used) All data expressed as mean ± SEM, non-cancer $n = 6$, cancer $n = 12$, * $p < 0.05$, ** $p < 0.01$, *** $p < 0.001$.

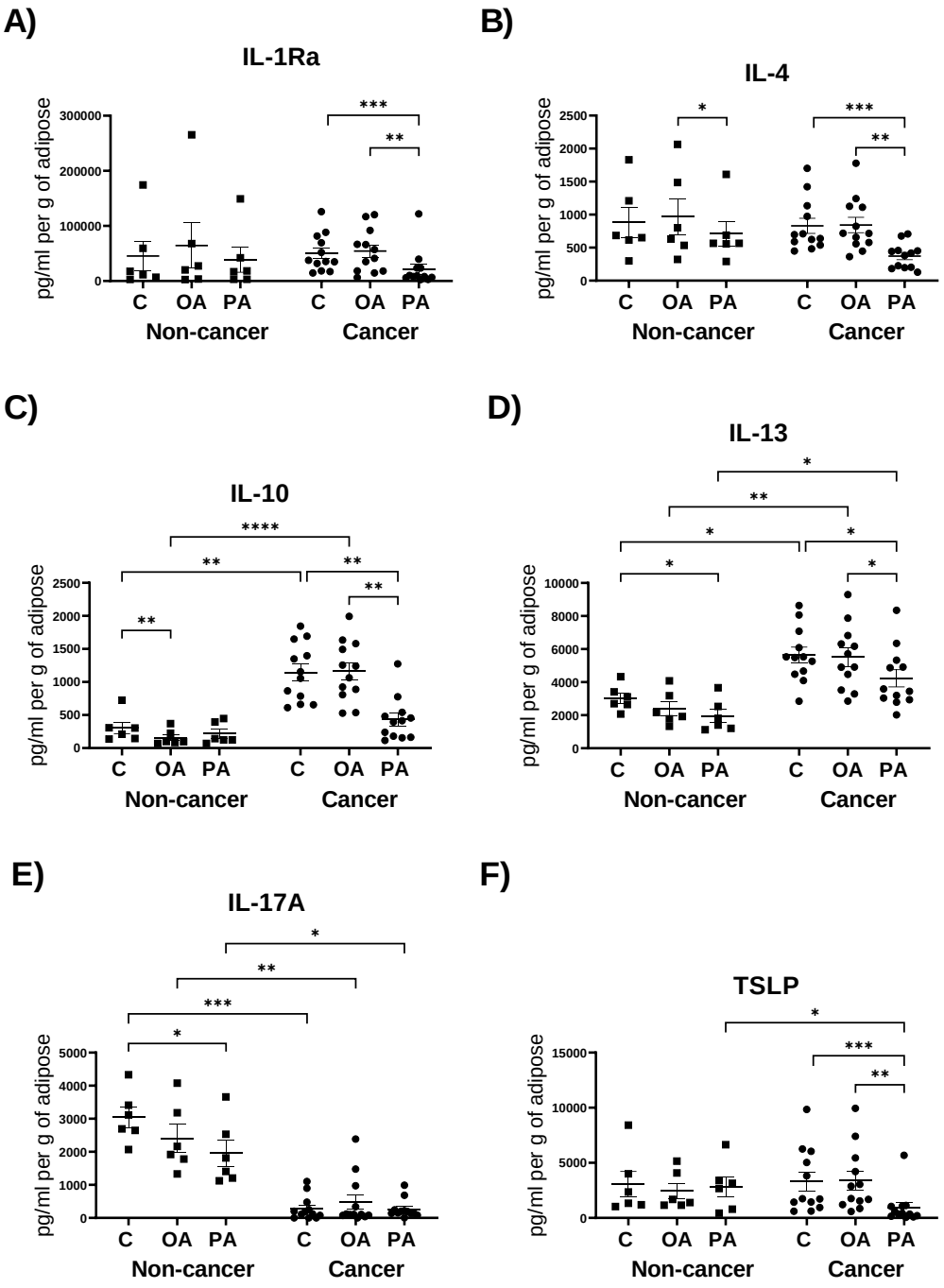


**Figure 3.4.6 Mediators of anti-inflammatory response are differentially expressed in the adipose secretome of non-cancer and cancer patients and are decreased in the cancer by palmitic acid.**

A-F) Secreted levels of IL-1Ra, IL-4, IL-10, IL-13, IL-17A, and TSLP from adipose tissue derived from non-cancer and OAC cancer patients treated with BSA Control (C), Oleic Acid (OA) or Palmitic Acid (PA).

(To assess fatty acid treatment in non-cancer and cancer cohorts Friedman test with Dunn's correction was used, to assess the difference between non-cancer compared with cancer cohorts Kruskal Wallis test with Dunn's correction was used) All data expressed as mean ± SEM, non-cancer $n = 6$, cancer $n = 12$, * $p < 0.05$, ** $p < 0.01$, *** $p < 0.001$, **** $p < 0.0001$.

### 3.4.3 *The immunosuppressive effects of palmitic acid on key pro-inflammatory mediators are most apparent in the adipose secretome of obese OAC patients.*

Obesity is a known contributor to chronic low-grade inflammation. Therefore, to assess whether increased visceral adiposity levels effected the response of OA and PA treatments on adipose tissue secretome from OAC patients a 54-analyte multiplex against obesity status, classified by VFA.

Non-obese vs Obese

IL-17A was also observed to be increased in control ACM from obese compared with non-obese OAC patients (**Figure 3.4.10**).

Non-obese

In the PA treated adipose secretome of non-obese OAC patients decreased secretion of IL-4, IP-10, and TNF-a was observed against control ACM from non-obese OAC patients (**Figure 3.4.8 - 3.4.10**).

In the PA treated adipose secretome of non-obese OAC patients decreased secreted levels of Eotaxin, Eotaxin-3, GM-CSF, IFN-γ, IL-10, IL-12p70, IL-1Ra, IL-1a, IL-2, IL-4, IL-6, IP-10, MDC, MIP-1β, MIP-3α, TNF-a, and TSLP were observed compared with OA treated ACM from non-obese OAC patients (**Figure 3.4.7 - 3.4.10**).

Obese

In the PA treated adipose secretome of obese OAC patients decreased secretion of GM-CSF, IFN-γ, IL-10, IL-1α, IL-1β, IL-2, MIP-1β, MIP-3α, TNF-α, and TSLP was observed compared with control ACM from obese OAC patients (**Figure 3.4.7 - 3.4.10**).

Additionally in the PA treated adipose secretome of obese OAC patients decreased secreted levels of IFN-γ, IL-1β, MIP-1α and MIP-1β compared with OA treated ACM from obese OAC patients (**Figure 3.4.8, 3.4.9**).

*($p < 0.05$, ** $p < 0.01$. *** $p < 0.001$.)*

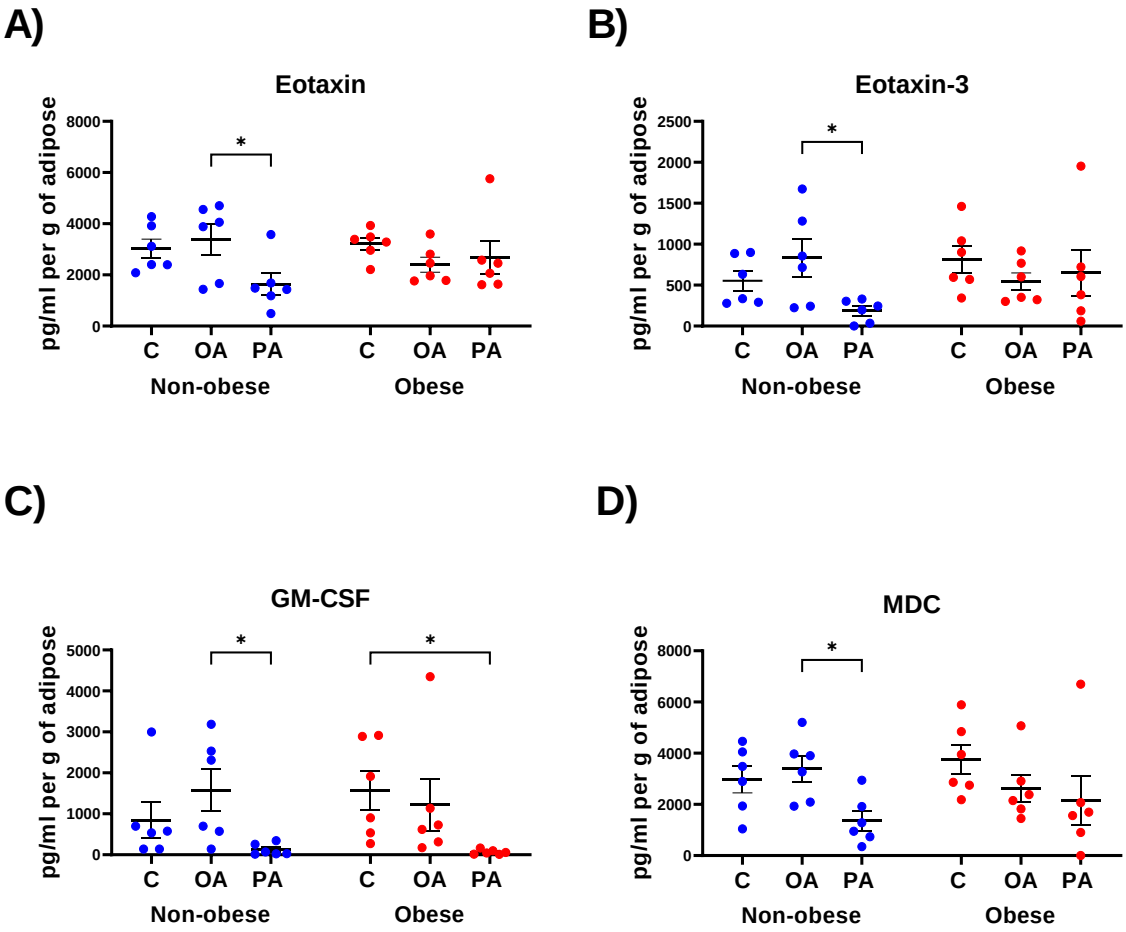


**Figure 3.4.7 Palmitic acid decreases secreted levels of mediators associated with immune cell recruitment in the adipose secretome of non-obese and obese cancer patients**

A-D) Secreted levels of Eotaxin, Eotaxin-3, GM-CSF, and MDC from adipose tissue derived from non-obese and obese OAC cancer patients treated with BSA Control (C), Oleic Acid (OA) or Palmitic Acid (PA).

To assess fatty acid treatment in non-obese cancer and obese cancer cohorts Friedman test with Dunn's correction was used, to assess the difference between non-obese cancer compared with obese cancer cohorts Kruskal Wallis test with Dunn's correction was used. All data expressed as mean ± SEM, non-obese cancer $n = 6$, obese cancer $n = 6$, * $p < 0.05$.

● symbols = non-obese OAC patients, ● symbols = obese OAC patients.

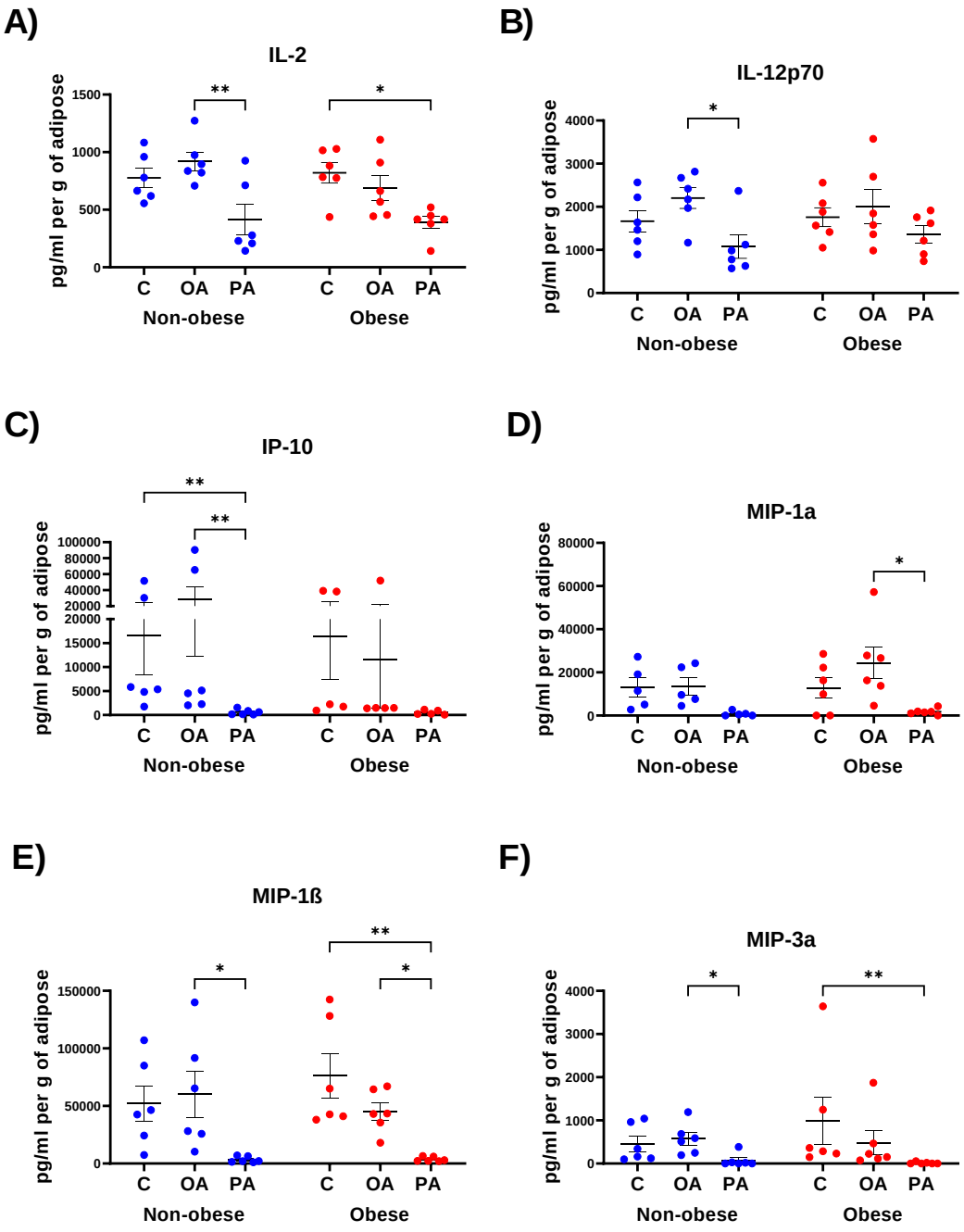


**Figure 3.4.8 Palmitic acid differentially decreases secreted levels of activators of Th1 immunity in the adipose secretome of non-obese and obese cancer patients**

A-F) Secreted levels of IL-2, IL-12p70, IP-10, MIP-1α, MIP-1β, and MIP-3α from adipose tissue derived from non-obese and obese cancer patients treated with BSA Control (C), Oleic Acid (OA) or Palmitic Acid (PA).

(To assess fatty acid treatment in non-obese cancer and obese cancer cohorts Friedman test with to assess fatty acid treatment in non-obese cancer and obese cancer cohorts Friedman test with Dunn's correction was used, to assess the difference between non-obese cancer compared with obese cancer cohorts Kruskal Wallis test with Dunn's correction was used. All data expressed as mean ± SEM, non-obese cancer $n = 6$, obese cancer $n = 6$, * $p < 0.05$, ** $p < 0.01$.

● symbols = non-obese OAC patients, ● symbols = obese OAC patients.

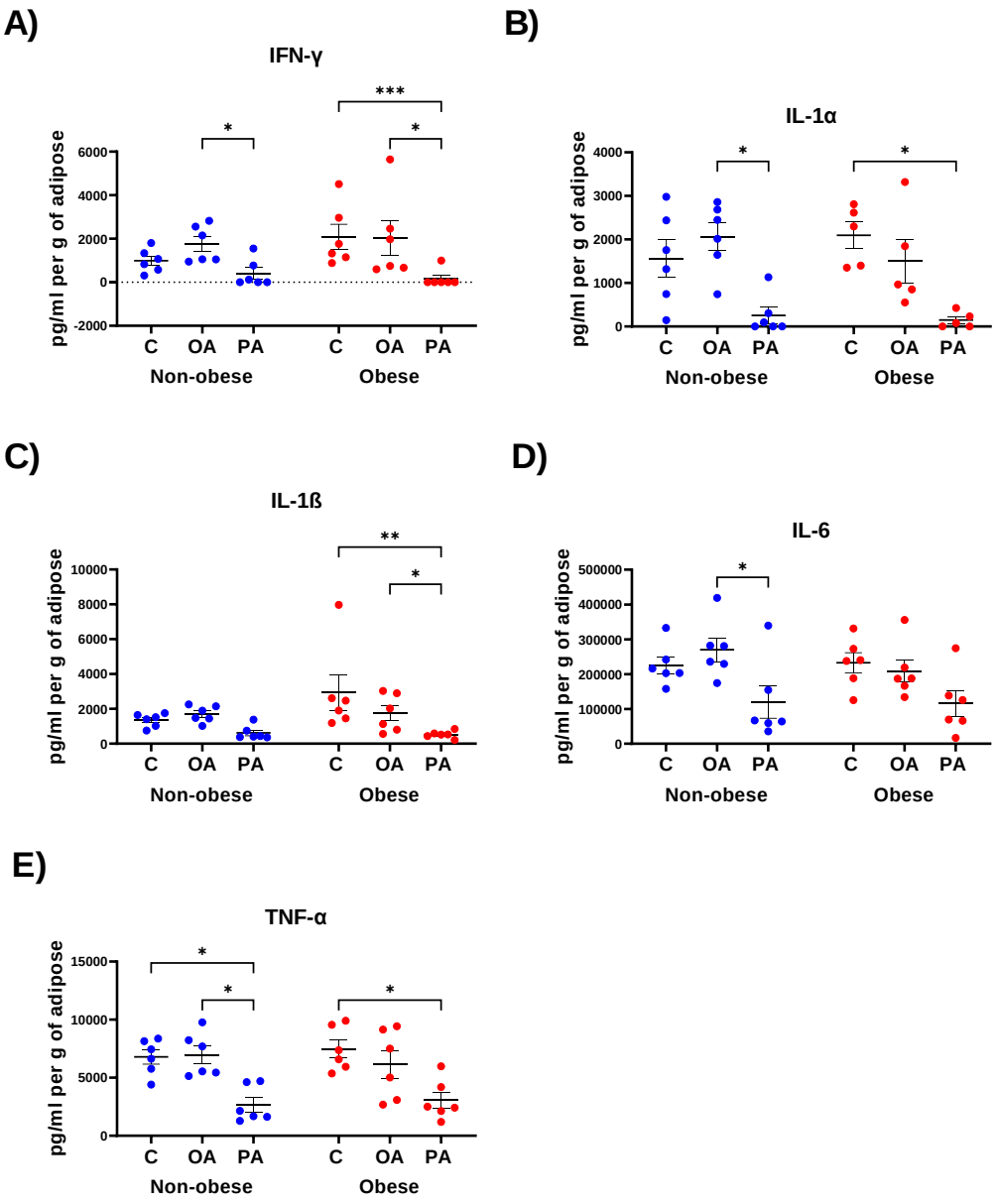


**Figure 3.4.9 Palmitic acid decreases secreted levels of pro-inflammatory mediators in the adipose secretome of obese OAC patients.**

A-E) Secreted levels of IFN-γ, IL-1α, IL-1β, IL-6, and TNF-α from adipose tissue derived from non-obese and obese cancer patients treated with BSA Control (C), Oleic Acid (OA) or Palmitic Acid (PA).

To assess fatty acid treatment in non-obese cancer and obese cancer cohorts Friedman test with Dunn's correction was used, to assess the difference between non-obese cancer compared with obese cancer cohorts Kruskal Wallis test with Dunn's correction was used. All data expressed as mean ± SEM, non-obese cancer $n = 6$, obese cancer $n = 6$, * $p < 0.05$, ** $p < 0.01$. *** $p < 0.001$.

● symbols = non-obese OAC patients, ● symbols = obese OAC patients.

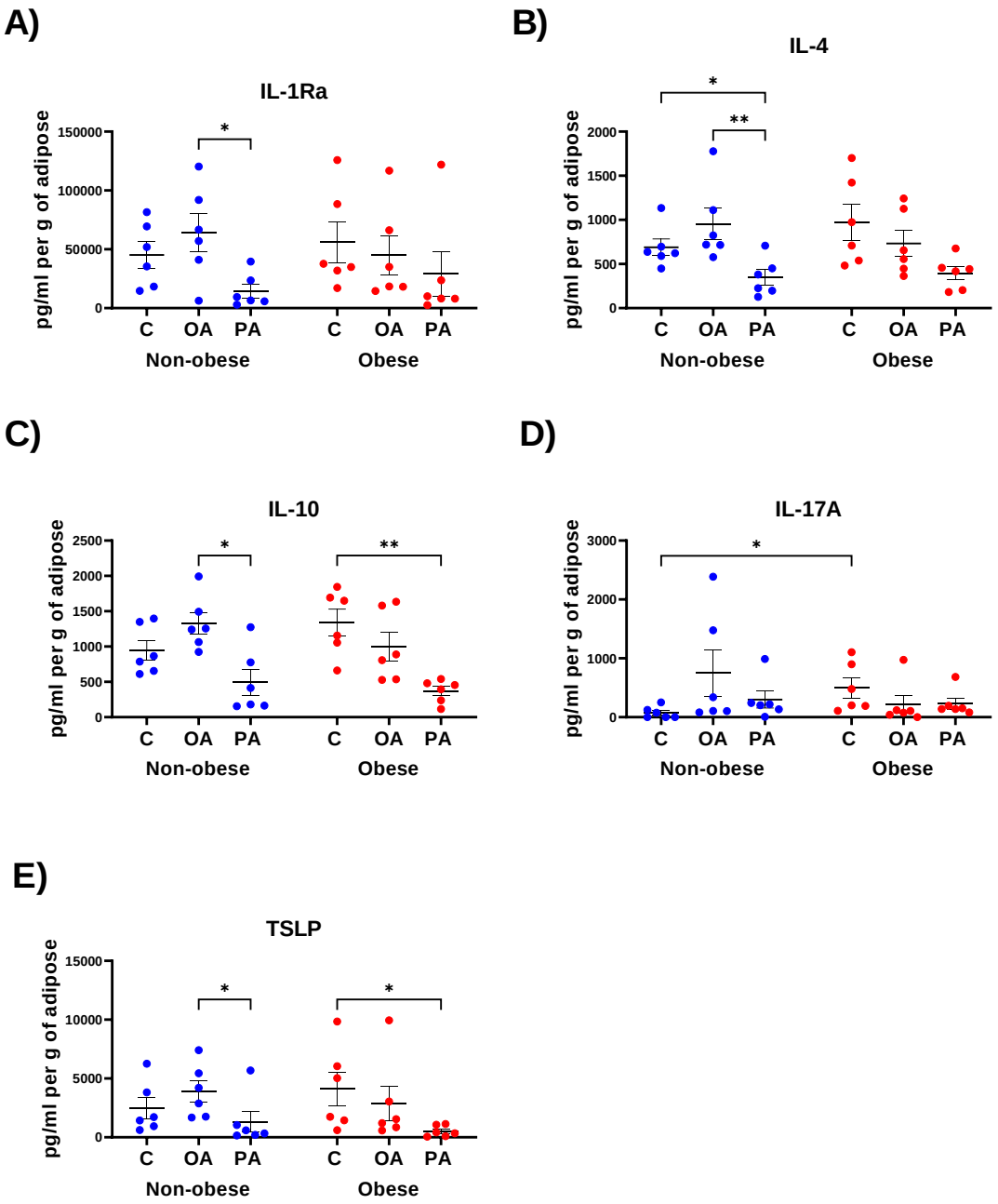


**Figure 3.4.10 Palmitic acid decreases secreted levels of anti-inflammatory mediators in the adipose secretome of non-obese OAC patients.**

A-E) Secreted levels of IL-1Ra, IL-4, IL-10, IL-17A, and TSLP from adipose tissue derived from non-obese and obese cancer patients treated with BSA Control (C), Oleic Acid (OA) or Palmitic Acid (PA).

To assess fatty acid treatment in non-obese cancer and obese cancer cohorts Friedman test with Dunn's correction was used, to assess the difference between non-obese cancer compared with obese cancer cohorts Kruskal Wallis test with Dunn's correction was used. All data expressed as mean ± SEM, non-obese cancer $n = 6$, obese cancer $n = 6$, * $p < 0.05$, ** $p < 0.01$.

● symbols = non-obese OAC patients, ● symbols = obese OAC patients.

### 3.4.4 *Maturation levels of dendritic cells is significantly inhibited by the adipose secretome of non-cancer patients treated with palmitic acid.*

DCs play a pivotal role in antigen presentation and anti-tumour immunity. To assess if fatty acid treatments which alter the adipose secretome influence DCs. Following DCs exposure to treated ACM from non-cancer and cancer patients, phenotypic and maturation markers were assessed via flow cytometry.

Non-cancer vs Cancer

OA treated ACM from non-cancer patients showed decreased DC expression of PD-L1 and increased expression of CD83, CD86, CD40, and CD54 compared to DCs cultured with OA treated ACM from OAC patients.

PA treated ACM from non-cancer patients showed decreased DC expression of CD80, CD80+CD86+, HLA-DR, CD11c, CD40, CD54, PD-L1, TIM-3, and increased expression of CD83 compared to DCs cultured with PA treated ACM from OAC patients (**Figure 3.4.12, 3.4.13**).

Non-cancer

OA treated ACM from non-cancer patients increased DC expression of CD80 compared with control ACM from non-cancer patients.

PA treated ACM from non-cancer patients decreased DC surface expression of CD80, CD86, HLA-DR, CD11c, CD40, CD54, and TIM-3 compared with OA treated ACM from non-cancer patients (**Figure 3.4.12, 3.4.13**).

Cancer

OA treated ACM from OAC patients showed significantly increased DC expression of CD83, PD-L1, and decreased expression of CD54 compared to DCs treated with control ACM from OAC patients  Control ACM from non-cancer patients showed decreased DC expression of CD80, PD-L1, and TIM-3, and increased expression of CD83 compared with DCs treated with control ACM from OAC patients (**Figure 3.4.12, 3.4.13**). The obesity status of OAC patients did not significantly impact DC expression of phenotypic, maturation, or immunoinhibitory markers.

(* $p < 0.05$, ** $p < 0.01$, *** $p < 0.001$.)

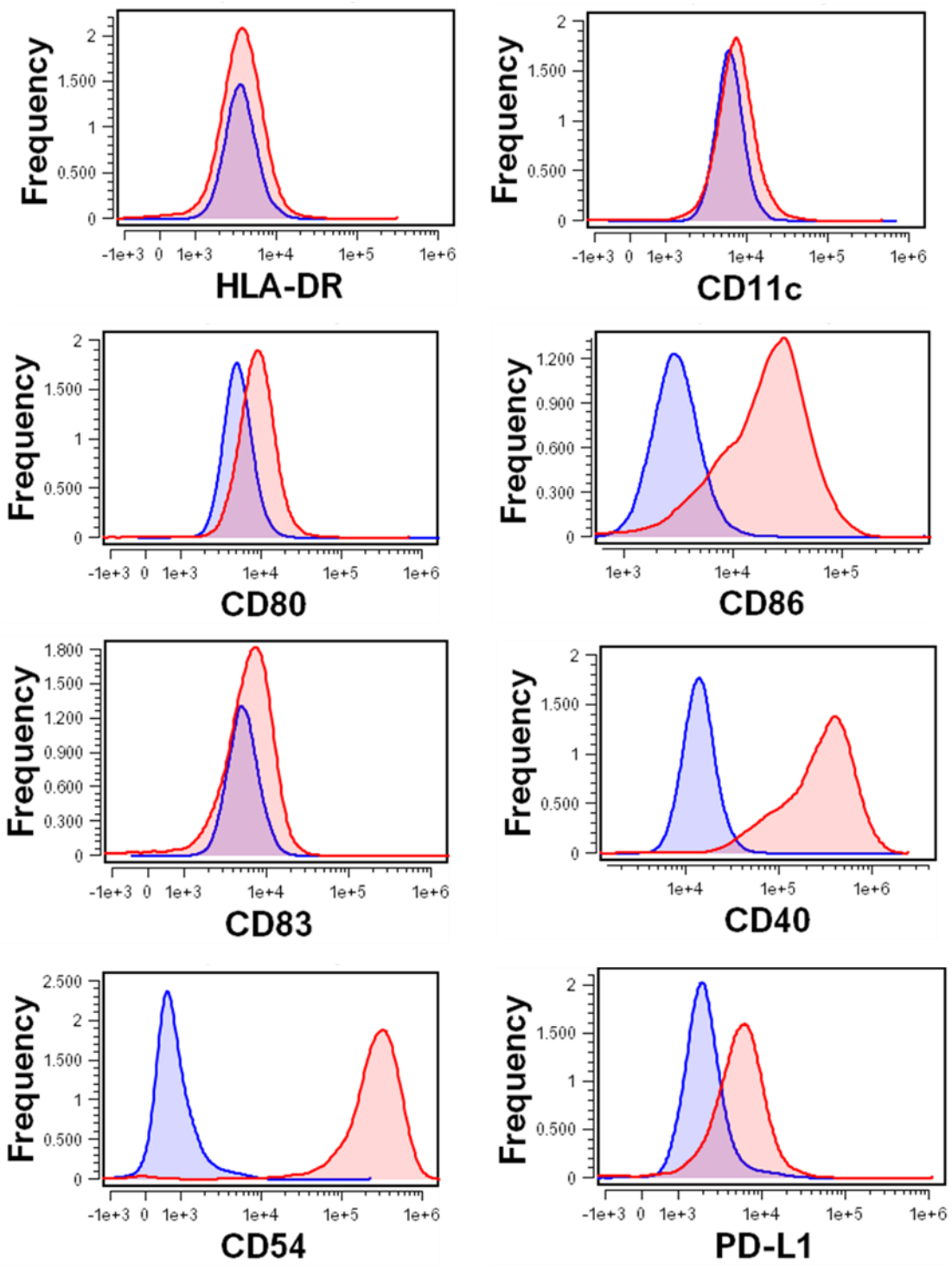


**Figure 3.4.11 Histograms of DC maturation markers following LPS stimulation**

Histograms displaying DC markers HLA-DR, CD11c, CD80, CD86 CD83, CD40, CD54 and PD-L1 which depict DCs response to LPS stimulation. (Blue peaks indicate unstimulated DCs and red peak indicate DCs following exposure to LPS stimulation)

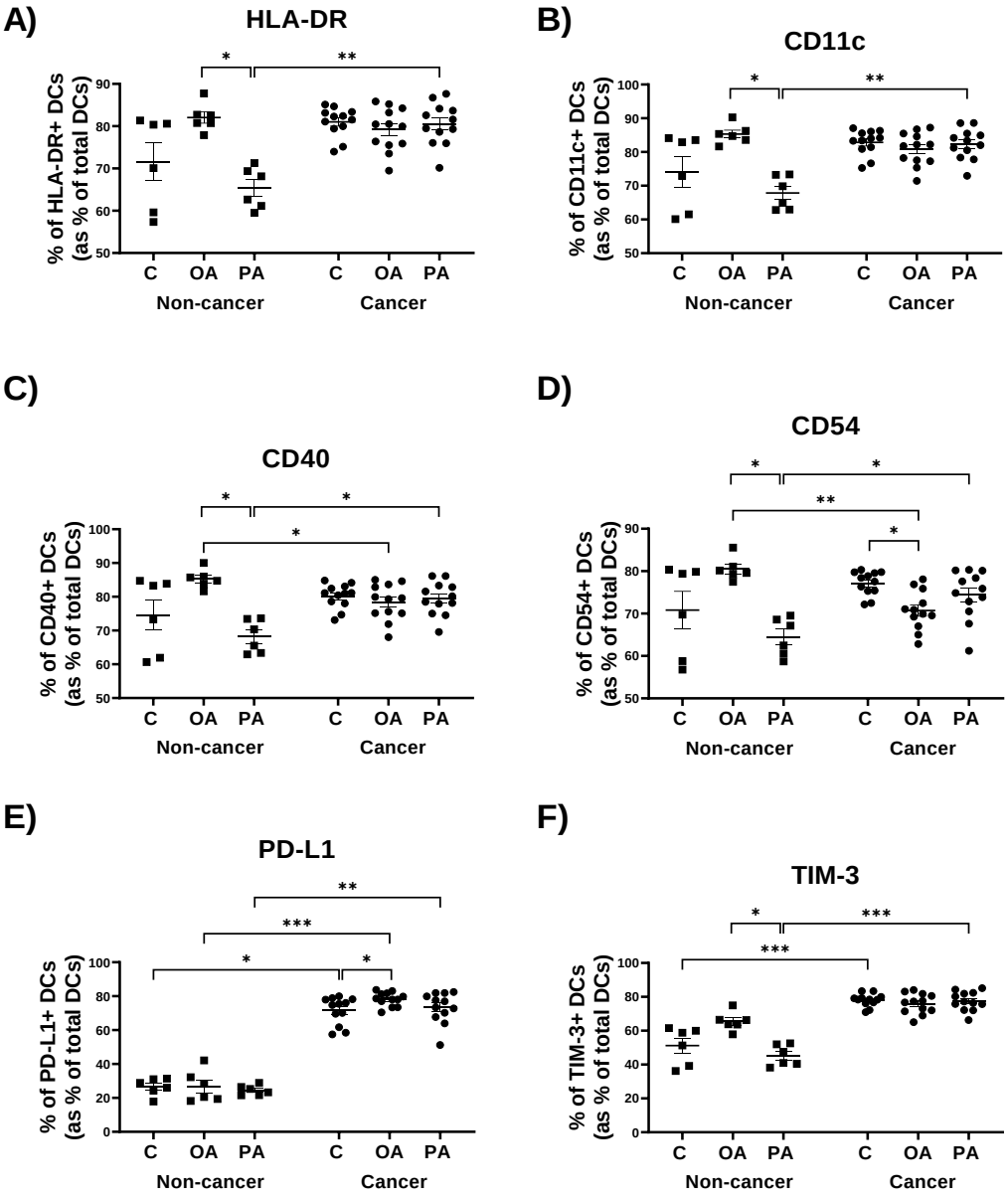


**Figure 3.4.12 The adipose secretome of cancer patients significantly increases the expression of immunoinhibitory markers on DCs.**

A-F) Expression of DC phenotypic and immunoinhibitory markers including HLA-DR, CD11c, CD40, CD54, TIM-3, and PD-L1 following exposure to adipose conditioned media in combination with BSA Control (C), Oleic Acid (OA) or Palmitic Acid (PA) derived from non-cancer and cancer patients.

(To assess fatty acid treatment in non-cancer and cancer cohorts Friedman test with Dunn's correction was used, to assess the difference between non-cancer compared with cancer cohorts Kruskal Wallis test with Dunn's correction was used) All data expressed as mean ± SEM, non-cancer $n = 6$, cancer $n = 12$, * $p < 0.05$, ** $p < 0.01$, *** $p < 0.001$.

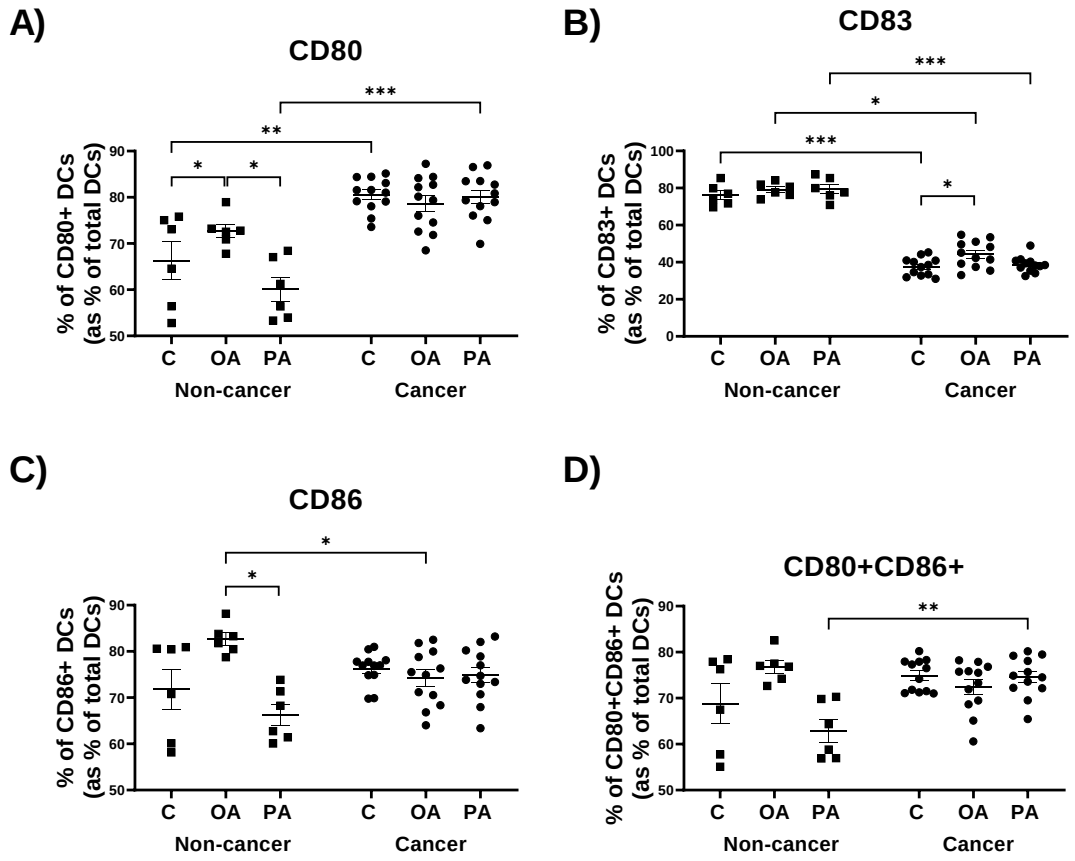


**Figure 3.4.13 The adipose secretome of non-cancer patients treated with palmitic acid decreases expression of maturation markers on DCs, an effect that is lost in the cancer setting.**

A-D) Expression of DC maturation markers including CD80, CD83, CD86 and co-expression of CD80+CD86+ following exposure to adipose conditioned media in combination with BSA Control (C), Oleic Acid (OA) or Palmitic Acid (PA) derived from non-cancer and cancer patients.

(To assess fatty acid treatment in non-cancer and cancer cohorts Friedman test with Dunn's correction was used, to assess the difference between non-cancer compared with cancer cohorts Kruskal Wallis test with Dunn's correction was used) All data expressed as mean ± SEM, non-cancer $n = 6$, cancer $n = 12$, * $p < 0.05$, ** $p < 0.01$, *** $p < 0.001$.

### 3.4.5 *Macrophages exposed to the adipose secretome of cancer patients treated with palmitic acid show decreased pro-inflammatory M1-like and increased anti-inflammatory M2-like markers.*

The paradoxical roles of Mϕ in the tumour microenvironment have been reported to play a pivotal role in antigen presentation and anti-tumour immunity. To assess what influence PA and OA treatments on the adipose secretome have on Mϕ polarisation, Mϕ were cultured in these treated ACM with typical pro-inflammatory and anti-inflammatory associated polarisation markers assessed via flow cytometry.

Non-cancer vs Cancer

Control ACM from non-cancer patients showed decreased Mϕ expression of HLA-DR, CD80, CD86, CD80+CD86+, CD163, CD206, CD163+CD206+, and increased Mϕ expression of CD68 compared with Mϕ treated with control ACM from OAC patients.

OA treated ACM from non-cancer patients showed increased Mϕ expression of CD68 and CD11b compared with Mϕ cultured with OA treated ACM from OAC patients.

PA treated ACM from non-cancer patients showed decreased Mϕ expression of HLA-DR, CD86, CD163, CD163+CD206+ and increased Mϕ expression of CD68 compared with Mϕ cultured with PA treated ACM from OAC patients (**Figure 3.4.14, 3.4.15**).

Non-cancer

OA treated ACM from non-cancer patients showed increased Mϕ expression of CD11b, and CD206 compared with matched control ACM treated Mϕ. OA treated ACM from non-cancer patients also showed increased Mϕ expression of CD11b, HLA-DR, and CD163 compared with Mϕ cultured with PA treated ACM from non-cancer patients (**Figure 3.4.14, 3.4.15**).

Cancer

PA treated ACM from OAC patients showed decreased Mϕ expression of CD80, and C80+CD86+ and increased expression of CD206, and CD163+CD206+ compared with matched control ACM treated Mϕ. PA treated ACM from OAC patients also showed decreased Mϕ expression of CD80 compared with Mϕ cultured with OA treated ACM from OAC patients (**Figure 3.4.14, 3.4.15**).

Cancer non-obese vs obese

Within the cancer cohort PA treatment on ACM derived from non-obese OAC patients significantly decreased Mϕ expression of CD80 compared with Mϕ cultured with OA treated ACM from non-obese OAC patients. PA treated ACM derived from non-obese OAC patients significantly decreased Mϕ expression of CD86 compared with Mϕ cultured with PA treated ACM from obese OAC patients. Also, within the cancer cohort PA treated ACM derived from non-obese OAC patients significantly increased Mϕ expression of CD206 compared with Mϕ cultured with PA treated ACM from obese OAC patients (**Figure 3.4.16**).

(* $p < 0.05$, ** $p < 0.01$, *** $p < 0.001$.)

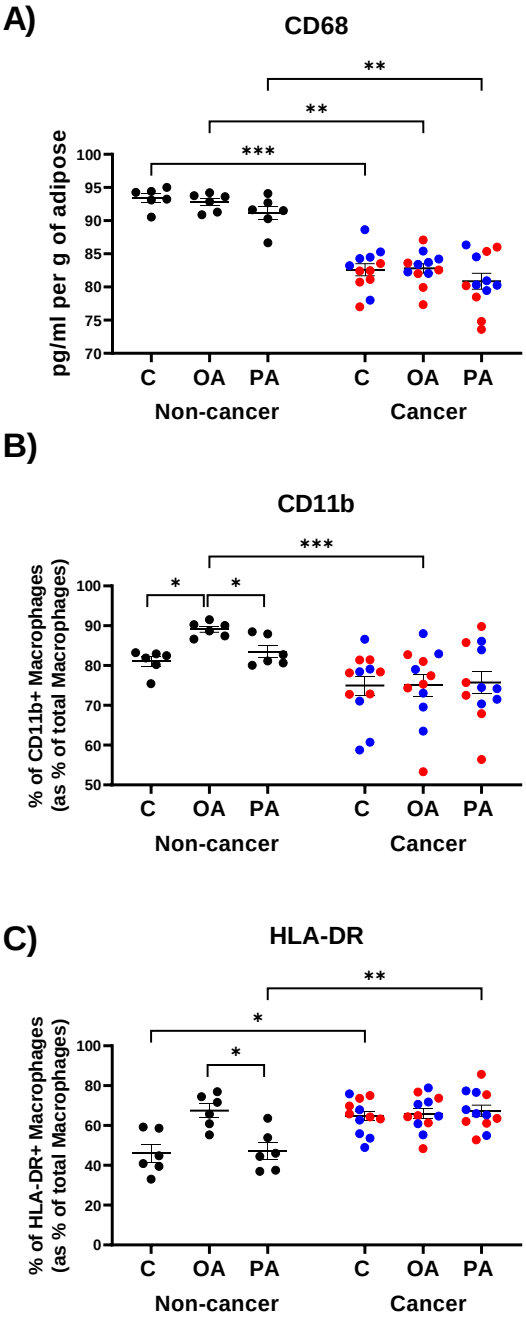


**Figure 3.4.14 The adipose secretome of non-cancer patients treated with oleic acid increases phenotypic markers of Mϕ, an effect that is lost in the cancer setting.**

A-C) Expression of Mϕ phenotypic markers including CD68, CD11b, and HLA-DR following exposure to adipose conditioned media in combination with BSA Control (C), Oleic Acid (OA) or Palmitic Acid (PA) derived from non-cancer and cancer patients.

(To assess fatty acid treatment in non-cancer and cancer cohorts Friedman test with Dunn's correction was used, to assess the difference between non-cancer compared with cancer cohorts Kruskal Wallis test with Dunn's correction was used) All data expressed as mean ± SEM, non-cancer $n$ = 6, cancer $n$ = 12, * $p < 0.05$, ** $p < 0.01$, *** $p < 0.001$.

● symbols = non-obese OAC patients, ● symbols = obese OAC patients.

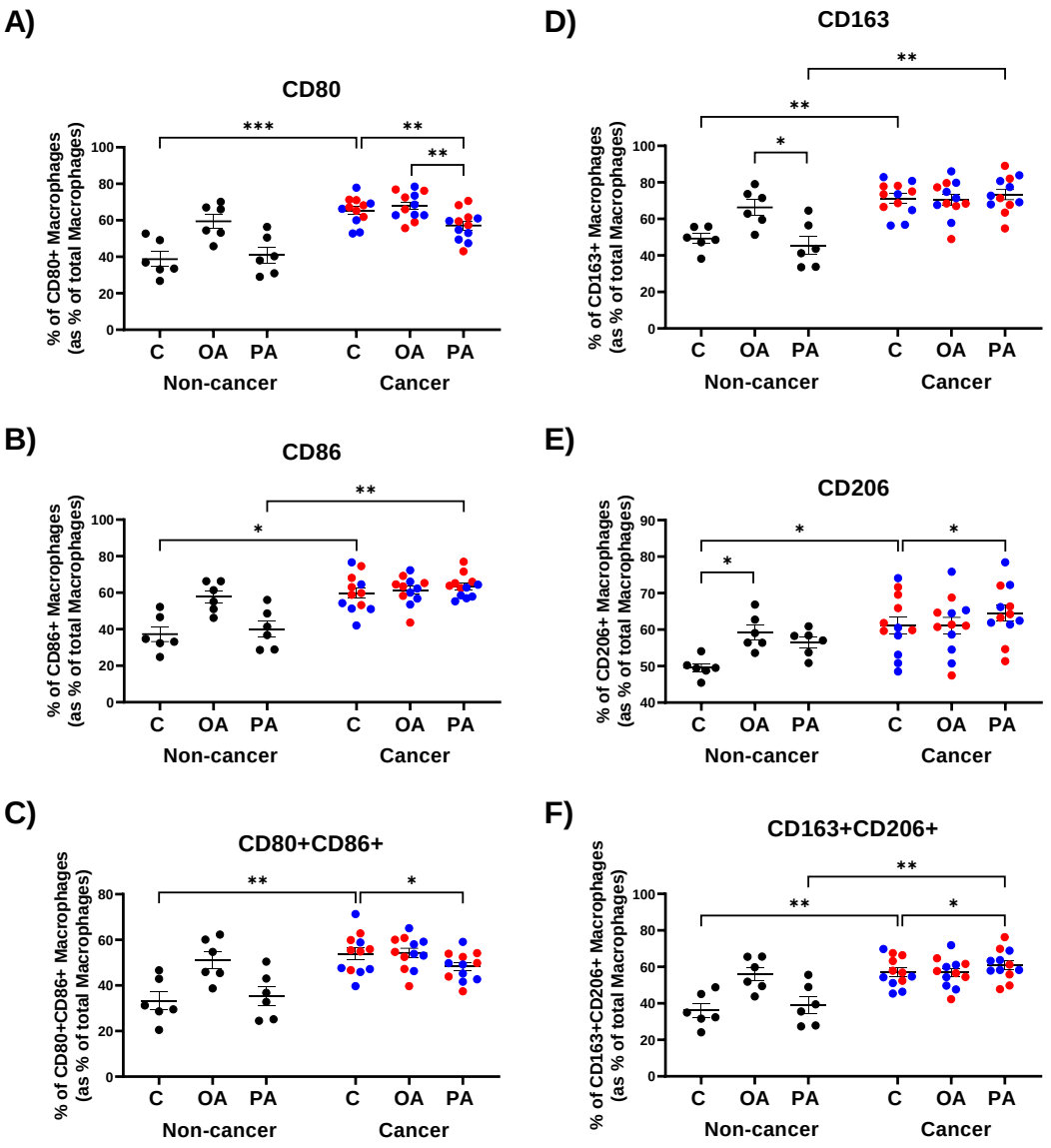


**Figure 3.4.15 The adipose secretome of cancer patients treated with palmitic acid decreases pro-inflammatory and increases anti-inflammatory markers on Mϕ.**

A-F) Expression of Mϕ polarisation markers including pro-inflammatory associated markers CD80, CD86, co-expression of CD80+CD86+, and anti-inflammatory associated CD163, CD206, co-expression of CD163+CD206+ following exposure to adipose conditioned media in combination with BSA Control (C), Oleic Acid (OA) or Palmitic Acid (PA) derived from non-cancer and cancer patients.

(To assess fatty acid treatment in non-cancer and cancer cohorts Friedman test with Dunn's correction was used, to assess the difference between non-cancer compared with cancer cohorts Kruskal Wallis test with Dunn's correction was used) All data expressed as mean ± SEM, non-cancer $n = 6$, cancer $n = 12$, * $p < 0.05$, ** $p < 0.01$, *** $p < 0.001$.

● symbols = non-obese OAC patients, ● symbols = obese OAC patients.

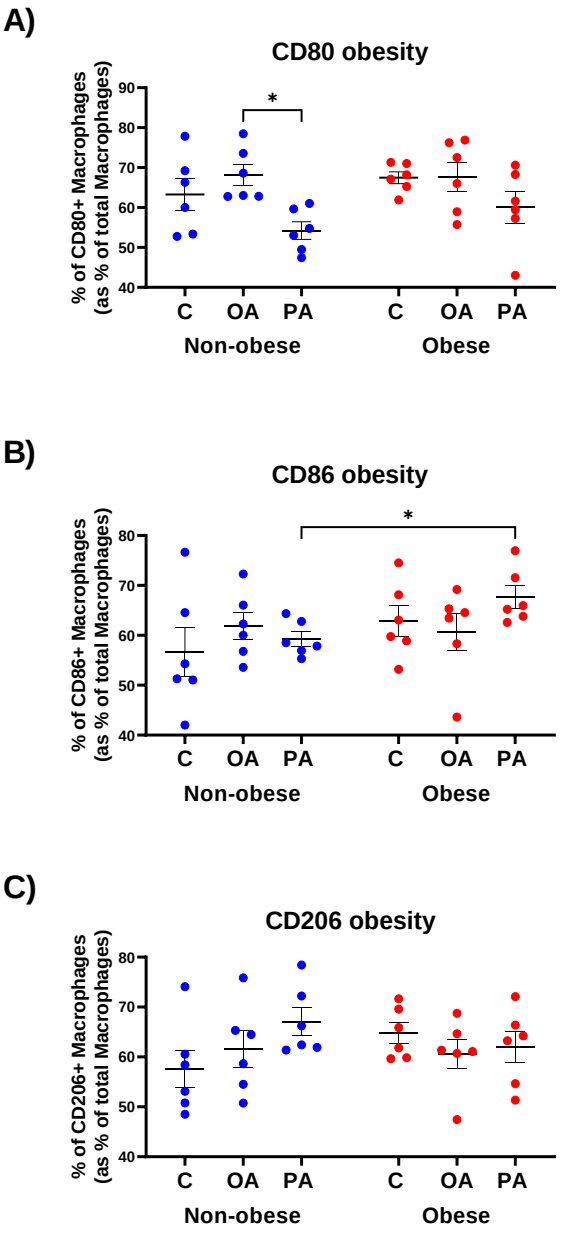


**Figure 3.4.16 The adipose secretome of non-obese and obese cancer patients treated with palmitic induces differential expression of decreases pro-inflammatory and increases anti-inflammatory markers on Mϕ.**

A-C) Expression of Mϕ polarisation markers including pro-inflammatory associated markers CD80, CD86, and anti-inflammatory associated CD206 following exposure to adipose conditioned media in combination with BSA Control (C), Oleic Acid (OA) or Palmitic Acid (PA) derived from non-obese and obese OAC cancer patients.

To assess fatty acid treatment in non-obese cancer and obese cancer cohorts Friedman test with Dunn's correction was used, to assess the difference between non-obese cancer compared with obese cancer cohorts Kruskal Wallis test with Dunn's correction was used. All data expressed as mean ± SEM, non-cancer $n = 6$, cancer $n = 12$, * $p < 0.05$, ** $p < 0.01$, *** $p < 0.001$.

● symbols = non-obese OAC patients, ● symbols = obese OAC patients

### 3.5 Summary of main findings

- PA diminishes OCR metabolism in adipose explants derived from cancer patients but not in non-cancer patients.
- The diminishing effect of PA on adipose utilisation of OCR metabolism are more apparent in obese OAC patients than non-obese OAC patients.
- PA promotes an immunosuppressive effect on the adipose secretome which is most apparent in adipose tissue from cancer patients.
- The obesity status of OAC patients differentially effects adipose tissue response to the immunosuppressive influence of PA.
- Maturation levels of DCs is significantly inhibited by the adipose secretome of non-cancer patients treated with palmitic acid. The adipose secretome of cancer patients promotes expression of immunoinhibitory markers compared with non-cancer patients.
- Mϕ exposed to the adipose secretome of cancer patients treated with palmitic acid show decreased pro-inflammatory M1-like and increased anti-inflammatory M2-like markers.
- The obesity status of OAC patients' effects Mϕ response to PA treatment stimulating differential expression of pro-inflammatory and anti-inflammatory markers.

### 3.6 Discussion

Adipose tissue is regarded as an immunosuppressive environment, that recruits immune cells and deleteriously impairs their functionality [81–85]. This study for the first-time reports that exogenous PA treatment on adipose tissue diminishes metabolic profiling and enhances an immunosuppressive secretome. Furthermore, Mϕ cultured in this PA treated adipose secretome showed increased expression of anti-inflammatory markers which may play a significant role in potentiating anti-tumour immunity.

PA has previously been identified to cause mitochondrial dysfunction using in vitro models, an effect that has not been seen with OA [402,403]. In our study, PA treatment significantly decreases the OCR profile of adipose tissue from cancer patients compared to untreated controls and OA treatment. This was coupled with decreased ECAR profiles. Neither of these treatment effects were mirrored in adipose explants derived from non-cancer patients. However, PA treatment significantly decreased OCR and ECAR profiles in OAC adipose explants compared with adipose tissue from non-cancer patients. Moreover, OCR was increased in the most viscerally obese of OAC patients compared with non-obese OAC patients, an effect significantly decreased by PA treatment. Collectively, this may indicate that adipose tissue from cancer patients particularly obese OAC patients may have aberrant biological functionality that is more effected by PA treatment. Previously our lab has identified decreased secreted levels of glutamine in obese OAC patients. Glutamine oxidation has been identified to maintain the TCA cycle during impaired mitochondrial functioning [404] which may be caused by PA treatment, thus leading to these diminished metabolic outputs.

As previously mentioned, fatty acid levels in circulation and within adipose tissue have also been reported to be abrogated by obesity. One of the most common saturated fatty acids found in the human body is PA, which has been observed to be increased in circulation in obese patients [68], however its expression at tissue level is tightly regulated. In contrast OA one of the most commonly found monounsaturated fatty acid in the human body has previously been reported to be increased in adipose tissue of obese mouse models [69]. This increase with OA has also been associated with a corresponding increase in Δ 9 desaturated lipids [69] which is catalysed by Stearoyl-CoA desaturase (SCD1) supported by ELOLV6, with OA being its main product [70,71]. These findings may also suggest that adipose tissue that has been treated with PA is actively undergoing fatty acid synthesis, catalysing this exogenous PA into OA, which may account for the diminished levels of OCR observed in the cancer setting. It has been reported that cancer stimulates the release of fatty acids to support its growth, proliferation, and metastasis [405]. Therefore, it could be postulated that adipose tissue from cancer patients may have diminished

fatty acid levels, which could promote fatty acid synthesis to compensate for this loss and could explain why this effect is not apparent in the adipose tissue of non-cancer patients.

The pro-inflammatory action of PA has been widely reported [65,284]. PA has many downstream effects on cancer and immune cells increasing IL-6, IL-1β, TNF-α and priming for pro-inflammatory immune responses [65]. However, adipose tissue has been reported to be immunosuppressive with deleterious downstream effects for immune cells [81–83]. Within this study, PA has been identified to have extensive immunosuppressive effects on adipose tissue derived from non-cancer patients and even more apparently in adipose tissue from OAC patients. PA treatment on adipose tissue from non-cancer patients significantly decreased Eotaxin-3, IL-4, IL-6, IL-13, MCP-1, MCP-4, and MDC compared to either matched control or OA treated ACM from non-cancer patients. Within the PA treated adipose secretome of OAC patients decreased secreted levels of IL-1β, IL-2, IL-4, IL-6, IL-10, IL-13, MCP-1, MDC, MIP-1α, MIP-1β, MIP-3α, and TNF-α were observed compared with control and OA treated adipose secretome of OAC patients. Eotaxin-3 was also observed to be decreased in the PA treated adipose secretome compared with control ACM from OAC patients. PA has been reported to induce the production of Reactive oxygen species(ROS) [406]. The induction of ROS in pre-adipocytes has been shown to impar proliferation, whilst in mature adipocytes ROS reduces oxygen consumption and blocks fatty acid oxidation, leading to lipid accumulation [407,408]. Increased oxidative stress in adipocytes has previously been linked to decreased secretion of adipokines [56], which may contribute to the diminished inflammatory outputs seen within our study. However reports have indicated that immunosuppressive cells such as tumour associated macrophages and myeloid derived suppressor cells have greater reliance on fatty acid oxidation(FAO) [409]. PA is a key fuel for FAO which could be utilised in the cancer microenvironment to perpetuate an immunosuppressive milieu diminishing anti-tumour immunity.

This study further reports that within the adipose secretome of non-cancer patients control ACM and PA treated ACM were both observed to have higher secreted levels of IL-1β compared with matched OA treated ACM. This effect was not mirrored in the cancer setting. Previous research has indicated that OA should possess inhibitory effects of IL-1β secretion in cells including macrophages [410]. However, the differential effects observed in the adipose secretome of OAC patients compared with non-cancer patients does require further research to further understand how this adipose secretome could perpetuate cancer development and progression. Particularly, this study reports increased secreted levels of IL-13 and decreased levels Eotaxin-3, IL-2, and IL-17A in the adipose secretome of OAC patients compared with non-

cancer patients, regardless of fatty acid treatment. IL-13 is a pleiotropic cytokine and more recently has been linked to diminished tumour immune surveillance as well as increasing invasion and metastasis [411]. It has also been reported to promote anti-inflammatory macrophage differentiation in adipose tissue [412] which could ameliorate low grade inflammation in obese adipose tissue but also attenuate anti-tumour immunity in the wider tumour microenvironment. IL-17a has been linked to augmenting adipose tissue inflammation and promoting cancer progression [271,413]. Eotaxin-3 and IL-2 play critical roles in immune cell activation and recruitment. Previous work from our lab has identified that obese adipose OAC tissue has decreased secreted levels of Eotaxin-3, whilst increased circulating levels of this cytokine have been linked with better overall survival in OAC patients [232]. The depleted levels of these cytokines in the adipose secretome of OAC patients compared with non-cancer patients poses interesting questions on how these cytokines levels have been altered so dramatically. Additionally, this study reports increased levels of IL-10 and MCP-4 in the control and OA treated ACM of OAC patients compared with matched non-cancer ACM. Both of these pleiotropic cytokines have been reported to possess potent anti-inflammatory effects, recruiting immune cells to resolve inflammation and hindering effective anti-tumour immunity [414,415]. However, further research is required to assess if these cytokines levels are affected by cancer progression or secreted into the wider tumour microenvironment which may enhance immune cell recruitment to adipose tissue leading to diminished functionality [312].

As previously mentioned, obesity is linked to a low-grade chronic inflammatory state. Within this study, the PA treated adipose secretome from non-obese OAC patients showed decreased secretion of Eotaxin, Eotaxin-3, GM-CSF, IFN-γ, IL-1Ra, IL-1α, IL-2, IL-4, IL-6, IL-10, IL-12p70, IP-10, MDC, MIP-1β, MIP-3α, TNF-α, and TSLP compared with matched control or OA treated ACM. In the obese setting similar decreases were observed for some of these analytes following PA treatment except Eotaxin, Eotaxin-3, IL-1Ra, IL-4, IL-6, IL-12p70, IP-10, and MDC. Many of these cytokines and chemokines are involved in recruitment of immune cells [329,416–418], mitigating inflammatory response [419] as well as activating NK and T cells [420]. The decreased secreted levels of these analytes following PA treatment in non-obese but not in the obese adipose tissue poses an interesting question as to how the obese adipose microenvironment may be more resistant to these immunosuppressive changes. Obesity and adipose tissue have previously been implicated in sequestering and diminishing the functionality of a series of immune cells [421], particularly in the cancer setting [422]. This postulates the question if a stunted response to the immunosuppressive of PA treatment could be due aberrant tolerance within adipose tissue to exogenous levels fatty acids. Additionally, IL-1β was observed to be significantly decreased by

PA treatment in the obese OAC adipose secretome compared with control and OA treatment. PA has typically been reported to increase IL-1β secretion in DCs and Mϕ [65,423], this dysfunctional response could be related to the altered secretome accompanying increased visceral adiposity.

Overall, PA seems to propagate an immunosuppressive environment within the adipose secretome which may hold implications for immune cell function within visceral adipose depots and the wider tumour microenvironment. Adipose tissue has been widely reported to recruit and sequester immune cells whilst diminishing their functionality [81–83], potentially through aberrant secretions of inflammatory mediators. This study reports that DCs cultured with PA treated ACM from non-cancer patients decreased expression of a series of maturation and functional markers including CD80, CD86, HLA-DR, CD11c, CD40, and CD54 compared with OA treated ACM. PA seems to propagate an immunosuppressive effect in the adipose secretome of non-cancer patients that significantly decreased DC maturation and functionality. However, ACM derived from OAC patients regardless of PA treatment demonstrated no significant difference compared to control OAC ACM on DC maturation levels. Potentially this could be linked to earlier findings, where the PA treated adipose secretome in cancer patients promotes an immunosuppressive environment. Or it could be indicative of the altered underlying biology of adipose tissue in cancer patients, which has been reported to be transformed to support the development of premetastatic niches to aid tumour growth and immune evasion [307]. Previous research has shown that DCs from cancer patients have higher amounts of triglycerides than non-cancer patients, which negatively impacted DCs antigen presenting and T-cell stimulating capabilities [282]. Further research is required to interrogate how cancer progression modulates adipose tissue secretome, its reaction to PA treatment and what downstream effects this poses for DCs maturation and FAO in DCs. Additionally, this study observed that DCs cultured in OA treated ACM from OAC patients showed decreased expression of CD54 compared matched control ACM and non-cancer OA treated ACM. OA has previously been identified to decrease CD54 expression in human aortic endothelial cells [67] and recent research has shown that whilst CD54 is necessary to maintain adhesions with CD8 T-cells this is not required for cytotoxic and central memory lymphocytes [424].

DCs cultured in ACM from OAC patients, regardless of fatty acid treatment, showed decreased expression of CD83 compared with ACM from non-cancer patients. However, DCs cultured with OA treated ACM from OAC patients did significantly increase CD83 compared with matched control ACM. CD83 is a characteristic marker of activated DCs and increased expression of CD83+ tumour infiltrating DCs has been associated with increased overall survival [425]. This

diminished expression of CD83 on DCs following exposure to OAC ACM may play a role in potentiating anti-tumour immunity but more research in this field is required. Within this study increased expression of TIM-3 was reported in DCs cultured with control and palmitic acid treated ACM from OAC patients compared with similarly treated ACM from non-cancer patients. Tim-3 expression on DCs has been reported to inhibit antitumour immunity by inhibiting inflammasome activation [426]. Furthermore, this study reports increased expression of PD-L1 on DCs cultured with ACM from OAC patients compared with ACM from non-cancer patients regardless of fatty acid treatment. PD-L1 expression on DCs has been shown to attenuate T cell activation [427]. It is of interest to note that ACM derived from OAC patients significantly increases the expression of these markers that attenuate anti-tumour immunity, an effect that is not seen in DCs treated with ACM from non-cancer patients.

Mϕ have been denoted as a key effector cell in propagating inflammation in adipose tissue microenvironment, particularly in obesity [244]. Within this study, Mϕ cultured with OA treated ACM from non-cancer patients showed increased expression of CD11b, HLA-DR, and anti-inflammatory associated markers CD163 and CD206 compared to either matched control or PA treated ACM. Previous reports have identified dietary OA increases anti-inflammatory marker CD206 on Mϕ in adipose tissue [285] and OA has also been reported to increases CD163 at a protein level in Mϕ [428]. However, in the cancer setting, Mϕ cultured with PA treated ACM showed decreased expression of pro-inflammatory associated markers CD80 and CD80+CD86+, and increased expression of anti-inflammatory associated markers CD206 and CD163+D206+ compared with matched control ACM. Further to this, Mϕ cultured with PA treated ACM from OAC patients showed increased expression of HLA-DR, CD163, CD163+CD206+ compared with Mϕ cultured in non-cancer PA treated ACM. These contradictory effects on Mϕ polarisation mirrors the findings in DCs within this study, where the influence of PA treatment on the adipose secretome of non-cancer and cancer patients have paradoxical effects. This further augments the postulation that PA treatment in the adipose secretome of OAC patients primes for an immunosuppressive environment which would be aided by anti-inflammatory M2-like Mϕ phenotype.

Furthermore, the complexities of ACM derived from OAC patients can particularly be seen when comparing Mϕ expression of polarisation markers compared against Mϕ cultured in non-cancer ACM. Mϕ cultured in control ACM from OAC patients had increased expression of HLA-DR, CD80, CD86 CD80+CD86+ CD163, CD206, CD163+CD206+ compared with Mϕ cultured in control ACM from non-cancer patients. ACM derived from OAC patients appears to enhance expression of anti and pro-inflammatory associated makers on Mϕ due to increases of anti and pro-

inflammatory associated cytokines including IL-10, IL-13 and TNF-α. IL-10 and IL-13 have both been reported to enhance M2-like Mϕ [235,429] and TNF-α is known to aid polarisation and be expressed by M1-like Mϕ [430] as well as negatively regulating M2 expression [431]. This shows a conflicting dynamic that is being driven by dysregulated ACM derived from OAC patients, that could potentiate anti-tumour efficacy.

Within the cancer cohort, Mϕ cultured with PA treated ACM from non-obese OAC patients showed decreased expression of CD80 and increased expression of CD206 compared to matched OA treated ACM and control ACM, respectively. Mϕ cultured in PA treated ACM from non-obese patients showed decreased expression of CD86 compared with Mϕ cultured in PA treated ACM from obese OAC patients. The decreased expression of pro-inflammatory M1 markers and increased expression of anti-inflammatory markers observed in Mϕ cultured with PA treated ACM from non-obese OAC patients may be indicative of the underlying biological changes obesity has on adipose tissue. The absence of the low grade chronic inflammatory state associated with obesity may make the adipose tissue derived from non-obese OAC patients more responsive to the immunosuppressive effects of PA treatment. This hypothesis could be further strengthened by the finding that PA treated ACM from obese OAC patients significantly increased CD86 expression on Mϕ compared to those cultured in PA treated ACM derived from non-obese OAC patients. M1 macrophages are known to increase in obesity [432], with the possibility that the ACM derived from obese OAC patients may be more amenable to M1 polarisation.

Conclusively, this study has indicated that exogenous PA treatment possesses differential effects on adipose tissue metabolism, significantly decreasing metabolic profiles of adipose tissue explants derived from OAC patients. PA treatment can also be observed to have a significant immunosuppressive effect on the adipose secretome of both non-cancer and OAC patients, with key anti-inflammatory cytokines being significantly decreased in the adipose secretome of OAC patients compared with non-cancer patients. PA treatment in the adipose secretome also lead to the observation of paradoxical effects on DC maturation and Mϕ polarisation between OAC and non-cancer patients. This study has shown for the first time that exogenous fatty acids in the adipose microenvironment could lead to detrimental immunosuppressive effects that could potentiate anti-tumour immunity and aid cancer progression.

*Chapter 4*

# *The differential influences of oleic and palmitic acid on the metabolism and secretome of adipose tissue explants of patients with oesophageal adenocarcinoma is augmented by increasing radiation.*

## 4.1 Objective and specific aims:

**Objective:**

The overall objective of this chapter was to assess whether increasing irradiation would affect the influence of exogenous fatty acids on immuno-metabolic profiles of adipose explant oesophageal cancer patients using real-time metabolic profiles and multiplex ELISA. As well as determining whether these altered immuno-metabolic profiles were influenced by increased visceral adiposity. This chapter further looks to assess how increasing irradiation and alterations in these treated adipose secretome effect immune cell function.

**Specific Aims**

- To assess metabolic profiles including oxidative phosphorylation and glycolysis of adipose explants derived from cancer patients in real time following culture with dietary fats Oleic Acid (OA) and Palmitic acid (PA) in combination with increasing irradiation.
- To assess the secreted profiles of these adipose explants for mediators of inflammation, metabolism, angiogenesis, and immune response and whether increasing irradiation effects the influence of OA and in particular the immunosuppressive nature of PA.
- To determine whether obesity differentially effects the metabolic and secreted profiles of adipose explants derived from cancer patients in response to OA and PA treatment combined with increasing irradiation.
- To evaluate whether the adipose secretome of cancer patients treated with OA and PA once combined with increasing irradiation influences dendritic cell (DC) expression of maturation markers, and whether this is altered by obesity.
- To evaluate whether the adipose secretome of cancer patients treated with OA and PA once combined with increasing irradiation influences macrophage (Mϕ) polarisation towards a pro-inflammatory (M1-like) or anti-inflammatory (M2-like) phenotype, and whether this is altered by obesity.

## 4.2 Introduction

Radiation therapy is one of the most commonly used modalities of therapy used to treat solid cancers. Radiation has been shown to deleteriously effect adipose tissue leading to a reduction in proliferating cells, increase in apoptotic cells and altering the hematopoietic population [433]. Further to this, adipocytes have been reported to have increased lipid accumulation following high dose radiation [434]. It has been reported that cancer cells promote free fatty acid release from pre-adipocytes in to form pre-metastatic niches and aid gastric cancer metastasis [435]. One such fatty acid is palmitic acid (PA) which has been reported to be increased in circulation with obesity and with cancer patients [399,436]. Oesophageal adenocarcinoma is one of the most closely associated cancers with obesity associated with poor prognosis and a five year survival of approximately 20% [7]. Currently the standard of care for treatment involves neoadjuvant treatment with either chemotherapy alone or combination chemoradiotherapy for locally advanced tumours [19]. Unfortunately, only approximately 30% of patients show a complete response to these current treatment modalities, leaving a large proportion of patients with no therapeutic gain and a possible delay to surgery [309,310].

Metabolism and mitochondrial pathways have been highlighted to affect the efficacy of radiotherapy by inducing radio-resistance in cancer cells [190]. Previously we have seen aberrant adipose tissue metabolism in OAC patients associated with a series of clinical factors including obesity, metabolic dysfunction and in relation to treatment response. Research has indicated that the adipocyte secretome increases cancer cell metabolism and confers cancer cells with enhanced survival and resistance to radiation induced oxidative stress [177]. On a cellular level many of the factors that have been suggested to enhance radio-resistance are associated with adipose secretome. One effect of the adipocyte secretome that is highly exploited by cancer cells, is adipocytes' ability to secrete factors that can alter the pro-inflammatory landscape of the tumour environment [181]. The adipocyte secretome of obese patients in known to be in a low-grade chronic state of inflammation, which has also been suggested to aid cancer cell survival by enabling protective mechanisms to allow them to evade the toxicity of radiotherapy [231].

Adipose tissue has been reported to recruit immune cells whilst having deleterious effects on their function which can potentiate anti-tumour immunity [81–85]. However, radiation therapy through its induction of radiation induced inflammation has been reported to promote anti-tumour immunity [434,437]. In particular, macrophages have been reported to play a vital role in radiation induced inflammation inducing an anti-tumour immunity response through the generation of an inflammatory response promoting classical activation and increased

expression of pro-inflammatory mediators [247]. We have reported that PA and Oleic Acid (OA) illicit differential secretion of inflammatory mediators from adipose tissue, these factors directly affect the antigen presenting abilities and polarisation of cells like Dendritic Cells (DCs) and Macrophages (Mϕ) [236]. Increased free fatty acids, which have been reported in obesity, have been shown to enhance Mϕ polarisation towards M1-like phenotype [283]. Further to this free fatty acids have also been shown to lead to lipid -loaden DCs with diminished antigen presenting capabilities and reduced capacity to effectively stimulate T cells [282].

This study for the first time looks to investigate if adipose tissue from non-obese (n=6) and obese(n=6) OAC patients have differential metabolic and secreted inflammatory profiles and whether exposure to increasing radiation alters these profiles. As well as examining whether the addition of exogenous fatty acids including PA and OA differentially alter metabolic preferences or secretome of these adipose explants with or without increasing radiation. Further to this, this study aims to assess how these treated adipose secretome exposed to increasing radiation effect dendritic cells (DCs) maturation and macrophage (Mϕ) polarisation and again whether this is affected by increasing visceral adiposity.

## 4.3 Materials and Methods

### 4.3.1 *Ethics Statement and Patient Recruitment*

Ethical approval was granted by the St James's Hospital/AMNCH ethical review board (Ethics number: REC_2019-07 List 25(27)) and written informed consent was collected from all patients in this study. 12 cancer patients were recruited within the period between 3rd of April 2021 and 14th of January 2023, patient demographics are listed in Table 4.3.1. Fresh adipose tissues were taken from all patients at the start of the surgical procedure. All OAC patients were being treated with curative intent. Obesity was defined via visceral fat area (VFA) measurements with cut-off value for VFA of 163.8 $cm^2$ in males and 80.1 $cm^2$ for females as previously categorised[318] with adipose tissue from 6 obese and 6 non-obese patients being collected .

**Table 4.3.1 Clinical demographics associated with OAC patients**

| **Patient Clinical Parameters** | |
|---|---|
| **Diagnosis** | OAC = 6<br>OGJ = 6 |
| **Sex** | Male = 8<br>Female = 4 |
| **Obesity Status via Visceral Fat Area** | Obese = 6<br>Non-obese = 6 |
| **Age at diagnosis** | 55-81 (Mean = 68.5) |
| **Post-treatment BMI** | 22.34-34.29 (Mean = 27.56) |
| **Weight** | 58.4–113 kg (Mean = 77.85) |
| **Mean VFA** | 71.86–303 (Mean = 138.1) |
| **Treatment** | Naïve *n* = 5<br>FLOT *n* = 5<br>CROSS *n* = 2 |
| **Tumour Regression Grading (TRG)** | TRG 1 *n* = 3 (CROSS *n* = 2, FLOT *n* = 1)<br>TRG 2 *n* = 3 (CROSS *n* = 1, FLOT *n* = 2)<br>TRG 3 *n* = 8 (CROSS *n* = 3, FLOT *n* = 5)<br>TRG 4 *n* = 3 (CROSS *n* = 2, FLOT *n* = 1)<br>TRG 5 *n* = 3 (CROSS *n* = 0, FLOT *n* = 3) |
| **Clinical Stage (T)** | T1 *n* = 5<br>T2 *n* = 0<br>T3 *n* = 7 |
| **Clinical Stage (N)** | N0 *n* = 7<br>N1 *n* = 1<br>N2 *n* = 4 |
| **Path stage (T)** | T0 *n* = 1<br>T1 *n* = 5<br>T2 *n* = 0<br>T3 *n* = 6<br>T4 *n* = 0 |
| **Path Stage (N)** | N0 *n* = 5<br>N1 *n* = 2<br>N2 *n* = 3<br>N3 *n* = 2 |

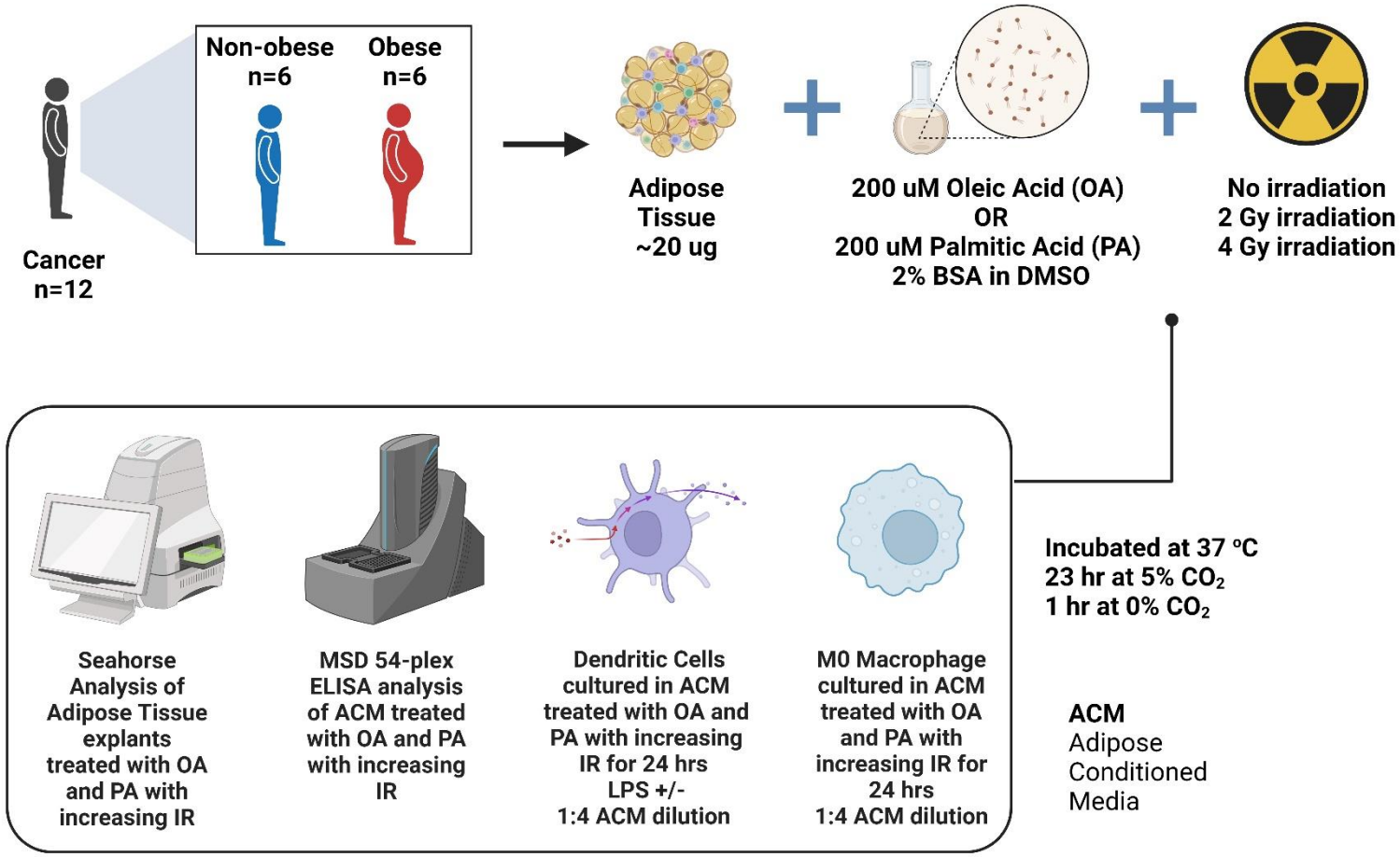


**Figure 4.3.1 Schematic of experimental methodology workflow associated with Chapter 4**

Real time metabolic and secreted profiles of adipose explants from OAC or OGJ cancer patients were assessed by Agilent seahorse, MSD multiplex ELISA following exogenous fatty acid treatment with OA And PA, with or without exposure to increasing irradiation (mock irradiated 0 Gy, 2 Gy, 4 Gy). The influence of these treated adipose secretome on dendritic cell maturation and macrophage polarisation were then assessed via flow cytometry.

### 4.3.2 *Lipid treatment*

Methodology carried out as per section *3.3.2 Lipid treatment.*

### 4.3.3 *Seahorse Analysis of metabolic profiles from adipose tissue explants and generation of Adipose Conditioned Media (ACM)*

Fresh omental tissue was collected from theatre and processed within 30 minutes by dissecting into pieces weighing approximately 20 µg. Tissue was plated in triplicates in 1 ml of M199 (supplemented with 0.1% gentamicin (Lonza, Switzerland), in a 24 well plate (Sarstedt, Germany). Adipose explants were then treated with 0.01% DMSO 2% BSA control or 200 µM OA or PA in 0.01% DMSO 2% BSA in M199. Following 2 hours incubation adipose explants were mock irradiated or irradiated at 2 or 4 Gy at a dose rate of 1.73Gy/minute (XStrahl (RS225), Atlanta, United States). Adipose explants were cultured for 24 hours at 37ºC at 5% Carbon Dioxide in a humidified incubator (Thermofisher, Massachusetts, USA). In the last hour of culture, adipose tissue and ACM was transferred to islet capture microplate with capture screens (Agilent Technologies, California, United States) and incubated in a non-CO2 incubator at 37$^{o}$C (Whitley, United Kingdom) prior to analysis. Seahorse Xfe24 analyser was used to assess metabolic profiles in adipose explants, (Agilent Technologies, California, United States) following a 12 minute equilibrate step, three basal measurements of OCR and ECAR were taken over 24 minutes consisting of three repeats of the following sequence “mix (3 min) / wait (2 min) / measurement (3 min)” to establish basal respiration. Adipose Conditioned Media (ACM) was extracted in a sterile environment and tissue weighed using a benchtop analytical balance (Radwag, Poland) and snap frozen. All samples were then stored at -80$^{o}$C for further processing.

### 4.3.4 *Multiplex ELISA*

Methodology carried out as per section *2.3.4 Multiplex ELISA.*

### 4.3.5 *Isolation of monocytes*

Methodology carried out as per section *3.3.5 Isolation of monocytes.*

### 4.3.6 *Dendritic cell culture*

Methodology carried out as per section *3.3.6 Dendritic cell culture.*

### 4.3.7 *Macrophage culture*

Methodology carried out as per section *3.3.7 Macrophage culture.*

### 4.3.8 *Flow cytometry*

Methodology carried out as per section *3.3.8 Flow cytometry*

### 4.3.9 *Statistical analysis*

All statistics were conducted using GraphPad Prism 9.5 (GraphPad Software, California, United States). A significance level of $p<0.05$ was used in all analysis and all p-values reported were two-tailed. Friedman testing with Dunn's post hoc correction, was employed for non-parametric testing between paired cohorts (Control vs. OA vs. PA within the non-cancer cohort and Control vs. OA vs. PA within the cancer cohort). For statistical testing between unpaired non-parametric cohorts, Kruskal Wallis test with Dunn's correction was used (Control/OA/PA non-cancer vs Control/OA/PA cancer. and between fatty acids treatments in non-obese and obese cancer cohorts). Details of specific statistical tests are given in each corresponding figure legend.

## 4.4 Results

### 4.4.1 *PA treatment alters OCR metabolism in adipose tissue, an effect that is augmented by 4 Gy radiation and patient obesity.*

Adipose tissue explants derived from OAC patients were assessed via Agilent Seahorse Xfe24 analyser to examine the influence of OA and PA treatments on their metabolic profiles under increasing doses of radiation. The impact of obesity, classified by VFA, on the action of these fatty acids in combination with increasing radiation on adipose metabolism was also investigated using real-time metabolic parameters.

In adipose tissue explants derived from OAC patients PA treatment significantly decreased OCR profiles compared to control and OA treated adipose explants in an unirradiated setting. PA treatment was also observed to decrease OCR profiles compared to control and OA treated adipose explants following 4 Gy radiation. In adipose tissue explants derived from OAC patients PA treatment was also observed to significantly decrease ECAR profiles compared to OA treated adipose explants in an unirradiated setting (**Figure 4.4.1 A, B**).

PA treatment in unirradiated adipose tissue explants from non-obese OAC patients significantly decreased OCR compared with matched OA treatment. In unirradiated adipose explants from obese OAC patients PA treatment significantly decreased OCR levels compared to matched OA treated adipose explants. PA treatment on adipose explants exposed to 4 Gy radiation decreased OCR profiles compared with matched control adipose. Additionally increased OCR profiles were observed in unirradiated adipose explants from obese OAC patients compared with non-obese patients. OA treatment on adipose explants exposed to 4 Gy radiation significantly increased ECAR profiles compared with matched control adipose. Additionally increased ECAR profiles were observed in control adipose explants from obese OAC patients compared with non-obese patients following exposure to 4 Gy radiation (**Figure 4.4.2 A, B**).

(* $p < 0.05$, ** $p < 0.01$.)

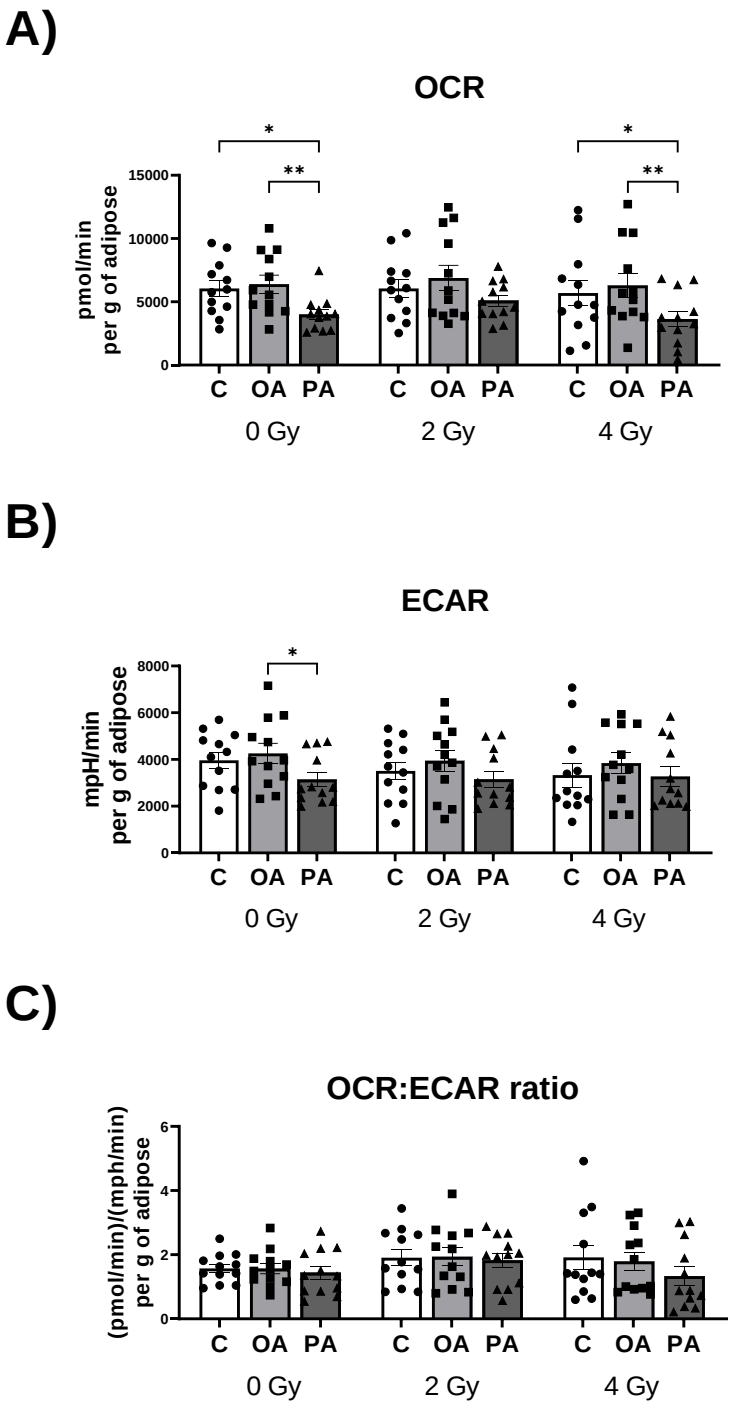


**Figure 4.4.1 The diminishing effect of palmitic acid on OCR metabolism in adipose tissue of OAC patients is augmented by high dose radiation.**

A-C) OCR, ECAR and OCR:ECAR ratio profiles of adipose tissue derived from non-obese and obese OAC cancer patients exposed to mock irradiated, 2 Gy irradiation or 4 Gy irradiation in combination with BSA Control (C = □), Oleic Acid (OA= ▒) or Palmitic Acid (PA= ■) in combination.

Friedman test with Dunn's correction, all data expressed as mean ± SEM, $n$ = 12, * $p$ < 0.05, ** $p$ <0.01.

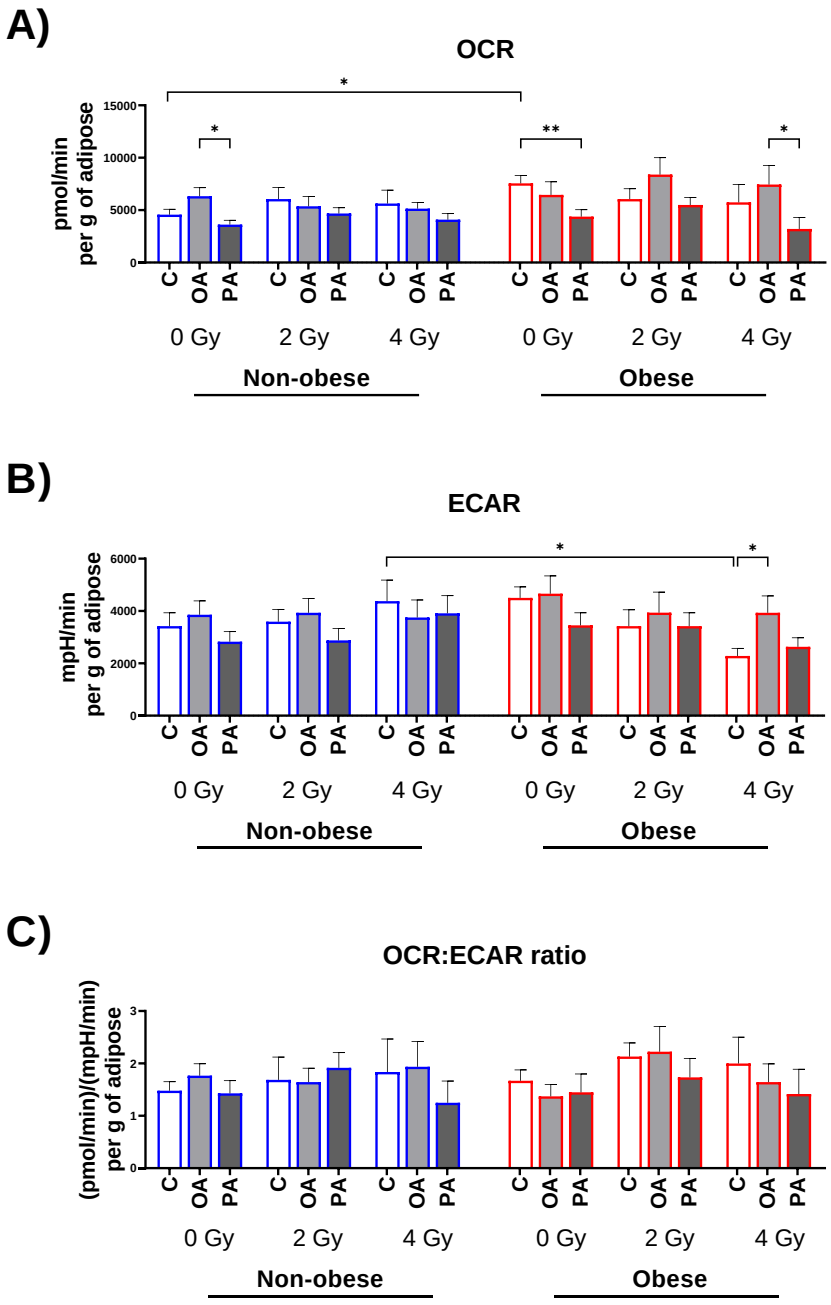


**Figure 4.4.2 The obesity status of OAC differentially effects adipose tissue metabolic response to exogenous fatty acids and increasing irradiation**

A-C) OCR, ECAR and OCR:ECAR ratio profiles of adipose tissue derived from non-obese and obese OAC cancer patients exposed to mock irradiated, 2 Gy irradiation or 4 Gy irradiation in combination with BSA Control (C = □), Oleic Acid (OA= ▒) or Palmitic Acid (PA= ■) in combination.

To assess fatty acid treatment in non-obese cancer and obese cancer cohorts Friedman test with Dunn's correction was used, to assess the difference between non-obese cancer compared with obese cancer cohorts Kruskal Wallis test with Dunn's correction was used. All data expressed as mean ± SEM, non-obese $n = 6$, obese $n = 6$, * $p < 0.05$, ** $p < 0.01$.

Blue border □ = non-obese, Red border □ = obese

### 4.4.2 *Increasing radiation enhances the immunosuppressive effects of PA treatment on the adipose secretome from OAC patients.*

As previously mentioned, the presence of PA and OA in circulation have been reported to play a role in augmenting or suppressing inflammatory mediators. In order to determine whether increasing doses of radiation augmented OA and PA treatments influence on the adipose secretome of cancer patients a 54-analyte multiplex was used to assess inflammatory mediators.

Control (0 Gy vs 2 Gy vs 4 Gy)

ACM from control adipose exposed to 2 Gy radiation showed decreased Eotaxin-3, and increased MCP-1 compared with unirradiated control adipose. Control ACM exposed to 4 Gy radiation showed decreased TNF-α and increased IL-4 compared with unirradiated adipose. Decreased secreted levels of IL-8 were observed in the control adipose secretome exposed to 4 Gy radiation compared to matched control exposed to 2 Gy radiation (**Figure 4.3.3, 4.3.5, 4.3.6**).

OA (0 Gy vs 2 Gy vs 4 Gy)

Following OA treatment in adipose explants exposed to 2 Gy radiation decreased IL-12p70 and IL-13 were observed compared with unirradiated OA treated adipose. Following OA treatment in adipose explants exposed to 4 Gy radiation decreased IL-2, and TNF-α as well as increased IL-4 was observed compared with unirradiated OA treated adipose. Decreased secreted levels of IL-8 were observed in the adipose secretome of explants treated with OA exposed to 4 Gy radiation compared to matched OA treated explants treated with 2 Gy radiation (**Figure 4.3.4 , 4.3.6**).

PA (0 Gy vs 2 Gy vs 4 Gy)

Following PA treatment in adipose explants exposed to 4 Gy radiation decreased IL-8, and increased MIP-3α, were observed compared with unirradiated PA treated adipose. Decreased secreted levels of IL-8 were observed in the adipose secretome of explants treated with PA exposed to 4 Gy radiation compared to matched PA treated explants treated with 2 Gy radiation (**Figure 4.3.4 - 4.3.5**).

Comparisons between fatty acids in the mock irradiated setting

In the unirradiated setting, the PA treated adipose secretome compared with control showed decreased expression of Eotaxin-3, GM-CSF, IFN-γ, IL-1α, IL-1β, IL-1Ra, IL-2, IL-6, IL-10, IL-13, IP-10, MDC, MIP-1β, MIP-3α, TNF-α, and TSLP (Figure 4.3.3 - 4.3.6). In the unirradiated setting, the PA treated adipose secretome compared with OA treated showed decreased expression of GM-CSF, IFN-γ, IL-1α, IL-1β, IL-1Ra, IL-2, IL-3, IL-6, IL-10, IL-12p70, IP-10, MIP-1β, TNF-α, and TSLP (**Figure 4.3.3 - 4.3.6**).

Comparisons between fatty acids following exposure to 2 Gy irradiation

Following exposure to 2 Gy radiation, the PA treated adipose secretome compared with control showed decreased expression of GM-CSF, IFN-γ, IL-1α, IL-1β, IL-1Ra, IL-2, IL-3, IL-4, IL-6, IL-10, IL-13, IP-10, MCP-1, MCP-4, MDC, MIP-1α, MIP-1β, MIP-3α, TNF-α, and TSLP (**Figure 4.3.3 - 4.3.6**).

Following exposure to 2 Gy radiation, the PA treated adipose secretome compared with OA treated showed decreased expression of GM-CSF, IFN-γ, IL-1α, IL-1β, IL-1Ra, IL-2, IL-3, IL-4, IL-6, IL-10, IL-12p70, IP-10, MCP-1, MCP-4, MDC, MIP-1α, MIP-1β, MIP-3α, TNF-α, and TSLP (**Figure 4.3.3 - 4.3.6**).

Comparisons between fatty acids following exposure to 4 Gy irradiation

Following exposure to 4 Gy radiation, the PA treated adipose secretome compared with control showed decreased expression of Eotaxin-3, GM-CSF, IFN-γ, IL-1α, IL-1β, IL-1Ra, IL-2, IL-4, IL-6, IL-10, IL-12p70, IP-10, MCP-4, MDC, MIP-1α, MIP-1β, TNF-α, and TSLP (**Figure 4.3.3 - 4.3.6**).

Following exposure to 4 Gy radiation, the PA treated adipose secretome compared with OA treated showed decreased expression of Eotaxin-3, GM-CSF, IFN-γ, IL-1α, IL-1β, IL-1Ra, IL-4, IL-6, IL-12p70, IP-10, MCP-4, MIP-1α, MIP-1β, TSLP and VEGF (**Figure 4.3.3 - 4.3.6**).

(* $p < 0.05$, ** $p < 0.01$, *** $p < 0.001$, **** $p < 0.0001$.)

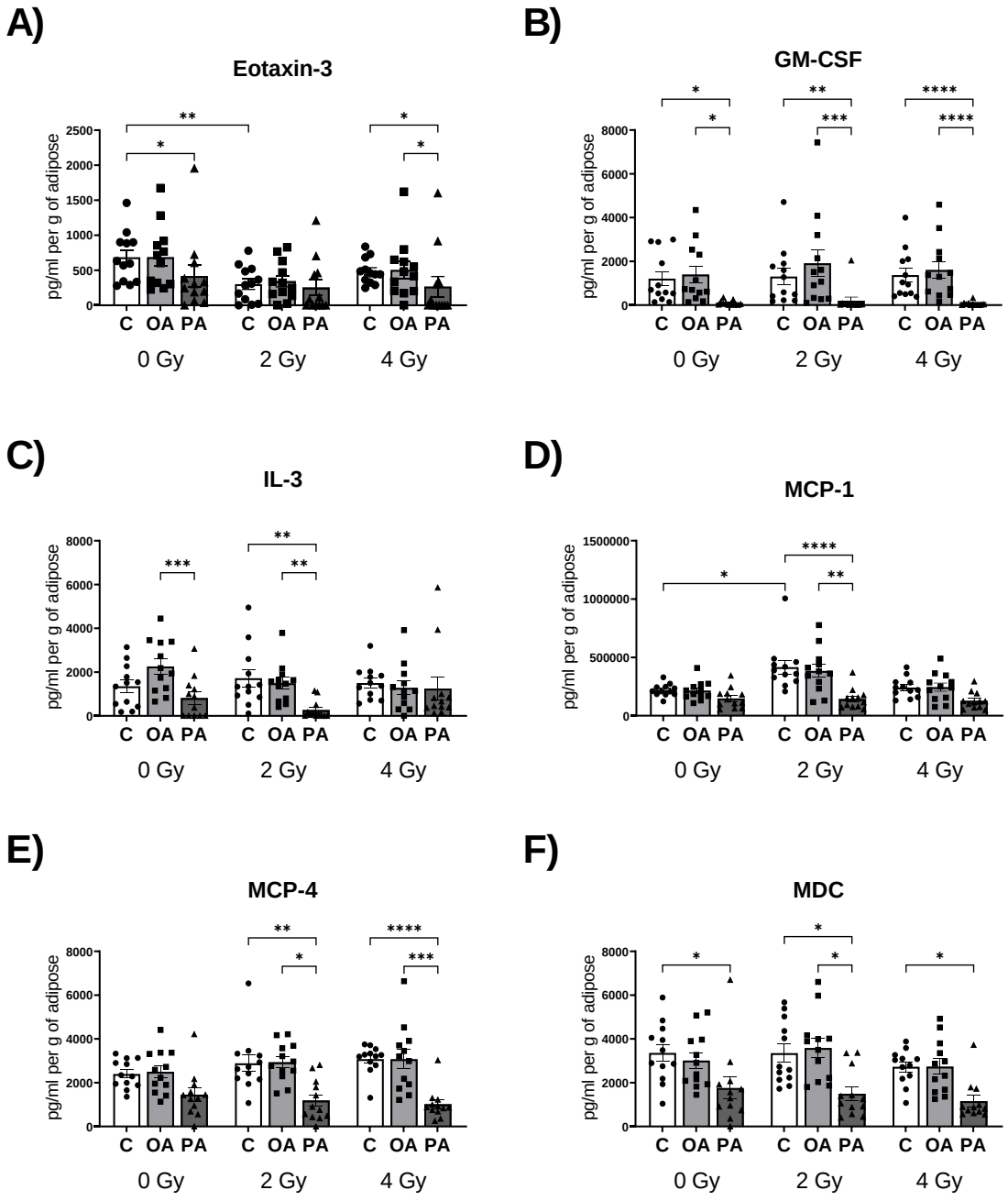


**Figure 4.4.3 Palmitic acid decreases secreted levels of mediators of immune cell recruitment in the adipose secretome of OAC patients.**

A-F) Secreted levels of Eotaxin, Eotaxin-3, GM-CSF, MCP-1, MCP-4, and MDC from adipose tissue derived from OAC cancer patients exposed to mock irradiation, 2 Gy irradiation or 4 Gy irradiation in combination with BSA Control (C = □), Oleic Acid (OA= ▒) or Palmitic Acid (PA= ■). Friedman test with Dunn's correction, all data expressed as mean ± SEM, $n$ = 12, * $p$ < 0.05, ** $p$ <0.01, *** $p$ <0.001, **** $p$ <0.0001.

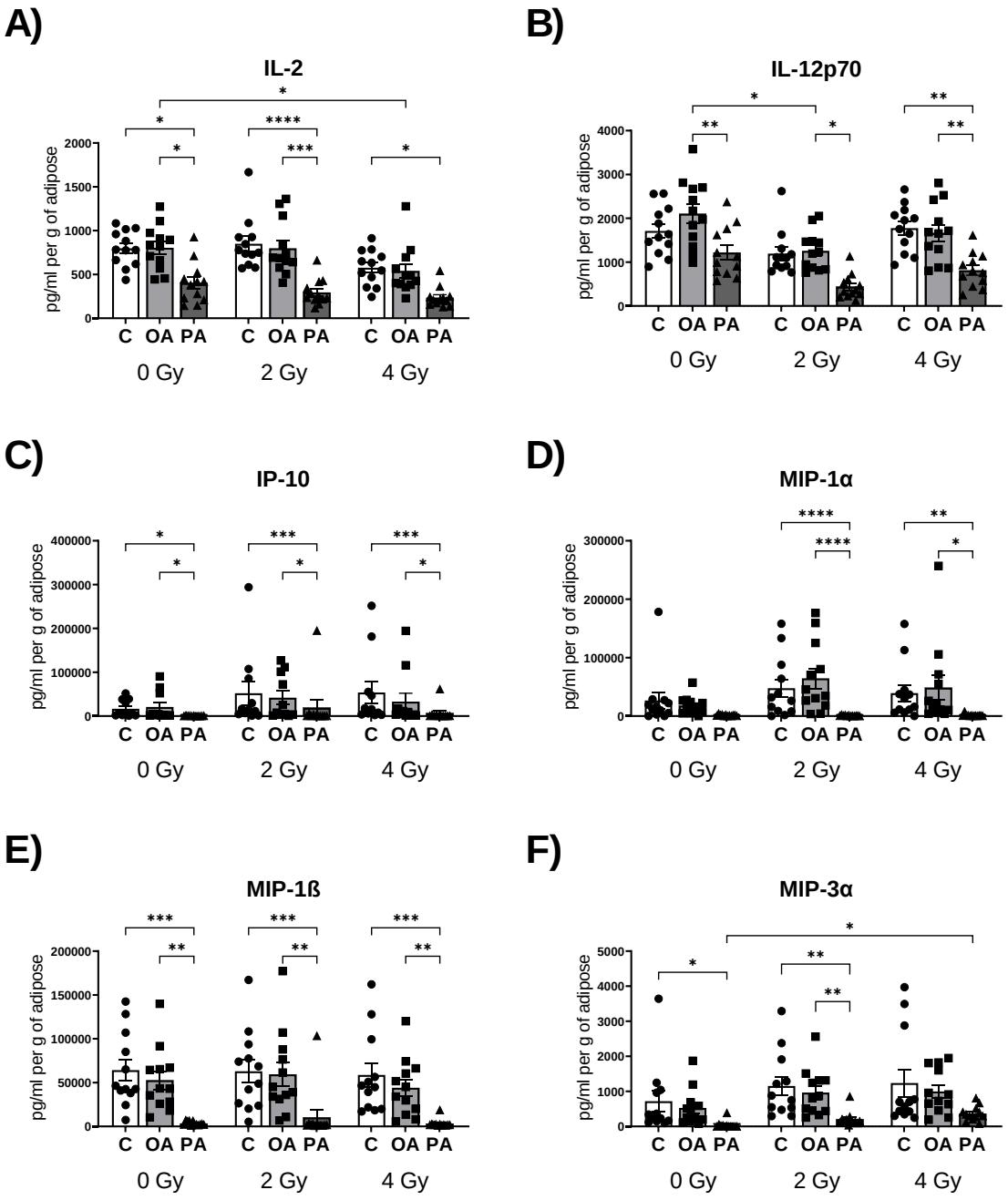


**Figure 4.4.4 Palmitic acid decreases secreted levels of factors associated with immune activation in the adipose secretome of OAC patients.**

A-F) Secreted levels of IL-2, IL12p70, IP-10, MIP-1α, MIP-1β, and MIP-3α from adipose tissue derived from OAC cancer patients exposed to mock irradiated, 2 Gy irradiation or 4 Gy irradiation in combination with BSA Control (C = ☐), Oleic Acid (OA= ▒) or Palmitic Acid (PA= ■) in combination.

Friedman test with Dunn's correction, all data expressed as mean ± SEM, $n$ = 12, * $p$ < 0.05, ** $p$ <0.01, *** $p$ <0.001, **** $p$ <0.0001.

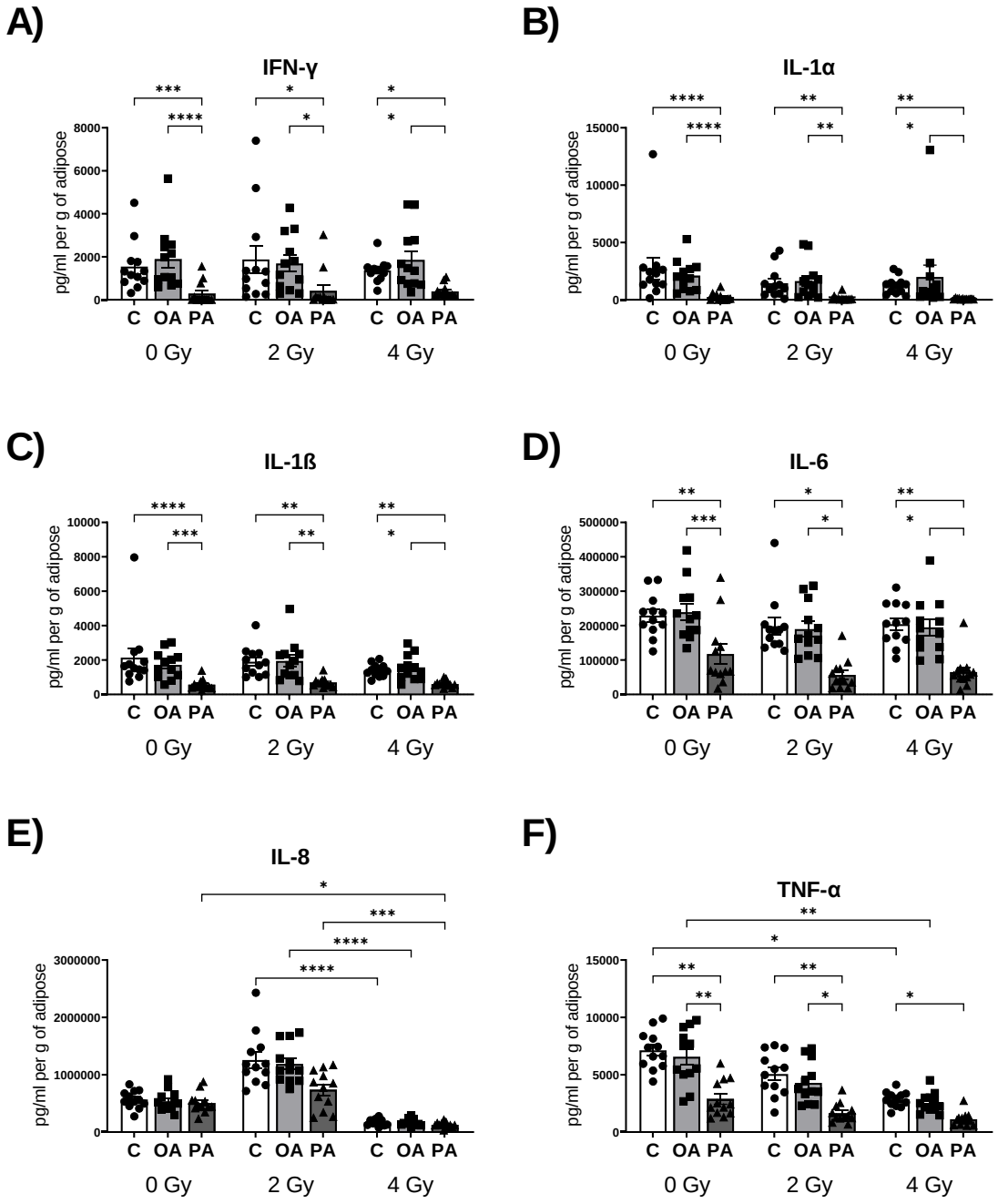


**Figure 4.4.5 Palmitic acid decreases secreted levels of pro-inflammatory mediators in the adipose secretome of OAC patients.**

A-F) Secreted levels of Eotaxin, Eotaxin-3, GM-CSF, MCP-1, MCP-4, and MDC from adipose tissue derived from OAC cancer patients exposed to mock irradiated, 2 Gy irradiation or 4 Gy irradiation in combination with BSA Control (C = ☐), Oleic Acid (OA= ▢) or Palmitic Acid (PA= ■) in combination.

Friedman test with Dunn's correction, all data expressed as mean ± SEM, *n* = 12, * *p* < 0.05, ** *p* <0.01, *** *p* <0.001, **** *p* <0.0001.

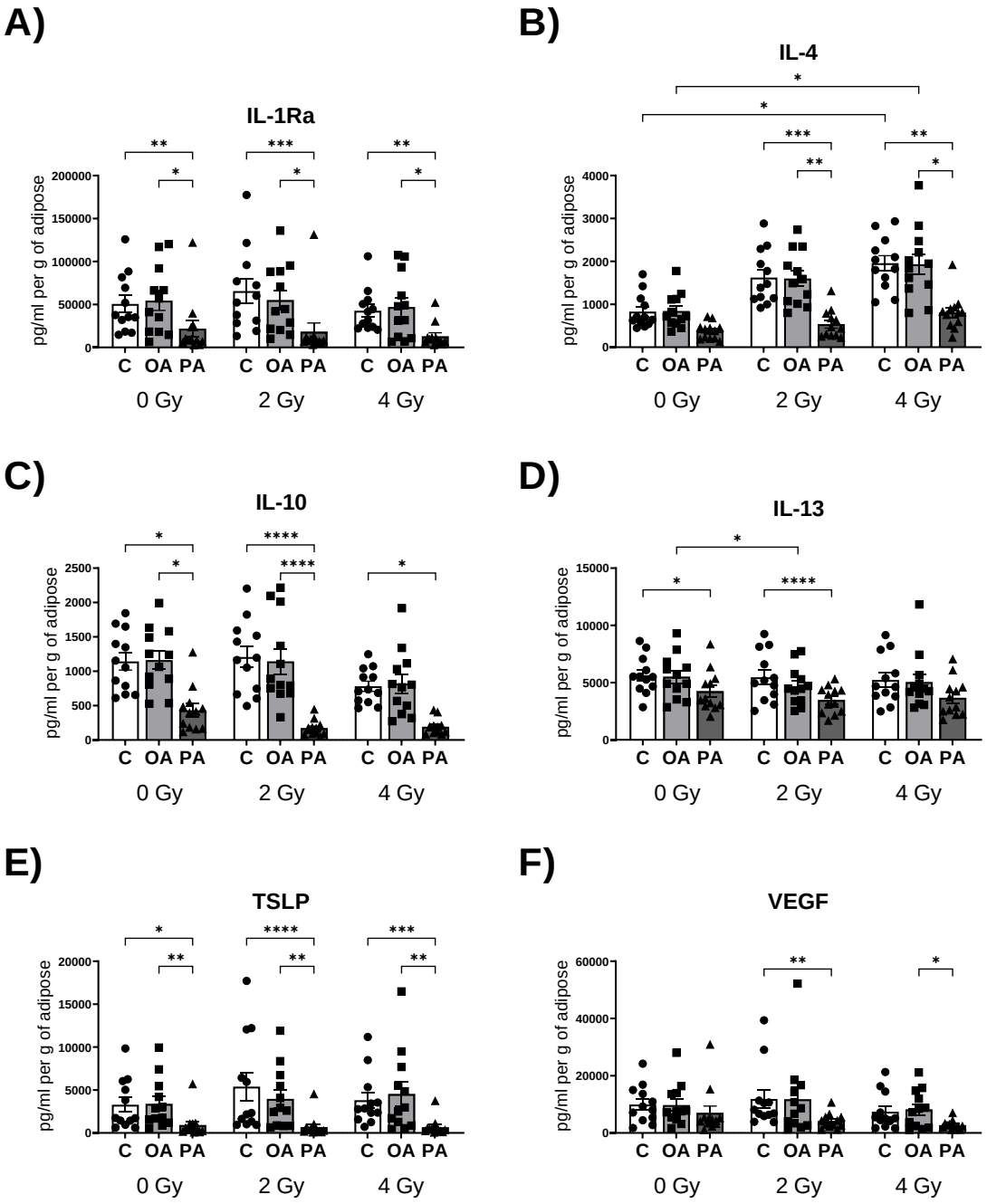


**Figure 4.4.6 Palmitic acid decreases secreted levels of anti-inflammatory and angiogenic mediators in the adipose secretome of OAC patients.**

A-F) Secreted levels of IL-1Ra, IL-4, IL-10,IL-13, TSLP, and VEGF from adipose tissue derived from OAC cancer patients exposed to mock irradiated, 2 Gy irradiation or 4 Gy irradiation in combination with BSA Control (C = □), Oleic Acid (OA= ▒) or Palmitic Acid (PA= ■) in combination.

Friedman test with Dunn's correction, all data expressed as mean ± SEM, $n$ = 12, * $p$ < 0.05, ** $p$ <0.01, *** $p$ <0.001, **** $p$ <0.0001.

### 4.4.3 *Increasing radiation leads to elevated secreted levels of angiogenic and vascular injury associated mediators in the adipose secretome of OAC patients.*

Radiation is a known inducer of key vascular injury and angiogenic associated mediators. In order to determine whether OA and PA treatments augmented the release of these factors into the adipose secretome following exposure to increasing radiation a 54-analyte multiplex was used to assess these mediators.

Control (0 Gy vs 2 Gy vs 4 Gy)

Control ACM exposed to 2 Gy radiation significantly increased secreted levels of bFGF, Flt-1, PIGF, CRP, SAA, sICAM-1, and sVCAM-1 compared with unirradiated control ACM. Control ACM exposed to 4 Gy radiation significantly increased secreted levels of bFGF, Flt-1, PIGF, VEGF-C, CRP, SAA, sICAM-1, and sVCAM-1 compared with unirradiated control ACM. Secreted levels of VEGF-C were also observed to be decreased in the adipose secretome of control treated ACM exposed to 4 Gy radiation compared with control ACM exposed to 2 Gy radiation (**Figure 4.4.7-4.4.8**).

OA (0 Gy vs 2 Gy vs 4 Gy)

OA treated ACM exposed to 2 Gy radiation significantly increased secreted levels of bFGF, Flt-1, PIGF, CRP, SAA, sICAM-1, and sVCAM-1 compared with unirradiated OA treated ACM. OA treated ACM exposed to 4 Gy radiation significantly increased secreted levels of bFGF, Flt-1 PIGF, VEGF-C, CRP, SAA, sICAM-1, and sVCAM-1 compared with unirradiated OA treated ACM. Secreted levels of VEGF-C were also observed to be decreased in the adipose secretome of OA treated ACM exposed to 4 Gy radiation compared with OA treated ACM exposed to 2 Gy radiation (**Figure 4.4.7-4.4.8**).

PA (0 Gy vs 2 Gy vs 4 Gy)

PA treated ACM exposed to 2 Gy radiation significantly increased secreted levels of bFGF, Flt-1, PIGF, CRP, and SAA compared with unirradiated PA treated ACM. PA treated ACM exposed to 4 Gy radiation significantly increased secreted levels of bFGF, Flt-1, PIGF, VEGF-C, CRP, and SAA compared with unirradiated PA treated ACM (**Figure 4.4.7-4.4.8**).

No differential secretion of angiogenic or vascular injury mediators were observed between any fatty acid treatments at any level of radiation exposure.

(* $p < 0.05$, ** $p < 0.01$, *** $p < 0.001$, **** $p < 0.0001$.)

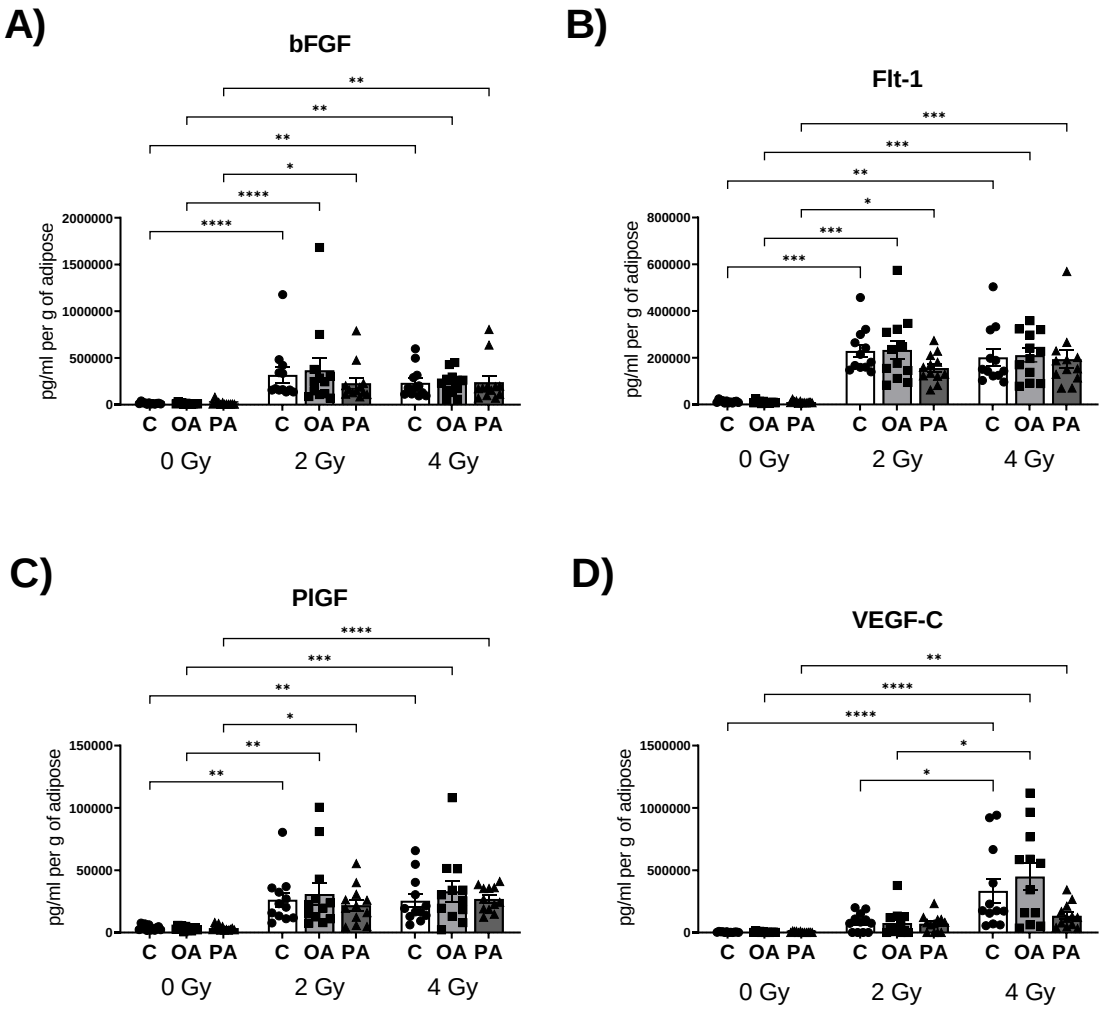


**Figure 4.4.7 Increasing irradiation increases secretion of angiogenic mediators in the adipose secretome of OAC regardless of fatty acid treatment.**

A-D) Secreted levels of bFGF, FLt-1, PIGF, and VEGF-C from adipose tissue derived from OAC cancer patients exposed to mock irradiated, 2 Gy irradiation or 4 Gy irradiation in combination with BSA Control (C = □), Oleic Acid (OA= ▒) or Palmitic Acid (PA= ■) in combination.

Friedman test with Dunn's correction, all data expressed as mean ± SEM, $n$ = 12, * $p$ < 0.05, ** $p$ <0.01, *** $p$ <0.001, **** $p$ <0.0001.

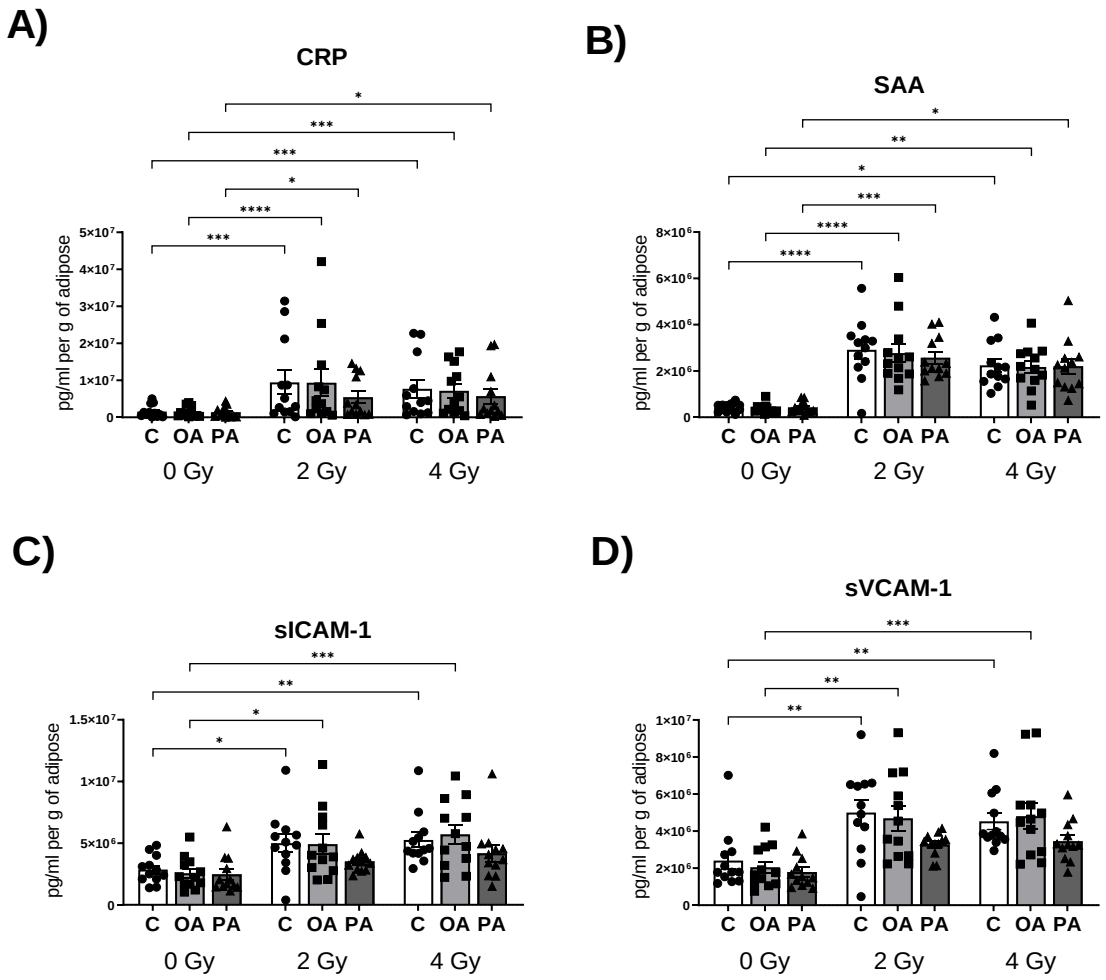


**Figure 4.4.8 Increasing irradiation increases secretion of factors associated with vascular injury in the adipose secretome of OAC regardless of fatty acid treatment.**

A-D) Secreted levels of CRP, SAA, sICAM-1, and sVCAM-1 from adipose tissue derived from OAC cancer patients exposed to mock irradiated, 2 Gy irradiation or 4 Gy irradiation in combination with BSA Control (C = □), Oleic Acid (OA= ▒) or Palmitic Acid (PA= ■) in combination.

Friedman test with Dunn's correction, all data expressed as mean ± SEM, *n* = 12, * *p* < 0.05, ** *p* <0.01, *** *p* <0.001, **** *p* <0.0001.

### 4.4.4 *PA treatment augmented by radiation differentially alters the secretion of key pro-inflammatory and anti-inflammatory mediators in the ACM of obese and non-obese OAC patients.*

Obesity is a known contributor to chronic low-grade inflammation. Therefore, to assess whether increased visceral adiposity effected the influence of increasing radiation doses in combination with OA and PA treatments on adipose tissue secretome from OAC patients a 54-analyte multiplex was used with obesity being classified by VFA.

PA (0 Gy vs 2 Gy vs 4 Gy)

Following PA treatment in combination with 4 Gy radiation decreased secreted levels of IL-3 in adipose explants of obese patients compared with non-obese patients (**Figure 4.4.9**).

Comparisons between fatty acids in the mock irradiated setting

Non-obese

In the unirradiated setting PA treated adipose tissue from non-obese patients secreted lower levels of IL-1α, and IP-10 compared with matched control ACM. Also, in the unirradiated setting PA treated adipose tissue from non-obese patients secreted lower levels of Eotaxin-3, GM-CSF, IFN-γ, IL-1α, IL-1β, IL-1Ra, IL-2, IL-3, IL-6, IL-12p70, IP-10, and MDC compared with matched OA treated ACM (**Figure 4.4.9, 4.4.10, 4.4.11, 4.4.13, 4.4.14**).

Obese

In the unirradiated setting PA treated adipose tissue from obese patients, secreted lower levels of GM-CSF, IFN-γ, IL-1α, IL-1β, IL-2, IL-10, MIP-1β, MIP-3α, and TLSP compared with matched control ACM. Also, in the unirradiated setting PA treated adipose tissue from obese patients, lower secreted levels of IFN-γ, IL-1α, and IL-1β compared with matched OA treated ACM. In PA treated adipose tissue exposed to 2 Gy radiation from obese patients, lower levels of GM-CSF, IFN-γ, IL-1α, IL-1β, IL-1Ra, IL-2, IL-10, MCP-1, MIP-1α, MIP-1β, MIP-3α, and TLSP were observed compared with matched control ACM (**Figure 4.4.9 - 4.4.15**).

Comparisons between fatty acids following exposure to 2 Gy irradiation

Non-obese

In PA treated adipose tissue exposed to 2 Gy radiation from non-obese patients, lower levels of IL-2, IL-3, IL-4, IL-6, IL-10, MCP-1, and TSLP were observed compared with matched control ACM. Also, in PA treated adipose tissue exposed to 2 Gy radiation from non-obese patients, lower secreted levels of IL-3, and IL-10 were observed compared with matched OA treated ACM (**Figure 4.4.9, 4.4.10, 4.4.11, 4.4.13, 4.4.15**).

Obese

In PA treated adipose tissue exposed to 2 Gy radiation from obese patients, lower secreted levels of GM-CSF, IFN-γ, IL-1α, IL-1β, IL-2, IL-10, MCP-1, MDC, MIP-1α, MIP-1β, and MIP-3α were observed compared with matched OA treated ACM (**Figure 4.4.9 - 4.4.15**).

.

Comparisons between fatty acids following exposure to 4 Gy irradiation

Non-obese

In PA treated adipose tissue exposed to 4 Gy radiation from non-obese patients, lower levels of GM-CSF, IL-1Ra, IL-2, IL-4, IL-6, IL-12p70, IL-15, MCP-1, MCP-4, and TLSP were observed compared with matched control ACM. Also, in PA treated adipose tissue exposed to 4 Gy radiation from non-obese patients, lower secreted levels of GM-CSF, IL-15, MCP-4, and TLSP were observed compared with matched OA treated ACM (**Figure 4.4.9, 4.4.10, 4.4.11, 4.4.13, 4.4.14, 4.4.15**).

Obese

In PA treated adipose tissue exposed to 4 Gy radiation from obese patients, lower levels of GM-CSF, IL-1α, MCP-4, MDC, MIP-1α, and MIP-1β were observed compared with matched control ACM. Also, in PA treated adipose tissue exposed to 4 Gy radiation from obese patients, lower secreted levels of GM-CSF, MCP-4, and MIP-1β were observed compared with matched OA treated ACM (**Figure 4.4.9, 4.4.10, 4.4.14**).

(* $p < 0.05$, ** $p < 0.01$, *** $p < 0.001$.)

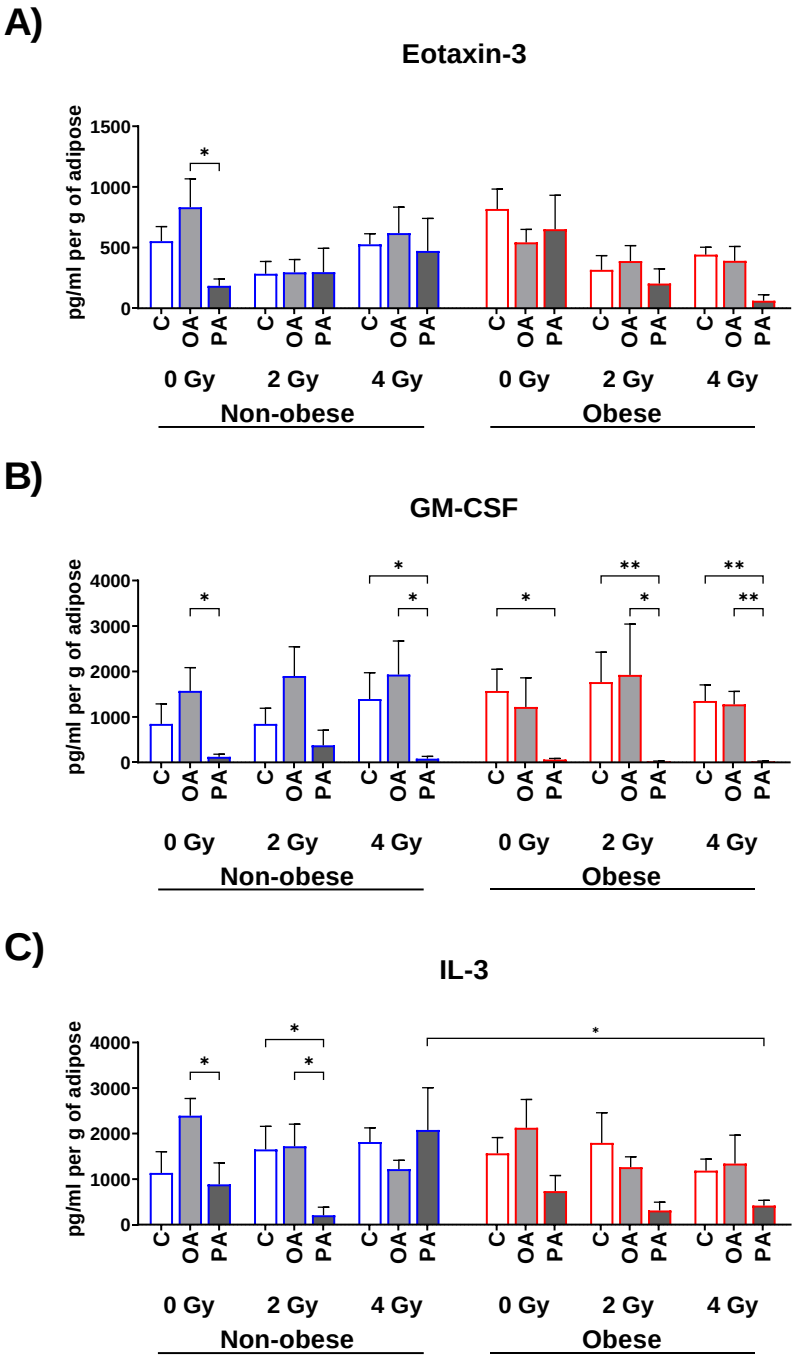


**Figure 4.4.9 Palmitic acid decreases section of factors associated with immune recruitment and activation most apparently in the adipose secretome of non-obese OAC patients.**

A-C) Secreted levels of Eotaxin-3, GM-CSF, and IL-3 from adipose tissue derived from non-obese and obese OAC cancer patients exposed to mock irradiation, 2 Gy irradiation or 4 Gy irradiation in combination with BSA Control (C = ☐), Oleic Acid (OA= ▒) or Palmitic Acid (PA= ■).

To assess fatty acid treatment within non-obese cancer and obese cancer cohorts Friedman test with Dunn's correction was used, to assess the difference between non-obese cancer compared with obese cancer cohorts Kruskal Wallis test with Dunn's correction was used. All data expressed as mean ± SEM, non-obese $n = 6$, obese $n = 6$, * $p < 0.05$, ** $p < 0.01$.

Blue border ☐ = non-obese, Red border ☐ = obese

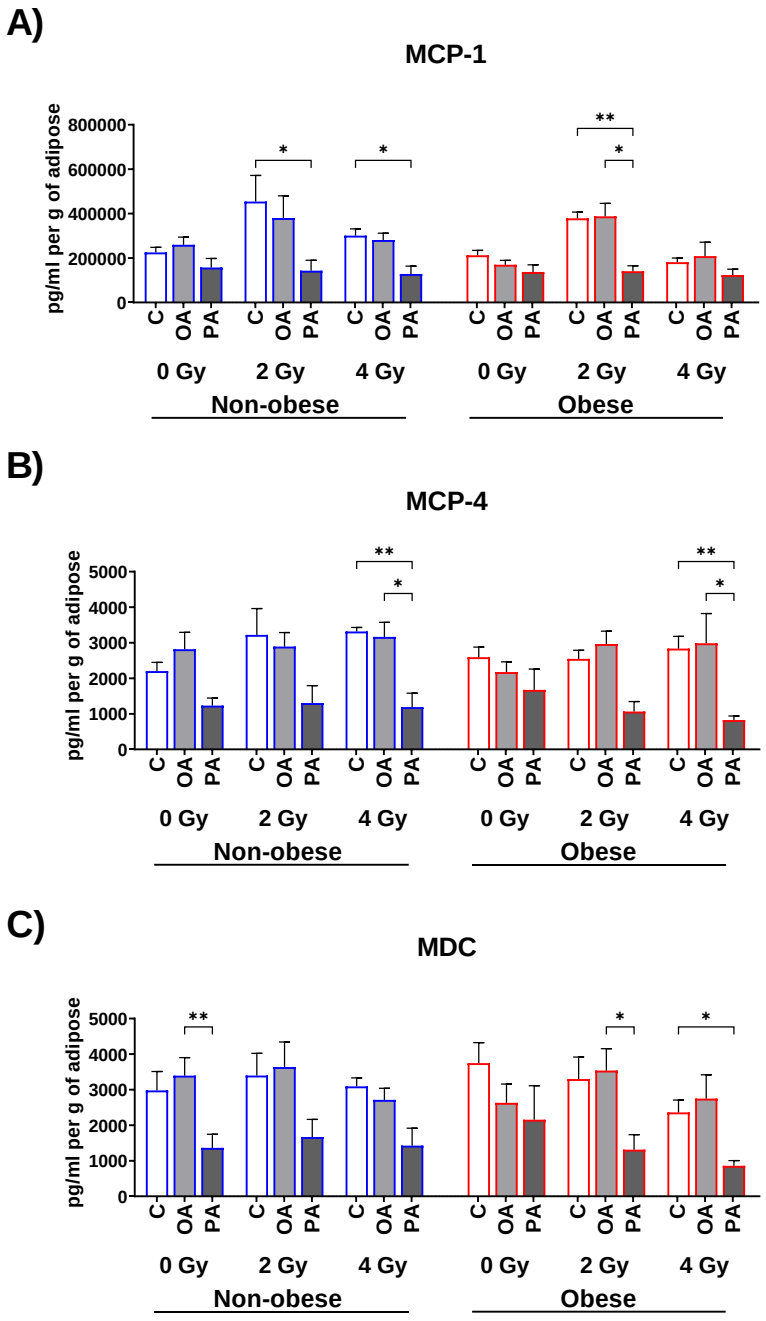


**Figure 4.4.10 Increasing radiation in combination with palmitic acid decreases secreted levels of chemotactic chemokines in the adipose secretome of non-obese and obese OAC patients.**

A-C) Secreted levels of MCP-1, MCP-4, and MDC from adipose tissue derived from non-obese and obese OAC cancer patients exposed to mock irradiation, 2 Gy irradiation or 4 Gy irradiation in combination with BSA Control (C = ☐), Oleic Acid (OA= ▒) or Palmitic Acid (PA= ■).

To assess fatty acid treatment within non-obese cancer and obese cancer cohorts Friedman test with Dunn's correction was used, to assess the difference between non-obese cancer compared with obese cancer cohorts Kruskal Wallis test with Dunn's correction was used. All data expressed as mean ± SEM, non-obese $n = 6$, obese $n = 6$, * $p < 0.05$, ** $p < 0.01$.

Blue border ☐ = non-obese, Red border ☐ = obese

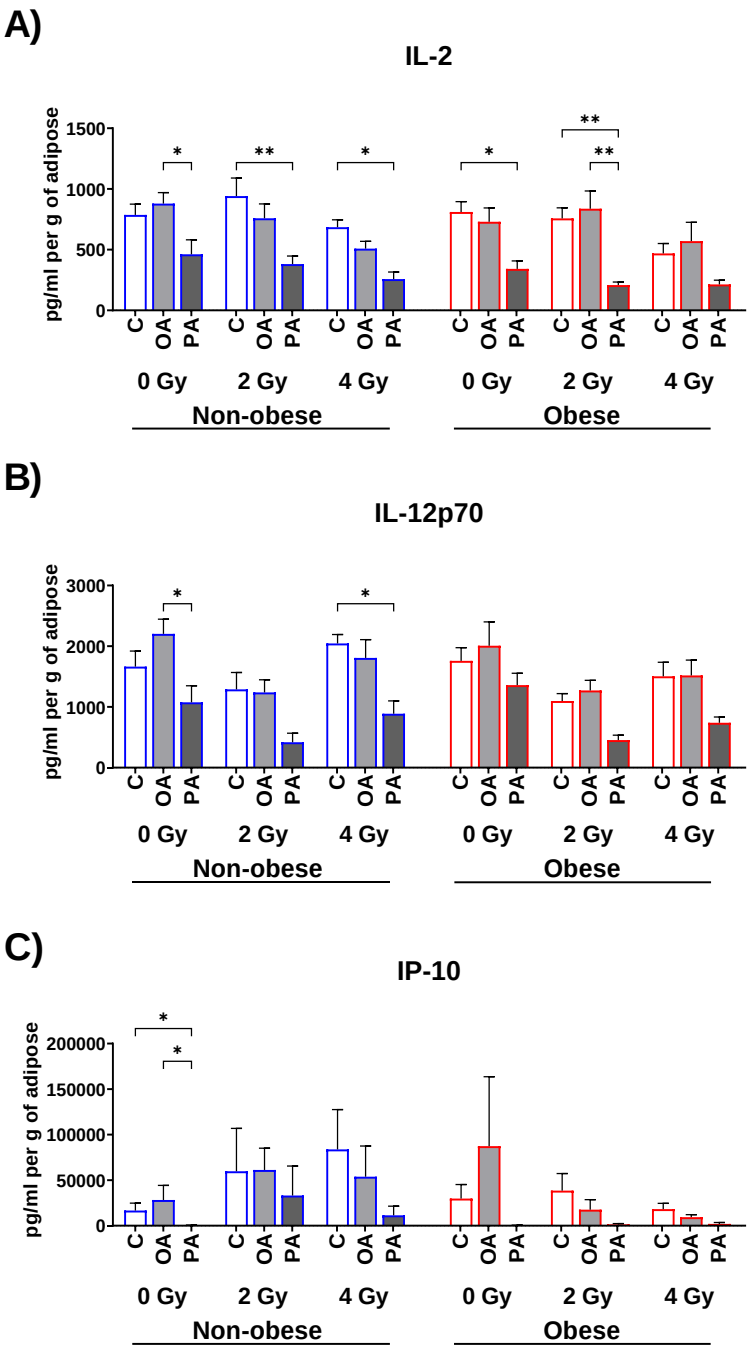


**Figure 4.4.11 The immunosuppressive effects of palmitic acid on secreted levels of immune activating factors is most apparent in the non-obese adipose secretome.**

A-C) Secreted levels of IL-2, IL-12p70 and IP-10 from adipose tissue derived from non-obese and obese OAC cancer patients exposed to mock irradiation, 2 Gy irradiation or 4 Gy irradiation in combination with BSA Control (C = ☐), Oleic Acid (OA= ▒) or Palmitic Acid (PA= ■).

To assess fatty acid treatment within non-obese cancer and obese cancer cohorts Friedman test with Dunn's correction was used, to assess the difference between non-obese cancer compared with obese cancer cohorts Kruskal Wallis test with Dunn's correction was used. All data expressed as mean ± SEM, non-obese $n = 6$, obese $n = 6$, * $p < 0.05$, ** $p < 0.01$.

Blue border ☐ = non-obese, Red border ☐ = obese

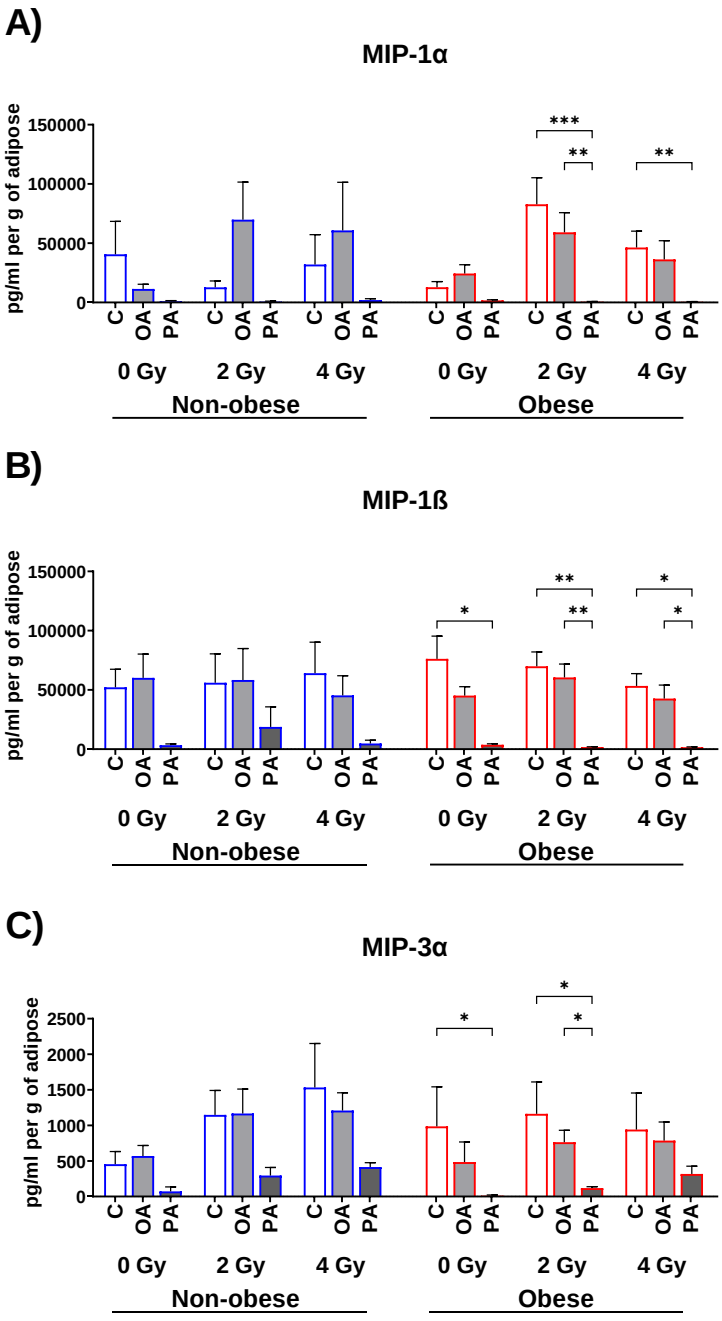


**Figure 4.4 12 The immunosuppressive effects of palmitic acid on secreted levels of MIP family members is most apparent in the obese adipose secretome.**

A-C) Secreted levels of MIP-1α, MIP-1β, and MIP-3α from adipose tissue derived from non-obese and obese OAC cancer patients exposed to mock irradiation, 2 Gy irradiation or 4 Gy irradiation in combination with BSA Control (C = □), Oleic Acid (OA= ▒) or Palmitic Acid (PA= ■).

To assess fatty acid treatment within non-obese cancer and obese cancer cohorts Friedman test with Dunn's correction was used, to assess the difference between non-obese cancer compared with obese cancer cohorts Kruskal Wallis test with Dunn's correction was used. All data expressed as mean ± SEM, non-obese $n = 6$, obese $n = 6$, * $p < 0.05$, ** $p < 0.01$, *** $p < 0.001$.

Blue border □ = non-obese, Red border □ = obese

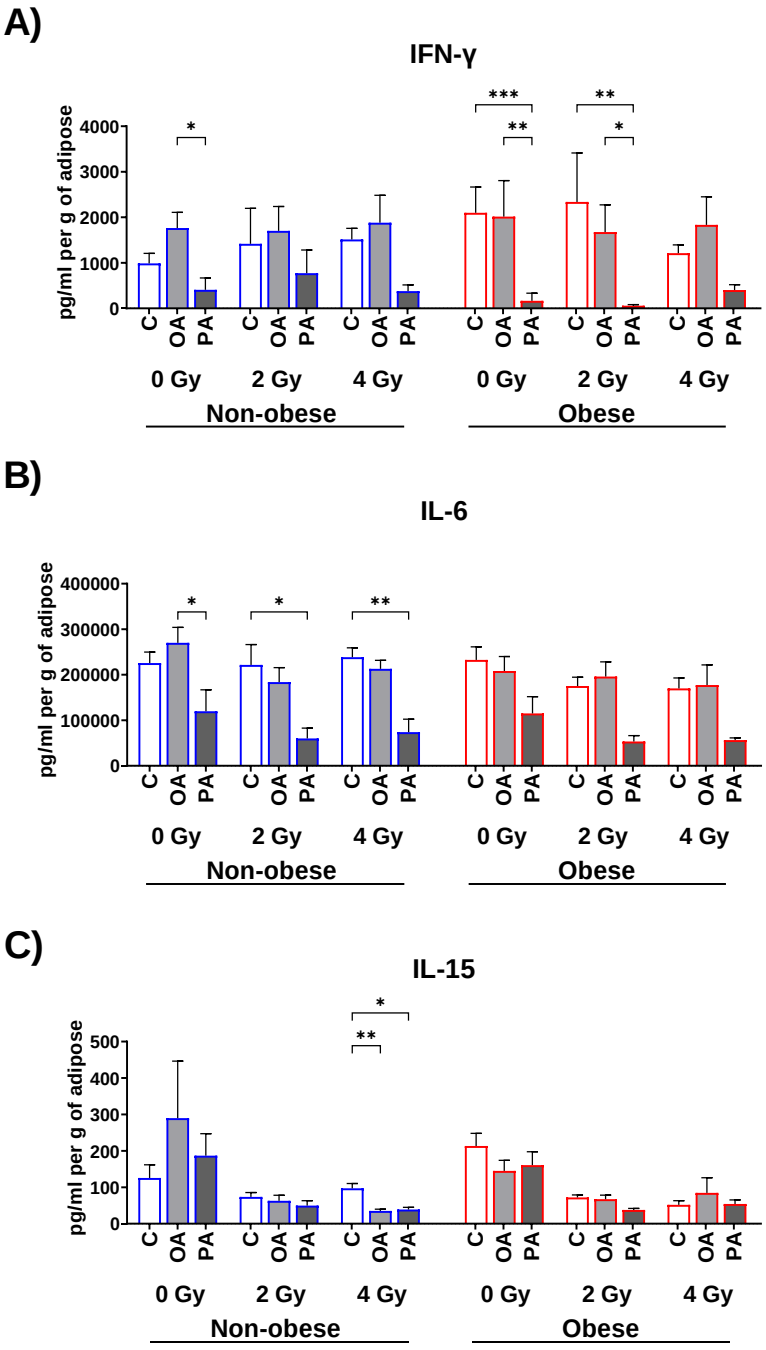


**Figure 4.4.13 Palmitic acid differentially diminishes adipose tissue secretion of alternate instigators of NFκB activation in non-obese and obese OAC patients.**

A-C) Secreted levels of IFN-γ, IL-6, and IL-15 from adipose tissue derived from non-obese and obese OAC cancer patients exposed to mock irradiation, 2 Gy irradiation or 4 Gy irradiation in combination with BSA Control (C = □), Oleic Acid (OA= ▒) or Palmitic Acid (PA= ■).

To assess fatty acid treatment within non-obese cancer and obese cancer cohorts Friedman test with Dunn's correction was used, to assess the difference between non-obese cancer compared with obese cancer cohorts Kruskal Wallis test with Dunn's correction was used. All data expressed as mean ± SEM, non-obese $n = 6$, obese $n = 6$, * $p < 0.05$, ** $p < 0.01$, *** $p < 0.001$.

Blue border □ = non-obese, Red border □ = obese

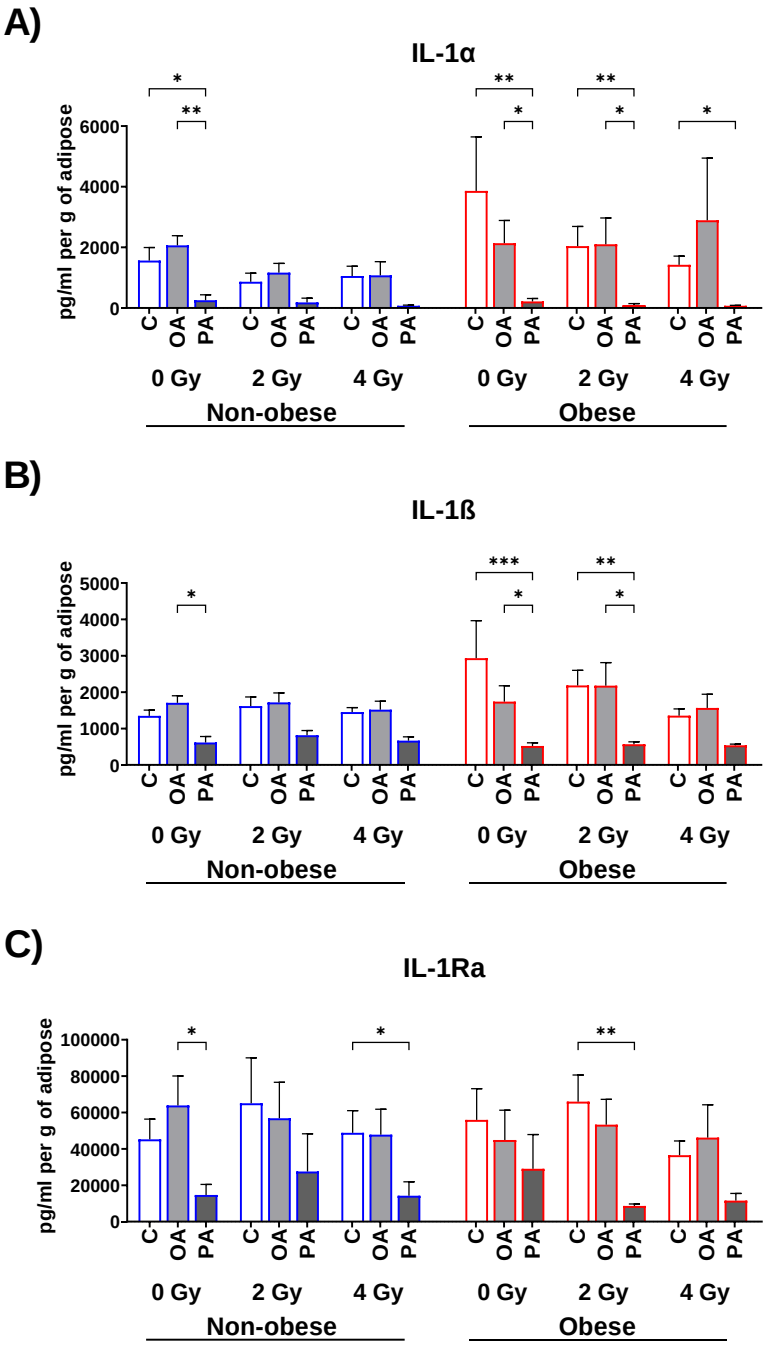


**Figure 4.4.14 The diminishing effect of palmitic acid on pro-inflammatory IL-1 family members is most apparent in the adipose secretome of obese OAC patients.**

A-C) Secreted levels of IL-1α, IL-1β, and IL-1Ra from adipose tissue derived from non-obese and obese OAC cancer patients exposed to mock irradiation, 2 Gy irradiation or 4 Gy irradiation in combination with BSA Control (C = ☐), Oleic Acid (OA= ▒) or Palmitic Acid (PA= ■).

To assess fatty acid treatment within non-obese cancer and obese cancer cohorts Friedman test with Dunn's correction was used, to assess the difference between non-obese cancer compared with obese cancer cohorts Kruskal Wallis test with Dunn's correction was used. All data expressed as mean ± SEM, non-obese $n = 6$, obese $n = 6$, * $p < 0.05$, ** $p < 0.01$, *** $p < 0.001$.

Blue border ☐ = non-obese, Red border ☐ = obese

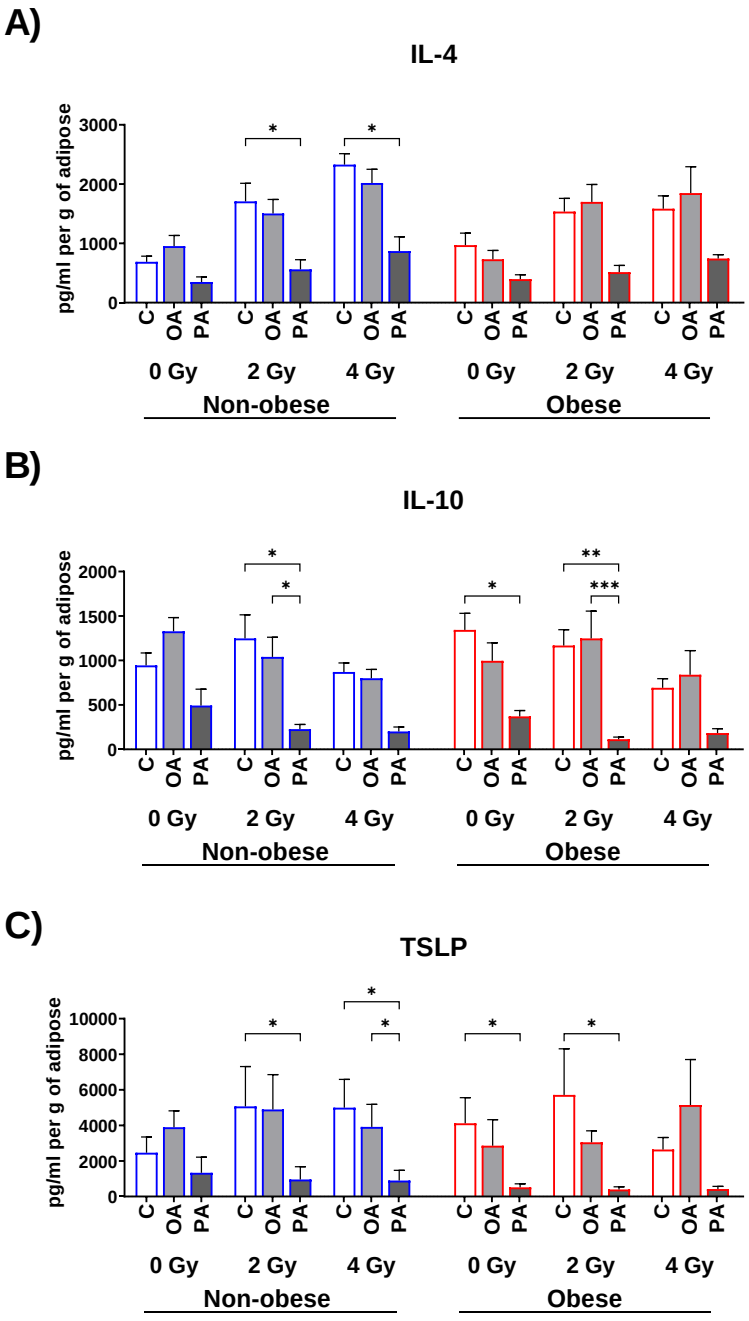


**Figure 4.4.15 Increasing radiation and obesity effect the decreased secretion of anti-inflammatory in the adipose secretome of non-obese and obese OAC patients in response to palmitic acid.**

A-C) Secreted levels of IL-4, IL-10, and TSLP from adipose tissue derived from non-obese and obese OAC cancer patients exposed to mock irradiation, 2 Gy irradiation or 4 Gy irradiation in combination with BSA Control (C = ☐), Oleic Acid (OA= ▒) or Palmitic Acid (PA= ■).

To assess fatty acid treatment within non-obese cancer and obese cancer cohorts Friedman test with Dunn's correction was used, to assess the difference between non-obese cancer compared with obese cancer cohorts Kruskal Wallis test with Dunn's correction was used. All data expressed as mean ± SEM, non-obese $n = 6$, obese $n = 6$, * $p < 0.05$, ** $p < 0.01$, *** $p < 0.001$.

Blue border ☐ = non-obese, Red border ☐ = obese

### 4.4.5 *Increasing radiation in combination with OA treatment on the adipose secretome of OAC patients augments expression of DC maturation markers.*

DCs play a pivotal role in antigen presentation and anti-tumour immunity. To assess what influence increasing radiation in combination with OA and PA treatments in the adipose secretome have on DCs function, DCs were cultured in these treated ACM and a series of phenotypic and maturation markers were assessed via flow cytometry.

Control (0 Gy vs 2 Gy vs 4 Gy)

DCs cultured with control ACM exposed to 2 Gy radiation showed decreased CD54 expression compared with DCs cultured in unirradiated control ACM. DCs cultured with control ACM exposed to 4 Gy radiation showed increased HLA-DR, CD11c, CD80, CD86, CD40, PD-L1, TIM-3 and decreased CD83 compared with unirradiated control ACM (**Figure 4.4.17 - 4.4.19**).

OA (0 Gy vs 2 Gy vs 4 Gy)

DCs cultured with OA treated ACM exposed to 2 Gy radiation showed increased HLA-DR, CD11c, CD80, CD86, CD80+CD86+, CD40, PD-L1, and TIM-3 expression compared with DCs cultured with unirradiated OA treated ACM. DCs cultured with OA treated ACM exposed to 4 Gy radiation showed increased HLA-DR, CD11c, CD80, CD86, CD80+CD86+, CD40, PD-L1, TIM-3 and decreased CD83 compared with unirradiated OA treated ACM. OA treated ACM exposed to 4 Gy radiation also significantly decreased DC viability compared with OA treated ACM exposed to 2 Gy radiation (**Figure 4.4.17 - 4.4.19**).

PA (0 Gy vs 2 Gy vs 4 Gy)

DCs cultured with PA treated ACM exposed to 4 Gy radiation showed increased CD80, TIM-3, and decreased CD83 compared with unirradiated OA treated ACM (**Figure 4.4.18 - 4.4.19**).

Comparisons between fatty acids in the mock irradiated setting

DCs cultured in unirradiated OA treated ACM also showed significantly decreased expression of CD54 compared with unirradiated control ACM (**Figure 4.4.19**).

Comparisons between fatty acids following exposure to 2 Gy irradiation

PA treated ACM exposed to 2 Gy radiation significantly decreased DC viability compared with matched 2 Gy irradiated control ACM, and OA treated ACM (**Figure 4.4.17**).

(* $p < 0.05$, ** $p < 0.01$, *** $p < 0.001$, **** $p < 0.0001$.)

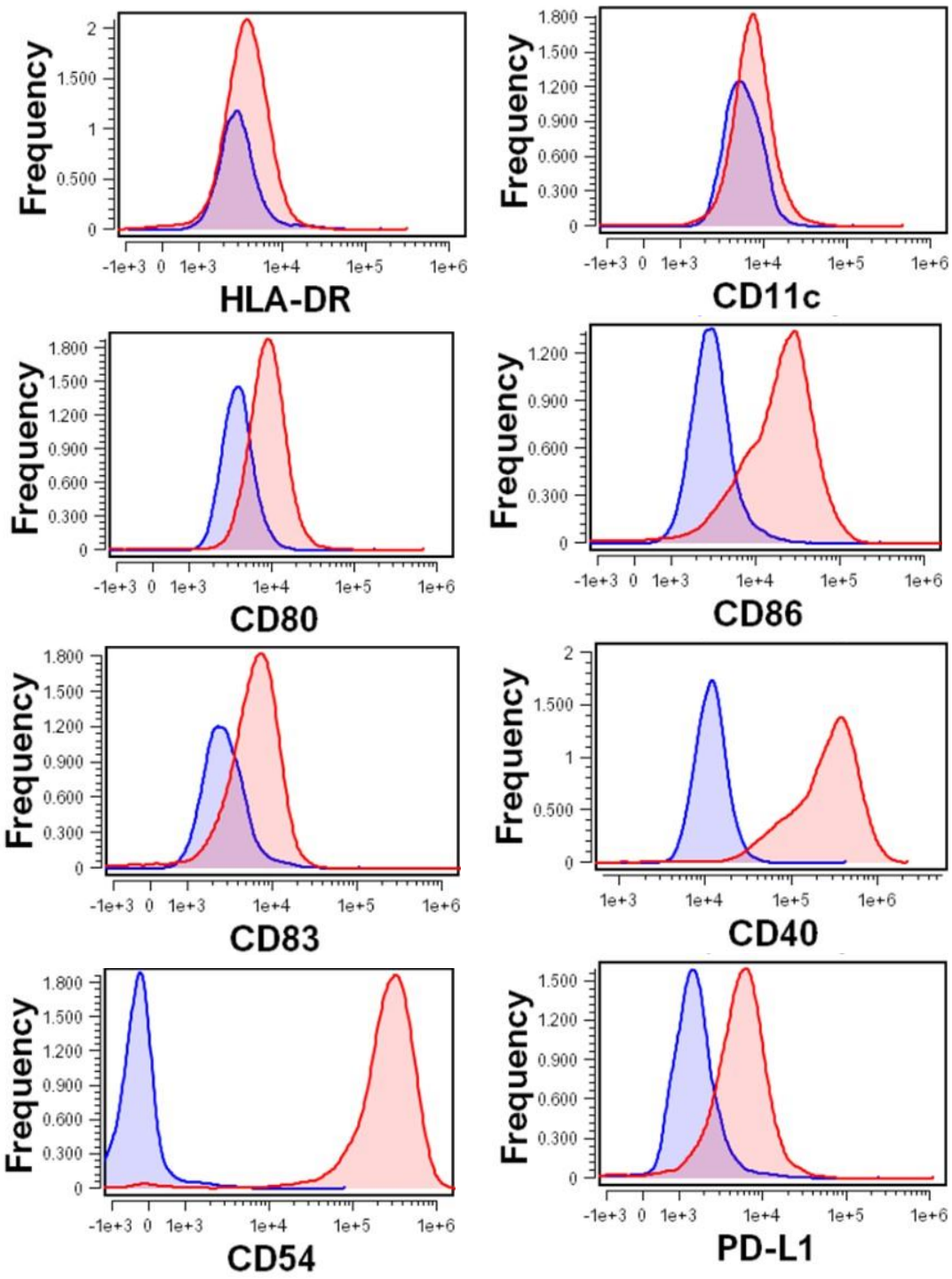


**Figure 4.4.16 Histograms of DC maturation markers following LPS stimulation**
Histograms displaying DC markers HLA-DR, CD11c, CD80, CD86 CD83, CD40, CD54 and PD-L1 which depict DCs response to LPS stimulation. (Blue peaks indicate unstimulated DCs and red peak indicate DCs following exposure to LPS stimulation)

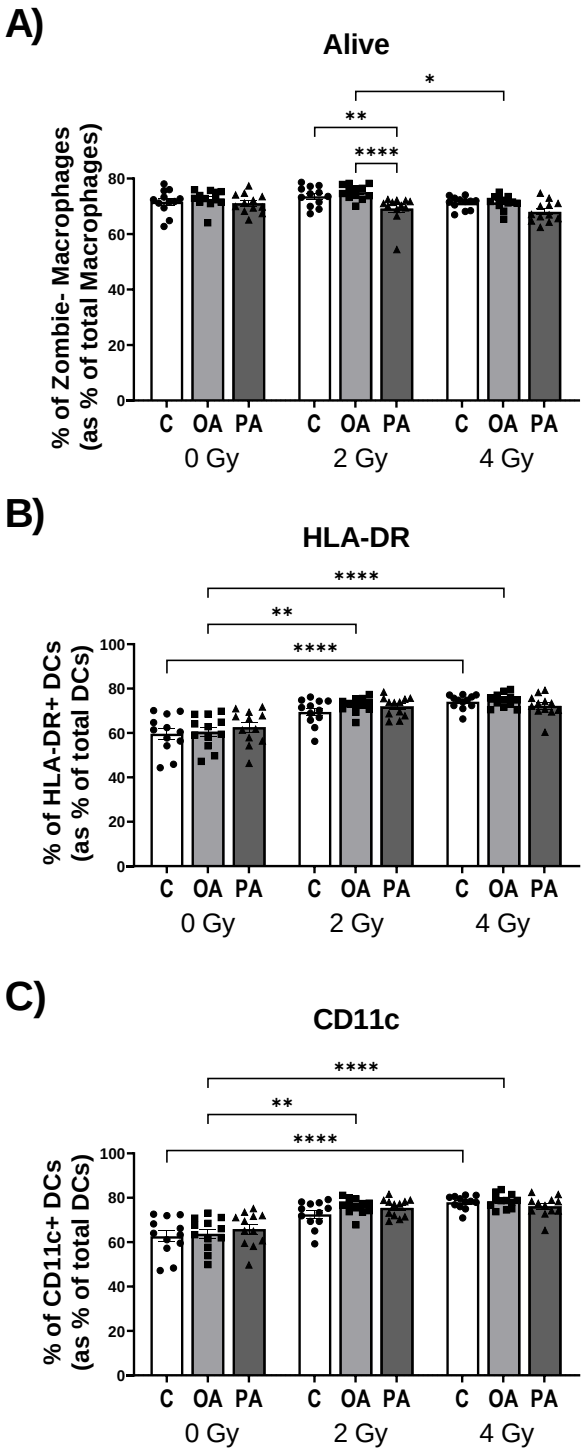


**Figure 4.4.17 The adipose secretome of OAC patients treated with oleic acid and increasing irradiation increases DC expression of phenotypic markers.**

A-C) Expression of DC viability and phenotypic markers including HLA-DR, and CD11c following culture with the adipose secretome of cancer patients exposed to mock irradiation, 2 Gy irradiation or 4 Gy irradiation in combination with BSA Control (C = □), Oleic Acid (OA= ▩) or Palmitic Acid (PA= ■) in combination.

Friedman test with Dunn's correction, all data expressed as mean ± SEM, $n$ = 12, * $p$ < 0.05, ** $p$ <0.01, *** $p$ <0.001, **** $p$ <0.0001.

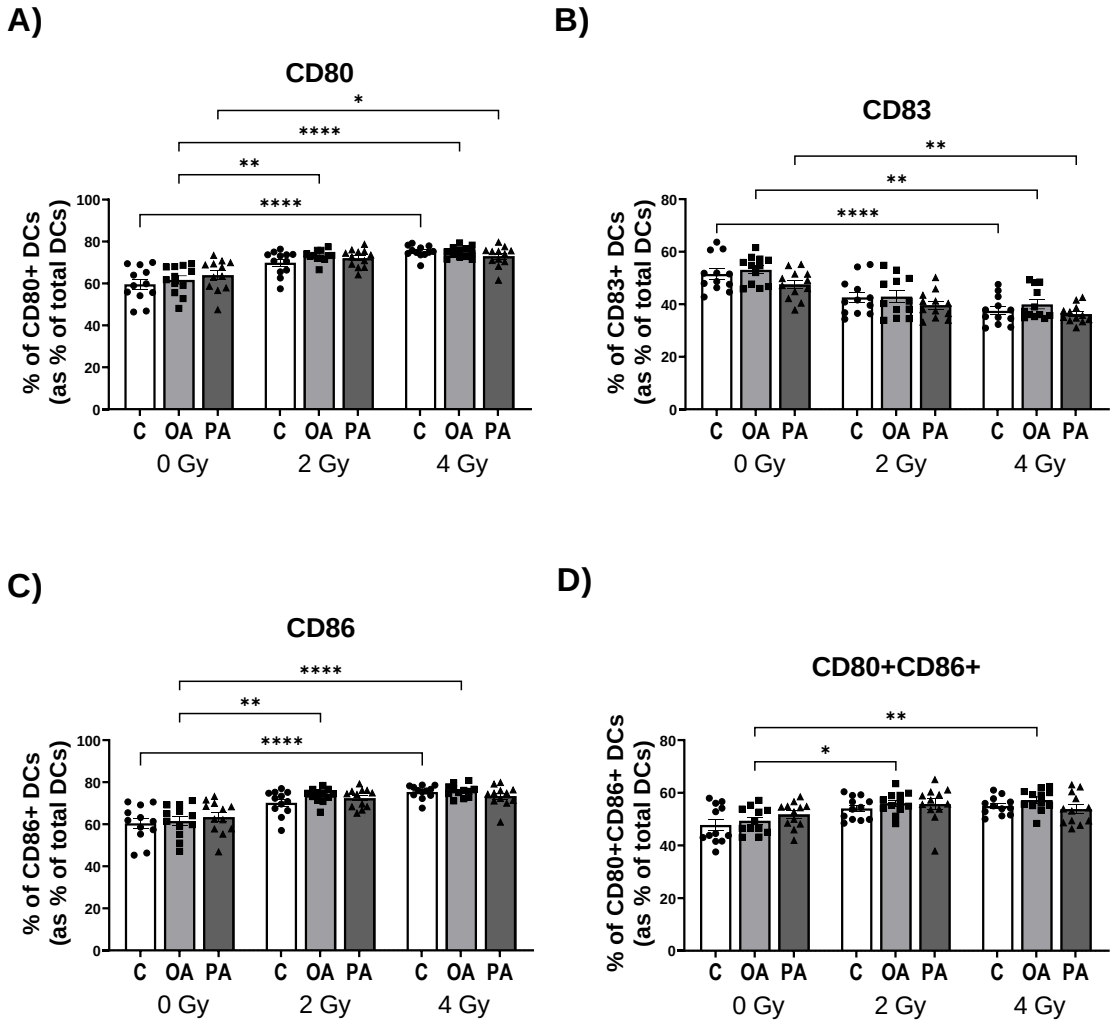


**Figure 4.4.18 The adipose secretome of OAC patients treated with oleic acid and increasing irradiation increases DC expression of maturation markers.**

A-D) Expression of DC maturation markers including CD80, CD83, CD86 and co-expression of CD80+CD86+ following culture with the adipose secretome of cancer patients exposed to mock irradiation, 2 Gy irradiation or 4 Gy irradiation in combination with BSA Control (C = ☐), Oleic Acid (OA= ☐) or Palmitic Acid (PA= ■) in combination.

Friedman test with Dunn's correction, all data expressed as mean ± SEM, $n$ = 12, * $p$ < 0.05, ** $p$ <0.01, *** $p$ <0.001, **** $p$ <0.0001.

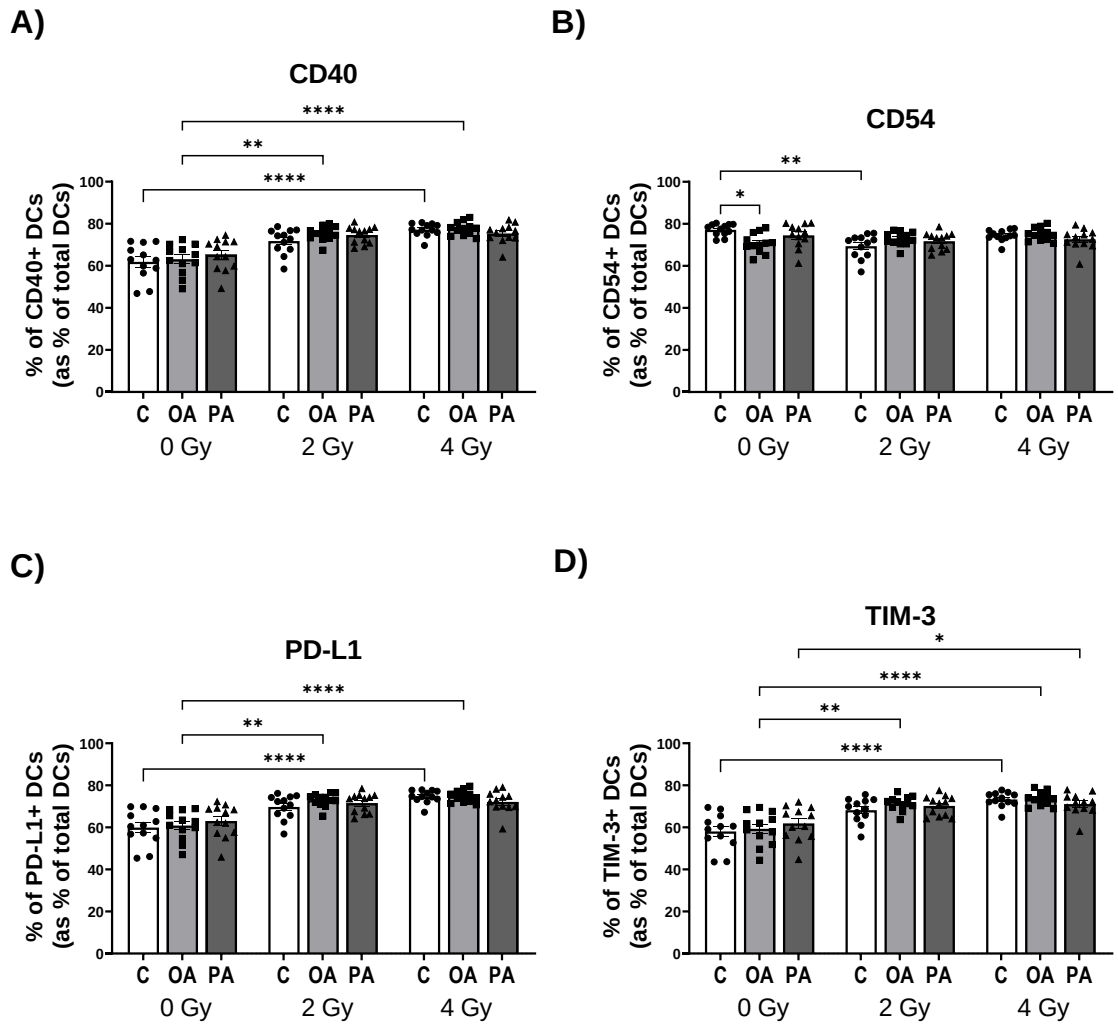


**Figure 4.4.19 The adipose secretome of OAC patients treated with oleic acid and increasing irradiation increases DC expression of CD40 and immunoinhibitory markers.**

A-D) Expression of DC adhesion and immunoinhibitory markers including CD40, CD54, TIM-3, and PD-L1 following culture with the adipose secretome of cancer patients exposed to mock irradiation, 2 Gy irradiation or 4 Gy irradiation in combination with BSA Control (C = ☐), Oleic Acid (OA= ☐) or Palmitic Acid (PA= ■) in combination.

Friedman test with Dunn's correction, all data expressed as mean ± SEM, $n$ = 12, * $p$ < 0.05, ** $p$ <0.01, *** $p$ <0.001, **** $p$ <0.0001.

### 4.4.6 *The PA treated adipose secretome of non-obese and obese OAC patients paradoxically polarise Mϕ towards anti-inflammatory and pro-inflammatory states with and without radiation.*

Obesity is a known contributor to chronic low-grade inflammation that deleteriously effects DC function and inhibits DC maturation. Therefore, to assess whether increased visceral adiposity augmented the influence of increasing radiation in combination with OA and PA treatments in the adipose secretome and the effects this holds for DCs function, DCs were cultured in these treated ACM and a series of phenotypic and maturation markers were assessed via flow cytometry.

DCs cultured with PA treated ACM from non-obese patients showed decreased viability compared with matched control and OA treated ACM exposed to 2 Gy radiation (**Figure 4.4.20**).

DCs cultured with PA treated ACM from obese patients showed decreased viability compared with matched unirradiated OA treated ACM. DCs cultured with PA treated ACM from obese patients exposed to 2 Gy irradiation also showed decreased viability compared with matched control and OA treated ACM exposed to 2 Gy radiation (**Figure 4.4.20**).

DCs cultured in unirradiated OA treated ACM from obese patients showed significantly decreased expression of CD54 compared with unirradiated matched control ACM and PA treated ACM. DCs cultured control ACM from non-obese patients showed decreased expression of CD80+CD86+ compared with DCs cultured in unirradiated control ACM from obese patients. DCs cultured control ACM from non-obese patients showed decreased expression of CD80+CD86+ compared with DCs cultured with matched PA treated ACM (**Figure 4.4.21 - 4.4.22**).

(* $p < 0.05$, ** $p < 0.01$, *** $p < 0.001$.)

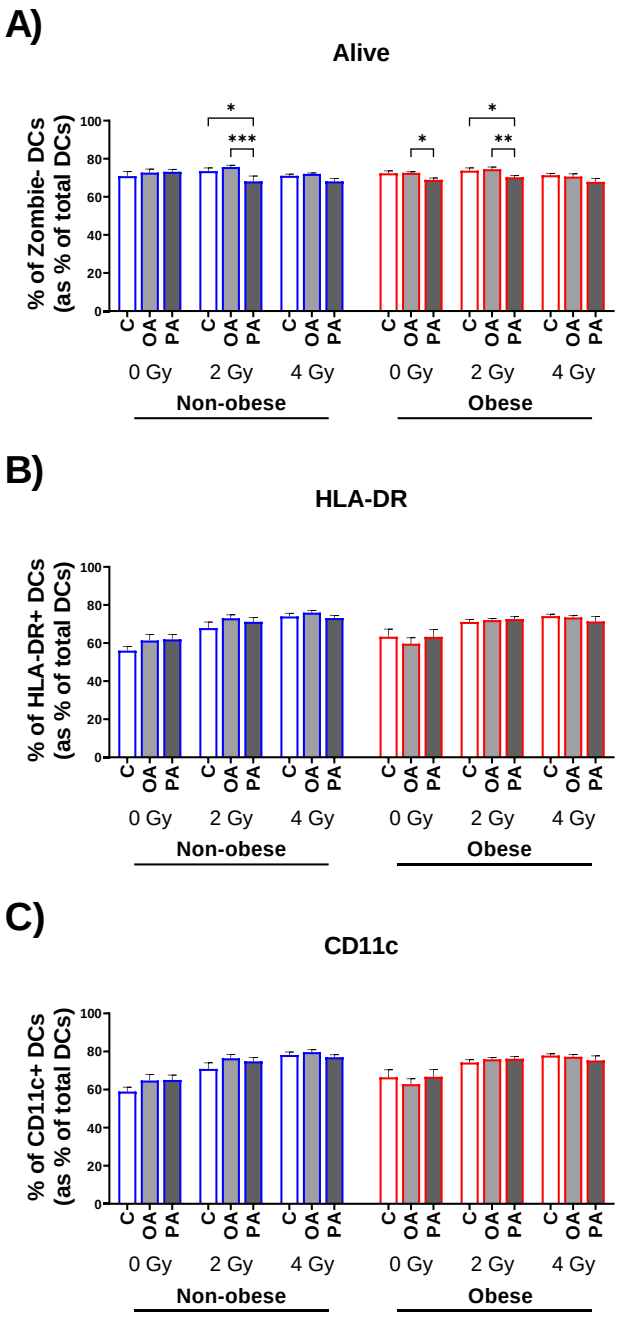


**Figure 4.4.20 The adipose secretome of non-obese and obese OAC patients treated with palmitic acid and 2 Gy irradiation decreases DC viability.**

A-C) Expression of DC viability, and phenotypic markers including HLA-DR, and CD11c following culture with the adipose secretome of non-obese and obese cancer patients exposed to mock irradiation, 2 Gy irradiation or 4 Gy irradiation in combination with BSA Control (C = ☐), Oleic Acid (OA= ▒) or Palmitic Acid (PA= ■) in combination.

To assess fatty acid treatment within non-obese cancer and obese cancer cohorts Friedman test with Dunn's correction was used, to assess the difference between non-obese cancer compared with obese cancer cohorts Kruskal Wallis test with Dunn's correction was used. All data expressed as mean ± SEM, non-obese $n = 6$, obese $n = 6$, * $p < 0.05$, ** $p < 0.01$, *** $p < 0.001$.

Blue border ☐ = non-obese, Red border ☐ = obese

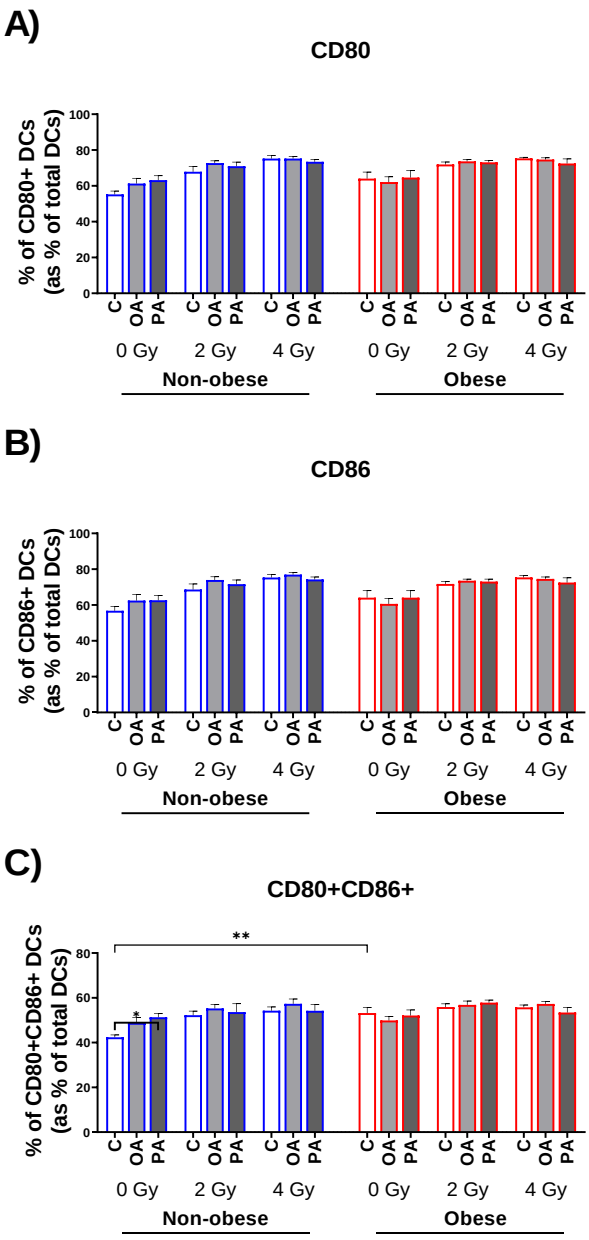


**Figure 4.4.21 The adipose secretome of non-obese OAC patients the showed decreased DC expression of CD80+CD86+ compared with obese patients, an effect that is ameliorated by PA.**

A-C) Expression of DC adhesion and maturation markers including, CD80, CD86 and co-expression of CD80+CD86+ following culture with the adipose secretome of non-obese and obese cancer patients exposed to mock irradiation, 2 Gy irradiation or 4 Gy irradiation in combination with BSA Control (C = ☐), Oleic Acid (OA= ▒) or Palmitic Acid (PA= ■) in combination.

To assess fatty acid treatment within non-obese cancer and obese cancer cohorts Friedman test with Dunn's correction was used, to assess the difference between non-obese cancer compared with obese cancer cohorts Kruskal Wallis test with Dunn's correction was used. All data expressed as mean ± SEM, non-obese $n$ = 6, obese $n$ = 6, * $p$ < 0.05, ** $p$ <0.01, *** $p$ <0.001.

Blue border ☐ = non-obese, Red border ☐ = obese

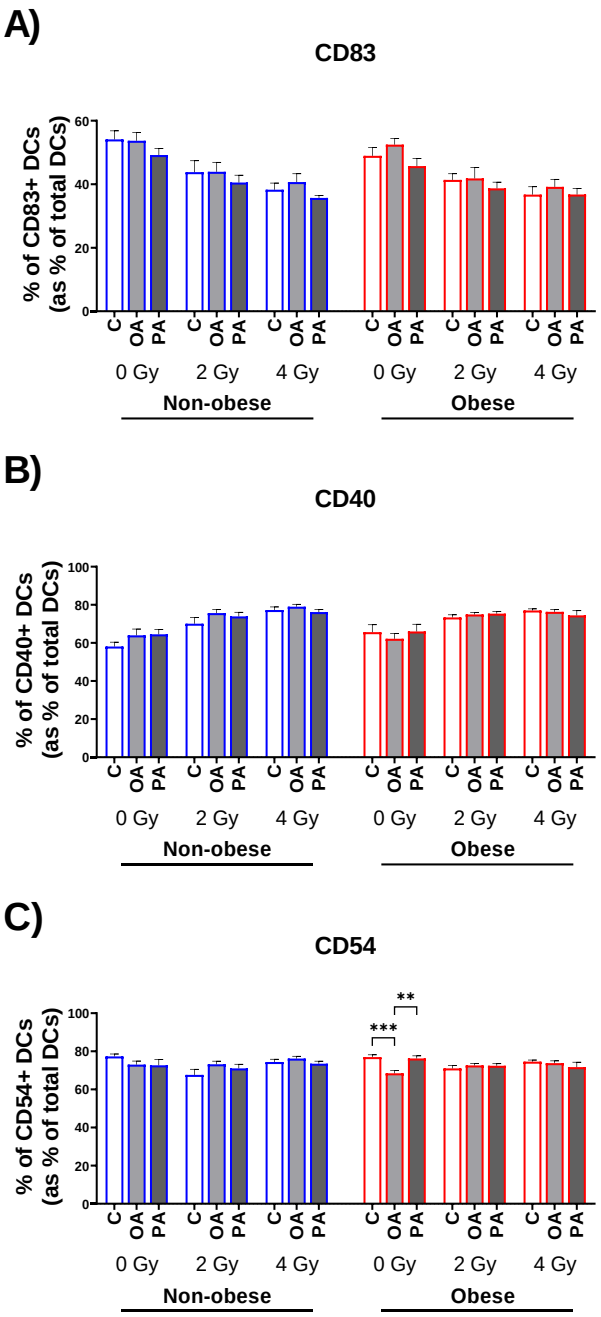


**Figure 4.4.22 The adipose secretome of obese OAC patients treated with OA decreased DC expression of CD54 in the unirradiated setting.**

A-C) Expression of DC adhesion and maturation markers including, CD83, CD40 and CD54 following culture with the adipose secretome of non-obese and obese cancer patients exposed to mock irradiation, 2 Gy irradiation or 4 Gy irradiation in combination with BSA Control (C = ☐), Oleic Acid (OA= ▢) or Palmitic Acid (PA= ■) in combination.

To assess fatty acid treatment within non-obese cancer and obese cancer cohorts Friedman test with Dunn's correction was used, to assess the difference between non-obese cancer compared with obese cancer cohorts Kruskal Wallis test with Dunn's correction was used. All data expressed as mean ± SEM, non-obese $n = 6$, obese $n = 6$, * $p < 0.05$, ** $p < 0.01$, *** $p < 0.001$.

Blue border ☐ = non-obese, Red border ☐ = obese

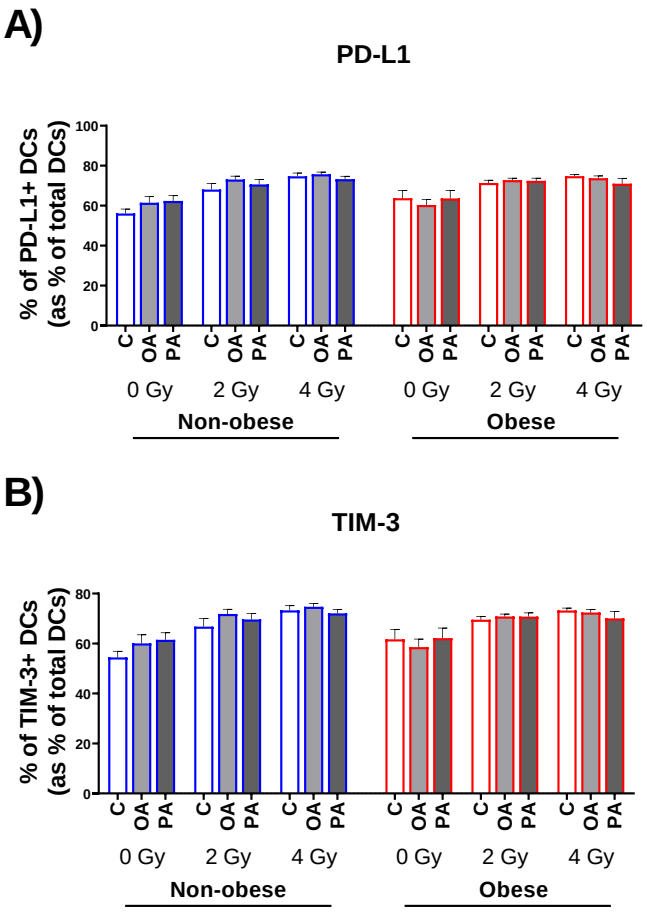


**Figure 4.4.23 Obesity status of OAC patients does not affect DC expression of immunoinhibitory markers in response to fatty acids with or without irradiation.**

A-B) Expression of DC immunoinhibitory markers including PD-L1, and TIM-3 following culture with the adipose secretome of non-obese and obese cancer patients exposed to mock irradiation, 2 Gy irradiation or 4 Gy irradiation in combination with BSA Control (C = ☐), Oleic Acid (OA= ☐) or Palmitic Acid (PA= ☐) in combination.

To assess fatty acid treatment within non-obese cancer and obese cancer cohorts Friedman test with Dunn's correction was used, to assess the difference between non-obese cancer compared with obese cancer cohorts Kruskal Wallis test with Dunn's correction was used. All data expressed as mean ± SEM, non-obese $n = 6$, obese $n = 6$, * $p < 0.05$, ** $p < 0.01$, *** $p < 0.001$.

Blue border ☐ = non-obese, Red border ☐ = obese

### 4.4.7 *Adipose treated with exogenous fatty acids and increasing radiation augments pro-inflammatory and anti-inflammatory Mϕ polarisation compared with the unirradiated adipose secretome.*

The paradoxical roles of Mϕ in the tumour microenvironment have been reported to play a pivotal role in antigen presentation and anti-tumour immunity. To assess the effect of increasing radiation in combination with OA and PA treatments on the adipose secretome have on Mϕ polarisation, Mϕ were cultured in these treated ACM with typical pro-inflammatory and anti-inflammatory associated polarisation markers assessed via flow cytometry.

Control (0 Gy vs 2 Gy vs 4 Gy)

Mϕ cultured with control ACM exposed to 4 Gy radiation showed increased CD11b, CD11c, HLA-DR, TIM-3, CD163, and CD206 compared with unirradiated control ACM (**Figure 4.4.24 - 4.4.25**).

OA (0 Gy vs 2 Gy vs 4 Gy)

Mϕ cultured with OA treated ACM exposed to 2 Gy radiation showed increased CD11c, HLA-DR, TIM-3, CD80+CD86+, CD163, CD206, and CD163+CD206+ expression compared with Mϕ cultured with unirradiated OA treated ACM. Mϕ cultured with OA treated ACM exposed to 4 Gy radiation showed increased CD11b, CD11c, HLA-DR, TIM-3, CD86, CD80+CD86+, CD163, CD206, and CD163+CD206+ expression compared with Mϕ cultured with unirradiated OA treated ACM. OA treated ACM exposed to 4 Gy radiation also significantly decreased Mϕ viability compared with Mϕ cultured in matched unirradiated OA treated ACM (**Figure 4.4.24 - 4.4.25**).

PA (0 Gy vs 2 Gy vs 4 Gy)

Mϕ cultured with PA treated ACM exposed to 2 Gy radiation showed increased CD11b, CD11c, HLA-DR, TIM-3, CD80, CD86, CD80+CD86+, CD206, and CD163+CD206+ expression compared with Mϕ cultured with unirradiated PA treated ACM. Mϕ cultured with PA treated ACM exposed to 4 Gy radiation showed increased CD11b, CD11c, TIM-3, and CD80 expression compared with Mϕ cultured with unirradiated PA treated ACM. PA treated ACM exposed to 4 Gy radiation also significantly decreased Mϕ viability compared with Mϕ cultured in matched unirradiated PA treated ACM (**Figure 4.4.24 - 4.4.25**).

Comparisons between fatty acids in the mock irradiated setting

In the unirradiated setting Mϕ cultured with PA treated ACM showed decreased expression of CD80, CD80+CD86+, and increased expression of CD206, CD163+CD206+ compared with matched control ACM. Additionally, in the unirradiated setting Mϕ cultured with PA treated ACM showed decreased expression of CD80 compared with matched OA treated ACM. (**Figure 4.4.25**).

(* $p < 0.05$, ** $p < 0.01$, *** $p < 0.001$, **** $p < 0.0001$.)

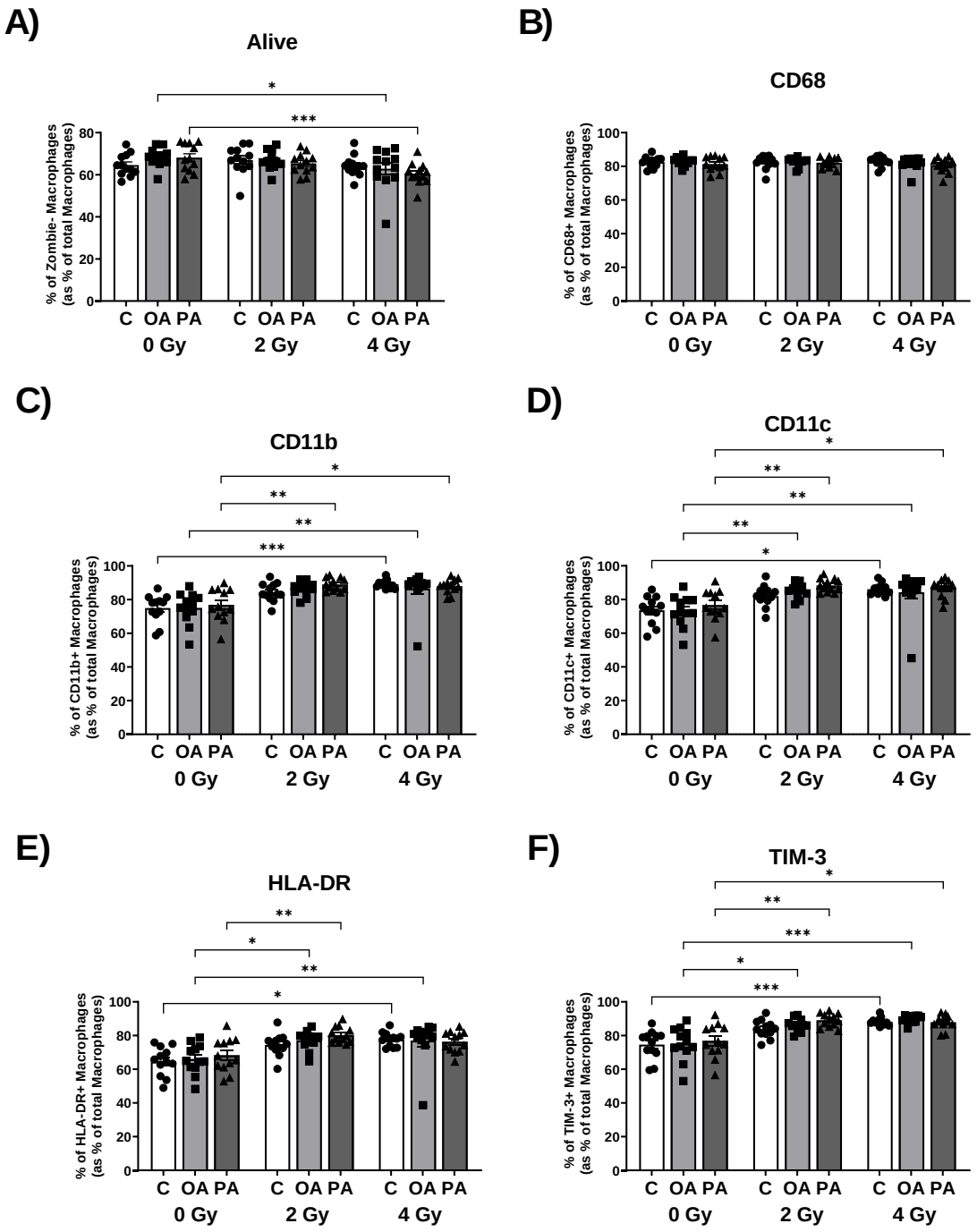


**Figure 4.4.24 The adipose secretome treated with fatty acids and increasing irradiation increases Mϕ expression of TIM-3.**

A-F) Expression of Mϕ viability, phenotypic and immunoinhibitory markers including CD68, CD11b, CD11c, HLA-DR, and TIM-3, following culture with the adipose secretome of OAC cancer patients exposed to mock irradiation, 2 Gy irradiation or 4 Gy irradiation in combination with BSA Control (C = □), Oleic Acid (OA= ▨) or Palmitic Acid (PA= ■) in combination.

To assess fatty acid treatment within non-obese cancer and obese cancer cohorts Friedman test with Dunn's correction was used, to assess the difference between non-obese cancer compared with obese cancer cohorts Kruskal Wallis test with Dunn's correction was used. All data expressed as mean ± SEM, $n$ = 12, * $p < 0.05$, ** $p < 0.01$, *** $p < 0.001$.

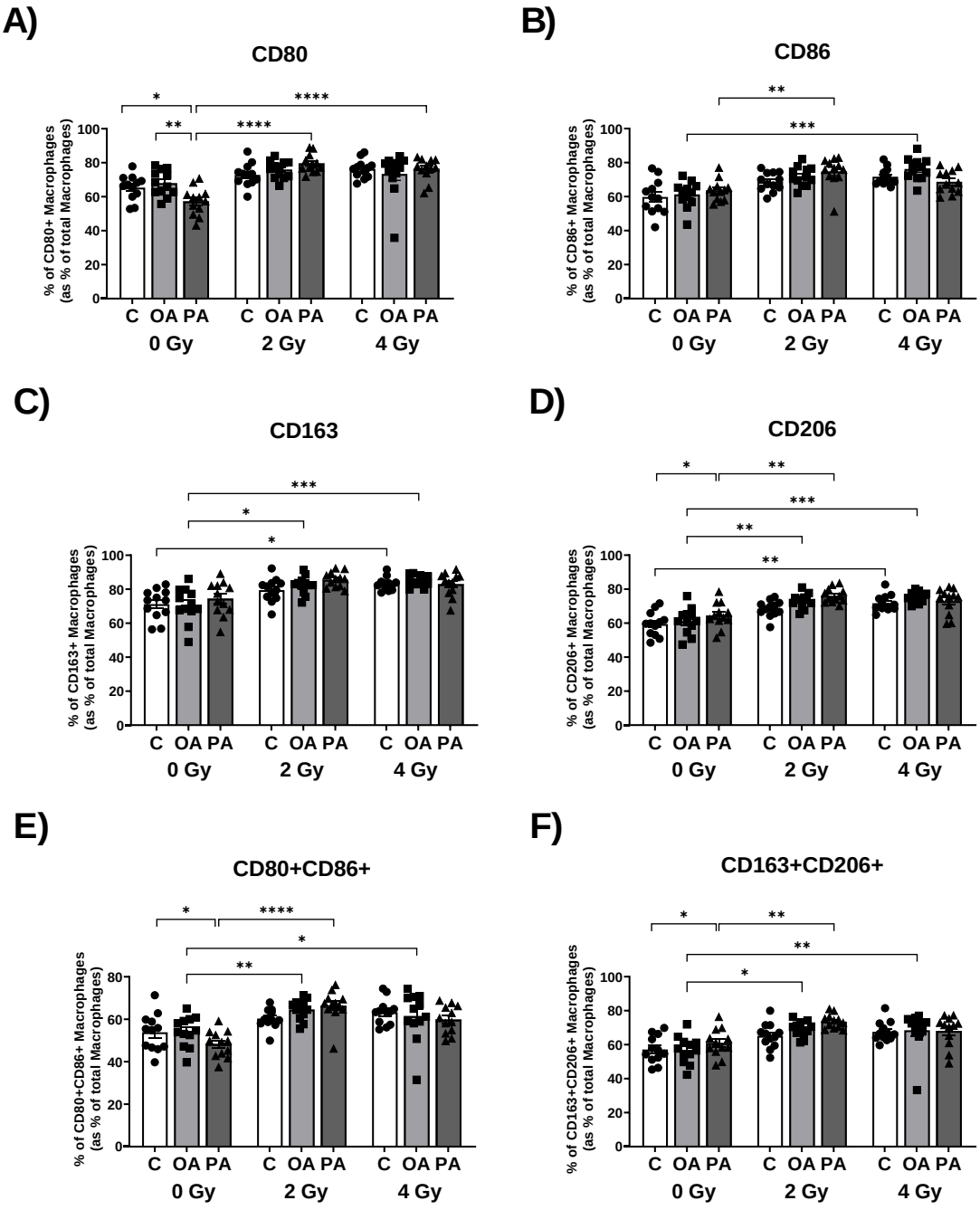


**Figure 4.4.25 Increasing radiation on the adipose secretome leads to palmitic acid inducing pro-inflammatory effects and oleic acid inducing anti-inflammatory effects in Mϕ.**

A-F) Expression of Mϕ pro-inflammatory and anti-inflammatory markers including CD80, CD86, CD163, CD206 and co-expression of CD80+CD86+ and CD163+CD206+ following culture with the adipose secretome of OAC patients exposed to mock irradiation, 2 Gy irradiation or 4 Gy irradiation in combination with BSA Control (C = □), Oleic Acid (OA= ▒) or Palmitic Acid (PA= ■) in combination.

To assess fatty acid treatment within non-obese cancer and obese cancer cohorts Friedman test with Dunn's correction was used, to assess the difference between non-obese cancer compared with obese cancer cohorts Kruskal Wallis test with Dunn's correction was used. All data expressed as mean ± SEM, n = 12, * $p < 0.05$, ** $p < 0.01$, *** $p < 0.001$, **** $p < 0.0001$.

### 4.4.8 *Increasing radiation in combination with PA treatment in the adipose secretome augments pro-inflammatory Mϕ polarisation in non-obese patients only.*

Obesity is a known contributor to chronic low-grade inflammation which is augmented by the action of pro-inflammatory M1-like Mϕ. Therefore, to assess whether increased visceral adiposity augmented the influence of increasing radiation in combination with OA and PA treatments in the adipose secretome and the effects this holds for Mϕ phenotype, Mϕ were cultured in these treated ACM and a series of phenotypic and maturation markers were assessed via flow cytometry.

In the non-obese setting Mϕ cultured with control ACM showed decreased viability compared with matched OA, and PA treated ACM. Additionally, Mϕ cultured with PA treated ACM from non-obese patients showed decreased expression of CD80 compared with matched OA treated ACM and increased expression of CD206 compared with matched control (**Figure 4.4.29**). In the obese setting Mϕ cultured with PA treated ACM from non-obese patients exposed to 2 Gy radiation showed increased expression of CD86, and CD80+CD86+ compared with matched control (**Figure 4.4.28**). In the obese setting Mϕ cultured with PA treated ACM exposed to 2 Gy radiation showed increased expression of CD206, and CD163+CD206+ compared with matched control (**Figure 4.4.29**). Mϕ cultured with unirradiated OA treated ACM from non-obese patients showed decreased expression of CD68 compared with OA treated ACM from obese patients. Mϕ cultured with unirradiated PA treated ACM from non-obese patients showed decreased expression of CD68, and CD86 compared with PA treated ACM from obese patients (**Figure 4.4.26, 4.4.28**).

(* $p < 0.05$.)

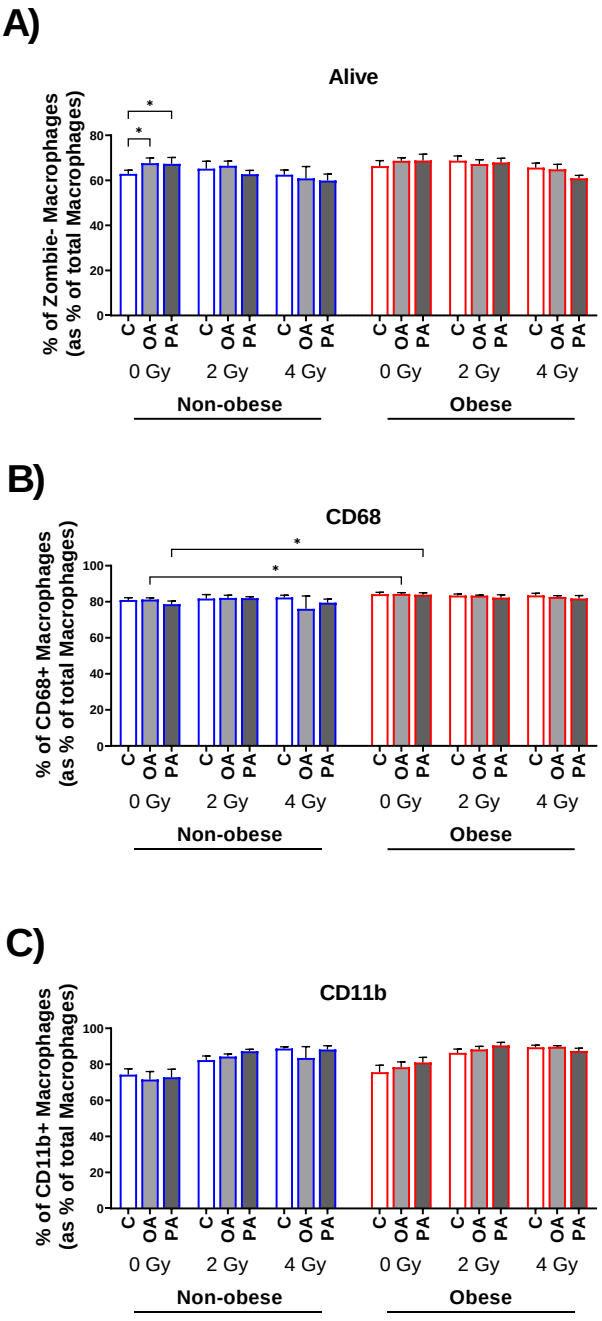


**Figure 4.4.26 The influence of the adipose secretome exposed to increasing irradiation and exogenous fatty acids on Mϕ expression of phenotypic markers is not impacted by obesity**

A-C) Expression of Mϕ viability and phenotypic markers including CD68, CD11b following culture with the adipose secretome of non-obese and obese cancer patients exposed to mock irradiation, 2 Gy irradiation or 4 Gy irradiation in combination with BSA Control (C = ☐), Oleic Acid (OA= ▢) or Palmitic Acid (PA= ■) in combination.

To assess fatty acid treatment within non-obese cancer and obese cancer cohorts Friedman test with Dunn's correction was used, to assess the difference between non-obese cancer compared with obese cancer cohorts Kruskal Wallis test with Dunn's correction was used. All data expressed as mean ± SEM, non-obese $n = 6$, obese $n = 6$, * $p < 0.05$.

Blue border ☐ = non-obese, Red border ☐ = obese

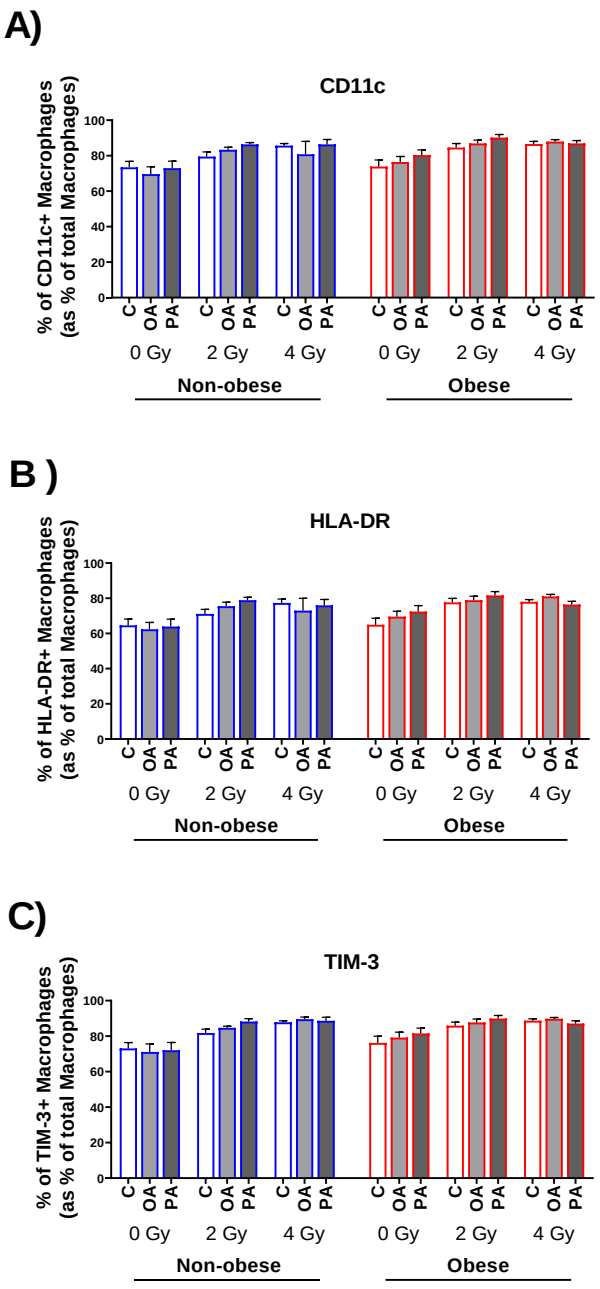


**Figure 4.4.27 Obesity does not affect Mϕ expression of phenotypic and immunoinhibitory markers in response to the adipose secretome exposed to increasing irradiation and exogenous fatty acids.**

A-C) Expression of Mϕ viability, phenotypic and immunoinhibitory markers including CD11c, HLA-DR, and TIM-3, following culture with the adipose secretome of non-obese and obese cancer patients exposed to mock irradiation, 2 Gy irradiation or 4 Gy irradiation in combination with BSA Control (C = ☐), Oleic Acid (OA= ▒) or Palmitic Acid (PA= ■) in combination.

To assess fatty acid treatment within non-obese cancer and obese cancer cohorts Friedman test with Dunn's correction was used, to assess the difference between non-obese cancer compared with obese cancer cohorts Kruskal Wallis test with Dunn's correction was used. All data expressed as mean ± SEM, non-obese $n = 6$, obese $n = 6$, * $p < 0.05$.

Blue border ☐ = non-obese, Red border ☐ = obese

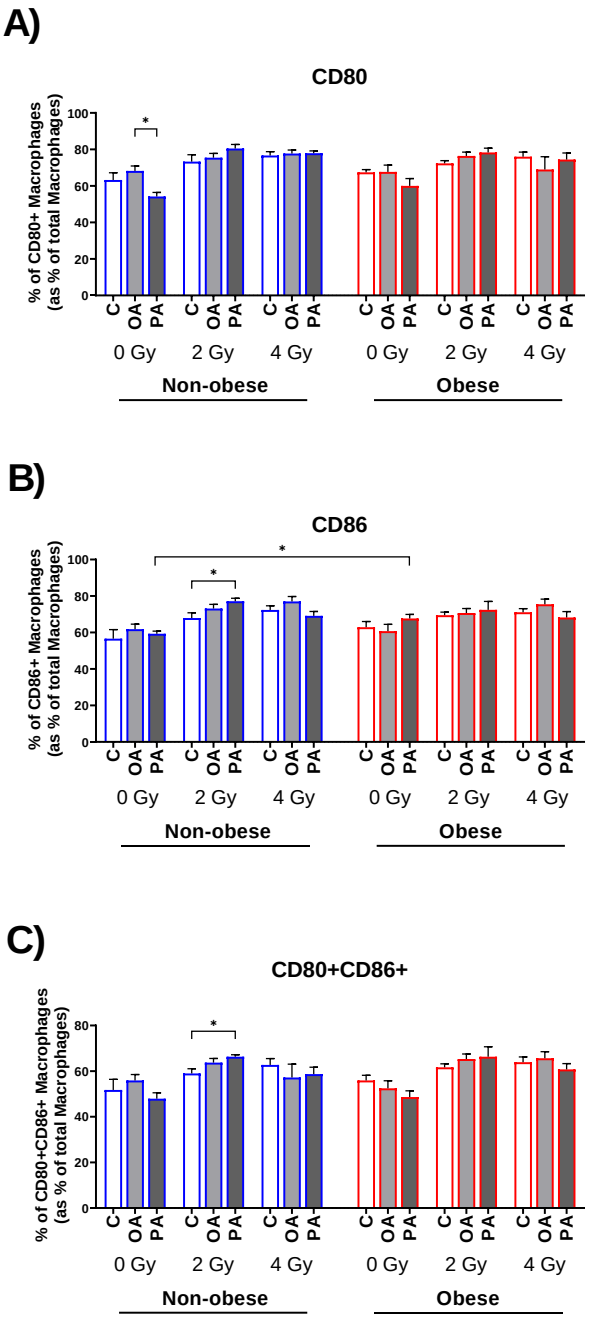


**Figure 4.4.28 Obesity differentially effects Mϕ expression of pro-inflammatory markers in response to the adipose secretome exposed to increasing irradiation and palmitic acid.**

A-C) Expression of Mϕ pro-inflammatory markers including CD80, CD86, and co-expression of CD80+CD86+ following culture with the adipose secretome of non-obese and obese cancer patients exposed to mock irradiation, 2 Gy irradiation or 4 Gy irradiation in combination with BSA Control (C = ☐), Oleic Acid (OA= ▩) or Palmitic Acid (PA= ■) in combination.

To assess fatty acid treatment within non-obese cancer and obese cancer cohorts Friedman test with Dunn's correction was used, to assess the difference between non-obese cancer compared with obese cancer cohorts Kruskal Wallis test with Dunn's correction was used. All data expressed as mean ± SEM, non-obese $n = 6$, obese $n = 6$, * $p < 0.05$.

Blue border ☐ = non-obese, Red border ☐ = obese

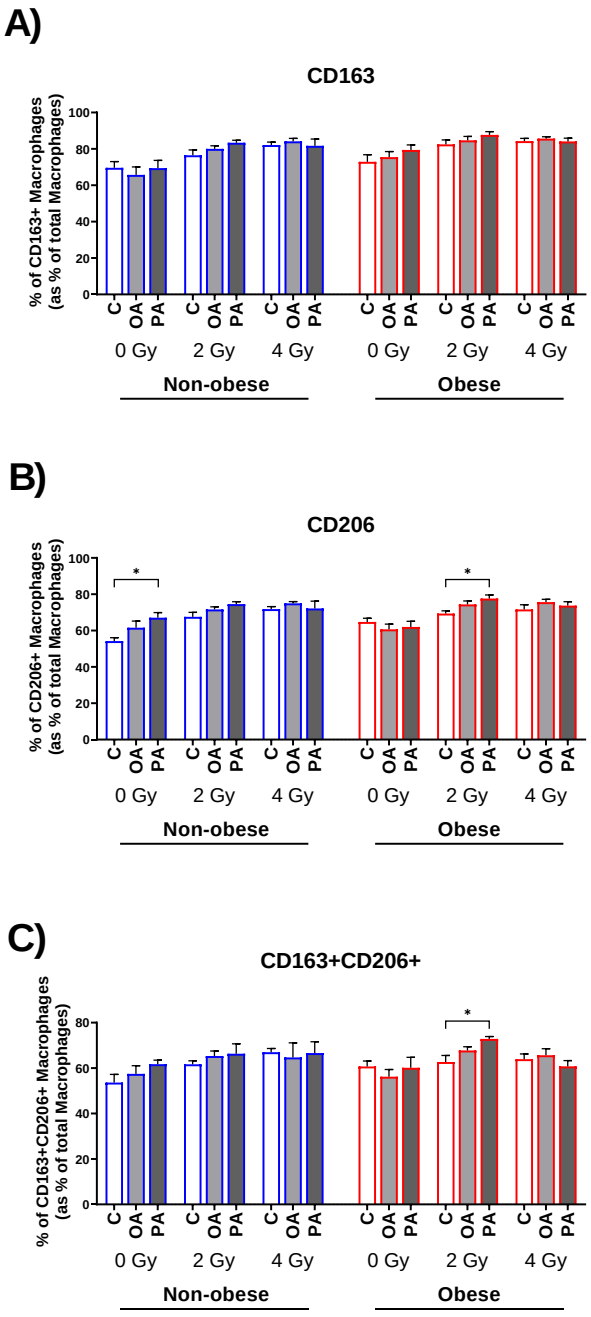


**Figure 4.4.29 Obesity differentially effects Mϕ expression of anti-inflammatory markers in response to the adipose secretome exposed to increasing irradiation and palmitic acid.**

A-C) Expression of Mϕ anti-inflammatory markers including CD163, CD206 and co-expression CD163+CD206+ following culture with the adipose secretome of non-obese and obese cancer patients exposed to mock irradiation, 2 Gy irradiation or 4 Gy irradiation in combination with BSA Control (C = ☐), Oleic Acid (OA= ▢) or Palmitic Acid (PA= ■) in combination.

To assess fatty acid treatment within non-obese cancer and obese cancer cohorts Friedman test with Dunn's correction was used, to assess the difference between non-obese cancer compared with obese cancer cohorts Kruskal Wallis test with Dunn's correction was used. All data expressed as mean ± SEM, non-obese $n = 6$, obese $n = 6$, * $p < 0.05$.

Blue border ☐ = non-obese, Red border ☐ = obese

## 4.5 Summary of main findings

- PA diminishes OCR metabolism in adipose explants derived from OAC patients an effect that is augmented by increasing irradiation.
- Obesity differential effects adipose explants utilisation of OCR and ECAR metabolism in the unirradiated setting and following 4 Gy irradiation. Obesity further effects adipose explants metabolic responses to exogenous fatty acids in the unirradiated setting and following 4 Gy irradiation.
- However exogenous fatty acid treatment does not affect adipose secretion of angiogenic, and vascular injury associated mediators, in the unirradiated setting or following irradiation.
- The obesity status of OAC patients differentially effects adipose tissue response to the immunosuppressive influence of PA.
- The adipose secretome of OAC patients treated with oleic acid and increasing irradiation increases DC expression of phenotypic, maturation and immunoinhibitory markers.
- The adipose secretome of non-obese and obese OAC patients treated with palmitic acid and 2 Gy irradiation decreases DC viability. Whilst the adipose secretome of non-obese OAC patients the showed decreased DC expression of CD80+CD86+ compared with obese patients, an effect that is ameliorated by PA.
- The adipose secretome treated with fatty acids and increasing irradiation increases Mϕ expression of TIM-3. Whilst exposure of the adipose secretome to increasing radiation in combination with palmitic acid induces pro-inflammatory effects and in combination with oleic acid induces anti-inflammatory effects in Mϕ.
- The influence of the adipose secretome exposed to increasing irradiation and exogenous fatty acids on Mϕ expression of phenotypic and immunoinhibitory markers is not impacted by obesity. However, obesity differentially effects Mϕ expression of pro-inflammatory and anti-inflammatory markers in response to the adipose secretome exposed to increasing irradiation and palmitic acid.

## 4.6 Discussion

This study for the first time reports the effect of increasing radiation on exogenous fatty acid treatment and how this influences adipose tissue metabolism and secretome. As well as looking at how this altered secretome is affected by increased visceral adiposity. This research further examines how this treated adipose secretome effects the maturation of DCs and polarisation of Mϕ and whether obesity alters these effects.

Palmitate has been reported to impair fatty acid oxidation (FAO) and citric acid cycle flux through diacylglycerides mediated Protein Kinase C activation and not oxidative stress [438]. This induced impairment of FAO may be aided through decreased glutamine in the obese adipose secretome of OAC patients. This study reports significantly decreased OCR metabolism in adipose explants treated with PA compared with control and OA treatment in both the unirradiated setting and after exposure to 4 Gy radiation. Fatty acid overload induced particularly by OA or PA has previously been shown to lead to accumulation of triacylglycerides in HepG2 cells, however, only PA mediated mitochondrial dysfunction and fragmentation [439]. This study reports in the unirradiated setting, OCR metabolism was significantly increased in control adipose explants from obese patients compared with non-obese patients. Additionally, in the unirradiated setting PA treated adipose from non-obese patients showed decreased OCR metabolism compared with matched OA treated adipose. In adipose derived from obese patients decreased OCR was observed in PA treated adipose compared with matched control. Palmitate in high doses has been reported to inhibit FAO and CPT-1 activity whilst still leading to increased intracellular lipid accumulation [440]. Significantly decreased OCR metabolism was also observed in PA treated adipose from obese patients compared with matched OA treated adipose following exposure to 4 Gy radiation. It has been reported that radiation leads to transient elevated glycolysis to facilitate DNA damage repair [295,441]. Following exposure to 4 Gy radiation, adipose explants from non-obese patients showed increased ECAR metabolism compared with adipose from obese patients. However adipose tissue from obese patients following OA treatment at 4 Gy radiation showed significant increases compared with matched control. well as significant increases in OCR compared with PA treated. This could indicate that OA treatment may aid in promoting transient glycolysis to facilitate DNA damage repair as the aberrant biological function of obese adipose tissue may impede its ability to mechanistically react in a similar manner as non-obese adipose tissue. However, previous research has also indicated that saturated membrane lipids may be less sensitive to external oxidative stress [442]. Oxidative stress is a direct result of radiation, which could infer that PA being a saturated fatty acid is protective during radiation exposure leading to these decreased metabolic profiles in adipose tissue treated with PA.

Radiotherapy has previously been linked to the induction of a series of cytokines, that aid tumour aggressiveness and metastasis [443]. Research has indicated that unsaturated fatty acids increase the radio-responsiveness of glioma cancer cells [444]. Previously we have seen that PA treatment augments an immunosuppressive effect on adipose tissue from both non-cancer and cancer patients. However, it has been reported that adipocytes undergoing oxidative stress have diminished secretion of adipokines [56]. Within this study again the immunosuppressive effects of PA treatment on adipose secretome were observed with decreased secreted levels of Eotaxin-3, GM-CSF, IFN-γ, IL-1α, IL-1β, IL-1Ra, IL-2, IL-3, IL-6, IL-10, IL-12p70, IL-13, IP-10, MDC, MIP-1β, MIP-3α TNF-α, and TSLP being reported compared with control ACM or OA treated ACM in either the unirradiated setting or with some level of increasing radiation. Many of these secreted factors have pleiotropic effects that aid in pro-inflammatory or anti-inflammatory biological actions, with many have critical roles in immune cell recruitment, modulation of anti-tumour immunity as well as correlating with a series of patient clinical outcomes [112,232,327]. In this study, increased secreted levels of IL-4 were observed in control and OA treated ACM exposed to 4 Gy radiation compared with unirradiated matched ACM. Interestingly, following exposure to 2 and 4 Gy radiation PA treatment significantly reduced secreted levels of IL-4 compared with matched control and OA treated ACM. IL-4 has previously been reported to be highly expressed in cancer cells following radiation treatment and high expression of IL-4 in cancer patients is correlated with poor survival [445]. PA treatments diminishing this effect in adipose tissue may be multi-faceted particularly in the case of obesity, as IL-4 may potentiate the low-grade chronic inflammation associated with it. However, decreased secreted IL-4 may possess beneficial effects for anti-tumour immunity. Interestingly, in control ACM increased secreted levels of MCP-1 were observed following 2 Gy radiation which was coupled with PA treatment significantly decreasing MCP-1 and VEGF secreted levels compared with control ACM also at 2 Gy radiation. MCP-1 is a key chemokine that regulates migration and infiltration of monocytes and macrophages [446], an action supported by MCP-4, which has previously been reported to be increased in obesity [447]. Previously, in meningioma cell lines, radiation was reported to induce increased expression of MCP-1 which led to induced VEGF expression [448]. This decrease in secreted levels of MCP-1 could potentiate immune cell recruitment to adipose tissue and again enable anti-tumour immunity.

Herein, secreted levels of MIP-1α are reported to be decreased following PA treatment and exposure to 2 and 4 Gy radiation compared with matched control and OA treated adipose secretome. MIP-1α and its interaction with its receptor has previously been reported to mitigate radiation-induced lung inflammation in mice models [449]. A reduction in the secreted levels of

MIP-1α could ameliorate the effects of radiation induced inflammation and corresponding secreted factors. Previous research has indicated that an ester of retinol and palmitic acid ameliorated the rectal symptoms of radiation proctopathy [450]. Interestingly, following exposure to 2 or 4 Gy radiation OA treated adipose explants showed increased secreted levels of IL-4 as well as decreased IL-2, IL-12p70, and TNF-α compared to the secretome of unirradiated adipose explants treated with OA. IL-2 possesses a critical role in T cell expansion and differentiation as well as aiding in stimulating cytotoxic effector cells [451]. IL-12p70 is an essential output of functional antigen presenting DCs and acts to induce NK cells [420] and cytotoxic CD8+ T cells [452]. TNF-α has been widely reported for its pro-inflammatory effects and its regulation of macrophage function [453] and as previously mentioned, IL-4 is a powerful anti-inflammatory agent. Such an increase in IL-4 coupled with decreases in immune and pro-inflammatory activating mediators could lead to a microenvironment primed to support anti-inflammatory action and potentiate anti-tumour immunity. However, OA has previously been reported to attenuate inflammation [454] and the alteration of these significant mediators of inflammation may speak to its method of action.

Secreted levels of IL-8 were also observed to be decreased in adipose explants exposed to 4 Gy radiation compared to 2 Gy radiation regardless of fatty acid treatment. Previous studies have indicated that IL-8 induction following radiation may be mitigated by IL-1Ra production or diminished IL-1α [455]. IL-1Ra was shown to be quit highly secreted in adipose tissue in this study particularly following 2 Gy radiation which could potentially mitigate this response. Interestingly, increasing radiation was shown to significantly increase secreted levels of a series of angiogenic associated mediators including bFGF, Flt-1, PlGF, and VEGF-C. bFGF has been shown to inhibit radiation induced apoptosis of HUVECs [456]. PlGF has been reported to be increased in vitro and in-vivo and inhibition synergistically decreases tumour growth with radiation [457]. Similarly, VEGF-C has been reported to be increased following radiation in lung cancer cells [458]. However very little research has looked at the influence of radiation on VEGF receptor FLT-1, it has been reported that that FLT-1 is upregulated in response to oxidative stress, promoting a more immunosuppressive phenotype in myeloid cells [459]. The promotion of potent pro-angiogenic factors such as bFGF, FLT-1, PlGF and VEGF-C by radiation could lead to an adipose secretome primed to promote angiogenesis and metastasis in the local tumour microenvironment. However, more research is required to fully understand if this occurrence within adipose tissue could be therapeutically targeted. Perhaps unsurprisingly, increased secreted levels of CRP, and SAA were also observed following radiation, both markers having previously been associated with vascular injury induced by radiation [460,461]. Higher levels of CRP

have been reported to be a poor prognostic indicator in oesophageal cancer patients treated with radiotherapy [462]. Decreased levels of SAA have been reported to negatively correlate with longer overall survival in patients receiving thoracic radiotherapy for non-small cell lung cancer [463]. Control and OA treated ACM were also observed to have significantly increased secreted levels of sICAM-1 and sVCAM-1 with increasing radiation whereas this effect was not observed in the PA treated adipose secretome. ICAM-1 and VCAM-1 are both essential for cell adhesion in a series of cells but also has been reported to have a major role in initiating metastasis [464,465]. Increased visceral adiposity is known to act in a detrimental capacity in a series of metabolic disorders. In the non-obese setting the adipose secretome treated with PA showed decreased secreted levels of Eotaxin-3, IL-3, IL-4, IL-6, IL-12p70, IL-15, and IP-10 compared with matched control or OA treated ACM either with or without radiation exposure. These effects were not mirrored in the obese setting. Eotaxin-3, IP-10, IL-3, and IL-15 are known to promote recruitment, development and differentiation of immune cells [233,466–468].

IL-4 as previously discussed is a powerful anti-inflammatory mediator and is known to regulate lipid metabolism by inhibiting adipogenesis [469]. IL-6 is known for its major pro-inflammatory effects and is widely reported to be elevated in adipose tissue of obese individuals [470]. In the obese setting the adipose secretome treated with PA showed decreased secreted levels of IFN-γ, IL-1α, IL-1β, IL-10, MIP-1α, MIP-1β, and MIP-3α compared with matched control or OA treated ACM either with or without radiation exposure. These effects were more apparent in the obese patients than the non-obese patients. IFN-γ, IL-1α and IL-1β have all been widely reported to be elevated in obesity and promote a pro-inflammatory response [471–473]. MIP-1α, MIP-1β and MIP-3α have shown to be elevated with obesity [474,475] and are known to recruit macrophages with MIP-1β being postulated to aid the infiltration of tumour associated macrophage into tumour tissue [476]. These divergent profiles of secreted factors following PA treatment in combination with exposure to radiation in non-obese and obese OAC patients poses an intriguing question into the underpinning mechanistic biology of adipose tissue that appears aberrantly altered by obesity. Key anti-inflammatory mediators and immune recruiting and differentiating factors are reduced in the adipose secretome of non-obese patients may diminish immune cell recruitment to the adipose tissue as well as decreasing anti-inflammatory primed immune cells which could ameliorate anti-tumour immunity. However, in the obese adipose secretome key pro-inflammatory and macrophage recruiting factors are diminished by PA which could potentiate anti-tumour immunity by bolstering anti-inflammatory immune responses. These differential responses of obese and non-obese adipose tissue may have implications in patients' response

to current modalities of therapy, but further research is required to fully interrogate this link and whether it may be therapeutically targeted.

Research has indicated that radiation may augment maturation as well as enhancing homing ability and T cell activating capacity of DCs [437,477]. This study reports that DCs cultured in control or OA treated ACM exposed to 4 Gy radiation significantly increased a series of phenotypic and functional markers including HLA-DR, CD11c, CD80, CD86, CD40, PD-L1, and TIM-3 compared with DCs cultured in unirradiated matched ACM. However, PA treatment in combination with exposure to 4 Gy radiation only showed a significant increase in DC expression of CD80, and TIM-3 compared with matched unirradiated ACM. Here it is observed that PA treatment on adipose tissue diminishes the influence of radiation to increase maturation markers on DCs, which may potentiate anti-tumour immunity [478]. Particularly, when this effect of PA treatment is coupled with increasing TIM-3 expression, a ligand known to diminish activation and the efficacy of chemotherapy [479,480]. DC expression of CD83 was significantly decreased by ACM exposed to 4 Gy radiation compared with matched unirradiated ACM regardless of fatty acid treatment. The influence on radiation or the adipose secretome on CD83 expression has not been widely reported in the literature. However, new insights show CD83 knockout in mice models lead to DCs secreting elevated IL-2, as well as highly expressing CD25 and OX40L known to induce antigen specific T cell response [481].

In the unirradiated setting, DCs cultured with control ACM from non-obese patients showed significantly decreased co-expression of CD80+CD86+ compared with matched PA treated ACM and control ACM from obese patients. Co-stimulatory molecules have been widely reported in literature to be vital for DC antigen presentation and T cell activation [482]. However, these interactions require further research to assess whether PA treatment or the effect of obesity on adipose secretome itself is more of an influencing force in this interaction. Further to this, DCs cultured in OA treated ACM from obese patients showed decreased expression of CD54 compared matched control ACM and PA treated ACM. OA has previously been identified to decrease CD54 expression in human aortic endothelial cells [67] and recent research has shown that whilst CD54 is necessary to maintain adhesions with CD8 T-cells this is not required for cytotoxic and central memory lymphocytes [424]. Increasing CD54 has further been reported to correlate with increasing BMI and abdominal fat mass in mice models. With increased pro-inflammatory factors and immune cell infiltration in adipose tissue also being reported in mice with increased CD54 [483]. The decreased expression of CD54 on DCs by OA treated ACM from obese patients could potentially be linked to anti-inflammatory effects.

Macrophages have been reported to play a vital role in radiation induced inflammation, inducing an anti-tumour immunity through the generation of an inflammatory response [247]. This study reports that Mϕ cultured with control ACM exposed to 4 Gy radiation showed significantly increased expression of CD11b, CD11c, HLA-DR, TIM-3, CD163, and CD206 compared with matched unirradiated ACM. It is of note, that irradiated control ACM that has significantly increased secreted levels of IL-2 promote Mϕ expression of CD163 and CD206. CD163 and CD206 are key markers of M2-like macrophages or Tumour Associated Macrophages (TAMs) and indicate a macrophage phenotype that is known to be tumour promoting. Further to this, TIM-3 has previously been reported in colon cancer to evoke the development of TAMs and expression of TIM-3 on TAMs has been correlated with more aggressive cancers and poorer survival rates in patients with hepatocellular carcinoma. Collectively, the irradiated adipose secretome could aid the development of TAMs, promoting a pro-tumorigenic immune response that could facilitate tumour growth and metastasis.

Similar effects were observed in Mϕ cultured with OA treated ACM exposed to 2 or 4 Gy radiation showed significantly increased expression of CD11b, CD11c, HLA-DR, TIM-3, CD86, CD80+CD86+, CD163, CD206, and CD163+CD206+ compared with matched unirradiated OA treated ACM. This increase in pro-inflammatory as well as anti-inflammatory associated ligands again may be related back to the adipose secretome of OA treated explants where a series of cytokines showed similar expression compared with control ACM. Interestingly, in this study Mϕ cultured with unirradiated PA treated ACM showed significantly decreased expression of CD80, CD80+CD86+, and increased expression of CD206, CD163+CD206+ compared with unirradiated control ACM or OA treated ACM. This deviation from the normally reported effects of PA on macrophages [65] is only seen in the unirradiated setting and may be linked to the immunosuppressive effects observed in the pro-inflammatory mediators observed in the adipose secretome. PA treatment in combination with the adipose secretome may promote a more anti-inflammatory TAM like phenotype that could potentiate anti-tumour immunity, but further research is required to interrogate this effect as it is diminished by the introduction of radiation.

PA is a known instigator of inflammatory response largely associated with obesity, driving macrophages towards classical activation and increasing pro-inflammatory ligands such as CD80 and CD86 [65]. Nonetheless, again in this study we report divergent effects of the action of the non-obese and obese adipose secretome on immune cell function seeing altering Mϕ phenotype. In the unirradiated setting, Mϕ cultured with PA treated ACM from non-obese patients showed decreases in pro-inflammatory associated markers compared with matched

OA treated ACM as well as compared with obese PA treated ACM. Additionally, Mϕ cultured with PA treated ACM from non-obese patients showed increases in anti-inflammatory associated markers compared with matched control ACM. However, following 2 Gy irradiation, Mϕ cultured with PA treated ACM from non-obese patients showed increases in pro-inflammatory associated markers compared with matched control ACM. Whilst Mϕ cultured with PA treated ACM from obese patients showed increases in anti-inflammatory associated markers compared with matched control ACM. Still, as previously mentioned these interactions require further research to assess whether this effect is linked to PA treatment on adipose tissue or the influence of obesity on adipose secretome itself and most importantly whether these interactions could be exploited for therapeutic gain.

To conclude, this study has indicated that exogenous PA treatment possesses significant anti-metabolic effects on adipose tissue from OAC patients in the unirradiated setting and following high dose radiation. As well as displaying significant immunosuppressive effects on the adipose secretome of OAC patients augmented by increasing radiation. However, increasing radiation in control ACM and OA treated ACM did show increases in key anti-inflammatory markers that may diminish anti-tumour immune responses. OA treatment on the adipose secretome in combination with increasing radiation was observed to significantly increase DC maturation. Whilst PA had differential effects on Mϕ polarisation, inducing anti-inflammatory phenotypes in the unirradiated setting and increasing expression of pro-inflammatory markers as well following exposure to radiation. However, it is of intertest to note that PA treatment induced differential responses in adipose tissue metabolism and secretome of non-obese and obese OAC patients, which were more pronounced following exposure to increasing radiation. Adipose tissue from obese patients displayed higher reliance on  in the unirradiated and decreased reliance on glycolysis following high dose radiation compared with adipose tissue from non-obese patients. However, this diminished reliance on glycolysis in adipose tissue from obese patients was reinvigorated by OA treatment which could be important to facilitate for DNA damage repair.

Additionally, PA treated adipose secretome from non-obese patients appeared to diminish pro-inflammatory polarisation in the unirradiated setting whilst increasing anti-inflammatory markers an effect that was reversed following exposure to 2 Gy radiation. In contrast, the opposite effects were observed in Mϕ treated with PA treated ACM from obese patients. Collectively, this could indicate the obese and non-obese adipose secretome may have very opposing mechanisms of response to exposure to increasing radiation in combination with PA treatment, which could be related to the differential secretion of key inflammatory mediators.

Cumulatively, this research indicates that the influence saturated fatty acids in combination with radiation in the adipose microenvironment could lead to detrimental immunosuppressive effects that could bolster pro-tumour immunity aiding in cancer growth and metastasis, particularly for patients with increased visceral adiposity.

*Chapter 5*

# *The obese adipose secretome differentially alters primary and metastatic oesophageal cancer cells metabolism and invasive capacity in response to fatty acids, increasing irradiation and inhibition of fatty acid oxidation.*

## 5.1 Objective and specific aims:

**Objective:**

The overall objective of this chapter was to assess the influence of the treated adipose secretome generated in chapter 4 on primary and metastatic cancer cell metabolism and invasive capacity. As well as identifying whether these responses could be affected through the introduction of increasing irradiation with or without exogenous fatty acids. This chapter also looked to assess whether the obesity status of patients classified by VFA biologically effected the underlying adipose secretome and whether this effect altered the response of adipose tissue to irradiation or fatty acids and what downstream effects this held for primary cancer and metastatic cell biological function.

**Specific Aims**

- To assess if the adipose secretome treated with PA (palmitic acid) and OA (oleic acid) in combination with increasing irradiation differentially effects primary cancer and metastatic cell metabolism and invasive capacity and whether this is altered by fatty acid oxidation (FAO) inhibition.
- To examine if obesity effects the adipose secretome response to PA and OA in combination with increasing irradiation and what downstream effects this has for primary cancer and metastatic cell metabolism and invasive capacity and if this is altered by FAO inhibition.
- To profile the adipose secretome treated with PA and OA in combination with increasing irradiation to assess how this modulates secreted levels of CD147 and whether this is affected by obesity.

## 5.2 Introduction

Adipose tissue has been reported to aid the development of metastatic niches [307] and diminish the efficacy of current cancer treatment [484] by supporting flexibility in cancer cell metabolism [485]. Previously we have observed that treatment with exogenous OA and PA in combination with increasing radiation differentially effects the adipose secretome, an effect that is further augmented by patient obesity status. The adipocyte secretome which is altered by obesity, has been suggested to aid cancer cell survival by enabling protective mechanisms to allow them to evade toxic cancer treatments [177,486]. Previously cancer cells have been shown to be conferred with added survival advantages following culture with adipocyte conditioned media allowing them to evade radiation induced inflammatory stress by evoking increased metabolic activity [177]. Moreover, certain chemotherapy treatments have been reported to dysregulate adipose tissue and adipocytes, leading to disruption in lipid storage and elevated free fatty acid levels which may aid in cancer cell metabolism and proliferation [136].

OAC is one of the most closely associated cancers with obesity [311], making it an exemplar model to study the effects of obesity and adipose tissue biology on cancer progression and metastasis. Due to the proximity of the visceral adipose tissue to gastrointestinal (GI) tract, OAC and other upper GI cancers have been shown to utilise the adipose enriched microenvironment to aid cancer cell growth and develop pre-metastatic niches to support migration and distant metastasis [435].

In addition to this, the adipose secretome has also been reported to influence the tumour microenvironment, particularly the visceral adipose tissue microenvironment due to its anatomical distribution and proximity to organs known to develop obesity associated carcinogenesis [79,487]. One effect of the adipocyte secretome that is highly evoked in cancer cells, is the adipocyte's ability to secrete factors that can alter the pro-inflammatory landscape of the tumour environment as well as releasing a series of free fatty acids to support cancer metabolism [112]. As previously shown OA and PA invoke differential secretion of these factors, with PA acts in an immunosuppressive manner on the secretome from visceral adipose explants. Primary cancer cells have been reported to heavily rely on glycolytic metabolism in order to grow and survive, even inducing this metabolic reliance in the face of oxidative stress evoked by radiation induced inflammation order to aid DNA damage repair [295]. Metastatic cancer cells however have been shown to rely more so on oxidative phosphorylation associated metabolism and fatty acid oxidation [302,303].

Whilst flexibility in energy metabolism has been reported to be critical in aiding cancer cell's ability to undergo epithelial to mesenchymal transition and migration in order to facilitate distant metastasis[304], other factors have also been identified to enhance this process. Previously secreted levels of CD147 have been linked to invasion and metastasis [488]. CD147 has been reported to promote invasion through cathepsin B [489], a factor known to lead to mitochondrial dysfunction and apoptosis [490]. CD147 has also been reported to be increased both in circulation and within visceral adipose depots of obese patients [491]. Further to this, previous research has shown that exposure to radiation enhances the invasive tendencies of cancer cells [492]. These invading cells have elevated lipid metabolism and increased reliance on free fatty acids [493], an effect that could be augmented by patient obesity which has been associated with increased circulating levels of free fatty acid PA [494].

This chapter assessed the dynamic interplay between the adipose secretome and cancer cell metabolism and invasive capacity, by utilising the treated adipose conditioned media generated in chapter 4. We assessed the culminative effect of exogenous fatty acid treatment and increasing irradiation on the adipose secretome and what downstream effects this has for primary cancer cells (FLO-1) and matched liver derived metastatic (FLO-LM) cancer cells [495] metabolism, FAO dependency and invasive capacity. Additionally, we asked the question if obesity status augments or attenuates these treatments effects on the adipose secretome and how this impacts primary and metastatic cancer cells functionality.

## 5.3 Materials and Methods

### 5.3.1 *Ethics Statement and Patient Recruitment*

Ethical approval was granted by the St James's Hospital/AMNCH ethical review board (Ethics number: REC_2019-07 List 25(27)) and written informed consent was collected from all patients in this study. 12 cancer patients were recruited within the period between 3rd of April 2021 and 14th of January 2023, patient demographics are listed in Table 1. Fresh adipose tissues were taken from all patients at the start of the surgical procedure. All OAC patients were being treated with curative intent. Obesity was defined via visceral fat area (VFA) measurements with cut-off value for VFA of 163.8 $cm^2$ in males and 80.1 $cm^2$ for females as previously categorised[318] with adipose tissue from 6 obese and 6 non-obese patients being collected.

**Table 5.3. 1 Clinical demographics associated with OAC patients**

| **Patient Clinical Parameters** | |
|---|---|
| **Diagnosis** | OAC = 6 |
| **Sex** | Male = 4<br>Female = 2 |
| **Age at diagnosis** | 55-81 (Mean = 68.5) |
| **Post-treatment BMI** | 22.34-34.29 (Mean = 27.56) |
| **Weight** | 58.4–113 kg (Mean = 77.85) |
| **Treatment** | Naïve *n* = 6 |
| **Clinical Stage (T)** | T1 *n* = 6 |
| **Clinical Stage (N)** | N0 *n* = 6 |
| **Path stage (T)** | T0 *n* = 1<br>T1 *n* = 5 |
| **Path Stage (N)** | N0 *n* = 5<br>N1 *n* = 1 |

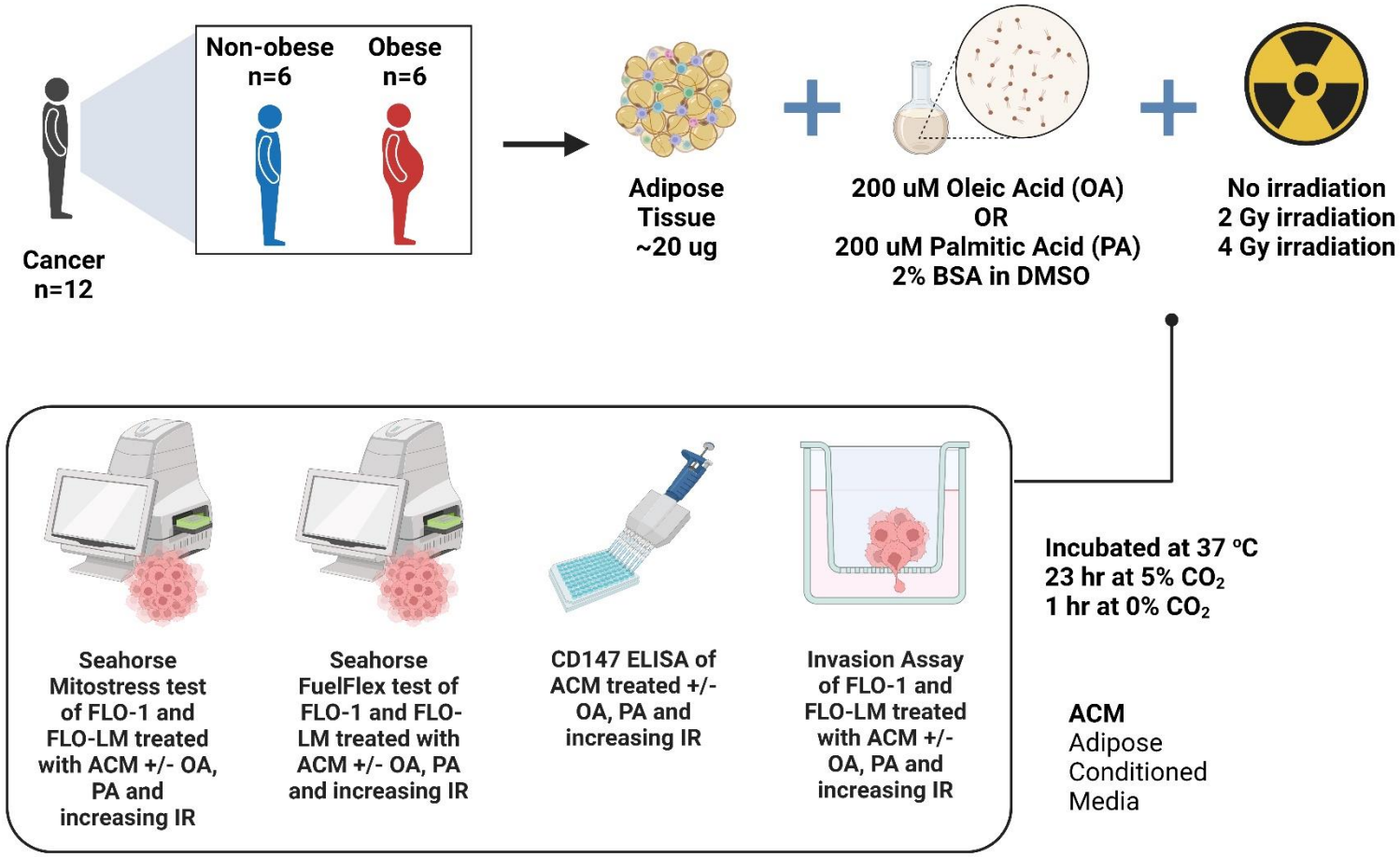


**Figure 5.3.1 Schematic of experimental methodology workflow associated with Chapter 5**

Mitochondrial parameters and fatty acid oxidation reliance of FLO-1 primary OAC cancer cells and FLO-LM matched liver derived metastatic cell line were assessed in response to culture with the adipose secretome of OAC patients which had been treated with dietary fatty acids and exposed to increasing irradiation using Agilent seahorse technology. The level of invasion associated CD147 was assessed in these treated ACM via ELISA as well as assessing their influence on the invasive capacity of these cell lines via an invasion assay.

### 5.3.2 *Lipid Treatment*

Methodology carried out as per section 3.3.2 Lipid treatment.

### 5.3.3 *Seahorse Analysis of metabolic profiles from adipose tissue explants and generation of Adipose Conditioned Media (ACM)*

Methodology carried out as per section 4.3.2 Seahorse Analysis of metabolic profiles from adipose tissue explants and generation of Adipose Conditioned Media (ACM)

### 5.3.4 *Secondary Cell Culture Methods*

#### 5.3.4.1 Growth Conditions

37ºC at 5% Carbon Dioxide in a humidified incubator, in DMEM supplemented with 10% FBS, and 1% Pen/Strep in t-75 culture dishes. All tissue culture was conducted in a laminar flow under sterile conditions with sterile or autoclaved materials and chemicals sterilized with 70% ethanol. Cell lines included in this study; FLO-1 originated from primary distal oesophageal adenocarcinoma FLO-LM derived from a FLO-1 liver metastasis (Peter MacCallum Cancer Centre, Australia)

#### 5.3.4.2 Thawing Cells

Cells are removed from Liquid Nitrogen or -80ºC and transferred immediately to 37 ºC water bath to defrost cells quickly to minimise exposure to DMSO. Cells were then removed from water bath with a small ice crystal remaining and transferred to 15 ml falcon tube in hood, with 7 ml of prewarmed media added drop wise to prevent osmotic shock. Suspension was then centrifuged at 12000 rpm for 3 minutes, media aspirated, leaving cell pellet undisturbed. 1 ml of pre-warmed media was added dropwise to cells, which were then re-suspended and brought up to an appropriate volume and transferred to culture vessel dependent on freezing instructions.

#### 5.3.4.3 Passaging Cells

Harvest as outlined above. The required volume of cell suspension was removed for a split ratio suited to the cells doubling time, then transferred to new plate with supplementary pre-warmed media with cell line, passage number, date, split ratio, and operator initials labelled on dish. Cells were gently migrated in north south fashion to ensure even distribution throughout the dish.

#### 5.3.4.4 Harvesting Cells

Media was extracted and washed with room temperature PBS, PBS extracted, method repeated, room temperature trypsin was added volume depending on size of vessel. Flasks replaced in incubator for approximately 5 minutes depending on cell lines adherence, flasks removed and tapped gently, inspected under microscope to ensure all cells had lifted and separated, trypsin was quenched with pre-warmed media approximately 3 times the volume of trypsin used.

#### 5.3.4.5 Cell Counting

Cells were harvested as outlined above, ensuring suspension was homogenous and 10 µl of sample transferred to an Eppendorf tube containing 90 µl of trypan blue. 10 µl of sample was placed on the gridded plate of a Hemacytometer, with cover slip placed on top at 45 º angle to prevent air bubbles. Each of the 16 square corner grids were counted and divided by four then multiplied by 10000 to find the average cell viability per ml.

#### 5.3.4.6 Freezing Cells

Prepare Freezing Media, as outlined in chemical reagents, allowed to cool before adding to cell suspension. Harvest cells as outlined above. Cell suspension was transferred to 15 ml falcon tube and centrifuged at 12000 rpm for 3 minutes. Media aspirated, leaving cell pellet untouched, then re-suspended in 1 ml of freezing media and transferred to a 1.5 ml cryovial. Labelled with cell line, passage number, date, initials of operator and dish to be used when cells are thawed.

### 5.3.5 *Analysis of mitochondrial function of oesophageal cancer and liver derived metastasis cell lines using Seahorse MitoStress test*

FLO-1 and FLO-LM cells were seeded at a density of 18,000 in 24 well XFe24 cell culture microplate plate (Agilent Technologies, California, United States) in a volume of 100 µl cDMEM and allowed to adhere for 3 hours before an additional 150 µl of media was added. Cells were rested overnight (approx. 18 hours). Media was extracted and replaced with 100 µl M199 control or appropriate treated ACM sample in technical replicates and allowed to incubate for a further 24 hours. Following this, cells were washed with Agilent Seahorse XF DMEM Medium supplemented with 10 mM glucose, 1 mM sodium pyruvate, and 2 mM L-glutamine (Agilent Technologies, California, United States) and incubated for 1 hour in a non-CO2 incubator at 37$^{o}$C. OCR, ECAR, basal respiration, ATP production, maximal respiration, proton leak and non-mitochondrial respiration were assessed using a Seahorse Biosciences XFe24 Extracellular Flux Analyser (Agilent Technologies, California, United States). Three basal measurements of OCR

and ECAR were taken over 24 minutes consisting of three repeats of mix (3 min) / wait (2 min) / measurement (3 min) to establish basal respiration. Three additional measurements in the same manner were obtained following the injection of 50 µl of 3 mitochondrial inhibitors including 1.8 µM oligomycin (Sigma Aldrich, California, United States), 4 µM Carbonyl cyanide 4- (trifluoromethoxy) phenylhydrazone (FCCP) (Sigma Aldrich, California, United States) and 2 µM Antimycin-A (Sigma Aldrich, California, United States). All inhibitors were diluted in Agilent DMEM. All measurements were normalised to cell number via crystal violet staining.

### 5.3.6 *Analysis of fatty acid dependency of oesophageal cancer and liver derived metastasis cell lines using Seahorse Fuel Flex test*

FLO-1 and FLO-LM cells were seeded at a density of 18,000 in 24 well XFe24 cell culture microplate plate (Agilent Technologies, California, United States) in a volume of 100 µl cDMEM and allowed to adhere for 3 hours before an additional 150 µl of media was added. Cells were rested overnight (approx. 18 hours). Media was extracted and replaced with 100 µl M199 control or appropriate treated ACM sample in technical replicates and allowed to incubate for a further 24 hours. Following this, cells were washed with Agilent Seahorse XF-DMEM Medium supplemented with 10 mM glucose, 1 mM sodium pyruvate, and 2 mM L-glutamine (Agilent Technologies, California, United States) and incubated for 1 hour in a non-CO2 incubator at 37$^{o}$C. Cells dependency on fatty acid oxidation was assessed using a Seahorse Biosciences XFe24 Extracellular Flux Analyser (Agilent Technologies, California, United States). Three basal measurements of OCR and ECAR were taken over 24 minutes consisting of three repeats of mix (3 min) / wait (2 min) / measurement (3 min) to establish basal respiration. Two additional measurements in the same manner were obtained following the injection of 50 µl of 4 µM etomoxir followed by a second 50 µl injection comprising of 3 µM BPTES combined with 2 µM UK5099 (Generon, Ireland). All inhibitors were diluted in Agilent XF-DMEM. All measurements were normalised to cell number via crystal violet staining.

### 5.3.7 *Crystal Violet Assay*

Supernatants were extracted in a sterile environment and stored at -80$^{o}$C for further processing. Cells were fixed with 50 µl of 1 % glutaraldehyde in PBS for 15 minutes at room temperature. Fixative was removed and cells washed twice with PBS and stained with 50 µl of 0.1% crystal violet solution for 30 minutes at room temperature. Crystal violet was then removed, and cells washed twice with dH2O and allowed to air dry overnight. Cells well then incubated with 50 µl of Triton-X 100 in PBS on a plate shaker at 450 rpm for 1 hour. The eluant was then transferred

to a 96 well flat bottom plate and read on a plate reader at 595 nm (VersaMax microplate reader, Molecular Devices, California, United States).

### 5.3.8 *Invasion Assay*

Prior to running the assay cells were serum starved for 24 hours and grown to 80% confluency. All reagents were equilibrated to room temperature prior to use. The "Cell Migration Chamber" (Figure 5.3.2) was dissembled under sterile conditions and 40 µl of Basement Membrane solution was added to bottom of the wells in the "Top Chamber". The chamber was then reassembled and incubated for 1 hour at 37 $^{o}$C to allow the basement membrane to gel. Cells were then harvested and centrifuged at 1000 x g, for 5 minutes to pellet. Cells were then resuspended in 100,000 per ml in serum free media. Again, under sterile conditions the cell migration chamber was disassembled and 50 µl of cell suspension was added to the wells of the top chamber (50,000 cells per well). These wells were brought up to a final volume of 100 µl with either a serum free media or serum free media containing 4 µM etomoxir (Generon, Ireland). The wells of the "Bottom Chamber" were filled with 200 µl of ACM from explants that had been treated with OA or PA in combination with increasing irradiation. The chamber was reassembled and incubated at 37 $^{o}$C for 48 hours. Using the above cell suspensions, cells standard curves were prepared in wash buffer and following 1 hour incubation at 37 $^{o}$C with cell dye, fluorescence was read at Ex/Em = 530/590 nm. Following, 48 hours incubation, media was aspirated from the "Top Chamber", and it was set aside. The "Bottom chamber" was centrifuged at 1000 x g for 5 minutes, media was aspirated and 200 µl of wash buffer was added. Again, the "Bottom Chamber" was centrifuged at 1000 x g for 5 minutes, wash buffer was aspirated and 100 µl of 10 % cell dye in cell dissociation solution was added. The full "Cell Migration Chamber" was the reassembled and allowed to incubate for 1 hour at 37 $^{o}$C, after which the chamber was disassembled and the fluorescence of the "Bottom Chamber" was read at Ex/Em = 530/590 nm.

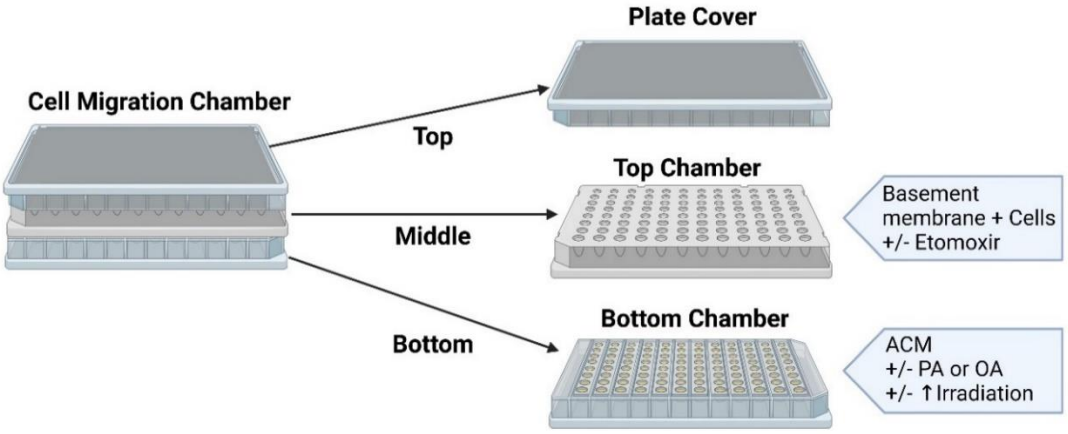


**Figure 5.3.2 schematic of invasion chamber apparatus and set-up showing location of cells, treated ACM and inhibitor etomoxir.**

### 5.3.9 *Statistical Analysis*

All statistics were conducted using GraphPad Prism 9.5 (GraphPad Software, California, United States). A significance level of $p<0.05$ was used in all analysis and all p-values reported were two-tailed. Friedman testing with Dunn's post hoc correction, was employed for non-parametric testing between paired cohorts. For statistical testing between unpaired non-parametric cohorts, Kruskal Wallis test with Dunn's correction was used. Details of specific statistical tests are given in each corresponding figure legend.

## 5.4 Results

### 5.4.1 *Basally oesophageal primary cancer cell lines show greater reliance on glycolysis compared to the matched liver metastasis cells*

Seahorse MitoStress test was used to assess the metabolic profiles of the primary cancer cell line FLO-1 and matched liver derived metastatic cell line FLO-LM. This test assesses a series of mitochondrial parameters that indicate cells preference of oxidative phosphorylation or glycolysis, respiratory capabilities, and indications of mitochondrial health.

- Basal respiration shows energetic demand and OCR oxygen consumption of the cell under baseline conditions.
- ATP linked respiration indicates the decrease in OCR following addition of oligomycin, it represents the portion of basal respiration that was being used to drive ATP production to meet the energetic needs of the cell. Proton leak is a measure of remaining basal respiration not coupled to ATP production.
- Proton leak can be a sign of mitochondrial damage or can be used as a mechanism to regulate the mitochondrial ATP production.
- Maximal respiration shows the maximum rate of respiration that the cell can achieve by adding the uncoupler FCCP that mimics a physiological “energy demand” or “stress”.
- Spare respiratory capacity is a measurement that indicates the capability of the cell to respond to an energetic demand it can be an indicator of cell fitness or flexibility.
- Non-mitochondrial respiration is oxygen consumption that persists due to a subset of cellular enzymes that continue to consume oxygen after the addition of antimycin A.
- ECAR is an indicator of extracellular acidification which is associated with lactate efflux, increases indicate cellular activation and proliferation.
- OCR:ECAR ratio a measure of metabolic phenotype used to detect metabolic changes and preferences in utilisation of oxidative phosphorylation or glycolysis.

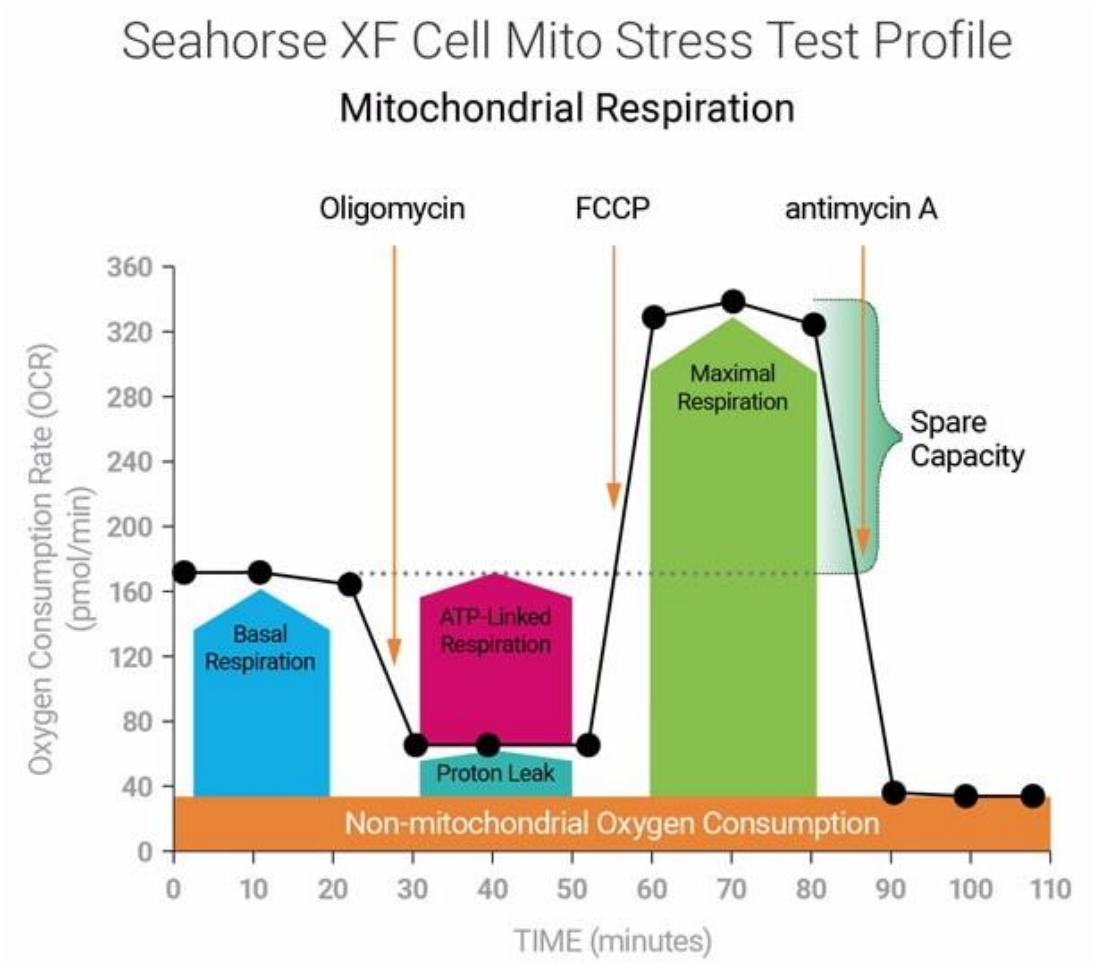


**Figure 5.4.1 An explanatory figure depicting the MitoStress Test process.**
This figure details the mitochondrial response to inhibitors Oligomycin, FCCP, and Antimycin and the ensuing measurements of basal respiration, ATP linked respiration, proton leak, maximal respiration, spare respiratory capacity, and non-mitochondrial consumption following their injection.

FLO-1 cells showed elevated ECAR profiles, an indicator of glycolytic metabolism compared with FLO-LM cells. However, FLO-LM demonstrated increased spare respiratory capacity and OCR:ECAR ratio compared with FLO-1 cells, an indicator that a cell can produce more ATP and overcome more stress in addition to having increased reliance on oxidative phosphorylation compared with glycolytic metabolism (Figure 5.4.2).

(* $p < 0.05$)

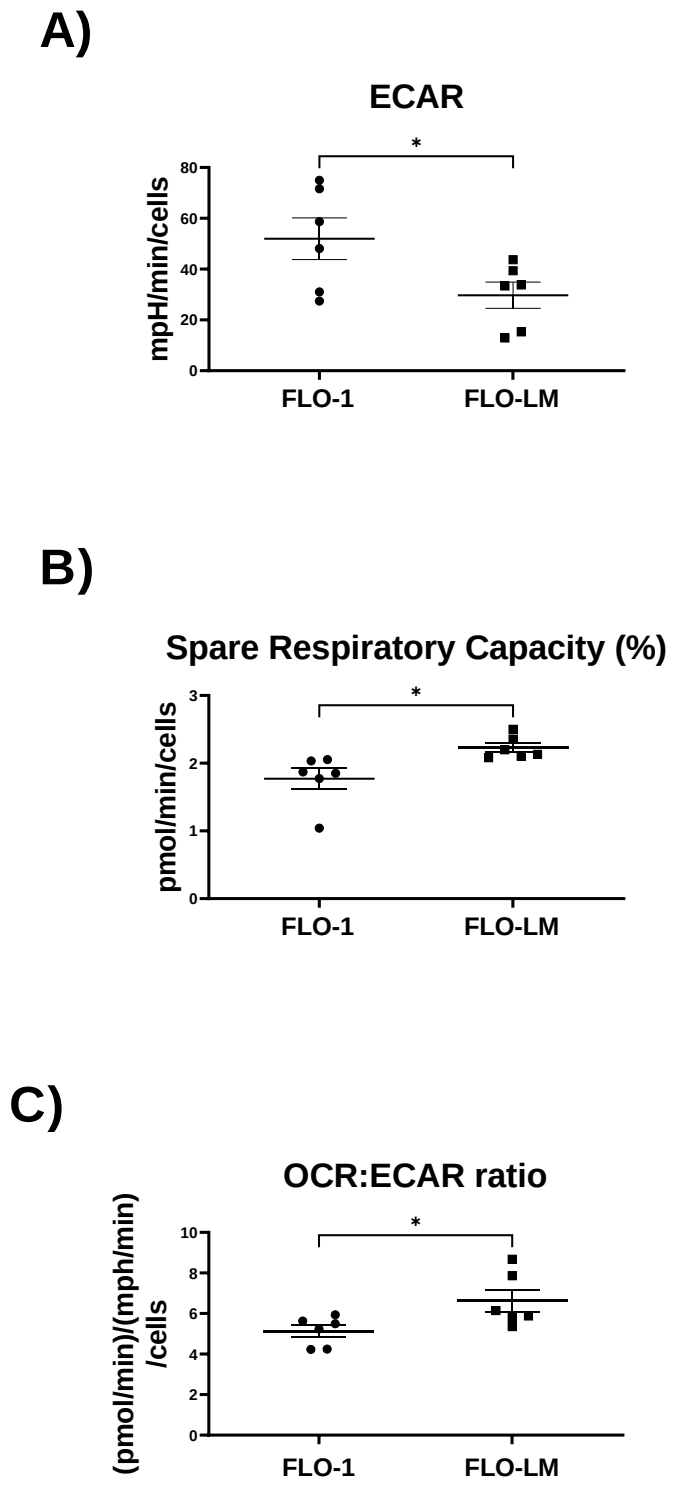


**Figure 5.4.2 Basally oesophageal cancer cell lines show greater reliance on glycolysis than liver metastasis cell line**

A) ECAR metabolic profiles of untreated FLO-1 and FLO-LM cell lines. B) Spare respiratory capacity of untreated FLO-1 and FLO-LM cell lines. C) OCR:ECAR ratio metabolic profiles of untreated FLO-1 and FLO-LM cell lines. (Unpaired t-test) All data expressed as mean ± SEM, n=6, * $p < 0.05$. Circle symbols indicate FLO-1 cell line (●), square symbols indicate FLO-LM(■).

### 5.4.2 *The adipose secretome exposed to fatty acids and increasing irradiation differentially alters oesophageal cancer and metastatic cells glycolytic capacity and mitochondrial parameters.*

Adipose tissue has been linked to aiding cancer cell growth, invasion ad treatment resistance through metabolic interactions. These interactions that aid growth and ATP production by invading adipose tissue have been linked to inducing the release of free fatty acids from adipocytes. To examine the influence of the adipose secretome which was exposed to increasing radiation in the presence or absence of OA and PA on FLO-1 and FLO-LM cell lines metabolic parameters, cells were cultured with the treated ACM previously generated in chapter 4 for 24 hours and assessed using Seahorse MitoStress test.

In FLO-1 cells OCR was observed to be decreased following culture with PA treated ACM exposed to 2 and 4 Gy irradiation compared with unirradiated matched ACM. In FLO-LM cells OCR was increased following culture with 2 Gy irradiated ACM compared with matched unirradiated ACM and following culture with OA treated ACM exposed to 2 Gy irradiation compared with OA treated ACM exposed to 4 Gy irradiation and PA treated ACM exposed to 2 Gy irradiation (**Figure 5.4.3**). In FLO-1 cells increased non-mitochondrial oxygen consumption was observed following culture with OA and PA treated unirradiated ACM compared with control unirradiated ACM. In FLO-LM cells decreased non-mitochondrial oxygen consumption was observed following culture with OA treated ACM exposed to 4 Gy irradiation and PA treated ACM in the unirradiated setting and following exposure to 2 and 4 Gy irradiation compared with similarly treated FLO-1 cells (**Figure 5.4.3**). In FLO-1 cells ATP linked respiration was decreased following culture with PA treated ACM exposed to 4 Gy irradiation compared with PA treated unirradiated ACM. In FLO-LM cells increased ATP linked respiration was observed following culture with OA treated ACM exposed to 2 Gy irradiation compared with OA treated ACM exposed to 4 Gy irradiation and PA treated ACM exposed to 2 Gy irradiation **(Figure 5.4.4**). In FLO-1 and FLO-LM cells proton leak was observed to be increased following culture with control ACM exposed to 2 Gy irradiation compared with control ACM exposed with 4 Gy or control unirradiated in FLO-LM cells. In FLO-LM cells proton leak was increased following culture with OA treated ACM exposed to 2 Gy irradiated ACM compared with OA treated ACM exposed to 4 Gy irradiation. In FLO-1 cells increased proton leak was observed following culture with PA treated unirradiated ACM compared with FLO-1 cells cultured with control unirradiated ACM, PA treated ACM exposed to 4 Gy irradiation and in FLO-LM cells cultured with PA treated unirradiated ACM (**Figure 5.4.4**). In FLO-1 cells decreased maximal respiration was observed following culture with PA treated

ACM exposed to 4 Gy irradiation compared with PA treated unirradiated ACM. In FLO-LM cells decreased maximal respiration was observed following culture with OA treated ACM exposed to 4 Gy irradiation compared with OA treated ACM exposed to 2 Gy irradiation (**Figure 5.4.5**). In FLO-LM cells increased spare respiratory capacity was observed following culture with control or OA treated ACM in the unirradiated setting or following 2 or 4 Gy irradiation compared with similarly treated FLO-1 cells. In FLO-LM cells spare respiratory capacity was decreased following culture with PA treated unirradiated ACM compared with control and OA treated unirradiated ACM. Additionally in FLO-LM cells spare respiratory capacity was decreased following culture with PA treated ACM exposed to 4 Gy irradiation compared with OA treated ACM exposed to 4 Gy irradiation (**Figure 5.4.5**). All treatments in FLO-1 cells showed increased ECAR profiles compared with FLO-LM cells except for ACM treated with OA and exposed to 2 Gy irradiation (**Figure 5.4.6**). In FLO-LM cells increased OCR:ECAR ratio was observed following culture with control ACM regardless of irradiation exposure and following culture with OA or PA treated ACM exposed to 2 Gy irradiation compared with similarly treated FLO-1 cells. In FLO-LM cells decreased OCR:ECAR ratio was observed following culture with PA treated unirradiated ACM compared with unirradiated control and OA treated ACM. Additionally, in FLO-LM cells decreased OCR:ECAR ratio was observed following culture with PA treated ACM exposed to 2 Gy irradiation compared with OA treated ACM exposed to 2 Gy irradiation. Furthermore, in FLO-LM cells decreased OCR:ECAR ratio was observed following culture with PA treated ACM exposed to 4 Gy irradiation compared with control ACM exposed to 4 Gy irradiation (**Figure 5.4.6**).

(* $p < 0.05$, ** $p < 0.01$, *** $p < 0.001$.)

A)

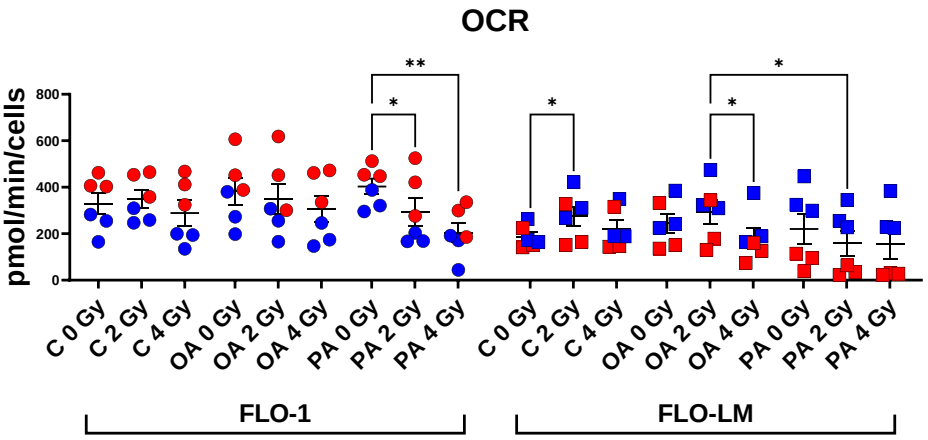


B)

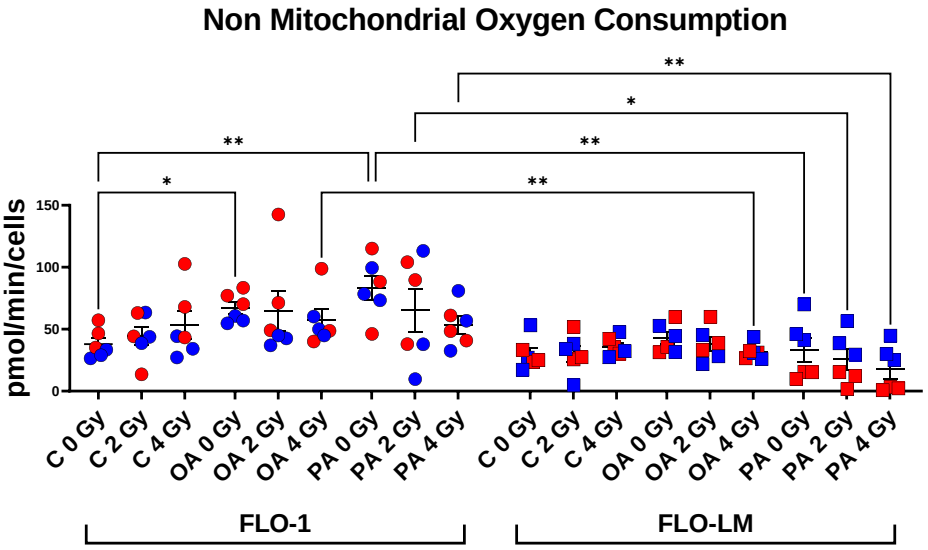


**Figure 5.4.3 The adipose secretome exposed to fatty acids and increasing irradiation differentially alters oesophageal cancer and metastatic cell lines basal respiration and non-mitochondrial associated oxygen consumption.**

FLO-1 and FLO-LM cell lines cultured with ACM treated with Control (C), Oleic Acid (OA), or Palmitic Acid (PA) in combination with mock irradiation, 2 Gy irradiation or 4 Gy irradiation. Mitochondrial parameters were assessed using Seahorse MitoStress test including (A-B) basal respiration, and non-mitochondrial oxygen consumption (Kruskal Wallis test with Dunn's correction). Blue circle symbols indicate FLO-1 cell line treated with ACM from non-obese patients (●), red circle symbols indicate FLO-1 treated with ACM from obese patients (●). Blue square symbols indicate FLO-LM cell line treated with ACM from non-obese patients (■), red square symbols indicate FLO-LM treated with ACM from obese patients (■). All data expressed as mean ± SEM, n=6* $p < 0.05$, ** $p < 0.01$, *** $p < 0.001$.

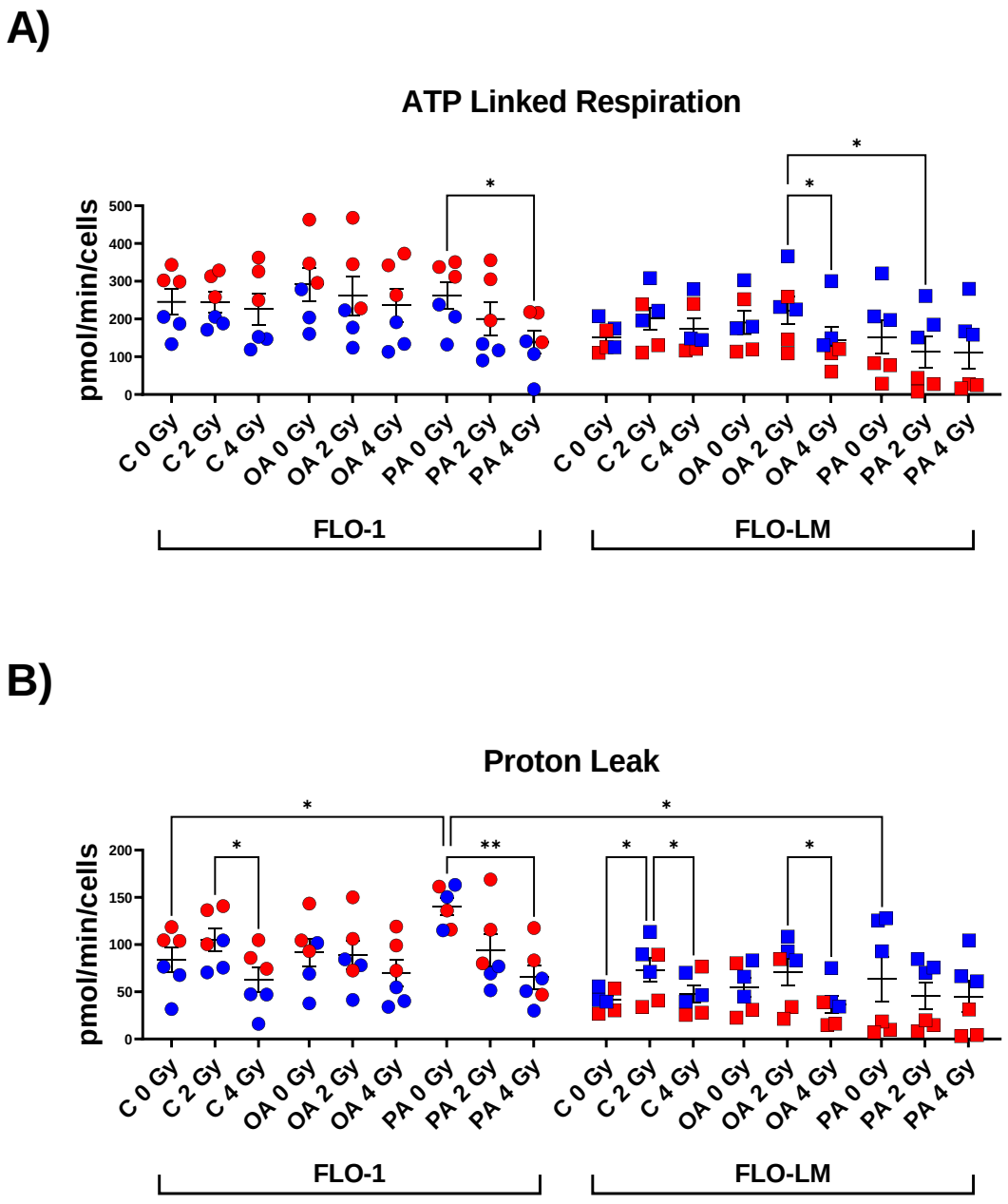


**Figure 5.4.4 The adipose secretome exposed to fatty acids and increasing irradiation differentially alters oesophageal cancer and metastatic cell lines ATP linked respiration and proton leak.**

FLO-1 and FLO-LM cell lines cultured with ACM treated with Control (C), Oleic Acid (OA), or Palmitic Acid (PA) in combination with mock irradiation, 2 Gy irradiation or 4 Gy irradiation. Mitochondrial parameters were assessed using Seahorse MitoStress test including (A-B) ATP linked respiration, and proton leak (Kruskal Wallis test with Dunn's correction). Blue circle symbols indicate FLO-1 cell line treated with ACM from non-obese patients (●), red circle symbols indicate FLO-1 treated with ACM from obese patients (●). Blue square symbols indicate FLO-LM cell line treated with ACM from non-obese patients (■), red square symbols indicate FLO-LM treated with ACM from obese patients (■). All data expressed as mean ± SEM, n=6, * $p < 0.05$, ** $p < 0.01$, *** $p < 0.001$.

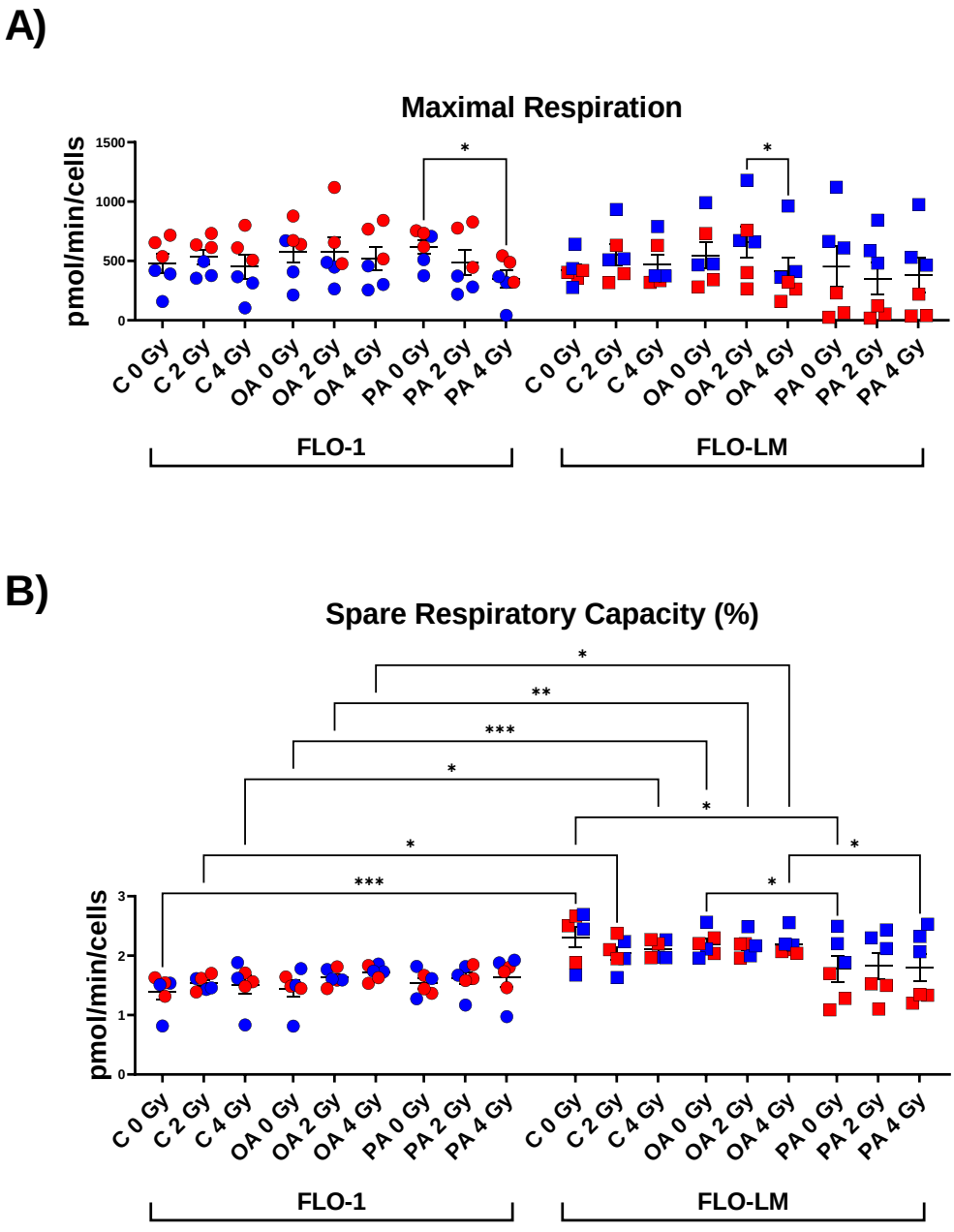


**Figure 5.4.5 The adipose secretome exposed to fatty acids and increasing irradiation differentially alters oesophageal cancer and metastatic cell lines maximal respiration and spare respiratory capacity.**

FLO-1 and FLO-LM cell lines cultured with ACM treated with Control (C), Oleic Acid (OA), or Palmitic Acid (PA) in combination with mock irradiation, 2 Gy irradiation or 4 Gy irradiation. Mitochondrial parameters were assessed using Seahorse MitoStress test including (A-B) maximal respiration and spare respiratory capacity (Kruskal Wallis test with Dunn's correction). Blue circle symbols indicate FLO-1 cell line treated with ACM from non-obese patients (●), red circle symbols indicate FLO-1 treated with ACM from obese patients (●). Blue square symbols indicate FLO-LM cell line treated with ACM from non-obese patients (■), red square symbols indicate FLO-LM treated with ACM from obese patients (■). All data expressed as mean ± SEM, n=6* $p < 0.05$, ** $p < 0.01$, *** $p < 0.001$.

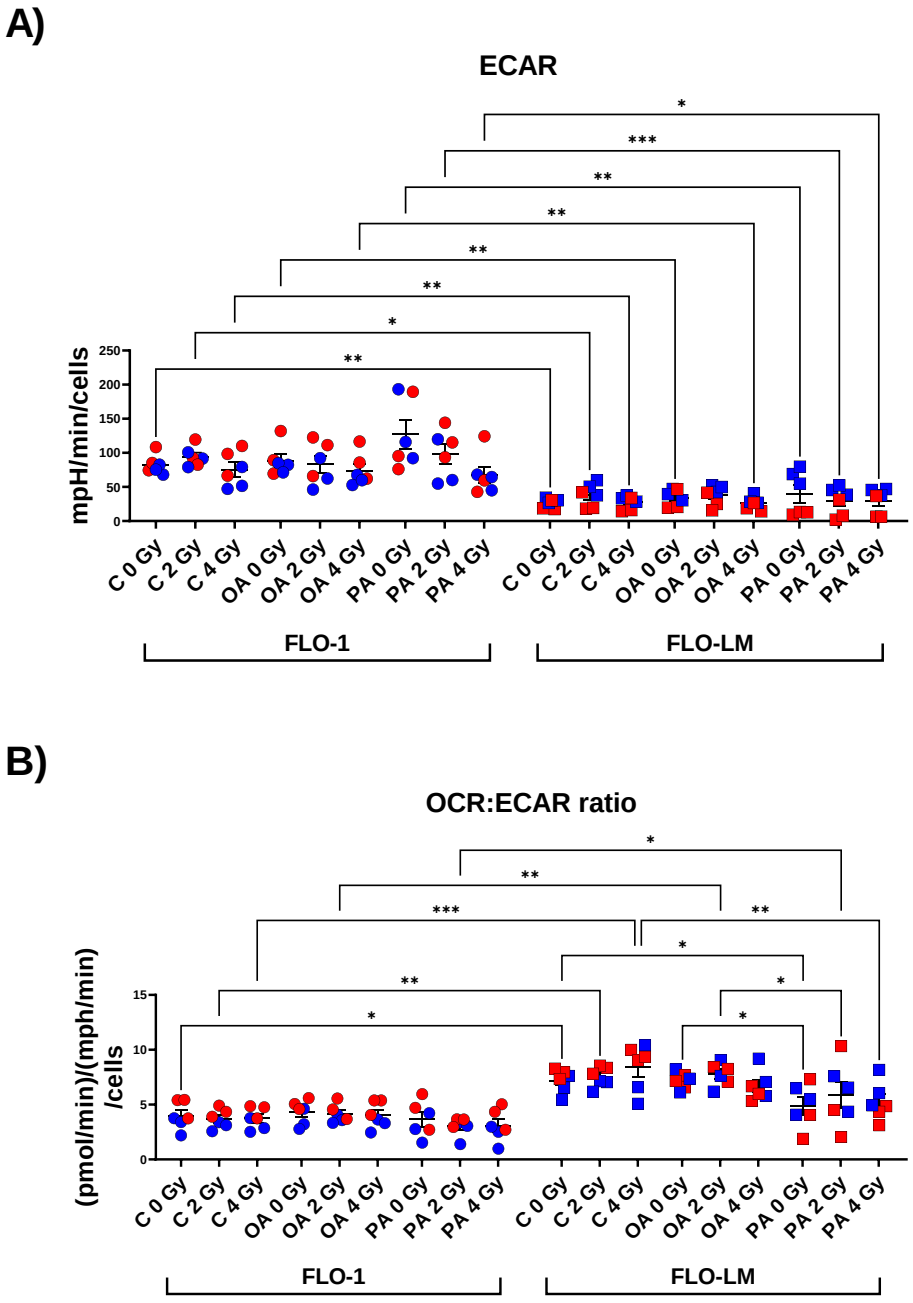


**Figure 5.4.6 The adipose secretome exposed to fatty acids and increasing irradiation differentially alters oesophageal cancer and metastatic cell lines glycolytic capacity.**
FLO-1 and FLO-LM cell lines cultured with ACM treated with Control (C), Oleic Acid (OA), or Palmitic Acid (PA) in combination with mock irradiation, 2 Gy irradiation or 4 Gy irradiation. Mitochondrial parameters were assessed using Seahorse MitoStress test including (A-B) ECAR and OCR:ECAR ratio (Kruskal Wallis test with Dunn's correction). Blue circle symbols indicate FLO-1 cell line treated with ACM from non-obese patients (●), red circle symbols indicate FLO-1 treated with ACM from obese patients (●). Blue square symbols indicate FLO-LM cell line treated with ACM from non-obese patients (■), red square symbols indicate FLO-LM treated with ACM from obese patients (■). All data expressed as mean ± SEM, n=6* $p < 0.05$, ** $p < 0.01$, *** $p < 0.001$.

### 5.4.3 *The non-obese adipose secretome in combination with fatty acids increases oxidative phosphorylation preferences in metastatic cell lines compared with primary cancer cells.*

The visceral adipose depot of non-obese patients possesses decreased fatty acid content and has been reported to have differential secretion of inflammatory mediators. To examine the influence of the adipose secretome derived from non-obese patients which was exposed to increasing radiation in the presence or absence of OA and PA on FLO-1 and FLO-LM cell lines metabolic parameters, cells were cultured with these treated ACM for 24 hours and assessed using Seahorse MitoStress test.

Within these figures all ACM was derived from non-obese OAC patients. In FLO-1 cells OCR was decreased following culture with PA treated ACM exposed to 2 and 4 Gy irradiation compared with unirradiated matched ACM. In FLO-LM cells OCR was increased following culture with 2 Gy irradiated ACM compared with matched unirradiated ACM and following culture with PA treated unirradiated ACM compared with unirradiated control ACM. Additionally, in FLO-LM cells OCR was decreased following culture with OA treated ACM exposed to 4 Gy irradiation compared with OA treated ACM exposed to 2 Gy irradiation (**Figure 5.4.7**). In FLO-1 cells increased non-mitochondrial oxygen consumption was observed following culture with OA and PA treated unirradiated ACM compared with control unirradiated ACM. In FLO-LM cells decreased non-mitochondrial oxygen consumption was observed following culture with OA treated ACM exposed to 4 Gy irradiation compared with similarly treated FLO-1 cells. In FLO-LM cells decreased non-mitochondrial oxygen consumption was observed following culture with PA treated ACM exposed to 4 Gy irradiation compared with PA treated ACM in the unirradiated setting (**Figure 5.4.7**). In FLO-1 cells ATP linked respiration was decreased following culture with PA treated ACM exposed to 2 Gy irradiation compared with PA treated unirradiated ACM. In FLO-LM cells increased ATP linked respiration was observed following culture with PA treated unirradiated ACM compared unirradiated control. In FLO-LM cells increased ATP linked respiration was observed following culture with OA treated ACM exposed to 2 Gy irradiation compared with OA treated ACM exposed to 4 Gy irradiation. In FLO-LM cells increased ATP linked respiration was observed following culture with OA and PA treated ACM exposed to 2 Gy irradiation compared with similarly treated FLO-1 cells (**Figure 5.4.8**). In FLO-1 and FLO-LM cells proton leak was observed to be increased following culture with control ACM exposed to 2 Gy irradiation compared with control ACM exposed with 4 Gy or control unirradiated and PA treated unirradiated ACM in FLO-LM cells. In FLO-1 cells increased proton leak was observed

following culture with PA treated unirradiated ACM compared with control unirradiated ACM, OA treated unirradiated ACM, PA treated ACM exposed to 2 and 4 Gy irradiation. In FLO-LM cells proton leak was increased following culture with OA treated ACM exposed to 2 Gy irradiated ACM compared with OA treated ACM exposed to 4 Gy irradiation. In FLO-LM cells increased maximal respiration was observed following culture with PA treated unirradiated ACM compared with unirradiated control ACM (**Figure 5.4.8**). In FLO-1 cells decreased maximal respiration was observed following culture with PA treated ACM exposed to 2 and 4 Gy irradiation and OA treated ACM exposed to 2 Gy irradiation compared with similarly treated FLO-LM cells (**Figure 5.4.9**). In FLO-LM cells increased spare respiratory capacity was observed following culture with control unirradiated ACM, OA treated ACM in the unirradiated setting or following 2 Gy irradiation, and PA treated ACM following exposure to 2 or 4 Gy irradiation compared with similarly treated FLO-1 cells (**Figure 5.4.9**). In FLO-1 cells increased ECAR profiles were observed following culture with PA treated unirradiated ACM compared with control and OA treated unirradiated ACM. Additionally, decreased ECAR was observed in FLO-LM cells following culture with control unirradiated ACM, control ACM exposed to 2 Gy irradiation, OA treated unirradiated ACM and OA treated ACM exposed to 4 Gy irradiation compared with similarly treated FLO-1 cells (**Figure 5.4.10**). In FLO-LM cells increased OCR:ECAR ratio was observed following culture with control, OA treated, and PA treated ACM exposed to 2 or 4 Gy irradiation compared with similarly treated FLO-1 cells (**Figure 5.4.10**).

(* $p < 0.05$, ** $p < 0.01$)

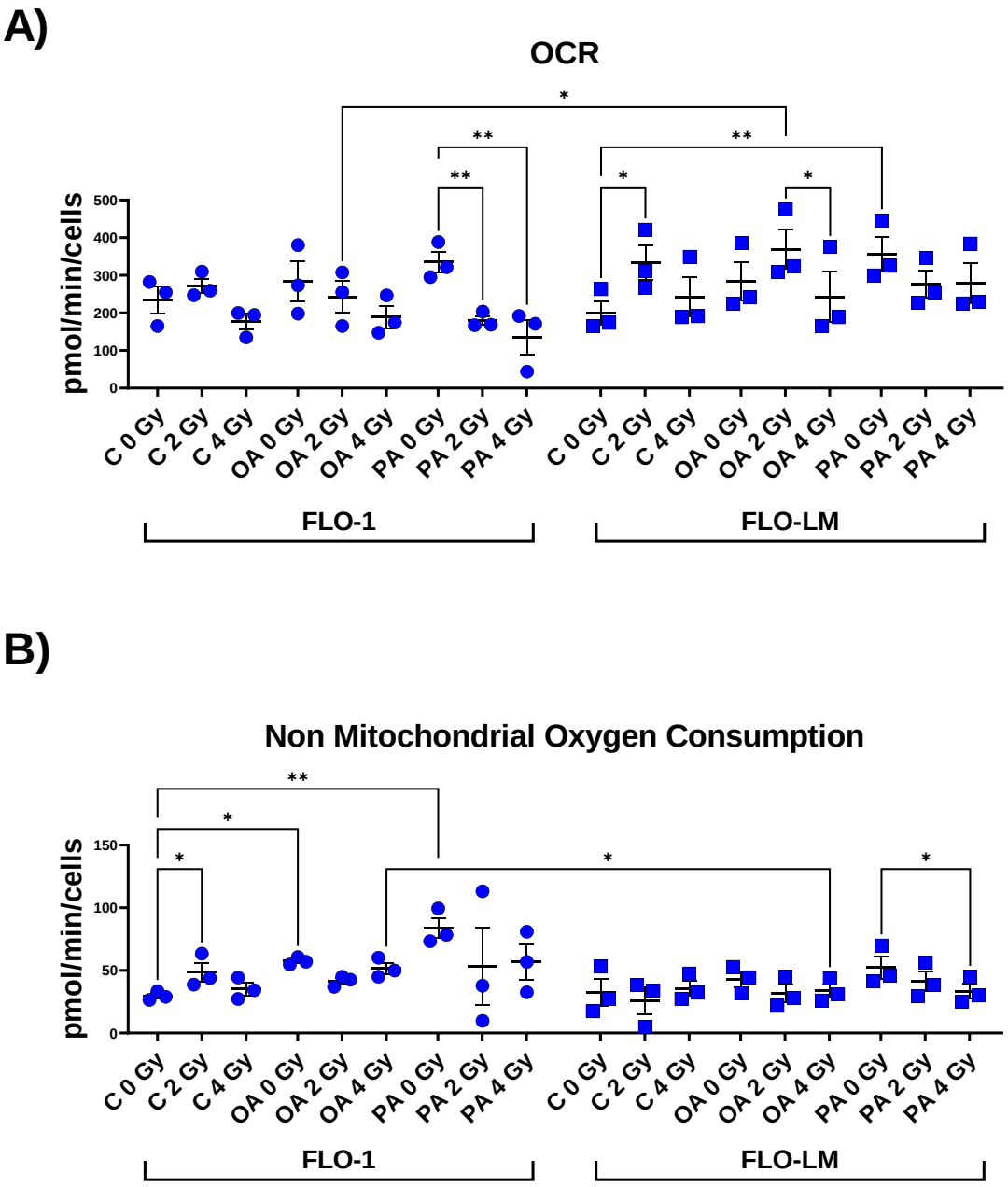


**Figure 5.4.7 Palmitic acid and increasing irradiation on the non-obese adipose secretome differentially decreases basal respiration and non-mitochondrial oxygen consumption in primary and metastatic cell lines.**

FLO-1 and FLO-LM cell lines cultured with ACM from non-obese patients treated with Control (C), Oleic Acid (OA), or Palmitic Acid (PA) in combination with mock irradiation, 2 Gy irradiation or 4 Gy irradiation. Mitochondrial parameters were assessed using Seahorse MitoStress test including (A-B) basal respiration, and non-mitochondrial oxygen consumption (Kruskal Wallis test with Dunn's correction). Blue circle symbols indicate FLO-1 cell line treated with ACM from non-obese patients (●), blue square symbols indicate FLO-LM treated with ACM from non-obese patients (■). All data expressed as mean ± SEM, n=3, * $p < 0.05$, ** $p < 0.01$.

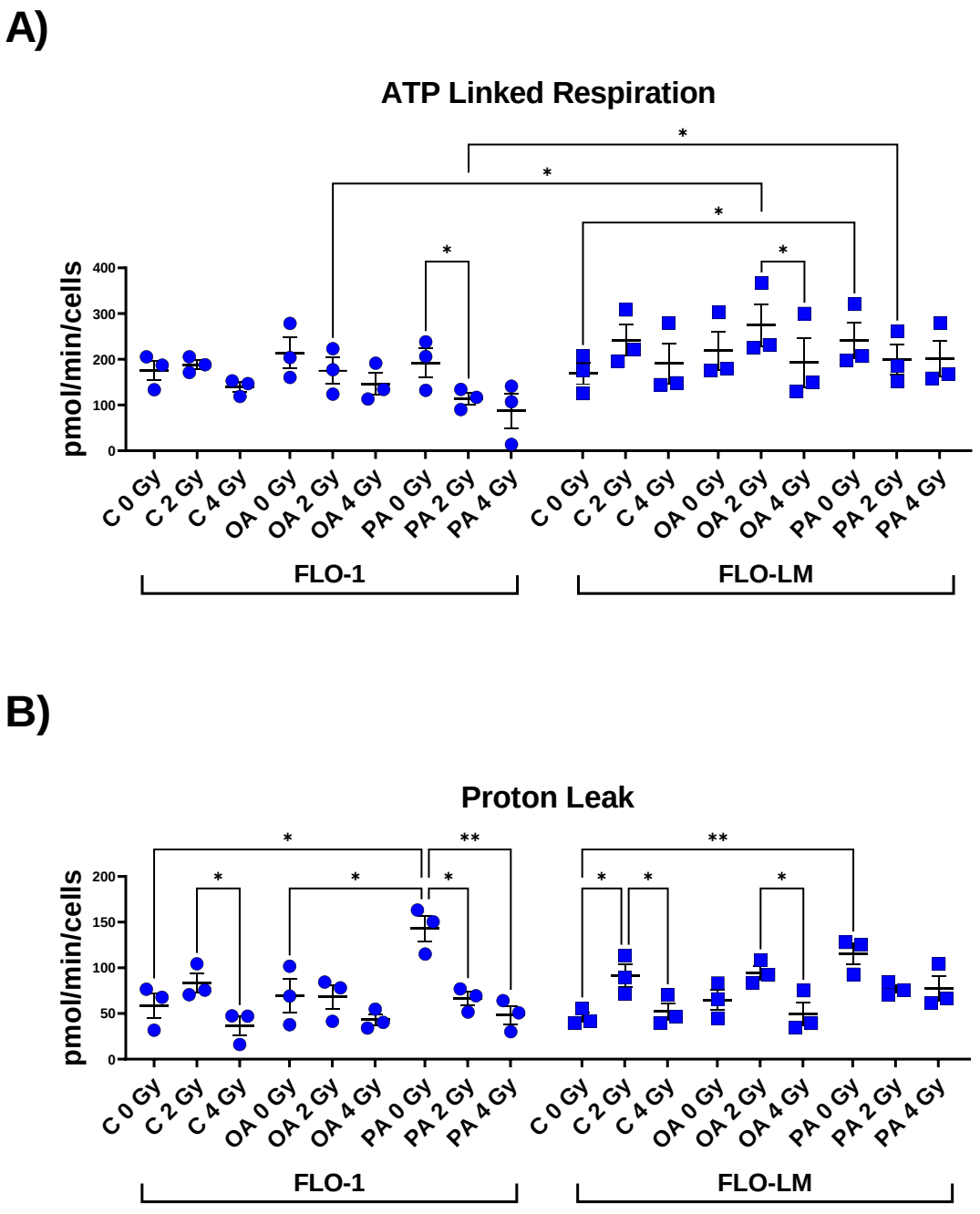


**Figure 5.4.8 Palmitic acid and increasing irradiation on the non-obese adipose secretome decreases ATP -linked respiration and proton leak in primary cancer cell lines.**

FLO-1 and FLO-LM cell lines cultured with ACM from non-obese patients treated with Control (C), Oleic Acid (OA), or Palmitic Acid (PA) in combination with mock irradiation, 2 Gy irradiation or 4 Gy irradiation. Mitochondrial parameters were assessed using Seahorse MitoStress test including (A-B) ATP production and proton leak (Kruskal Wallis test with Dunn's correction). Blue circle symbols indicate FLO-1 cell line treated with ACM from non-obese patients (●), blue square symbols indicate FLO-LM treated with ACM from non-obese patients (■). All data expressed as mean ± SEM, n=3, * $p < 0.05$, ** $p < 0.01$.

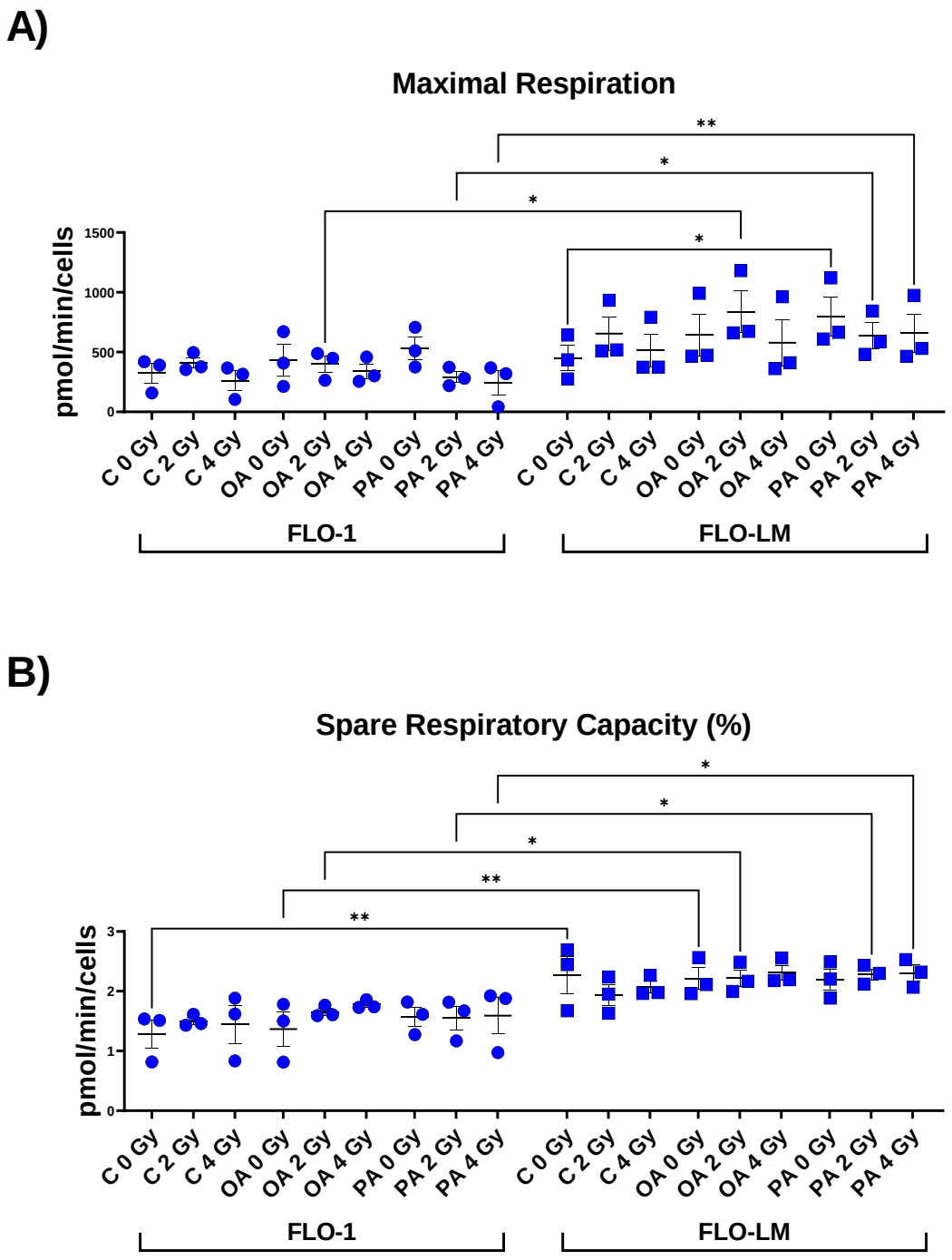


**Figure 5.4.9 Palmitic acid and increasing irradiation on the non-obese adipose secretome increases maximal respiration and spare respiratory capacity in metastatic cancer cell lines.** FLO-1 and FLO-LM cell lines cultured with ACM from non-obese patients treated with Control (C), Oleic Acid (OA), or Palmitic Acid (PA) in combination with mock irradiation, 2 Gy irradiation or 4 Gy irradiation. Mitochondrial parameters were assessed using Seahorse MitoStress test including (A-B) maximal respiration, and spare respiratory capacity (Kruskal Wallis test with Dunn's correction). Blue circle symbols indicate FLO-1 cell line treated with ACM from non-obese patients (●), blue square symbols indicate FLO-LM treated with ACM from non-obese patients (■). All data expressed as mean ± SEM, n=3, * $p < 0.05$, ** $p < 0.01$.

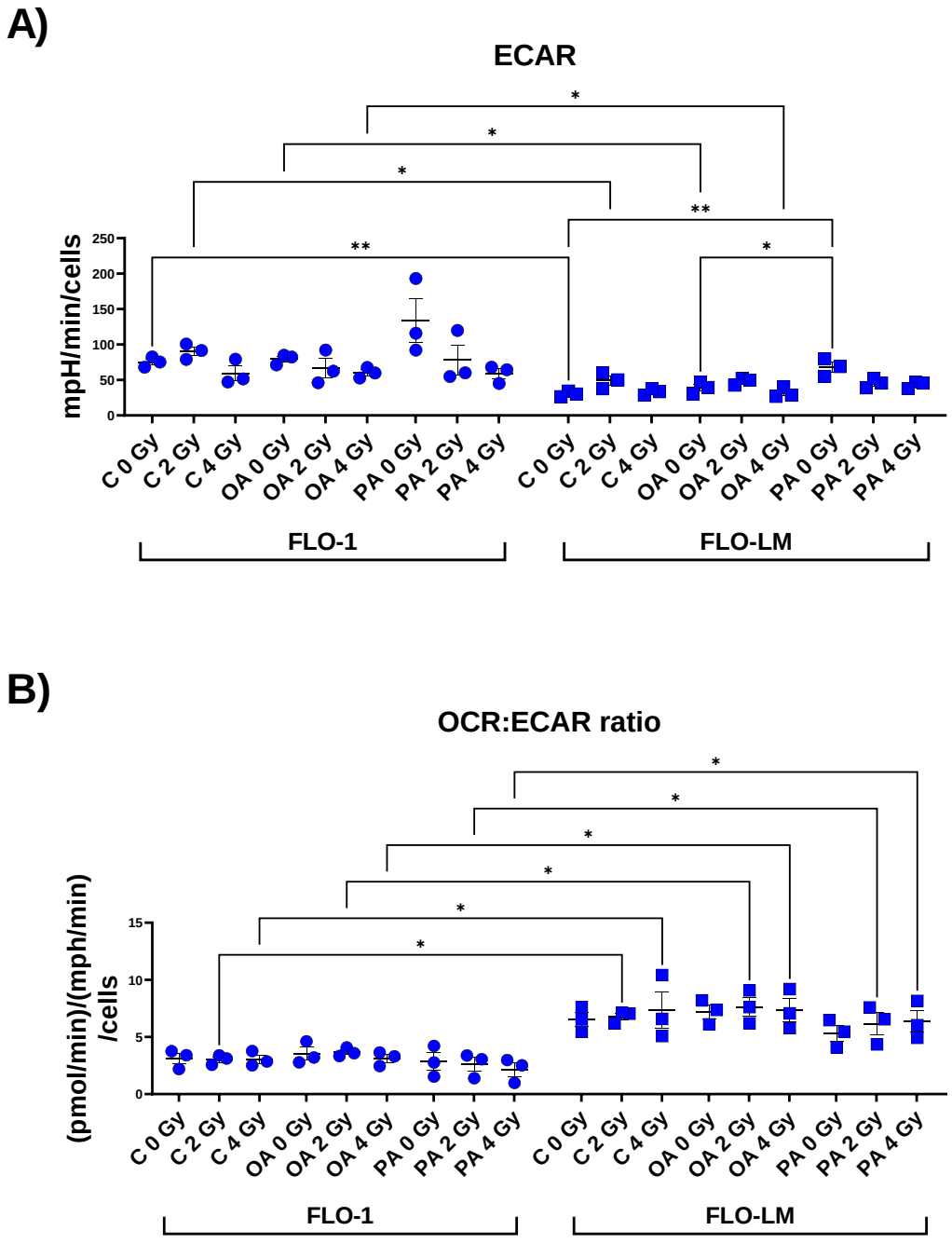


**Figure 5.4.10 The non-obese adipose secretome in combination with fatty acids increases oxidative phosphorylation preferences in metastatic cells compared with primary cancer cells.**

FLO-1 and FLO-LM cell lines cultured with ACM from non-obese patients treated with Control (C), Oleic Acid (OA), or Palmitic Acid (PA) in combination with mock irradiation, 2 Gy irradiation or 4 Gy irradiation. Mitochondrial parameters were assessed using Seahorse MitoStress test including (A-B) ECAR and OCR:ECAR ratio (Kruskal Wallis test with Dunn's correction). Blue circle symbols indicate FLO-1 cell line treated with ACM from non-obese patients (●), blue square symbols indicate FLO-LM treated with ACM from non-obese patients (■). All data expressed as mean ± SEM, n=3, * $p < 0.05$, ** $p < 0.01$.

### 5.4.4 *The obese adipose secretome in combination with PA decreases mitochondrial profiles and glycolytic metabolism in metastatic cell lines compared with primary cancer cells.*

Visceral adipose tissue has been reported to be in a state of chronic low-grade inflammation. Increased levels of saturated fatty acid PA within circulation has been reported in correlation with obesity. To examine the influence of the adipose secretome derived from obese patients which was exposed to increasing radiation in the presence or absence of OA and PA on FLO-1 and FLO-LM cell lines metabolic parameters, cells were cultured with these treated ACM for 24 hours and assessed using Seahorse MitoStress test.

Within this figure all ACM was derived from obese OAC patients. In FLO-LM cells decreased OCR, ATP-linked respiration and maximal respiration were observed following culture with OA treated ACM exposed to 4 Gy irradiation and PA treated ACM exposed to 2 or 4 Gy irradiation compared with similarly treated FLO-1 cells (**Figure 5.4.11 - 5.4.13**). In FLO-LM cells decreased non-mitochondrial oxygen consumption and ECAR profiles observed following culture with PA treated ACM in either the unirradiated setting or following exposure to 2 or 4 Gy irradiation compared with similarly treated FLO-1 cells (**Figure 5.4.11, 5.4.14**). In FLO-LM cells decreased proton leak was observed following culture with OA treated ACM exposed to 4 Gy irradiation and PA treated ACM in either the unirradiated setting or following exposure to 2 or 4 Gy irradiation compared with similarly treated FLO-1 cells (**Figure 5.4.12**). In FLO-LM cells increased spare respiratory capacity was observed following culture with control and OA unirradiated ACM and control ACM exposed to 2 Gy irradiation compared with similarly treated FLO-1 cells. In FLO-LM cells decreased spare respiratory capacity was observed following culture with PA treated ACM in either the unirradiated setting or following exposure to 2 or 4 Gy irradiation compared with similarly unirradiated or irradiated control and OA treated ACM (**Figure 5.4.13**). In FLO-LM cells increased OCR:ECAR ratio was observed following culture with control ACM exposed to 2 or 4 Gy irradiation compared with similarly treated FLO-1 cells. In FLO-LM cells decreased OCR:ECAR ratio was observed following culture with PA treated ACM in either the unirradiated setting or following exposure to 4 Gy irradiation compared with similarly unirradiated or 4 Gy irradiated control ACM (**Figure 5.4.14**).

(* $p < 0.05$, ** $p < 0.01$, *** $p < 0.001$.)

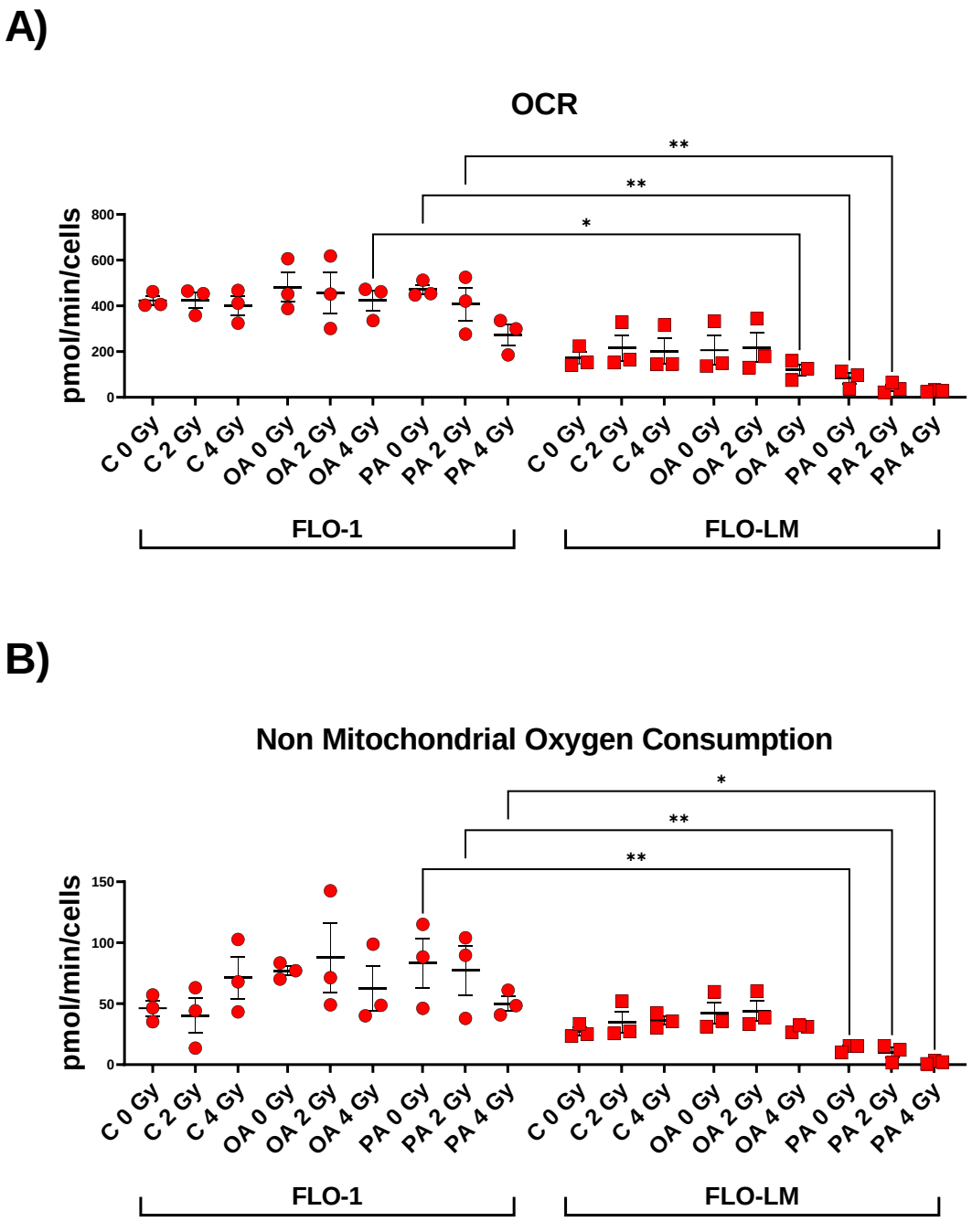


**Figure 5.4.11 The obese adipose secretome in combination with PA and increasing irradiation decreases basal respiration and non-mitochondrial oxygen consumption in metastatic cells compared to matched primary cancer cells.**

FLO-1 and FLO-LM cell lines cultured with ACM from obese patients treated with Control (C), Oleic Acid (OA), or Palmitic Acid (PA) in combination with mock irradiation, 2 Gy irradiation or 4 Gy irradiation. Mitochondrial parameters were assessed using Seahorse MitoStress test including (A-B) basal respiration and non-mitochondrial oxygen consumption (Kruskal Wallis test with Dunn's correction). Red circle symbols indicate FLO-1 cell line treated with ACM from obese patients (●), red square symbols indicate FLO-LM treated with ACM from obese patients (■). All data expressed as mean ± SEM, n=3, * $p < 0.05$, ** $p < 0.01$.

A)

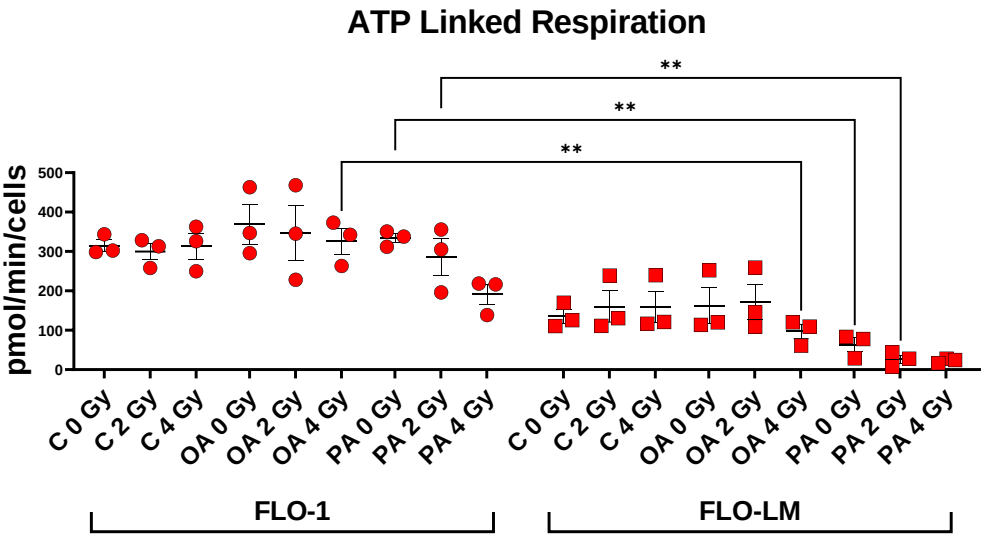


B)

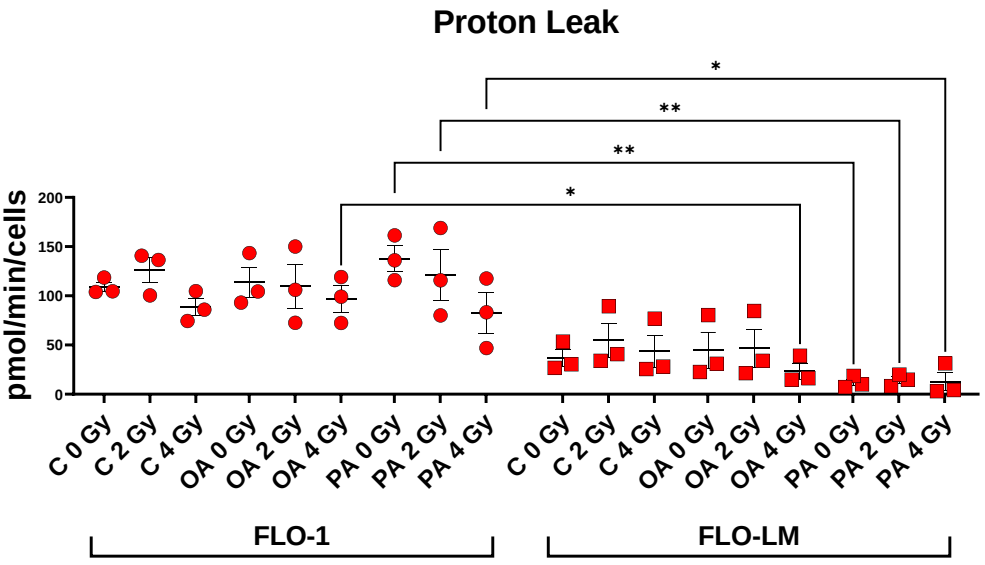


**Figure 5.4.12 The obese adipose secretome in combination with PA and increasing irradiation decreases ATP linked respiration and proton in metastatic cancer cells.**
FLO-1 and FLO-LM cell lines cultured with ACM from obese patients treated with Control (C), Oleic Acid (OA), or Palmitic Acid (PA) in combination with mock irradiation, 2 Gy irradiation or 4 Gy irradiation. Mitochondrial parameters were assessed using Seahorse MitoStress test including (A-B) ATP linked respiration, and proton leak (Kruskal Wallis test with Dunn's correction). Red circle symbols indicate FLO-1 cell line treated with ACM from obese patients (●), red square symbols indicate FLO-LM treated with ACM from obese patients (■). All data expressed as mean ± SEM, n=3, * $p < 0.05$, ** $p < 0.01$.

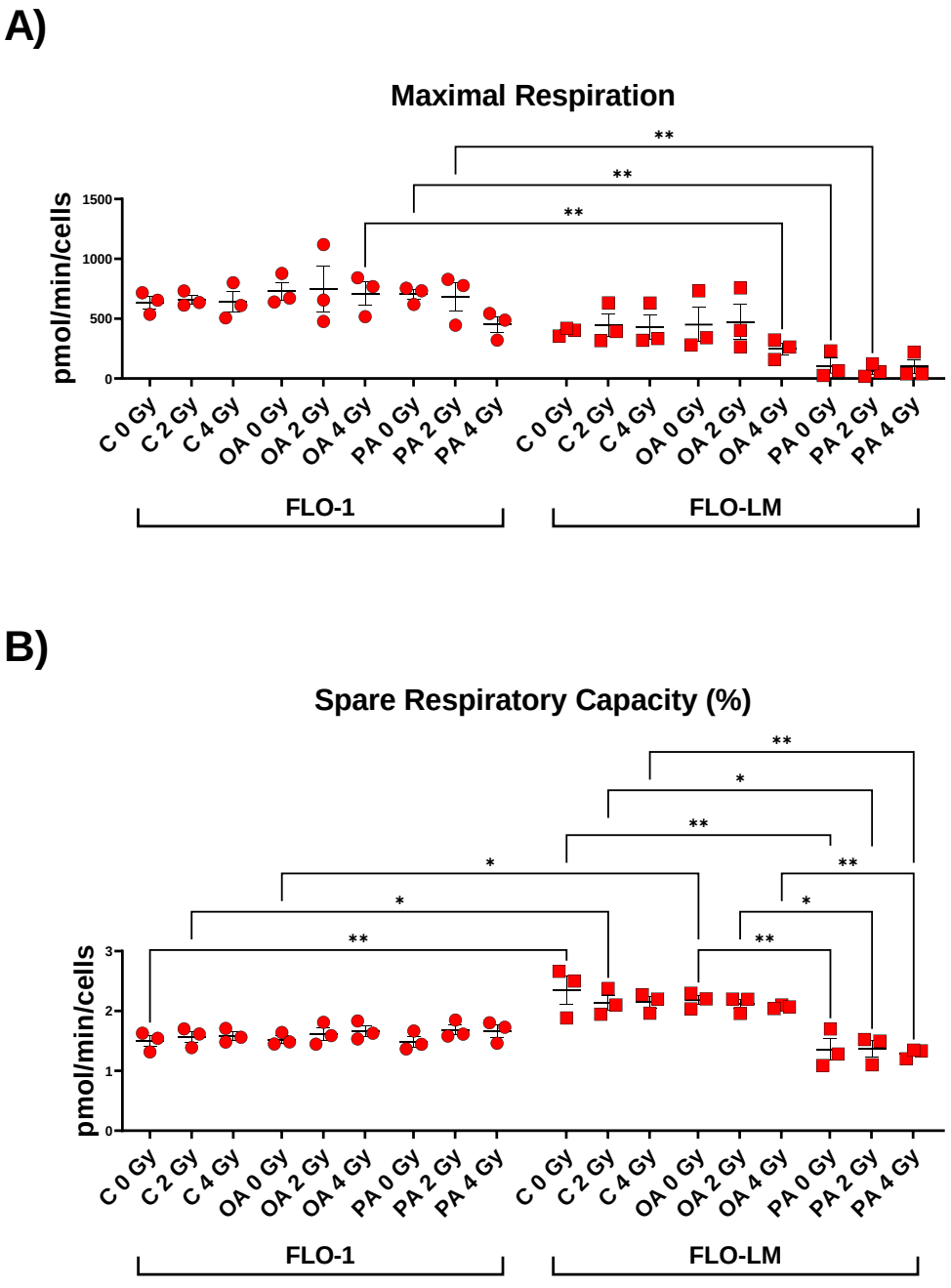


**Figure 5.4.13 The obese adipose secretome in combination with PA and increasing irradiation decreases maximal respiration and spare respiratory capacity in metastatic cells compared to matched primary cancer cells.**

FLO-1 and FLO-LM cell lines cultured with ACM from obese patients treated with Control (C), Oleic Acid (OA), or Palmitic Acid (PA) in combination with mock irradiation, 2 Gy irradiation or 4 Gy irradiation. Mitochondrial parameters were assessed using Seahorse MitoStress test including (A-B) maximal respiration, and spare respiratory capacity (Kruskal Wallis test with Dunn's correction). Red circle symbols indicate FLO-1 cell line treated with ACM from obese patients (●), red square symbols indicate FLO-LM treated with ACM from obese patients (■). All data expressed as mean ± SEM, n=3, * $p < 0.05$, ** $p < 0.01$.

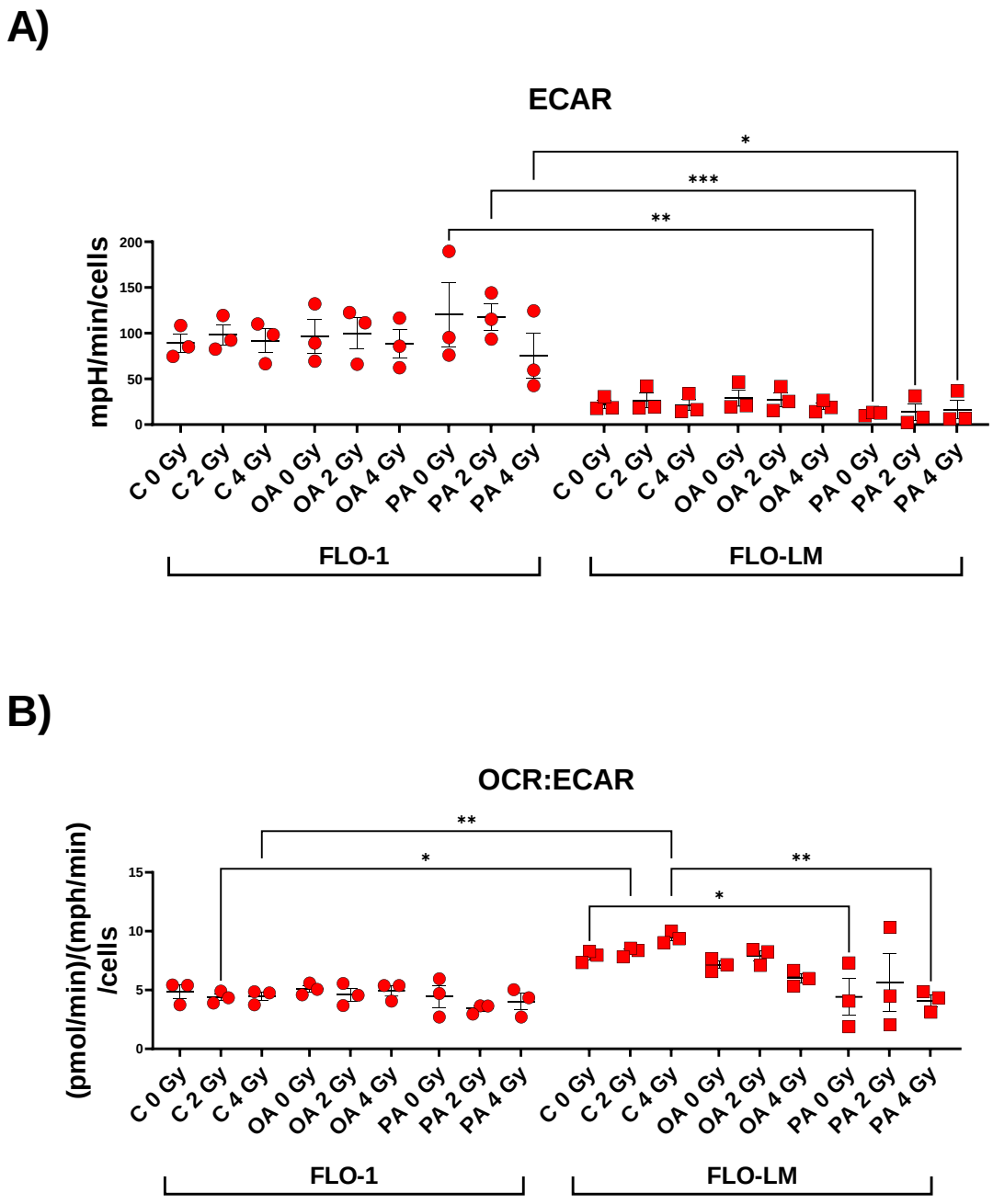


**Figure 5.4.14 The obese adipose secretome in combination with PA and increasing irradiation decreases glycolytic metabolism in metastatic cells compared to matched primary cancer cells.**

FLO-1 and FLO-LM cell lines cultured with ACM from obese patients treated with Control (C), Oleic Acid (OA), or Palmitic Acid (PA) in combination with mock irradiation, 2 Gy irradiation or 4 Gy irradiation. Mitochondrial parameters were assessed using Seahorse MitoStress test including (A-B) ECAR and OCR:ECAR ratio (Kruskal Wallis test with Dunn's correction). Red circle symbols indicate FLO-1 cell line treated with ACM from obese patients (●), red square symbols indicate FLO-LM treated with ACM from obese patients (■). All data expressed as mean ± SEM, n=3, * $p < 0.05$, ** $p < 0.01$, *** $p < 0.001$.

### 5.4.5 *The obese adipose secretome in combination with fatty acids and increasing irradiation increases reliance on oxidative phosphorylation in oesophageal cancer cells compared with non-obese ACM.*

Obesity has been linked to development and progression of a series of obesity associated cancers. To examine whether the adipose secretome derived from non-obese and obese patients which was exposed to increasing radiation in the presence or absence of OA and PA had differential effects on primary cancer cell line FLO-1 cell line metabolic parameters, cells were cultured with these treated ACM for 24 hours and assessed using Seahorse MitoStress test.

In FLO-1 cells increased OCR was observed following culture with control unirradiated ACM, control ACM exposed to 4 Gy irradiation, OA in combination with 4 Gy irradiation as well as PA treatment combined with 2 Gy irradiation from obese patients compared with similarly treated ACM from non-obese patients (**Figure 5.4.15**). In FLO-1 cells increased non-mitochondrial oxygen consumption was observed following culture with OA or PA unirradiated ACM from non-obese patients compared with unirradiated control ACM from non-obese patients (**Figure 5.4.15**). In FLO-1 cells increased ATP linked respiration was observed following culture with control ACM exposed to 4 Gy irradiation, OA in combination with 2 or 4 Gy irradiation as well as PA treatment combined with 2 Gy irradiation from obese patients compared with similarly treated ACM from non-obese patients (**Figure 5.4.16**). In FLO-1 cells increased proton leak was observed following culture with PA treated unirradiated ACM from non-obese patients compared with control unirradiated ACM, OA treated unirradiated ACM, PA treated ACM exposed to 2 and 4 Gy irradiation (**Figure 5.4.16**). In FLO-1 cells increased maximal respiration was observed following culture with control ACM exposed to 4 Gy irradiation, OA in combination with 4 Gy irradiation as well as PA treatment combined with 2 Gy irradiation from obese patients compared with similarly treated ACM from non-obese patients (**Figure 5.4.17**). In FLO-1 cells increased ECAR was observed following culture with PA treated unirradiated ACM from non-obese patients compared with PA treated ACM exposed to 4 Gy irradiation (**Figure 5.4.18**). In FLO-1 cells increased OCR:ECAR ratio was observed following culture with ACM treated with OA in combination with 4 Gy irradiation from obese patients compared with similarly treated ACM from non-obese patients (**Figure 5.4.18**).

(* $p < 0.05$, ** $p < 0.01$.)

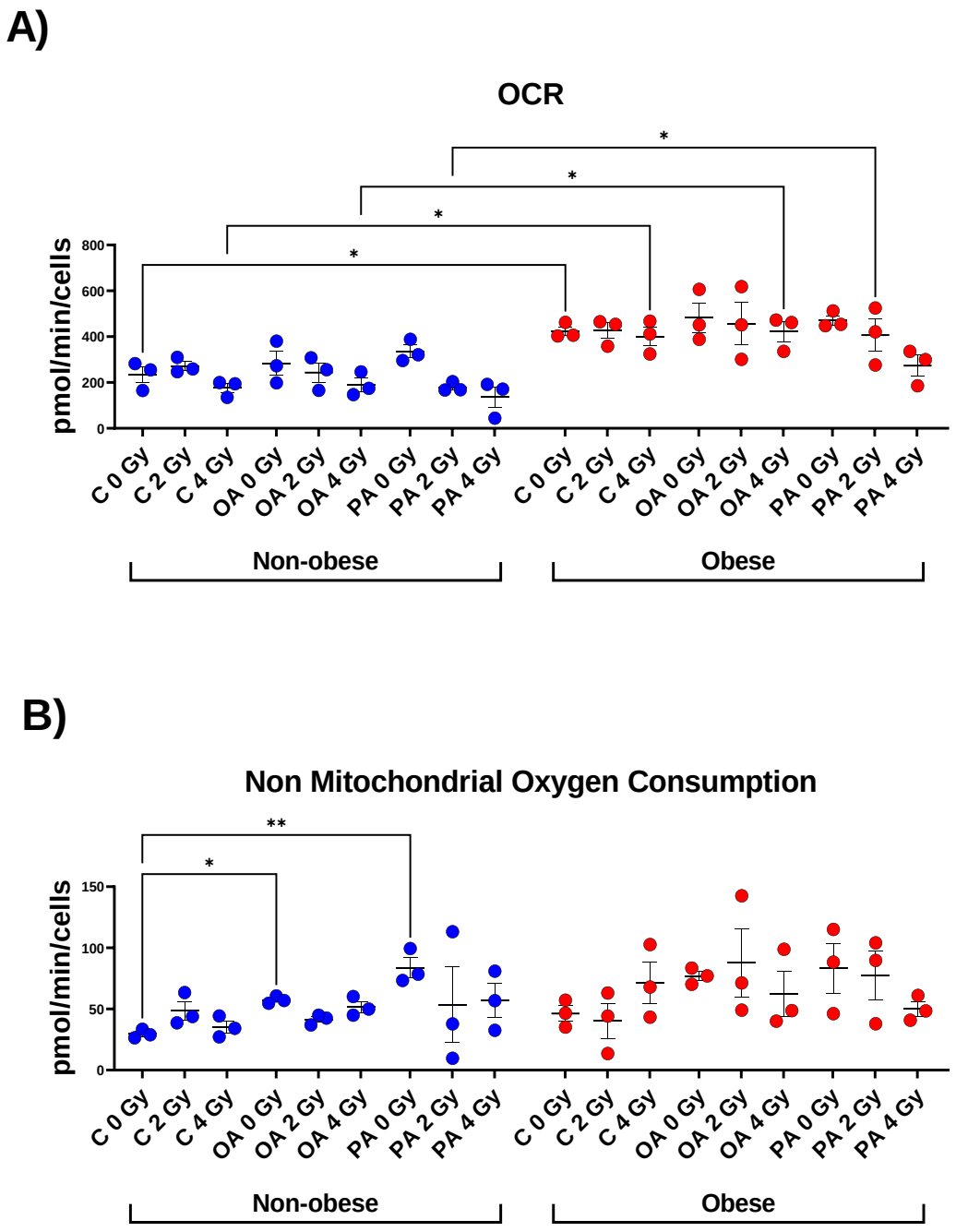


**Figure 5.4.15 The obese adipose secretome in combination with fatty acids and increasing irradiation increases reliance on oxidative phosphorylation in primary cancer cells compared with non-obese ACM.**

FLO-1 cell line cultured with ACM treated with Control (C), Oleic Acid (OA), or Palmitic Acid (PA) in combination with mock irradiation, 2 Gy irradiation or 4 Gy irradiation. Mitochondrial parameters were assessed using Seahorse MitoStress test including (A-B) basal respiration and non-mitochondrial oxygen consumption (Kruskal Wallis test with Dunn's correction). Blue circle symbols indicate FLO-1 cell line treated with ACM from non-obese patients (●), red circle symbols indicate FLO-1 treated with ACM from obese patients (●). All data expressed as mean ± SEM, n=3, * $p < 0.05$, ** $p < 0.01$.

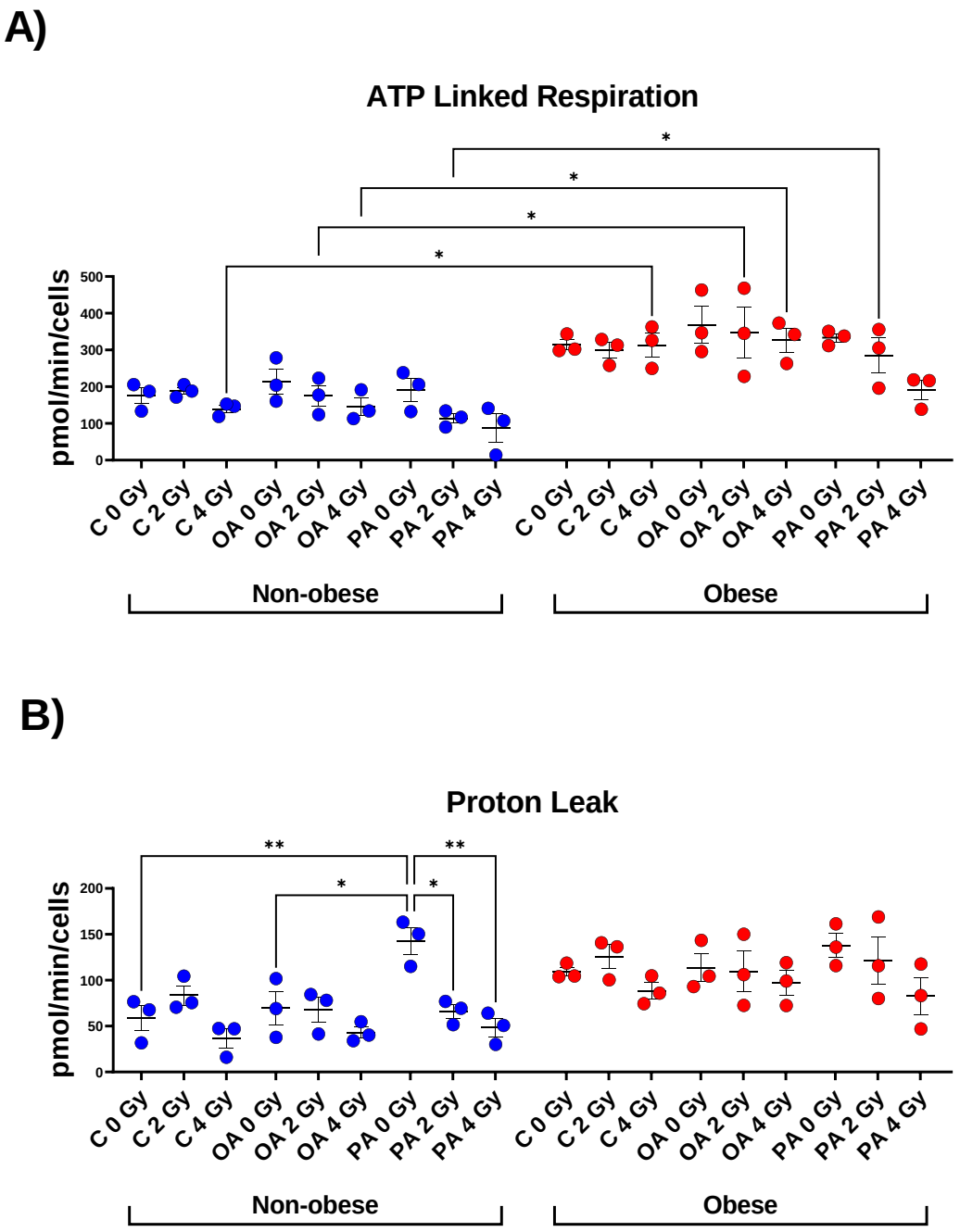


**Figure 5.4.16 The non-obese adipose secretome in combination with fatty acids and increasing irradiation decreases ATP linked respiration oesophageal cancer cells compared with obese ACM.**

FLO-1 cell line cultured with ACM treated with Control (C), Oleic Acid (OA), or Palmitic Acid (PA) in combination with mock irradiation, 2 Gy irradiation or 4 Gy irradiation. Mitochondrial parameters were assessed using Seahorse MitoStress test including (A-B) ATP linked respiration, and proton leak (Kruskal Wallis test with Dunn's correction). Blue circle symbols indicate FLO-1 cell line treated with ACM from non-obese patients (●), red circle symbols indicate FLO-1 treated with ACM from obese patients (●). All data expressed as mean ± SEM, n=3, * $p < 0.05$, ** $p < 0.01$.

A)

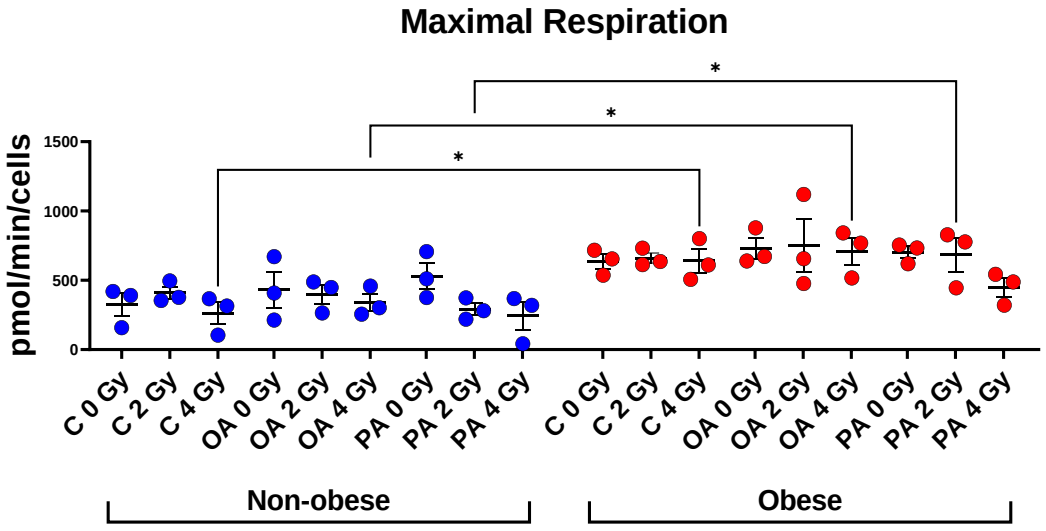


B)

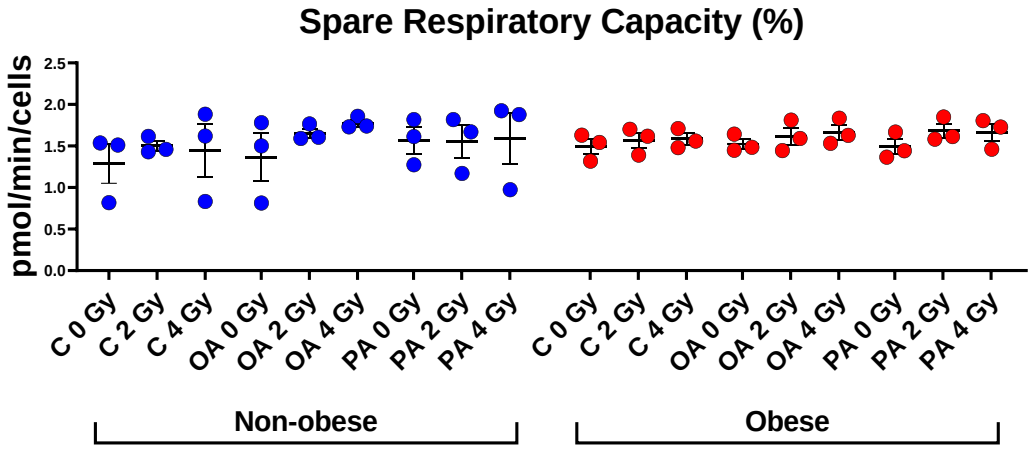


**Figure 5.4.17 The obese adipose secretome in combination with increasing irradiation increases oesophageal cancer cells utilisation of maximal respiration compared with non-obese ACM.**

FLO-1 cell line cultured with ACM treated with Control (C), Oleic Acid (OA), or Palmitic Acid (PA) in combination with mock irradiation, 2 Gy irradiation or 4 Gy irradiation. Mitochondrial parameters were assessed using Seahorse MitoStress test including (A-B) maximal respiration, and spare respiratory capacity (Kruskal Wallis test with Dunn's correction). Blue circle symbols indicate FLO-1 cell line treated with ACM from non-obese patients (●), red circle symbols indicate FLO-1 treated with ACM from obese patients (●). All data expressed as mean ± SEM, n=3, * $p < 0.05$, ** $p < 0.01$.

A)

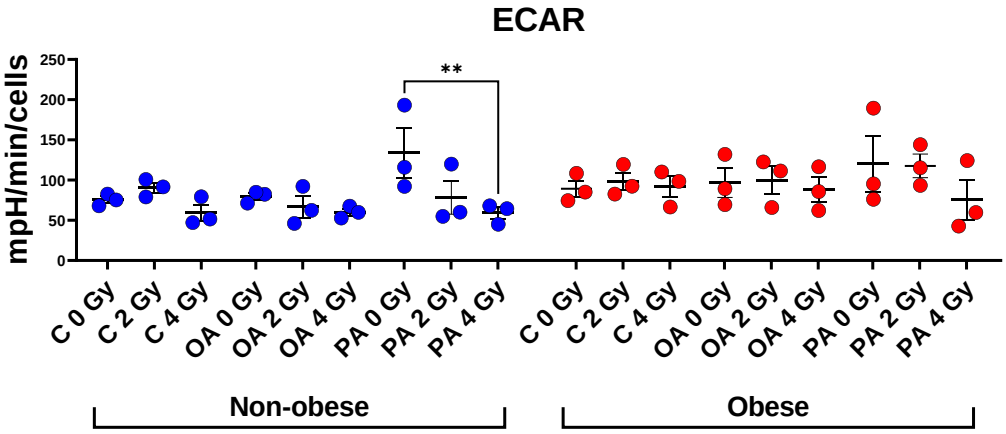


B)

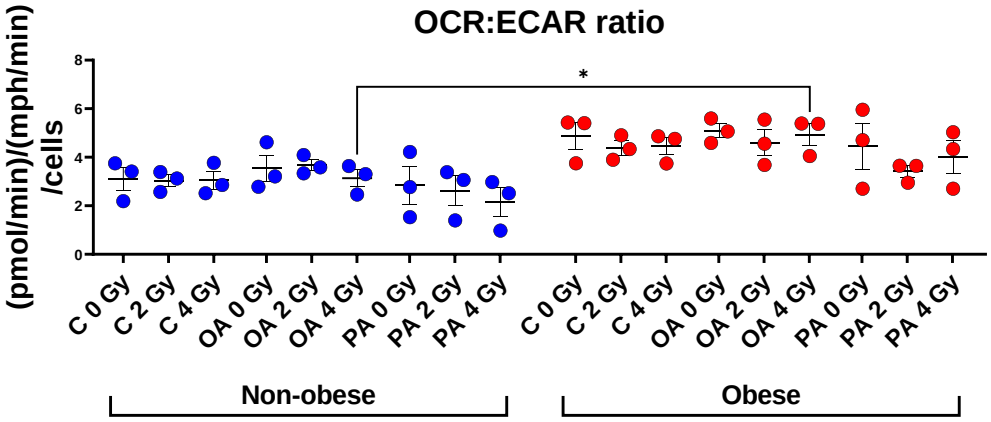


**Figure 5.4.18 The non-obese adipose secretome in combination with palmitic acid and increasing irradiation decreases reliance on glycolysis in primary cancer cells compared with non-obese ACM.**

FLO-1 cell line cultured with ACM treated with Control (C), Oleic Acid (OA), or Palmitic Acid (PA) in combination with mock irradiation, 2 Gy irradiation or 4 Gy irradiation. Mitochondrial parameters were assessed using Seahorse MitoStress test including (A-B) ECAR and OCR:ECAR ratio (Kruskal Wallis test with Dunn's correction). Blue circle symbols indicate FLO-1 cell line treated with ACM from non-obese patients (●), red circle symbols indicate FLO-1 treated with ACM from obese patients (●). All data expressed as mean ± SEM, n=3, * $p < 0.05$, ** $p < 0.01$.

### 5.4.6 *The obese adipose secretome in combination with PA and increasing irradiation decreases OCR profiles in metastatic cancer cells compared with non-obese ACM.*

Obesity related factors that augment dysfunctional adipose biology have been postulated to support cancer metastasis [307]. To examine whether the adipose secretome derived from non-obese and obese patients which was exposed to increasing radiation in the presence or absence of OA and PA had differential effects on liver derived metastatic cell line FLO-LM metabolic parameters, cells were cultured with these treated ACM for 24 hours and assessed using Seahorse MitoStress test.

In FLO-LM cells decreased OCR, ATP linked respiration, proton leak, maximal respiration, spare respiratory capacity and ECAR were observed following culture with PA treated ACM in either the unirradiated setting or following exposure to 2 or 4 Gy irradiation from obese patients compared with similarly treated ACM from non-obese patients (**Figure 5.4.19 – 5.4.22**). In FLO-LM cells increased non-mitochondrial oxygen consumption was observed following culture with PA unirradiated ACM from non-obese patients compared with PA unirradiated ACM from obese patients. Additionally, decreased non-mitochondrial oxygen consumption was observed following culture with PA unirradiated ACM and PA treated ACM exposed to 2 Gy irradiation from obese patients compared with OA unirradiated ACM and OA treated ACM exposed to 2 Gy irradiation also from obese patients. Furthermore, decreased non-mitochondrial oxygen consumption was also observed following culture with PA treated ACM exposed to 4 Gy irradiation from obese patients compared with control ACM exposed to 4 Gy irradiation also from obese patients (**Figure 5.4.19**). In FLO-LM cells decreased spare respiratory capacity was observed following culture with PA unirradiated ACM from obese patients compared with control and OA treated unirradiated ACM also from obese patients. Additionally, decreased spare respiratory capacity was observed following culture with PA treated ACM exposed to 4 Gy irradiation from obese patients compared with control ACM exposed to 4 Gy irradiation also from obese patients (**Figure 5.4.21**). In FLO-LM cells increased ECAR ratio was observed following culture with PA unirradiated ACM from non-obese patients compared with control unirradiated ACM also from non-obese patients (**Figure 5.4.22**). In FLO-LM cells decreased OCR:ECAR ratio was observed following culture with PA unirradiated ACM from obese patients compared with control unirradiated ACM also from obese patients. Additionally, decreased OCR:ECAR ratio was observed following culture with OA and PA treated ACM exposed to 4 Gy irradiation from obese patients compared with control ACM exposed to 4 Gy irradiation also from obese patients (**Figure 5.4.22**).

(* $p < 0.05$, ** $p < 0.01$, *** $p < 0.001$.)

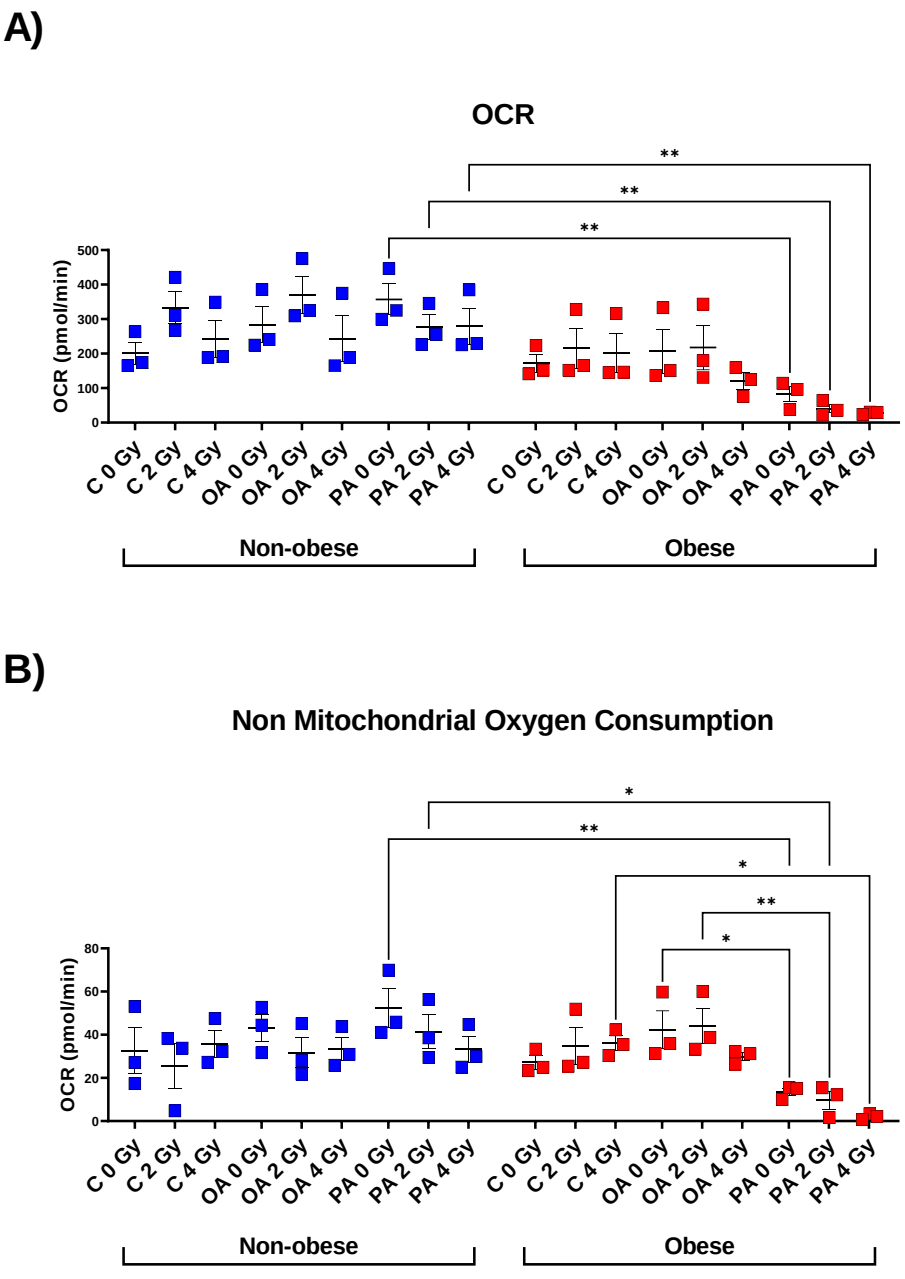


**Figure 5.4.19 The obese adipose secretome in combination with PA and increasing irradiation decreases basal respiration and non-mitochondrial oxygen consumption in metastatic cancer cells compared with non-obese ACM.**

FLO-LM cell line cultured with ACM from non-obese and obese treated with Control (C), Oleic Acid (OA), or Palmitic Acid (PA) in combination with mock irradiation, 2 Gy irradiation or 4 Gy irradiation. Mitochondrial parameters were assessed using Seahorse MitoStress test including (A-B) basal respiration, non-mitochondrial oxygen consumption (Kruskal Wallis test with Dunn's correction). Blue square symbols indicate FLO-LM cell line treated with ACM from non-obese patients (■), red square symbols indicate FLO-LM treated with ACM from obese patients (■). All data expressed as mean ± SEM, n=3, * $p < 0.05$, ** $p < 0.01$.

A)

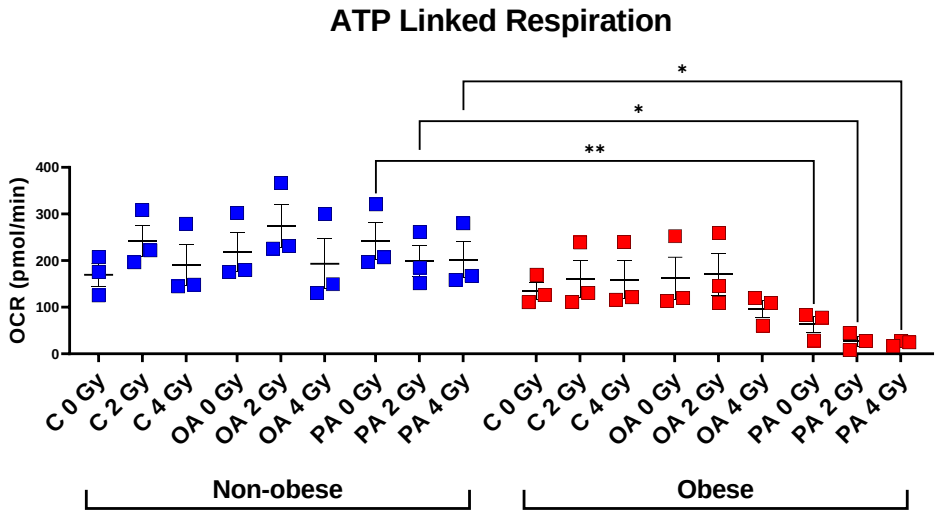


B)

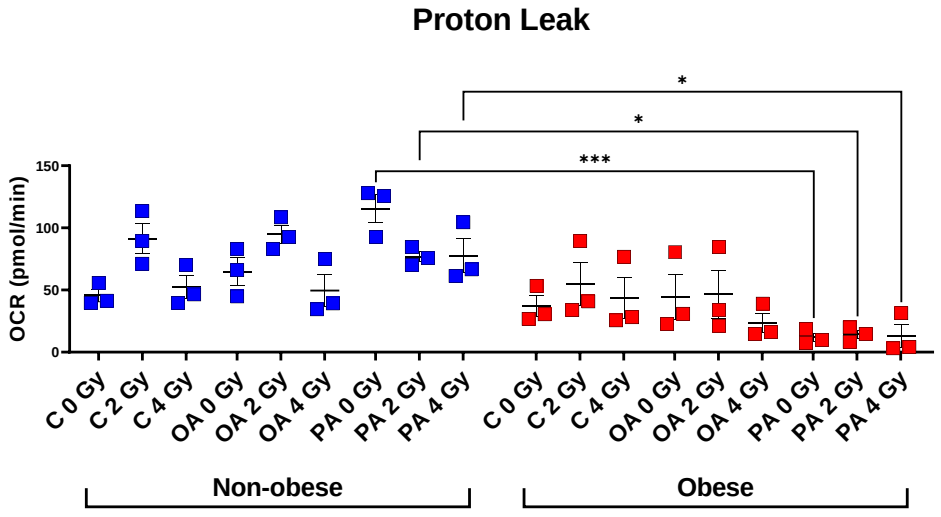


**Figure 5.4.20 The obese adipose secretome in combination with PA and increasing irradiation decreases ATP linked respiration and proton leak in metastatic cancer cells compared with non-obese ACM.**

FLO-LM cell line cultured with ACM from non-obese and obese treated with Control (C), Oleic Acid (OA), or Palmitic Acid (PA) in combination with mock irradiation, 2 Gy irradiation or 4 Gy irradiation. Mitochondrial parameters were assessed using Seahorse MitoStress test including (A-B) ATP linked respiration, and proton leak o (Kruskal Wallis test with Dunn's correction). Blue square symbols indicate FLO-LM cell line treated with ACM from non-obese patients (■), red square symbols indicate FLO-LM treated with ACM from obese patients (■). All data expressed as mean ± SEM, n=3, * $p < 0.05$, ** $p < 0.01$.

A)

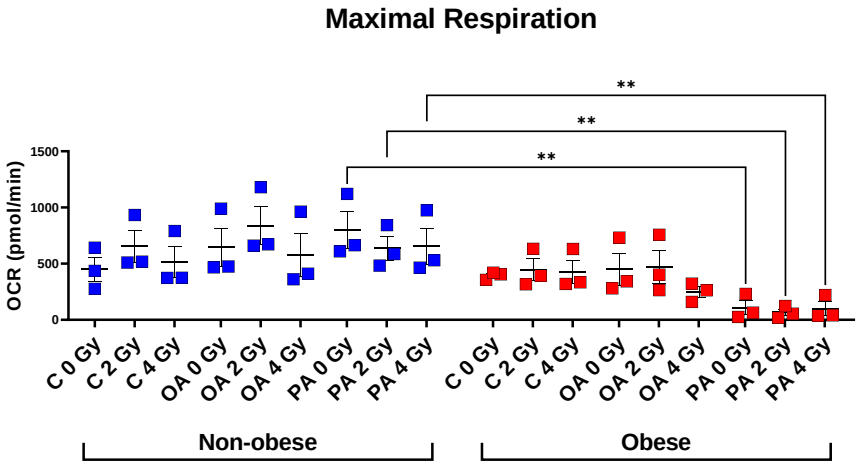


B)

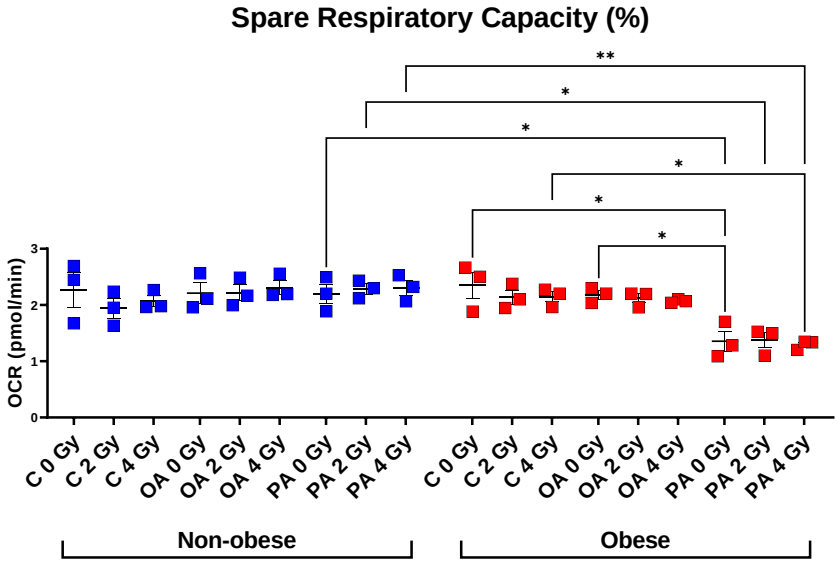


**Figure 5.4.21 The obese adipose secretome in combination with PA and increasing irradiation decreases maximal respiration and spare respiratory capacity in metastatic cancer cells compared with non-obese ACM.**

FLO-LM cell line cultured with ACM from non-obese and obese treated with Control (C), Oleic Acid (OA), or Palmitic Acid (PA) in combination with mock irradiation, 2 Gy irradiation or 4 Gy irradiation. Mitochondrial parameters were assessed using Seahorse MitoStress test including (A-B maximal respiration, and spare respiratory capacity (Kruskal Wallis test with Dunn's correction). Blue square symbols indicate FLO-LM cell line treated with ACM from non-obese patients (■), red square symbols indicate FLO-LM treated with ACM from obese patients (■). All data expressed as mean ± SEM, n=3, * $p < 0.05$, ** $p < 0.01$.

A)

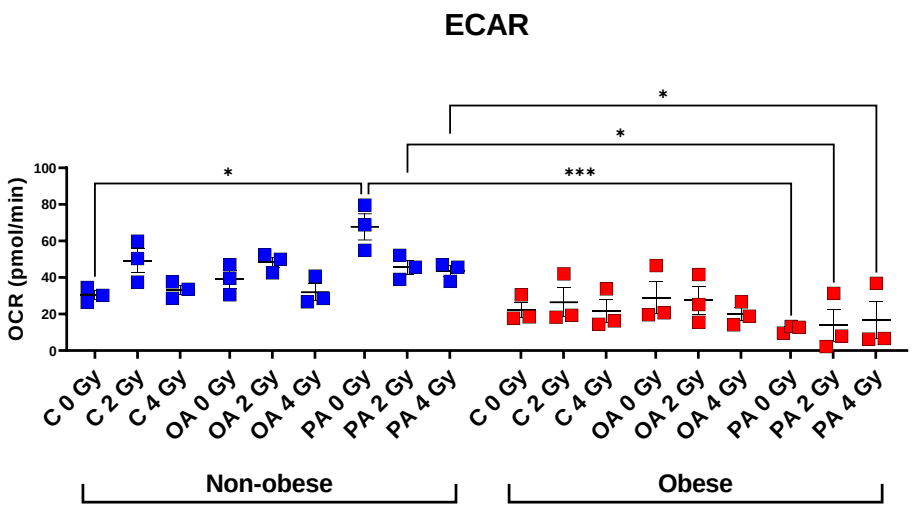


B)

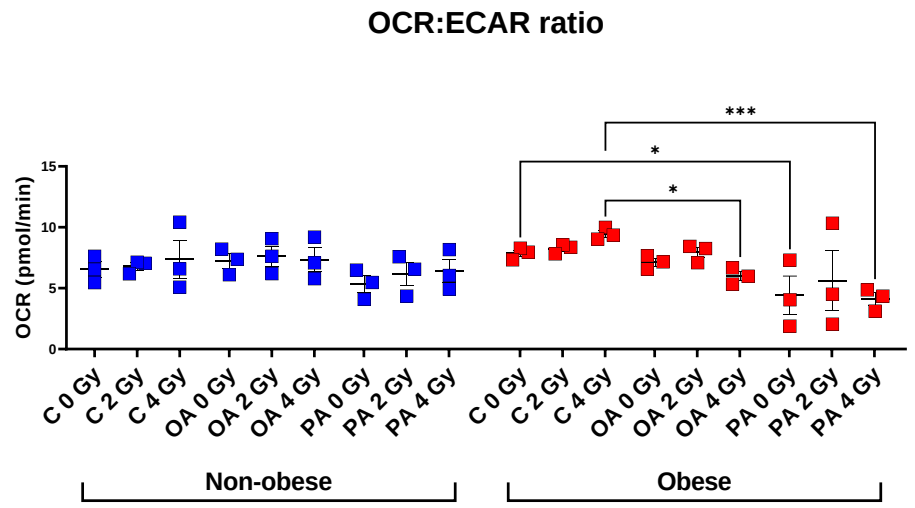


**Figure 5.4.22 The obese adipose secretome in combination with PA and increasing irradiation decreases metastatic cancer cells glycolytic metabolism compared with non-obese ACM.**

FLO-LM cell line cultured with ACM from non-obese and obese treated with Control (C), Oleic Acid (OA), or Palmitic Acid (PA) in combination with mock irradiation, 2 Gy irradiation or 4 Gy irradiation. Mitochondrial parameters were assessed using Seahorse MitoStress test including (A-B) ECAR and OCR:ECAR ratio (Kruskal Wallis test with Dunn's correction). Blue square symbols indicate FLO-LM cell line treated with ACM from non-obese patients (■), red square symbols indicate FLO-LM treated with ACM from obese patients (■). All data expressed as mean ± SEM, n=3, * $p < 0.05$, ** $p < 0.01$.

### 5.4.7 *The adipose secretome exposed to increasing irradiation and exogenous fatty acids differentially alter fatty acid dependency of cancer and metastatic cell lines*

Adipocytes and exogenous fatty acids aid cancer cells metabolic flexibility and metastasis [493,496]. To examine whether the adipose secretome derived from non-obese and obese patients which was exposed to increasing radiation in the presence or absence of OA and PA had differential effects on FLO-1 and FLO-LM metabolic parameters, cells were cultured with these treated ACM for 24 hours and assessed using Seahorse Mito FuelFlex test. The Mito FuelFlex test determines the rate of oxidation of a targeted fuel by measuring mitochondrial respiration of cells in the presence or absence of fuel pathway inhibitors in real time. Here, Fuel Dependency is an indication of cells' reliance on a fuel pathway to maintain baseline respiration, in the context of measuring fatty acid oxidation dependency, this is measured following the injection of etomoxir. Fuel capacity demonstrates a cells' ability to use a fuel pathway to meet metabolic demand when other fuel pathways are inhibited. In the context of establishing fatty acid dependency, BPTES which inhibits glutamine metabolism and UK5099 which inhibits glycolysis through inhibition of pyruvate transport into the mitochondrial and injected after etomoxir.

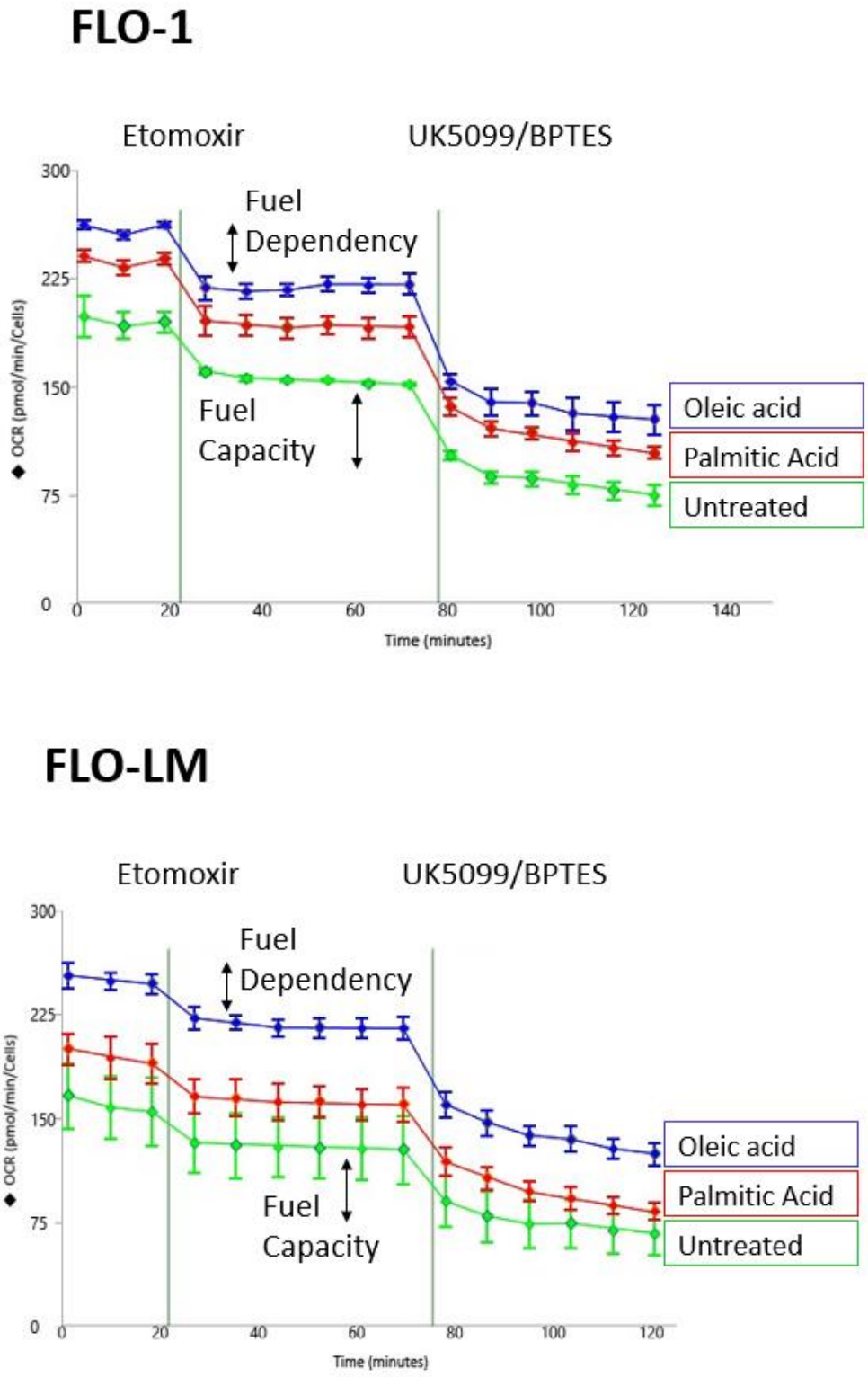


**Figure 5.4.23 An explanatory figure depicting the FuelFlex Test process.**
This figure details the mitochondrial response to inhibitors of fatty acid oxidation (Etomoxir) followed by shutdown of glucose metabolism (UK5099) and glutamine metabolism (BPTES) the ensuing measurements of fuel dependency and fuel capacity following their injection.

In FLO-LM cells decreased dependency of fatty acid oxidation was observed following culture with control ACM exposed to 2 Gy irradiation, OA treated ACM exposed to 4 Gy irradiation and PA treated ACM both in the unirradiated state and following exposure to 2 and 4 Gy irradiation compared with similarly treated FLO-1 cells. Additionally in FLO-LM cells decreased dependency of fatty acid oxidation was observed following culture with control ACM exposed to 2 Gy irradiation compared with FLO-LM cultured with control ACM exposed to 4 Gy irradiation (**Figure 5.4.24**). In FLO-LM cells decreased dependency of fatty acid oxidation was observed following culture with PA treated ACM exposed to 2 Gy irradiation compared with OA treated ACM exposed to 2 Gy irradiation from non-obese patients. Additionally, in FLO-LM decreased dependency of fatty acid oxidation was observed following culture with PA treated ACM exposed to 2 Gy irradiation from non-obese patients compared with similarly treated FLO-1 cells (**Figure 5.4.25**). In FLO-LM cells decreased dependency of fatty acid oxidation was observed following culture with OA treated ACM from obese patients exposed to 4 Gy irradiation and PA treated ACM from obese patients both in the unirradiated state and following exposure to 2 and 4 Gy irradiation compared with similarly treated FLO-1 cells (**Figure 5.4.25**). In FLO-1 cells decreased dependency of fatty acid oxidation was observed following culture with control ACM and OA treated ACM from obese patients exposed to 2 and 4 Gy irradiation compared with compared with FLO-1 cells cultured with similarly treated ACM from non-obese patients (**Figure 5.4.26**). In FLO-LM cells decreased dependency of fatty acid oxidation was observed following culture with control ACM, OA treated ACM and PA treated ACM from obese patients exposed to 4 Gy irradiation compared with compared with FLO-LM cells cultured with similarly treated ACM from non-obese patients (**Figure 5.4.26**).

(* $p < 0.05$, ** $p < 0.01$.)

A)

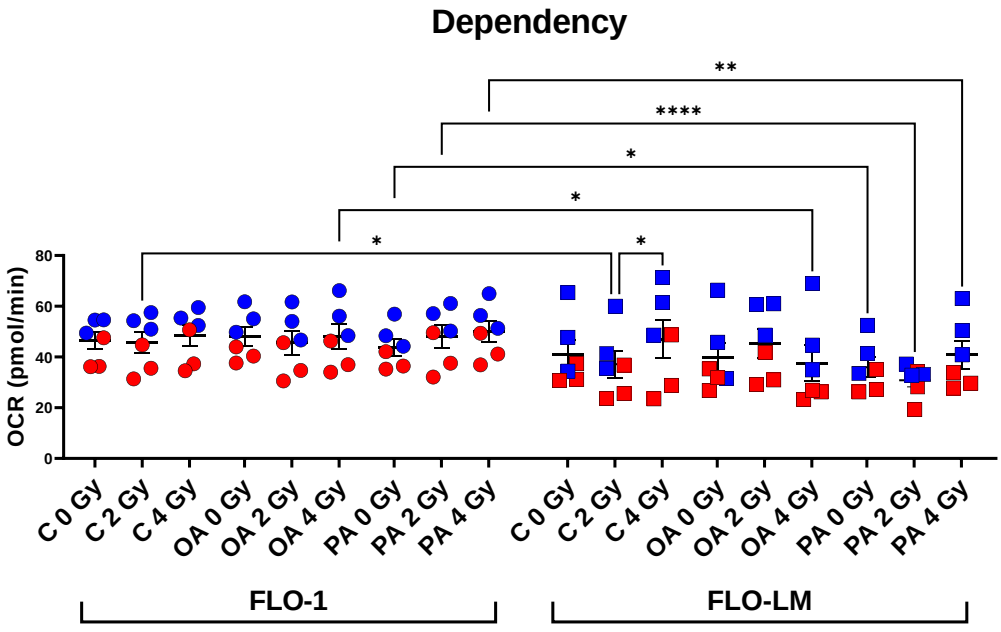


**Figure 5.4.24 The adipose secretome exposed to increasing irradiation and exogenous fatty acids differentially alter fatty acid dependency of cancer and metastatic cell lines**

FLO-1 and FLO-LM cell lines cultured with ACM treated with Control (C), Oleic Acid (OA), or Palmitic Acid (PA) in combination with mock irradiation, 2 Gy irradiation or 4 Gy irradiation. Mitochondrial dependency on fatty acids as a fuel source was assessed using Seahorse FuelFlex test. A) FLO-1 and FLO-LM cells cultured with ACM treated with fatty acids and increasing irradiation (n=6), Blue circle symbols indicate FLO-1 cell line treated with ACM from non-obese patients (●), red circle symbols indicate FLO-1 treated with ACM from obese patients (●). Blue square symbols indicate FLO-LM cell line treated with ACM from non-obese patients (■), red square symbols indicate FLO-LM treated with ACM from obese patients (■). All data expressed as mean ± SEM, * $p < 0.05$, ** $p < 0.01$.

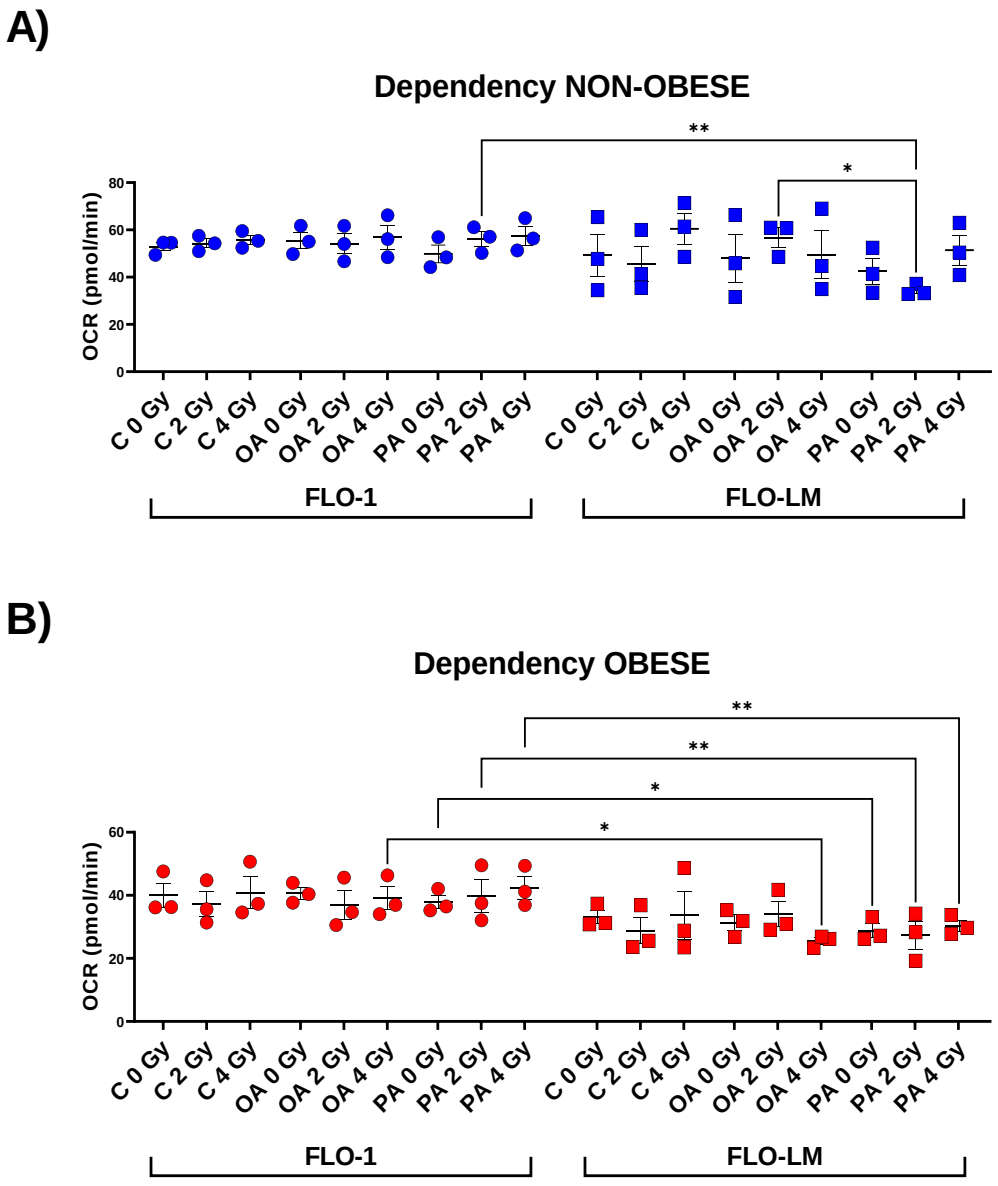


**Figure 5.4.25 The obese adipose secretome exposed to increasing irradiation and palmitic acid decrease reliance on fatty acid oxidation in metastatic cell s compared with primary cancer cells.**

FLO-1 and FLO-LM cell lines cultured with ACM treated with Control (C), Oleic Acid (OA), or Palmitic Acid (PA) in combination with mock irradiation, 2 Gy irradiation or 4 Gy irradiation. Mitochondrial dependency on fatty acids as a fuel source was assessed using Seahorse FuelFlex test. A) FLO-1 and FLO-LM cells cultured with ACM from non-obese patients treated with fatty acids and increasing irradiation, (n=3) B) FLO-1 and FLO-LM cells cultured with ACM from non-obese patients treated with fatty acids and increasing irradiation (n=3) (Kruskal Wallis test with Dunn's correction). Blue circle symbols indicate FLO-1 cell line treated with ACM from non-obese patients (●), red circle symbols indicate FLO-1 treated with ACM from obese patients (●). Blue square symbols indicate FLO-LM cell line treated with ACM from non-obese patients (■), red square symbols indicate FLO-LM treated with ACM from obese patients (■). All data expressed as mean ± SEM, * $p < 0.05$, ** $p < 0.01$.

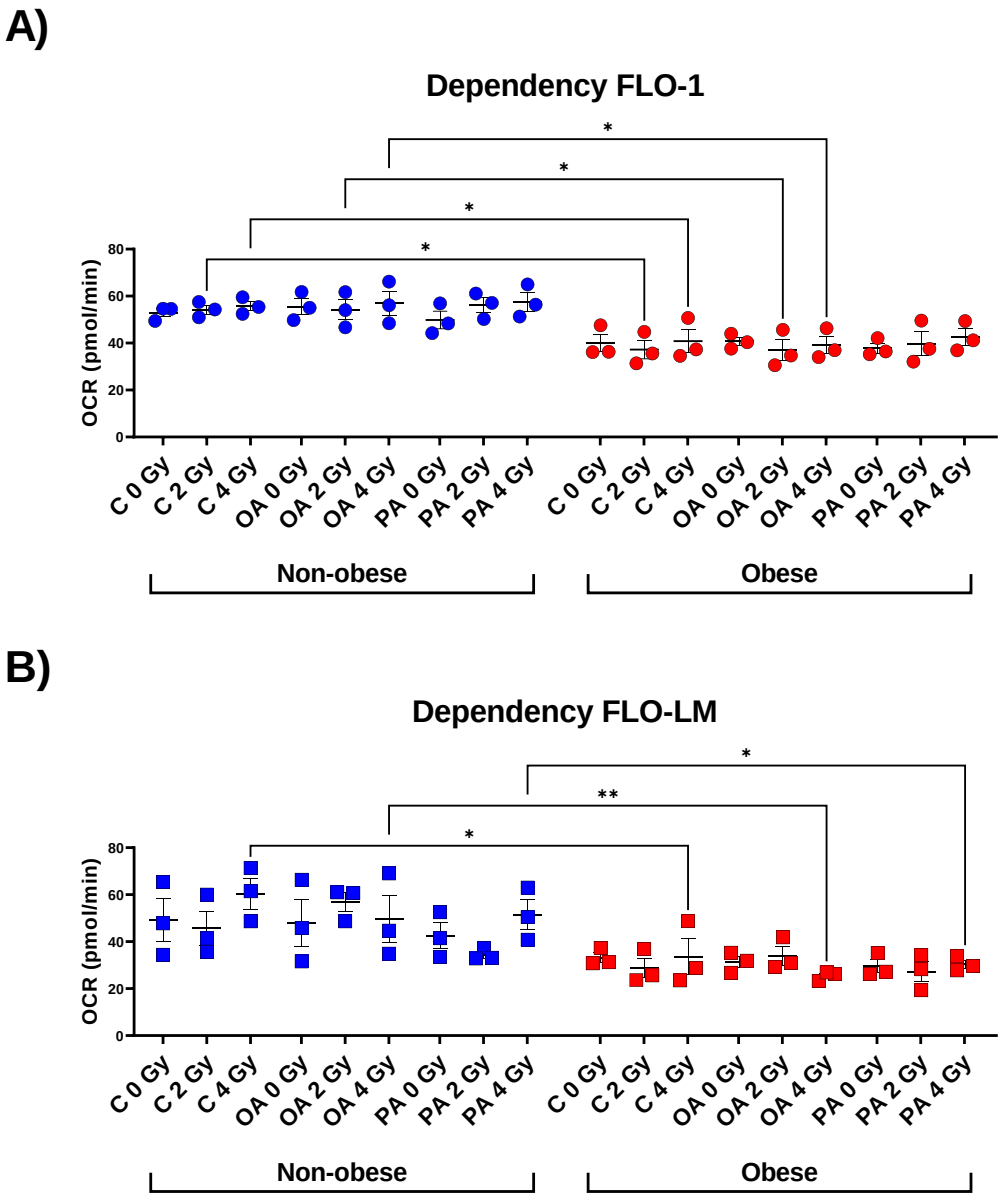


**Figure 5.4.26 The adipose secretome of obese and non-obese patients exposed to increasing irradiation and exogenous fatty acids differentially alter fatty acid dependency of primary and metastatic cell lines.**

FLO-1 and FLO-LM cell lines cultured with ACM treated with Control (C), Oleic Acid (OA), or Palmitic Acid (PA) in combination with mock irradiation, 2 Gy irradiation or 4 Gy irradiation. Mitochondrial dependency on fatty acids as a fuel source was assessed using Seahorse FuelFlex test. A) FLO-1 cells cultured with ACM from non-obese and obese patients treated with fatty acids and increasing irradiation, (n=3), B) FLO-LM cells cultured with ACM from non-obese and obese patients treated with fatty acids and increasing irradiation, (n=3). (Kruskal Wallis test with Dunn's correction). Blue circle symbols indicate FLO-1 cell line treated with ACM from non-obese patients (●), red circle symbols indicate FLO-1 treated with ACM from obese patients (●). Blue square symbols indicate FLO-LM cell line treated with ACM from non-obese patients (■),

red square symbols indicate FLO-LM treated with ACM from obese patients (■). All data expressed as mean ± SEM, * $p < 0.05$, ** $p < 0.01$.

### 5.4.8 *Adipose explants from obese OAC patients exposed to increasing irradiation and palmitic acid have higher secreted levels of CD147*

Previously secreted levels of CD147 have been linked to invasion and metastasis [488]. CD147 has been reported to promote invasion through cathepsin B [489], a factor known to lead to mitochondrial dysfunction and apoptosis [490]. CD147 has also been reported to be increased in circulation and within visceral adipose depots in obese patients [491]. Adipose explants treated with OA and PA and exposed to increasing irradiation were assessed for secreted levels of CD147 by ELISA and was further interrogated based on patient obesity as classified by VFA.

Increased secreted levels of CD147 were observed from adipose explants exposed to 2 or 4 Gy irradiation compared with unirradiated explants. Additionally increased secreted levels of CD147 were observed in unirradiated adipose explants treated with OA or PA compared with unirradiated control (**Figure 5.4.27 A**). In adipose explants derived from obese OAC patients increased secreted levels of CD147 were observed following PA treatment compared with matched obese control and PA treated adipose explants from non-obese patients (**Figure 5.4.27 B**). Increased secreted levels of CD147 were also observed from adipose explants from obese patients following exposure to increasing irradiation of 2 or 4 Gy samples compared with matched control unirradiated adipose explants. Adipose explants from obese patients treated with PA in the unirradiated setting or following exposure to 2 or 4 Gy irradiation also showed increased secreted levels of CD147 compared with unirradiated matched control adipose explants (**Figure 5.4.27 C**).

(* $p < 0.05$, ** $p < 0.01$, *** $p < 0.001$.)

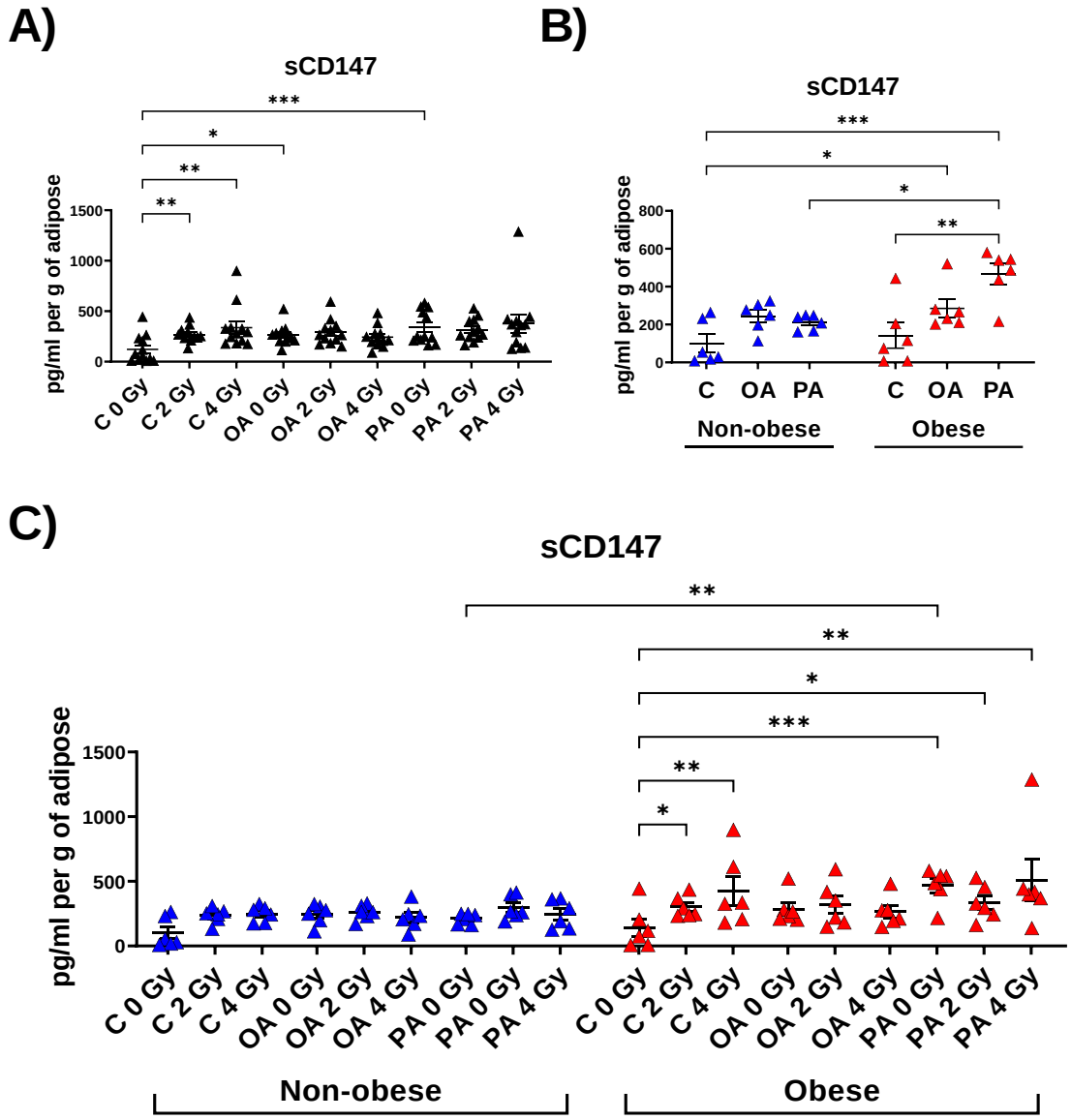


**Figure 5.4.27 Exposure of adipose explants from obese patients to increasing irradiation and PA upregulates secreted levels of CD147**

Adipose conditioned media was assessed for secreted levels of CD147 following treatment with Control (C), Oleic Acid (OA), or Palmitic Acid (PA) in combination with mock irradiation, 2 Gy irradiation or 4 Gy irradiation. A) ACM treated with fatty acids and increasing irradiation (n=12), B) ACM non-obese and obese patients treated with fatty acids (non-obese n=6, obese n=6) C) ACM from non-obese and obese patients treated with fatty acids and increasing irradiation (non-obese n=6, obese n=6), (Kruskal Wallis test with Dunn's correction). Triangle symbols indicate ACM samples (▲). Blue triangle symbols indicate ACM from non-obese patients (▲), red triangle symbols indicate ACM from obese patients (▲). All data expressed as mean ± SEM, * $p < 0.05$, ** $p < 0.01$, *** $p < 0.001$.

### 5.4.9 *Inhibition of fatty acid oxidation increases invasiveness of primary oesophageal cancer cell lines cultured with OA and PA treated ACM*

Invading cancer cells have been reported to have enhanced lipid metabolism and increased reliance on free fatty acids[493]. To assess the influence of adipose secretome, free fatty acids and dependency on FAO on invasive capacity, both FLO-1 and FLO-LM cells lines were cultured with OA and PA treated ACM in an uninhibited setting and with inhibition of FAO by etomoxir. The influences of these treatments were assessed using an invasion chamber with basement membrane for a better reflection of the environment these cells would invade.

FLO-1 cells showed increased invasive capacity towards PA treated ACM compared with matched control. However, inhibition of FAO increased invasiveness of FLO-1 towards OA and PA treated ACM compared with matched inhibited and uninhibited control (**Figure 5.4.28 A**). Additionally, inhibition of FAO increases invasiveness of FLO-LM cells towards ACM treated with OA and PA compared with matched uninhibited control. Whilst inhibition of FAO increased FLO-LM cells invasiveness towards PA treated ACM compared with uninhibited FLO-LM cells towards PA treated ACM (**Figure 5.4.28 B**). FLO-1 cells were also observed to have increased invasive capacity towards PA treated ACM compared with uninhibited cells treated with control ACM, however following the inhibition of FAO this effect was observed with both OA and PA treated ACM. Additionally, regardless of FAO inhibition PA treated ACM decreased FLO-LM invasiveness compared with similarly treated FLO-1 cells (**Figure 5.4.28 C, D**).

(* $p < 0.05$, ** $p < 0.01$, *** $p < 0.001$.)

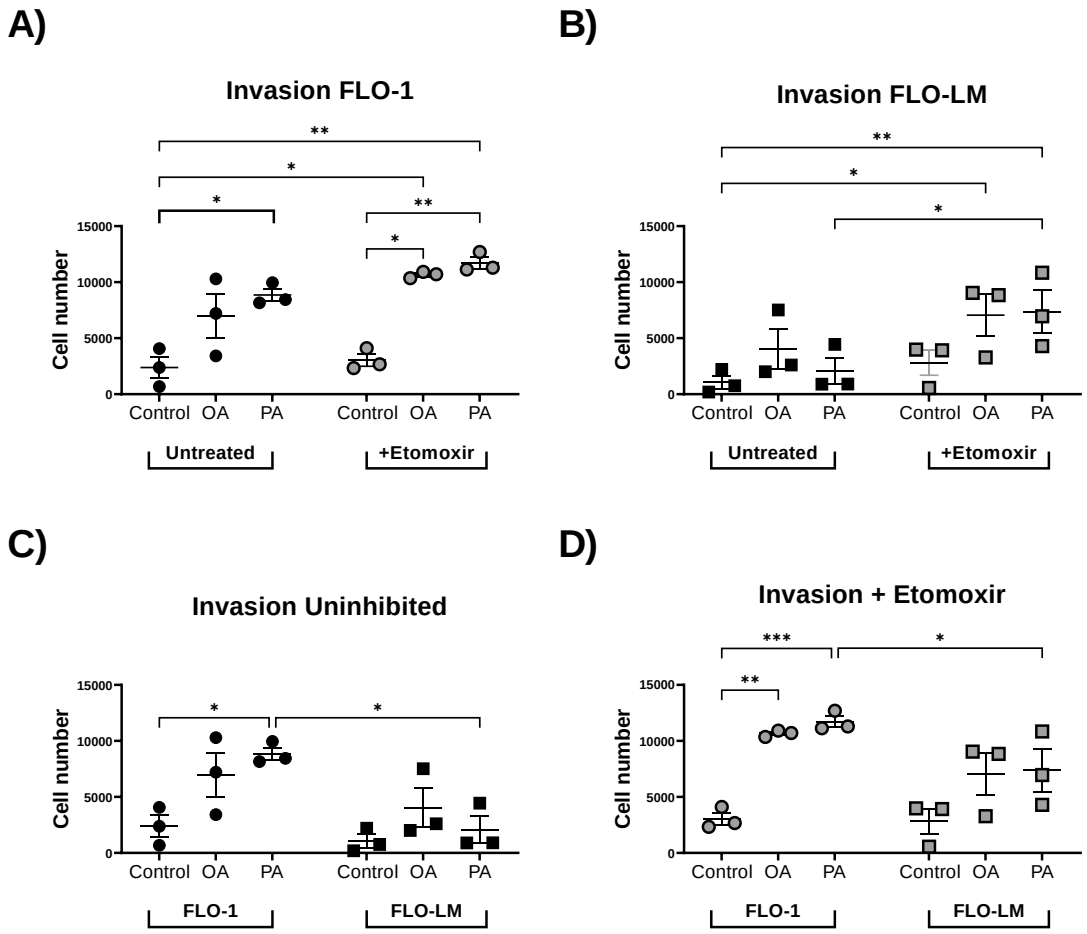


**Figure 5.4.28 Inhibition of fatty acid oxidation increases invasiveness of primary oesophageal cancer cell lines cultured with OA and PA treated ACM**

FLO-1 and FLO-LM cell lines cultured with ACM treated with Control (C), Oleic Acid (OA), or Palmitic Acid (PA) in combination with mock irradiation, 2 Gy irradiation or 4 Gy irradiation. Invasive capacity of these cells was then assessed using an invasion assay either with or without inhibition of fatty acid oxidation. A) FLO-1 cells cultured with ACM treated with fatty acids with or without etomoxir, B) FLO-LM cells cultured with ACM treated with fatty acids with or without etomoxir, C) FLO-1 and FLO-LM cells cultured with ACM treated with fatty acids without inhibition, D) FLO-1 and FLO-LM cells cultured with ACM treated with fatty acids under conditions of fatty acid inhibition, (Kruskal Wallis test with Dunn's correction). Black circle symbols indicate FLO-1 cell line cultured with fatty acids without inhibition (●), Grey circle symbols indicate FLO-1 cell line cultured with fatty acids with inhibition of fatty acid oxidation (●). Black square symbols indicate FLO-LM cultured with fatty acids without inhibition (■), Grey square symbols indicate FLO-LM cultured with fatty acids with inhibition of fatty acid oxidation (■). All data expressed as mean ± SEM, n=3, * $p < 0.05$, ** $p < 0.01$, *** $p < 0.001$.

### 5.4.10 *The adipose secretome treated with PA and increasing irradiation augments the invasive capacities of oesophageal cancer and metastatic cell lines*

Previously, exposure to radiation has been shown to enhance the invasive capacity of cells [492]. To assess the influence of increasing radiation on how the adipose secretome, free fatty acids and FAO dependency alters FLO-1 and FLO-LM cells lines invasive capacity, cells were cultured with OA and PA treated ACM exposed to increasing irradiation in an uninhibited setting and with inhibition of FAO by etomoxir. The influences of these treatments were assessed using an invasion chamber with basement membrane for a better reflection of the environment these cells would invade.

FLO-1 cells showed increased invasive capacity towards control ACM exposed to 4 Gy irradiation and with PA treated ACM compared with matched unirradiated control. However, inhibition of FAO increased invasiveness of FLO-1 towards control ACM exposed to 2 or 4 Gy irradiation and OA and PA treated unirradiated ACM compared with matched unirradiated control. Additionally, inhibition of FAO decreased invasiveness of FLO-1 cells towards OA treated ACM exposed to 4 Gy irradiation compared with OA treated unirradiated ACM and OA treated ACM exposed to 2 Gy irradiation (**Figure 5.4.29 A**). FLO-LM cells showed increased invasive capacity under FAO inhibition towards control ACM exposed to 4 Gy irradiation compared with control unirradiated ACM. FLO-LM cells showed increased invasive capacity towards PA treated ACM exposed to 4 Gy irradiation compared with PA unirradiated ACM and PA treated ACM exposed to 2 Gy irradiation. Additionally, FLO-LM cells showed increased invasive capacity towards PA treated unirradiated ACM following inhibition of FAO compared with FLO-LM cells treated with PA unirradiated ACM in the uninhibited state (**Figure 5.4.29 B**). FLO-1 cells showed increased invasive capacity in the uninhibited state towards OA treated ACM exposed to 2 Gy irradiation and PA treated unirradiated ACM compared with similarly treated FLO-LM cells (**Figure 5.4.30 A**). FLO-1 cells showed increased invasive capacity under FAO inhibition towards PA treated unirradiated ACM and PA treated ACM exposed to 2 Gy irradiation compared with similarly treated FLO-LM cells (**Figure 5.4.30 B**).

(* $p < 0.05$, ** $p < 0.01$, *** $p < 0.001$.)

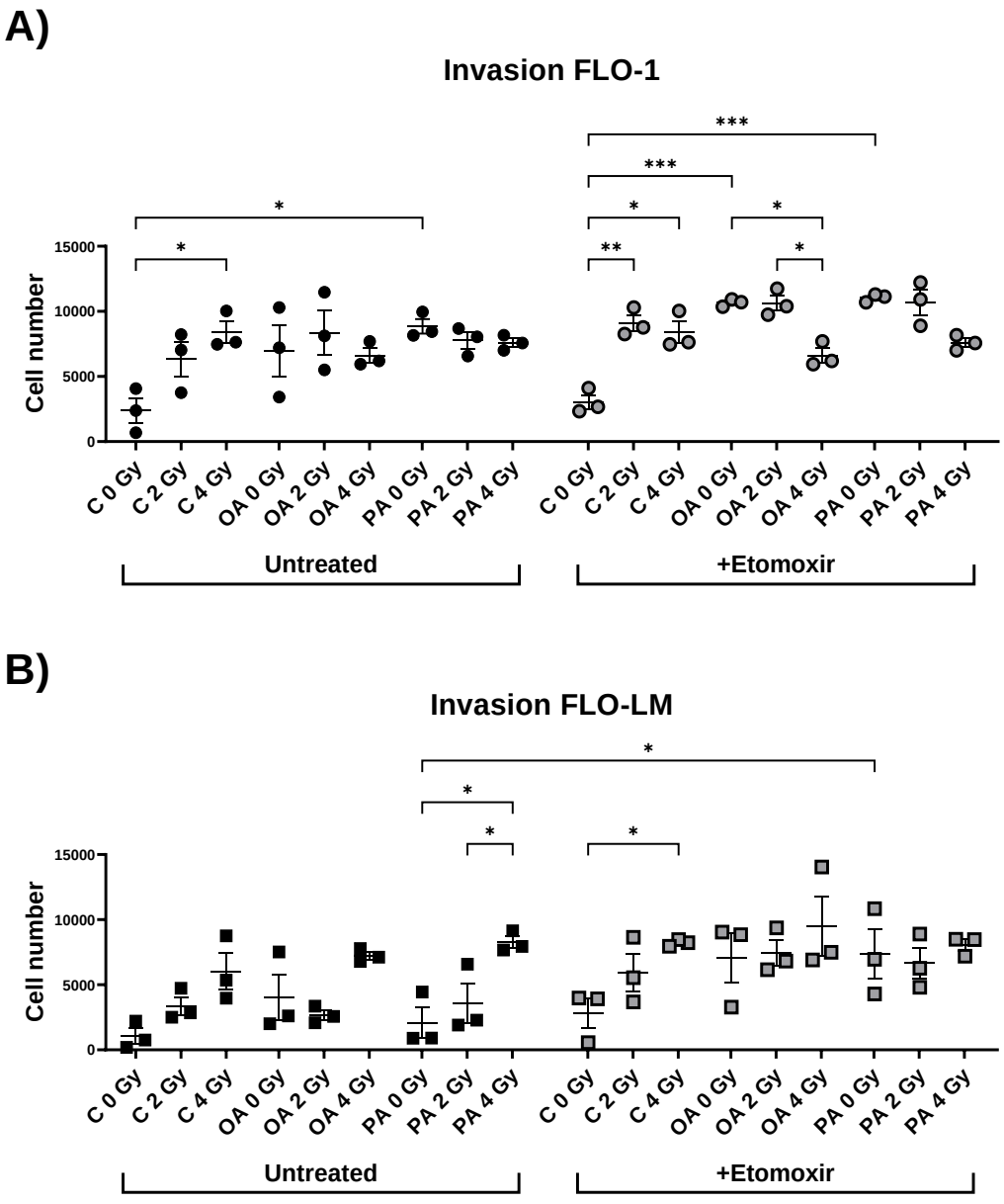


**Figure 5.4.29 The adipose secretome treated with PA and increasing irradiation increases the invasive capacities of oesophageal cancer and metastatic cell line.**

FLO-1 and FLO-LM cell lines cultured with ACM treated with Control (C), Oleic Acid (OA), or Palmitic Acid (PA) in combination with mock irradiation, 2 Gy irradiation or 4 Gy irradiation. Invasive capacity of these cells was then assessed using an invasion assay either with or without inhibition of fatty acid oxidation. A) FLO-1 cells cultured with ACM treated with fatty acids with or without etomoxir, B) FLO-LM cells cultured with ACM treated with fatty acids with or without etomoxir (Kruskal Wallis test with Dunn's correction). Black circle symbols indicate FLO-1 cell line cultured with fatty acids without inhibition (●), Grey circle symbols indicate FLO-1 cell line cultured with fatty acids with inhibition of fatty acid oxidation (●). Black square symbols indicate FLO-LM cultured with fatty acids without inhibition (■), Grey square symbols indicate FLO-LM cultured with fatty acids with inhibition of fatty acid oxidation (■). All data expressed as mean ± SEM, n=3, * $p < 0.05$, ** $p < 0.01$.

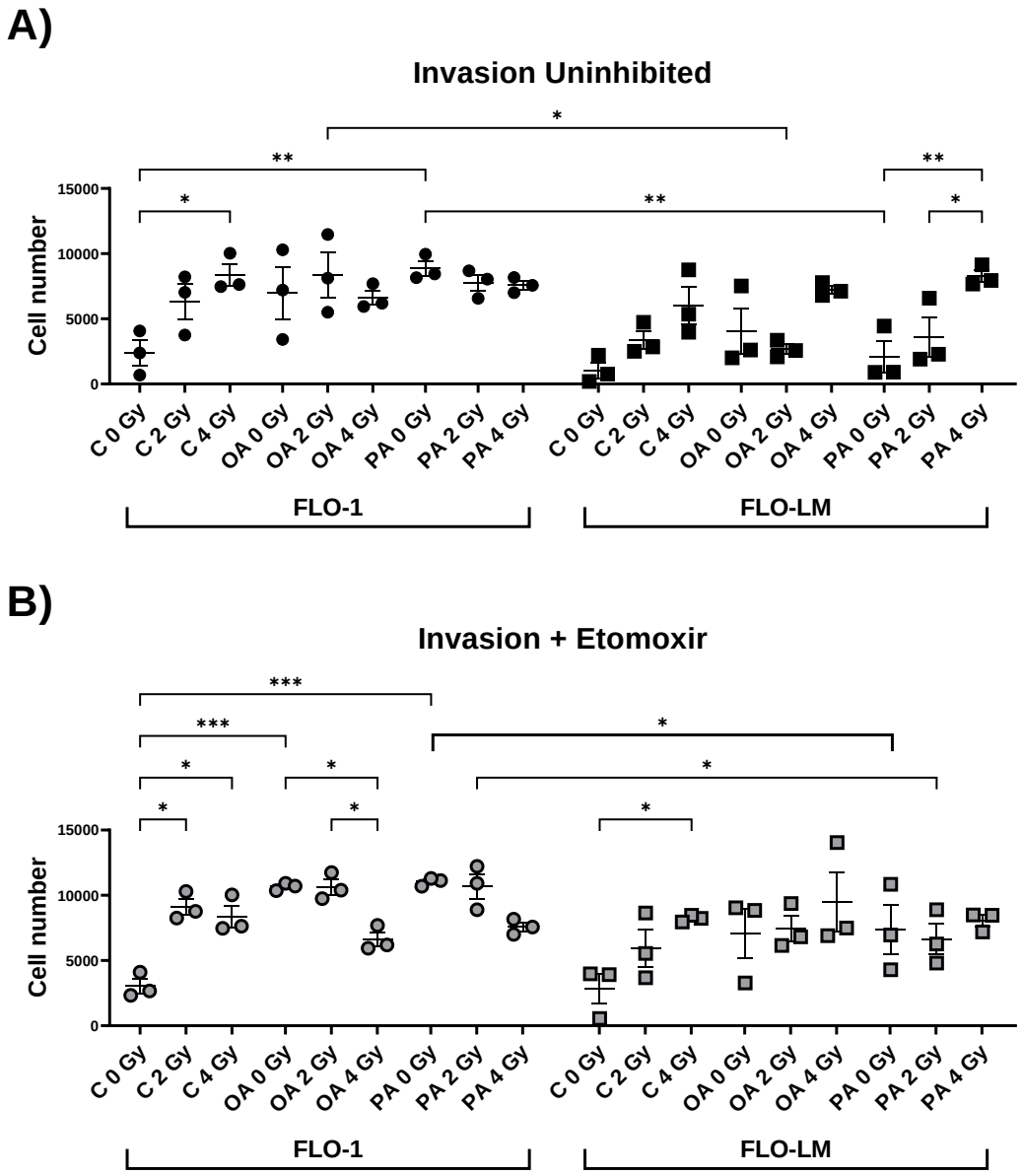


**Figure 5.4.30 Under inhibition of FAO, the adipose secretome treated with PA and 4 Gy irradiation decreases primary cancer and increases metastatic cells invasive capacity.**
FLO-1 and FLO-LM cell lines cultured with ACM treated with Control (C), Oleic Acid (OA), or Palmitic Acid (PA) in combination with mock irradiation, 2 Gy irradiation or 4 Gy irradiation. Invasive capacity of these cells was then assessed using an invasion assay either with or without inhibition of fatty acid oxidation. A) FLO-1 and FLO-LM cells cultured with ACM treated with fatty acids without inhibition, B) FLO-1 and FLO-LM cells cultured with ACM treated with fatty acids under conditions of fatty acid inhibition, (Kruskal Wallis test with Dunn's correction). Black circle symbols indicate FLO-1 cell line cultured with fatty acids without inhibition (●), Grey circle symbols indicate FLO-1 cell line cultured with fatty acids with inhibition of fatty acid oxidation (●). Black square symbols indicate FLO-LM cultured with fatty acids without inhibition (■), Grey square symbols indicate FLO-LM cultured with fatty acids with inhibition of fatty acid oxidation (■). All data expressed as mean ± SEM, n=3, * $p < 0.05$, ** $p < 0.01$.

### 5.4.11 *FAO differentially effects the invasive capacity of primary and metastatic cell lines exposed to PA treated non-obese and obese ACM*

As mentioned invading cancer cells have elevated lipid metabolism and increased reliance on free fatty acids [493]. Obesity has also been reported to elevate free fatty acids in circulation [494]. To assess the influence of obesity on how the adipose secretome, free fatty acids and FAO dependency alters FLO-1 and FLO-LM cells lines invasive capacity, cells were cultured with PA treated ACM from obese and non-obese patients in an uninhibited setting and with inhibition of FAO by etomoxir. The influences of these treatments were assessed using an invasion chamber with basement membrane for a better reflection of the environment these cells would invade.

FLO-1 cells in the uninhibited state showed increased invasive capacity towards PA treated ACM from obese patients compared with matched control and control ACM from non-obese patients (**Figure 5.4.31 A**). However, following inhibition of FAO this observed effect was lost. Interestingly FLO-1 cells under FAO inhibition did show increased invasive capacity towards PA treated ACM from non-obese patients compared with control ACM from obese patients (**Figure 5.4.31 A, B**). Similarly, FLO-LM cells in the uninhibited state did show increased invasive capacity towards PA treated ACM from non-obese patients compared with control ACM from obese patients as well as PA treated ACM from obese patients (**Figure 5.4.31 C**). FLO-LM cells in the uninhibited state and following inhibition of FAO showed increased invasive capacity towards PA treated ACM from non-obese and obese patients compared with matched controls (**Figure 5.4.31 D**).

(* $p < 0.05$, ** $p < 0.01$.)

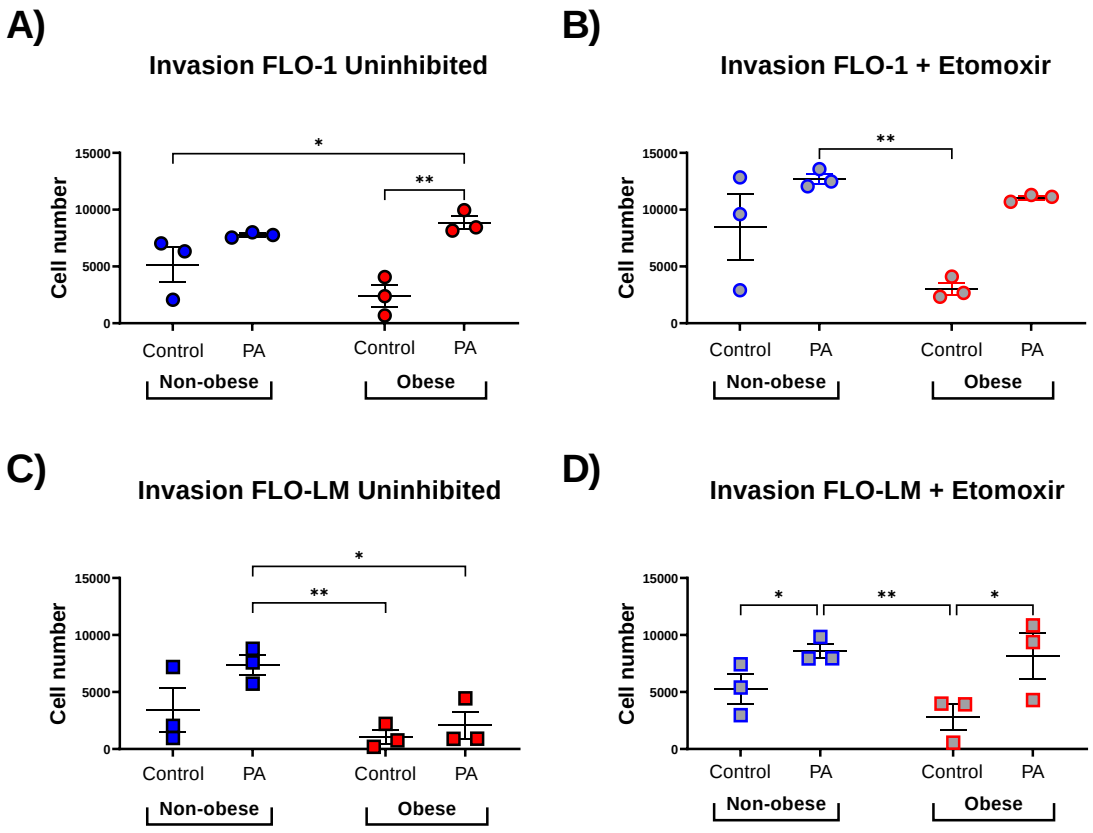


**Figure 5.4.31 FAO differentially effects the invasive capacity of primary and metastatic cell lines exposed to PA treated non-obese and obese ACM**

FLO-1 and FLO-LM cell lines cultured with ACM from non-obese and obese patients treated with Control (C), or Palmitic Acid (PA) in combination with mock irradiation, 2 Gy irradiation or 4 Gy irradiation. Invasive capacity of these cells was then assessed using an invasion assay either with or without inhibition of fatty acid oxidation. A) FLO-1 cells cultured with ACM treated with fatty acids with or without etomoxir, B) FLO-LM cells cultured with ACM treated with fatty acids with or without etomoxir, C) FLO-1 and FLO-LM cells cultured with ACM treated with fatty acids without inhibition, D) FLO-1 and FLO-LM cells cultured with ACM treated with fatty acids under conditions of fatty acid inhibition, (Kruskal Wallis test with Dunn's correction). Blue circle symbols indicate FLO-1 cell line cultured with ACM from non-obese patients treated with fatty acids without inhibition (●), red circle symbols indicate FLO-1 cell line cultured with ACM from obese patients treated with fatty acids without inhibition (●). Blue square symbols indicate FLO-LM cell line cultured with ACM from non-obese patients treated with fatty acids without inhibition (■), red circle symbols indicate FLO-LM cell line cultured with ACM from obese patients treated with fatty acids without inhibition (■). Blue circle symbols indicate FLO-1 cell line cultured with ACM from non-obese patients treated with fatty acids under inhibition of fatty acid oxidation (●), red circle symbols indicate FLO-1 cell line cultured with ACM from obese patients treated with fatty acids under inhibition of fatty acid oxidation (●). Blue square symbols indicate FLO-LM cell line cultured with ACM from non-obese patients treated with fatty acids under inhibition of fatty acid oxidation (■), red circle symbols indicate FLO-LM cell line cultured with ACM from obese patients treated with fatty acids under inhibition of fatty acid oxidation (■). All data expressed as mean ± SEM, n=3, * $p < 0.05$, ** $p < 0.01$.

### 5.4.12 *The obese adipose secretome treated with increasing irradiation and PA differentially affects only metastatic cells under FAO*

As mentioned, increasing radiation enhances the invasive tendencies of cancer cells [492]. These invading cells have elevated lipid metabolism and increased reliance on free fatty acids [493], with increased PA in circulation being associated with obesity [494]. To assess the influence of the culminating effect of obesity, PA, increasing radiation and FAO dependency on FLO-1 and FLO-LM cells lines invasive capacity, cells were cultured with PA treated ACM exposed to increasing radiation from obese and non-obese patients in an uninhibited setting and with inhibition of FAO by etomoxir. The influences of these treatments were assessed using an invasion chamber with basement membrane for a better reflection of the environment these cells would invade.

FLO-1 cells in the uninhibited setting showed increased invasion towards control ACM exposed to 4 Gy irradiation from both non-obese and obese patients (**Figure 5.4.32 A**). However, following inhibition of FAO, FLO-1 cells appeared to have greater invasion towards treated ACM from non-obese patients regardless of irradiation. However, increased invasion was still observed towards control ACM exposed to 4 Gy irradiation from obese patients compared to matched control, similar to the uninhibited setting (**Figure 5.4.32 B**). Additionally, FLO-1 displayed increased invasive capacity towards PA treated unirradiated ACM compared with matched control from obese patients only (**Figure 5.4.32 A**). Following inhibition of FAO, this effect is lost in FLO-1 cells towards PA treated ACM from obese patients. However, FLO-1 cells showed decreased invasion towards PA treated ACM exposed to 4 Gy irradiation from obese patients compared with similarly treated ACM from non-obese patients (**Figure 5.4.32 B**). In FLO-LM cells in the uninhibited state showed increased invasiveness towards PA treated ACM exposed to 4 Gy irradiation compared with control ACM exposed to 4 Gy irradiation from non-obese patients. Interestingly, FLO-LM cells showed increased invasion towards ACM from obese patients exposed to increasing irradiation and treated with PA combined with increasing irradiation in a dose dependent manner (**Figure 5.4.33 A**). Under FAO inhibition the observed effect of PA treated ACM exposed to increasing irradiation which augmented FLO-LM cells invasive capacity in a dose dependant manner was lost regardless of exposure to irradiation. However, control ACM exposed to 4 Gy irradiation from obese patients still enhanced FLO-LM invasion in a dose dependant manner regardless of FAO inhibition (**Figure 5.4.33 B**).

(* $p < 0.05$, ** $p < 0.01$.)

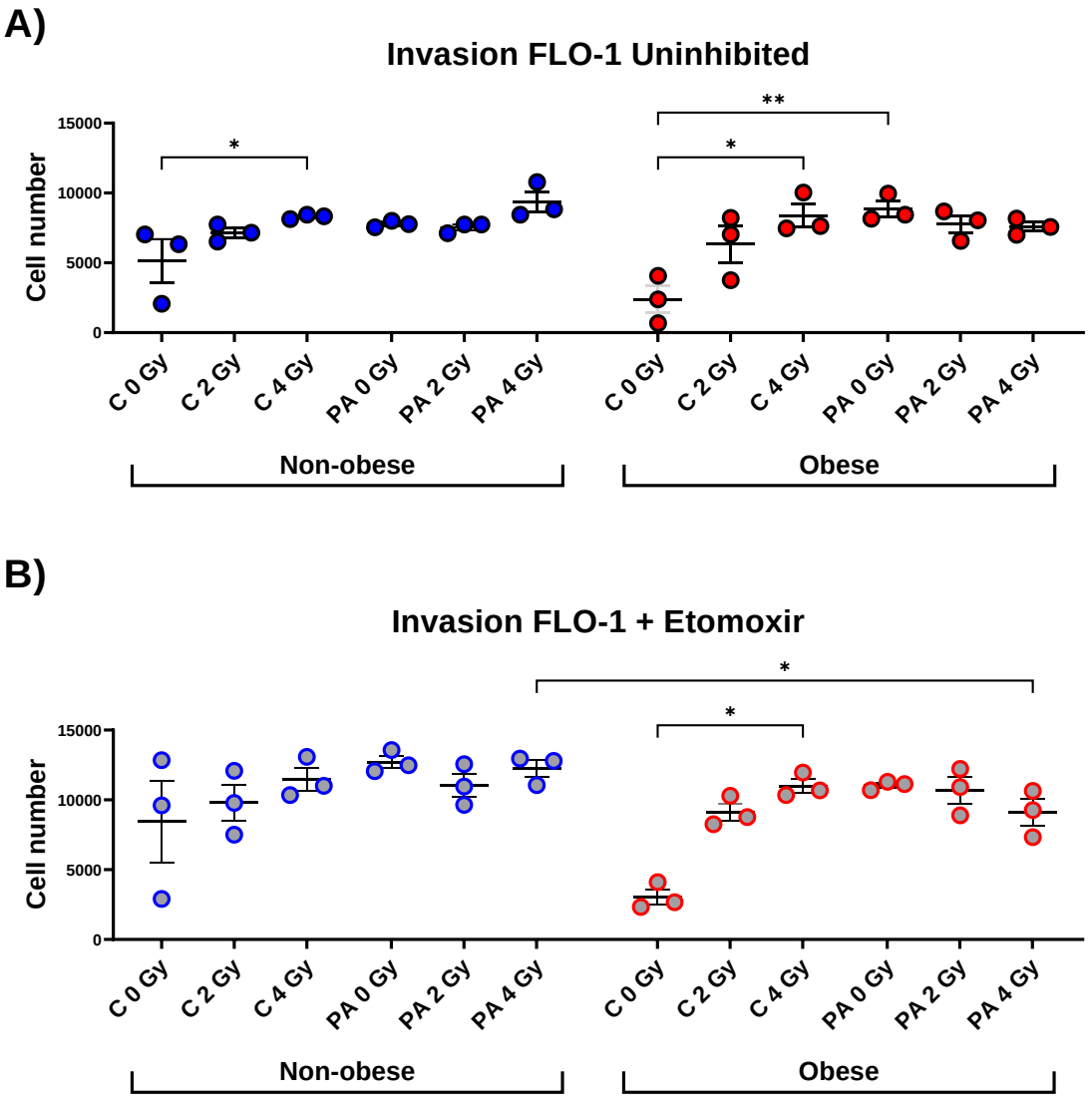


**Figure 5.4.32 Inhibition of FAO does not affect primary cancer cells invasive capacity towards non-obese or obese adipose secretome treated with increasing irradiation and PA**

FLO-1 cell lines were cultured with ACM from non-obese and obese patients treated with Control (C), Oleic Acid (OA), or Palmitic Acid (PA) in combination with mock irradiation, 2 Gy irradiation or 4 Gy irradiation. Invasive capacity of these cells was then assessed using an invasion assay either with or without inhibition of fatty acid oxidation. A) FLO-1 cells cultured with ACM treated with fatty acids without etomoxir, B) FLO-1 cells cultured with ACM treated with fatty acids with etomoxir (Kruskal Wallis test with Dunn's correction). Blue circle symbols indicate FLO-1 cell line cultured with ACM from non-obese patients treated with fatty acids without inhibition (●), red circle symbols indicate FLO-1 cell line cultured with ACM from obese patients treated with fatty acids without inhibition (●).Blue circle symbols indicate FLO-1 cell line cultured with ACM from non-obese patients treated with fatty acids under inhibition of fatty acid oxidation (●), red circle symbols indicate FLO-1 cell line cultured with ACM from obese patients treated with fatty acids under inhibition of fatty acid oxidation (●). All data expressed as mean ± SEM, n=3, * $p < 0.05$, ** $p < 0.01$.

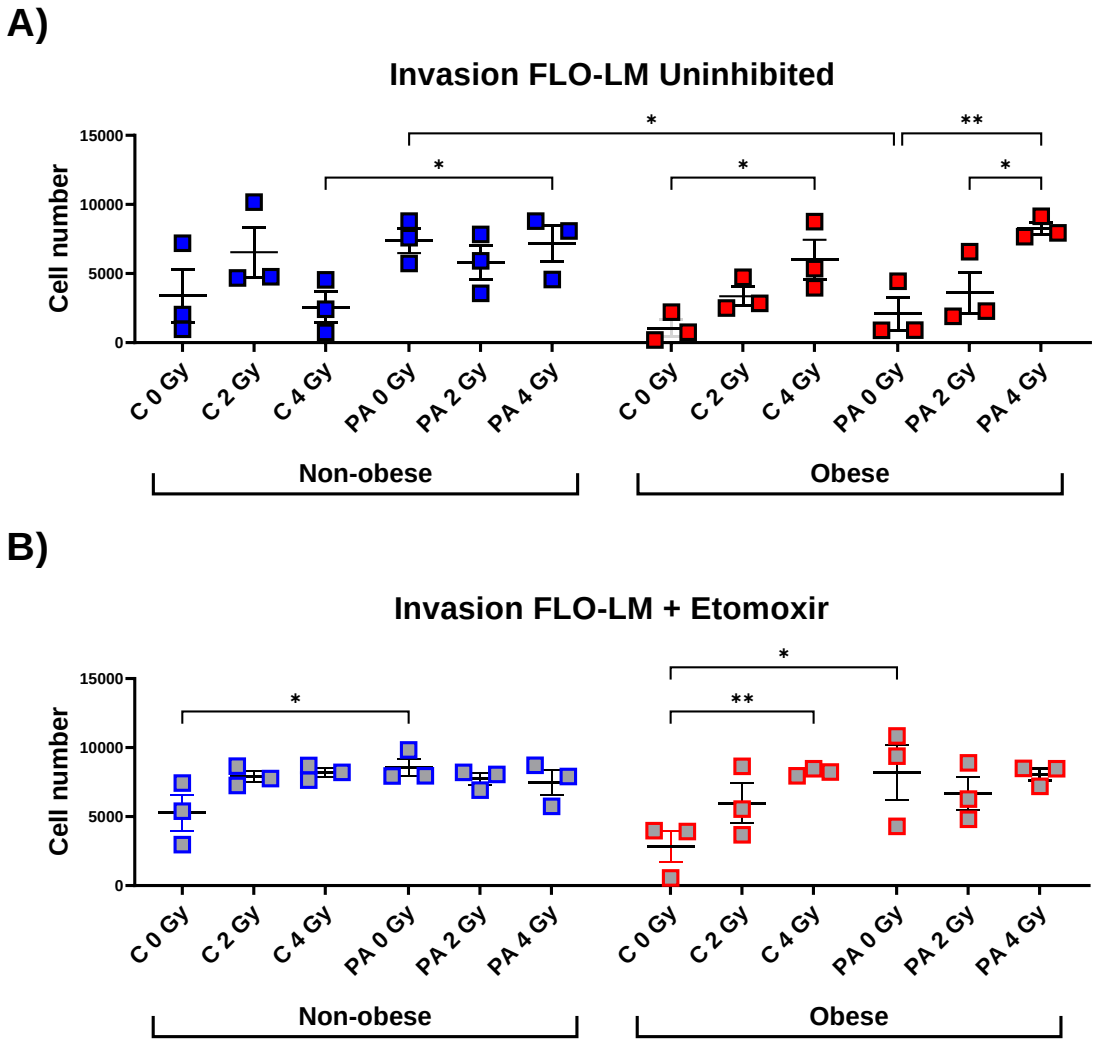


**Figure 5.4.33 The inhibition of FAO differentially effects metastatic cells invasive capacity towards the obese adipose secretome treated with increasing irradiation and PA.**

FLO-LM cell line was cultured with ACM from non-obese and obese patients treated with Control (C), Oleic Acid (OA), or Palmitic Acid (PA) in combination with mock irradiation, 2 Gy irradiation or 4 Gy irradiation. Invasive capacity of these cells was then assessed using an invasion assay either with or without inhibition of fatty acid oxidation. A) FLO-LM cells cultured with ACM treated with fatty acids without inhibition, B) FLO-LM cells cultured with ACM treated with fatty acids under conditions of fatty acid inhibition, (Kruskal Wallis test with Dunn's correction). Blue square symbols indicate FLO-LM cell line cultured with ACM from non-obese patients treated with fatty acids without inhibition (■), red circle symbols indicate FLO-LM cell line cultured with ACM from obese patients treated with fatty acids without inhibition (■).Blue square symbols indicate FLO-LM cell line cultured with ACM from non-obese patients treated with fatty acids under inhibition of fatty acid oxidation (■), red circle symbols indicate FLO-LM cell line cultured with ACM from obese patients treated with fatty acids under inhibition of fatty acid oxidation (■). All data expressed as mean ± SEM, n=3, * $p < 0.05$, ** $p < 0.01$.

## 5.5 Summary of main findings

- Primary and metastatic cancer cells utilise different metabolic pathways, with primary cancer cells showing greater reliance on glycolysis whilst metastatic cells show increased preference for oxidative phosphorylation with a greater spare respiratory capacity.

- PA treated ACM derived from non-obese and obese patients evokes differential metabolic functionality in metastatic cancer cells, with non-obese PA treated ACM increasing metastatic cells utilisation of oxidative phosphorylation associated metabolism and obese PA treated ACM decreasing this.

- Increasing radiation in combination with PA, particularly in the obese setting, decreases metastatic cells dependency on fatty acid oxidation compared with primary cancer cells. Interestingly control and OA treated ACM from obese patients in combination with radiation decreased primary cancer cells dependency on FAO compared with similarly treated ACM from non-obese patients. However, control, OA, and PA treated ACM from obese patients in combination with 4 Gy irradiation decreased metastatic cells dependency on FAO compared with similarly treated ACM from non-obese patients.

- Increased secreted levels of CD147 are most apparent in the obese adipose secretome following exposure to increasing irradiation or PA treatment with or without irradiation.

- Primary cancer cells showed enhanced invasion towards the PA enriched adipose secretome regardless of exposure to irradiation, inhibition of FAO or patient obesity status.

- Metastatic cells only demonstrated increased invasive capacity towards the PA enriched adipose secretome following either increasing irradiation, FAO inhibition or if ACM was derived from non-obese patients.

## 5.6 Discussion

This results chapter assessed the dynamic interplay between the adipose secretome and cancer cell metabolism and invasive capacity. Adipose tissue has been reported to aid the development of metastatic niches [307] and diminish the efficacy of current cancer treatment [484] by supporting flexibility in cancer cell metabolism [485]. Previously we have observed that treatment with exogenous OA and PA in combination with increasing radiation differentially effects the adipose secretome, an effect that is further augmented by patient obesity status. This chapter assessed the culminative effect of exogenous fatty acid treatment and increasing irradiation on the adipose secretome and what downstream effects this has on primary cancer cells (FLO-1) and liver derived metastatic (FLO-LM) cancer cells metabolism, FAO dependency and invasive capacity.

Primary cancer cells have been reported to rely heavily on glycolytic metabolism [497], whilst recent studies have indicated that metastatic cells preferentially utilise oxidative phosphorylation [302]. Interestingly, oesophageal primary cancer cell lines in this study did show greater reliance on glycolysis compared to metastatic cells. These metastatic cells had an increased OCR:ECAR ratio indicating a metabolic preference towards oxidative phosphorylation, both findings which lie in line with literature. Interestingly, the metastatic cells also shown increased spare respiratory capacity compared with primary cancer cells. Spare respiratory capacity is depleted under oxidative stress when oxidative phosphorylation fails to reach the threshold required to sustain the energetic needs of the cell, leading to the induction of glycolysis to meet energy demands [498]. Higher spare respiratory capacity indicates that a cell can produce increased ATP via oxidative phosphorylation upon increased energy demand. This enhanced spare reserve may be indicative of how metastatic cells utilise enhanced metabolic parameters to support migratory capacity.

Fatty acid metabolism has been implicated in promoting aggressive cancers in addition to diminishing treatment efficacy [499]. We observed that PA treated ACM regardless of irradiation increases primary cancer cells non-mitochondrial oxygen consumption and glycolytic metabolism whilst decreasing oxidative phosphorylation preferences compared with metastatic cells. Non-mitochondrial oxygen consumption involves oxygen consuming process that are not associated with the mitochondria [500]. Potentially this elevated non-mitochondrial oxygen consumption observed in primary cancer cells could be linked to increased fatty acid uptake and FAO following the introduction of PA. However. PA overload has also been linked to inducing oxidative stress which may explain the enhanced reliance these primary cancer cells have on glycolytic metabolism [501]. As previously shown, the visceral adipose depot of non-obese

patients has differential secretion of inflammatory mediators and is not associated with increased release of free fatty acids into circulation as is observed in obese patients [68]. This study observed that the non-obese adipose secretome treated with OA and PA exposed to increasing irradiation increased metastatic cells reliance on oxidative phosphorylation as well as increasing maximal respiration and spare respiratory capacity compared with similarly treated primary cells. Interestingly, this may indicate that metastatic cells may be more evasive to the oxidative stress induced by fatty acid treatment and irradiation in the presence of the adipose secretome derived from non-obese patients. Additionally, PA treatment on the non-obese unirradiated adipose secretome was observed to increase proton leak in both primary cancer cells and metastatic cells compared with control ACM. Visceral adipose tissue has been reported to be in a state of chronic low-grade inflammation [398]. Increased levels of saturated fatty acid PA within circulation has been reported in correlation with obesity [68], which has been reported to aid cancer metastasis. Here, PA treatment on the obese adipose secretome in combination with increasing radiation was observed to significantly decrease metabolic parameters of metastatic cells compared with primary cancer cells, and spare respiratory capacity was also decreased compared with matched metastatic cell control. Previously PA has been linked to enhance migratory ability in primary tumour cells [502], which may be indicative of why these primary cells have been conferred with this enhanced metabolic phenotype which may aid in their development into metastatic cells.

Obesity has been linked to development of a series of obesity associated primary cancers [58] as well as aiding their growth and evasion of cytotoxic therapies [503]. Within this study, the obese adipose secretome in combination with fatty acids and increasing irradiation increased oxidative phosphorylation, ATP linked respiration and maximal respiration in oesophageal primary cancer cells compared with non-obese ACM. However, PA treatment on non-obese ACM in the unirradiated setting significantly increased proton leak an effect not observed in the obese setting. The overall increases in utilisation of metabolic parameters associated with oxidative phosphorylation by primary cancer cells following incubation with obese ACM exposed to increasing irradiation indicate these cells have been conferred with the ability to create increased energy supplies. Previously, we have identified increased glutamate in the adipose secretome of obese patients, glutamate has previously been linked to enhancing mitochondrial ATP production [504] which could be contributory factor in this phenomenon. Further to this, obesity related factors that augment dysfunctional adipose biology have been postulated to support cancer metastasis [307]. Here we identified that the obese adipose secretome in combination with PA and increasing irradiation decreases oxidative phosphorylation, non-

mitochondrial oxygen consumption, ATP linked respiration, proton leak maximal respiration, spare respiratory capacity, ECAR in metastatic cancer cells compared with non-obese ACM. It is of interested that PA treatment in combination with non-obese ACM and obese ACM have these differential responses on metastatic cells preferences for oxidative phosphorylation associated metabolism, potentially this may be linked to the differential composition of fatty acids in the adipose secretome prior to the addition of exogenous PA. As metastatic cells have been reported to rely more heavily on FAO, they may be more susceptible to PA overload as prolonged exposure to PA has been reported to impair FAO. PA overload has also previously been linked to increased lipid droplet formation and mitochondrial fragmentation [439] as well as being associated with inducing lipotoxicity, altered lipid metabolism and ER stress [305].

Cancer cells have been reported to have reliance on three major fuel sources glucose, glutamine and fatty acids [505], their flexibility in metabolising these fuels is critical mechanism that aids their survival and resistance to current cancer treatments [485,506]. Adipocytes and exogenous fatty acids have been reported to aid cancer cells metabolic flexibility as well as aiding in metastasis [493,496]. Within this study, PA treated ACM in the unirradiated setting and following exposure to increasing radiation decreased metastatic cell line's dependency on FAO compared with primary cell lines. This decreased dependency on FAO following PA treatment was mirrored in the setting of obese ACM. FAO has been linked to aiding cancer cell metastasis [303], however this decreased dependency on FAO by metastatic cells following culture with PA treated ACM exposed to increasing irradiation, particularly in the obese setting draws into question what the basal fatty acid content is composed of. As well as whether there are other factors such as glutamate that are aiding this decreased reliance on FAO, however further research is required to fully assess mechanism and whether targeting these factors synergistically may prove as an attractive therapeutic target to diminish cancer cell metastasis. Interestingly primary cancer cells showed decreased dependency on FAO following treatment with control and OA treated ACM derived from obese patients following exposure to 2 and 4 Gy irradiation compared with similarly treated cells exposed to ACM from non-obese patients. Whilst metastatic cells showed decreased FAO dependency following culture with control, OA, and PA treated ACM from obese patients exposed to 4 Gy irradiation compared with similarly treated cells exposed to non-obese ACM. Both primary and metastatic cancer cells showing decreased dependency on FAO following culture with obese ACM exposed to 4 Gy irradiation regardless of fatty acid treatment may indicate a switch in metabolic preference due to the alteration caused in the adipose secretome exposed to high dose irradiation. Cancer cells have previously been reported to evoke increased reliance on glycolytic metabolism following radiation induced inflammatory

stress [507], a mechanism known to confer radioresistance by aiding DNA repair [295]. As previously mentioned, we have identified increased secreted levels of glutamate in the ACM of obese OAC patients which has been linked to augmented oxidative glycolytic metabolism [508]. Potentially the oxidative stress caused by irradiation on the adipose secretome could augment this response however further research is required to mechanistically assess this reaction.

Previously secreted levels of CD147 have been linked to invasion and metastasis [488]. CD147 has also been reported to be increased following exposure to irradiation [509] as well as contributing to reprogramming of fatty acid metabolism [510]. Within this study, exposure to increasing irradiation significantly increased secreted levels of CD147 in ACM as did OA and PA treatment in the unirradiated state, which is of interest considering the earlier effects these treatments were observed to have on mitochondrial parameters. CD147 has been reported to promote invasion through cathepsin B and β-catenin [489], factors known to lead to mitochondrial dysfunction and apoptosis through the induction of bid and bax [490]. β-catenin has also been reported to activate vimentin [511], a filament known to regulate epithelial to mesenchymal transition which induces migration and invasion [512]. CD147 has further been reported to be increased in circulation and within visceral adipose depots of obese patients [491]. Here we report that PA treatment significantly increased CD147 in the secretome of adipose explants from obese patients compared with non-obese patients as well as against control ACM from obese patients. Further to this, increasing irradiation and PA treatment in combination with increasing irradiation significantly increased secreted levels of CD147 in the adipose secretome of obese patients, an effect not observed in the secretome of adipose explants derived from non-obese patients. It is of interest that increases in CD147 are most apparent in the adipose secretome of obese OAC patients, as obesity has been widely reported to support the development of metastatic niches that support invading cancer cells [307].

Invading cancer cells have been reported to have enhanced lipid metabolism and increased reliance on free fatty acids [493]. Within this study primary cancer cells showed increased invasion towards PA treated ACM regardless of FAO inhibition. Whilst inhibition of FAO in primary cancer cells significantly increased invasiveness towards OA treated ACM. Utilisation of FAO has been more strongly linked with metastatic cells, however PA has been previously reported to enhance metastasis [502]. Potentially inhibition of FAO may induce stress in primary cancer cells stimulating their movement towards a fatty acid enriched environment, as FAO has been reported to protect cancer cells from apoptosis by increasing mitochondrial membrane lipids [506]. Interestingly, this study observed inhibition of FAO increased metastatic cancer cells invasion towards PA treated ACM compared with uninhibited cells movement towards PA

treated ACM. However, regardless of inhibition of FAO primary cancer cells showed enhanced invasion towards PA treated ACM compared with metastatic cancer cells. Considering that metastatic cells have been reported to preferentially utilise FAO, it is of interest that only following inhibition of this mechanism do these cells move towards the PA enriched adipose secretome. This could be indicative of the altered biology of metastatic cells and their increased reliance on FAO that only when energy source is blocked do they migrate towards more fatty acid enriched environments. Additionally, the observation that primary cells invade more towards PA enriched ACM than their metastatic counterparts pose an interesting question about their basal energy needs and preferential fuel sources. This decreased invasion by metastatic cells could be linked to their metabolic plasticity and flexibility which alters as that migrate throughout the body to distant sites of metastasis [513], an enhancement that could aid their resistance to current cancer treatments.

Previously, exposure to radiation has been reported to enhance the invasive capacity of cancer cells [492]. Here we report that primary cancer cells showed increased invasiveness towards control ACM exposed to 4 Gy irradiation regardless of FAO inhibition. Whilst metastatic cancer cells only showed enhanced invasion towards control ACM exposed to 4 Gy irradiation following inhibition of FAO.
This could suggest that the migratory capacity of primary cancer cells is stimulated by irradiated adipose secretome which possesses elevated levels of inflammatory mediators (supplemental figure), that have been linked to aiding metastasis in oesophageal cancer [514]. Whilst again the reliance of metastatic cells on FAO is evident, as their invasive capacity is enhanced following inhibition of FAO. Metastatic cancer cells also showed increased invasiveness towards PA treated ACM exposed to 4 Gy irradiation in the uninhibited setting, however, following inhibition of FAO metastatic cancer cells showed increased invasion towards PA treated ACM regardless of irradiation exposure. Again, we observed that metastatic cancer cells with the ability to utilise FAO demonstrate less motility. However, PA in combination with radiation elicits the same effect as FAO inhibition on these metastatic cells enhancing their invasive capacity. Further research is required to interrogate what similar mechanisms these treatments induce in metastatic and whether blocking these processes could be utilised for therapeutic gain. In contrast, primary cancer cells following FAO inhibition showed decreased invasiveness towards OA treated ACM exposed to 4 Gy irradiation. OA has previously been linked to having anti-cancer properties as well as ameliorated the pro-inflammatory effects induced by saturated fatty acids [64,515]. It is of interest that the combination of OA and 4 Gy irradiation on the adipose secretome created a microenvironment that diminished the invasion of primary cancer cells but

did not affect metastatic cells. This could be indicative that that OA could be beneficial in diminishing the invasiveness induced by radiation and potentiate pre-metastatic niche development in visceral adipose tissue, however, further research is required to identify if this could be therapeutically targeted. Metastatic cancer cells also showed decreased invasiveness towards PA treated ACM in the unirradiated setting compared with primary cancer cells in an uninhibited state. Similarity, following inhibition of FAO metastatic cancer cells showed decreased invasiveness compared with primary cancer cells towards PA treated unirradiated ACM and PA treated ACM exposed to 2 Gy irradiation. This mirrors previous observations where this decreased invasion by metastatic cells could be linked to their altered metabolic plasticity and flexibility which is developed during migration [513].

As mentioned invading cancer cells have elevated lipid metabolism and increased reliance on free fatty acids [493]. Obesity has also been reported to elevate free fatty acids in circulation [494]. Within this study primary cancer cells showed increased invasive capacity towards PA treated ACM derived from obese patients an effect that was not observed with PA treated ACM from non-obese patients. Interestingly following FAO inhibition this effect was lost. Obesity has previously been linked to the expansion of metastasis-initiating cells [516], which may account for this enhanced migration of primary cells towards the PA enriched adipose secretome of obese patients. In contrast, metastatic cells did not demonstrate increased invasive capacity towards PA treated ACM derived from non-obese or obese patients in the uninhibited state. However, following FAO inhibition of FAO metastatic cells showed increased invasiveness towards PA treated ACM derived from non-obese or obese patients. This differential response of primary and metastatic cancer cells towards PA treated ACM from obese patients which was dependant on FAO inhibition, again may be indicative of underlying metabolic preferences. This contrasting response may indicate that inhibition of FAO may mitigate the invasive capacity of primary tumour cells and may make them more susceptible to the cytotoxic effects of current therapies. FAO has previously been linked to chemoresistance and inhibition of this has been shown to enhance chemosensitivity in drug resistant cancers [517,518]. However, again this response highlights that metastatic cells possess enhanced invasive capacity when they are prevented from utilising FAO, which calls into question if inhibition of FAO in combination with current cancer therapies may exacerbate cancer metastasis as cells evoke invasion to find additional fuel sources.

Increasing radiation enhances invasive phenotypes in cancer cell which rely on lipid metabolism and increased free fatty acids, one such fatty acid PA has been reported to be increased in circulation in obese individuals [492–494]. Within this study, both primary and metastatic cancer

cells showed significantly increased invasion towards obese control ACM exposed to 4 Gy irradiation regardless of FAO inhibition. Primary and metastatic cancer cells showed similar levels of invasion towards PA treated ACM from non-obese patients regardless of increasing irradiation or inhibition of FAO. Similarly primary cancer cells showed comparable levels of invasion towards PA treated ACM from obese patients regardless of increasing irradiation or inhibition of FAO. However metastatic cells showed decreased invasiveness towards PA treated unirradiated ACM from obese patients compared with PA treated ACM from obese patients exposed to 2 or 4 Gy irradiation. This effect was not observed following the inhibition of FAO as metastatic cells showed comparable invasion at all does of irradiation. Highlighting again that PA in combination with radiation elicits the same effect as FAO inhibition on these metastatic cells enhancing their invasive capacity, an effect that is augmented by the obese adipose secretome. Obesity has been linked to enhanced metastasis as a result of the many biologically processes it aberrantly effects including lipid metabolism [519]. However, further analysis is required to assess if these cells utilise different fuel sources to compensate in the presence of FAO inhibition to interrogate if dual blockade of these metabolic pathways could be harnessed for therapeutic gain.

This study has aimed to elucidate how the adipose secretome influences the metabolic and invasive parameters of primary oesophageal cancer and liver derived metastatic cells. We have highlighted these cells employ different metabolic mechanisms with primary cells being more reliant on glycolysis, whilst metastatic cells utilise oxidative phosphorylation associated mechanisms as well as being acutely affected by inhibition of FAO. Elevated secreted levels of CD147 a factor known to drive metastasis, was observed in ACM treated with PA and exposed to increasing radiation, which was most apparent in the obese adipose secretome. Inhibition of FAO, a mechanism known to support metastasis, was seen to have differential response in enhancing invasion of primary and metastatic towards the PA enriched adipose secretome, an effect that was further amplified by patient obesity. These findings pose the question whether FAO inhibitors which have been proposed to enhance the efficacy of current cancer therapies, may exacerbate cancer cell invasion, and increase distant metastasis particularly in the most viscerally obese of patients.

*Chapter 6*

# *Palmitic acid evokes divergent metabolic and secreted profiles in adipose tissue explants of oesophageal adenocarcinoma patients in response to chemotherapy and chemoradiotherapy.*

## 6.1 Objective and specific aims:

**Objective:**

The overall objective of this chapter was to assess whether increasing irradiation would affect the influence of exogenous fatty acids on immuno-metabolic profiles of adipose explant oesophageal cancer patients using real-time metabolic profiles and multiplex ELISA. As well as determining whether these altered immuno-metabolic profiles were influenced by increased visceral adiposity. This chapter further looks to assess how increasing irradiation and alterations in these treated adipose secretome effect immune cell function.

**Specific Aims**

- To assess metabolic profiles including oxidative phosphorylation and glycolysis of adipose explants from treatment naïve OAC patients following culture with FLOT chemotherapy regimen and CROSS chemoradiotherapy regimen in combination with OA (oleic acid) and PA (palmitic acid).
- To assess the influence of chemotherapy and chemoradiotherapy on the secreted profiles of these adipose explants for mediators of inflammation, metabolism, angiogenesis, and immune response and whether this in influenced by exogenous fatty acids.
- To examine the influence of these chemotherapy and chemoradiotherapy treated adipose secretome on oesophageal cancer cell lines metabolism and whether this in influenced by exogenous fatty acids.
- To evaluate whether the adipose secretome of cancer patients treated with chemotherapy or chemoradiotherapy combined with OA or PA influences dendritic cell (DC) expression of maturation markers.
- To evaluate whether the adipose secretome of cancer patients treated with chemotherapy or chemoradiotherapy combined with OA or PA influences macrophage (Mϕ) polarisation towards a pro-inflammatory (M1-like) or anti-inflammatory (M2-like) phenotype.

## 6.2 Introduction

Chemotherapy and chemoradiotherapy are two of the most historic and commonly used therapies used to treat cancer [87,166]. Currently the standard of care for OAC involves neoadjuvant treatment with either chemotherapy alone, including FLOT regimen, or combination chemoradiotherapy, including CROSS regimen, for locally advanced tumours [19]. Adipose tissue is a regulatory organ with many downstream functions that are not fully understood, including its response to chemotherapy and radiotherapy. However, increased visceral adiposity has been reported to have deleterious effects on the efficacy of current cancer treatments such as chemotherapy and chemoradiotherapy [231]. Particularly, the efficacy of chemotherapy has been reported to be mitigated by adipose tissue, with adipocytes sequestering and metabolising these drugs diminishing their cytotoxic effects [484]. Further to this chemotherapy has been reported to diminish lipid storage as well as depleting expression of proteins associated with ATP generation and fatty acid oxidation [520], both key pathways associated with adipocyte metabolism

The adipose secretome has also been reported to influence the tumour microenvironment, particularly visceral adipose tissue due to its anatomical distribution and proximity to organs known to develop obesity associated carcinogenesis [79,487]. Chemotherapy and chemoradiotherapy have been reported to augment the secretion of factors from adipose tissue in such a manner that aids cancer metastasis and survival from cytotoxic interventions [78]. The adipose secretome has even been postulated as a potential attractive therapeutic target to potentiate tumour progression and enhance treatment efficacy [79]. Cancer associated adipocytes (CAAs) are one factor that is being actively targeted to improve treatment responses. Targeting of CD36 and its associated mechanisms is currently being explored to mitigate tumour cells lipid uptake from CAAs. CD36 has been linked to promoting chemoresistance in cancer cells and inhibition of CD36 has been reported to evoke immunostimulatory effects and decreased tumour aggressiveness *in-vitro* [521,522]. Recent reports have also linked treatment resistance in tumour cells with their ability to invoke a metabolic switch from glycolysis to lipid metabolism to evade the cytotoxic effects of chemotherapy. Inhibition of Fatty acid synthase (FASN) in combination with chemotherapy has been reported to increase the efficacy of these chemotherapy in treatment resistant cancers both in *in-vitro* and *in-vivo* [523,524]. Fatty acids are a principal component of the adipose secreted profile and saturated fatty acid palmitic acid (PA), and mono-unsaturated fatty acid oleic acid (OA) are two of the main components of these profiles. Previously, PA has been reported to enhances the efficacy of chemotherapy [525], whilst OA has been reported to have significant anti-tumour effects [64].

Mitochondrial dysfunction is commonly induced by cancer cells to aid tumour progression [286]. Aberrant cellular metabolism has been widely reported to be induced by cancer in order to evade the cytotoxic effects of chemotherapy and chemoradiotherapy [191,287]. Particularly, lipid metabolism and fatty acid oxidation has recently been reported to enhance cancer cell resistance to current cancer treatments [288]. PA has previously been reported to lead to enhanced uptake of fatty acids [305] and upregulation of lipid metabolism genes that has been reported to aid in the initiation of metastasis [306], making it an attractive target to diminish cancer cells ability to evade current treatments. Adipose tissue has also been reported to recruit immune cells whilst having deleterious effects on their function which can potentiate anti-tumour immunity [81–85]. Dendritic cells possess a critical role in initiating anti-tumour immunity, through antigen presentation. Chemotherapy has previously been reported to increase DC antigen presentation [242], however induction of DC response following radiotherapy was shown to be dependent on an active immune infiltrate already being present [243].Macrophages in both their pro-inflammatory and anti-inflammatory phenotypes play a central role in cancer progression and treatment resistance. Anti-inflammatory or tumour associated macrophages (TAMs) have reported to be induced by chemotherapy [245] as well as mediating chemoresistance [246]. However, radiation therapy through its initiation of radiation induced inflammation has been linked to the promotion of classically activated macrophages and increased expression of pro-inflammatory mediators which enhance anti-tumour immunity [247,434,437].

This study for the first-time reports on the effects of chemotherapy and chemoradiotherapy on adipose tissue metabolism and its secretome and the effects of exogenous fatty acids on this adipose microenvironment including metabolism, dendritic cell maturation and macrophage polarisation. This data provides information on whether adipose tissue is the mitigating factor in the obesity-cancer link that deleteriously effects the efficacy of current therapies.

## 6.3 Materials and Methods

### 6.3.1 *Ethics Statement and Patient Recruitment*

Ethical approval was granted by the St James's Hospital/AMNCH ethical review board (Ethics number: REC_2019-07 List 25(27)) and written informed consent was collected from all patients in this study. 6 cancer patients were recruited within the period between 8th of January 2022 and 16th of September 2022, patient demographics are listed in Table 6.3.1. Fresh adipose tissues were taken from all patients at the start of surgical resection. All OAC patients were being treated with curative intent and had received no treatment prior to surgical resection.

**Table 6.3.1 Clinical demographics associated with OAC patients**

| **Patient Clinical Parameters** | |
|---|---|
| **Diagnosis** | OAC = 6 |
| **Sex** | Male = 5<br>Female = 1 |
| **Age at diagnosis** | 53-88 (Mean = 72.5) |
| **Post-treatment BMI** | 25.7-32 (Mean = 29.9) |
| **Weight** | 63–97.2 kg (Mean = 82.15) |
| **Treatment** | Naïve *n* = 6 |
| **Clinical Stage (T)** | T1 *n* = 4<br>T3 *n* = 2 |
| **Clinical Stage (N)** | N0 *n* = 5<br>N1 *n* = 0<br>N2 *n* = 1 |
| **Path stage (T)** | T0 *n* = 0<br>T1 *n* = 4<br>T2 *n* = 2<br>T3 *n* = 0<br>T4 *n* = 0 |
| **Path Stage (N)** | N0 *n* = 4<br>N1 *n* = 1<br>N2 *n* = 1<br>N3 *n* = 0 |

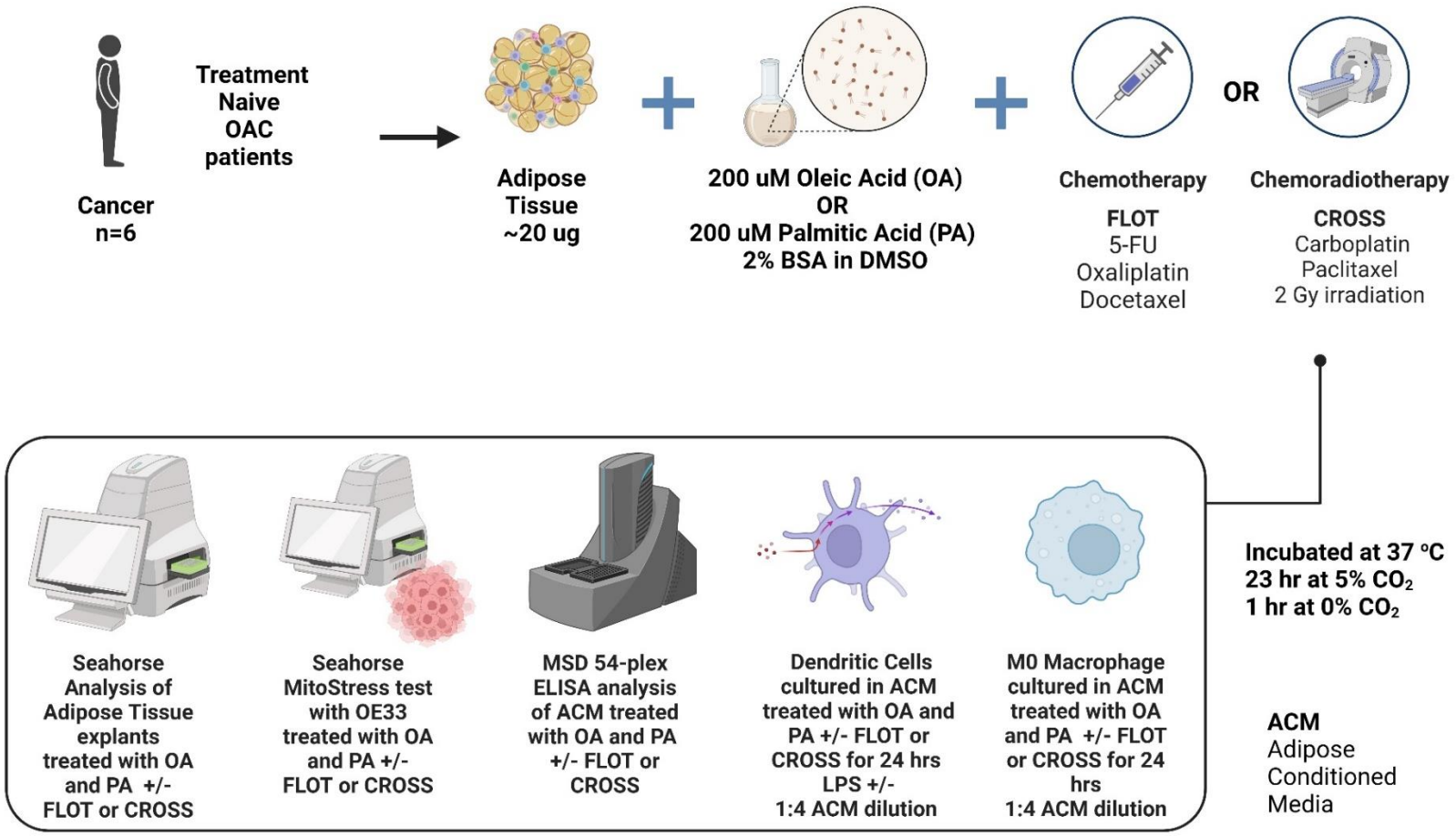


**Figure 6.3.1 Schematic of experimental methodology workflow associated with Chapter 6**

Real time metabolic and secreted profiles of adipose explants from OAC treatment naïve cancer patients were assessed by Agilent seahorse, MSD multiplex ELISA following culture with chemotherapy FLOT regimen or chemoradiotherapy CROSS regimen combined with exogenous fatty acid treatment with OA And PA, with or without exposure to increasing irradiation (mock irradiated 0 Gy, 2 Gy, 4 Gy). The influence of these treated adipose secretome on cancer cell metabolism, dendritic cell maturation and macrophage polarisation were then assessed via Agilent Seahorse technology or flow cytometry.

### 6.3.2 *Lipid treatment*

Methodology carried out as per section *3.3.2 Lipid treatment.*

### 6.3.3 *Seahorse Analysis of metabolic profiles from adipose tissue explants and generation of Adipose Conditioned Media (ACM)*

Fresh omental tissue was collected from theatre and processed within 30 minutes by dissecting into pieces weighing approximately 20 mg. Tissue was plated in triplicates in 1 ml of M199 (supplemented with 0.1% gentamicin (Lonza, Switzerland), in a 24 well plate (Sarstedt, Germany). Adipose explants were then treated with treated with vehicle, FLOT combination chemotherapy (0.08249 µM 5-fluorouracil, 2 µM oxaliplatin, 0.001 µM docetaxel) or CROSS combination chemoradiotherapy (0.001 µM paclitaxel, 1000 µM carboplatin + 2 Gy irradiation). These combination doses were previously optimised in downstream target cells OE33 to achieve 50% cell death [526]. In addition to this samples were also treated with 0.01% DMSO 2% BSA control or 200 µM OA or PA in 0.01% DMSO 2% BSA in M199. Following 2 hours incubation adipose explants CROSS treated samples were irradiated with 2 Gy at a dose rate of 1.73Gy/minute (XStrahl (RS225), Atlanta, United States). Adipose explants were cultured for 24 hours at 37ºC at 5% Carbon Dioxide in a humidified incubator (Thermofisher, Massachusetts, USA). In the last hour of culture, adipose tissue and ACM was transferred to islet capture microplate with capture screens (Agilent Technologies, California, United States) and incubated in a non-CO2 incubator at 37$^{o}$C (Whitley, United Kingdom) prior to analysis. Seahorse Xfe24 analyser was used to assess metabolic profiles in adipose explants, (Agilent Technologies, California, United States) following a 12 minute equilibrate step, three basal measurements of OCR and ECAR were taken over 24 minutes consisting of three repeats of the following sequence “mix (3 min) / wait (2 min) / measurement (3 min)” to establish basal respiration. Adipose Conditioned Media (ACM) was extracted in a sterile environment and tissue weighed using a benchtop analytical balance (Radwag, Poland) and snap frozen. All samples were then stored at -80$^{o}$C for further processing.

### 6.3.4 *Multiplex ELISA*

Methodology carried out as per section *2.3.4 Multiplex ELISA.*

## *6.4 Analysis of mitochondrial function of oesophageal cancer cells using Seahorse MitoStress test*

OE33 cells were seeded at a density of 20,000 in 24 well XFe24 cell culture microplate plate (Agilent Technologies, California, United States) in a volume of 100 µl cDMEM and allowed to

adhere for 3 hours before an additional 150 µl of media was added. Cells were rested overnight (approx. 18 hours). Media was extracted and replaced with 100 µl M199 control or appropriate treated ACM sample in technical replicates and allowed to incubate for a further 24 hours. Following this, cells were washed with Agilent Seahorse XF DMEM Medium supplemented with 10 mM glucose, 1 mM sodium pyruvate, and 2 mM L-glutamine (Agilent Technologies, California, United States) and incubated for 1 hour in a non-CO2 incubator at 37$^{o}$C. OCR, ECAR, basal respiration, ATP production, maximal respiration, proton leak and non-mitochondrial respiration were assessed using a Seahorse Biosciences XFe24 Extracellular Flux Analyser (Agilent Technologies, California, United States). Three basal measurements of OCR and ECAR were taken over 24 minutes consisting of three repeats of mix (3 min) / wait (2 min) / measurement (3 min) to establish basal respiration. Three additional measurements in the same manner were obtained following the injection of 50 µl of 3 mitochondrial inhibitors including 1.8 µM oligomycin (Sigma Aldrich, California, United States), 4 µM Carbonyl cyanide 4-(trifluoromethoxy) phenylhydrazone (FCCP) (Sigma Aldrich, California, United States) and 2 µM Antimycin-A (Sigma Aldrich, California, United States). All inhibitors were diluted in Agilent DMEM. All measurements were normalised to cell number via crystal violet staining.

#### 6.3.5 *Crystal Violet Assay*

Methodology carried out as per section 5.3.7 Crystal Violet Assay.

#### 6.3.6 *Isolation of monocytes*

Methodology carried out as per section *3.3.5 Isolation of monocytes.*

#### 6.3.7 *Dendritic cell culture*

Methodology carried out as per section *3.3.6 Dendritic cell culture.*

#### 6.3.8 *Macrophage culture*

Methodology carried out as per section *3.3.7 Macrophage culture.*

#### 6.3.9 *Flow cytometry*

Methodology carried out as per section *3.3.8 Flow cytometry*

#### 6.3.10 *Statistical Analysis*

All statistics were conducted using GraphPad Prism 9.5 (GraphPad Software, California, United States). A significance level of $p<0.05$ was used in all analysis and all p-values reported were

two-tailed. Friedman testing with Dunn's post hoc correction, was employed for non-parametric testing between paired cohorts. Details of specific statistical tests are given in each corresponding figure legend.

## 6.5 Results

### 6.4.1 *Chemotherapy diminishes oxidative phosphorylation in adipose tissue explants which is by oleic acid.*

Chemotherapy and chemoradiotherapy are known to detrimentally effect adipose tissue function as well as potentiating the efficacy of these treatments. To assess the influence of chemotherapy or chemoradiotherapy on the metabolic profiles and phenotypes of adipose tissue, seahorse technology was used. Whether exogenous fatty acids altered adipose tissue response to these treatments was also assessed using these real-time metabolic parameters.

FLOT regimen significantly decreased OCR metabolism in adipose explants whilst FLOT and CROSS regimens significantly decreased adipose explants reliance on oxidative phosphorylation over glycolysis (**Figure 6.4.1**). OA in combination with FLOT increased adipose explants OCR and ECAR metabolic profiles (**Figure 6.4.2**). However, PA treatments in combination with CROSS significantly decreased adipose explants OCR metabolic profiles compared with matched control and PA treatment in combination with FLOT regimen (**Figure 6.4.2**).

(* $p < 0.05$, ** $p < 0.01$)

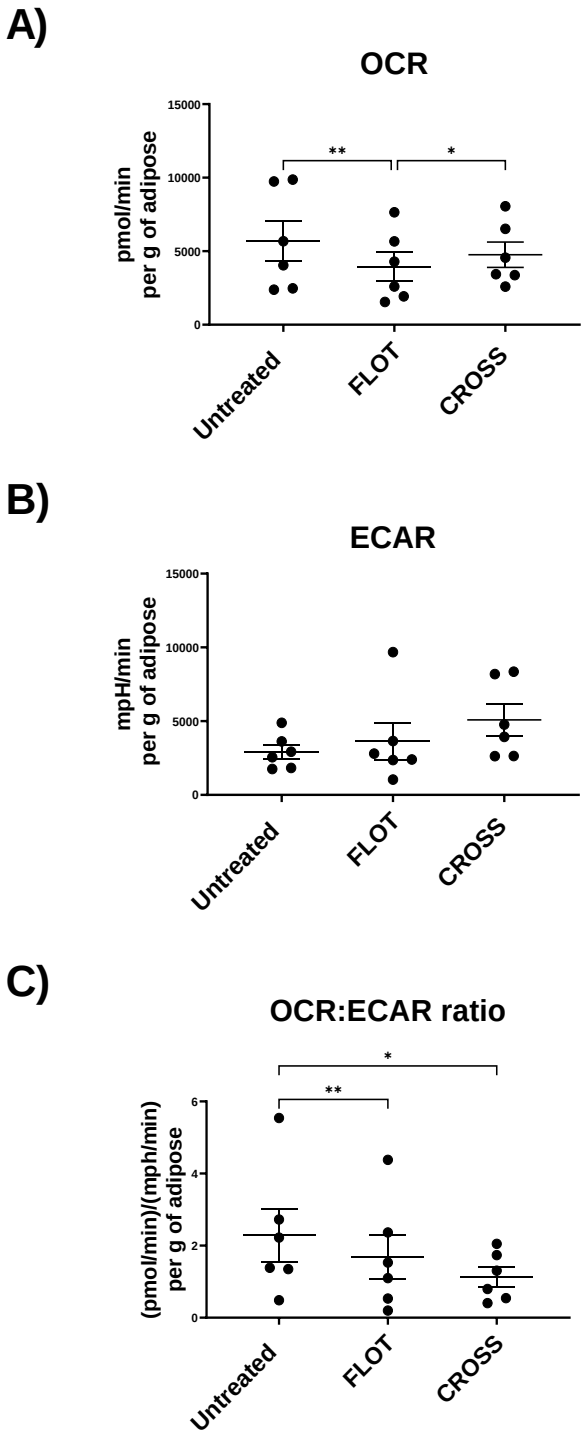


**Figure 6.41 Chemotherapy diminishes oxidative phosphorylation in adipose tissue explants, whilst both therapies increase glycolytic preferences in adipose explants.**

A-C) OCR, ECAR and OCR:ECAR ratio profiles of untreated, chemotherapy treated (FLOT) and chemoradiotherapy treated (CROSS) adipose explants,

(Friedman test with Dunn's correction) All data expressed as mean ± SEM, n=6, * $p < 0.05$, ** $p < 0.01$.

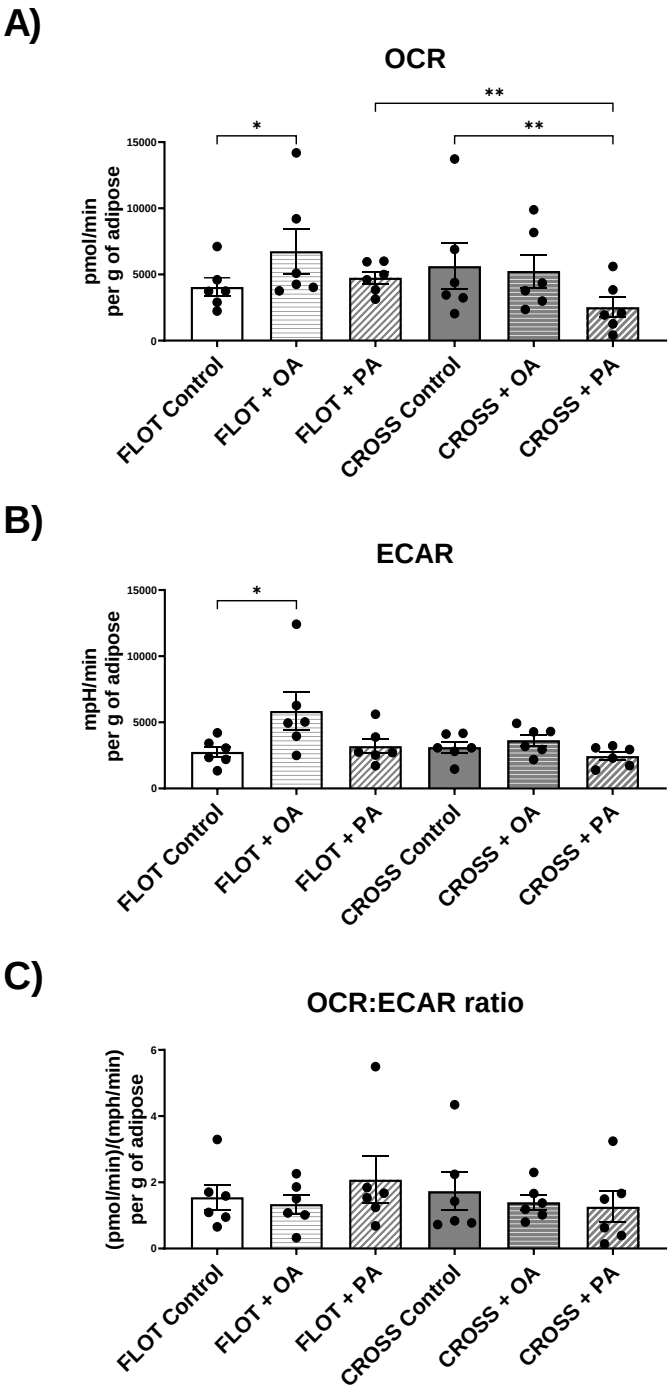


**Figure 6.4.2 Chemotherapy in combination with OA increases OCR and ECAR profiles in adipose explants, whilst Chemoradiotherapy in combination with PA decreases adipose tissues OCR profiles.**

A-C) OCR, ECAR and OCR:ECAR ratio profiles of chemotherapy treated (FLOT) and chemoradiotherapy treated (CROSS) adipose explants in combination with BSA Control, Oleic Acid (OA) or Palmitic Acid (PA).

(Friedman test with Dunn's correction) All data expressed as mean ± SEM, n=6, * $p < 0.05$, ** $p <$ yes this is the way to display the pvalues 0.01.

### 6.4.2 *Chemoradiotherapy increases the secreted levels of pro-inflammatory mediators in the adipose secretome*

Chemotherapy and Chemoradiotherapy have been established to have widespread effects on the tumour microenvironment through the alteration of a series of pro-inflammatory, immune-inhibitory, and angiogenic mediators both in circulation and at tissue level. To establish a baseline to examine the effects of chemotherapy and chemoradiotherapy on the adipose secretome of cancer patients a 54-analyte multiplex was used to assess inflammatory mediators comparing against a matched untreated adipose secretome

FLOT regimen significantly decreased adipose secreted levels of anti-inflammatory, immunoinhibitory and angiogenic mediators compared with untreated adipose, including IL-13, TARC, and VEGF (**Figure 6.4.5 B, Figure 6.4.3 C, F**). CROSS regimen significantly decreased adipose secreted levels of a series of anti-inflammatory and angiogenic mediators compared with untreated adipose, including IL-1Ra, PIGF, VEGF, and VEGF-C (**Figure 6.4.5 B, Figure 6.4.3 D - F)** CROSS regimen further showed diminished adipose secreted levels of anti-inflammatory and angiogenic associated mediators compared with FLOT treated adipose tissue, including IL-1Ra and VEGF-C (**Figure 6.4.5 B, Figure 6.4.3 F**).

CROSS regimen significantly increased adipose secreted levels of a series of pro-inflammatory and immune activating mediators compared with untreated adipose, including GM-CSF, IL-17A, IL-21, IL-23, and IL-31 (**Figure 6.4.3 A, Figure 6.4.5 C - F**). Interestingly, CROSS regimen showed significantly elevated adipose secreted levels of a series of pro-inflammatory, immune activating and vascular injury associated mediators compared with FLOT treated adipose tissue, including GM-CSF, IFN-γ, IL-1β, IL-7, IL-16, IL-17A, MDC, SAA, TNF-α, IL-31 (**Figure 6.4.3 A, Figure 6.4.4 A – F, Figure 6.4.5 F)**.

(* $p < 0.05$, ** $p < 0.01$)

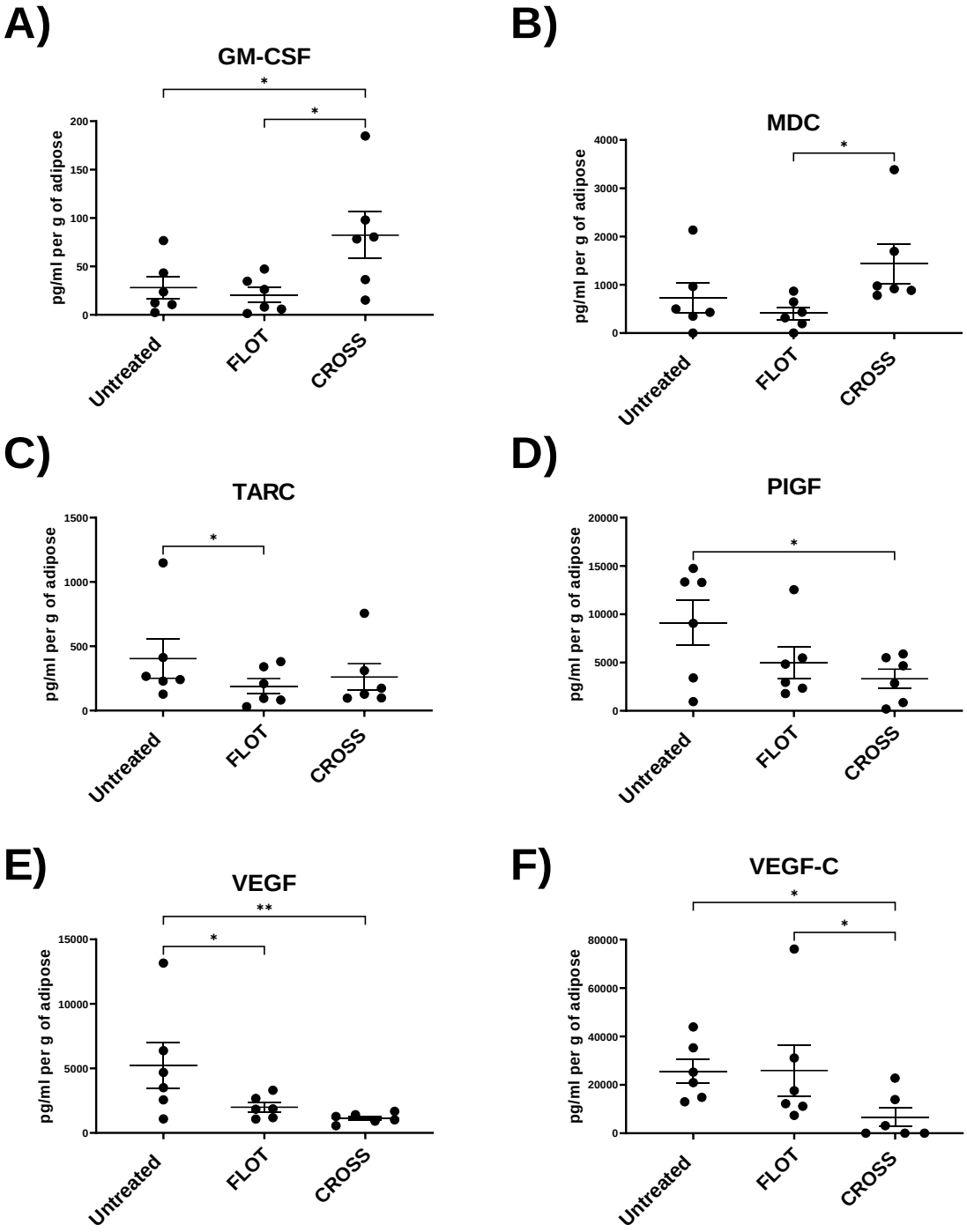


**Figure 6.4.3 Chemoradiotherapy increases the secreted levels of mediators of immune cell recruitment and decreases secretion of angiogenic mediators in the adipose secretome**

A-F) Secreted levels of GM-CSF, MDC, TARC, PIGF, VEGF, and VEGF-C of untreated, chemotherapy treated (FLOT) and chemoradiotherapy treated (CROSS) adipose explants. (Friedman test with Dunn's correction) All data expressed as mean ± SEM, n=6, * $p < 0.05$, ** $p < 0.01$.

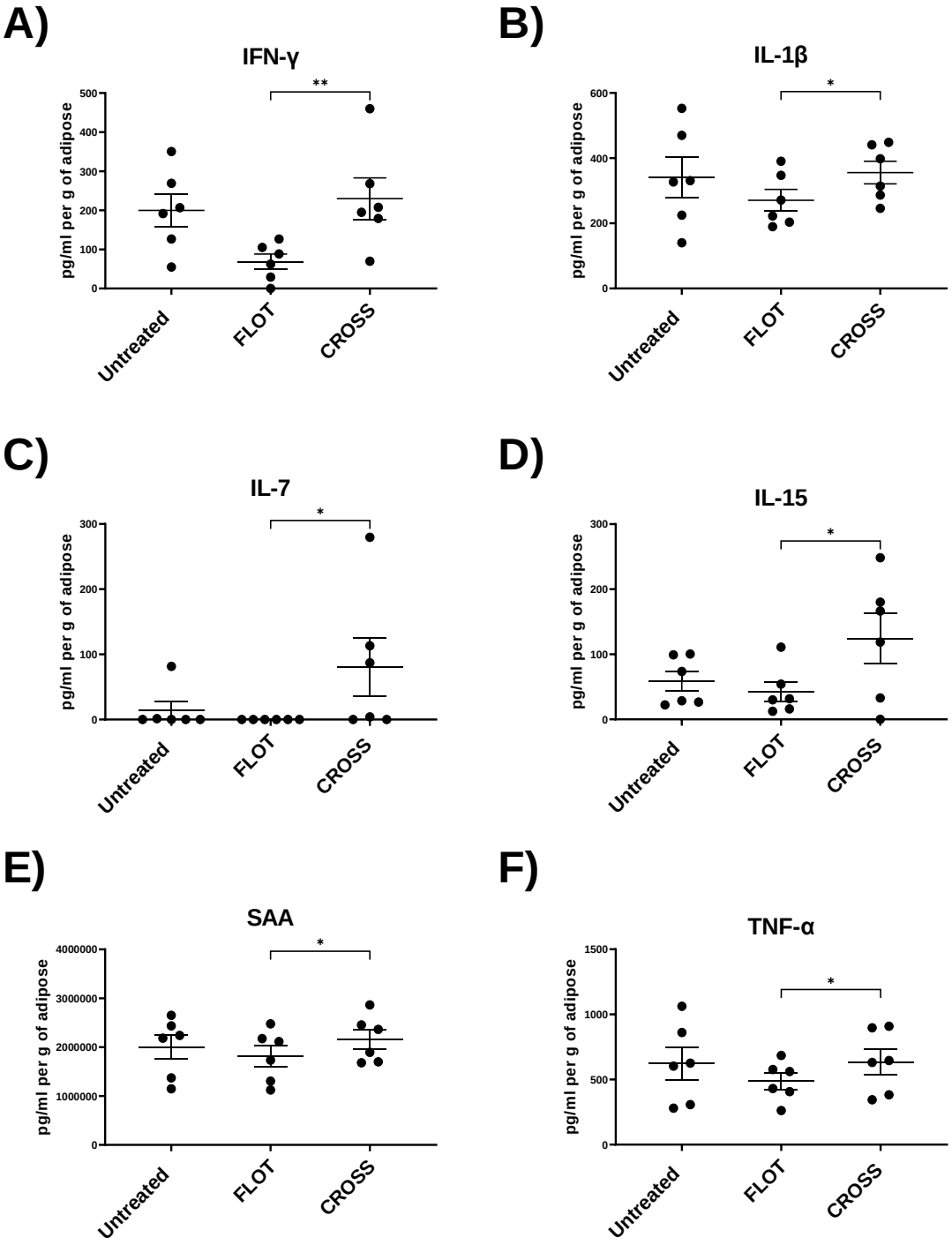


**Figure 6.4.4 Chemoradiotherapy increases the secreted levels of pro-inflammatory mediators in the adipose secretome compared with chemotherapy alone**

A-F) Secreted levels of IFN-γ, IL-1β, IL-7, IL-16, SAA, and TNF-α of untreated, chemotherapy treated (FLOT) and chemoradiotherapy treated (CROSS) adipose explants.

(Friedman test with Dunn's correction) All data expressed as mean ± SEM, n=6, * $p < 0.05$, ** $p < 0.01$.

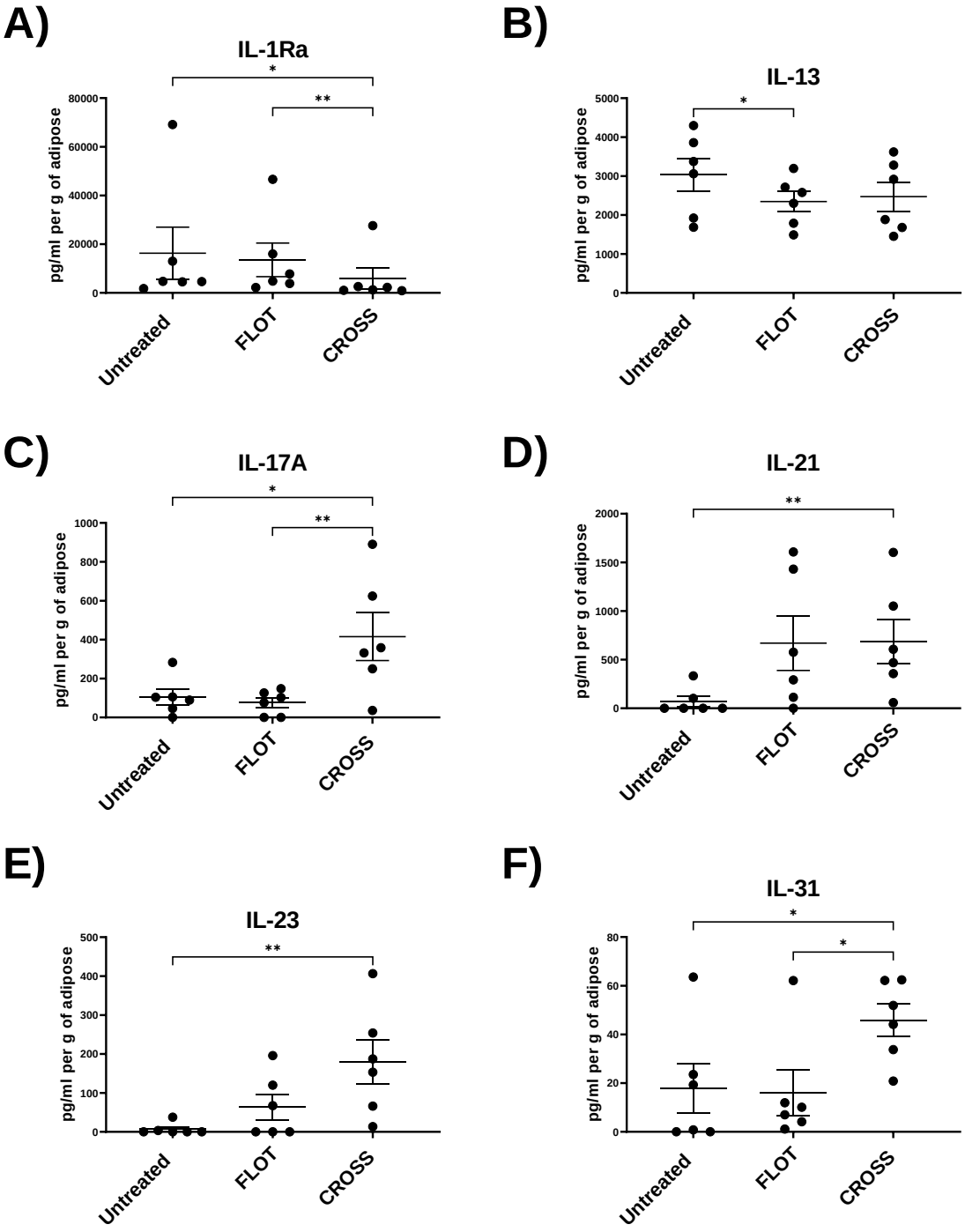


**Figure 6.4.5 Chemoradiotherapy increases the secreted levels of mediators involved in anti-inflammatory response, TH2 immunity and TH17 immunity in the adipose secretome**

A-F) Secreted levels of IL-1Ra, IL-13, IL-17A, IL-21 IL-23, IL-31, of untreated, chemotherapy treated (FLOT) and chemoradiotherapy treated (CROSS) adipose explants.

(Friedman test with Dunn's correction) All data expressed as mean ± SEM, n=6, * $p < 0.05$, ** $p < 0.01$.

### 6.4.3 *Chemotherapy and chemoradiotherapy differentially alter the adipose tissue response to exogenous fatty acids leading to divergent secreted levels of significant immune associated factors.*

As previously mentioned, chemotherapy and chemoradiotherapy are known to alter the secretion levels of a series of factors involved in inflammatory and immune recruitment, however whether the addition of exogenous fatty acids augments or diminishes these is not understood. To assess the effects of chemotherapy and chemoradiotherapy in combination with PA or OA treatment on the adipose secretome, levels of IL-4, IL-8 IL-12p70, IL-22, and MDC which were assessed by multiplex ELISA. This sentence reads like only these were measured.

FLOT in combination with PA treatment showed significantly increased adipose secreted levels of anti-inflammatory and immune stimulatory mediators IL-4, IL-12p70, and MDC, however, CROSS in combination with PA treatment showed significantly decreased secreted levels of these factors (**Figure 6.4.6 A, C, E**). FLOT in combination with PA treatment increased adipose secreted levels of IL-8 compared with adipose treated with FLOT in combination with OA, in contrast, CROSS in combination with PA treatment showed decreased secreted levels of IL-8 (**Figure 6.4.6. B**). FLOT in combination with OA treatment showed increased adipose secreted levels of IL-22 compared with matched control, opposingly in CROSS treated adipose in combination with OA secreted levels of IL-22 were significantly decreased (**Figure 6.4.6 D**).

(* $p < 0.05$, ** $p < 0.01$, ***$< 0.001$)

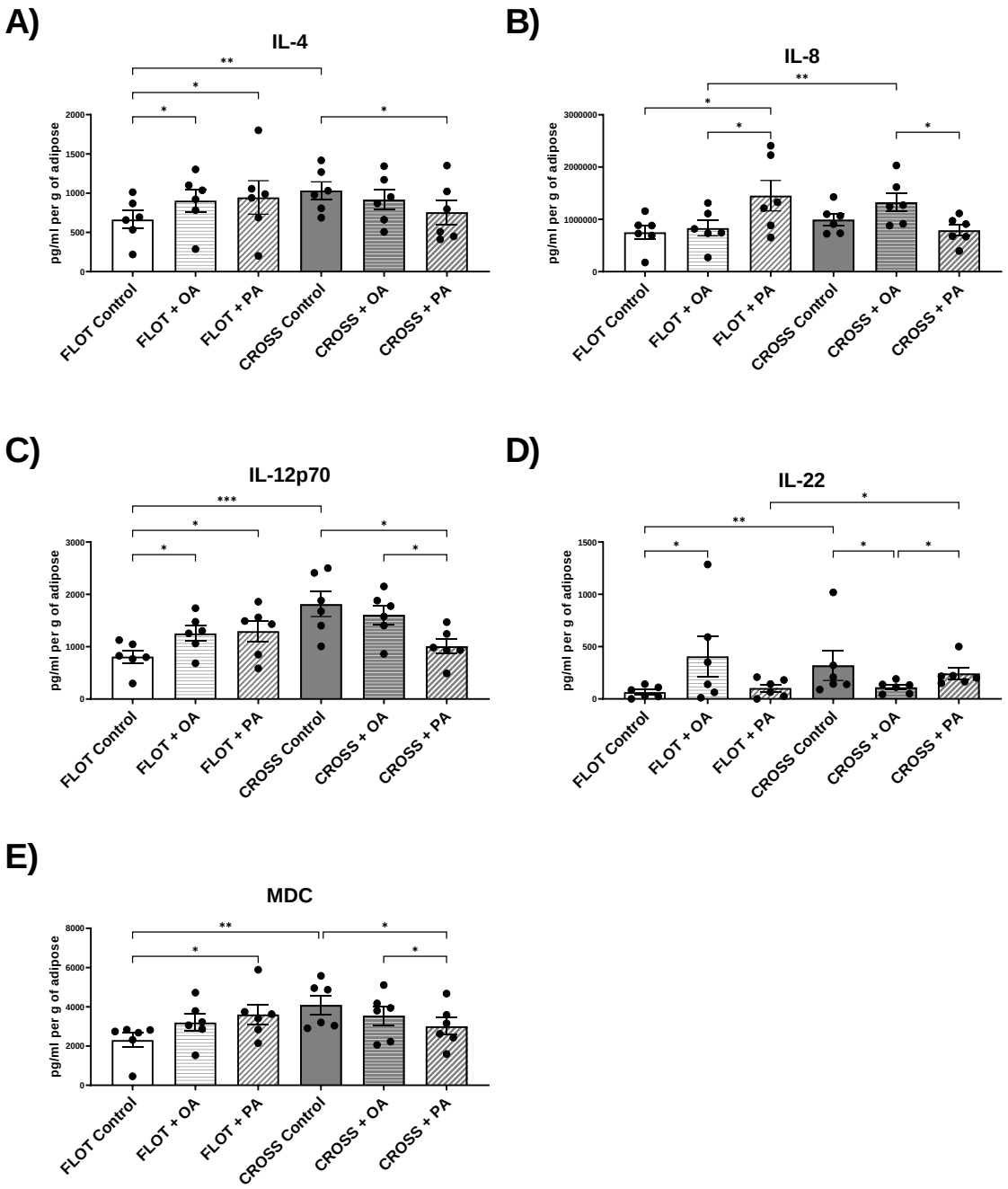


**Figure 6.4.6 Chemotherapy and chemoradiotherapy differentially alter the adipose tissue response to exogenous fatty acids leading to divergent secreted levels of significant immune associated factors.**

A-E) Secreted levels of IL-4, IL-8, IL-12p70, IL-22 and MDC of chemotherapy treated (FLOT) and chemoradiotherapy treated (CROSS) adipose explants in combination with BSA Control, Oleic Acid (OA) or Palmitic Acid (PA).

(Friedman test with Dunn's correction) All data expressed as mean ± SEM, n=6, ** $p < 0.05$, ** $p < 0.01$, *** < 0.0001.*

### 6.4.4 *Following both chemotherapy and chemoradiotherapy, exogenous fatty acids cause similar increases in mediators associated with Th17 immune responses.*

Previously we observed a series of inflammatory and immune recruiting factors differentially altered by chemotherapy and chemoradiotherapy combined with other PA or OA treatment. To assess the influence of chemotherapy and chemoradiotherapy in combination with PA or OA treatment on key mediators and promotors of Th17 associated immune response including IL-1β, IL-7 IL-15, IL-17A, and IL-17D, secreted levels in the adipose secretome were assessed by multiplex ELISA.

FLOT in combination with OA treatment showed significantly increased adipose secreted levels of significant pro-inflammatory factors IL-1β, and IL-17D, compared against either FLOT treated control or FLOT in combination with PA. A similar effect was observed in adipose tissue treated with CROSS in combination with OA (**Figure 6.4.7 A, E**). FLOT in combination with PA treatment showed significantly increased adipose secreted levels of pro-inflammatory and T cell stimulatory mediators including IL-7, IL-15, and IL-17A, an effect that was mirrored by adipose tissue treated with CROSS in combination with PA compared with matched control adipose secretome (**Figure 6.4.7 B, C, D**).

(* $p < 0.05$, ** $p < 0.01$)

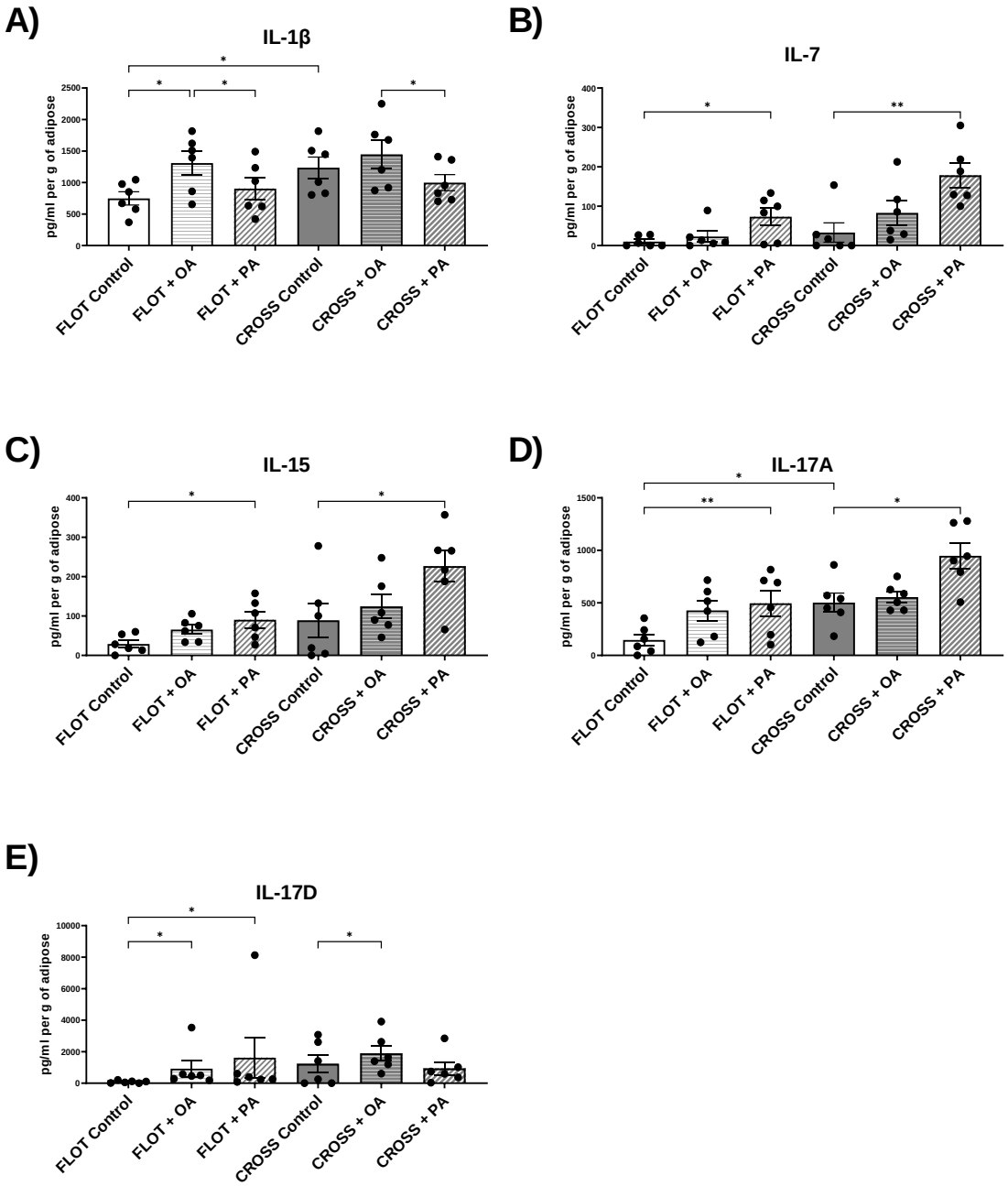


**Figure 6.4.7 Following both chemotherapy and chemoradiotherapy, exogenous fatty acids cause similar increases in mediators associated with Th17 immune responses.**

A-E) Secreted levels of IL-1β, IL-7, IL-15, IL-17A and IL-17D of chemotherapy treated (FLOT) and chemoradiotherapy treated (CROSS) adipose explants in combination with BSA Control, Oleic Acid (OA) or Palmitic Acid (PA).

(Friedman test with Dunn's correction) All data expressed as mean ± SEM, n=6, * $p < 0.05$, ** $p < 0.01$.

### 6.4.5 *Chemotherapy in combination with OA increases adipose secreted levels of pro-inflammatory, adhesion and angiogenic associated factors*

The influence of OA on chemotherapy efficacy as previously mentioned is contentiously reported in the literature. This study looked to assess the influence of chemotherapy and chemoradiotherapy in combination with OA treatment on secreted levels of factors involved in inflammatory, adhesion and immune-recruiting responses including Flt-1, IL-1α, IL-1Ra, MCP-4, sICAM-1, sVCAM-1, and VEGF which were assessed by multiplex ELISA.

FLOT in combination with OA treatment showed significantly increased adipose secreted levels of significant angiogenic, pro-inflammatory and adhesion associated factors including Flt-1, IL-1α, MCP-4, sICAM-1, sVCAM-1, and VEGF, compared with matched control (**Figure 6.4.8 A, B, D-G**). Additionally, FLOT in combination with PA treatment showed significantly increased secreted levels of sVCAM-1 (**Figure 6.4.8 F**). FLOT in combination with OA or PA treatment showed significantly increased adipose secreted levels of anti-inflammatory mediator IL-1Ra with similarly CROSS treated adipose tissue secretome (**Figure 6.4.8 C**).

(* $p < 0.05$, ** $p < 0.01$)

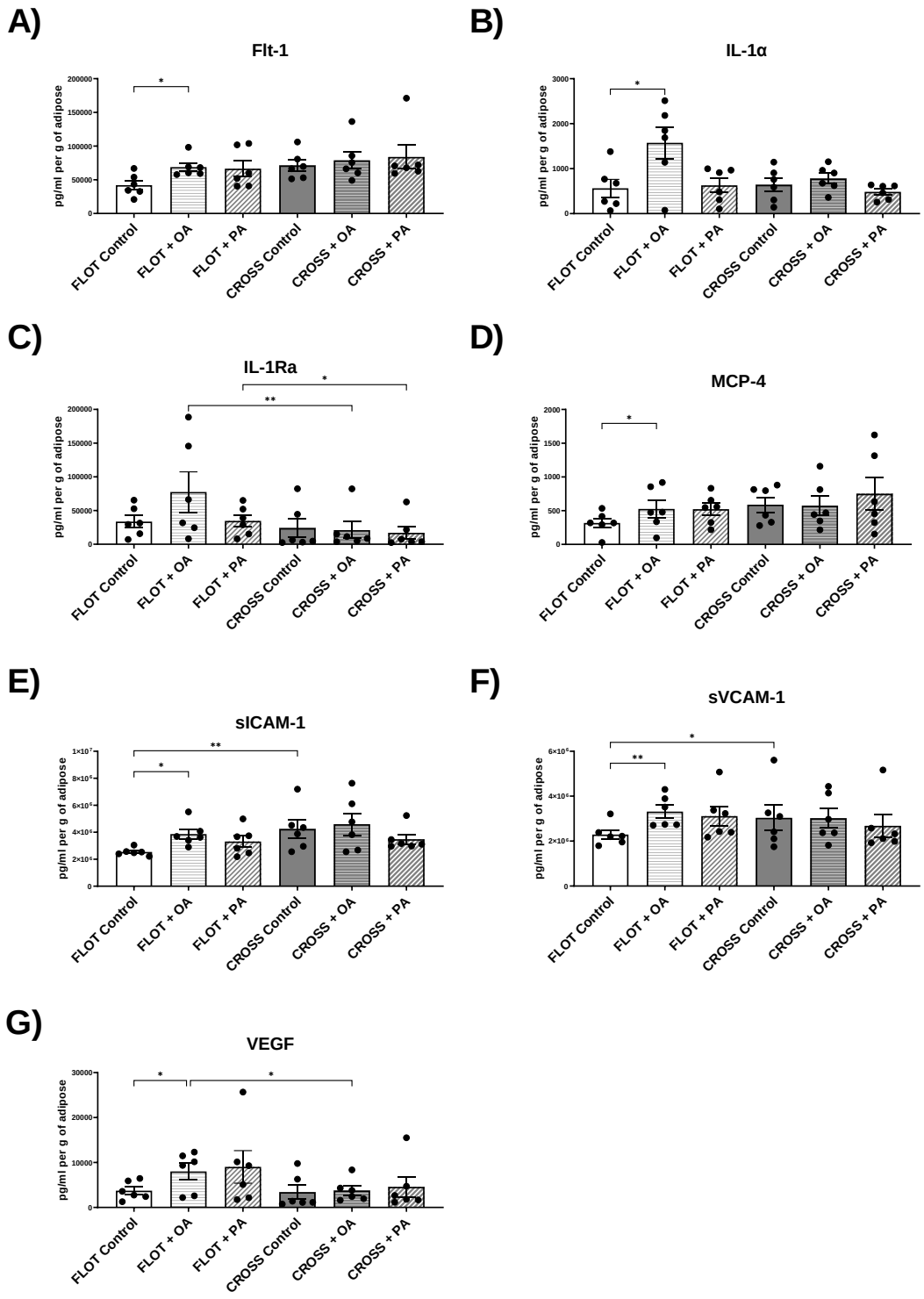


**Figure 6.4.8 Chemotherapy in combination with OA increases adipose secreted levels of pro-inflammatory, adhesion and angiogenic associated factors**

A-G) Secreted levels of FLt-1, IL-1α, IL-1Ra, MCP-4, sICAM-1, sVCAM-1, and VEGF of chemotherapy treated (FLOT) and chemoradiotherapy treated (CROSS) adipose explants in combination with BSA Control, Oleic Acid (OA) or Palmitic Acid (PA).

(Friedman test with Dunn's correction) All data expressed as mean ± SEM, n=6, * $p < 0.05$, ** $p < 0.01$.

### 6.4.6 *Chemotherapy in combination with PA increase adipose secreted levels of pro-inflammatory, angiogenic and immuno-modulatory mediators*

The influence of PA on cancer treatment efficacy again has been contentiously reported, with links to increasing cancer cell sensitivity to chemotherapy as well as aiding in metastasis. To assess the influence of chemotherapy in combination with PA treatment on secreted levels of factors involved in inflammatory, adhesion and immune-recruiting responses including IL-2, IL-6, MCP-1, TARC and TNF-α multiplex ELISA were utilised.

FLOT in combination with PA treatment showed increased adipose secreted levels of pro-inflammatory and immune activating mediators including IL-2, IL-6 MCP-1, TARC and TNF-α compared with either matched control or CROSS in combination with PA treatment (**Figure 6.4.9 A-E**). Additionally, decreased secreted levels of TNF-α were observed in the adipose secretome following exposure to CROSS in combination with PA treatment compared with matched control (**Figure 6.4.9 E**).

(* $p < 0.05$)

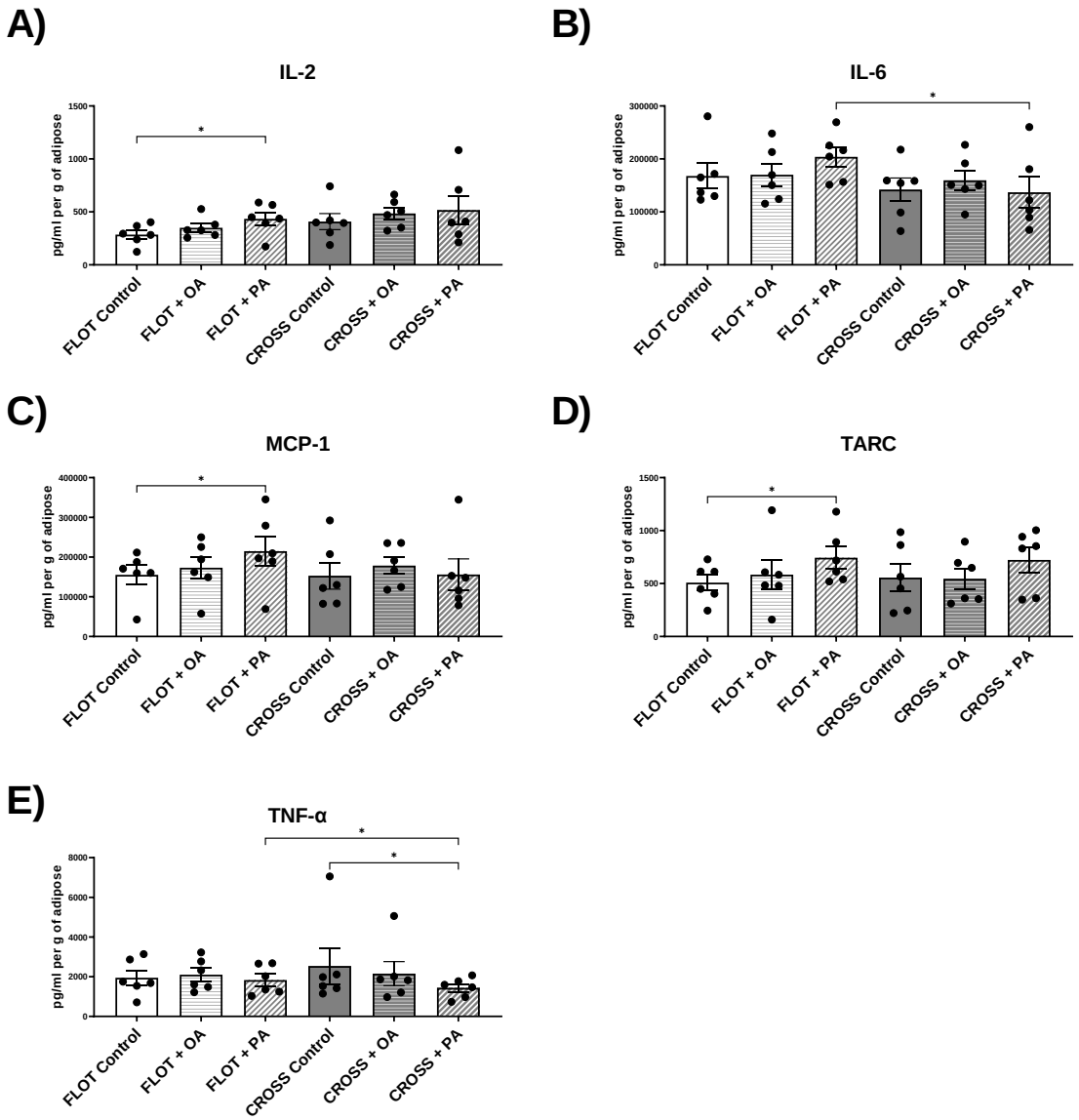


**Figure 6.4.9 Chemotherapy in combination with PA increase adipose secreted levels of pro-inflammatory, angiogenic and immuno-modulatory mediators**

A-E) Secreted levels of IL-2, IL-6, IL-1Ra, MCP-1, TARC, and TNF-α of chemotherapy treated (FLOT) and chemoradiotherapy treated (CROSS) adipose explants in combination with BSA Control, Oleic Acid (OA) or Palmitic Acid (PA).

(Friedman test with Dunn's correction) All data expressed as mean ± SEM, n=6, * $p < 0.05$.

### 6.4.7 *Chemoradiotherapy in combination with PA increases secreted levels of key inflammatory, angiogenic and vascular injury associated mediators compared with chemotherapy*

PA has been widely reported to have wide reaching inflammatory effects, an effect that has not been observed on the adipose secretome. This study looked to assess the influence of chemoradiotherapy in combination with PA treatment compared with chemotherapy combined with PA on the adipose secretome. Secreted levels in the adipose secretome of factors involved in pro-inflammatory response, angiogenesis and vascular injury response including IL-9, IL-17A/F, IL-17B, IL-21, IL-23, IL-27, IL-31, SAA, and VEGF-C were assessed by multiplex ELISA.

CROSS in combination with PA treatment significantly increased a series of pro-inflammatory, vascular injury and angiogenic mediators in the adipose secretome compared with either matched control or adipose tissue cultured with FLOT regimen combined with PA acid. These mediators included IL-9, IL-17A/F, IL-17B, IL-21, IL-23, IL-27, IL-31, SAA, and VEGF-C (**Figure 6.4.10 A-I**).

(***< 0.001, ** $p < 0.01$, * $p < 0.05$)

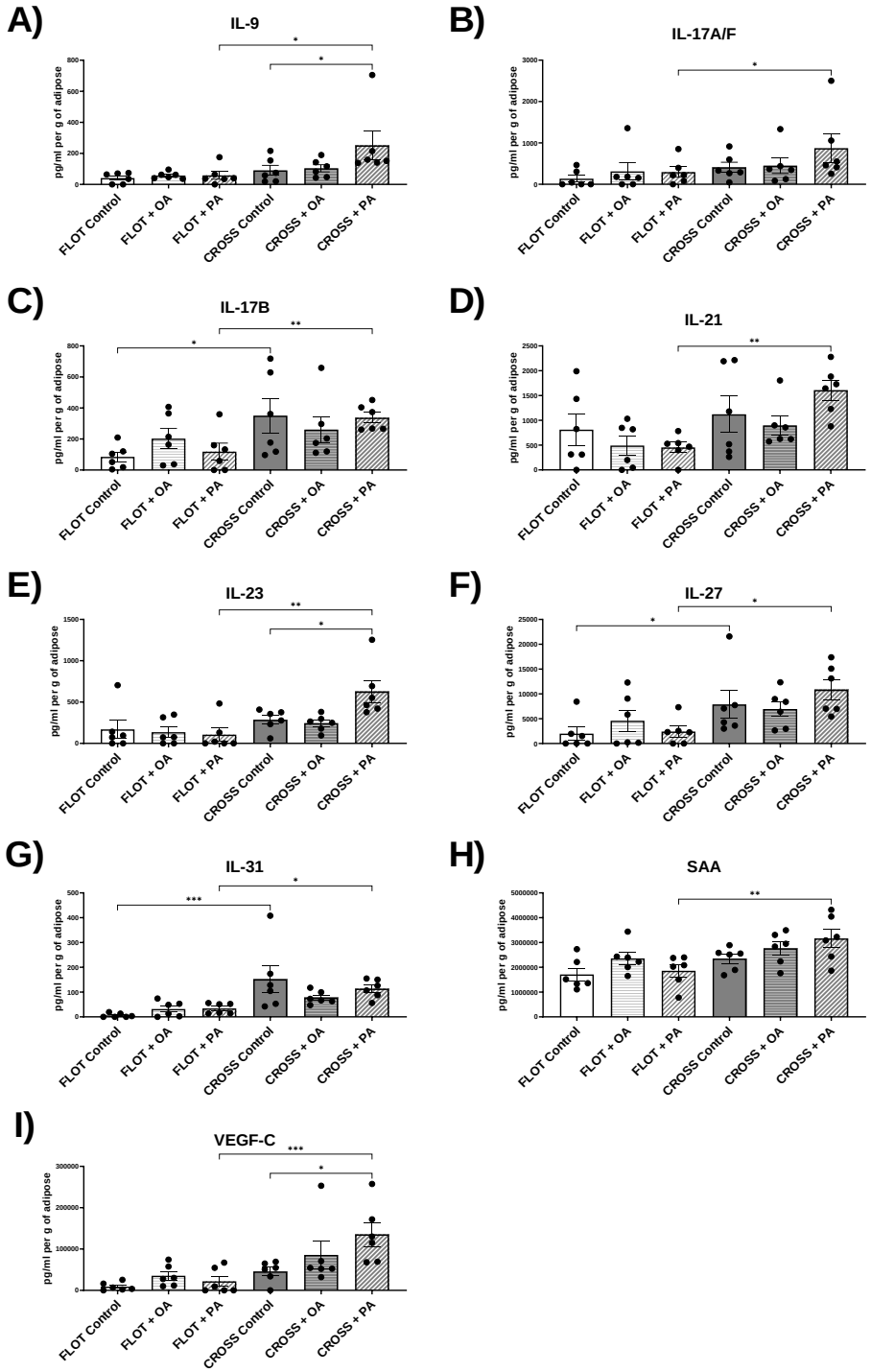


**Figure 6.4.10 Chemoradiotherapy in combination with PA increases secreted levels of key inflammatory, angiogenic and vascular injury associated mediators compared with chemotherapy**

A-I) Secreted levels of IL-9, IL-17A/F, IL-17B, IL-21, IL-23, IL-27, IL-31, SAA, and VEGF-C of chemotherapy treated (FLOT) and chemoradiotherapy treated (CROSS) adipose explants in combination with BSA Control, Oleic Acid (OA) or Palmitic Acid (PA).

(Friedman test with Dunn's correction) All data expressed as mean ± SEM, n=6, * $p < 0.05$, ** $p < 0.01$, *** $p < 0.001$

### 6.4.8 *The chemotherapy treated adipose secretome increases reliance on glycolysis and augments dysfunctional mitochondrial response to stress in oesophageal cancer cells.*

Chemotherapy has been reported to enhance cancer cell glycolytic metabolism. Whilst chemoradiotherapy has been shown to decrease cancer metabolism directly following irradiation with a subsequent enhanced glycolysis. To assess the influence of chemotherapy or chemoradiotherapy on the adipose secretome and how this alters cancer cell metabolic profiles MitoStress test and seahorse technology was used. Just be specific in cells

OE33 oesophageal cancer cells cultured with FLOT treated adipose secretome demonstrated metabolic profiles associated with mitochondrial dysfunction, including elevated glycolytic metabolism, increased maximal respiration, and increased proton leak (**Figure 6.4.10 B, C, F, G**). OE33 cells cultured with CROSS treated adipose showed increased ATP linked respiration, maximal respiration, and spare respiratory capacity, an indication that cells are still capable of utilising mitochondrial reserves (**Figure 6.4.10 C, D, F**).

(* $p < 0.05$)

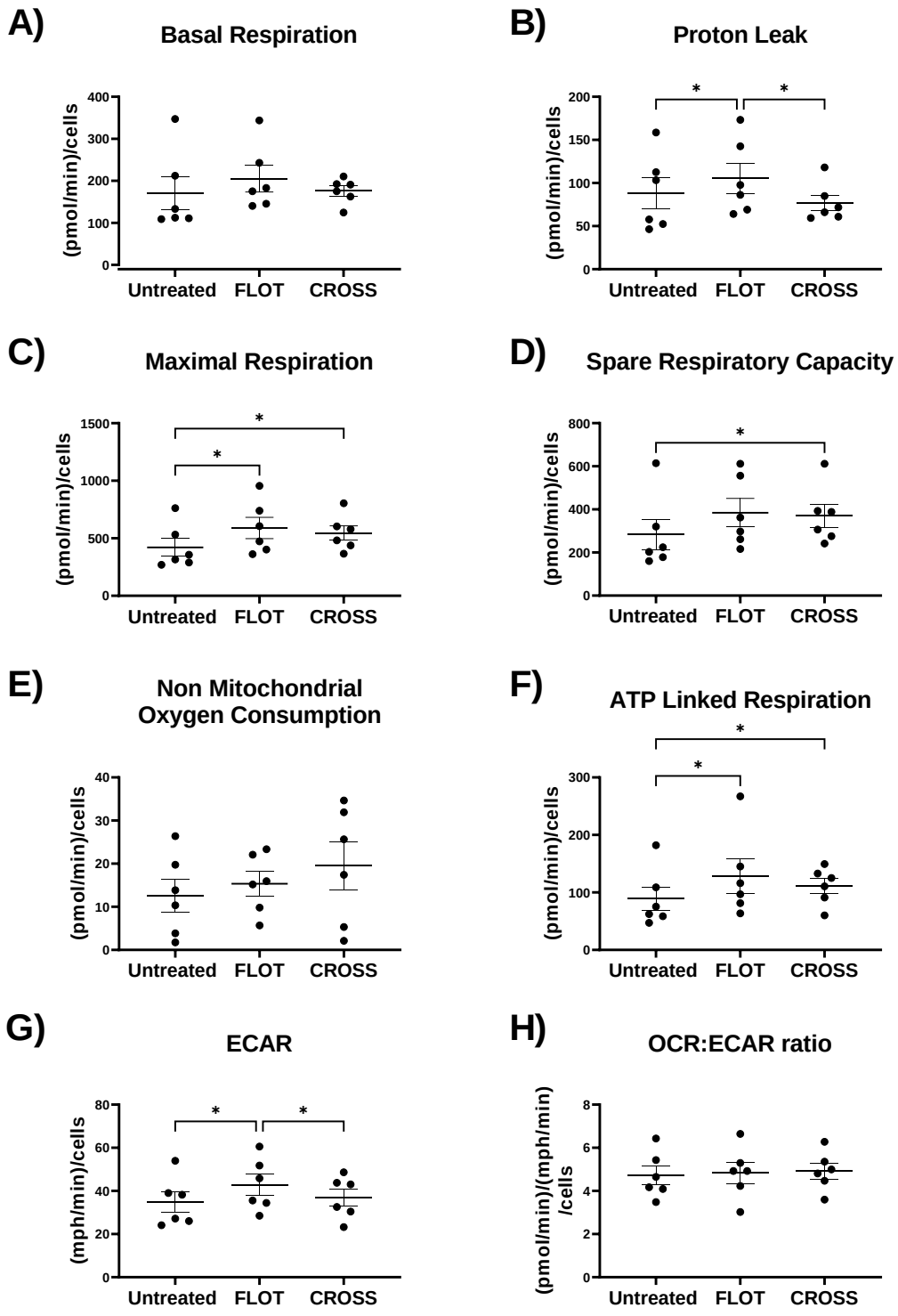


**Figure 6.4.11 The chemotherapy treated adipose secretome increases reliance on glycolysis and augments dysfunctional mitochondrial response to stress in oesophageal cancer cells.** A-H) Mitochondrial parameters including basal respiration, proton leak, maximal respiration, spare respiratory capacity, non-mitochondrial oxygen consumption, ATP linked respiration, ECAR and OCR:ECAR ratio of OE33 cell lines following exposure to untreated, chemotherapy treated (FLOT) and chemoradiotherapy treated (CROSS) adipose conditioned media

(Friedman test with Dunn's correction) All data expressed as mean ± SEM, n=6, * $p < 0.05$

### 6.4.9 *Chemoradiotherapy in combination with PA increases oesophageal cancer cells reliance on glycolytic pathways whilst chemotherapy in combination with OA induces mitochondrial dysfunction in response to stress.*

Chemotherapy ad chemoradiotherapy has been reported to enhance cancer cell glycolysis and fatty acid oxidation in response to the stress induced by these therapies. To assess the influence of chemotherapy or chemoradiotherapy in combination with OA or PA treatment on the adipose secretome and how this alters cancer cell metabolic profiles MitoStress test and seahorse technology was used.

OE33 cancer cells cultured with FLOT, and OA treated ACM showed decreased maximal respiration and spare respiratory capacity compared with matched control and PA treatment (**Figure 6.4.13 B, C**). Furthermore, OE33 cells cultured with FLOT, and OA treatment showed significantly increased non mitochondrial oxygen consumption compared to OE33 cultured with CROSS and OA treated ACM (**Figure 6.4.12 C**). OE33 cancer cells cultured with CROSS and PA treated ACM showed increased reliance on glycolytic metabolism compared with matched control (**Figure 6.4.14 A**). Additionally, OE33 cells cultured with FLOT, and PA treatment showed significantly increased basal respiration, ATP linked respiration and OCR:ECAR ratio compared to OE33 cultured with CROSS and OA treated ACM (**Figure 6.4.12 A, 6.4.13 A, 6.4.14 B**).

(** $p < 0.01$, * $p < 0.05$)

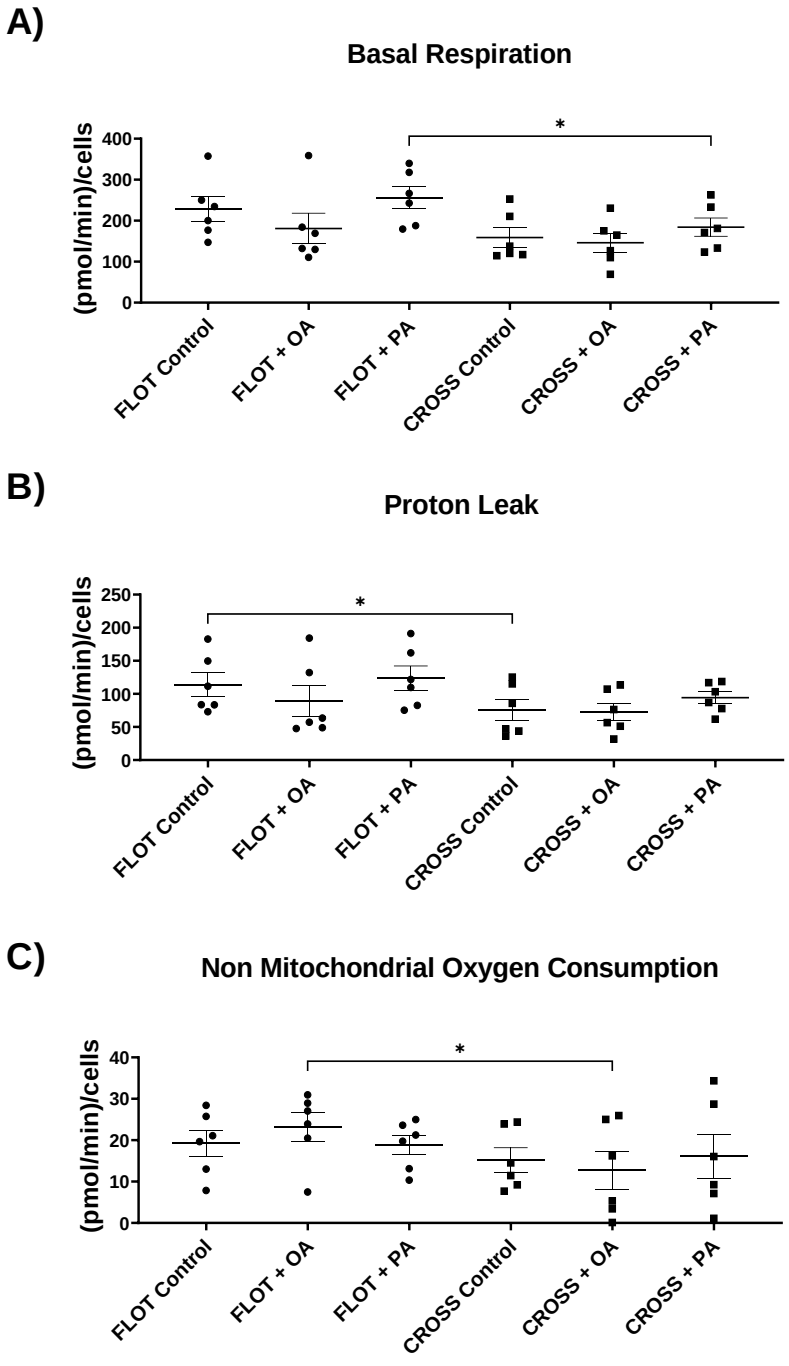


**Figure 6.4.12 Chemoradiotherapy in combination with PA decreases oesophageal cancer cells OCR profiles whilst chemoradiotherapy in combination with OA decreases no-mitochondrial oxygen consumption compared with chemotherapy in combination with fatty acids**

A-C) Mitochondrial parameters including basal respiration, proton leak, and non-mitochondrial oxygen consumption of OE33 cell lines following exposure to chemotherapy treated (FLOT) and chemoradiotherapy treated (CROSS) adipose conditioned media in combination with BSA Control, Oleic Acid (OA) or Palmitic Acid (PA).

(Friedman test with Dunn's correction) All data expressed as mean ± SEM, n=6, * $p < 0.05$, ** $p < 0.01$.

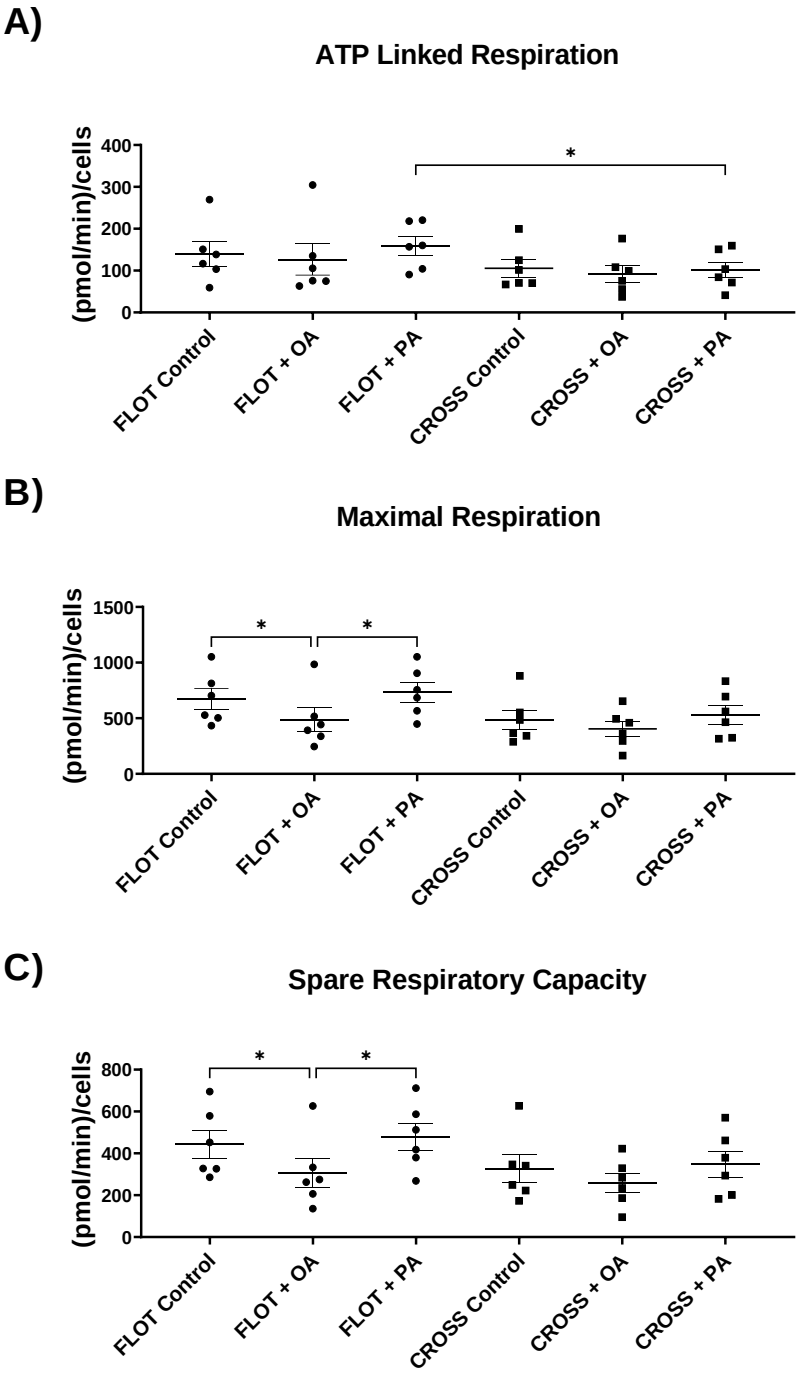


**Figure 6.4.13 Chemotherapy in combination with OA decreases cancer cells maximal respiration and spare respiratory capacity.**

A-C) Mitochondrial parameters including ATP linked respiration, maximal respiration, and spare respiratory capacity of OE33 cell lines following exposure to chemotherapy treated (FLOT) and chemoradiotherapy treated (CROSS) adipose conditioned media in combination with BSA Control, Oleic Acid (OA) or Palmitic Acid (PA).

(Friedman test with Dunn's correction) All data expressed as mean ± SEM, n=6, * $p < 0.05$, ** $p < 0.01$.

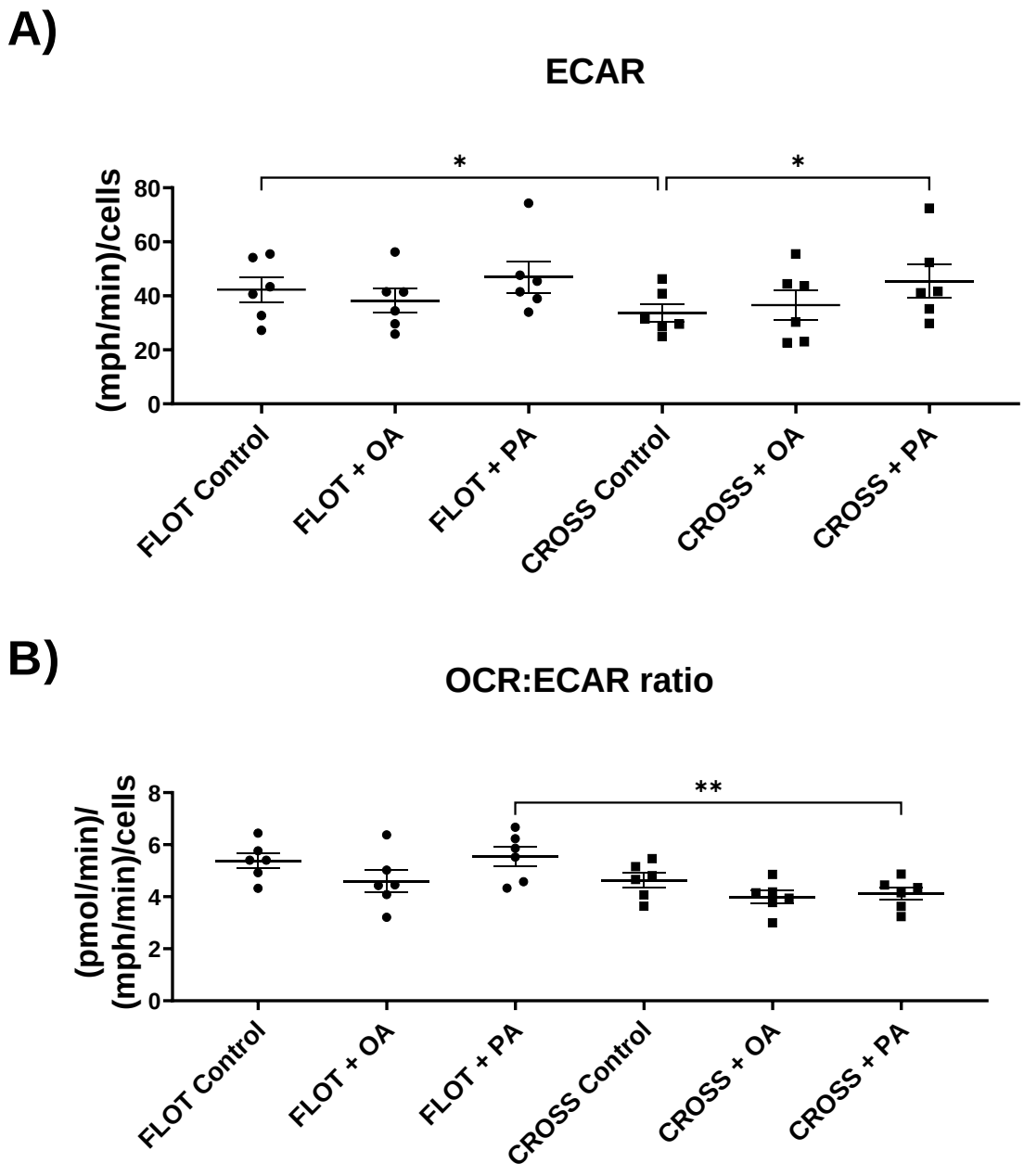


**Figure 6.4.14 Chemoradiotherapy in combination with PA increases oesophageal cancer cells reliance on glycolytic pathways.**

A-B) Mitochondrial parameters including ECAR and OCR:ECAR ratio of OE33 cell lines following exposure to chemotherapy treated (FLOT) and chemoradiotherapy treated (CROSS) adipose conditioned media in combination with BSA Control, Oleic Acid (OA) or Palmitic Acid (PA).

(Friedman test with Dunn's correction) All data expressed as mean ± SEM, n=6, * $p < 0.05$, ** $p < 0.01$.

### 6.4.10 *Chemotherapy increases DCs maturation markers, whilst all treatments increased immunoinhibitory ligand TIM-3.*

Chemotherapy and chemoradiotherapy have been reported to enhance DCs antigen presentation. To assess the influence of chemotherapy or chemoradiotherapy on the adipose secretome and how this alters DCs maturation, stimulated DCs were assessed via flow cytometry for a panel of phenotypic and maturation markers following exposure to these treated ACM.

DCs cultured with the FLOT treated adipose secretome showed significantly increased expression of a series of phenotype and maturation ligands including HLA-DR, CD11c, CD40, CD54, and CD86 (**Figure 6.4.16 B-D, Figure 6.4.17 C**). In addition to this, DCs cultured with both FLOT, and CROSS treated ACM showed increased expression on immunoinhibitory ligand TIM-3 (**Figure 6.4.17 E**).

(** $p < 0.01$, * $p < 0.05$)

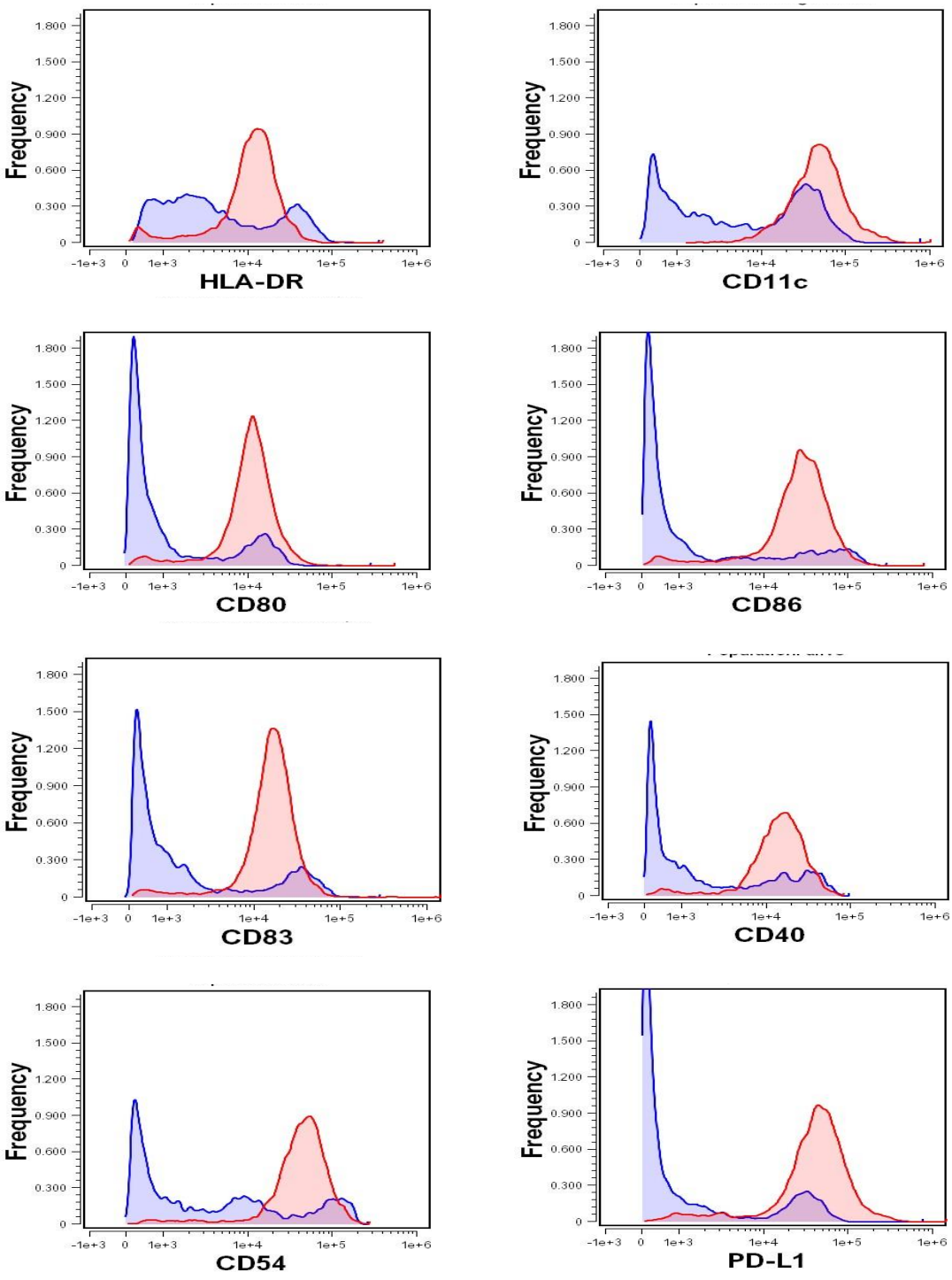


**Figure 6.4.15 Histograms of DC maturation markers following LPS stimulation**

Histograms displaying DC markers HLA-DR, CD11c, CD80, CD86 CD83, CD40, CD54 and PD-L1 which depict DCs response to LPS stimulation. (Blue peaks indicate unstimulated DCs and red peak indicate DCs following exposure to LPS stimulation)

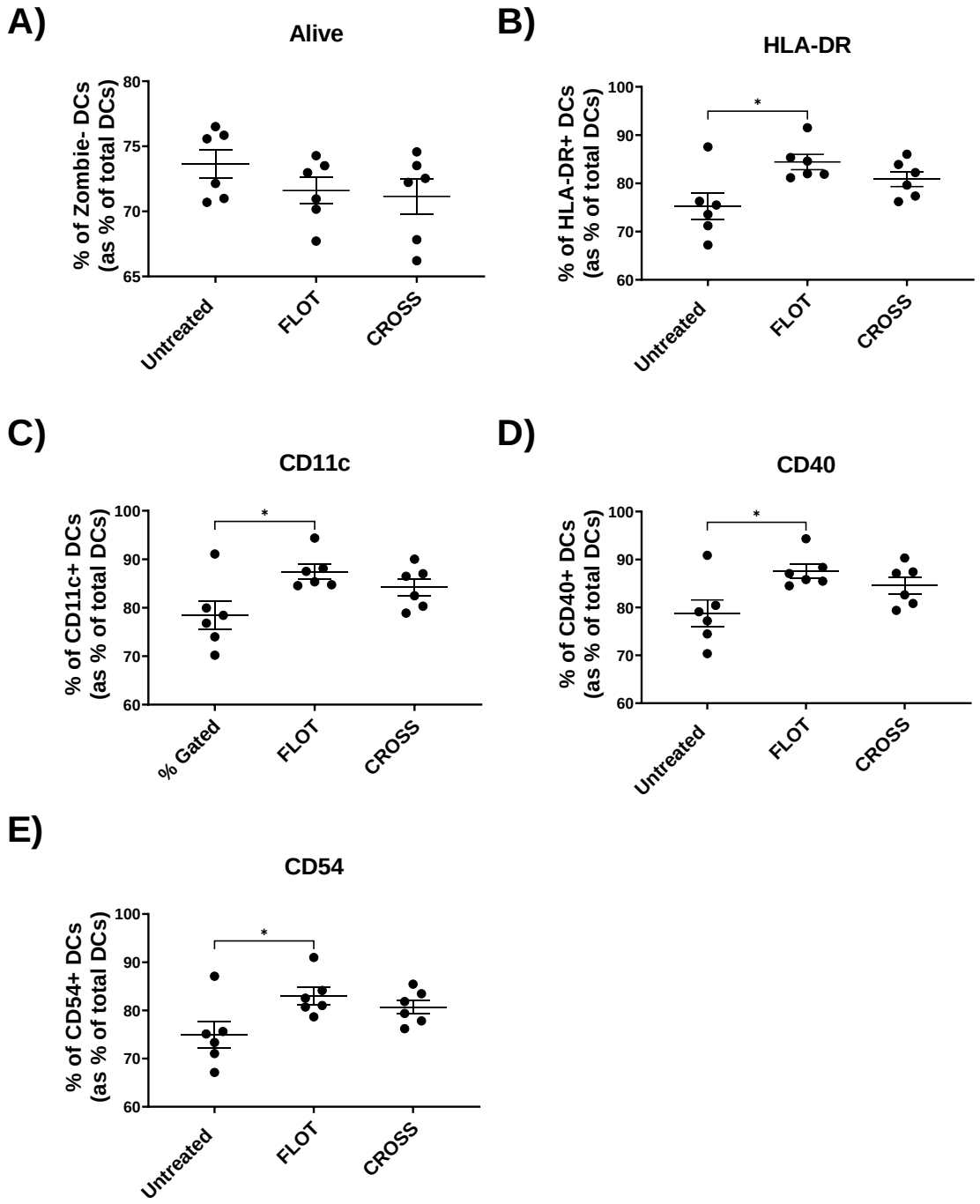


**Figure 6.4.16 Chemotherapy increases DCs expression of phenotypic and adhesion associated markers.**

A-E) Expression of DC phenotypic and maturation markers including viability, HLA-DR, CD11c, CD40, and CD54 following exposure to untreated, chemotherapy treated (FLOT) and chemoradiotherapy treated (CROSS) adipose conditioned media

(Friedman test with Dunn's correction) All data expressed as mean ± SEM, n=6, * $p < 0.05$, ** $p < 0.01$.

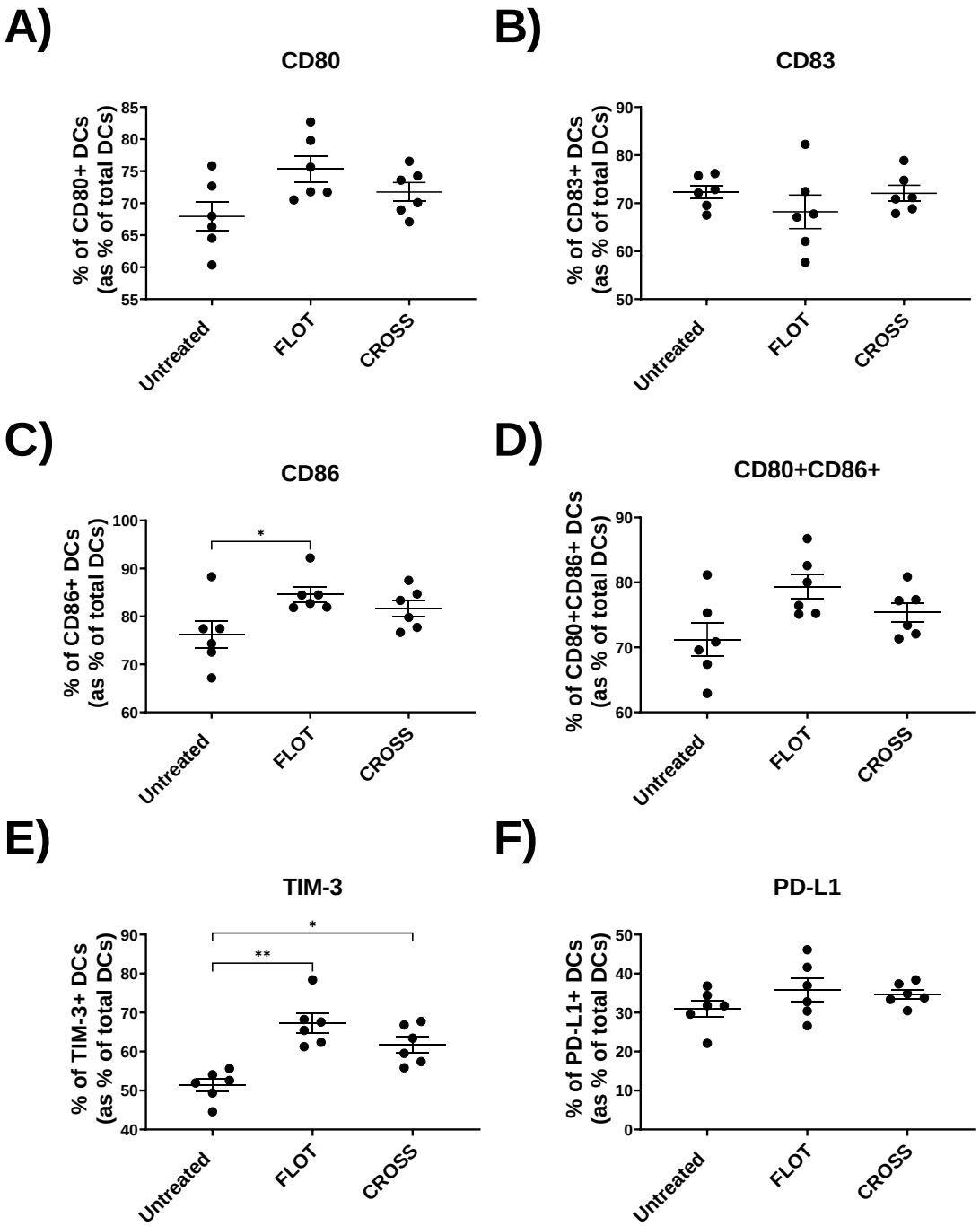


**Figure 6.4.17 Chemotherapy increases DCs maturation markers, whilst all treatments increased immunoinhibitory ligand TIM-3.**

A-F) Expression of DC phenotypic and maturation markers including CD80, CD83, CD86, CD80+CD86+, TIM-3 and PD-L1 following exposure to untreated, chemotherapy treated (FLOT) and chemoradiotherapy treated (CROSS) adipose conditioned media

(Friedman test with Dunn's correction) All data expressed as mean ± SEM, n=6, * $p < 0.05$, ** $p < 0.01$.

### 6.4.11 *Chemoradiotherapy in combination with PA treatment significantly decreases expression of DC maturation and immune inhibitory signals*

PA as previously mentioned has been shown to enhance DCs maturation. To assess the influence of chemotherapy or chemoradiotherapy in combination with OA or PA treatment on the adipose secretome and how this alters DCs maturation, stimulated DCs were assessed via flow cytometry for a panel of phenotypic and maturation markers following exposure to these treated ACM.

DCs cultured with FLOT, and PA treated ACM showed decreased expression of CD80 and CD80+CD86+ compared with matched control or OA treated (**Figure 6.4.19 A, D**). Whilst DCs cultured with CROSS and PA treated ACM showed significantly decreased expression of CD40, CD54, CD86, and CD80+CD86+ compared with matched control or OA treated (**Figure 6.4.18, D, E, Figure 6.4.19 C, D**). Additionally, DCs cultured with CROSS and PA treated ACM showed increased expression of CD83 compared with matched control (**Figure 6.4.19 B**). DCs cultured with FLOT, and PA treated ACM showed decreased expression of immuno-inhibitory ligands TIM-3 and PD-L1 compared with matched with matched control and OA treated ACM (**Figure 6.4.19 E, F**). Whilst DCs cultured with CROSS and PA treated ACM only showed decreased expression of TIM-3 compared with DCs cultured CROSS and OA treated ACM (**Figure 6.4.19 E**).

(* $p < 0.05$)

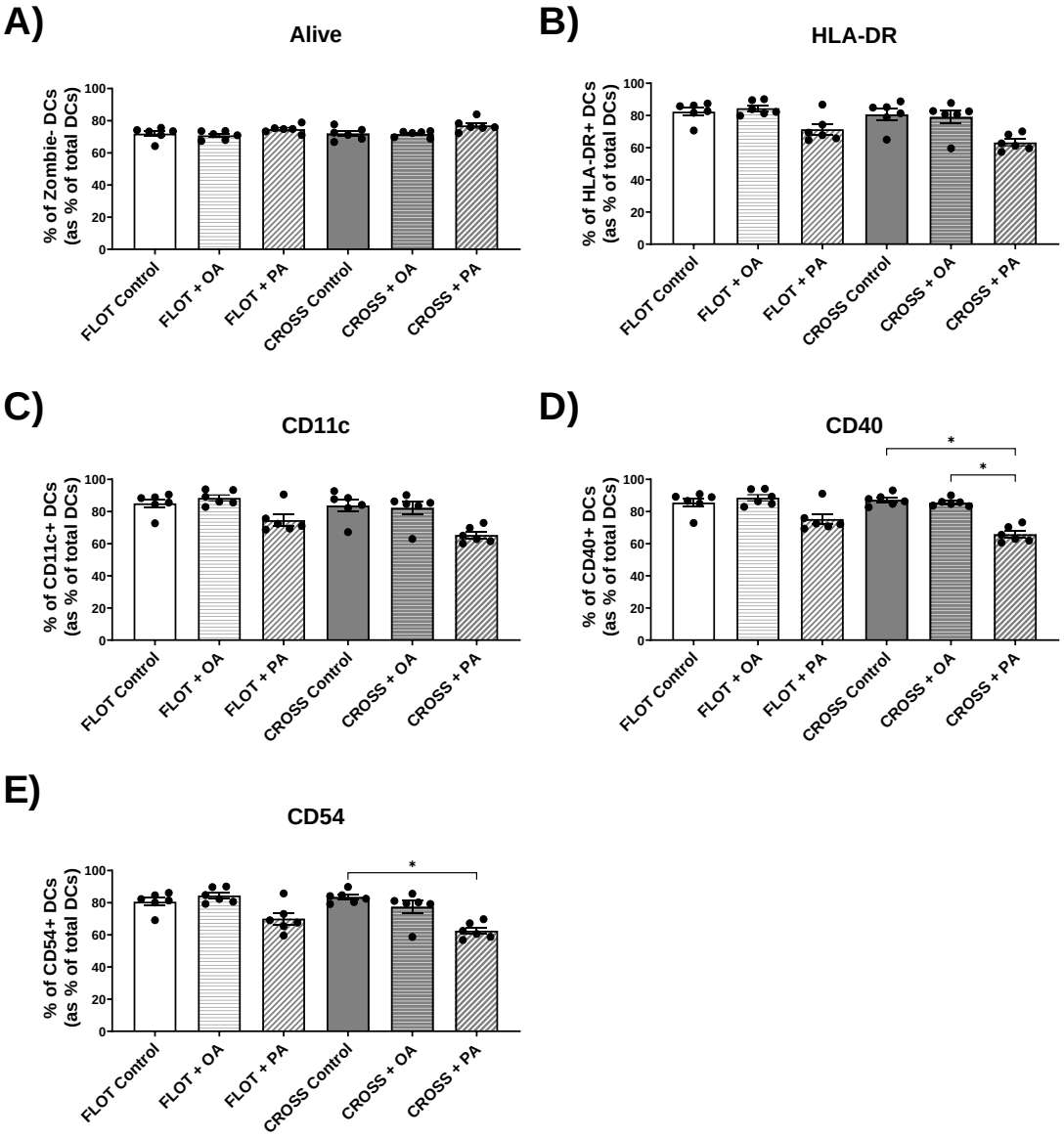


**Figure 6.4.18 The adipose secretome treated with chemoradiotherapy in combination with PA treatment significantly decreases DC expression of CD40.**

A-E) Expression of DC phenotypic and adhesion markers including viability, HLA-DR, CD11c, CD40, and CD54 and following exposure to chemotherapy treated (FLOT) and chemoradiotherapy treated (CROSS) adipose conditioned media in combination with BSA Control, Oleic Acid (OA) or Palmitic Acid (PA).

(Friedman test with Dunn's correction) All data expressed as mean ± SEM, n=6, * $p < 0.05$.

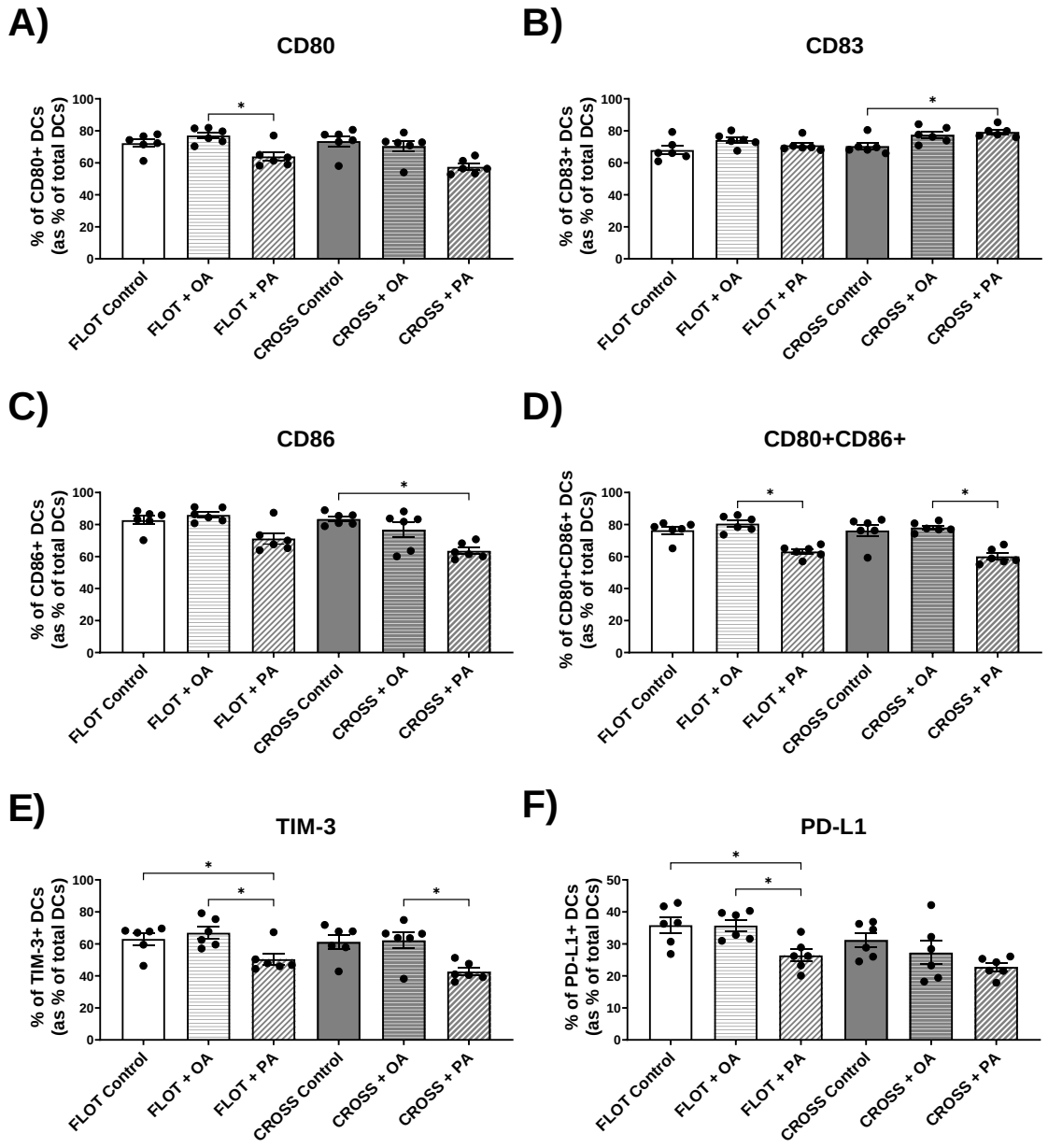


**Figure 6.4.19 The adipose secretome treated with chemotherapy in combination with PA treatment significantly decreases expression of DC maturation and immune inhibitory signals.**

A-F) Expression of DC phenotypic and maturation markers including CD80, CD83, CD86, CD80+CD86+, TIM-3, and PD-L1 following exposure to chemotherapy treated (FLOT) and chemoradiotherapy treated (CROSS) adipose conditioned media in combination with BSA Control, Oleic Acid (OA) or Palmitic Acid (PA).

(Friedman test with Dunn's correction) All data expressed as mean ± SEM, n=6, * $p < 0.05$.

### 6.4.12 *Chemotherapy ACM significantly increases anti-inflammatory markers on unpolarised Mϕ whilst chemoradiotherapy significantly increases pro-inflammatory markers*

Chemotherapy and chemoradiotherapy have been reported to have pleiotropic effects on Mϕ polarisation. To assess the influence of chemotherapy or chemoradiotherapy on the adipose secretome and how this alters Mϕ maturation, unpolarised Mϕ were assessed via flow cytometry for a panel of phenotypic, pro-inflammatory and anti-inflammatory markers following exposure to these treated ACM.

Unpolarised Mϕ cultured with FLOT treated ACM showed significantly increased co-expression of anti-inflammatory associated markers CD163+CD206+ (**Figure 6.4.21 F**). Unpolarised Mϕ cultured with CROSS treated ACM showed significantly decreased expression of phenotypic markers CD68, as well as increased expression of pro-inflammatory associated markers CD80, CD86, CD80+CD86+, and immune-inhibitory marker TIM-3 (**Figure 6.4.20, B, F, Figure 6.4.21 A, B, E**).

(* $p < 0.05$)

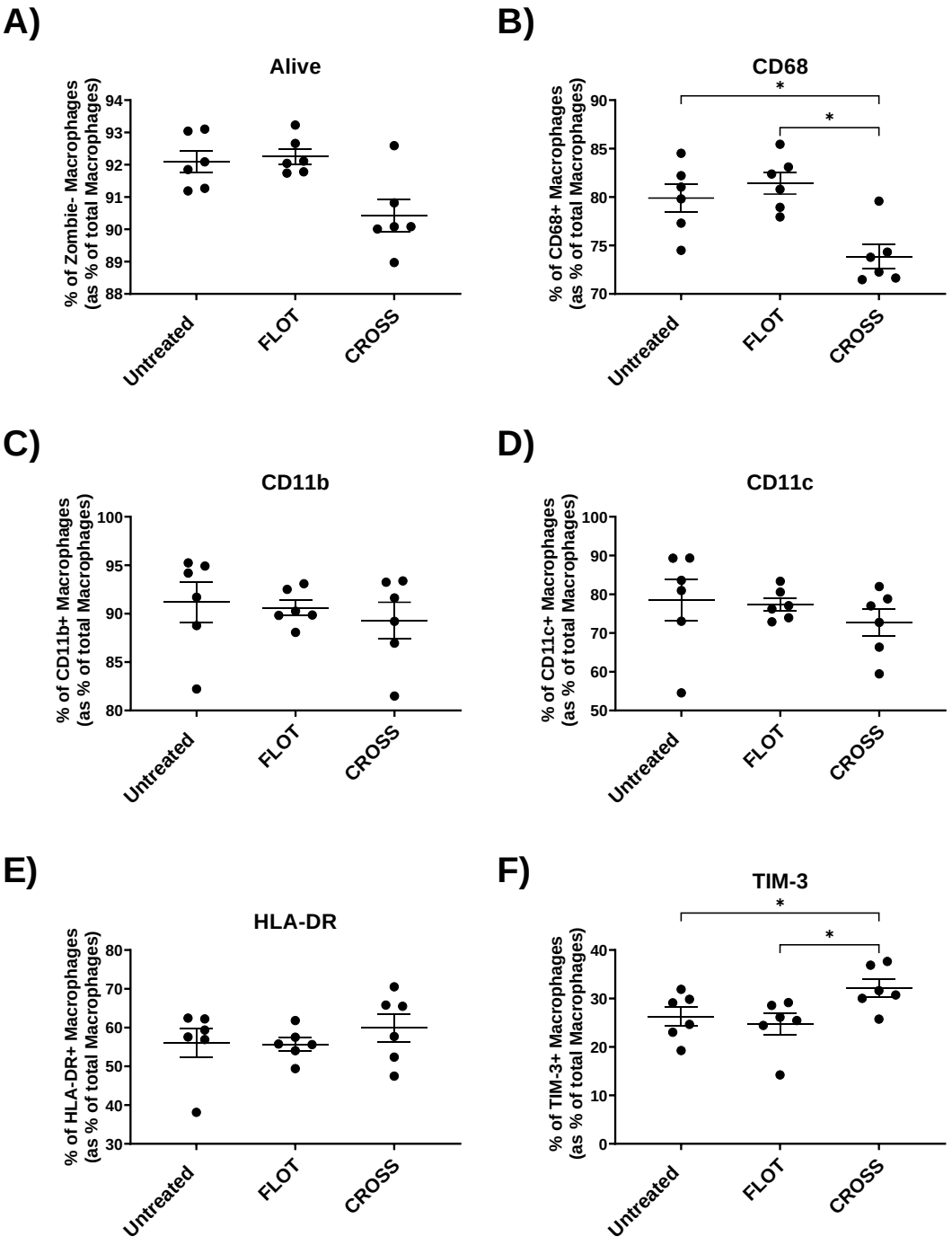


**Figure 6.4.20 Chemoradiotherapy treated adipose secretome significantly increases immunoinhibitory markers TIM-3 on unpolarised Mϕ.**

A-F) Expression of unpolarised Mϕ phenotypic and immunoinhibitory markers including viability, CD68, CD11b, CD11c, HLA-DR, and TIM-3 following exposure to untreated, chemotherapy treated (FLOT) and chemoradiotherapy treated (CROSS) adipose conditioned media

(Friedman test with Dunn's correction) All data expressed as mean ± SEM, n=6, * $p < 0.05$.

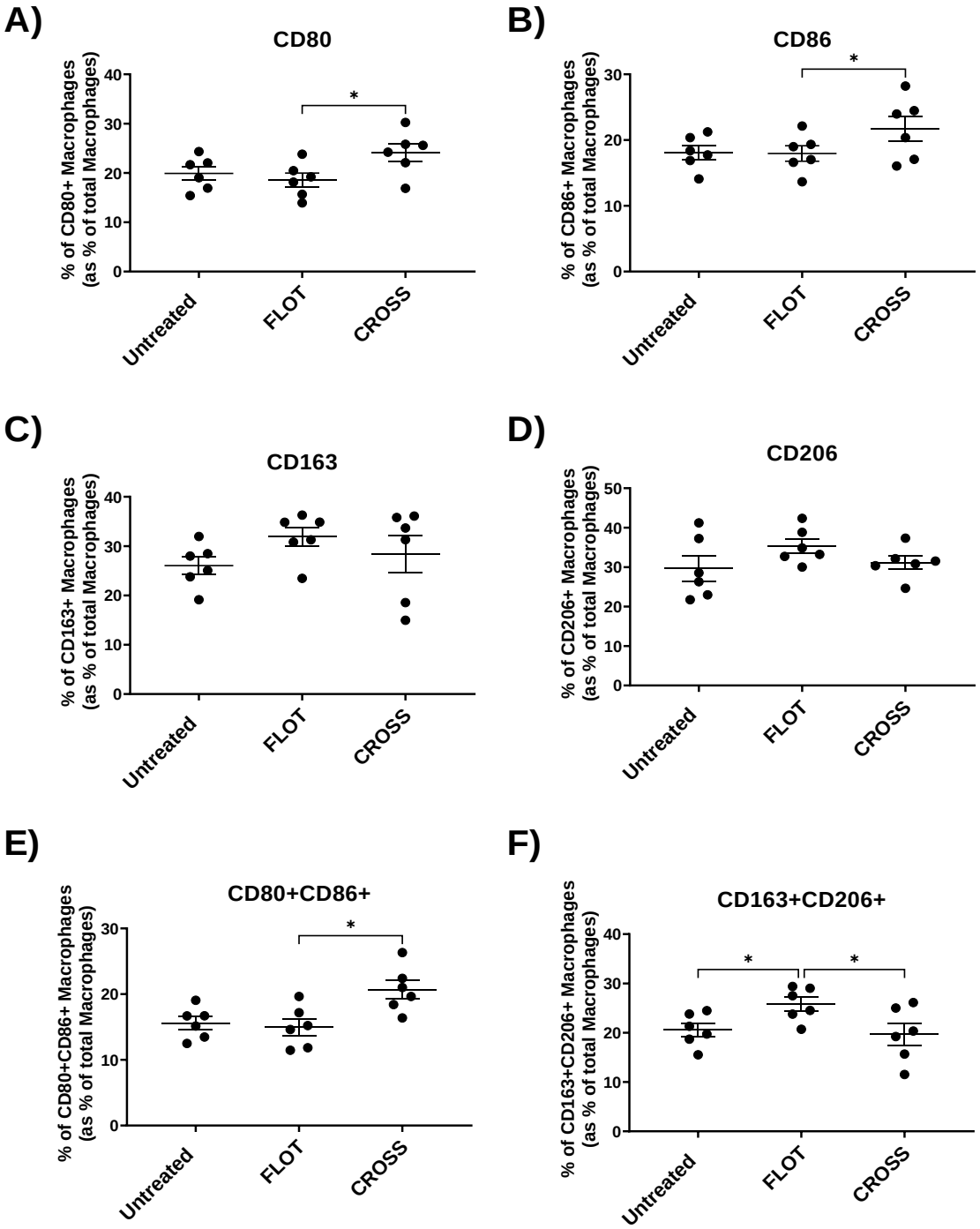


**Figure 6.4.21 Chemotherapy treated adipose secretome significantly increases anti-inflammatory markers on unpolarised Mϕ whilst chemoradiotherapy significantly increases pro-inflammatory markers.**

A-F) Expression of unpolarised Mϕ polarisation markers including CD80, CD86, CD163, CD206, CD80+CD86+, and CD163+CD206+ following exposure to untreated, chemotherapy treated (FLOT) and chemoradiotherapy treated (CROSS) adipose conditioned media

(Friedman test with Dunn's correction) All data expressed as mean ± SEM, n=6, * $p < 0.05$.

### 6.4.13 *Chemoradiotherapy in combination with PA significantly increases CD206 expression on unpolarised Mϕ*

Invoking fatty acid oxidation has been reported to be a central cellular metabolic change in response to the stress induced by chemotherapy or chemoradiotherapy. To assess the influence of chemotherapy or chemoradiotherapy in combination with OA or PA treatment on the adipose secretome and how this alters Mϕ maturation, unpolarised Mϕ were assessed via flow cytometry for a panel of phenotypic, pro-inflammatory and anti-inflammatory markers following exposure to these treated ACM.

Similar expression of pro-inflammatory and anti-inflammatory ligands were observed in unpolarised Mϕ cultured with FLOT and CROSS treated ACM as described in **Figure 6.4.20 - Figure 6.4.21**. However unpolarised Mϕ cultured with CROSS and PA treated ACM showed significantly increased expression of anti-inflammatory associated markers CD206 compared with matched control (**Figure 6.4.23 C**).

(* $p < 0.05$)

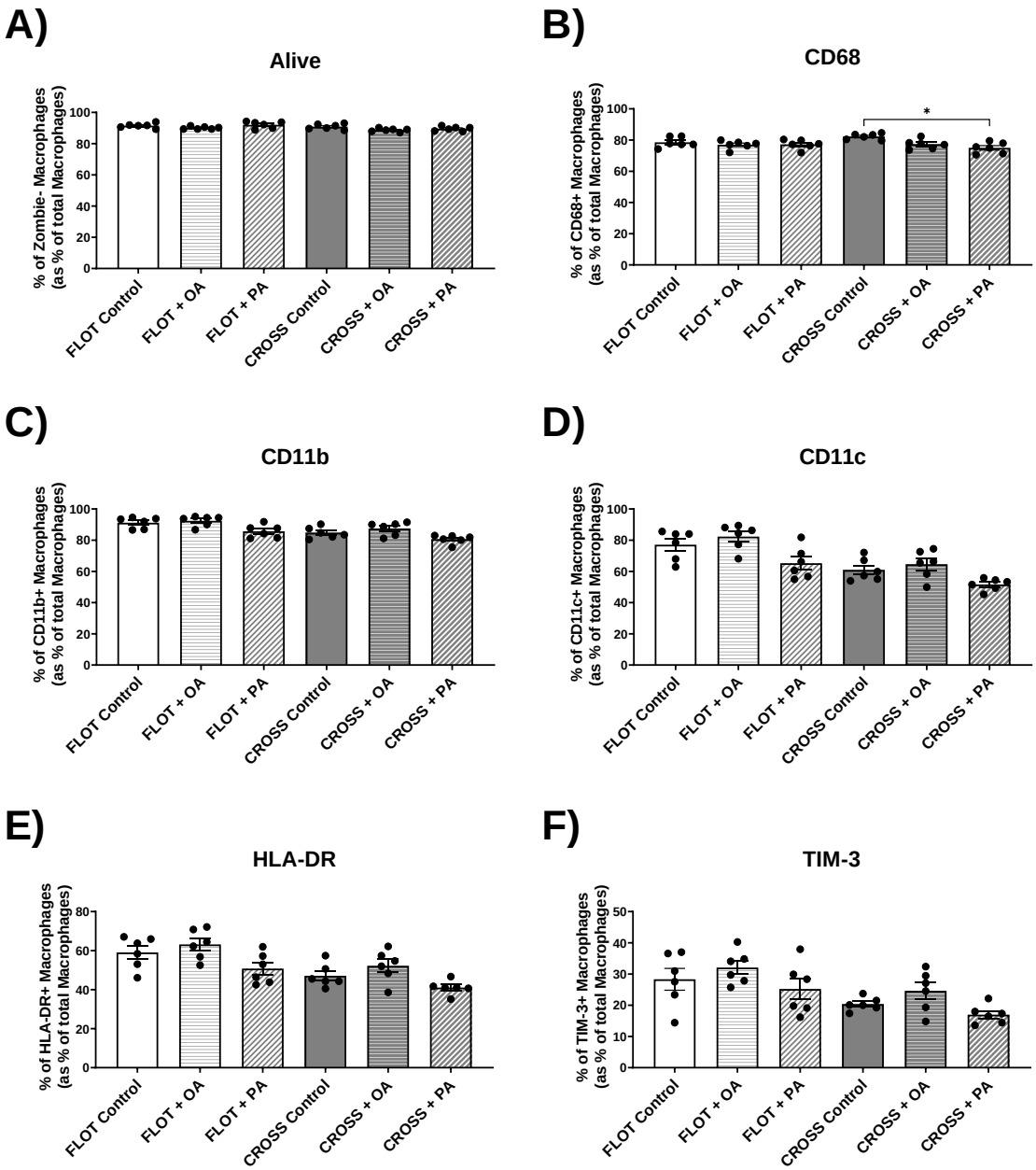


**Figure 6.4.22 The adipose secretome tretaed with chemoradiotherapy in combination with PA significantly decreased CD268 expression on unpolarised Mϕ.**

A-F) Expression of unpolarised Mϕ phenotypic and polarisation markers including viability, CD68, CD11b, CD11c, HLA-DR, and TIM-3 following exposure to chemotherapy treated (FLOT) and chemoradiotherapy treated (CROSS) adipose conditioned media in combination with BSA Control, Oleic Acid (OA) or Palmitic Acid (PA).

(Friedman test with Dunn's correction) All data expressed as mean ± SEM, n=6, * $p < 0.05$.

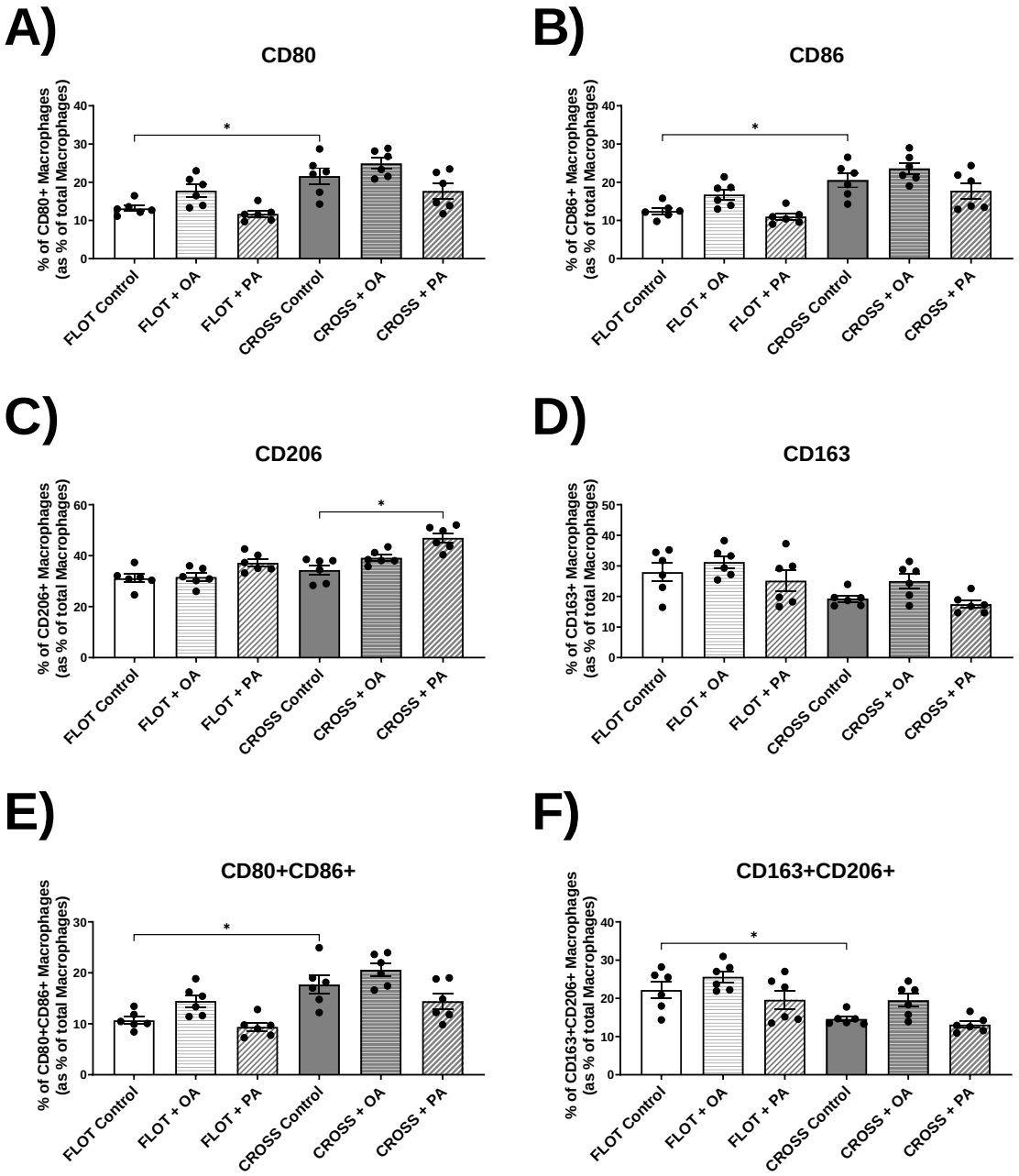


**Figure 6.4.23 Chemoradiotherapy in combination with PA significantly increases CD206 expression on unpolarised Mϕ**

A-F) Expression of unpolarised Mϕ phenotypic and polarisation markers including CD80, CD86, CD163, CD206, CD80+CD86+, and CD163+CD206+ following exposure to chemotherapy treated (FLOT) and chemoradiotherapy treated (CROSS) adipose conditioned media in combination with BSA Control, Oleic Acid (OA) or Palmitic Acid (PA).

(Friedman test with Dunn's correction) All data expressed as mean ± SEM, n=6, * $p < 0.05$.

### 6.4.14 *Chemotherapy significantly increases M1 polarised Mϕ expression of pro-inflammatory and immune-inhibitory ligands*

Chemoradiotherapy have been reported to evoke radiation induced inflammation, a response perpetuated by M1-like macrophages. To assess the influence of chemotherapy or chemoradiotherapy on the adipose secretome and how this alters Mϕ maturation, M1-polarised Mϕ by LPS were assessed via flow cytometry for a panel of phenotypic, and pro-inflammatory markers following exposure to these treated ACM.

M1-polarised Mϕ cultured with FLOT treated ACM also showed significantly decreased viability compared with Mϕ cultured with CROSS treated ACM (**Figure 6.4.24 A**). M1-polarised Mϕ cultured with FLOT treated ACM showed significantly increased expression of a series of Mϕ phenotypic and immune-inhibitory associated markers including CD11b, CD11c, HLA-DR, and TIM-3 compared with control ACM (**Figure 6.4.24 C, D, E, F**). M1-polarised Mϕ cultured with FLOT treated ACM showed significantly increased expression of a pro-inflammatory associated Mϕ markers including CD80, CD86, and co-expression of CD80+CD86+ compared with control ACM (**Figure 6.4.25 A, B, C**).

(* $p < 0.05$)

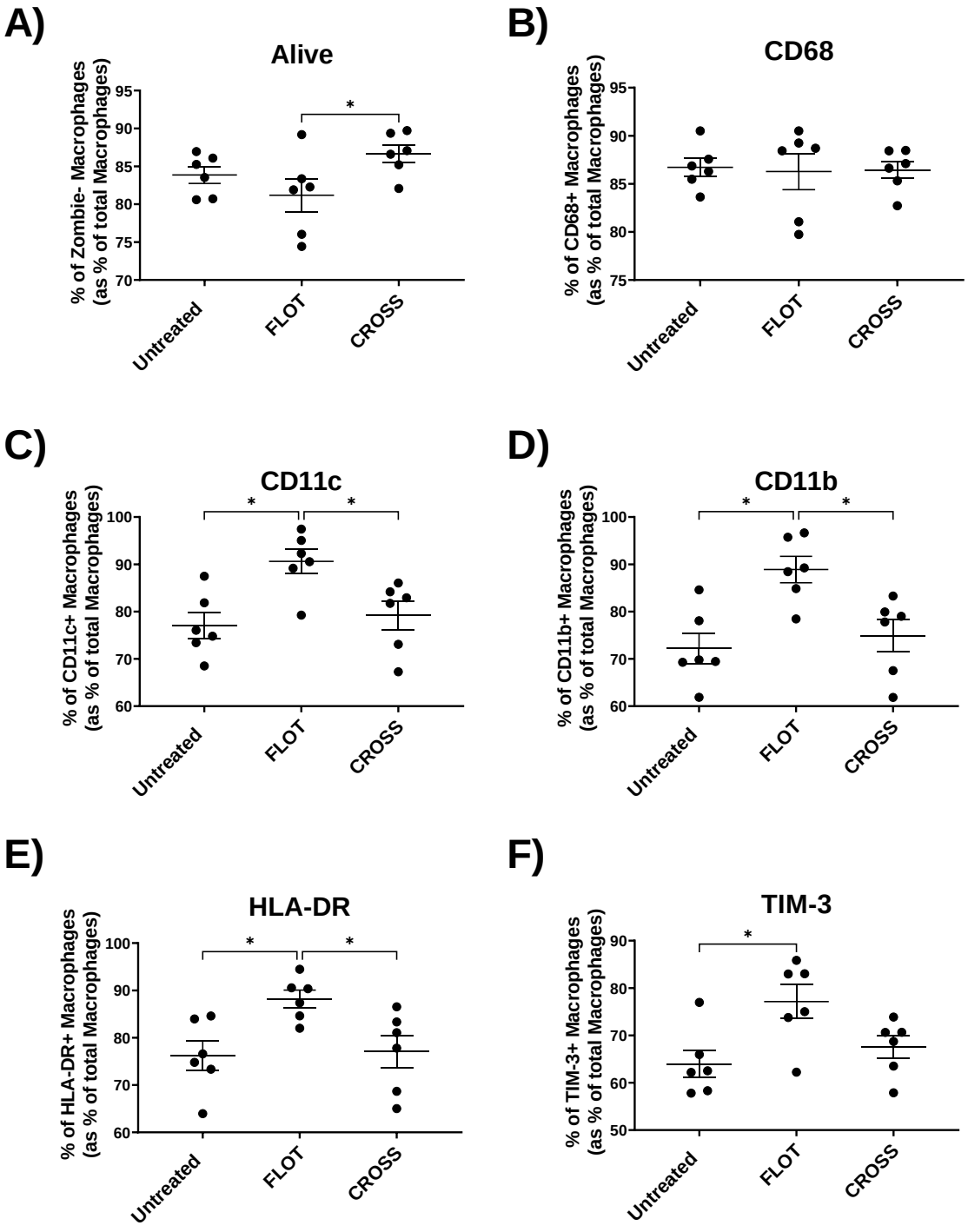


**Figure 6.4.24 Chemotherapy treated adipose secretome significantly increases M1 polarised Mϕ expression of phenotypic and immune-inhibitory ligands**

A-F) Expression of LPS M1 primed Mϕ phenotypic and immunoinhibitory markers including viability, CD68, CD11b, CD11c, HLA-DR, and TIM-3 exposure to untreated, chemotherapy treated (FLOT) and chemoradiotherapy treated (CROSS) adipose conditioned media

(Friedman test with Dunn's correction) All data expressed as mean ± SEM, n=6, * $p < 0.05$.

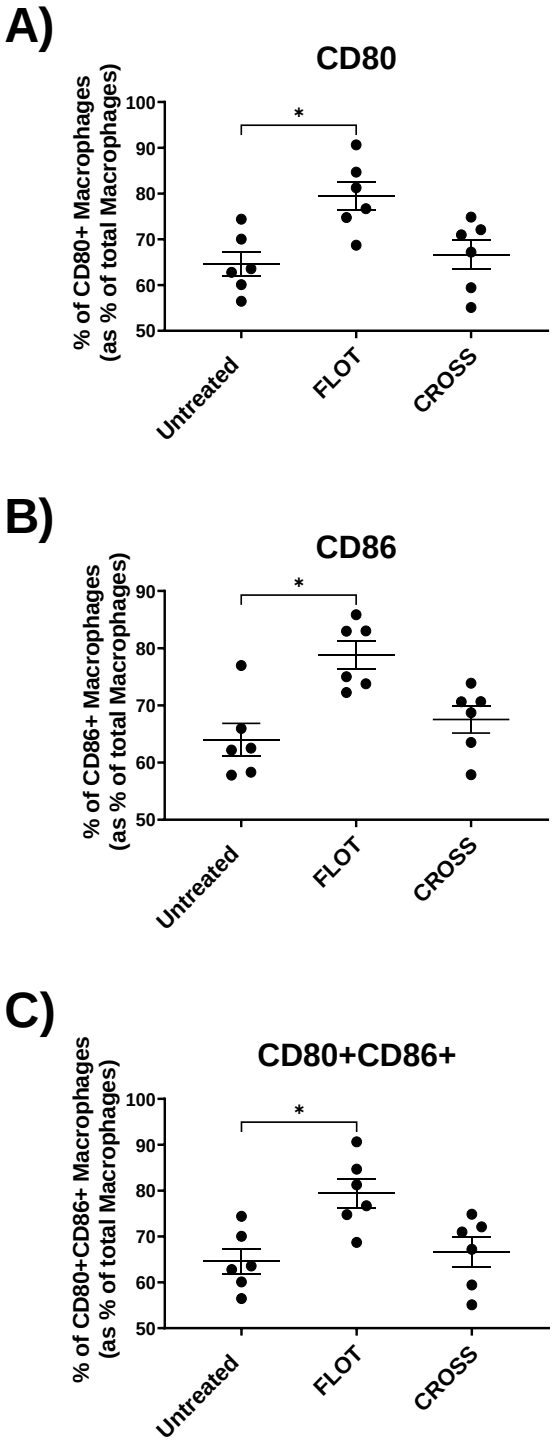


**Figure 6.4.25 Chemotherapy treated adipose secretome significantly increases M1 polarised Mϕ expression of pro-inflammatory ligands**

A-C) Expression of LPS M1 primed Mϕ polarisation markers including CD80, CD86, and CD80+CD86+ exposure to untreated, chemotherapy treated (FLOT) and chemoradiotherapy treated (CROSS) adipose conditioned media

(Friedman test with Dunn's correction) All data expressed as mean ± SEM, n=6, * $p < 0.05$.

### 6.4.15 *Chemoradiotherapy in combination with OA significantly decreases M1 polarised Mϕ expression of pro-inflammatory and immune-inhibitory ligands*

PA as previously mentioned, has been widely reported for its -pro-inflammatory effects, OA on the side has been shown to ameliorate pro-inflammatory response particularly in response to external stress. To assess the influence of chemotherapy or chemoradiotherapy in combination with OA or PA treatment on the adipose secretome and how this alters Mϕ maturation, M1-polarised Mϕ by LPS were assessed via flow cytometry for a panel of phenotypic, and pro-inflammatory markers following exposure to these treated ACM.

M1-polarised Mϕ cultured with CROSS and OA treated ACM showed significantly decreased expression of phenotypic marker CD68 compared to Mϕ cultured with FLOT and OA treated ACM (**Figure 6.4.26 B**). Additionally, these Mϕ cultured with CROSS and OA treated ACM showed decreased expression of pro-inflammatory associated markers CD80, CD86, CD80+CD86+, and immune-inhibitory marker TIM-3 compared with Mϕ cultured with FLOT and OA treated ACM (**Figure 6.4.27 A, B, C, Figure 6.4.26 F)**.

(* $p < 0.05$)

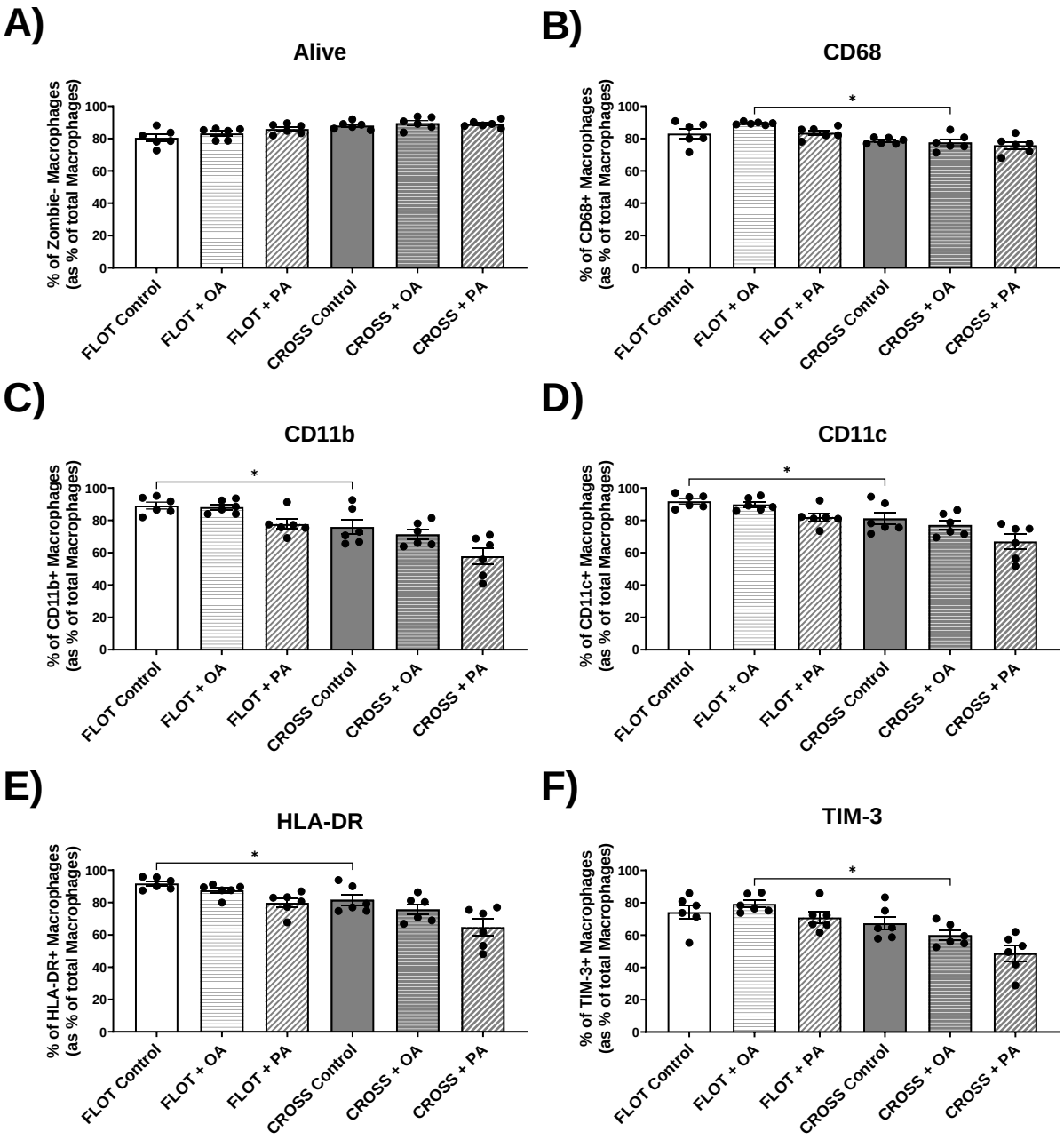


**Figure 6.4.26 Chemoradiotherapy treated adipose secretome in combination with OA significantly decreases M1 polarised Mϕ expression of immune-inhibitory TIM-3.**

A-F) Expression of LPS M1 primed Mϕ phenotypic and immuno-inhibitory markers including viability, CD68, CD11b, CD11c, HLA-DR, and TIM-3 following exposure to chemotherapy treated (FLOT) and chemoradiotherapy treated (CROSS) adipose conditioned media in combination with BSA Control, Oleic Acid (OA) or Palmitic Acid (PA).

(Friedman test with Dunn's correction) All data expressed as mean ± SEM, n=6, * $p < 0.05$.

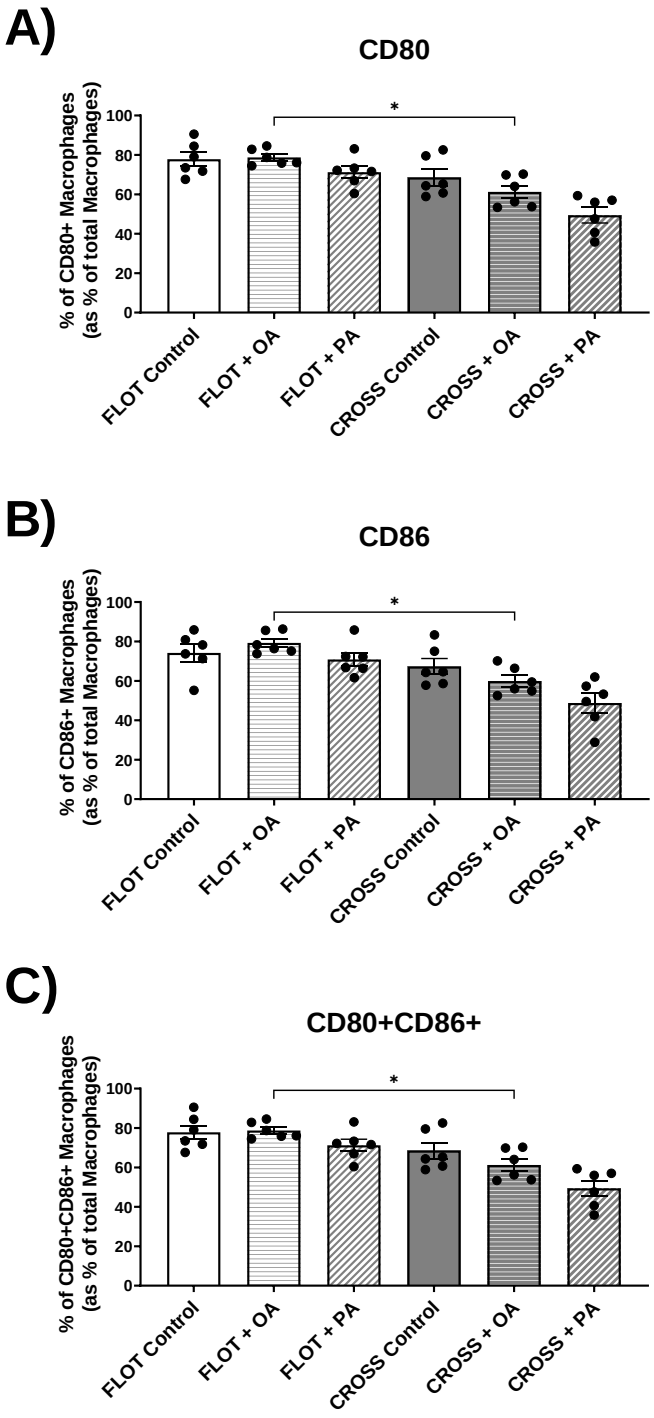


**Figure 6.4.27 Chemoradiotherapy treated adipose secretome in combination with OA significantly decreases M1 polarised Mϕ expression of pro-inflammatory markers.**

A-C) Expression of LPS M1 primed Mϕ phenotypic and polarisation markers including CD80, CD86, and CD80+CD86+ following exposure to chemotherapy treated (FLOT) and chemoradiotherapy treated (CROSS) adipose conditioned media in combination with BSA Control, Oleic Acid (OA) or Palmitic Acid (PA).

(Friedman test with Dunn's correction) All data expressed as mean ± SEM, n=6, * $p < 0.05$.

### 6.4.16 *Chemoradiotherapy significantly increases M2 polarised Mϕ expression of anti-inflammatory associated marker CD206*

Chemotherapy have been reported to decreases M2-like macrophages and increase pro-inflammatory responses, whilst radiotherapy has been reported to enhance M2-like recruitment. To assess the influence of chemotherapy or chemoradiotherapy on the adipose secretome and how this alters Mϕ maturation, M2-polarised Mϕ by IL-4 were assessed via flow cytometry for a panel of phenotypic, and anti-inflammatory markers following exposure to these treated ACM.

M2-polarised Mϕ cultured with FLOT treated ACM also showed significantly decreased viability compared with Mϕ cultured with CROSS treated ACM (**Figure 6.4.28 A**). M2-polarised Mϕ cultured with FLOT treated ACM also showed significantly increased expression of a series of Mϕ phenotypic markers including CD11c, and HLA-DR compared with control and CROSS treated ACM (**Figure 6.4.28 D, E**). However, M2-polarised Mϕ cultured with CROSS treated ACM showed significantly increased expression of anti-inflammatory associated marker CD206 compared with matched control (**Figure 6.4.29 B**).

(* $p < 0.05$)

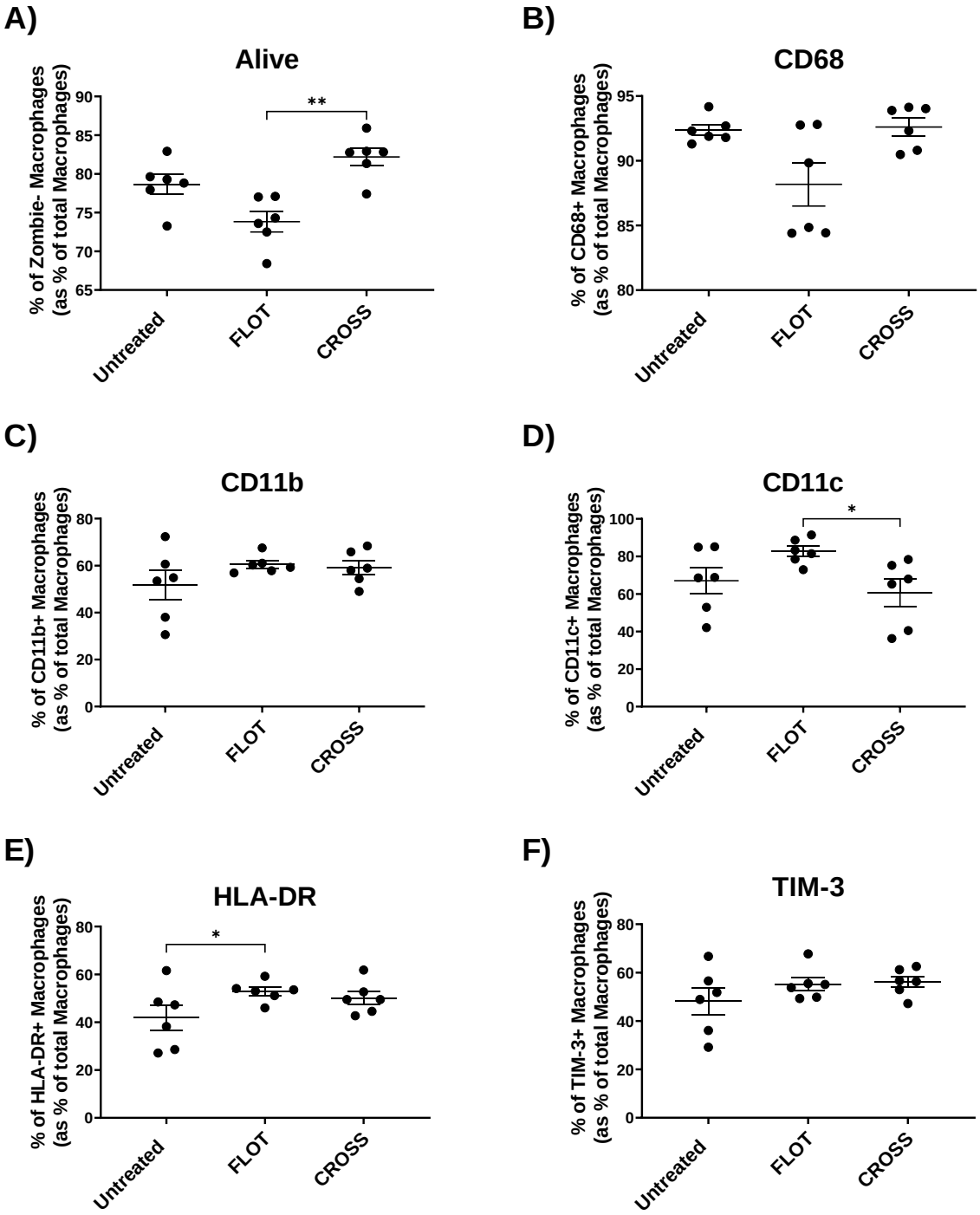


**Figure 6.4.28 Chemotherapy treated adipose secretome increases M2 polarised Mϕ expression of HLA-DR.**

A-F) Expression of IL-4 M2 primed Mϕ phenotypic and immunoinhibitory markers including viability, CD68, CD11b, CD11c, HLA-DR, and TIM-3 following exposure to chemotherapy treated (FLOT) and chemoradiotherapy treated (CROSS) adipose conditioned media in combination with BSA Control, Oleic Acid (OA) or Palmitic Acid (PA).

(Friedman test with Dunn's correction) All data expressed as mean ± SEM, n=6, * $p < 0.05$.

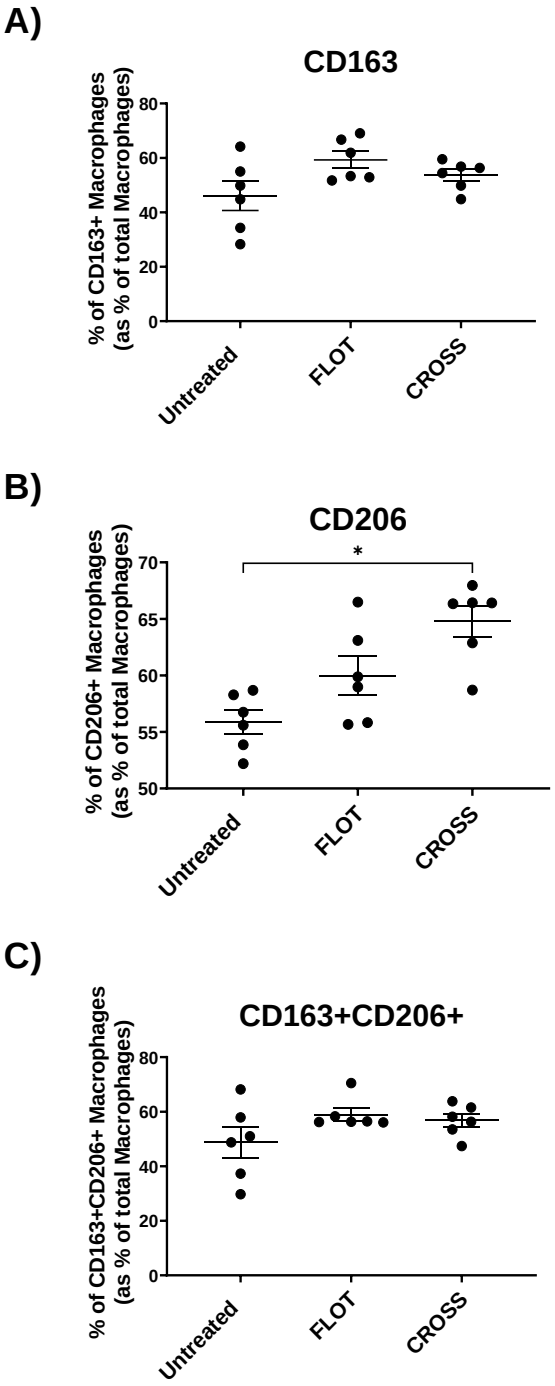


**Figure 6.4.29 Chemoradiotherapy treated adipose secretome significantly increases M2 polarised Mϕ expression of CD206.**

A-C) Expression of IL-4 M2 primed Mϕ anti-inflammatory polarisation markers including CD163, CD206, and CD163+CD206+ following exposure to chemotherapy treated (FLOT) and chemoradiotherapy treated (CROSS) adipose conditioned media in combination with BSA Control, Oleic Acid (OA) or Palmitic Acid (PA).

(Friedman test with Dunn's correction) All data expressed as mean ± SEM, n=6, * $p < 0.05$.

### 6.4.17 *Chemoradiotherapy in combination with PA significantly decreases M2 polarised Mϕ expression of anti-inflammatory and immune-inhibitory ligands*

Lipid loaded macrophages have been reported to be abundantly expressed in most tumours, conferring M2 like Mϕ with pathogenic features that aid tumour progression and enhance immunosuppression. To assess the influence of chemotherapy or chemoradiotherapy in combination with OA or PA treatment on the adipose secretome and how this alters Mϕ maturation, M2-polarised Mϕ by IL-4 were assessed via flow cytometry for a panel of phenotypic, and anti-inflammatory markers following exposure to these treated ACM.

M2 polarised Mϕ cultured with chemoradiotherapy in combination with PA showed increased viability compared with matched control. M2-polarised Mϕ cultured with CROSS and PA treated ACM showed significantly increased expression of phenotypic marker CD68 compared with matched control ACM and FLOT and PA treated ACM (**Figure 6.4.30 B**). Additionally, these Mϕ cultured with CROSS and PA treated ACM showed decreased expression of anti-inflammatory associated markers CD163, CD206, CD163+CD206+, and immunoinhibitory marker TIM-3 compared with Mϕ cultured with FLOT and PA treated ACM (**Figure 6.4.31 A, B, C, Figure 6.4.30 F**). Increased expression of immune-inhibitory TIM-3 was also observed on M2 polarised Mϕ cultured with CROSS and OA treated ACM compared to Mϕ cultured with CROSS and PA treated ACM (**Figure 6.4.30 F**).

(* $p < 0.05$)

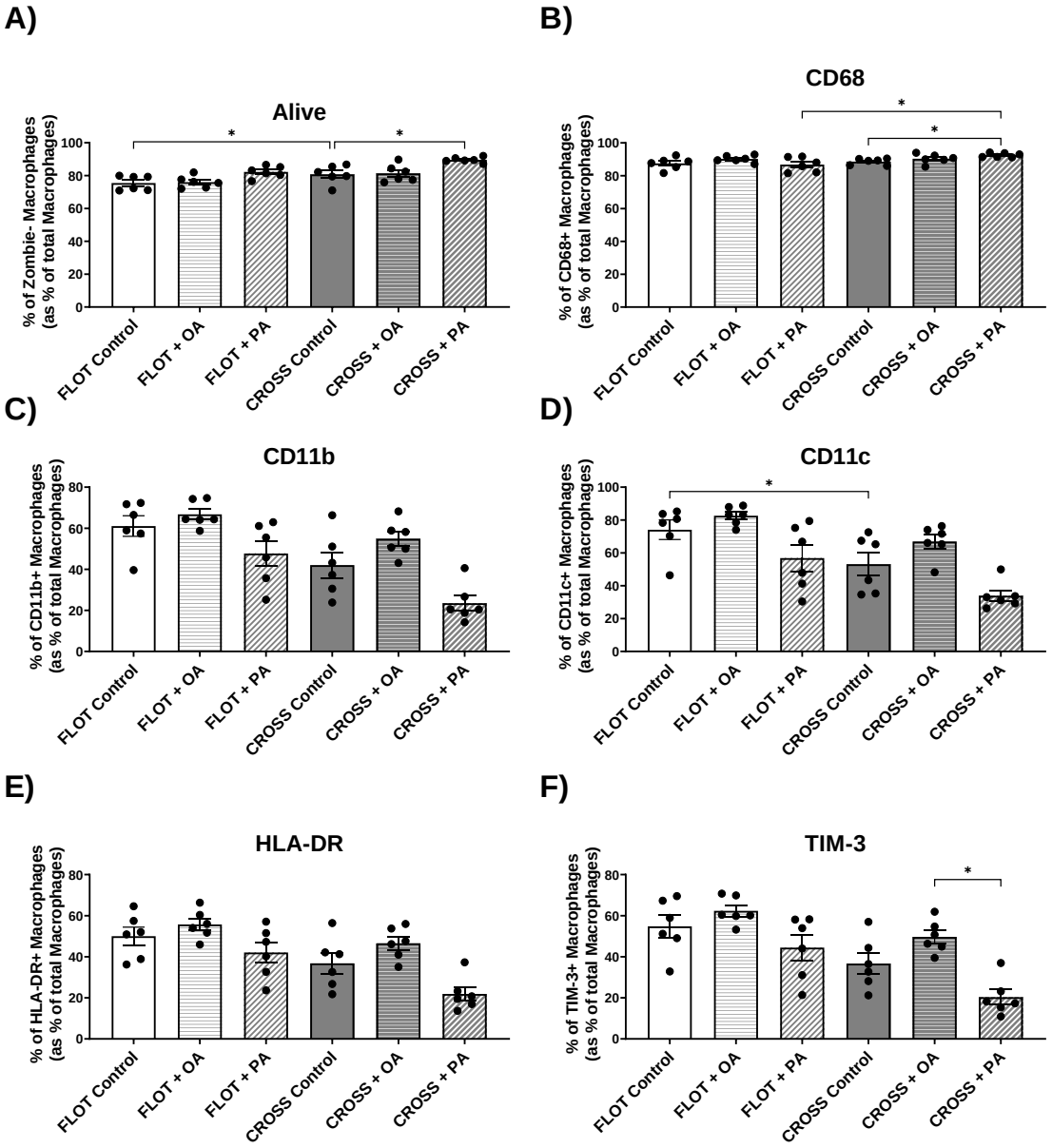


**Figure 6.4.30 Chemoradiotherapy treated adipose secretome in combination with PA significantly decreases M2 polarised Mϕ expression of immune-inhibitory TIM-3 and increased viability.**

A-F) Expression of IL-4 M2 primed Mϕ phenotypic and immunoinhibitory markers including viability, CD68, CD11b, CD11c, HLA-DR, and TIM-3 following exposure to chemotherapy treated (FLOT) and chemoradiotherapy treated (CROSS) adipose conditioned media in combination with BSA Control, Oleic Acid (OA) or Palmitic Acid (PA).

(Friedman test with Dunn's correction) All data expressed as mean ± SEM, n=6, * $p < 0.05$, *** $p < 0.001$.

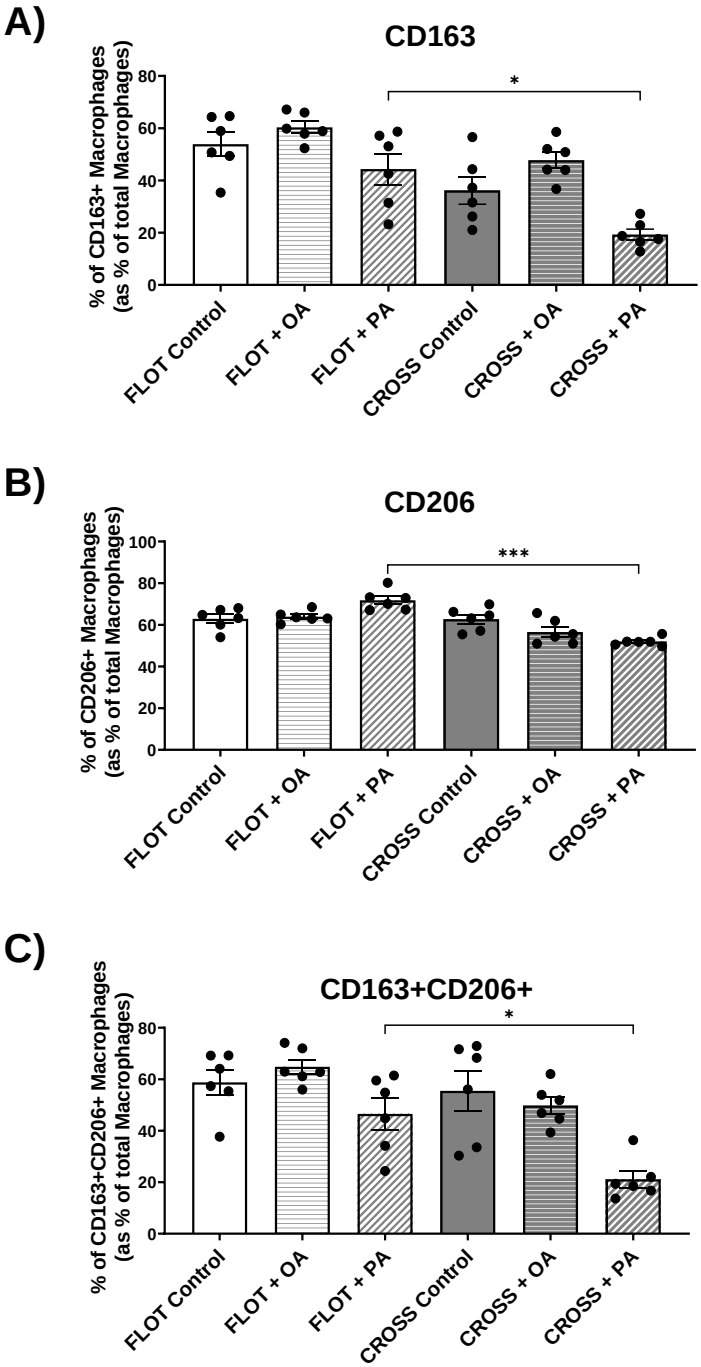


**Figure 6.4.31 Chemoradiotherapy treated adipose secretome in combination with PA significantly decreases M2 polarised Mϕ expression of anti-inflammatory associated markers.**

A-C) Expression of IL-4 M2 primed Mϕ phenotypic and polarisation markers including CD163, CD206, and CD163+CD206+ following exposure to chemotherapy treated (FLOT) and chemoradiotherapy treated (CROSS) adipose conditioned media in combination with BSA Control, Oleic Acid (OA) or Palmitic Acid (PA).

(Friedman test with Dunn's correction) All data expressed as mean ± SEM, n=6, * $p < 0.05$, *** $p < 0.001$.

## 6.6 Summary of main findings

- FLOT chemotherapy regimen decreased adipose tissue explants utilisation of oxidative phosphorylation and increased glycolytic preference. CROSS chemoradiotherapy regimen increased adipose tissue explants glycolytic preference.

- FLOT chemotherapy regimen in combination with OA increased adipose tissue explants utilisation of oxidative phosphorylation and increased glycolysis. CROSS chemoradiotherapy regimen in combination with PA decreased adipose tissue explants utilisation of oxidative phosphorylation.

- FLOT chemotherapy regimen decreased adipose tissue explants secretion of pro-inflammatory mediators. CROSS chemoradiotherapy regimen increased adipose tissue explants secretion of pro-inflammatory mediators.

- FLOT and CROSS regimens in combination with fatty acids differentially effected adipose tissue secretion of IL-4, IL-8, IL-12p70, IL-22 and MDC. However, both therapies combined with fatty acids increased adipose secretion of mediators of Th17 immune response.

- The adipose secretome treated with FLOT chemotherapy regimen increased oesophageal cancer cell proton leak and utilisation of glycolysis preference. The adipose secretome treated with CROSS chemoradiotherapy regimen increased oesophageal cancer cell spare respiratory capacity and utilisation of oxidative phosphorylation.

- The adipose secretome treated with FLOT chemotherapy regimen combined with OA decreased oesophageal cancer cell maximal respiration and spare respiratory capacity. The adipose secretome treated with CROSS chemoradiotherapy regimen in combination with PA decreased oesophageal cancer cell utilisation of oxidative phosphorylation and glycolytic preference.

- The adipose secretome treated with FLOT chemotherapy regimen increased DC expression of maturation and immunoinhibitory markers. The adipose secretome treated with CROSS chemoradiotherapy regimen increased DC expression of immunoinhibitory marker TIM-3.

- The adipose secretome treated with FLOT chemotherapy regimen combined with PA decreased DC expression of immunoinhibitory markers PD-L1 and TIM-3. The adipose secretome treated with CROSS chemoradiotherapy regimen with PA decreased DC expression of maturation and immunoinhibitory markers.

- The adipose secretome treated with FLOT chemotherapy regimen increased unpolarised Mϕ expression of anti-inflammatory associated markers as well as increasing M1-primed Mϕ expression of pro-inflammatory markers and TIM-3. The adipose secretome treated with CROSS chemoradiotherapy regimen increased unpolarised Mϕ expression of pro-inflammatory associated markers as well as increasing M2-primed Mϕ expression of anti-inflammatory markers.

- The adipose secretome treated with CROSS chemoradiotherapy regimen combined with OA increased unpolarised Mϕ expression of anti-inflammatory associated markers. The adipose secretome treated with CROSS chemoradiotherapy regimen combined with PA increased unpolarised Mϕ expression of anti-inflammatory associated markers but decreased M2-primed Mϕ expression of anti-inflammatory markers.

## 6.7 Discussion

The role of adipose tissue and the influence of obesity on cancer treatment response has been contentiously reported. For the first time this study examined the influence chemotherapy and chemoradiotherapy regimens on adipose tissue metabolism and its secretome. This study looked to further explore what implications this treated adipose secretome has for cancer cell metabolism, DC maturation and Mϕ polarisation. We further examined whether the addition of exogenous fatty acids could alter adipose tissue response to these cytotoxic therapies and what downstream effects this could hold for cancer and immune cell function.

In this study, FLOT chemotherapy regimen decreased OCR metabolism and OCR:ECAR ratio in adipose explants compared with untreated adipose. OCR a measurement of oxidative phosphorylation has been reported to be unregulated in more aggressive cancers, and inhibition of oxidative phosphorylation has been suggested to enhance the efficacy of chemotherapy [527]. However, a reduction in ROS production in the presence of prolonged chemotherapy has been shown to be a mitigating factor in its efficacy [528]. Additionally, chemoradiotherapy was observed to decrease OCR:ECAR ratio indicating a switch in preference to glycolysis. Radiation therapy has been shown to evoke a switch to glycolysis in cancer cells to survive the subsequent oxidative stress induced [507]. These diminished levels of OCR in adipose tissue following chemotherapy and elevated reliance on glycolysis following chemoradiotherapy may have more dynamic effects in the wider tumour microenvironment. This switch in metabolic preference could lead to an altered nutrient composition in the adipose tissue. Differential metabolism of metabolites such as glutamine that we have previously seen decreased in obese adipose tissue [80], or fatty acids could lead to an altered adipose milieu that may have opposing effects on cancer cell proliferation and migration.

We observed an increase in OCR and ECAR profiles in adipose explants treated with chemotherapy in combination with OA. Such an effect could be paradoxical as increased OCR with linked increased ROS induction could prove damaging within adipose tissue. However, increased levels of glycolysis could indicate adaptive change to counteract the induced damage, an effect not observed in adipose tissue treated with chemoradiotherapy in combination with OA. OA acid has been extensively researched as a solid lipid nanoparticle for the delivery of 5-FU and oxaliplatin, components of FLOT chemotherapy, with the hopes of reducing the rapid metabolism associated with these drugs and increasing treatment efficacy [529,530]. Further to this, decreased OCR levels were observed in adipose tissue following exposure to chemoradiotherapy in combination with PA compared with matched control and chemotherapy combined with PA. This noteworthy reaction between chemoradiotherapy and PA on OCR levels

echoes our previous research which indicated that irradiation may perpetuate the effects of PA on inhibiting OCR metabolism in adipose tissue. PA has previously been reported to confer cancer cells with enhanced survival to paclitaxel induced apoptosis [506] as well as inducing oxidative stress which may be enhanced by chemoradiotherapy. These differential metabolic reactions in adipose tissue in response to chemotherapy and chemoradiotherapy particularly in combination with exogenous fatty acids may be adaptions to survive the induction of reactive oxygen species (ROS) caused by these therapies. However, the damage induced as a by-product of these cytotoxic therapies may lead to detrimental changes in the adipose tissue biology and secreted factors that could aid the progression of cancer and diminish anti-tumour immunity. Further research is required to elucidate if these aberrant adipose metabolic changes following treatment exposure could be targeted for therapeutic gain.

The adipose secretome has also been reported to influence the tumour microenvironment, as well as mitigating cancer treatment response [79,231]. This study reports adipose tissue exposed to chemoradiotherapy showed increased secreted levels of a series of pro-inflammatory, vascular injury, immune recruiting and activating mediators GM-CSF, IFN-γ, IL-7, IL-16, IL-17A, IL-1β, IL-21, IL-23, IL-31, MDC, SAA, and TNF-α. Previously research has shown that following radiation therapy, increased leukocyte infiltration and myeloid cell activation [531]. GM-CSF and MDC are two key cytokines associated with immune cell recruitment and activation. Interestingly, GM-CSF is given in combination with radiotherapy to combat neutropenia, it has also been shown to not increase tumour cell migration [532]. Increases in secreted levels of GM-CSF from adipose tissue following chemoradiotherapy could act beneficially but further research is required to interrogate this link. Additionally, as would be expected following chemoradiotherapy, adipose tissue showed significant increases in secreted levels of pro-inflammatory cytokines including IFN-γ, IL-7, IL-16, IL-17A, IL-1β, IL-21, IL-23, IL-31, and TNF-α. Radiation induced inflammation is a known phenomenon [533], which is central to promoting anti-tumour immunity and regression [534]. Such increases in secretome of adipose tissue following chemoradiotherapy could enhance the circulatory pro-inflammatory response and aid in tumour cell death. Perhaps unsurprisingly, increased secreted levels of SAA were also observed following chemoradiotherapy, a factor that has previously be linked to radiation induced damage [461]. Decreased levels of SAA in circulation have previously been reported to be associated with diminished overall survival in patients receiving radiotherapy [463], so this increase in the adipose secretome may be influential in identifying pro-inflammatory response.

In addition to this adipose tissue exposed to chemoradiotherapy showed decreased secreted levels of anti-inflammatory and angiogenic mediators IL-1Ra, PIGF, SAA, VEGF, VEGF-C. IL-1Ra

has been reported to competitively inhibit pro-inflammatory responses from IL-1 family associated cytokines [535]. This decreased secretion by adipose tissue following exposure to chemoradiotherapy may aid in perpetuating radiation induced inflammation. PIGF, VEGF, and VEGF-C are known promotors of endothelial cell proliferation [536–538]. Previous research in rectal cancer biopsies has shown diminished endothelial cell proliferation after radiotherapy [531]. Interesting, these factors were decreased following chemoradiotherapy, asking the question if this response could ameliorate circulatory expression of these angiogenic mediators in the wider tumour microenvironment. Interestingly adipose tissue exposed to chemotherapy shown decreased secreted levels of immunoinhibitory mediators IL-13 and TARC. IL-13 plays a central role activating a Th2 response and inducing M2-like Mϕ polarisation, both critical factors in diminishing the efficacy of anti-tumour immunity [539]. Similarly, TARC has been reported to play a central role in stimulating Th2 driven immunity [540]. The influence of chemotherapy on the adipose secretome provokes some interesting questions. Here we observe that chemotherapy significantly decreases drivers of Th2 immunity, which are known to support pro-tumour immunity. Leading to the question whether this influence is adipose specific, how this could alter the inflammatory landscape of adipose tissue itself, specifically in obese OAC patients who suffer from a low grade pro-inflammatory state, as well as whether these effects have any bearing on the wider tumour microenvironment.

Exogenous lipids have been reported to promote the growth of cancer [209], as well as contributing to the efficacy of some therapies [525]. We have shown increased secreted levels of IL-22 in the adipose secretome of explants treated with chemotherapy and OA However, in the adipose secretome of explants treated with chemoradiotherapy with OA secreted levels of IL-22 were decreased. IL-22 has been reported for its pro-inflammatory as well as its pro-tumour effects, by inducing proliferation and inhibiting apoptotic effects [541]. Increased secreted levels of IL-4, IL-8, IL-12p70 and MDC were observed in the adipose secretome of explants treated with chemotherapy and PA compared with matched control. However, in the adipose secretome of explants treated with chemoradiotherapy with PA secreted levels of these factors were decreased compared with matched control. IL-12p70 is produced by dendritic cells and macrophages and are critical in aiding in the induction of NK cells and anti-tumour immunity [420]. However, IL-4 is a known promotor of M2-like Mϕ polarisation and central in promoting Th2 immunity, diminishing immune responses that may aid treatment efficacy [353,542]. IL-8 whilst a known promotor of pro-inflammatory response, has been reported to aid cancer growth whilst inhibiting the efficacy of cancer treatments [543]. Previous research has identified that IL-8 is significantly increased following chemotherapy and this increase is associated with

drug resistance, making it a an attractive potential target [544]. Additionally, MDC has been reported to be secreted by M2-like Mϕ and promotes Th2 immunity and Tregs activation [545], which also deleteriously affects anti-tumour immunity. These differentially secreted factors observed in the adipose secretome in response to chemotherapy and chemoradiotherapy in conjugation with exogenous fatty acids may indicate how the biology of adipose tissue responds to external stresses. However, a larger question which requires further research is how this altered adipose secretome could mitigate the efficacy of these cytotoxic treatments or aid cancer cells in evading their effects.

Within the adipose secretome of explants exposed to chemotherapy and chemoradiotherapy in combination with OA significant increased secreted levels of IL-1β and IL-17D were observed compared with control matched control. Similarly in the adipose secretome of explants exposed to chemotherapy and chemoradiotherapy in combination with PA increased secreted levels of IL-7, IL-15 and IL-17A were observed. These interleukins have been shown to significantly increase activation as well as sustaining Th17 immune responses [546–548]. Previously chemotherapy and chemoradiotherapy have been linked to increases in Th17 cell frequency which has been associated with therapy resistance and poor prognosis [549,550]. These elevated secreted levels of these mediators observed in the adipose secretome following exposure to cytotoxic therapies in the presence of OA and PA may have implications in wider tumour microenvironment by dampening anti-tumour immunity by promoting Th17 immunity which could enhance resistance to conventional cancer treatments.

Increased secreted levels of IL-1Ra were observed in the adipose secretome following chemotherapy combined with either OA or PA compared with the adipose secretome exposed to chemoradiotherapy combined with OA or PA. Both exposure to fatty acids and chemoradiotherapy have been shown to increase pro-inflammatory response [533]. A response which is dependent on diminished level of IL-1Ra [551], which may account for this differential levels in the adipose secretome in response to chemotherapy and chemoradiotherapy. Further to this, increased secreted levels of VEGF were observed in the adipose secretome following chemotherapy combined with either OA compared with the adipose secretome exposed to chemoradiotherapy combined with OA. VEGF expression has been reported to be upregulated following exposure to chemotherapy drugs in cancer cells [552] as well as OA in rat models [553]. In addition to this, this study reports increase secreted levels of IL-6 and TNF-α from adipose explants exposed to chemotherapy combined with PA compared with chemoradiotherapy combined with PA. PA and chemotherapy have previously been reported to enhance IL-6 and TNF-α production [284,554], both factors associated with pro-inflammatory response. In contrast,

as series of Th2 and Th17 associated mediators were observed to be increased in the secretome of adipose explants treated with chemoradiotherapy in combination with PA compared with adipose exposed to chemotherapy and PA including IL-9, IL-17A/F, IL-17B, IL-21. IL-23, and IL-31. IL-9 and IL-31 have both been reported to promote and sustain Th2 responses [555,556]. Whilst research has shown that IL-17, IL-21, and IL-23 play central roles in supporting Th17 immunity [557]. These increases in the adipose secretome could be promoted to ameliorate the radiation induced inflammation inflicted by oxidative stress generated by chemoradiotherapy in combination with PA. However, these increases could also impact the wider tumour microenvironment and detrimentally effect the efficacy of chemoradiotherapy. Interesting, IL-27 was also seen to be elevated in in the secretome of adipose explants treated with chemoradiotherapy in combination with PA compared with adipose exposed to chemotherapy and PA. IL-27, which has been widely reported to negatively inhibit both Th2 and Th17 immune responses [558,559] could play a potential role in mitigating the influence of these mediators that diminish the efficacy of anti-tumour immunity.

Additionally in this study OA in combination with chemotherapy was observed to increase secreted levels of FLT-1, IL-1α, MCP-4, sICAM-1, sVCAM-1, and VEGF compared with matched control. As previously mentioned, both chemotherapy and OA have been reported to increase VEGF [552,553]. So it is of interest that FLt-1, a receptor for VEGF is increased by similar stimuli. Further research is required to interrogate this link and whether this increase in angiogenic mediators secreted by adipose tissue could contribute to the angiogenesis caused by these treatments in the wider tumour microenvironment. These effects were not mirrored in the adipose secretome of explants exposed to chemoradiotherapy and OA treatment. In contrast, PA in combination with chemotherapy was observed to increase adipose secreted levels of IL-2, MCP-1, TARC and decrease TNF-α . IL-2 possesses a critical role in T cell expansion and differentiation as well as aiding in stimulating cytotoxic effector cells [451]. TNF-α has been widely reported for its pro-inflammatory effects and its regulation of macrophage function [453], Previous research has shown that docetaxel lead to increased IL-2 and decreased TNF-α in circulation [560], an effect which may be promoted by PA. MCP-1 is a key chemokine that regulates migration and infiltration of monocytes and macrophages [446] and as previously mentioned TARC has been reported to play a central role in stimulating Th2 driven immunity [540]. In addition to this, TARC has also been reported to be secreted by M2-like macrophages. PA and chemotherapy in combination leading to this enhanced levels of MCP-1 and TARC could potentiate anti-tumour immunity be promoting M2-like macrophages, known to mediate chemoresistance [246].

Interestingly these effects were not echoed in the adipose secretome of explants exposed to chemoradiotherapy and PA treatment. Instead, PA in combination with chemoradiotherapy showed increased secreted levels of IL-9, IL-23, and VEGF-C compared with matched control. As previously mentioned IL-9 and IL-23 have both been reported to promote and sustain Th2 and Th17 responses [555,557]. Indicating that PA could augment the radiation induced damage evoked by chemoradiotherapy and the induction of these cytokines could be amelioratory. However again, it brings into question what influence this altered adipose secretome has for the wider tumour microenvironment particularly cancer cell function and anti-tumour immunity.

Cellular metabolism is a multifaceted mitochondrial process and mitochondrial dysfunction commonly induced by cancer cells to aid tumour progression is an even more complex system [286,561]. This study reports increased maximal and ATP-linked respiration by oesophageal cancer cell line OE33 cultured within the secretome of adipose explants exposed to chemotherapy and chemoradiotherapy. Increased maximal respiration is an indication of response to external stress, whilst increased ATP-linked respiration indicates an increase in ATP demand, which can be linked to cellular proliferation [500]. Additionally, studies have shown that high ATP levels enhance cancer cells resistance to chemotherapy [562]. Interestingly OE33 exposed to chemotherapy treated ACM showed increased basal respiration and ECAR whilst cells cultured with chemoradiotherapy showed increased spare respiratory capacity. A high basal OCR indicates that cells are using a higher percentage of the maximal rate of respiration and indicates they may not have enough reserved capacity to meet the cellular energy demands required through oxidative phosphorylation alone [500]. Spare respiratory capacity is depleted under extreme oxidative stress, in this occurrence where oxidative phosphorylation fails to reach the threshold required to sustain the energetic needs of the cell, glycolysis is stimulated to meet energy demands [498]. This high basal OCR and switch to glycolysis in OE33 cultured with chemotherapy treated ACM may indicate a higher presence of oxidative stress and mitochondrial dysfunction. In addition to this OE33 cultured with chemotherapy treated ACM showed increased levels of proton leak. Proton leak has been linked to a series of factors such as damaged induced to the inner mitochondrial membrane or increased uncoupling protein activity [500]. Uncoupling proteins are known to interfere with ATP production by inducing proton leak, UCP2 in particular has been reported to be expressed in aggressive cancers and has been implicated in promoting chemoresistance [563]. Conclusively, chemotherapy treated ACM promotes mitochondrial dysfunction and increased reliance on glycolysis in OE33, effects that are not observed in cells cultured with chemoradiotherapy treated ACM. These effects which

may be perpetuated by the adipose secretome are essential mechanisms that are evoked by cancer cells to evade cell death and enhance chemoresistance.

OA has been reported to have anti-tumour effects [64]. OE33 cultured with ACM treated with chemoradiotherapy in combination with OA showed decreased maximal respiration, spare respiratory capacity compared with matched control. Further to this OE33 cultured with ACM treated with chemotherapy and OA showed increased non-mitochondrial oxygen consumption compared with OE33 cultured with ACM treated with chemoradiotherapy in combination with OA. Maximal respiration, a measure of a cell response to external stress, has been reported to be diminished in response to oxidative stress [564]. Spare respiratory capacity as previously mentioned has also been reported to be depleted under extreme oxidative stress [498]. Non-mitochondrial oxygen consumption involves oxygen consuming process that are not associated with the mitochondria [500]. These processes involve enzymes associated with the induction of inflammation, lipoxygenases and have particularly been reported to be increased in the presence of stressors like reactive oxygen species [565]. This profile shows enhanced mitochondrial dysfunction, which may indicate that OA enhances the oxidative stress induced chemotherapy in OE33 cells which could be further perpetuated by the adipose secretome. In contrast OE33 cultured with ACM treated with chemotherapy in combination with PA showed increased basal respiration, ATP linked respiration and OCR:ECAR ratio. These profiles indicate that whilst cells may require increased ATP potentially to recover and proliferate following exposure to ACM treated with chemotherapy and PA, oxidative phosphorylation levels are increased both basally and preferential over glycolysis. Interestingly, inhibition of oxygen consumption has been reported to be a potential target to combat tumour hypoxia, which is a known inducer of radioresistance [566]. This effect that could be enhanced by PA upregulation of fatty acid oxidation associated genes [567] which are also upregulated by hypoxia [568].

Dendritic cells possess a critical role in initiating anti-tumour immunity, through antigen presentation. Chemotherapy has previously been reported to increase DC antigen presentation [242], however induction of DC response following radiotherapy was shown to be dependent on an active immune infiltrate already being present [243]. DCs cultured with ACM treated with chemotherapy showed increased expression of HLA-DR, CD11c, CD40, CD54, CD86. CD40 plays an essential role in activating DC maturation leading to increased expression of CD80/CD86 and production of IL-12 [569], whilst CD54 supports DC adhesion and activation of T cells [424,570]. CD86 is widely reported for its role in DC maturation, polarisation of Th1 response and activation of NK cells [420]. This upregulation of a series of factors that promote DC maturation, and T cell priming may

indicate that the chemotherapy treated adipose secretome may aid in promoting anti-tumour immunity enhancing treatment efficacy. However, DCs cultured with ACM treated with chemotherapy or chemoradiotherapy showed increased expression of TIM-3. Tim-3 expression on DCs has been reported to inhibit antitumour immunity by inhibiting inflammasome activation [426], which may act as a diminishing influence on the cytotoxicity of these treatments.

Interestingly, DCs cultured with ACM treated with chemotherapy combined with PA showed decreased expression of TIM-3 and PD-L1. PD-L1 expression on DCs has been shown to attenuate T cell activation [427], and as previously mentioned TIM-3 also diminishes anti-tumour immunity. Depleted levels of these markers known to diminish the efficacy of DC antigen presentation could prove beneficial in revitalising anti-tumour immunity. However, DCs cultured with ACM treated with chemoradiotherapy combined with PA showed decreased expression of CD40, CD54, CD86 and increased CD83. Further to this DCs cultured with chemotherapy and chemoradiotherapy in combination with PA showed decreased co-expression of CD80 and CD86 co-stimulatory molecules compared with DCs cultured with chemotherapy and chemoradiotherapy combined with OA. Whilst PA seems to promote the decrease of immuno-inhibitory factors it also depletes levels of markers known to activate and sustain DC presentation and T cell activation. These paradoxical effects of the adipose secretome treated with chemoradiotherapy and PA on DC biology pose an interesting question on whether loss and gain of function could be interlinked.

Macrophages in both their pro-inflammatory and anti-inflammatory phenotypes play a central role in cancer progression and treatment resistance. Anti-inflammatory or TAMs have reported to be induced by chemotherapy [245] as well as mediating chemoresistance [246]. On the other hand, pro-inflammatory macrophages have been reported to play a vital role in radiation induced inflammation, inducing an anti-tumour immunity through the generation of an inflammatory response [247]. This study reports in unpolarised Mϕ, the adipose secretome of explants treated with chemoradiotherapy significantly decreased expression of phenotypic markers CD68 but increased expression of inflammatory markers CD80, CD86 and co-expression of CD80 and CD86. In contrast, Mϕ cultured with chemotherapy showed increased co-expression of CD163 and CD206 markers known to be associated with a TAM like phenotype. It is interesting to observe chemoradiotherapy treated ACM enhancing M1 associated markers and chemotherapy treated ACM upregulating expression of M2 associated markers which speaks to the opposing mechanisms of action these cytotoxic therapies induce. However, Mϕ cultured with chemotherapy and chemoradiotherapy treated ACM showed increased expression of TIM-3. TIM-3 has previously been reported to evoke the development of TAMs

[571] and expression of TIM-3 on TAMs has been correlated with more aggressive cancers and poorer survival rates in patients [572]. Additionally, Mϕ cultured with ACM treated with chemoradiotherapy combined with PA showed decreased expression of phenotypic marker CD68 and increased expression of anti-inflammatory marker CD206. This may indicate that the enhanced inflammatory response induced by chemoradiotherapy, and PA treated ACM on Mϕ may stimulate an anti-inflammatory reaction to compensate but further research is required is to interrogate this reaction.

Interestingly in M1-polarised Mϕ cultured with chemotherapy increased expression of CD11b, CD11c, HLA-DR, CD80, CD86, CD80+CD86+ and TIM-3 was observed. The chemotherapy treated ACM may perpetuate the effects of Mϕ priming towards a pro-inflammatory phenotype. Such an occurrence could prove as an attractive therapeutic target to diminish the induction of TAMs by chemotherapy regimens [245] but further research is required to investigate if there is any utility in this relationship. M2-polarised Mϕ cultured with chemotherapy showed increased expression of HLA-DR compared with matched control as well as decreased viability, CD68 and increased CD11c compared with Mϕ cultured with ACM treated with chemoradiotherapy. Whilst M2-polarised Mϕ cultured with chemoradiotherapy showed increased expression of anti-inflammatory associated marker CD206 compared with matched control. CD206 is a powerful inducer of anti-inflammatory response that stimulates the release of cytokines known to resolve inflammation such as IL-10, IL-13, and TGF-β [573]. Mϕ primed by IL-4 for anti-inflammatory response may upregulate expression of CD206 following exposure to ACM treated with chemoradiotherapy in an attempt to resolve the resulting radiation induced inflammatory signals. Intriguingly, M1-polarised Mϕ cultured with chemoradiotherapy in combination with OA significantly decreased M1 pro-inflammatory markers CD80, CD86 and CD80+CD86+ as well as CD68, TIM-3 compared with Mϕ cultured in chemotherapy in combination with OA. OA is known for its anti-inflammatory effects [574], potentially its action here is to resolve inflammatory responses incited by LPS stimulation in combination with inflammatory inducing chemoradiotherapy. In contrast, M2-polarised Mϕ cultured with chemoradiotherapy in combination with PA significantly decreased M2 anti-inflammatory markers CD163, CD206 and CD163+CD206+ as well as increasing CD68 compared with Mϕ cultured in chemotherapy in combination with PA. M2-polarised Mϕ cultured with chemoradiotherapy in combination with PA significantly decreased TIM-3 expression compared with Mϕ cultured with chemoradiotherapy combined with OA. PA has been widely reported for its pro-inflammatory effects particularly in macrophages [65]. It is of interest that ACM treated with PA combined with inflammation inducing chemoradiotherapy significantly decreased anti-inflammatory

associated markers [575] and TIM-3, a factor reported to induce M2 like TAMs [245] particularly under the inciting stimulus of IL-4.

Conclusively for the first time this study has shown that chemotherapy and chemoradiotherapy differential alter adipose tissue metabolism and secreted factors, with chemoradiotherapy significantly increasing pro-inflammatory associated mediators. Exogenous fatty acids were observed to differentially alter the adipose secretome in response to these therapies. However, both therapies combined with exogenous fatty acids showed significant increases in mediators of Th17 associated immune response. The chemotherapy treated adipose secretome enhanced mitochondrial dysfunction in cancer cells as well as increasing their reliance on glycolysis. Chemotherapy treated ACM significantly increased DC maturation markers and M2-like phenotypes in unpolarised Mϕ. Whilst chemoradiotherapy significantly increased M1-like phenotypes in unpolarised Mϕ, but in combination with OA it decreases M1 primed expression of pro-inflammatory and in combination with PA decreased M2 primed expression of anti-inflammatory markers. Adipose tissue is a regulatory organ with so many poorly understood downstream effects but is central to the development of so many obesity-associated cancers. We have demonstrated that chemotherapy, chemoradiotherapy and exogenous fatty acid treatment can significantly alter the metabolic preferences and secretome of adipose tissue. Alterations in the adipose secretome could potentiate anti-tumour immunity and treatment efficacy, therefore further interrogation is required to fully elucidate the influence adipose tissue may have in treatment response.

# *Chapter 7*

# *Discussion and future directions*

## 7.1 Discussion

Obesity is a major clinical challenge that confers increased risk for numerous metabolic and malignant diseases. Whilst many cancers have been linked to increased visceral adiposity, OAC is one of the most closely associated cancers with obesity [311], perhaps in part due to its close anatomical proximity to the visceral adipose depot. The influence of obesity in cancer progression and treatment response is an urgent clinical challenge, as the obesity epidemic is predicted to increase exponentially with the World Obesity Atlas of 2023 predicting that by 2035, 51% of the global population will be overweight or obese [576]. Adipose tissue is detrimentally effected by obesity leading to a dysfunctional biology, primed to support a chronic low-grade inflammatory state linked to metabolic disease and cancer development [73,74]. However, what precise roles adipose tissue plays in the development of disease and altering the efficacy of interventional treatments is an understudied area of translational research.

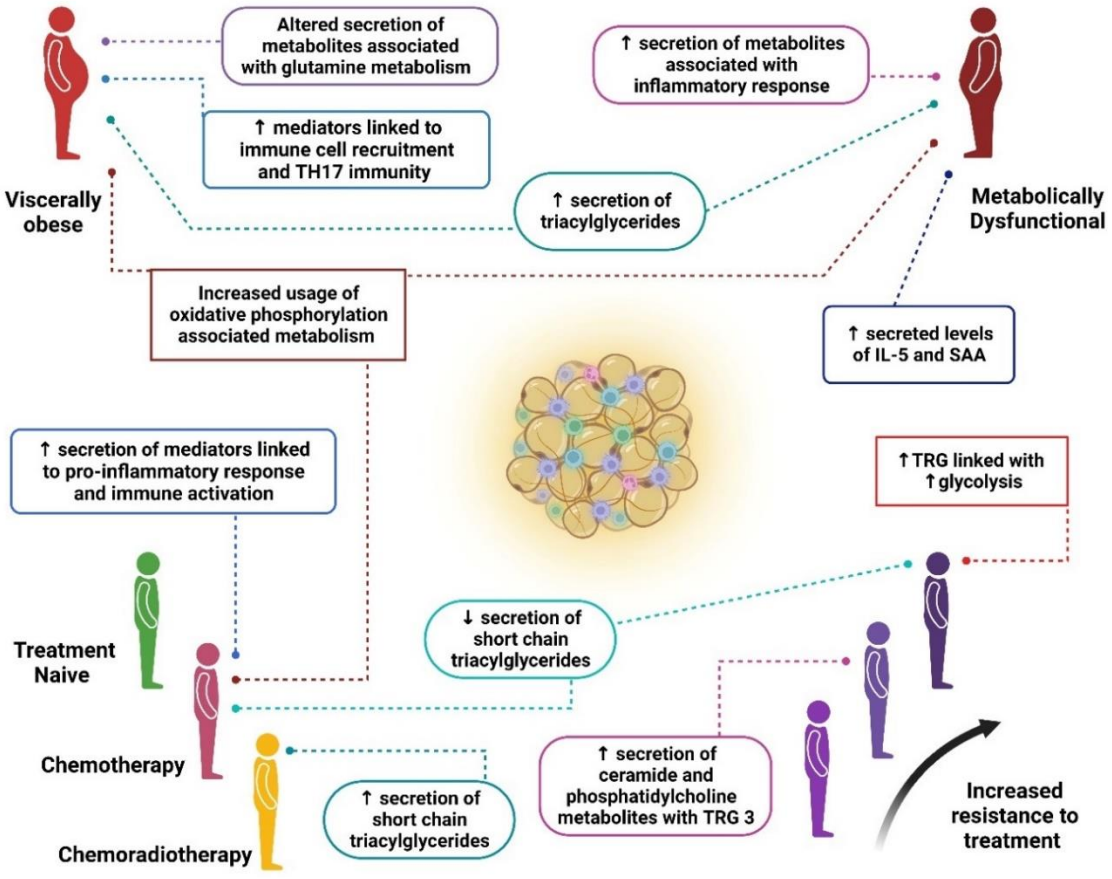


**Figure 7.1.1 Schematic figure depicting the main findings of chapter 2.**
This figure illustrates the associations observed between adipose tissue metabolism and its secreted factors compared with clinical demographics associated with OAC patients including obesity, metabolic dysfunction, previous treatment exposure and response to treatment.

In chapter 2, we examined the associations from adipose tissue metabolism and its secreted factors with detailed OAC patient demographics. Interestingly, we observed that visceral obesity, metabolic dysfunction, and previous exposure to chemotherapy regimen FLOT increased adipose tissue reliance on oxidative phosphorylation associated metabolism. Increased utilisation of oxidative phosphorylation has been linked to increased ROS production, a reaction that has previously been linked to obesity, metabolic diseases and chemotherapy [577,578]. Interestingly the induction of reactive oxygen species (ROS) has been linked to propagating inflammatory disorders [579] and could be indicative of a possible mechanism adipose tissue invokes to establish chronic low-grade inflammation. Increased ROS production has also been linked to chemotherapy exposure [580]. This type of induced oxidative stress has been linked to decreased secreted adipokines [56] that are known to support cancer growth and such a decrease maybe beneficial. However, aberrant adipokine secretion is linked to metabolic disorders such as diabetes [56], which can be induced by chemotherapy, and adipose tissue could aid in this response. Further to this, adipose tissue from patients who had the poorest response to treatment showed increased reliance on glycolytic metabolism. This could be indicative of biological changes in adipose tissue as it primes to support cancer development and metastatic movement. A metabolic shift towards glycolysis would signify increased energetic demand by the adipose tissue and could be linked to the release of free fatty acids or other fuel sources into the tumour microenvironment to support cancer growth, forcing this increased reliance on glycolysis.

The adipose secretome particularly in obese patients has been reported to be pro-tumorigenic through its secretion of chemokines, growth factors, and fatty acids that aid cancer cell growth [581]. In our studies, adipose tissue derived from the most viscerally obese of patients exhibited increased secreted levels of mediators associated with immune cell recruitment and TH17 response. Previously immune cells have been reported to be recruited to adipose tissue where they lose functionality, thus diminishing the anti-tumour immune response. Th17 immunity leads to the secretion of IL-17 that not only aids cancer progression but can stimulates myeloid cell infiltration [270,271] allowing the propagation of obesity associated inflammation. Increased levels of IL-5 and SAA were observed in the adipose secretome of metabolically dysfunctional OAC patients, both factors have previously been linked with metabolic disorders [341,582]. Elevated levels of SAA have been associated with poor overall survival in patients with solid malignancies [583], whilst IL-5 has been reported to be induced by inflammation and linked with increased metastatic activity [584]. Taken as a whole, the adipose secretome in patients who demonstrate metabolic dysfunction and obesity could diminish the efficacy of anti-tumour

immunity. In contrast, we observed that previous exposure to chemotherapy regimen FLOT increased secreted levels of mediators known to be associated with pro-inflammatory response and immune cell activation. This could prove a beneficial addition to the tumour environment by inciting anti-tumour immunity by increasing effector immune cells and leading to cancer cell death.

Additionally, obesity was observed to differentially alter the secretion of key metabolites associated with glutamine metabolism in the adipose secretome. Glutamine was observed to be decreased in the adipose secretome of obese patients which lies in line with literature [585], whilst glutamate was observed to be increased. The differentially expression of these metabolites might indicate that shifts in metabolic mechanisms and free glutamine in the adipose secretome of non-obese patients may be utilised by cancer cells undergoing malignant transformation [586]. However, it must be noted that increased secretion of glutamate may be indicative of increased glutamine metabolism leading to excess formation of its catalysed product [587]. Interestingly again we observed that metabolic dysfunction increases adipose explant secretion of key metabolites associated with pro-inflammatory response that perpetuate metabolic disorders. Obesity and metabolic dysfunction were further associated with increased secreted levels of triacylglycerides in the in the adipose secretome which is in line with literature [588,589]. This enriched adipose secretome could be postulated to support cancer growth and provide support in the establishment of metastasis. Interestingly increased levels of ceramides and phosphatidylcholines were observed in the adipose secretome of patients who showed a partial response to current modalities of cancer treatment. Ceramide metabolism has been reported to be cytotoxic and increased expression of ceramide has been associated with better prognosis for cancer patients [590,591]. Phosphatidylcholine metabolism on the other hand has been linked with regulating resistance to cancer treatment [379]. It is of interest that both metabolites are upregulated in the adipose secretome of patients who only partially respond to therapy, highlighting the key question whether the adipose secretome could aid in these opposing metabolic responses that might mitigate the efficacy of therapy? Additionally, previous exposure to chemotherapy treatment and poor responders to cancer treatment were observed to have decreased levels of short chain triacylglycerides. Chemoradiotherapy on the other hand showed increased secreted levels of short chain triacylglycerides in the secretome of adipose explants. Interestingly previous research has highlighted that short chain fatty acids have anti-tumour effects [592]. Therefore, it is noteworthy, that these short chain triacylglycerides are decreased in the adipose secretome of the poorest responders to therapy. However, the increased level of short chain triacylglycerides in the

adipose secretome of patients treated with chemoradiotherapy could prove beneficial in mediating an anti-tumour response. It may also potentially highlight a different mechanism of action compared with chemotherapy alone which had a conflicting result, seeing a decrease in these triacylglycerides.

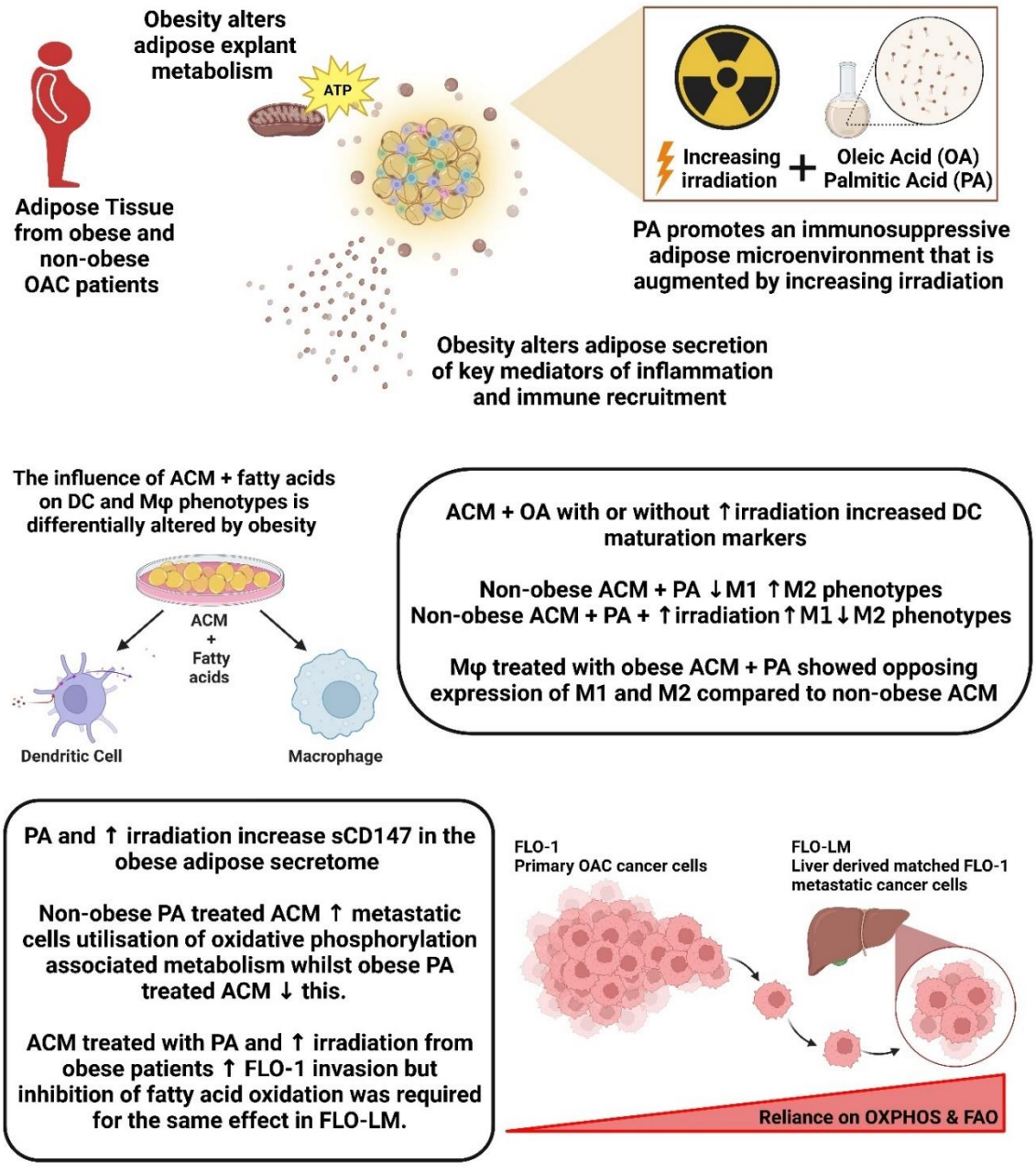


**Figure 7.1.2 Schematic figure depicting the main findings of chapter 3, 4 and 5.**
This figure illustrates the influence of exogenous fatty acids and increasing radiation on adipose tissue metabolism and its secreted factors. It details how this altered adipose secretome effects DC maturation, Mϕ polarisation and the metabolic and invasive capacity of primary OAC (FLO-1) and matched liver derived metastatic cancer cells (FLO-LM).

Adipose tissue possesses the ability to not only secrete factors that can alter the pro-inflammatory landscape of the tumour environment but also co-ordinate the release of free fatty acids that support cancer metabolism and growth [112,593]. Saturated fatty acids such as palmitic acid have been linked with pro-inflammatory response [65] whilst unsaturated fatty acids including oleic acid have been reported to act in anti-inflammatory manner [66] as well as ameliorating the pro-inflammatory effect of saturated fatty acids [67]. Further to this, fatty acid levels in the circulation and within adipose tissue have also been reported to be abrogated by obesity. Increased palmitic acid (PA) has been observed in circulation in obese patients [68] and increased Oleic Acid (OA) in adipose tissue of obese mouse models [69]. Within chapter 3 we observed PA diminishing adipose explant utilisation of oxidative phosphorylation associated metabolism in addition to eliciting an immunosuppressive effect. on the adipose secretome. These effects are most apparent in adipose tissue from OAC cancer patients compared with non-cancer patients which may be indicative of biological changes that prime adipose tissue to support the development of pre-metastatic niches. Particularly, we observed that PA reduced secreted levels of IFN-γ, IL-12p70, and TNF-α, mediators known to drive anti-tumour immunity. IFN-γ and TNF-α play a critical role in activating signalling pathways that trigger cell death by enhancing killing efficiency of tumour-infiltrating M1 Mϕ and priming TH1 responses [594,595]. IL-12p70 also aids anti-tumour immunity through promoting Th1 responses [353]. Decreased secreted levels of these mediators of anti-tumour immunity in the adipose secretome could lead to diminished functionality of immune cells that infiltrate adipose tissue as well as having wider more detrimental effects in tumour microenvironment.

Intriguingly, secreted levels of IL-1β were observed to be decreased by OA in the adipose secretome non-cancer patients compared with PA treatment, an effect that lies in line with literature. However, in the adipose secretome of OAC cancer patients PA treatment reduced secretion of IL-1β compared with OA. We hypothesise that the underlying biology of adipose tissue in OAC patients may undergo transformation to make it more amenable to support the growth and migration of cancer cells, which may alter phenotypical responses to exogenous treatment. Further to this, the adipose secretome of OAC patients demonstrated altered secretion of factors that could aid pro-tumour immunity. Particularly IL-2, known to promote TH1 responses was decreased in the adipose secretome of OAC patients compared with non-cancer patients [596]. Additionally, IL-10 and IL-13, known for their anti-inflammatory effects and their stimulation of pro-tumour immunity [597,598], were increased in the adipose secretome of OAC patients compared with non-cancer patients. This altered adipose milieu may amplify the immune evasive capacity of the tumour microenvironment diminishing the efficacy of anti-

tumour immunity. Interestingly, the immuno-inhibitory effects of PA on the adipose secretome were more evident in the adipose tissue of obese OAC patients compared with their non-obese counterparts. We observed decreased secreted levels of immunostimulatory cytokines IFN-γ, IL-1β, and IL-2 that stimulate anti-tumour immune responses. In chapter 4, we observed that the diminishing effect of PA on adipose utilisation of oxidative phosphorylation and the immunosuppressive effect of PA on the adipose secretome were further augmented by increasing irradiation. Intriguingly, increasing irradiation has been linked with enhancing systemic anti-tumour immunity [599] so this repressive effect of PA on the adipose secretome could potentiate the benefits induced by radiotherapy.

The immune system plays a pivotal role in both tumour initiation, progression and mitigating the effects of cancer treatment [600–602]. Adipose tissue recruits immune cells whilst having deleterious effects on their function, this can potentiate anti-tumour immunity [81–85]. We see this effect is increased in obese patients which may be linked to the elevated levels of immune recruiting cytokines, seen in chapter 2. Interestingly in chapter 3 and 4, we observed that the fatty acid treated adipose milieu led to downstream effects on innate immune cell function. OA treated ACM regardless of irradiation exposure was observed to increase DC expression of maturation markers. However, DCs cultured in the unirradiated OA treated adipose secretome demonstrated decreased expression of CD54 compared with control and non-cancer patients. Whilst an increase in maturation of DCs could prove beneficial in the tumour microenvironment, by increasing the efficacy of antigen presentation and cross priming of T cells. CD54 holds a significant role in creating strong adhesion interactions between DCs and T cells to allow for stimulation, which could mitigate the functionality of mature DCs. Therefore, it is of interest that following exposure to irradiation this decreased expression of CD54 is lost, which again could be indicative of the influence of increasing irradiation enhancing systemic anti-tumour immunity [599]. Intriguingly, ACM derived from OAC cancer patients also increased DC expression of immunoinhibitory markers PD-L1 and TIM-3 compared with non-cancer patients. PD-L1 expression on DCs is known to attenuate T cell activation [603], whilst TIM-3 inhibits anti-tumour immunity through regulation of inflammasome activity [426]. The adipose secretome of OAC patients appears to be altered in a manner that is supportive of immuno-inhibitory action. This could be a pro-tumour adaptation in adipose tissue to enhance cancer cell's ability to grow and metastasize in an environment with diminished immune surveillance.

Macrophages have been reported to play a vital role in radiation induced inflammation inducing an anti-tumour immunity response through the generation of an inflammatory response promoting classical activation and increased expression of pro-inflammatory mediators [247].

Additionally, increased free fatty acids, which have been reported in obesity, enhance Mϕ polarisation towards M1-like phenotype [283]. Therefore, it is of interest that within chapter 3 and 4 Mϕ phenotype and response towards exogenous PA appeared most profoundly altered by the exposure of the adipose secretome to increasing irradiation which demonstrated confounding effects that were further augmented by patient obesity. The adipose secretome of non-obese patients treated with PA decreased expression of markers associated with M1 phenotypes and increased markers associated with M2 phenotypes. In contrast, PA treated adipose secretome of obese patients differentially effected expression of these markers, increasing M1 markers and decreasing M2 markers. However, following exposure of these adipose explants to increasing irradiation in combination with PA treatment led to a non-obese adipose secretome that increased markers of M1 phenotypes and decreased expression of M2 associated markers. Opposing effects were observed in Mϕ following culture with similarly treated adipose secretome from obese patients, with decreased expression of M1 markers and increased expression of M2 markers. This opposing response of Mϕ towards the PA treated adipose secretome of non-obese and obese patients, an effect that is inversed following exposure to radiation, may indicate underlying adipose biology that could be exploited to enhance treatment planning and in turn its efficacy. The adipose secretome has previously been postulated as a potential attractive therapeutic target to potentiate tumour progression and enhance treatment efficacy [79]. Cancer associated adipocytes (CAAs) are one factor that is being actively targeted to improve treatment responses. Targeting of CD36, a central fatty acid transporter within the cell is currently being explored to mitigate tumour cells lipid uptake from CAAs. CD36 has been linked to promoting chemoresistance in cancer cells and inhibition of CD36 has been reported to evoke immunostimulatory effects and decreased tumour aggressiveness *in-vitro* [521,522]. Recent reports have also linked treatment resistance in tumour cells with their ability to invoke a metabolic switch from glycolysis to lipid metabolism actively relying on fatty acids within the cell to evade the cytotoxic effects of chemotherapy. Inhibition of Fatty acid synthase (FASN) in combination with chemotherapy has been reported to increase the efficacy of these chemotherapy in treatment resistant cancers both in *in-vitro* and *in-vivo* [523,524].

Primary and metastatic cells have been widely reported to utilise different metabolic pathways [513]. Metastatic cells in particular have been reported to have enhanced metabolic flexibility which aids their migratory capacity to establish distant metastasis [604]. Within chapter 5 we observed that primary and metastatic cells have differential metabolic preferences. Primary cells utilise glycolytic metabolism whilst metastatic cells have a greater reliance on oxidative phosphorylation which lies in line with literature [497,605]. Additionally metastatic cells were

observed to have greater spare respiratory capacity which is known to aid in radioresistance [606]. Under stress and increased energy demands, cells invoke this mitochondrial spare reserve. Oxidative stress has been reported to decrease spare respiratory capacity and increase cell reliance on glycolytic metabolism to overcome this strain and meet cellular energy needs. Oxidative stress is induced following cancer cell exposure to the cytotoxic effects of chemotherapy or radiation induced inflammation invoked by radiotherapy. It is of interest that metastatic cells are conferred with these altered metabolic preferences and spare reserves which could be indicative of why they are so resistant to current cancer treatments. Further to this, the PA treated adipose secretome of non-obese patients increased metastatic cells utilisation of oxidative phosphorylation associated metabolic pathways. However, PA treated adipose secretome of obese patients decreased this preference in metastatic cells. This differential utilisation of metabolic parameters by metastatic cells in the face of non-obese and obese adipose secretome following PA treatment again could be suggestive of the variation in their biological composition. Which potentially could be linked to the aberrant secretion of glutamine and glutamate that was observed in chapter 2 with obesity, which could indicate the utilisation of glutamine metabolic pathway or the tricarboxylic acid cycle, both of which are influenced by glutamate [607].

Whilst flexibility in energy metabolism is critical in aiding cancer cell's ability to migrate to facilitate distant metastasis [304], other factors have also been identified to enhance this process. Previously, secreted levels of CD147 have been linked to invasion and metastasis [488]. CD147 is increased both in circulation and within visceral adipose depots of obese patients [491]. In our work, secreted levels of CD147 were increased following exposure to fatty acid treatment or increasing radiation. Interestingly when patient cohorts were split into obese and non-obese, the effect of increasing radiation on sCD147 levels was only observed in the obese adipose secretome. Additionally, PA treatment on the adipose tissue from obese OAC patients showed increased secreted levels of sCD147 compared with similarly treated adipose tissue of non-obese OAC patients. CD147 has been linked to the promoting cathepsin B production through induction of β-catenin by reduction of GSK-3β [489] . Cathepsin B has also been linked with IL-1β activation and inflammatory response or alternatively, inducing apoptotic signalling to mitochondria by increasing bid and bax while inhibiting bcl-xl, leading to cell death [490]. This altered secretion of CD147 that are augmented by increasing radiation, obesity and PA treatment in the adipose secretome could prove an attractive therapeutic target to mitigate the invasive support adipose tissue affords cancer [489,491].

Adipose tissue and its secretome can prime the development of pre-metastatic niches and are utilised for their enriched environment that has inhibitory effects on immune cell function [307]. We observed increased invasion of both primary and metastatic cell lines towards the adipose secretome of non-obese patients regardless of fatty acid treatment, which may be linked to the increased level of glutamine observed in the adipose secretome of non-obese patients (chapter 2). Certain cancers have been shown to become addicted to glutamine during their transformation and depletion of this metabolite can inhibit invasion and migration [608,609]. Interestingly, PA treated adipose secretome of obese patients increased primary cancer cells invasive capacity. However, in metastatic cells increased invasion towards the PA treated adipose secretome of obese patients was only observed following inhibition of fatty acid oxidation (FAO). This could be indicative of the decreased availability of glutamine in the obese adipose secretome. However, it further indicates the reliance of metastatic cells on their spare respiratory reserve and only following inhibition of FAO is their metabolic needs jeopardised leading them to become more invasive. Additionally, this result showing primary cells increased invasive capacity towards the adipose secretome, demonstrates just how pivotal adipose tissue is in the development of primary metastatic niches that support the development of distant metastasis [610].

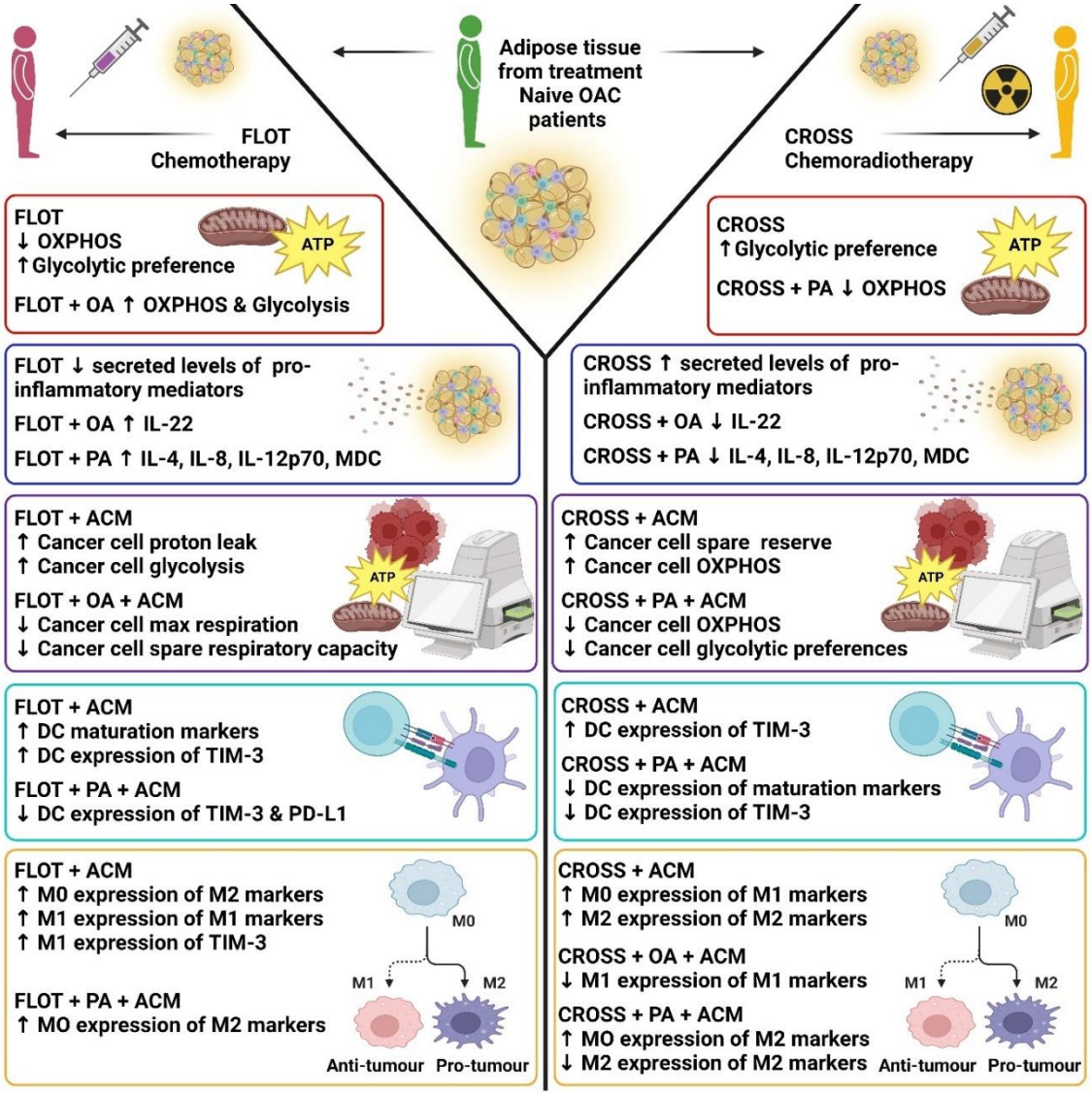


**Figure 7.1.3 Schematic figure depicting the main findings of chapter 6.**
This figure illustrates the influence of chemotherapy regimen FLOT and chemoradiotherapy CROSS on treatment naïve OAC adipose tissue metabolism and secreted factors and whether these treatments are influenced by exogenous fatty acid treatment. It further details how this altered adipose secretome effects DC maturation, Mϕ polarisation and the metabolic parameters of OAC cell line OE33.

Currently, the standard of care for treatment of OAC involves neo-adjuvant chemotherapy or combination chemo-radiotherapy for locally advanced tumours [19]. Unfortunately, only approximately 30% of patients show a complete response to these modalities of treatment, leaving a large proportion of patients with no therapeutic gain and a possible delay to surgery [309,310]. The question remains whether adipose tissue biology plays a role in treatment response, which has never been fully addressed in this field.

Within chapter 6, we observed that exposure of adipose explants to chemotherapy regimen FLOT decreased oxidative phosphorylation associated metabolism and increased its utilisation of glycolytic metabolism. Interestingly we had previously seen in chapter 2 that patients exposed to FLOT regimen had increased utilisation of oxidative phosphorylation compared with patients who were treatment naïve. This could be evidence of an initial response to the cytotoxic effects of the chemotherapy regimen as metabolism shifts towards a glycolytic preference to ameliorate oxidative stress and repair from chemically induced damage [295]. Similarly following adipose explant exposure to chemoradiotherapy regimen CROSS, we observed an increased preference for glycolytic metabolism. This could be indicative of a metabolic shift to compensate for radiation induced inflammation and oxidative stress.

Interestingly, when FLOT regimen was combined with OA treatment, adipose explants showed increased utilisation of both oxidative phosphorylation and glycolysis associated metabolic pathways. This could be indicative of improved mitochondrial health as both pathways are being utilised to provide the energetic needs of the cell whilst undergoing stress. However, when PA was combined with CROSS regimen a decreased utilisation of oxidative phosphorylation was observed in adipose explants. This mirrors previous findings in chapter 3 where PA in combination with increasing irradiation diminishes adipose explant's ability to use oxidative phosphorylation associated metabolism. This raises the question whether the impact of radiation with PA in the adipose explant is the causal factor in this setting and if the chemotherapeutic aspects of this regimen bear any influence. This diminishing effect of PA on oxidative phosphorylation in adipose explants was not observed following exposure to FLOT regimen.

Chemotherapy and chemoradiotherapy have been reported to deleteriously impact the adipose secretome in such a manner that aids cancer metastasis and survival from cytotoxic interventions [78]. The differential effects of these therapies were significantly evident in the secretome of these adipose explants, with FLOT regimen decreasing secreted levels of pro-inflammatory mediators and CROSS regimen increasing these. This could be indicative of the radiation induced inflammation commonly associated with radiotherapy [534]. Whilst both therapies in combination with fatty acids appeared to induce the secretion of factors associated with Th17 immune responses in the adipose secretome. Th17 immune responses can be paradoxical, stimulating tumour progression and regression [611]. The elevation of these factors in the adipose secretome could lead to confounding effects in the wider tumour microenvironment.

Interestingly, fatty acids in combination with these treatments stimulated differential secretion of key mediators associated with inflammatory response and immune activation. FLOT in combination with OA increased adipose secreted levels of IL-22, whilst CROSS and OA decreased these levels compared with their matched control. Additionally, FLOT in combination with PA increased levels of IL-4, IL-8, IL-12p70, and MDC, whereas CROSS and PA decreased the secretion of these analytes in the adipose secretome compared with their respective matched controls. It is of interest that chemotherapy in combination with exogenous fatty acids leads to an increase in factors that prime for immune activation and pro-inflammatory response, whilst an opposing effect is observed with chemoradiotherapy. Previously we observed that FLOT chemotherapy alone decreased the expression of pro-inflammatory mediators, but upon the introduction of these fatty acids that profile is reversed. When we further consider that fatty acids have been shown to be elevated in obese patients, this association may act as a beneficial contribution to the efficacy of chemotherapy. Studies have previously shown that obese patients show increased levels of complete pathological response and progression free survival in response to chemotherapy compared with non-obese patients [612,613], which further highlights the question does adipose tissue contribute to this outcome?.

Aberrant cellular metabolism has been widely reported to be induced by cancer in order to evade the cytotoxic effects of chemotherapy and chemoradiotherapy [191,287]. Interestingly, we observed that the FLOT treated adipose secretome increased cancer cells utilisation of glycolytic metabolism and increased proton leak. As previously mentioned, a switch to glycolytic metabolism has been reported to be induced under stress in order to meet the energetic demands of a cell and proton leak can be an indication of mitochondrial damage [500]. In contrast, the CROSS treated adipose secretome increased cancer cell utilisation of oxidative phosphorylation associated parameters and increase spare respiratory capacity. Increased spare respiratory capacity is indicative that a cell can survive increased stress without switching preferences to glycolytic reserves. These results indicate that adipose exposure to chemotherapy elicits a higher induction of oxidative stress and mitochondrial dysfunction which may enhance cancer cell death. The effect of chemoradiotherapy on the adipose secretome seems to confer cancer cells with greater survival advantages. Interestingly, the adipose secretome treated with FLOT in combination with OA decreased cancer cells maximal respiration and spare respiratory capacity. However, the adipose secretome treated with CROSS and PA decreased cancer cells oxidative phosphorylation associated metabolism and increased glycolysis and glycolic preference over oxidative phosphorylation. It is of interest that the damaging influence of FLOT is augmented by OA, whilst chemoradiotherapy which enhanced

metabolic parameters of cancer cells is reversed by PA, inciting cancer cells to shift their metabolic parameters to aid survival. These differential effects of exogenous fatty acids in combination with chemotherapy and chemoradiotherapy pose an interesting question, if the concentration of these fatty acids is differentially expressed in obesity [68,69] could this be exploited to improve the efficacy of cancer treatment?.

Dendritic cells play a critical role in initiating anti-tumour immunity, through antigen presentation and cross priming of T cells [614]. We observed that the FLOT treated adipose secretome increased DC expression of maturation markers, which is in line with the published literature as chemotherapy has previously been reported to increase DC antigen presentation [242]. However, both the FLOT and CROSS treated adipose secretome were observed to increase DC expression of immunoinhibitory marker TIM-3, as previously highlighted expression of this on DCs has been implicated in restraining anti-tumour immunity [426]. Intriguingly, the adipose secretome treated with FLOT in combination with PA showed decreased DC expression of TIM-3 and PD-L1, both associated with immuno-inhibitory effects. Whilst the adipose secretome treated with CROSS in combination with PA decreased DC expression of maturation markers and TIM-3. The influence of PA on the adipose secretome combined with either cancer therapy appears to constrain the expression of immuno-inhibitory markers on DCs. This could be related to the extreme immunosuppressive effects observed following PA treatment as discussed in chapter 3. PA has emerged as a regulator of innate immunity and inflammatory processes [615]. This influence could enhance anti-tumour immunity however it could also lead to increased inflammatory response which could mitigate the efficacy of therapy, making this result paradoxical in nature.

Macrophages with both their pro-inflammatory and anti-inflammatory phenotypes play a central role in cancer progression and treatment resistance. Anti-inflammatory or TAMs have reported to be induced by chemotherapy [245] as well as mediating chemoresistance [246]. Pro-inflammatory macrophages have been reported to play a vital role in radiation induced inflammation, inducing an anti-tumour immunity through the generation of an inflammatory response [247]. We observed that the FLOT treated adipose secretome increased the expression of markers associated with M2 phenotypes on unpolarised Mϕ, whilst the CROSS treated adipose secretome increased expression of M1 markers on unpolarised Mϕ, findings which lie in line with literature [245,247]. In contrast with the unpolarised state, M1 polarised Mϕ exposed to the FLOT treated adipose secretome demonstrated increased expression of M1 markers as well as Tim-3. Whilst in M2 polarised Mϕ, the CROSS treated adipose secretome increased expression of M2 markers. These opposing responses could be influenced by the underlying

biology of adipose tissue and how it responds to these therapies, which could be differentially affected by the introduction of external stimulus such as LPS and IL-4.

Interestingly the adipose secretome treated with CROSS in combination with PA increased expression of M2 markers on unpolarised Mϕ. In contrast, the adipose secretome treated with CROSS in combination with PA decreased expression of M2 markers on M2 polarised Mϕ. This conflicting result could indicate that PA may have more repressive effects on Mϕ primed towards an anti-inflammatory state. Anti-inflammatory Mϕ are key drivers of pro-tumour immunity supporting the development of radioresistance and chemoresistance [246,616], making them an attractive therapeutic target. However, understanding how the adipose secretome could influence their response in the wider tumour microenvironment and how this is affected by interventional therapy or external fuel sources like fatty acids could play a pivotal role in constraining their pro-tumour effects. Further to this, in M1 polarised Mϕ, the adipose secretome treated with CROSS in combination with OA was observed to decrease expression of markers associated with M1 phenotypes. OA has typically been reported for its anti-inflammatory properties and the resolution of inflammation caused by saturated fatty acids [66,67]. However, in a cancer setting, this reduction of pro-inflammatory Mϕ could prove detrimental by inhibiting anti-tumour immunity, particularly given that obese adipose tissue has been reported to have increased levels of oleic acid which could further diminish treatment efficacy.

To conclude, adipose tissue has the potential to act as an influential mediator of cancer progression and treatment resistance. The adipose secretome is enriched with a series of factors that impact inflammatory and immune responses which are heavily influenced by the heterogenous patient's demographics. Further to this, addition of external stresses such as exogenous fatty acids, increasing radiation or cytotoxic drugs can differentially affect the adipose secretome, priming it to repress anti-tumour immunity and conferring cancer cells with enhanced metabolic and invasive capacity. Most significantly, this thesis identifies that obesity is a fundamental cause of the aberrant adipose tissue biology. This phenomenon leads to a wider tumour microenvironment primed to support cancer progression and the establishment of metastasis highlighting the critical need to address the cancer-obesity link and if this can be exploited to improve treatment.

## 7.2 Limitations to this study

One of the limitations of this study is in the small sample size particularly in the non-cancer cohort and treatment naïve OAC patient cohort used to assess the influence of chemotherapy and chemoradiotherapy on adipose metabolism and secreted factors. In addition to this whilst the non-cancer cohort did not have a malignant oncologic disease, they were patients undergoing surgery for benign but inflammatory diseases which could skew the population. In future studies the inclusion of obese non-cancer patients undergoing bariatric surgery could also be included to further separation the influence of inflammatory diseases and the chronic low-grade inflammatory state that is associated with obesity.

Another limitation of this study is the model of adipose explant tissue, whilst studies within our group have shown that explant models are viable for up to 72 hours, mitochondrial function in adipose tissue explants is exacerbated following 24-hour culture. Due to this there is a very short time period to assess adipose response to the treatments applied within this study. Particularly in relation to the chemotherapy and chemotherapy regimens as this study was limited to the use of a single treatment which are not a full reflection of the regimen patients undergo. Therefore, it must be acknowledged that the full regimen of chemotherapy and chemoradiotherapy may induce different responses.

Potentially these results could be reassessed in adipocyte cell lines, adipocyte cell lines which would not be a true reflection of the adipose explants that are derived from cancer patients as they lack that previous interaction with the tumour microenvironment. This interaction has been linked to changes in the underlying biology and secreted factors in adipose tissue which promote the development of pre-metastatic niches that support cancer proliferation and migration to aid in the development of distant metastasis.

Additionally, the use of cancer cell lines model to reflect primary and metastatic states of this disease may not be the most appropriate model, as it does not reflect how the tumour microenvironment augments the progression of metastatic development. Potentially these results could be reassessed in mouse models to further confirm the validity of these findings.

## 7.3 Future Directions

This research for the first time has provided a in depth analysis of adipose tissue in non-cancer and particularly in cancer patients, looking at its metabolism, secreted factors, its response to exogenous fatty acids and how the secretome of these treated adipose tissues influence dendritic cell maturation and macrophage polarisation. As well as assessing the response of cancer adipose tissue to increasing irradiation and chemotherapy and how these are influenced by patient obesity. Thus, it has led to development of many future directions to further interrogate these findings

1. Firstly, further insight is required to assess the mechanism behind the immunosuppressive effects of PA on adipose tissue and its secretome. This could include assessing both the secretome and the adipose tissue at a transcriptional level to identify mitochondrial markers of damage which would give greater insight into which pathways are contributing to this response and whether this can be exploited for therapeutic gain. Further to this as literature has shown that higher levels of palmitic acid are observed in circulation of obese patients and higher levels of oleic acid are observed in obese adipose depots, it will be critical to discern the fatty acid content of both the adipose explants and its secretome. Also, to discern if there are changes in this fatty acid content between non-cancer and cancer patients to assess whether cancer changes the ratio of these fatty acids and whether this can be ameliorated to help decrease cancer cell migration to the adipose enriched pre-metastatic niches.

2. Following on from these findings, it would be of interest to assess the influence of obesity in a wider cohort of patients in response to chemotherapy and chemoradiotherapy. Whilst numerous trials have assessed whether patients have better response to either of these treatments few have looked at whether the obesity status of these patients confer any added survival advantage. It will also be of intertest to integrate the data that has been generated throughout this project, as a large proportion of the experiments conducted were carried out on the same patient cohort. The integration of this data could lead to the identification of a key signatures that could connect adipose biology to obesity and could be extrapolated to treatment respond. OAC is not the only obesity associated cancer, so it would also be of interest to see if these results could be recapitulated in other obesity associated cancers such as endometrial, colon and stomach.

3. Considering our findings of the effects of FAO inhibition on the metabolic dependency of primary and metastatic cancer cells, it would strengthen these findings to assess how the inhibition of glutamine and glucose would affect the metabolic and invasive capacity of these cells. Further to our findings of the differential secretion of glutamine and its associated metabolites in non-obese and obese patients, it would be of interest to assess the effects of reintroduction of glutamine into the obese adipose tissue. Particularly, in how this may alter immune and cancer cell function and metabolism.

4. In order to further interrogate on the adipose secretome support the migratory capacity of our primary and matched liver derived metastatic cell lines , it would prove intriguing if we pre-treated these cells with matched tumour conditioned media and then assess whether this differentially influences the invasive capacity of these cells towards our tretaed adipose conditioned media and whether inhibition of any of the metabolic pathways including fatty acid oxidation, glutamine and glucose metabolism would perturb this response.

5. Additionally, whilst we assessed the phenotypic response of dendritic cells and macrophages in response to the treated adipose secretome, it would further validify these findings to explore them on a metabolic and functional level. Particularly in assessing how these cells could signal and activate T cells, which subset of T cells they would invoke and whether it would influence the tumour killing capacity of T cells.

6. This research highly focused on palmitic and oleic acid due to the prevalence of these fatty acids in the normal diet and within the human body. However, poly-unsaturated fatty acids (PUFAs) have previously been indicated to have radio-sensitizing and anti-cancer properties. It would enhance the scope of this research to reassess these findings using PUFAs and whether they would differentially affect adipose tissue metabolic and secreted profiles, response to increasing irradiation and chemotherapy and what downstream effects this would have for cancer and immune cell function.

7. Finally, assessing the cumulative effect of administering chemotherapy and chemoradiotherapy regimens in combination with dietary fatty acids would be best represented in an *in-vivo* model. A recently developed mouse model of obesity associated oesophageal adenocarcinoma, would prove an excellent model to assess the influence of these results and whether the addition of dietary fats could augment treatment efficacy particularly in the obese setting.

## 8.0 Appendices

### 8.1 Appendix 1

To optimise adipose tissue normalisation strategies 3 different methods of normalisation were examined. For weight technique (w) tissue was weighed pre-incubation, incubated, assessed for metabolic read outs, weighed again and the output OCR/ECAR data for each piece of tissue was normalised to before and after weights (**Figure 8.1.1 – 8.1.2**) For protein technique (p) tissue was weighed pre-incubation, incubated, assessed for metabolic read outs and tissue was then lysed using RIPA buffer and protein content assessed using BCA assay. The output OCR/ECAR data for each piece of tissue was normalised to before weight and the after-incubation protein content. For RNA technique (r) tissue was weighed pre-incubation, incubated, assessed for metabolic read outs and tissue was then lysed using Qiazol reagent and RNA content assessed using nanodrop. The output OCR/ECAR data for each piece of tissue was normalised to before weight and the after-incubation RNA content. Following this post weight and RNA were selected as the most closely aligned selected for future methods of normalisation.

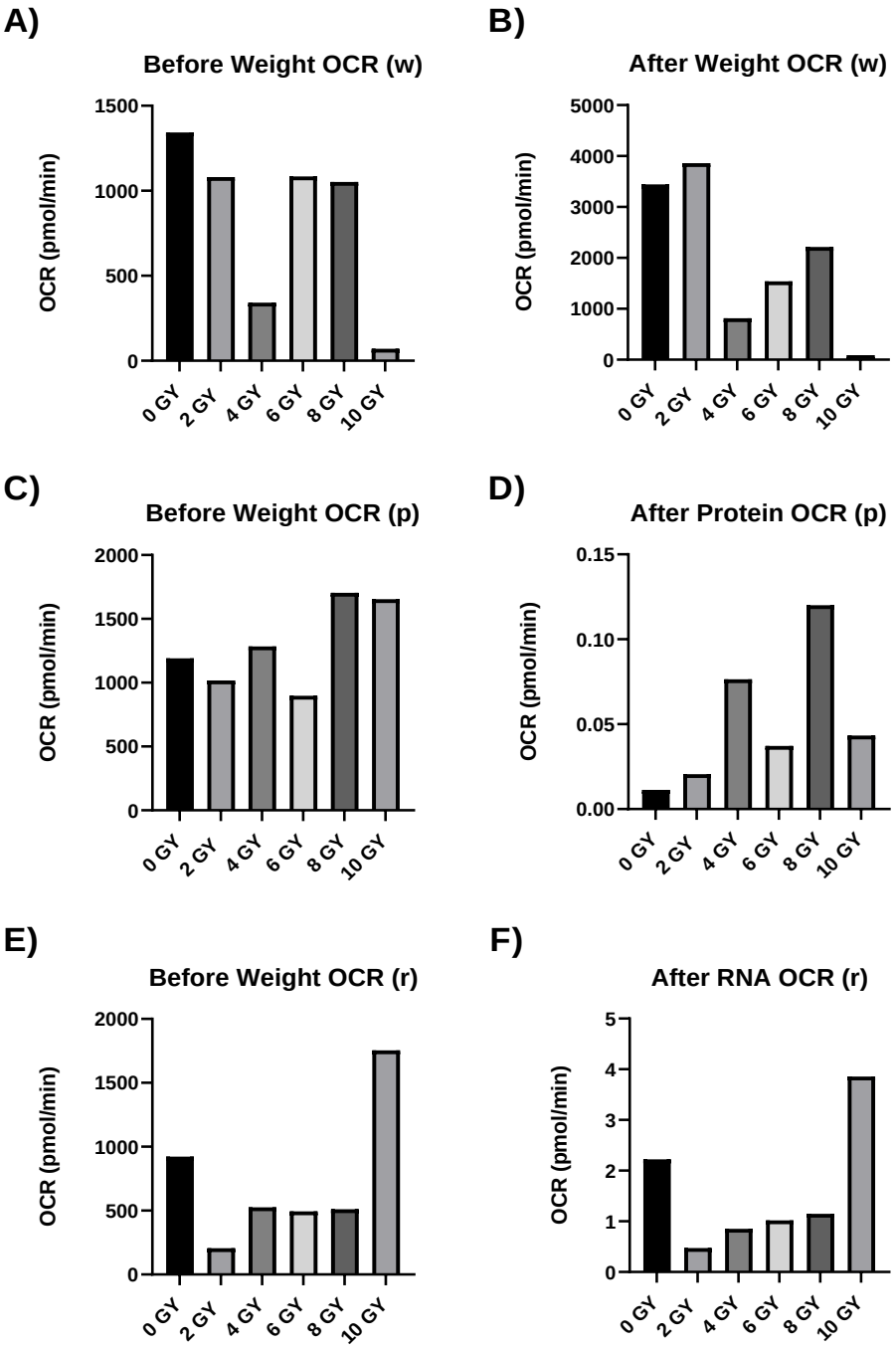


**Figure 8.1.1 Optimisation of adipose tissue normalisation for OCR measurements using pre-incubation weight, post-incubation weight, protein content and RNA concentration.**

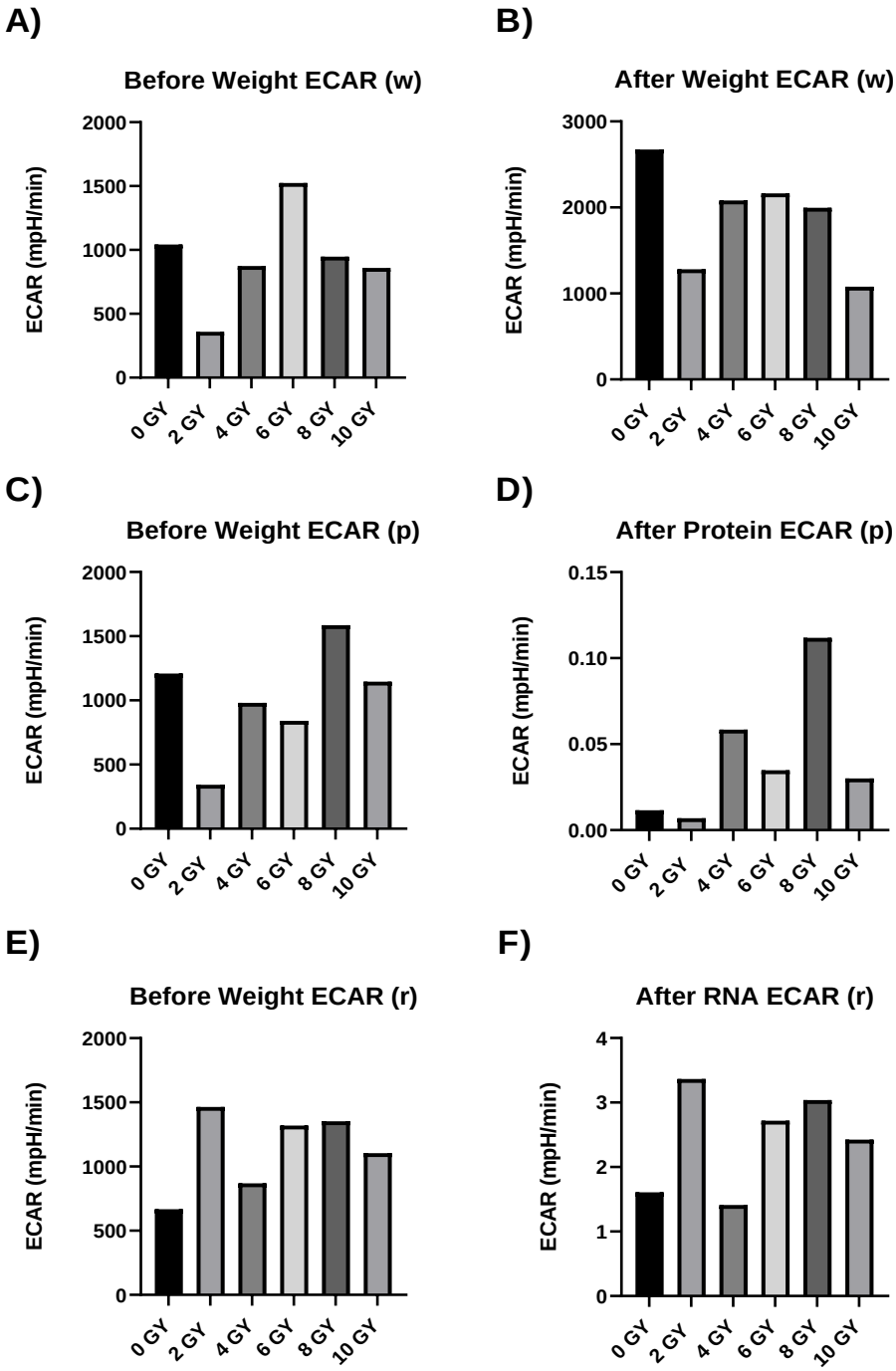


**Figure 8.1.2 Optimisation of adipose tissue normalisation for OCR measurements using pre-incubation weight, post-incubation weight, protein content and RNA concentration.**

## 8.2 Appendix 2

To assess the influence of low and high dose radiation of adipose tissue metabolism, a dose response was conducted where adipose tissue in triplicates was treated with increasing doses of radiation, 0 Gy, 2 Gy, 4 Gy, 6 Gy, 8 Gy and 10 Gy and whether this was influenced by obesity. In similar manner as above samples were cultured for 24 hours with OCR and ECAR assessed using Seahorse technology.

Adipose explants exposed to 4 Gy irradiation showed significant increase in OCR profiles compared to 0 Gy control, 6 Gy irradiated, and 10 Gy irradiated. Adipose explants exposed to 8 Gy radiation showed significant increase in OCR profiles 6 Gy irradiated (**Figure 8.2.1 A**). Similarly, 4 Gy irradiation showed significant increase in OCR:ECAR ratio in adipose tissue compared to 6 Gy and 10 Gy irradiated adipose (**Figure 8.2.1 C**) (n=20).

A significant increase in OCR was determined in obese adipose explants (n=10) versus non-obese patients' adipose explants (n=10) at 0 Gy, 2 Gy, and 4 Gy irradiation doses (**Figure 8.2.1 D**). A significant increase in ECAR was determined in obese adipose explants (n=10) versus non-obese patients' adipose explants (n=10) following 4 Gy irradiation (**Figure 8.2.1 E**). A significant increase in OCR:ECAR ratio was determined in obese adipose explants (n=10) versus non-obese patients' adipose explants (n=10) at 2 Gy, and 4 Gy irradiation doses (**Figure 8.2.1 F**). Obesity was determined using VFA parameters, significance was assessed using Kruskal Wallis testing between obese and non-obese cohorts and Friedman testing was used between matched samples at increasing radiation doses with Dunn's correction.

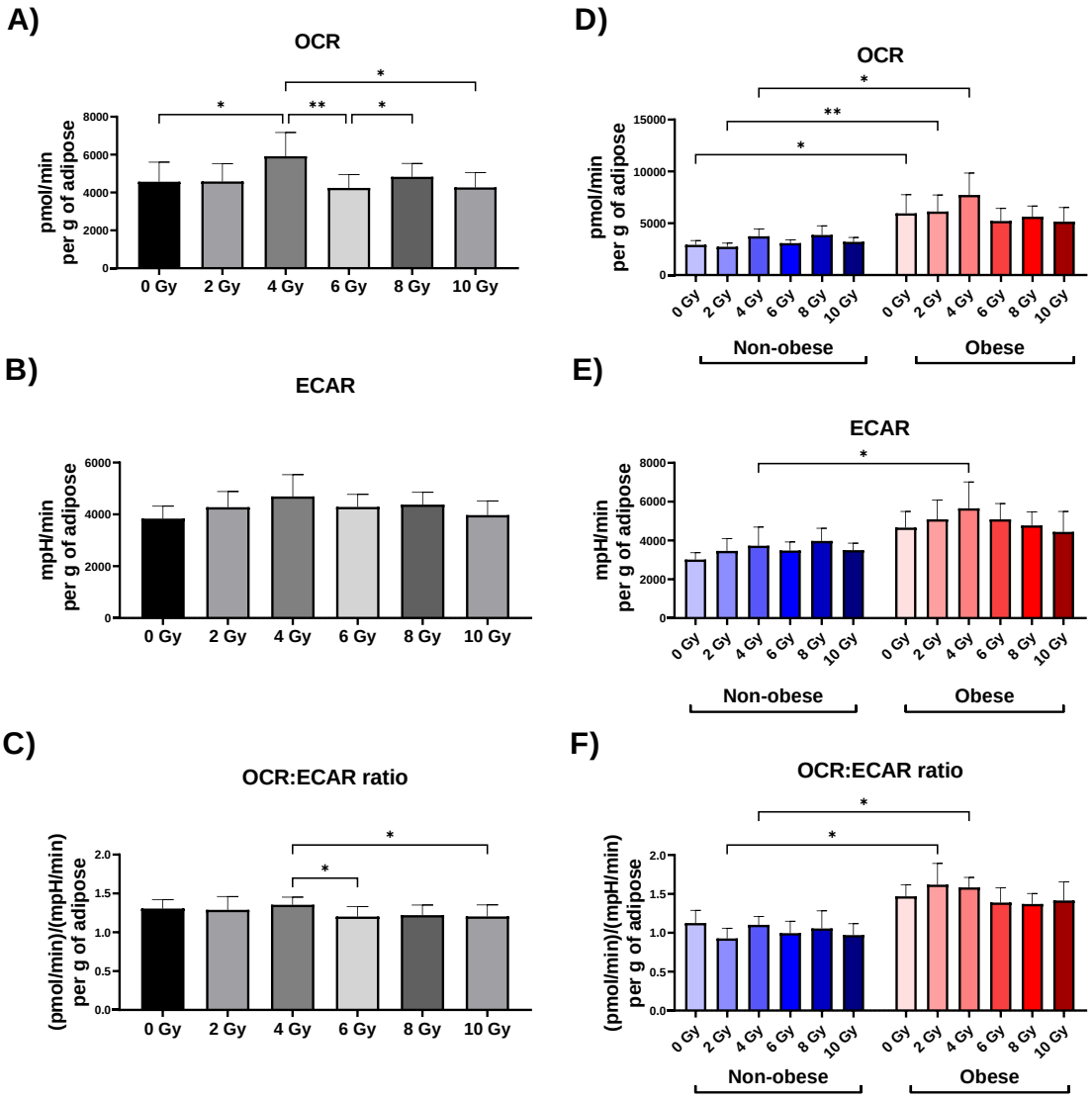


**Figure 8.2.1 Increasing radiation and obesity alter the metabolic profiles of visceral adipose explants derived from OAC patients.**

## 8.3 Appendix 3

To assess the influence of low and high dose radiation of adipose tissue secretome, a dose response was conducted where adipose tissue in triplicates was treated with increasing doses of radiation, 0 Gy, 2 Gy, 4 Gy, 6 Gy, 8 Gy and 10 Gy and whether this was influenced by obesity. Methodology carried out as per section 2.3.4 Multiplex ELISA

GM-CSF, IFN-γ, IL-1β, IL-2, IL-4, IL-6, IL-8, IL-12p70, IP-10 and MDC all display increased secretion with at more than one specific increased radiation dose.

Eotaxin-3 and VEGF-C display increased secretion with at least one specific increased radiation dose.

Significance was computed using Friedman testing with Dunn's correction on a cohort,

IL-23 and IL-27 display decreased secretion with at more than one specific increased radiation dose.

(n = 20) (**Figure 8.3.1**)

Eotaxin-3, IL-3, IL-17D, IL-27, MDC, SAA, TSLP, VEGF-D display increased secretion with at least one specific increased radiation dose in the obese adipose secretome compared with the non-obese adipose secretome of OAC patients.

IL12p70, IL-23, and MDC most apparently display altered secretion with at least one specific increased radiation dose in the non-obese adipose secretome of OAC patients.

IL-8, IL-27 and VEGF-D most apparently display altered secretion with at least one specific increased radiation dose in the obese adipose secretome of OAC patients.

GM-CSF, IL-4, and IL-6 display increased secretion with at least one specific increased radiation dose regardless of the obesity status of OAC patients

Significance was computed using Kruskal Wallis testing with Dunn's correction on a cohort non-obese n = 10, obese n=10. (**Figure 8.3.2**)

(* $p < 0.05$, ** $p < 0.01$, *** $p < 0.001$, **** $p < 0.0001$)

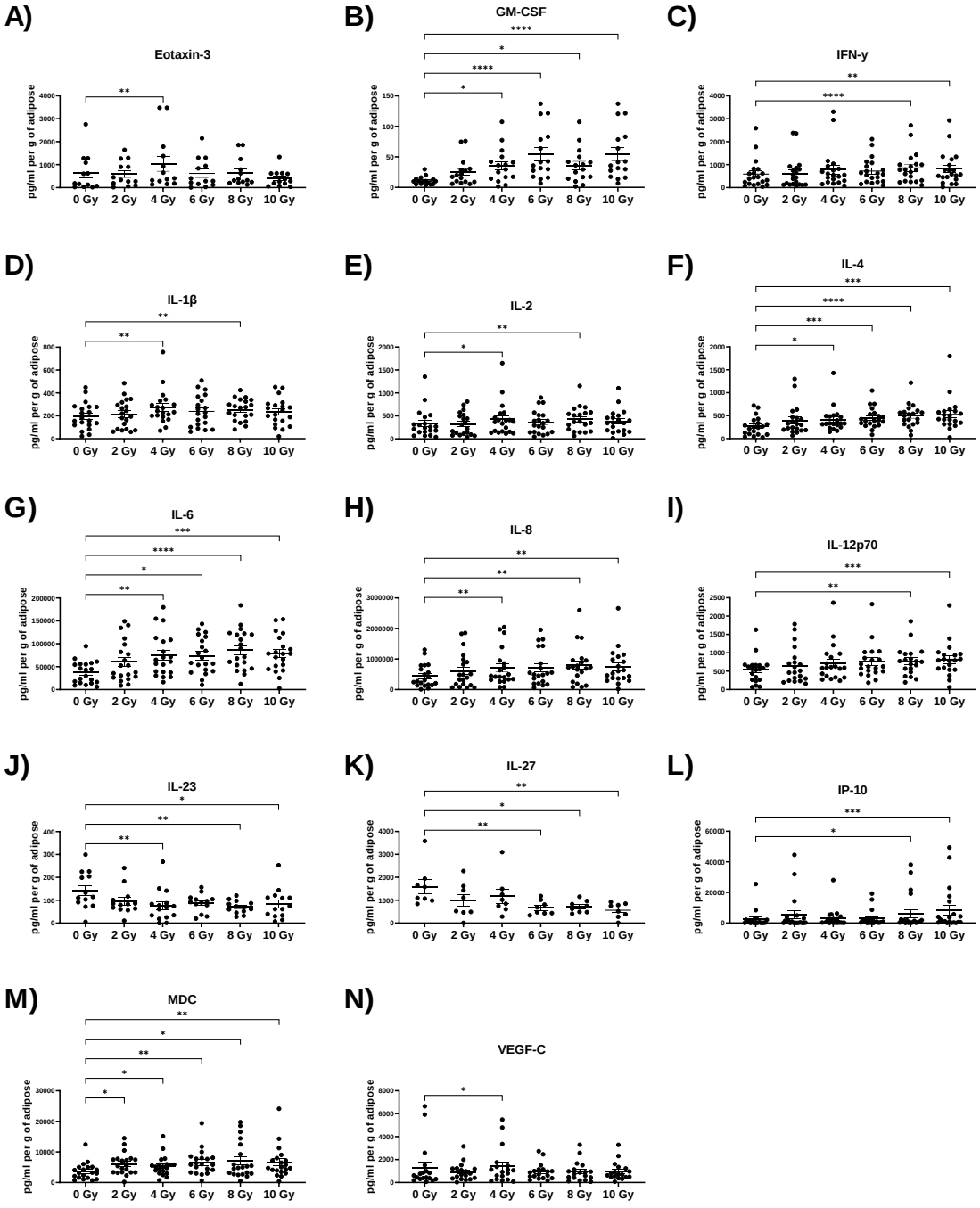


**Figure 8.3.1 Increasing radiation alters inflammatory mediators in the adipose secretome of OAC patients.**

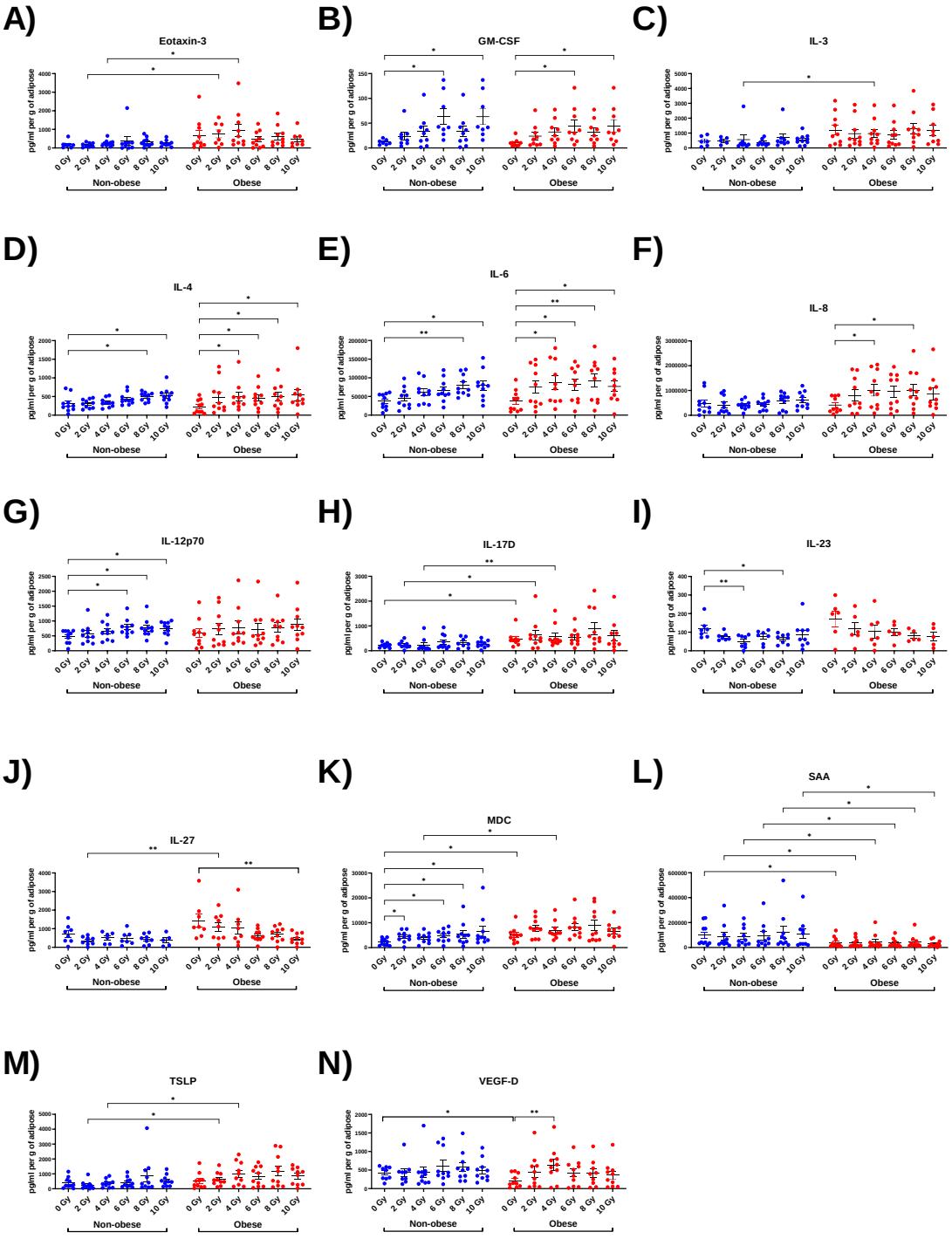


**Figure 8.3.2 Increasing radiation alters inflammatory mediators in the adipose secretome of non-obese and obese OAC patients.**

## 8.4 Appendix 4

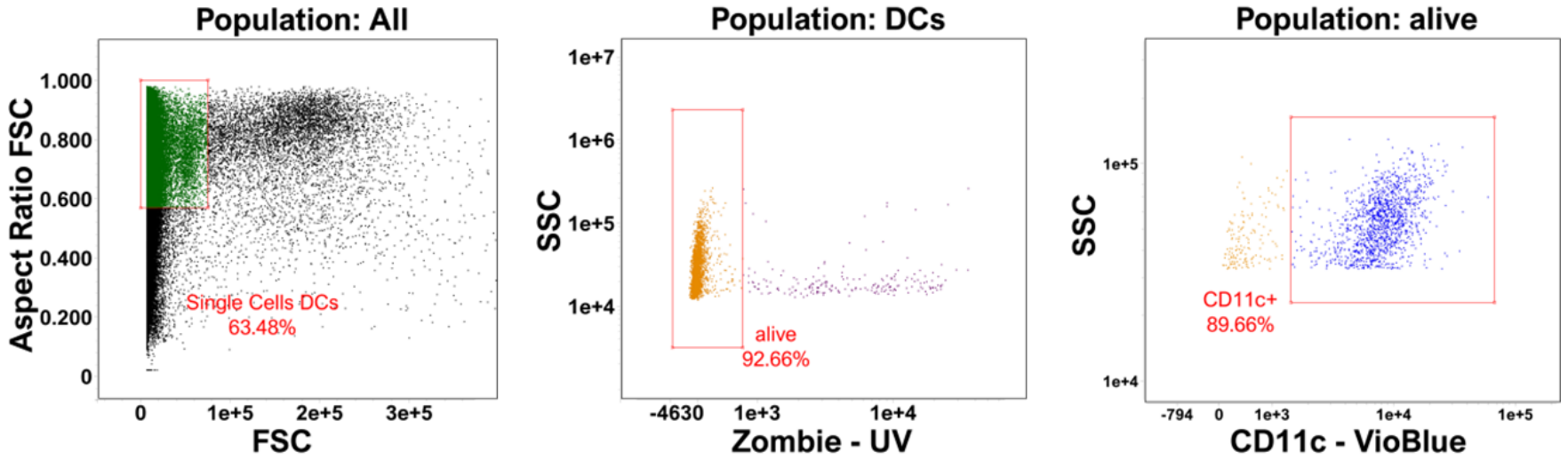


**Figure 8.4.1 Gating strategy for DC flow cytometry analysis**

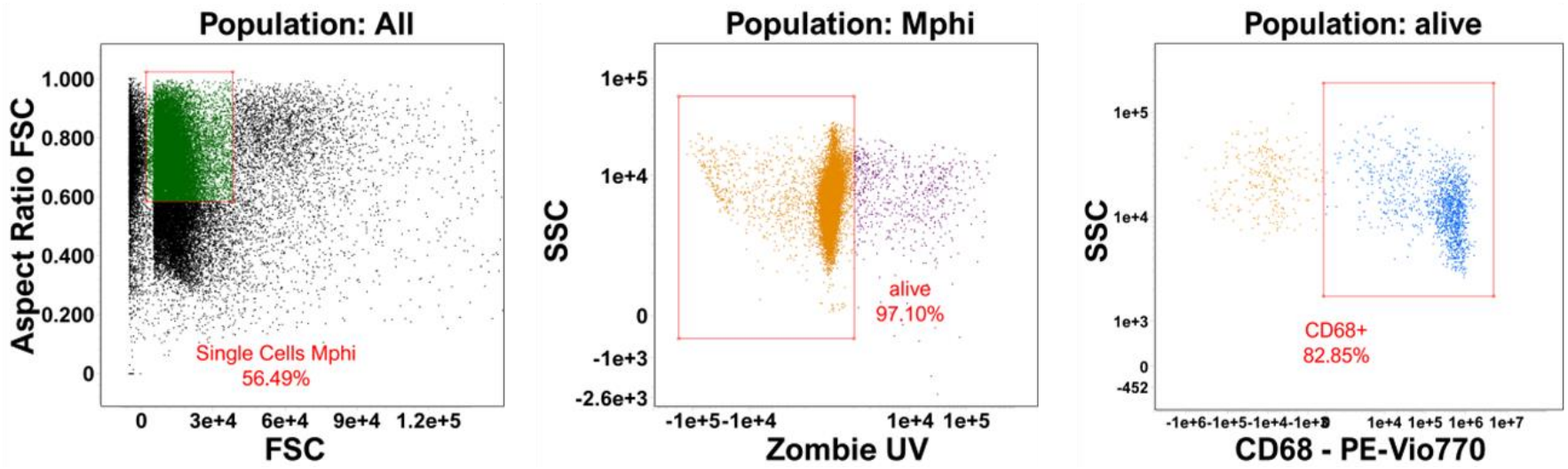


**Figure 8.4.2 Gating strategy for Mϕ flow cytometry analysis**

## 9.0 Bibliography


1. Sung H, Ferlay J, Siegel RL, Laversanne M, Soerjomataram I, Jemal A, et al. Global Cancer Statistics 2020: GLOBOCAN Estimates of Incidence and Mortality Worldwide for 36 Cancers in 185 Countries. CA Cancer J Clin [Internet] 2021 [cited 2023 Mar 21];71(3):209–49. Available from: https://onlinelibrary.wiley.com/doi/full/10.3322/caac.21660

2. Kim J, Bowlby R, Mungall AJ, Robertson AG, Odze RD, Cherniack AD, et al. Integrated genomic characterization of oesophageal carcinoma. Nat 2017 5417636 [Internet] 2017 [cited 2023 Mar 21];541(7636):169–75. Available from: https://www.nature.com/articles/nature20805

3. Zhao B, Zhang Z, Mo D, Lu Y, Hu Y, Yu J, et al. Optimal extent of transhiatal gastrectomy and lymphadenectomy for the stomach-predominant adenocarcinoma of esophagogastric junction: Retrospective single-institution study in China. Front Oncol 2019;9(JAN):639.

4. Bray F, Ferlay J, Soerjomataram I, Siegel RL, Torre LA, Jemal A. Global cancer statistics 2018: GLOBOCAN estimates of incidence and mortality worldwide for 36 cancers in 185 countries. CA Cancer J Clin 2018;68(6):394–424.

5. Thrift AP. The epidemic of oesophageal carcinoma: Where are we now? Cancer Epidemiol 2016;41:88–95.

6. McColl KEL. What is causing the rising incidence of esophageal adenocarcinoma in the West and will it also happen in the East? J Gastroenterol [Internet] 2019 [cited 2023 Mar 23];54(8):669–73. Available from: https://link.springer.com/article/10.1007/s00535-019-01593-7

7. Zhang Y. Epidemiology of esophageal cancer [Internet]. World J. Gastroenterol.2013 [cited 2021 Feb 28];19(34):5598–606. Available from: /pmc/articles/PMC3769895/

8. National Cancer Registry Ireland. Cancer in Ireland 1994-2020: Annual statistical report of the National Cancer Registry. 2022 [cited 2023 Mar 21];Available from: www.ncri.ie

9. Foley KG, Lewis WG, Fielding P, Karran A, Chan D, Blake P, et al. N-staging of oesophageal and junctional carcinoma: is there still a role for EUS in patients staged N0 at PET/CT? Clin Radiol [Internet] 2014 [cited 2023 Mar 23];69(9):959–64. Available from: https://pubmed.ncbi.nlm.nih.gov/24916652/

10. Abouzied MM, Fathala A, Alsugair A, Muhaideb AI Al, Qahtani MH Al. Role of Fluorodeoxyglucose-Positron Emission Tomography/Computed Tomography in the Evaluation of Head and Neck Carcinoma. World J Nucl Med [Internet] 2017 [cited 2023 Mar 23];16(4):257. Available from: /pmc/articles/PMC5639440/

11. Amin MB, Greene FL, Edge SB, Compton CC, Gershenwald JE, Brookland RK, et al. The Eighth Edition AJCC Cancer Staging Manual: Continuing to build a bridge from a population-based to a more "personalized" approach to cancer staging. CA Cancer J Clin [Internet] 2017 [cited 2023 Mar 23];67(2):93–9. Available from: https://pubmed.ncbi.nlm.nih.gov/28094848/

12. Rice TW, Ishwaran H, Ferguson MK, Blackstone EH, Goldstraw P. Cancer of the Esophagus and Esophagogastric Junction: An Eighth Edition Staging Primer. J Thorac Oncol 2017;12(1):36–42.

13. Berry MF. Esophageal cancer: staging system and guidelines for staging and treatment. J Thorac Dis [Internet] 2014 [cited 2023 Mar 21];6(Suppl 3):S289. Available from: /pmc/articles/PMC4037413/

14. Defize IL, Hillegersberg R van, Mook S, Meijer GJ, Lin SH, Ruurda JP, et al. Restaging after chemoradiotherapy for locally advanced esophageal cancer. Ann Transl Med [Internet] 2019 [cited 2023 Mar 23];7(Suppl 8):S288–S288. Available from: /pmc/articles/PMC6976470/

15. Pennathur A, Gibson MK, Jobe BA, Luketich JD. Oesophageal carcinoma. Lancet [Internet] 2013 [cited 2023 Mar 21];381(9864):400–12. Available from: http://www.thelancet.com/article/S0140673612606436/fulltext

16. Kim TJ, Kim HY, Lee KW, Kim MS. Multimodality Assessment of Esophageal Cancer: Preoperative Staging and Monitoring of Response to Therapy1. https://doi.org/101148/rg292085106 [Internet] 2009 [cited 2023 Mar 21];29(2):403–21. Available from: https://pubs.rsna.org/doi/10.1148/rg.292085106

17. Hoeppner J, Lordick F, Brunner T, Glatz T, Bronsert P, Röthling N, et al. ESOPEC: prospective randomized controlled multicenter phase III trial comparing perioperative chemotherapy (FLOT protocol) to neoadjuvant chemoradiation (CROSS protocol) in patients with adenocarcinoma of the esophagus (NCT02509286). BMC Cancer [Internet] 2016 [cited 2021 Feb 25];16(1):503. Available from: http://bmccancer.biomedcentral.com/articles/10.1186/s12885-016-2564-y

18. Donlon NE, Moran B, Kamilli A, Davern M, Sheppard A, King S, et al. Cross versus flot regimens in esophageal and esophagogastric junction adenocarcinoma a propensity-matched comparison. Ann Surg [Internet] 2022 [cited 2023 Mar 22];276(5):792–8. Available from: https://journals.lww.com/annalsofsurgery/Fulltext/2022/11000/CROSS_Versus_FLOT_Regimens_in_Esophageal_and.8.aspx

19. Reynolds J V., Preston SR, O'Neill B, Lowery MA, Baeksgaard L, Crosby T, et al. Neo-AEGIS (Neoadjuvant trial in Adenocarcinoma of the Esophagus and Esophago-Gastric Junction International Study): Preliminary results of phase III RCT of CROSS versus perioperative chemotherapy (Modified MAGIC or FLOT protocol). (NCT01726452). https://doi.org/101200/JCO20213915_suppl4004 2021;39(15_suppl):4004–4004.

20. Blum Murphy M, Xiao L, Patel VR, Maru DM, Correa AM, G. Amlashi F, et al. Pathological complete response in patients

with esophageal cancer after the trimodality approach: The association with baseline variables and survival—The University of Texas MD Anderson Cancer Center experience. Cancer [Internet] 2017 [cited 2023 Mar 25];123(21):4106–13. Available from: https://onlinelibrary.wiley.com/doi/full/10.1002/cncr.30953

21. Kelly RJ, Ajani JA, Kuzdzal J, Zander T, Van Cutsem E, Piessen G, et al. Adjuvant Nivolumab in Resected Esophageal or Gastroesophageal Junction Cancer. N Engl J Med [Internet] 2021 [cited 2023 Mar 25];384(13):1191–203. Available from: https://www.nejm.org/doi/full/10.1056/nejmoa2032125

22. Donlon NE, Davern M, Sheppard AD, O'Connell F, Dunne MR, Hayes C, et al. The Impact of Esophageal Oncological Surgery on Perioperative Immune Function; Implications for Adjuvant Immune Checkpoint Inhibition. Front Immunol 2022;13:114.

23. Hou Y, Nitta H, Parwani A V., Li Z. PD-L1 and CD8 are associated with deficient mismatch repair status in triple-negative and HER2-positive breast cancers. Hum Pathol [Internet] 2019 [cited 2023 Mar 25];86:108–14. Available from: https://pubmed.ncbi.nlm.nih.gov/30633926/

24. Beer A, Taghizadeh H, Schiefer AI, Puhr HC, Karner AK, Jomrich G, et al. PD-L1 and HER2 Expression in Gastroesophageal Cancer: a Matched Case Control Study. Pathol Oncol Res [Internet] 2020 [cited 2023 Mar 25];26(4):2225. Available from: /pmc/articles/PMC7471145/

25. Mandard AM, Dalibard F, Mandard JC, Marnay J, Henry-Amar M, Pefiot JF, et al. Pathologic Assessment of Tumor Regression after Preoperative Chemoradiotherapy of Esophageal Carcinoma Clinicopa thologic Correlations. Cancer [Internet] 1992 [cited 2023 Mar 21];73(11):2669–882. Available from: https://onlinelibrary.wiley.com/terms-and-conditions

26. Reynolds J V., Preston SR, O'Neill B, Baeksgaard L, Griffin SM, Mariette C, et al. ICORG 10-14: NEOadjuvant trial in Adenocarcinoma of the oEsophagus and oesophagoGastric junction International Study (Neo-AEGIS). BMC Cancer [Internet] 2017 [cited 2023 Mar 25];17(1). Available from: /pmc/articles/PMC5457631/

27. Schlottmann F, Molena D, Patti MG. Gastroesophageal reflux and Barrett's esophagus: a pathway to esophageal adenocarcinoma. Updates Surg [Internet] 2018 [cited 2023 Mar 26];70(3):339–42. Available from: https://link.springer.com/article/10.1007/s13304-018-0564-y

28. Grassi A, Ballardini G, Susca M, Bianchini F, Bonoli S, Bianchi FB, et al. Systematic review: proton-pump inhibitor failure in gastro-oesophageal reflux disease--where next? Aliment Pharmacol Ther [Internet] 2005 [cited 2023 Mar 22];22(2):79–82. Available from: https://pubmed.ncbi.nlm.nih.gov/16011666/

29. Zhang T, Zhang B, Tian W, Wei Y, Wang F, Yin X, et al. Trends in gastroesophageal reflux disease research: A bibliometric and visualized study. Front Med 2022;9:2879.

30. Ronkainen J, Talley NJ, Storskrubb T, Johansson SE, Lind T, Vieth M, et al. Erosive esophagitis is a risk factor for Barrett's esophagus: a community-based endoscopic follow-up study. Am J Gastroenterol [Internet] 2011 [cited 2023 Mar 22];106(11):1946–52. Available from: https://pubmed.ncbi.nlm.nih.gov/21946284/

31. Schneider JL, Corley DA. A review of the epidemiology of Barrett's oesophagus and oesophageal adenocarcinoma. Best Pract Res Clin Gastroenterol [Internet] 2015 [cited 2023 Mar 24];29(1):29. Available from: /pmc/articles/PMC5648333/

32. Killcoyne S, Fitzgerald RC. Evolution and progression of Barrett's oesophagus to oesophageal cancer. Nat Rev Cancer 2021 2111 [Internet] 2021 [cited 2023 Mar 22];21(11):731–41. Available from: https://www.nature.com/articles/s41568-021-00400-x

33. Phelan JJ, Feighery R, Eldin OS, Meachair S, Cannon A, Byrne R, et al. Examining the connectivity between different cellular processes in the Barrett tissue microenvironment. Cancer Lett [Internet] 2016 [cited 2023 Mar 25];371(2):334–46. Available from: https://pubmed.ncbi.nlm.nih.gov/26688097/

34. Sharma N, Ho KY. Risk Factors for Barrett's Oesophagus. Gastrointest Tumors [Internet] 2016 [cited 2023 Mar 22];3(2):103. Available from: /pmc/articles/PMC5121541/

35. Bhat S, Coleman HG, Yousef F, Johnston BT, McManus DT, Gavin AT, et al. Risk of Malignant Progression in Barrett's Esophagus Patients: Results from a Large Population-Based Study. JNCI J Natl Cancer Inst [Internet] 2011 [cited 2023 Mar 22];103(13):1049. Available from: /pmc/articles/PMC3632011/

36. Qiao Y, Hyder A, Bae SJ, Zarin W, O'Neill TJ, Marcon NE, et al. Surveillance in Patients With Barrett's Esophagus for Early Detection of Esophageal Adenocarcinoma: A Systematic Review and Meta-Analysis. Clin Transl Gastroenterol [Internet] 2015 [cited 2023 Mar 25];6(12). Available from: https://pubmed.ncbi.nlm.nih.gov/26658838/

37. Duits LC, Lao-Sirieix P, Wolf WA, O'Donovan M, Galeano-Dalmau N, Meijer SL, et al. A biomarker panel predicts progression of Barrett's esophagus to esophageal adenocarcinoma. Dis esophagus Off J Int Soc Dis Esophagus [Internet] 2019 [cited 2023 Mar 25];32(1). Available from: https://pubmed.ncbi.nlm.nih.gov/30496496/

38. Kane LE, Mellotte GS, Mylod E, O'Brien RM, O'Connell F, Buckley CE, et al. Diagnostic Accuracy of Blood-based Biomarkers for Pancreatic Cancer: A Systematic Review and Meta-analysis. Cancer Res Commun [Internet] 2022 [cited 2022 Nov 27];2(10):1229–43. Available from: https://aacrjournals.org/cancerrescommun/article/2/10/1229/709859/Diagnostic-Accuracy-of-Blood-based-Biomarkers-for

39. Budny A, Grochowski C, Kozłowski P, Kolak A, Kamińska M, Budny B, et al. Obesity as a tumour development triggering factor. Ann Agric Environ Med [Internet] 2019 [cited 2020 Mar 19];26(1):13–23. Available from:

http://www.ncbi.nlm.nih.gov/pubmed/30922023

40. O'Sullivan J, Lysaght J, Donohoe CL, Reynolds J V. Obesity and gastrointestinal cancer: the interrelationship of adipose and tumour microenvironments. Nat. Rev. Gastroenterol. Hepatol.2018;15(11):699–714.

41. World Health Organisation. Obesity [Internet]. [cited 2023 Mar 12];Available from: https://www.who.int/health-topics/obesity#tab=tab_1

42. Meldrum DR, Morris MA, Gambone JC. Obesity pandemic: causes, consequences, and solutions—but do we have the will? Fertil. Steril.2017;107(4):833–9.

43. Pal SK, Miller MJ, Agarwal N, Chang SM, Chavez-MacGregor M, Cohen E, et al. Clinical Cancer Advances 2019: Annual Report on Progress Against Cancer From the American Society of Clinical Oncology. J Clin Oncol [Internet] 2019 [cited 2020 Apr 21];37(10):834–49. Available from: http://www.ncbi.nlm.nih.gov/pubmed/30702028

44. Arnold M, Pandeya N, Byrnes G, Renehan AG, Stevens GA, Ezzati M, et al. Global burden of cancer attributable to high body-mass index in 2012: a population-based study. Lancet Oncol [Internet] 2015 [cited 2023 Mar 24];16(1):36–46. Available from: https://pubmed.ncbi.nlm.nih.gov/25467404/

45. Morris Brown L, Swanson CA, Gridley G, Swanson GM, Schoenberg JB, Greenberg RS, et al. Adenocarcinoma of the esophagus: Role of obesity and diet. J Natl Cancer Inst [Internet] 1995 [cited 2021 Feb 28];87(2):104–9. Available from: https://pubmed.ncbi.nlm.nih.gov/7707381/

46. Vaughan TL, Davis S, Kristal A, Thomas DB. Obesity, alcohol, and tobacco as risk factors for cancers of the esophagus and gastric cardia: adenocarcinoma versus squamous cell carcinoma. Cancer Epidemiol Prev Biomarkers 1995;4(2).

47. Ryan AM, Rowley SP, Fitzgerald AP, Ravi N, Reynolds J V. Adenocarcinoma of the oesophagus and gastric cardia: Male preponderance in association with obesity. Eur J Cancer [Internet] 2006 [cited 2021 Feb 28];42(8):1151–8. Available from: https://pubmed.ncbi.nlm.nih.gov/16630714/

48. Renehan AG, Roberts DL, Dive C. Obesity and cancer: Pathophysiological and biological mechanisms [Internet]. Arch. Physiol. Biochem.2008 [cited 2021 Feb 28];114(1):71–83. Available from: https://pubmed.ncbi.nlm.nih.gov/18465361/

49. Thrift AP, Shaheen NJ, Gammon MD, Bernstein L, Reid BJ, Onstad L, et al. Obesity and risk of esophageal adenocarcinoma and barrett's esophagus: A mendelian randomization study. J Natl Cancer Inst [Internet] 2014 [cited 2021 Feb 28];106(11). Available from: /pmc/articles/PMC4200028/

50. Iyengar NM, Gucalp A, Dannenberg AJ, Hudis CA. JOURNAL OF CLINICAL ONCOLOGY Obesity and Cancer Mechanisms: Tumor Microenvironment and Inflammation. J Clin Oncol [Internet] 2016 [cited 2019 Nov 21];34:4270–6. Available from: www.jco.org

51. Lennon H, Sperrin M, Badrick E, Renehan AG. The Obesity Paradox in Cancer: a Review. Curr. Oncol. Rep.2016;18(9).

52. Griggs JJ, Mangu PB, Temin S, Lyman GH. Appropriate Chemotherapy Dosing for Obese Adult Patients With Cancer: American Society of Clinical Oncology Clinical Practice Guideline. J Oncol Pract 2012;8(4):e59–61.

53. Lynam-Lennon N, Maher SG, Maguire A, Phelan J, Muldoon C, Reynolds J V., et al. Altered Mitochondrial Function and Energy Metabolism Is Associated with a Radioresistant Phenotype in Oesophageal Adenocarcinoma. PLoS One [Internet] 2014 [cited 2022 Sep 5];9(6):e100738. Available from: https://journals.plos.org/plosone/article?id=10.1371/journal.pone.0100738

54. Bochet L, Meulle A, Imbert S, Salles B, Valet P, Muller C. Cancer-associated adipocytes promotes breast tumor radioresistance. Biochem Biophys Res Commun [Internet] 2011 [cited 2020 Mar 16];411(1):102–6. Available from: http://www.ncbi.nlm.nih.gov/pubmed/21712027

55. Mongan AM, Lynam-Lennon N, Doyle SL, Casey R, Carr E, Cannon A, et al. Visceral adipose tissue modulates radiosensitivity in oesophageal adenocarcinoma. Int J Med Sci 2019;16(4):519–28.

56. Masschelin PM, Cox AR, Chernis N, Hartig SM. The Impact of Oxidative Stress on Adipose Tissue Energy Balance. Front Physiol [Internet] 2020 [cited 2023 Feb 6];10:1638. Available from: /pmc/articles/PMC6987041/

57. Park J, Morley TS, Kim M, Clegg DJ, Scherer PE. Obesity and cancer - Mechanisms underlying tumour progression and recurrence [Internet]. Nat. Rev. Endocrinol.2014 [cited 2020 Mar 19];10(8):455–65. Available from: http://www.ncbi.nlm.nih.gov/pubmed/24935119

58. Quail DF, Dannenberg AJ. The obese adipose tissue microenvironment in cancer development and progression [Internet]. Nat. Rev. Endocrinol.2019 [cited 2020 Mar 19];15(3):139–54. Available from: http://www.ncbi.nlm.nih.gov/pubmed/30459447

59. Khan S, Chan YT, Revelo XS, Winer DA. The Immune Landscape of Visceral Adipose Tissue During Obesity and Aging. Front Endocrinol (Lausanne) 2020;11:267.

60. Heeran AB, McCready J, Dunne MR, Donlon NE, Nugent TS, Bhardwaj A, et al. Opposing immune-metabolic signature in visceral versus subcutaneous adipose tissue in patients with adenocarcinoma of the oesophagus and the oesophagogastric junction. Metabolites [Internet] 2021 [cited 2022 Aug 31];11(11):768. Available from: https://www.mdpi.com/2218-1989/11/11/768/htm

61. Shah S, Cox AG. Article Commentary: A Role for IR-β in the Free Fatty Acid Mediated Development of Hepatic Insulin Resistance? Biochem Insights 2009;2:BCI.S2996.

62. Calder PC. Functional Roles of Fatty Acids and Their Effects on Human Health. JPEN J Parenter Enteral Nutr [Internet] 2015 [cited 2023 Mar 16];39(1 Suppl):18S-32S. Available from: https://pubmed.ncbi.nlm.nih.gov/26177664/

63. Lunn J, Theobald HE. The health effects of dietary unsaturated fatty acids. Nutr Bull [Internet] 2006 [cited 2023 Mar 22];31(3):178–224. Available from: https://onlinelibrary.wiley.com/doi/full/10.1111/j.1467-3010.2006.00571.x

64. Giulitti F, Petrungaro S, Mandatori S, Tomaipitinca L, de Franchis V, D'Amore A, et al. Anti-tumor Effect of Oleic Acid in Hepatocellular Carcinoma Cell Lines via Autophagy Reduction. Front Cell Dev Biol 2021;9:141.

65. Korbecki J, Bajdak-Rusinek K. The effect of palmitic acid on inflammatory response in macrophages: an overview of molecular mechanisms. Inflamm Res [Internet] 2019 [cited 2023 Jan 29];68(11):915. Available from: /pmc/articles/PMC6813288/

66. Santa-María C, López-Enríquez S, Montserrat-de la Paz S, Geniz I, Reyes-Quiroz ME, Moreno M, et al. Update on Anti-Inflammatory Molecular Mechanisms Induced by Oleic Acid. Nutr 2023, Vol 15, Page 224 [Internet] 2023 [cited 2023 Mar 12];15(1):224. Available from: https://www.mdpi.com/2072-6643/15/1/224/htm

67. Harvey KA, Walker CL, Xu Z, Whitley P, Pavlina TM, Hise M, et al. Oleic acid inhibits stearic acid-induced inhibition of cell growth and pro-inflammatory responses in human aortic endothelial cells. J Lipid Res [Internet] 2010 [cited 2023 Jan 29];51(12):3470. Available from: /pmc/articles/PMC2975719/

68. Kang M, Lee A, Yoo HJ, Kim M, Kim M, Shin DY, et al. Association between increased visceral fat area and alterations in plasma fatty acid profile in overweight subjects: A cross-sectional study. Lipids Health Dis [Internet] 2017 [cited 2023 Mar 2];16(1):1–10. Available from: https://lipidworld.biomedcentral.com/articles/10.1186/s12944-017-0642-z

69. Yew Tan C, Virtue S, Murfitt S, Robert LD, Phua YH, Dale M, et al. Adipose tissue fatty acid chain length and mono-unsaturation increases with obesity and insulin resistance. Sci Reports 2015 51 [Internet] 2015 [cited 2023 Mar 12];5(1):1–11. Available from: https://www.nature.com/articles/srep18366

70. Piccinin E, Cariello M, De Santis S, Ducheix S, Sabbà C, Ntambi JM, et al. Role of Oleic Acid in the Gut-Liver Axis: From Diet to the Regulation of Its Synthesis via Stearoyl-CoA Desaturase 1 (SCD1). Nutr 2019, Vol 11, Page 2283 [Internet] 2019 [cited 2023 Mar 16];11(10):2283. Available from: https://www.mdpi.com/2072-6643/11/10/2283/htm

71. Matsuzaka T. Role of fatty acid elongase Elovl6 in the regulation of energy metabolism and pathophysiological significance in diabetes. Diabetol Int [Internet] 2021 [cited 2023 Mar 16];12(1):68. Available from: /pmc/articles/PMC7790921/

72. Piccinin E, Cariello M, De Santis S, Ducheix S, Sabbà C, Ntambi JM, et al. Role of Oleic Acid in the Gut-Liver Axis: From Diet to the Regulation of Its Synthesis via Stearoyl-CoA Desaturase 1 (SCD1). Nutr 2019, Vol 11, Page 2283 [Internet] 2019 [cited 2023 Mar 21];11(10):2283. Available from: https://www.mdpi.com/2072-6643/11/10/2283/htm

73. Chait A, den Hartigh LJ. Adipose Tissue Distribution, Inflammation and Its Metabolic Consequences, Including Diabetes and Cardiovascular Disease. Front Cardiovasc Med 2020;7:22.

74. Khanna D, Khanna S, Khanna P, Kahar P, Patel BM. Obesity: A Chronic Low-Grade Inflammation and Its Markers. Cureus [Internet] 2022 [cited 2023 Mar 12];14(2). Available from: https://pubmed.ncbi.nlm.nih.gov/35386146/

75. Zhao C, Wu M, Zeng N, Xiong M, Hu W, Lv W, et al. Cancer-associated adipocytes: Emerging supporters in breast cancer. J Exp Clin Cancer Res [Internet] 2020 [cited 2023 Mar 22];39(1):1–17. Available from: https://jeccr.biomedcentral.com/articles/10.1186/s13046-020-01666-z

76. Obradovic M, Sudar-Milovanovic E, Soskic S, Essack M, Arya S, Stewart AJ, et al. Leptin and Obesity: Role and Clinical Implication. Front Endocrinol (Lausanne) [Internet] 2021 [cited 2023 Mar 22];12. Available from: /pmc/articles/PMC8167040/

77. Surmacz E. Obesity hormone leptin: A new target in breast cancer? Breast Cancer Res 2007;9(1):301.

78. Bochet L, Meulle A, Imbert S, Salles B, Valet P, Muller C. Cancer-associated adipocytes promotes breast tumor radioresistance. Biochem Biophys Res Commun 2011;411(1):102–6.

79. Lo Iacono M, Modica C, Porcelli G, Brancato OR, Muratore G, Bianca P, et al. Targeting of the Peritumoral Adipose Tissue Microenvironment as an Innovative Antitumor Therapeutic Strategy. Biomol 2022, Vol 12, Page 702 [Internet] 2022 [cited 2023 Feb 17];12(5):702. Available from: https://www.mdpi.com/2218-273X/12/5/702/htm

80. O'Connell F, Mylod E, Donlon NE, Heeran AB, Butler C, Bhardwaj A, et al. Energy Metabolism, Metabolite, and Inflammatory Profiles in Human Ex Vivo Adipose Tissue Are Influenced by Obesity Status, Metabolic Dysfunction, and Treatment Regimes in Patients with Oesophageal Adenocarcinoma. Cancers 2023, Vol 15, Page 1681 [Internet] 2023 [cited 2023 Mar 15];15(6):1681. Available from: https://www.mdpi.com/2072-6694/15/6/1681/htm

81. Conroy MJ, Fitzgerald V, Doyle SL, Channon S, Useckaite Z, Gilmartin N, et al. The microenvironment of visceral adipose tissue and liver alter natural killer cell viability and function. J Leukoc Biol [Internet] 2016 [cited 2023 Jan 29];100(6):1435–42. Available from: https://pubmed.ncbi.nlm.nih.gov/27365528/

82. Conroy MJ, Maher SG, Melo AM, Doyle SL, Foley E, Reynolds J V., et al. Identifying a Novel Role for Fractalkine (CX3CL1) in Memory CD8+ T Cell Accumulation in the Omentum of Obesity-Associated Cancer Patients. Front Immunol [Internet] 2018 [cited 2023 Jan 29];9(AUG). Available from: https://pubmed.ncbi.nlm.nih.gov/30150990/

83. Melo AM, Mylod E, Fitzgerald V, Donlon NE, Murphy DM, Foley EK, et al. Tissue distribution of γδ T cell subsets in oesophageal adenocarcinoma. Clin Immunol 2021;229:108797.

84. Mylod E, O'connell F, Donlon NE, Butler C, Reynolds J V., Lysaght J, et al. The Omentum in Obesity-Associated Cancer: A Hindrance to Effective Natural Killer Cell Migration towards Tumour Which Can Be Overcome by CX3CR1 Antagonism. Cancers 2022, Vol 14, Page 64 [Internet] 2021 [cited 2022 Aug 31];14(1):64. Available from: https://www.mdpi.com/2072-6694/14/1/64/htm

85. Davern M, Bracken-Clarke D, Donlon NE, Sheppard AD, Butler C, Donohoe C, et al. Visceral adipose tissue secretome from early and late-stage oesophageal cancer patients differentially affects effector and regulatory T cells. 2022;

86. Essa N, O'Connell F, Prina-Mello A, O'Sullivan J, Marcone S. Gold nanoparticles and obese adipose tissue microenvironment in cancer treatment. Cancer Lett 2022;525:1–8.

87. DeVita VT, Chu E. A history of cancer chemotherapy. Cancer Res.2008;68(21):8643–53.

88. Kieler M, Unseld M, Bianconi D, Schindl M, Kornek G V., Scheithauer W, et al. Impact of New Chemotherapy Regimens on the Treatment Landscape and Survival of Locally Advanced and Metastatic Pancreatic Cancer Patients. J Clin Med [Internet] 2020 [cited 2020 Mar 21];9(3):648. Available from: https://www.mdpi.com/2077-0383/9/3/648

89. Kurnit KC, Sinno AK, Fellman B, Stone RL, Sood AK, Gershenson DM, et al. Gastrointestinal adjuvant chemotherapy regimens improve survival outcomes in women with mucinous ovarian cancer. Gynecol Oncol 2019;154:248–9.

90. Schiller JH, Harrington D, Belani CP, Langer C, Sandler A, Krook J, et al. Comparison of Four Chemotherapy Regimens for Advanced Non–Small-Cell Lung Cancer. N Engl J Med [Internet] 2002 [cited 2020 Mar 21];346(2):92–8. Available from: http://www.nejm.org/doi/abs/10.1056/NEJMoa011954

91. Lengyel E, Makowski L, DiGiovanni J, Kolonin MG. Cancer as a Matter of Fat: The Crosstalk between Adipose Tissue and Tumors. Trends in Cancer2018;4(5):374–84.

92. Karatas F, Erdem GU, Sahin S, Aytekin A, Yuce D, Sever AR, et al. Obesity is an independent prognostic factor of decreased pathological complete response to neoadjuvant chemotherapy in breast cancer patients. Breast 2017;32:237–44.

93. Litton JK, Gonzalez-Angulo AM, Warneke CL, Bondy M. Relationship Between Obesity and Pathologic Response to Neoadjuvant Chemotherapy Among Women With Operable Breast Cancer "From Mother to Child Project" View project Cancer vaccines View project SEE PROFILE. Artic J Clin Oncol [Internet] 2008 [cited 2020 Mar 18];Available from: https://www.researchgate.net/publication/23223679

94. Vaysse C, Muller C, Fallone F. Obesity: An heavyweight player in breast cancer's chemoresistance [Internet]. Oncotarget2019 [cited 2020 Mar 16];10(35):3207–8. Available from: http://www.ncbi.nlm.nih.gov/pubmed/31143368

95. Lyman GH, Sparreboom A. Chemotherapy dosing in overweight and obese patients with cancer. Nat. Rev. Clin. Oncol.2013;10(8):451–9.

96. Tavitian S, Denis A, Vergez F, Berard E, Sarry A, Huynh A, et al. Impact of obesity in favorable-risk AML patients receiving intensive chemotherapy. Am J Hematol [Internet] 2016 [cited 2020 Mar 18];91(2):193–8. Available from: http://doi.wiley.com/10.1002/ajh.24228

97. Estey EH. Acute myeloid leukemia: 2019 update on risk-stratification and management. Am J Hematol [Internet] 2018 [cited 2020 Mar 22];93(10):1267–91. Available from: http://doi.wiley.com/10.1002/ajh.25214

98. Sheng X, Tucci J, Parmentier JH, Ji L, Behan JW, Heisterkamp N, et al. Adipocytes cause leukemia cell resistance to daunorubicin via oxidative stress response. Oncotarget [Internet] 2016 [cited 2021 Aug 11];7(45):73147. Available from: /pmc/articles/PMC5341969/

99. X S, JH P, J T, H P, O CT, CM DC, et al. Adipocytes Sequester and Metabolize the Chemotherapeutic Daunorubicin. Mol Cancer Res [Internet] 2017 [cited 2021 Aug 11];15(12):1704–13. Available from: https://pubmed.ncbi.nlm.nih.gov/29117945/

100. Hanley MJ, Abernethy DR, Greenblatt DJ. Effect of obesity on the pharmacokinetics of drugs in humans. Clin. Pharmacokinet.2010;49(2):71–87.

101. Porter DJ, Wilson M. Effect of capping chemotherapy dose on chemotherapy effect in morbidly obese women with breast cancer. J Clin Oncol [Internet] 2013 [cited 2020 Mar 21];31(15_suppl):1081–1081. Available from: http://ascopubs.org/doi/10.1200/jco.2013.31.15_suppl.1081

102. Meyerhardt JA, Tepper JE, Niedzwiecki D, Hollis DR, McCollum AD, Brady D, et al. Impact of body mass index on outcomes and treatment-related toxicity in patients with stage II and III rectal cancer: Findings from intergroup trial 0114. J Clin Oncol 2004;22(4):648–57.

103. Meyerhardt JA, Catalano PJ, Haller DG, Mayer RJ, Benson AB, Macdonald JS, et al. Influence of body mass index on outcomes and treatment-related toxicity in patients with colon carcinoma. Cancer [Internet] 2003 [cited 2020 Mar 21];98(3):484–95. Available from: http://doi.wiley.com/10.1002/cncr.11544

104. Georgiadis MS, Steinberg SM, Hankins LA, Ihde DC, Johnson BE. Obesity and therapy-related toxicity in patients treated for small-cell lung cancer. J Natl Cancer Inst [Internet] 1995 [cited 2020 Mar 21];87(5):361–6. Available from: http://www.ncbi.nlm.nih.gov/pubmed/7853417

105. Wenzell CM, Gallagher EM, Earl M, Yeh JY, Kusick KN, Advani AS, et al. Outcomes in obese and overweight acute myeloid leukemia patients receiving chemotherapy dosed according to actual body weight. Am J Hematol [Internet] 2013 [cited 2020 Mar 22];88(10):906–9. Available from: http://www.ncbi.nlm.nih.gov/pubmed/23828018

106. Wang J, Myles B, Wei C, Chang JY, Hofstetter WL, Ajani JA, et al. Obesity and outcomes in patients treated with chemoradiotherapy for esophageal carcinoma. Dis Esophagus 2014;27(2):168–75.

107. Griggs JJ, Sorbero MES, Lyman GH. Undertreatment of obese women receiving breast cancer chemotherapy. Arch Intern Med [Internet] 2005 [cited 2020 Mar 23];165(11):1267–73. Available from: http://www.ncbi.nlm.nih.gov/pubmed/15956006

108. Cao Y. Adipocyte and lipid metabolism in cancer drug resistance. J. Clin. Invest.2019;129(8):3006–17.

109. Ouchi N, Parker JL, Lugus JJ, Walsh K. Adipokines in inflammation and metabolic disease. Nat. Rev. Immunol.2011;11(2):85–97.

110. Maury E, Brichard SM. Adipokine dysregulation, adipose tissue inflammation and metabolic syndrome. Mol. Cell. Endocrinol.2010;314(1):1–16.

111. Unamuno X, Gómez-Ambrosi J, Rodríguez A, Becerril S, Frühbeck G, Catalán V. Adipokine dysregulation and adipose tissue inflammation in human obesity. Eur J Clin Invest [Internet] 2018 [cited 2020 Apr 8];48(9):e12997. Available from: http://doi.wiley.com/10.1111/eci.12997

112. Nieman KM, Romero IL, Van Houten B, Lengyel E. Adipose tissue and adipocytes support tumorigenesis and metastasis. Biochim. Biophys. Acta - Mol. Cell Biol. Lipids2013;1831(10):1533–41.

113. Considine R V., Sinha MK, Heiman ML, Kriauciunas A, Stephens TW, Nyce MR, et al. Serum Immunoreactive-Leptin Concentrations in Normal-Weight and Obese Humans. N Engl J Med [Internet] 1996 [cited 2020 Sep 7];334(5):292–5. Available from: http://www.nejm.org/doi/abs/10.1056/NEJM199602013340503

114. Gogas H, Trakatelli M, Dessypris N, Terzidis A, Katsambas A, Chrousos GP, et al. Melanoma risk in association with serum leptin levels and lifestyle parameters: a case-control study. Ann Oncol 2007;19:384–9.

115. Carino C, Olawaiye AB, Cherfils S, Serikawa T, Lynch MP, Rueda BR, et al. Leptin regulation of proangiogenic molecules in benign and cancerous endometrial cells. Int J Cancer 2008;123(12):2782–90.

116. Yeh WL, Lu DY, Lee MJ, Fu WM. Leptin induces migration and invasion of glioma cells through MMP-13 production. Glia 2009;57(4):454–64.

117. Gu F, Zhang H, Yao L, Jiang S, Lu H, Xing X, et al. Leptin contributes to the taxol chemoresistance in epithelial ovarian cancer. Oncol Lett [Internet] 2019 [cited 2020 Mar 16];18(1):561–70. Available from: http://www.ncbi.nlm.nih.gov/pubmed/31289528

118. Cleary MP, Juneja SC, Phillips FC, Hu X, Grande JP, Maihle NJ. Leptin Receptor-Deficient MMTV-TGF-α/LeprdbLepr db Female Mice Do Not Develop Oncogene-Induced Mammary Tumors. Exp Biol Med 2004;229(2):182–93.

119. Otvos L, Kovalszky I, Riolfi M, Ferla R, Olah J, Sztodola A, et al. Efficacy of a leptin receptor antagonist peptide in a mouse model of triple-negative breast cancer. Eur J Cancer 2011;47(10):1578–84.

120. Lipsey CC, Harbuzariu A, Robey RW, Huff LM, Gottesman MM, Gonzalez-Perez RR. Leptin Signaling Affects Survival and Chemoresistance of Estrogen Receptor Negative Breast Cancer. Int J Mol Sci [Internet] 2020 [cited 2020 Nov 22];21(11):3794. Available from: https://www.mdpi.com/1422-0067/21/11/3794

121. VanSaun MN. Molecular pathways: Adiponectin and leptin signaling in cancer. Clin. Cancer Res.2013;19(8):1926–32.

122. Surmacz E. Leptin and adiponectin: Emerging therapeutic targets in breast cancer. J Mammary Gland Biol Neoplasia [Internet] 2013 [cited 2020 Apr 1];18(3–4):321–32. Available from: http://www.ncbi.nlm.nih.gov/pubmed/24136336

123. Otake S, Takeda H, Fujishima S, Fukui T, Orii T, Sato T, et al. Decreased levels of plasma adiponectin associated with increased risk of colorectal cancer. World J Gastroenterol 2010;16(10):1252–7.

124. Gelsomino L, Naimo GD, Catalano S, Mauro L, Andò S. The emerging role of adiponectin in female malignancies. Int J Mol Sci 2019;20(9).

125. Booth A, Magnuson A, Fouts J, Foster M. Adipose tissue, obesity and adipokines: Role in cancer promotion. Horm Mol Biol Clin Investig 2015;21(1):57–74.

126. Yang IP, Miao ZF, Huang CW, Tsai HL, Yeh YS, Su WC, et al. High blood sugar levels but not diabetes mellitus significantly enhance oxaliplatin chemoresistance in patients with stage III colorectal cancer receiving adjuvant FOLFOX6 chemotherapy. Ther Adv Med Oncol [Internet] 2019 [cited 2020 Nov 22];11. Available from: /pmc/articles/PMC6704420/?report=abstract

127. Bråkenhielm E, Veitonmäki N, Cao R, Kihara S, Matsuzawa Y, Zhivotovsky B, et al. Adiponectin-induced antiangiogenesis and antitumor activity involve caspase-mediated endothelial cell apoptosis. Proc Natl Acad Sci U S A [Internet] 2004 [cited 2020 Nov 22];101(8):2476–81. Available from: /pmc/articles/PMC356975/?report=abstract

128. Lee YC, Chen YJ, Wu CC, Lo S, Hou MF, Yuan SSF. Resistin expression in breast cancer tissue as a marker of prognosis and hormone therapy stratification. In: Gynecologic Oncology. Elsevier; 2012. page 742–50.

129. Wang CH, Wang PJ, Hsieh YC, Lo S, Lee YC, Chen YC, et al. Resistin facilitates breast cancer progression via TLR4-mediated induction of mesenchymal phenotypes and stemness properties. Oncogene 2018;37(5):589–600.

130. Liu Z, Shi A, Song D, Han B, Zhang Z, Ma L, et al. Resistin confers resistance to doxorubicin-induced apoptosis in human breast cancer cells through autophagy induction. Am J Cancer Res 2017;7(3):574–83.

131. Su YC, Davuluri GVN, Chen CH, Shiau DC, Chen CC, Chen CL, et al. Galectin-1-induced autophagy facilitates cisplatin resistance of hepatocellular carcinoma. PLoS One 2016;11(2).

132. Pang J, Shi Q, Liu Z, He J, Liu H, Lin P, et al. Resistin induces multidrug resistance in myeloma by inhibiting cell death and upregulating ABC transporter expression. Haematologica 2017;102(7):1273–80.

133. Nath A, Li I, Roberts LR, Chan C. Elevated free fatty acid uptake via CD36 promotes epithelial-mesenchymal transition in hepatocellular carcinoma. Sci Rep 2015;5.

134. Ladanyi A, Mukherjee A, Kenny HA, Johnson A, Mitra AK, Sundaresan S, et al. Adipocyte-induced CD36 expression drives ovarian cancer progression and metastasis. Oncogene 2018;37(17):2285–301.

135. Kubo M, Gotoh K, Eguchi H, Kobayashi S, Iwagami Y, Tomimaru Y, et al. Impact of CD36 on Chemoresistance in Pancreatic Ductal Adenocarcinoma. Ann Surg Oncol 2020;27(2):610–9.

136. Mentoor I, Engelbrecht AM, van Jaarsveld PJ, Nell T. Chemoresistance: Intricate Interplay Between Breast Tumor Cells and Adipocytes in the Tumor Microenvironment. Front Endocrinol (Lausanne) 2018;9:758.

137. Aiwei YB, Behjatolah MK, Hedges RA, Rogers LJ, Kadlubar SA, Thomas KE. Adipocyte hypoxia promotes epithelial-mesenchymal transition-related gene expression and estrogen receptor-negative phenotype in breast cancer cells. Oncol Rep 2015;33(6):2689–94.

138. Majmundar AJ, Wong WJ, Simon MC. Hypoxia-Inducible Factors and the Response to Hypoxic Stress. Mol. Cell2010;40(2):294–309.

139. Selvendiran K, Bratasz A, Kuppusamy ML, Tazi MF, Rivera BK, Kuppusamy P. Hypoxia induces chemoresistance in ovarian cancer cells by activation of signal transducer and activator of transcription 3. Int J Cancer [Internet] 2009 [cited 2020 Nov 22];125(9):2198–204. Available from: /pmc/articles/PMC2893222/?report=abstract

140. Krock BL, Skuli N, Simon MC. Hypoxia-Induced Angiogenesis: Good and Evil. Genes and Cancer 2011;2(12):1117–33.

141. Lin C, McGough R, Aswad B, Block JA, Terek R. Hypoxia induces HIF-1α and VEGF expression in chondrosarcoma cells and chondrocytes. J Orthop Res 2004;22(6):1175–81.

142. Mamede AC, Abrantes AM, Pedrosa L, Casalta-Lopes JE, Pires AS, Teixo RJ, et al. Beyond the Limits of Oxygen: Effects of Hypoxia in a Hormone-Independent Prostate Cancer Cell Line. ISRN Oncol [Internet] 2013 [cited 2020 Nov 22];2013:1–8. Available from: /pmc/articles/PMC3791829/?report=abstract

143. Liu L, Ning X, Sun L, Zhang H, Shi Y, Guo C, et al. Hypoxia-inducible factor-1α contributes to hypoxia-induced chemoresistance in gastric cancer. Cancer Sci [Internet] 2007 [cited 2020 Nov 22];0(0):071113200242006-??? Available from: http://doi.wiley.com/10.1111/j.1349-7006.2007.00643.x

144. Hosogai N, Fukuhara A, Oshima K, Miyata Y, Tanaka S, Segawa K, et al. Adipose tissue hypoxia in obesity and its impact on adipocytokine dysregulation. Diabetes 2007;56(4):901–11.

145. Denduluri SK, Idowu O, Wang Z, Liao Z, Yan Z, Mohammed MK, et al. Insulin-like growth factor (IGF) signaling intumorigenesis and the development ofcancer drug resistance. Genes Dis.2015;2(1):13–25.

146. Doyle SL, Donohoe CL, Finn SP, Howard JM, Lithander FE, Reynolds J V., et al. IGF-1 and its receptor in esophageal cancer: association with adenocarcinoma and visceral obesity. Am J Gastroenterol [Internet] 2012 [cited 2023 Mar 25];107(2):196–204. Available from: https://pubmed.ncbi.nlm.nih.gov/22146489/

147. Vigneri PG, Tirrò E, Pennisi MS, Massimino M, Stella S, Romano C, et al. The insulin/IGF system in colorectal cancer development and resistance to therapy. Front. Oncol.2017;5(OCT):230.

148. Shen K, Cui D, Sun L, Lu Y, Han M, Liu J. Inhibition of IGF-IR increases chemosensitivity in human colorectal cancer cells through MRP-2 promoter suppression. J Cell Biochem 2012;113(6):2086–97.

149. Samuel S, Fan F, Dang LH, Xia L, Gaur P, Ellis LM. Intracrine vascular endothelial growth factor signaling in survival and chemoresistance of human colorectal cancer cells. Oncogene 2011;30(10):1205–12.

150. Nusrat O, Belotte J, Fletcher NM, Memaj I, Saed MG, Diamond MP, et al. The Role of Angiogenesis in the Persistence of Chemoresistance in Epithelial Ovarian Cancer. Reprod Sci 2016;23(11):1484–92.

151. Zhang Y, Daquinag AC, Amaya-Manzanares F, Sirin O, Tseng C, Kolonin MG. Stromal progenitor cells from endogenous adipose tissue contribute to pericytes and adipocytes that populate the tumor microenvironment. Cancer Res 2012;72(20):5198–208.

152. Khairoun M, S Korevaar S. Human Bone Marrow- and Adipose Tissue-derived Mesenchymal Stromal Cells are Immunosuppressive In vitro and in a Humanized Allograft Rejection Model. J Stem Cell Res Ther 2013;Suppl 6(1).

153. Mele V, Muraro MG, Calabrese D, Pfaff D, Amatruda N, Amicarella F, et al. Mesenchymal stromal cells induce epithelial-to-mesenchymal transition in human colorectal cancer cells through the expression of surface-bound TGF-β. Int J Cancer [Internet] 2014 [cited 2020 Mar 26];134(11):2583–94. Available from: http://www.ncbi.nlm.nih.gov/pubmed/24214914

154. Kucerova L, Skolekova S, Matuskova M, Bohac M, Kozovska Z. Altered features and increased chemosensitivity of human breast cancer cells mediated by adipose tissue-derived mesenchymal stromal cells. BMC Cancer 2013;13(1):1–13.

155. Su F, Ahn S, Saha A, DiGiovanni J, Kolonin MG. Adipose stromal cell targeting suppresses prostate cancer epithelial-mesenchymal transition and chemoresistance. Oncogene [Internet] 2019 [cited 2020 Mar 16];38(11):1979–88. Available

from: http://www.ncbi.nlm.nih.gov/pubmed/30361686

156. Incio J, Liu H, Suboj P, Chin SM, Chen IX, Pinter M, et al. Obesity-induced inflammation and desmoplasia promote pancreatic cancer progression and resistance to chemotherapy. Cancer Discov [Internet] 2016 [cited 2020 Mar 16];6(8):852–69. Available from: http://www.ncbi.nlm.nih.gov/pubmed/27246539

157. Gaianigo N, Melisi D, Carbone C. EMT and Treatment Resistance in Pancreatic Cancer. Cancers (Basel) [Internet] 2017 [cited 2020 Mar 22];9(12):122. Available from: http://www.mdpi.com/2072-6694/9/9/122

158. Ansari D, Carvajo M, Bauden M, Andersson R. Pancreatic cancer stroma: controversies and current insights. Scand. J. Gastroenterol.2017;52(6–7):641–6.

159. Bain GH, Collie-Duguid E, Murray GI, Gilbert FJ, Denison A, McKiddie F, et al. Tumour expression of leptin is associated with chemotherapy resistance and therapy-independent prognosis in gastro-oesophageal adenocarcinomas. Br J Cancer 2014;110(6):1525–34.

160. Sokolova O, Naumann M. NF-κB signaling in gastric cancer [Internet]. Toxins (Basel).2017 [cited 2020 Mar 16];9(4). Available from: http://www.ncbi.nlm.nih.gov/pubmed/28350359

161. Renehan AG, Dive C. Obesity, insulin and chemoresistance in colon cancer. J Gastrointest Oncol [Internet] 2011 [cited 2020 Mar 16];2(1):8–10. Available from: http://www.ncbi.nlm.nih.gov/pubmed/22811820

162. Incio J, Liu H, Suboj P, Chin SM, Chen IX, Pinter M, et al. Obesity-induced inflammation and desmoplasia promote pancreatic cancer progression and resistance to chemotherapy. Cancer Discov 2016;6(8):852–69.

163. Rizi BS, Caneba C, Nowicka A, Nabiyar AW, Liu X, Chen K, et al. Nitric oxide mediates metabolic coupling of omentum-derived adipose stroma to ovarian and endometrial cancer cells. Cancer Res 2015;75(2):456–71.

164. Yang J, Zaman MM, Vlasakov I, Roy R, Huang L, Martin CR, et al. Adipocytes promote ovarian cancer chemoresistance. Sci Rep 2019;9(1).

165. Yu W, Cao DD, Li Q bai, Mei H ling, Hu Y, Guo T. Adipocytes secreted leptin is a pro-tumor factor for survival of multiple myeloma under chemotherapy. Oncotarget 2016;7(52):86075–86.

166. Connell PP, Hellman S. Advances in radiotherapy and implications for the next century: A historical perspective. Cancer Res.2009;69(2):383–92.

167. Ross KH, Gogineni K, Subhedar PD, Lin JY, McCullough LE. Obesity and cancer treatment efficacy: Existing challenges and opportunities [Internet]. Cancer2019 [cited 2020 Mar 18];125(10):1588–92. Available from: https://onlinelibrary.wiley.com/doi/abs/10.1002/cncr.31976

168. Lin LL, Hertan L, Rengan R, Teo BKK. Effect of body mass index on magnitude of setup errors in patients treated with adjuvant radiotherapy for endometrial cancer with daily image guidance. Int J Radiat Oncol Biol Phys 2012;83(2):670–5.

169. Moszyńska-Zielińska M, Chaułbińska-Fendler J, Gottwald L, Zytko L, Bigos E, Fijuth J. Does obesity hinder radiotherapy in endometrial cancer patients? The implementation of new techniques in adjuvant radiotherapy - Focus on obese patients. Prz Menopauzalny 2014;18(2):96–100.

170. Wang LS, Murphy CT, Ruth K, Zaorsky NG, Smaldone MC, Sobczak ML, et al. Impact of obesity on outcomes after definitive dose-escalated intensity-modulated radiotherapy for localized prostate cancer. Cancer 2015;121(17):3010–7.

171. Choi Y, Lee YH, Park SK, Cho H, Ahn KJ. Association between obesity and local control of advanced rectal cancer after combined surgery and radiotherapy. Radiat Oncol J [Internet] 2016 [cited 2020 Mar 19];34(2):113–20. Available from: http://www.ncbi.nlm.nih.gov/pubmed/27306771

172. Hicks DF, Bakst R, Doucette J, Kann BH, Miles B, Genden E, et al. Impact of obesity on outcomes for patients with head and neck cancer. Oral Oncol 2018;83:11–7.

173. Von Gruenigen VE, Tian C, Frasure H, Waggoner S, Keys H, Barakat RR. Treatment effects, disease recurrence, and survival in obese women with early endometrial carcinoma: A Gynecologic Oncology Group Study. Cancer 2006;107(12):2786–91.

174. Silberg J, Nowak K, Larose M, Wright C, Simone NL. Effect of elevated BMI on radiation toxicity in early stage breast cancer patients. J Clin Oncol 2016;34(15_suppl):1049–1049.

175. AA DG, L FG, ÁM L, J SS, R C, E DCP, et al. Breast Radiotherapy-Related Cardiotoxicity. When, How, Why. Risk Prevention and Control Strategies. Cancers (Basel) [Internet] 2021 [cited 2021 Aug 10];13(7). Available from: https://pubmed.ncbi.nlm.nih.gov/33916644/

176. Hayashi Y, Iijima H, Isohashi F, Tsujii Y, Fujinaga T, Nagai K, et al. The heart's exposure to radiation increases the risk of cardiac toxicity after chemoradiotherapy for superficial esophageal cancer: A retrospective cohort study. BMC Cancer [Internet] 2019 [cited 2020 Mar 19];19(1):195. Available from: https://bmccancer.biomedcentral.com/articles/10.1186/s12885-019-5421-y

177. Coelho P, Silva L, Faria I, Vieria M, Monteiro A, Pinto G, et al. Adipocyte Secretome Increases Radioresistance of Malignant Melanocytes by Improving Cell Survival and Decreasing Oxidative Status. Radiat Res 2017;187(5):581.

178. Kosmacek EA, Oberley-Deegan RE. Adipocytes protect fibroblasts from radiation-induced damage by adiponectin secretion. Sci Reports 2020 101 [Internet] 2020 [cited 2021 Aug 11];10(1):1–12. Available from: https://www.nature.com/articles/s41598-020-69352-w

179. Z L, KKL W, X J, A X, KKY C. The role of adipose tissue senescence in obesity- and ageing-related metabolic disorders. Clin Sci (Lond) [Internet] 2020 [cited 2021 Aug 11];134(2):315–30. Available from: https://pubmed.ncbi.nlm.nih.gov/31998947/

180. Wu Q, Li B, Sun S, Sun S. Unraveling Adipocytes and Cancer Links: Is There a Role for Senescence? Front Cell Dev Biol 2020;0:282.

181. Dirat B, Bochet L, Dabek M, Daviaud D, Dauvillier S, Majed B, et al. Cancer-associated adipocytes exhibit an activated phenotype and contribute to breast cancer invasion. Cancer Res [Internet] 2011 [cited 2020 Mar 27];71(7):2455–65. Available from: http://www.ncbi.nlm.nih.gov/pubmed/21459803

182. Russo SM, Tepper JE, Baldwin AS Jr, Liu R, Adams J, Elliott P, et al. Enhancement of radiosensitivity by proteasome inhibition: Implications for a role of NF-κB. Int J Radiat Oncol Biol Phys 2001;50(1):183–93.

183. Voboril R, Weberova-Voborilova J. Constitutive NF-kappaB activity in colorectal cancer cells: impact on radiation-induced NF-kappaB activity, radiosensitivity, and apoptosis. Neoplasma [Internet] 2006 [cited 2020 Mar 21];53(6):518–23. Available from: http://www.ncbi.nlm.nih.gov/pubmed/17167722

184. Bonner JA, Trummell HQ, Willey CD, Plants BA, Raisch KP. Inhibition of STAT-3 results in radiosensitization of human squamous cell carcinoma. Radiother Oncol 2009;92(3):339–44.

185. Wunderlich CM, Hövelmeyer N, Wunderlich FT. Mechanisms of chronic JAK-STAT3-SOCS3 signaling in obesity. JAK-STAT 2013;2(2):e23878.

186. Zeng L, Beggs RR, Cooper TS, Weaver AN, Yang ES. Combining Chk1/2 inhibition with cetuximab and radiation enhances in vitro and in vivo cytotoxicity in head and neck squamous cell carcinoma. Mol Cancer Ther 2017;16(4):591–600.

187. Yang HY, Qu RM, Lin XS, Liu TX, Sun QQ, Yang C, et al. IGF-1 from Adipose-derived mesenchymal stem cells promotes radioresistance of breast cancer cells. Asian Pacific J Cancer Prev 2014;15(23):10115–9.

188. Richardson RB, Harper ME. Mitochondrial stress controls the radiosensitivity of the oxygen effect: Implications for radiotherapy. Oncotarget 2016;7(16):21469–83.

189. Harada H, Itasaka S, Zhu Y, Zeng L, Xie X, Morinibu A, et al. Treatment regimen determines whether an HIF-1 inhibitor enhances or inhibits the effect of radiation therapy. Br J Cancer 2009;100(5):747–57.

190. Tang L, Wei F, Wu Y, He Y, Shi L, Xiong F, et al. Role of metabolism in cancer cell radioresistance and radiosensitization methods. J. Exp. Clin. Cancer Res.2018;37(1):1–15.

191. Shimura T, Noma N, Sano Y, Ochiai Y, Oikawa T, Fukumoto M, et al. AKT-mediated enhanced aerobic glycolysis causes acquired radioresistance by human tumor cells. Radiother Oncol 2014;112(2):302–7.

192. Cruz-Gregorio A, Martínez-Ramírez I, Pedraza-Chaverri J, Lizano M. Reprogramming of energy metabolism in response to radiotherapy in head and neck squamous cell carcinoma. Cancers (Basel).2019;11(2):182.

193. Lynam-Lennon N, Connaughton R, Carr E, Mongan AM, O'Farrell NJ, Porter RK, et al. Excess visceral adiposity induces alterations in mitochondrial function and energy metabolism in esophageal adenocarcinoma. BMC Cancer [Internet] 2014 [cited 2019 Apr 12];14:907. Available from: http://www.ncbi.nlm.nih.gov/pubmed/25471892

194. Mongan AM, Lynam-Lennon N, Doyle SL, Casey R, Carr E, Cannon A, et al. Visceral adipose tissue modulates radiosensitivity in oesophageal adenocarcinoma. Int J Med Sci [Internet] 2019 [cited 2020 Mar 16];16(4):519–28. Available from: http://www.ncbi.nlm.nih.gov/pubmed/31171903

195. Naumann P, Habermehl D, Welzel T, Debus J, Combs SE. Outcome after neoadjuvant chemoradiation and correlation with nutritional status in patients with locally advanced pancreatic cancer. Strahlentherapie und Onkol 2013;189(9):745–52.

196. Dandapani S V, Zhang Y, Jennelle R, Lin YG. Radiation-Associated Toxicities in Obese Women with Endometrial Cancer: More Than Just BMI? ScientificWorldJournal [Internet] 2015 [cited 2020 Mar 19];2015:483208. Available from: http://www.ncbi.nlm.nih.gov/pubmed/26146653

197. Al-Ammar Y, Al-Mansour B, Al-Rashood O, Tunio MA, Islam T, Al-Asiri M, et al. Impact of body mass index on survival outcome in patients with differentiated thyroid cancer. Braz J Otorhinolaryngol 2018;84(2):220–6.

198. Chowdhury PS, Chamoto K, Honjo T. Combination therapy strategies for improving PD-1 blockade efficacy: a new era in cancer immunotherapy. J Intern Med [Internet] 2018 [cited 2023 Mar 22];283(2):110–20. Available from: https://pubmed.ncbi.nlm.nih.gov/29071761/

199. Mirsoian A, Bouchlaka MN, Sckisel GD, Chen M, Pai CCS, Maverakis E, et al. Adiposity induces lethal cytokine storm after systemic administration of stimulatory immunotherapy regimens in aged mice. J Exp Med 2014;211(12):2373–83.

200. Guiu B, Petit JM, Bonnetain F, Ladoire S, Guiu S, Cercueil JP, et al. Visceral fat area is an independent predictive biomarker of outcome after first-line bevacizumab-based treatment in metastatic colorectal cancer. Gut 2010;59(3):341–7.

201. Incio J, Ligibel JA, McManus DT, Suboj P, Jung K, Kawaguchi K, et al. Obesity promotes resistance to anti-VEGF therapy in breast cancer by up-regulating IL-6 and potentially FGF-2. Sci Transl Med 2018;10(432).

202. E. Griner S, J. Wang K, P. Joshi J, Nahta R. Mechanisms of Adipocytokine-Mediated Trastuzumab Resistance in HER2-Positive Breast Cancer Cell Lines. Curr Pharmacogenomics Person Med 2013;11(1):31–41.

203. Schernthaner-Reiter MH, Kasses D, Tugendsam C, Riedl M, Peric S, Prager G, et al. Growth differentiation factor 15 increases following oral glucose ingestion: Effect of meal composition and obesity. Eur J Endocrinol 2016;175(6):623–31.

204. Bougaret L, Delort L, Billard H, Le Huede C, Boby C, De la Foye A, et al. Adipocyte/breast cancer cell crosstalk in obesity interferes with the anti-proliferative efficacy of tamoxifen. PLoS One 2018;13(2).

205. Efstathiou JA, Bae K, Shipley WU, Hanks GE, Pilepich M V., Sandler HM, et al. Obesity and mortality in men with locally advanced prostate cancer: Analysis of RTOG 85-31. Cancer 2007;110(12):2691–9.

206. Mangiola S, Stuchbery R, McCoy P, Chow K, Kurganovs N, Kerger M, et al. Androgen deprivation therapy promotes an obesity-like microenvironment in periprostatic fat. Endocr Connect 2019;8(5):547–58.

207. Halabi S, Ou SS, Vogelzang NJ, Small EJ. Inverse correlation between body mass index and clinical outcomes in men with advanced castration–recurrent prostate cancer. Cancer [Internet] 2007 [cited 2020 Apr 20];110(7):1478–84. Available from: http://doi.wiley.com/10.1002/cncr.22932

208. Groß JP, Nattenmüller J, Hemmer S, Tichy D, Krzykalla J, Goldschmidt H, et al. Body fat composition as predictive factor for treatment response in patients with newly diagnosed multiple myeloma – subgroup analysis of the prospective GMMG MM5 trial. Oncotarget 2017;8(40):68460.

209. Zhao J, Zhi Z, Wang C, Xing H, Song G, Yu X, et al. Exogenous lipids promote the growth of breast cancer cells via CD36. Oncol Rep 2017;38(4):2105–15.

210. Liang Y, Han H, Liu L, Duan Y, Yang X, Ma C, et al. CD36 plays a critical role in proliferation, migration and tamoxifen-inhibited growth of ER-positive breast cancer cells. Oncogenesis 2018;7(12):1–14.

211. Yang J, Park KW, Cho S. Inhibition of the CD36 receptor reduces visceral fat accumulation and improves insulin resistance in obese mice carrying the BDNF-Val66Met variant. J Biol Chem 2018;293(34):13338–48.

212. Murphy KA, James BR, Sjaastad F V., Kucaba TA, Kim H, Brincks EL, et al. Cutting Edge: Elevated Leptin during Diet-Induced Obesity Reduces the Efficacy of Tumor Immunotherapy. J Immunol [Internet] 2018 [cited 2020 Mar 17];201(7):1837–41. Available from: http://www.ncbi.nlm.nih.gov/pubmed/30135180

213. Canter RJ, Le CT, Beerthuijzen JMT, Murphy WJ. Obesity as an immune-modifying factor in cancer immunotherapy [Internet]. J. Leukoc. Biol.2018 [cited 2020 Mar 16];104(3):487–97. Available from: http://www.ncbi.nlm.nih.gov/pubmed/29762866

214. Wang Z, Monjazeb AM, Murphy WJ. The complicated effects of obesity on cancer and immunotherapy [Internet]. Immunotherapy2019 [cited 2020 Mar 17];11(1):11–4. Available from: http://www.ncbi.nlm.nih.gov/pubmed/30702013

215. Yan Z, Cao J, Cheng H, Qiao J, Zhang H, Wang Y, et al. A combination of humanised anti-CD19 and anti-BCMA CAR T cells in patients with relapsed or refractory multiple myeloma: a single-arm, phase 2 trial. Lancet Haematol 2019;6(10):e521–9.

216. Lee DW, Kochenderfer JN, Stetler-Stevenson M, Cui YK, Delbrook C, Feldman SA, et al. T cells expressing CD19 chimeric antigen receptors for acute lymphoblastic leukaemia in children and young adults: A phase 1 dose-escalation trial. Lancet 2015;385(9967):517–28.

217. Mirsoian A, Murphy WJ. Obesity and cancer immunotherapy toxicity. Immunotherapy2015;7(4):319–22.

218. Andersen R, Donia M, Westergaard MCW, Pedersen M, Hansen M, Svane IM. Tumor infiltrating lymphocyte therapy for ovarian cancer and renal cell carcinoma. Hum Vaccin Immunother [Internet] 2015 [cited 2020 Apr 19];11(12):2790–5. Available from: http://www.tandfonline.com/doi/full/10.1080/21645515.2015.1075106

219. Zhang J, Wang L. The emerging world of TCR-T cell trials against cancer: A systematic review. Technol. Cancer Res. Treat.2019;18.

220. Shimasaki N, Jain A, Campana D. NK cells for cancer immunotherapy. Nat. Rev. Drug Discov.2020;19(3):200–18.

221. Murphy WJ, Longo DL. The Surprisingly Positive Association between Obesity and Cancer Immunotherapy Efficacy [Internet]. JAMA - J. Am. Med. Assoc.2019 [cited 2020 Mar 17];321(13):1247–8. Available from: http://www.ncbi.nlm.nih.gov/pubmed/30882850

222. Cortellini A, Bersanelli M, Buti S, Cannita K, Santini D, Perrone F, et al. A multicenter study of body mass index in cancer patients treated with anti-PD-1/PD-L1 immune checkpoint inhibitors: When overweight becomes favorable. J Immunother Cancer [Internet] 2019 [cited 2020 Mar 18];7(1):57. Available from: http://jitc.bmj.com/lookup/doi/10.1186/s40425-019-0527-y

223. Wang Z, Aguilar EG, Luna JI, Dunai C, Khuat LT, Le CT, et al. Paradoxical effects of obesity on T cell function during tumor progression and PD-1 checkpoint blockade. Nat Med 2019;25(1):141–51.

224. Wu B, Sun X, Gupta HB, Yuan B, Li J, Ge F, et al. Adipose PD-L1 Modulates PD-1/PD-L1 Checkpoint Blockade Immunotherapy Efficacy in Breast Cancer. Oncoimmunology [Internet] 2018 [cited 2020 Mar 18];7(11):e1500107. Available from: https://www.tandfonline.com/doi/full/10.1080/2162402X.2018.1500107

225. Dirix LY, Takacs I, Jerusalem G, Nikolinakos P, Arkenau HT, Forero-Torres A, et al. Avelumab, an anti-PD-L1 antibody, in patients with locally advanced or metastatic breast cancer: A phase 1b JAVELIN solid tumor study. Breast Cancer Res Treat 2018;167(3):671–86.

226. Donnelly D, Bajaj S, Yu J, Hsu M, Balar A, Pavlick A, et al. The complex relationship between body mass index and

response to immune checkpoint inhibition in metastatic melanoma patients. J Immunother Cancer [Internet] 2019 [cited 2020 Mar 21];7(1):222. Available from: http://jitc.bmj.com/lookup/doi/10.1186/s40425-019-0699-5

227. Richtig G, Hoeller C, Wolf M, Wolf I, Rainer BM, Schulter G, et al. Body mass index may predict the response to ipilimumab in metastatic melanoma: An observational multi-centre study. PLoS One 2018;13(10).

228. Fujii M, Inoguchi T, Batchuluun B, Sugiyama N, Kobayashi K, Sonoda N, et al. CTLA-4Ig immunotherapy of obesity-induced insulin resistance by manipulation of macrophage polarization in adipose tissues. Biochem Biophys Res Commun 2013;438(1):103–9.

229. Bayan CAY, Lopez AT, Gartrell RD, Komatsubara KM, Bogardus M, Rao N, et al. The Role of Oncolytic Viruses in the Treatment of Melanoma. Curr Oncol Rep [Internet] 2018 [cited 2020 Apr 20];20(10):80. Available from: http://link.springer.com/10.1007/s11912-018-0729-3

230. Sprooten J, Ceusters J, Coosemans A, Agostinis P, De Vleeschouwer S, Zitvogel L, et al. Trial watch: dendritic cell vaccination for cancer immunotherapy. Oncoimmunology2019;8(11).

231. O'Connell F, O'Sullivan J. Help or hindrance: The obesity paradox in cancer treatment response. Cancer Lett 2021;522:269–80.

232. Donlon NE, Sheppard A, Davern M, O'connell F, Phelan JJ, Power R, et al. Linking Circulating Serum Proteins with Clinical Outcomes in Esophageal Adenocarcinoma—An Emerging Role for Chemokines. Cancers 2020, Vol 12, Page 3356 [Internet] 2020 [cited 2021 Nov 15];12(11):3356. Available from: https://www.mdpi.com/2072-6694/12/11/3356/htm

233. Gentili A, Zaibi MS, Alomar SY, De Vuono S, Ricci MA, Alaeddin A, et al. Circulating Levels of the Adipokines Monocyte Chemotactic Protein-4 (MCP-4), Macrophage Inflammatory Protein-1β (MIP-1β), and Eotaxin-3 in Severe Obesity and Following Bariatric Surgery. Horm Metab Res [Internet] 2016 [cited 2022 Sep 6];48(12):847–53. Available from: https://pubmed.ncbi.nlm.nih.gov/27300476/

234. Peng JC, Abu Bakar S, Richardson MM, Jonsson JJ, Frazer IH, Nielsen LK, et al. IL10 and IL12B polymorphisms each influence IL-12p70 secretion by dendritic cells in response to LPS. Immunol Cell Biol 2006;84(2):227–32.

235. Little AC, Pathanjeli P, Wu Z, Bao L, Goo LE, Yates JA, et al. IL-4/IL-13 stimulated macrophages enhance breast cancer invasion via rho-GTPase regulation of synergistic VEGF/CCL-18 signaling. Front Oncol 2019;9(MAY):456.

236. Mittal SK, Cho KJ, Ishido S, Roche PA. Interleukin 10 (IL-10)-mediated Immunosuppression: MARCH-I INDUCTION REGULATES ANTIGEN PRESENTATION BY MACROPHAGES BUT NOT DENDRITIC CELLS*. J Biol Chem [Internet] 2015 [cited 2022 Sep 22];290(45):27158. Available from: /pmc/articles/PMC4646393/

237. Ostrand-Rosenberg S. Immune Surveillance: A Balance Between Pro- and Anti-tumor Immunity. Curr Opin Genet Dev [Internet] 2008 [cited 2023 Mar 22];18(1):11. Available from: /pmc/articles/PMC2699403/

238. Ma YL, Huang FJ, Cong L, Gong WC, Bai HM, Li J, et al. IL-4–Producing Dendritic Cells Induced during Schistosoma japonica Infection Promote Th2 Cells via IL-4–Dependent Pathway. J Immunol [Internet] 2015 [cited 2023 Mar 22];195(8):3769–80. Available from: https://journals.aai.org/jimmunol/article/195/8/3769/105128/IL-4-Producing-Dendritic-Cells-Induced-during

239. Keswani T, Sarkar S, Sengupta A, Bhattacharyya A. Role of TGF-β and IL-6 in dendritic cells, Treg and Th17 mediated immune response during experimental cerebral malaria. Cytokine [Internet] 2016 [cited 2023 Mar 22];88:154–66. Available from: https://pubmed.ncbi.nlm.nih.gov/27632786/

240. Bailey SR, Nelson MH, Himes RA, Li Z, Mehrotra S, Paulos CM. Th17 cells in cancer: The ultimate identity crisis. Front Immunol 2014;5(JUN):276.

241. Kushwah R, Hu J. Role of dendritic cells in the induction of regulatory T cells. Cell Biosci [Internet] 2011 [cited 2023 Mar 22];1(1):1–10. Available from: https://cellandbioscience.biomedcentral.com/articles/10.1186/2045-3701-1-20

242. Liang YH, Tsai JH, Cheng YM, Chan KY, Hsu WL, Lee CC, et al. Chemotherapy agents stimulate dendritic cells against human colon cancer cells through upregulation of the transporter associated with antigen processing. Sci Reports 2021 111 [Internet] 2021 [cited 2023 Feb 16];11(1):1–13. Available from: https://www.nature.com/articles/s41598-021-88648-z

243. Blair TC, Bambina S, Alice AF, Kramer GF, Medler TR, Baird JR, et al. Dendritic Cell Maturation Defines Immunological Responsiveness of Tumors to Radiation Therapy. J Immunol [Internet] 2020 [cited 2023 Feb 16];204(12):3416. Available from: /pmc/articles/PMC7571541/

244. Liang W, Qi Y, Yi H, Mao C, Meng Q, Wang H, et al. The Roles of Adipose Tissue Macrophages in Human Disease. Front Immunol 2022;13:2831.

245. Heath O, Berlato C, Maniati E, Lakhani A, Pegrum C, Kotantaki P, et al. Chemotherapy induces tumor-associated macrophages that aid adaptive immune responses in ovarian cancer. Cancer Immunol Res [Internet] 2021 [cited 2023 Feb 16];9(6):665. Available from: /pmc/articles/PMC7611478/

246. Larionova I, Cherdyntseva N, Liu T, Patysheva M, Rakina M, Kzhyshkowska J. Interaction of tumor-associated macrophages and cancer chemotherapy. Oncoimmunology [Internet] 2019 [cited 2023 Feb 15];8(7). Available from: /pmc/articles/PMC6527283/

247. Shi X, Shiao SL. The Role of Macrophage Phenotype in Regulating the Response to Radiation Therapy. Transl Res [Internet] 2018 [cited 2023 Feb 6];191:64. Available from: /pmc/articles/PMC6018060/

248. Ostrand-Rosenberg S. Myeloid derived-suppressor cells: their role in cancer and obesity. Curr Opin Immunol 2018;51:68–75.

249. Xia S, Sha H, Yang L, Ji Y, Ostrand-Rosenberg S, Qi L. Gr-1+ CD11b+ myeloid-derived suppressor cells suppress inflammation and promote insulin sensitivity in obesity. J Biol Chem [Internet] 2011 [cited 2023 Jun 25];286(26):23591–9. Available from: http://www.jbc.org/article/S0021925819488923/fulltext

250. Bao Y, Mo J, Ruan L, Li G. Increased monocytic CD14+HLADRlow/- myeloid-derived suppressor cells in obesity. Mol Med Rep [Internet] 2015 [cited 2023 Jun 25];11(3):2322–8. Available from: http://www.spandidos-publications.com/10.3892/mmr.2014.2927/abstract

251. Yan D, Adeshakin AO, Xu M, Afolabi LO, Zhang G, Chen YH, et al. Lipid Metabolic Pathways Confer the Immunosuppressive Function of Myeloid-Derived Suppressor Cells in Tumor. Front Immunol [Internet] 2019 [cited 2023 Jun 25];10(JUN):1399. Available from: /pmc/articles/PMC6593140/

252. Chen H, Sun L, Feng L, Yin Y, Zhang W. Role of Innate lymphoid Cells in Obesity and Insulin Resistance. Front Endocrinol (Lausanne) [Internet] 2022 [cited 2023 Jun 26];13. Available from: /pmc/articles/PMC9091334/

253. Wang H, Shen L, Sun X, Liu F, Feng W, Jiang C, et al. Adipose group 1 innate lymphoid cells promote adipose tissue fibrosis and diabetes in obesity. Nat Commun 2019 101 [Internet] 2019 [cited 2023 Jun 27];10(1):1–14. Available from: https://www.nature.com/articles/s41467-019-11270-1

254. Wilhelm C, Harrison OJ, Schmitt V, Pelletier M, Spencer SP, Urban JF, et al. Critical role of fatty acid metabolism in ILC2-mediated barrier protection during malnutrition and helminth infection. J Exp Med [Internet] 2016 [cited 2023 Jun 27];213(8):1409. Available from: /pmc/articles/PMC4986525/

255. Robinette ML, Fuchs A, Cortez VS, Lee JS, Wang Y, Durum SK, et al. Transcriptional programs define molecular characteristics of innate lymphoid cell classes and subsets. Nat Immunol [Internet] 2015 [cited 2023 Jun 27];16(3):306–17. Available from: https://pubmed.ncbi.nlm.nih.gov/25621825/

256. Terabe M, Park JM, Berzofsky JA. Role of IL-13 in regulation of anti-tumor immunity and tumor growth. Cancer Immunol Immunother [Internet] 2004 [cited 2023 Jun 27];53(2):79–85. Available from: https://pubmed.ncbi.nlm.nih.gov/14610620/

257. Li Y, Wang W, Yang F, Xu Y, Feng C, Zhao Y. The regulatory roles of neutrophils in adaptive immunity. Cell Commun Signal [Internet] 2019 [cited 2023 Jun 28];17(1):1–11. Available from: https://biosignaling.biomedcentral.com/articles/10.1186/s12964-019-0471-y

258. Sanchez-Pino MD, Richardson WS, Zabaleta J, Puttalingaiah RT, Chapple AG, Liu J, et al. Increased inflammatory low-density neutrophils in severe obesity and effect of bariatric surgery: Results from case-control and prospective cohort studies. eBioMedicine [Internet] 2022 [cited 2023 Jun 28];77. Available from: http://www.thelancet.com/article/S2352396422000949/fulltext

259. Talukdar S, Oh DY, Bandyopadhyay G, Li D, Xu J, McNelis J, et al. Neutrophils mediate insulin resistance in mice fed a high-fat diet through secreted elastase. Nat Med [Internet] 2012 [cited 2023 Jun 28];18(9):1407–12. Available from: https://pubmed.ncbi.nlm.nih.gov/22863787/

260. Rice CM, Davies LC, Subleski JJ, Maio N, Gonzalez-Cotto M, Andrews C, et al. Tumour-elicited neutrophils engage mitochondrial metabolism to circumvent nutrient limitations and maintain immune suppression. Nat Commun [Internet] 2018 [cited 2023 Jun 29];9(1). Available from: /pmc/articles/PMC6269473/

261. Xiong S, Dong L, Cheng L. Neutrophils in cancer carcinogenesis and metastasis. J Hematol Oncol 2021 141 [Internet] 2021 [cited 2023 Jun 30];14(1):1–17. Available from: https://jhoonline.biomedcentral.com/articles/10.1186/s13045-021-01187-y

262. Vivier E, Tomasello E, Baratin M, Walzer T, Ugolini S. Functions of natural killer cells. Nat Immunol 2008 95 [Internet] 2008 [cited 2023 Jun 27];9(5):503–10. Available from: https://www.nature.com/articles/ni1582

263. Lee BC, Kim MS, Pae M, Yamamoto Y, Eberlé D, Shimada T, et al. Adipose natural killer cells regulate adipose tissue macrophages to promote insulin resistance in obesity. Cell Metab [Internet] 2016 [cited 2023 Jun 27];23(4):685. Available from: /pmc/articles/PMC4833527/

264. Lynch LA, O'Connell JM, Kwasnik AK, Cawood TJ, O'Farrelly C, O'Shea DB. Are natural killer cells protecting the metabolically healthy obese patient? Obesity (Silver Spring) [Internet] 2009 [cited 2023 Jun 27];17(3):601–5. Available from: https://pubmed.ncbi.nlm.nih.gov/19238145/

265. Kobayashi T, Lam PY, Jiang H, Bednarska K, Gloury R, Murigneux V, et al. Increased lipid metabolism impairs NK cell function and mediates adaptation to the lymphoma environment. Blood [Internet] 2020 [cited 2023 Jun 27];136(26):3004–17. Available from: https://pubmed.ncbi.nlm.nih.gov/32818230/

266. Conroy MJ, Fitzgerald V, Doyle SL, Channon S, Useckaite Z, Gilmartin N, et al. The microenvironment of visceral adipose tissue and liver alter natural killer cell viability and function. J Leukoc Biol [Internet] 2016 [cited 2022 Sep 6];100(6):1435–42. Available from: https://pubmed.ncbi.nlm.nih.gov/27365528/

267. Zhang N, Bevan MJ. CD8(+) T cells: foot soldiers of the immune system. Immunity [Internet] 2011 [cited 2023 Jun 30];35(2):161–8. Available from: https://pubmed.ncbi.nlm.nih.gov/21867926/

268. Luckheeram RV, Zhou R, Verma AD, Xia B. CD4+T Cells: Differentiation and Functions. Clin Dev Immunol [Internet] 2012 [cited 2023 Jun 30];2012:12. Available from: /pmc/articles/PMC3312336/

269. Howie D, Bokum A Ten, Necula AS, Cobbold SP, Waldmann H. The role of lipid metabolism in T lymphocyte differentiation and survival. Front Immunol 2018;8(JAN):322986.

270. Veldhoen M. Interleukin 17 is a chief orchestrator of immunity. Nat Immunol [Internet] 2017 [cited 2023 Mar 12];18(6):612–21. Available from: https://pubmed.ncbi.nlm.nih.gov/28518156/

271. Zhao J, Chen X, Herjan T, Li X. The role of interleukin-17 in tumor development and progression. J Exp Med [Internet] 2020 [cited 2023 Jan 29];217(1). Available from: https://doi.org/10.1084/jem.20190297

272. Wu L, Van Kaer L. Contribution of lipid-reactive natural killer T cells to obesity-associated inflammation and insulin resistance. Adipocyte [Internet] 2013 [cited 2023 Jun 27];2(1):12. Available from: /pmc/articles/PMC3661135/

273. Lynch L, O'Shea D, Winter DC, Geoghegan J, Doherty DG, O'Farrelly C. Invariant NKT cells and CD1d(+) cells amass in human omentum and are depleted in patients with cancer and obesity. Eur J Immunol [Internet] 2009 [cited 2023 Jun 27];39(7):1893–901. Available from: https://pubmed.ncbi.nlm.nih.gov/19585513/

274. Fu S, He K, Tian C, Sun H, Zhu C, Bai S, et al. Impaired lipid biosynthesis hinders anti-tumor efficacy of intratumoral iNKT cells. Nat Commun 2020 111 [Internet] 2020 [cited 2023 Jun 27];11(1):1–15. Available from: https://www.nature.com/articles/s41467-020-14332-x

275. Hinks TSC, Zhang XW. MAIT Cell Activation and Functions. Front Immunol 2020;11:534723.

276. Bergin R, Kinlen D, Kedia-Mehta N, Hayes E, Cassidy FC, Cody D, et al. Mucosal-associated invariant T cells are associated with insulin resistance in childhood obesity, and disrupt insulin signalling via IL-17. Diabetologia [Internet] 2022 [cited 2023 Jun 27];65(6):1012–7. Available from: https://pubmed.ncbi.nlm.nih.gov/35305128/

277. Toubal A, Kiaf B, Beaudoin L, Cagninacci L, Rhimi M, Fruchet B, et al. Mucosal-associated invariant T cells promote inflammation and intestinal dysbiosis leading to metabolic dysfunction during obesity. Nat Commun 2020 111 [Internet] 2020 [cited 2023 Jun 27];11(1):1–20. Available from: https://www.nature.com/articles/s41467-020-17307-0

278. Riffelmacher T, Paynich Murray M, Wientjens C, Chandra S, Cedillo-Castelán V, Chou TF, et al. Divergent metabolic programmes control two populations of MAIT cells that protect the lung. Nat Cell Biol 2023 256 [Internet] 2023 [cited 2023 Jun 28];25(6):877–91. Available from: https://www.nature.com/articles/s41556-023-01152-6

279. Petley E V., Koay HF, Henderson MA, Sek K, Todd KL, Keam SP, et al. MAIT cells regulate NK cell-mediated tumor immunity. Nat Commun 2021 121 [Internet] 2021 [cited 2023 Jun 28];12(1):1–15. Available from: https://www.nature.com/articles/s41467-021-25009-4

280. Yan J, Allen S, McDonald E, Das I, Mak JYW, Liu L, et al. MAIT cells promote tumor initiation, growth and metastases via tumor MR1. Cancer Discov [Internet] 2020 [cited 2023 Jun 28];10(1):124–41. Available from: https://dx.doi.org/10.1158/2159-8290.CD-19-0569

281. Macdougall CE, Wood EG, Loschko J, Scagliotti V, Cassidy FC, Robinson ME, et al. Visceral Adipose Tissue Immune Homeostasis Is Regulated by the Crosstalk between Adipocytes and Dendritic Cell Subsets. Cell Metab 2018;27(3):588-601.e4.

282. Herber DL, Cao W, Nefedova Y, Novitskiy S V., Nagaraj S, Tyurin VA, et al. Lipid accumulation and dendritic cell dysfunction in cancer. Nat Med 2010 168 [Internet] 2010 [cited 2023 Jan 30];16(8):880–6. Available from: https://www.nature.com/articles/nm.2172

283. Xia W, Lu Z, Chen W, Zhou J, Zhao Y. Excess fatty acids induce pancreatic acinar cell pyroptosis through macrophage M1 polarization. BMC Gastroenterol [Internet] 2022 [cited 2023 Jan 31];22(1):1–16. Available from: https://bmcgastroenterol.biomedcentral.com/articles/10.1186/s12876-022-02146-8

284. Zhou BR, Zhang JA, Zhang Q, Permatasari F, Xu Y, Wu D, et al. Palmitic Acid Induces Production of Proinflammatory Cytokines Interleukin-6, Interleukin-1β, and Tumor Necrosis Factor-α via a NF-κB-Dependent Mechanism in HaCaT Keratinocytes. Mediators Inflamm [Internet] 2013 [cited 2023 Jan 30];2013. Available from: /pmc/articles/PMC3774064/

285. Camell C, Smith CW. Dietary Oleic Acid Increases M2 Macrophages in the Mesenteric Adipose Tissue. PLoS One [Internet] 2013 [cited 2023 Jan 30];8(9):75147. Available from: /pmc/articles/PMC3787090/

286. Hsu CC, Tseng LM, Lee HC. Role of mitochondrial dysfunction in cancer progression. Exp Biol Med [Internet] 2016 [cited 2023 Feb 15];241(12):1281. Available from: /pmc/articles/PMC4950268/

287. Desbats MA, Giacomini I, Prayer-Galetti T, Montopoli M. Metabolic Plasticity in Chemotherapy Resistance. Front Oncol [Internet] 2020 [cited 2023 Feb 17];10. Available from: /pmc/articles/PMC7068907/

288. Germain N, Dhayer M, Boileau M, Fovez Q, Kluza J, Marchetti P. Lipid Metabolism and Resistance to Anticancer Treatment. Biology (Basel) [Internet] 2020 [cited 2023 Feb 17];9(12):1–23. Available from: /pmc/articles/PMC7766644/

289. Luo X, Cheng C, Tan Z, Li N, Tang M, Yang L, et al. Emerging roles of lipid metabolism in cancer metastasis. Mol Cancer [Internet] 2017 [cited 2023 Mar 13];16(1):1–10. Available from: https://molecular-cancer.biomedcentral.com/articles/10.1186/s12943-017-0646-3

290. Batista-Gonzalez A, Vidal R, Criollo A, Carreño LJ. New Insights on the Role of Lipid Metabolism in the Metabolic Reprogramming of Macrophages. Front Immunol 2020;10:2993.

291. O'Sullivan D, vanderWindt GWJ, Huang SCC, Curtis JD, Chang CH, Buck MDL, et al. Memory CD8(+) T cells use cell-intrinsic lipolysis to support the metabolic programming necessary for development. Immunity [Internet] 2014 [cited

2023 Mar 23];41(1):75–88. Available from: https://pubmed.ncbi.nlm.nih.gov/25001241/

292. Kempkes RWM, Joosten I, Koenen HJPM, He X. Metabolic Pathways Involved in Regulatory T Cell Functionality. Front Immunol 2019;10:2839.

293. Warburg O. On the origin of cancer cells. Science [Internet] 1956 [cited 2023 Mar 23];123(3191):309–14. Available from: https://pubmed.ncbi.nlm.nih.gov/13298683/

294. Lin J, Xia L, Liang J, Han Y, Wang H, Oyang L, et al. The roles of glucose metabolic reprogramming in chemo- and radio-resistance. J Exp Clin Cancer Res 2019 381 [Internet] 2019 [cited 2023 Mar 23];38(1):1–13. Available from: https://jeccr.biomedcentral.com/articles/10.1186/s13046-019-1214-z

295. Bhatt AN, Chauhan A, Khanna S, Rai Y, Singh S, Soni R, et al. Transient elevation of glycolysis confers radio-resistance by facilitating DNA repair in cells. BMC Cancer [Internet] 2015 [cited 2023 Feb 6];15(1):1–12. Available from: https://bmccancer.biomedcentral.com/articles/10.1186/s12885-015-1368-9

296. Koundouros N, Poulogiannis G. Reprogramming of fatty acid metabolism in cancer [Internet]. Br. J. Cancer2020 [cited 2021 Feb 24];122(1):4–22. Available from: https://doi.org/10.1038/s41416-019-0650-z

297. Mayas MD, Ortega FJ, Macías-Gonzlez M, Bernal R, Gámez-Huelgas R, Fernndez-Real JM, et al. Inverse relation between FASN expression in human adipose tissue and the insulin resistance level. Nutr Metab [Internet] 2010 [cited 2023 Mar 23];7(1):1–7. Available from: https://nutritionandmetabolism.biomedcentral.com/articles/10.1186/1743-7075-7-3

298. Mobbs C V., Makimura H. Block the FAS, lose the fat. Nat Med 2002 84 [Internet] 2002 [cited 2023 Mar 23];8(4):335–6. Available from: https://www.nature.com/articles/nm0402-335

299. Khasawneh J, Schulz MD, Walch A, Rozman J, Hrabe De Angelis M, Klingenspor M, et al. Inflammation and mitochondrial fatty acid β-oxidation link obesity to early tumor promotion. Proc Natl Acad Sci U S A [Internet] 2009 [cited 2023 Mar 23];106(9):3354–9. Available from: https://www.pnas.org/doi/abs/10.1073/pnas.0802864106

300. Ghazy HF, El-Hadaad HA, Wahba HA, Abbas R, Abbas OA. Metastatic Esophageal Carcinoma: Prognostic Factors and Survival. J Gastrointest Cancer [Internet] 2022 [cited 2023 Mar 3];53(2):446–50. Available from: https://pubmed.ncbi.nlm.nih.gov/33847917/

301. Massagué J, Obenauf AC. Metastatic Colonization. Nature [Internet] 2016 [cited 2023 Mar 23];529(7586):298. Available from: /pmc/articles/PMC5029466/

302. Hu Y, Xu W, Zeng H, He Z, Lu X, Zuo D, et al. OXPHOS-dependent metabolic reprogramming prompts metastatic potential of breast cancer cells under osteogenic differentiation. Br J Cancer 2020 12311 [Internet] 2020 [cited 2023 Mar 2];123(11):1644–55. Available from: https://www.nature.com/articles/s41416-020-01040-y

303. Li M, Xian H chun, Tang YJ, Liang X hua, Tang Y ling. Fatty acid oxidation: driver of lymph node metastasis. Cancer Cell Int 2021 211 [Internet] 2021 [cited 2023 Mar 2];21(1):1–13. Available from: https://cancerci.biomedcentral.com/articles/10.1186/s12935-021-02057-w

304. Parlani M, Jorgez C, Friedl P. Plasticity of cancer invasion and energy metabolism. Trends Cell Biol [Internet] 2022 [cited 2023 Mar 3];Available from: https://pubmed.ncbi.nlm.nih.gov/36328835/

305. Nissar AU, Sharma L, Tasduq SA. Palmitic acid induced lipotoxicity is associated with altered lipid metabolism, enhanced CYP450 2E1 and intracellular calcium mediated ER stress in human hepatoma cells. Toxicol Res (Camb) [Internet] 2015 [cited 2023 Feb 17];4(5):1344–58. Available from: https://academic.oup.com/toxres/article/4/5/1344/5573527

306. Pascual G, Avgustinova A, Mejetta S, Martín M, Castellanos A, Attolini CSO, et al. Targeting metastasis-initiating cells through the fatty acid receptor CD36. Nature [Internet] 2017 [cited 2023 Feb 17];541(7635):41–5. Available from: https://pubmed.ncbi.nlm.nih.gov/27974793/

307. Annett S, Moore G, Robson T. Obesity and Cancer Metastasis: Molecular and Translational Perspectives. Cancers (Basel) [Internet] 2020 [cited 2023 Feb 21];12(12):1–30. Available from: /pmc/articles/PMC7766668/

308. de Vegt F, Gommers JJJ, Groenewoud H, Siersema PD, Verbeek ALM, Peters Y, et al. Trends and projections in the incidence of oesophageal cancer in the Netherlands: An age-period-cohort analysis from 1989 to 2041. Int J cancer [Internet] 2022 [cited 2022 Nov 10];150(3):420–30. Available from: https://pubmed.ncbi.nlm.nih.gov/34605022/

309. Noble F, Lloyd MA, Turkington R, Griffiths E, O'Donovan M, O'Neill JR, et al. Multicentre cohort study to define and validate pathological assessment of response to neoadjuvant therapy in oesophagogastric adenocarcinoma. Br J Surg [Internet] 2017 [cited 2023 Jan 23];104(13):1816. Available from: /pmc/articles/PMC5725679/

310. Donohoe CL, O'Farrell NJ, Grant T, King S, Clarke L, Muldoon C, et al. Classification of pathologic response to neoadjuvant therapy in esophageal and junctional cancer: assessment of existing measures and proposal of a novel 3-point standard. Ann Surg [Internet] 2013 [cited 2023 Jan 23];258(5):784–92. Available from: https://pubmed.ncbi.nlm.nih.gov/24045450/

311. Fang X, Wei J, He X, Lian J, Han D, An P, et al. Quantitative association between body mass index and the risk of cancer: A global Meta-analysis of prospective cohort studies. Int J Cancer 2018;143(7):1595–603.

312. Mylod E, O'connell F, Donlon NE, Butler C, Reynolds J V., Lysaght J, et al. The Omentum in Obesity-Associated Cancer: A Hindrance to Effective Natural Killer Cell Migration towards Tumour Which Can Be Overcome by CX3CR1 Antagonism. Cancers 2022, Vol 14, Page 64 [Internet] 2021 [cited 2022 May 10];14(1):64. Available from: https://www.mdpi.com/2072-6694/14/1/64/htm

313. Heeran AB, McCready J, Dunne MR, Donlon NE, Nugent TS, Bhardwaj A, et al. Opposing Immune-Metabolic Signature in Visceral Versus Subcutaneous Adipose Tissue in Patients with Adenocarcinoma of the Oesophagus and the Oesophagogastric Junction. Metabolites [Internet] 2021 [cited 2022 Mar 19];11(11). Available from: https://pubmed.ncbi.nlm.nih.gov/34822426/

314. Lashinger LM, Rossi EL, Hursting SD. Obesity and resistance to cancer chemotherapy: Interacting roles of inflammation and metabolic dysregulation. Clin Pharmacol Ther [Internet] 2014 [cited 2020 Mar 16];96(4):458–63. Available from: http://www.ncbi.nlm.nih.gov/pubmed/24960521

315. Böhm A, Keuper M, Meile T, Zdichavsky M, Fritsche A, Häring HU, et al. Increased mitochondrial respiration of adipocytes from metabolically unhealthy obese compared to healthy obese individuals. Sci Reports 2020 101 [Internet] 2020 [cited 2022 Aug 18];10(1):1–10. Available from: https://www.nature.com/articles/s41598-020-69016-9

316. Buckley AM, Dunne MR, Morrissey ME, Kennedy SA, Nolan A, Davern M, et al. Real-time metabolic profiling of oesophageal tumours reveals an altered metabolic phenotype to different oxygen tensions and to treatment with Pyrazinib. Sci Reports 2020 101 [Internet] 2020 [cited 2022 Dec 9];10(1):1–16. Available from: https://www.nature.com/articles/s41598-020-68777-7

317. Finkelstein EA, Khavjou OA, Thompson H, Trogdon JG, Pan L, Sherry B, et al. Obesity and severe obesity forecasts through 2030. Am J Prev Med [Internet] 2012 [cited 2022 Dec 9];42(6):563–70. Available from: https://pubmed.ncbi.nlm.nih.gov/22608371/

318. Doyle SL, Bennett AM, Donohoe CL, Mongan AM, Howard JM, Lithander FE, et al. Establishing computed tomography–defined visceral fat area thresholds for use in obesity-related cancer research. Nutr Res 2013;33(3):171–9.

319. Grundy SM, Cleeman JI, Daniels SR, Donato KA, Eckel RH, Franklin BA, et al. Diagnosis and Management of the Metabolic Syndrome. Circulation [Internet] 2005 [cited 2022 Nov 18];112(17). Available from: https://www.ahajournals.org/doi/abs/10.1161/CIRCULATIONAHA.105.169405

320. R Core Team. R: A language and environment for statistical computing. [Internet]. 2019;Available from: https://www.rproject.org/

321. Harrell Jr FE, with contributions from Charles Dupont, many others. Hmisc: Harrell Miscellaneous [Internet]. 2020;Available from: https://cran.r-project.org/package=Hmisc

322. Wei T, Simko V. R package "corrplot": Visualization of a Correlation Matrix [Internet]. 2017;Available from: https://github.com/taiyun/corrplot

323. Ashton TM, Gillies McKenna W, Kunz-Schughart LA, Higgins GS. Oxidative phosphorylation as an emerging target in cancer therapy. Clin Cancer Res [Internet] 2018 [cited 2022 Sep 5];24(11):2482–90. Available from: https://aacrjournals.org/clincancerres/article/24/11/2482/80659/Oxidative-Phosphorylation-as-an-Emerging-Target-in

324. Choi MJ, Jung SB, Lee SE, Kang SG, Lee JH, Ryu MJ, et al. An adipocyte-specific defect in oxidative phosphorylation increases systemic energy expenditure and protects against diet-induced obesity in mouse models. Diabetologia [Internet] 2020 [cited 2022 Sep 5];63(4):837–52. Available from: https://pubmed.ncbi.nlm.nih.gov/31925461/

325. Vellinga TT, De Boer VCJ, Fatrai S, Van Schelven S, Trumpi K, Verheem A, et al. SIRT1/PGC1a-Dependent increase in oxidative phosphorylation supports chemotherapy resistance of colon cancer. Clin Cancer Res [Internet] 2015 [cited 2022 Sep 5];21(12):2870–9. Available from: https://aacrjournals.org/clincancerres/article/21/12/2870/261524/SIRT1-PGC1-Dependent-Increase-in-Oxidative

326. Chen Y, Yu CY, Deng WM. The role of pro-inflammatory cytokines in lipid metabolism of metabolic diseases. Int Rev Immunol [Internet] 2019 [cited 2022 Dec 9];38(6):249–66. Available from: https://pubmed.ncbi.nlm.nih.gov/31353985/

327. Gentili A, Zaibi MS, Alomar SY, De Vuono S, Ricci MA, Alaeddin A, et al. Circulating Levels of the Adipokines Monocyte Chemotactic Protein-4 (MCP-4), Macrophage Inflammatory Protein-1β (MIP-1β), and Eotaxin-3 in Severe Obesity and Following Bariatric Surgery. Horm Metab Res [Internet] 2016 [cited 2021 Mar 1];48(12):847–53. Available from: https://pubmed.ncbi.nlm.nih.gov/27300476/

328. Lan Q, Lai W, Zeng Y, Liu L, Li S, Jin S, et al. CCL26 Participates in the PRL-3-Induced Promotion of Colorectal Cancer Invasion by Stimulating Tumor-Associated Macrophage Infiltration. Mol Cancer Ther [Internet] 2018 [cited 2022 Sep 6];17(1):276–89. Available from: https://pubmed.ncbi.nlm.nih.gov/29051319/

329. Godiska R, Chantry D, Raport CJ, Sozzani S, Allavena P, Leviten D, et al. Human Macrophage–derived Chemokine (MDC), a Novel Chemoattractant for Monocytes, Monocyte-derived Dendritic Cells, and Natural Killer Cells. J Exp Med [Internet] 1997 [cited 2022 Sep 6];185(9):1595–604. Available from: http://rupress.org/jem/article-pdf/185/9/1595/1111525/5512.pdf

330. Yoshimura T, Imamichi T, Weiss JM, Sato M, Li L, Matsukawa A, et al. Induction of monocyte chemoattractant proteins in macrophages via the production of granulocyte/macrophage colony-stimulating factor by breast cancer cells. Front Immunol 2016;7(JAN):2.

331. Chehimi M, Vidal H, Eljaafari A. Pathogenic Role of IL-17-Producing Immune Cells in Obesity, and Related Inflammatory Diseases. J Clin Med [Internet] 2017 [cited 2021 Mar 1];6(7):68. Available from: /pmc/articles/PMC5532576/

332. Carolan E, Tobin LM, Mangan BA, Corrigan M, Gaoatswe G, Byrne G, et al. Altered distribution and increased IL-17 production by mucosal-associated invariant T cells in adult and childhood obesity. J Immunol [Internet] 2015 [cited 2022 Sep 6];194(12):5775–80. Available from: https://pubmed.ncbi.nlm.nih.gov/25980010/

333. Punt S, Langenhoff JM, Putter H, Fleuren GJ, Gorter A, Jordanova ES. The correlations between IL-17 vs. Th17 cells and cancer patient survival: a systematic review. Oncoimmunology [Internet] 2015 [cited 2022 Sep 6];4(2):1–10. Available from: https://pubmed.ncbi.nlm.nih.gov/25949881/

334. Coffelt SB, Kersten K, Doornebal CW, Weiden J, Vrijland K, Hau CS, et al. IL-17-producing γδ T cells and neutrophils conspire to promote breast cancer metastasis. Nature [Internet] 2015 [cited 2022 Sep 6];522(7556):345–8. Available from: https://pubmed.ncbi.nlm.nih.gov/25822788/

335. Lotti F, Jarrar AM, Pai RK, Hitomi M, Lathia J, Mace A, et al. Chemotherapy activates cancer-associated fibroblasts to maintain colorectal cancer-initiating cells by IL-17A. J Exp Med [Internet] 2013 [cited 2022 Sep 6];210(13):2851–72. Available from: https://pubmed.ncbi.nlm.nih.gov/24323355/

336. Lee EJ, Park HJ, Lee IJ, Kim WW, Ha SJ, Suh YG, et al. Inhibition of IL-17A suppresses enhanced-tumor growth in low dose pre-irradiated tumor beds. PLoS One [Internet] 2014 [cited 2022 Sep 6];9(9). Available from: https://pubmed.ncbi.nlm.nih.gov/25181290/

337. Gómez-Ambrosi J, Catalán V, Rodríguez A, Ramírez B, Silva C, Gil MJ, et al. Involvement of serum vascular endothelial growth factor family members in the development of obesity in mice and humans. J Nutr Biochem [Internet] 2010 [cited 2022 Sep 6];21(8):774–80. Available from: https://pubmed.ncbi.nlm.nih.gov/19615882/

338. Stacker SA, Caesar C, Baldwin ME, Thornton GE, Williams RA, Prevo R, et al. VEGF-D promotes the metastatic spread of tumor cells via the lymphatics. Nat Med 2001 72 [Internet] 2001 [cited 2022 Sep 6];7(2):186–91. Available from: https://www.nature.com/articles/nm0201_186

339. Rozenberg P, Reichman H, Zab-Bar I, Itan M, Pasmanik-Chor M, Bouffi C, et al. CD300f:IL-5 cross-talk inhibits adipose tissue eosinophil homing and subsequent IL-4 production. Sci Rep [Internet] 2017 [cited 2022 Sep 6];7(1). Available from: /pmc/articles/PMC5517555/

340. Zaynagetdinov R, Sherrill TP, Gleaves LA, McLoed AG, Saxon JA, Habermann AC, et al. Interleukin-5 Facilitates Lung Metastasis by Modulating the Immune Microenvironment. Cancer Res [Internet] 2015 [cited 2022 Sep 6];75(8):1624. Available from: /pmc/articles/PMC4401663/

341. Deetman PE, Bakker SJL, Dullaart RPF. High sensitive C-reactive protein and serum amyloid A are inversely related to serum bilirubin: effect-modification by metabolic syndrome. Cardiovasc Diabetol [Internet] 2013 [cited 2022 Sep 6];12(1). Available from: https://pubmed.ncbi.nlm.nih.gov/24209691/

342. Malle E, De Beer FC. Human serum amyloid A (SAA) protein: a prominent acute-phase reactant for clinical practice. Eur J Clin Invest [Internet] 1996 [cited 2022 Sep 6];26(6):427–35. Available from: https://onlinelibrary.wiley.com/doi/full/10.1046/j.1365-2362.1996.159291.x

343. Lucas S, Taront S, Magnan C, Fauconnier L, Delacre M, Macia L, et al. Interleukin-7 Regulates Adipose Tissue Mass and Insulin Sensitivity in High-Fat Diet-Fed Mice through Lymphocyte-Dependent and Independent Mechanisms. PLoS One [Internet] 2012 [cited 2022 Sep 6];7(6):40351. Available from: /pmc/articles/PMC3386973/

344. Morre M, Beq S. Interleukin-7 and immune reconstitution in cancer patients: a new paradigm for dramatically increasing overall survival. Target Oncol [Internet] 2012 [cited 2022 Sep 6];7(1):55. Available from: /pmc/articles/PMC3304058/

345. Ke B, Wei T, Huang Y, Gong Y, Wu G, Liu J, et al. Interleukin-7 resensitizes non-small-cell lung cancer to cisplatin via inhibition of ABCG2. Mediators Inflamm 2019;2019.

346. Karaman S, Hollmén M, Yoon SY, Alkan HF, Alitalo K, Wolfrum C, et al. Transgenic overexpression of VEGF-C induces weight gain and insulin resistance in mice. Sci Rep [Internet] 2016 [cited 2022 Sep 6];6. Available from: /pmc/articles/PMC4980670/

347. Su JL, Yen CJ, Chen PS, Chuang SE, Hong CC, Kuo IH, et al. The role of the VEGF-C/VEGFR-3 axis in cancer progression. Br J Cancer 2007 964 [Internet] 2006 [cited 2022 Sep 6];96(4):541–5. Available from: https://www.nature.com/articles/6603487

348. Wang CA, Harrell JC, Iwanaga R, Jedlicka P, Ford HL. Vascular endothelial growth factor C promotes breast cancer progression via a novel antioxidant mechanism that involves regulation of superoxide dismutase 3. Breast Cancer Res [Internet] 2014 [cited 2022 Sep 6];16(1):1–17. Available from: https://breast-cancer-research.biomedcentral.com/articles/10.1186/s13058-014-0462-2

349. Kobold S, Völk S, Clauditz T, Küpper NJ, Minner S, Tufman A, et al. Interleukin-22 is frequently expressed in small- and large-cell lung cancer and promotes growth in chemotherapy-resistant cancer cells. J Thorac Oncol [Internet] 2013 [cited 2022 Sep 6];8(8):1032–42. Available from: https://pubmed.ncbi.nlm.nih.gov/23774470/

350. Kim EY, Noh HM, Choi B, Park JE, Kim JE, Jang Y, et al. Interleukin-22 Induces the Infiltration of Visceral Fat Tissue by a Discrete Subset of Duffy Antigen Receptor for Chemokine-Positive M2-Like Macrophages in Response to a High Fat Diet. Cells [Internet] 2019 [cited 2022 Sep 6];8(12). Available from: https://pubmed.ncbi.nlm.nih.gov/31817755/

351. Buhrmann C, Yazdi M, Popper B, Shayan P, Goel A, Aggarwal BB, et al. Evidence that TNF-β induces proliferation in colorectal cancer cells and resveratrol can down-modulate it. Exp Biol Med [Internet] 2019 [cited 2022 Sep 6];244(1):1–12. Available from: https://journals.sagepub.com/doi/10.1177/1535370218824538

352. Baker KJ, Houston A, Brint E. IL-1 Family Members in Cancer; Two Sides to Every Story. Front Immunol [Internet] 2019 [cited 2022 Sep 6];10(JUN):1197. Available from: /pmc/articles/PMC6567883/

353. Tugues S, Burkhard SH, Ohs I, Vrohlings M, Nussbaum K, Vom Berg J, et al. New insights into IL-12-mediated tumor

suppression. Cell Death Differ [Internet] 2015 [cited 2022 Sep 6];22(2):237. Available from: /pmc/articles/PMC4291488/

354. Clish CB. Metabolomics: an emerging but powerful tool for precision medicine. Cold Spring Harb Mol Case Stud [Internet] 2015 [cited 2022 Sep 7];1(1):a000588. Available from: /pmc/articles/PMC4850886/

355. Maltais-Payette I, Boulet MM, Prehn C, Adamski J, Tchernof A. Circulating glutamate concentration as a biomarker of visceral obesity and associated metabolic alterations. Nutr Metab [Internet] 2018 [cited 2022 Sep 7];15(1):1–7. Available from: https://nutritionandmetabolism.biomedcentral.com/articles/10.1186/s12986-018-0316-5

356. Ren W, Xia Y, Chen S, Wu G, Bazer FW, Zhou B, et al. Glutamine Metabolism in Macrophages: A Novel Target for Obesity/Type 2 Diabetes. Adv Nutr [Internet] 2019 [cited 2022 Sep 7];10(2):321–30. Available from: https://europepmc.org/articles/PMC6416106

357. Daniele G, Campi B, Saba A, Codini S, Ciccarone A, Giusti L, et al. Plasma N-Acetylaspartate Is Related to Age, Obesity, and Glucose Metabolism: Effects of Antidiabetic Treatment and Bariatric Surgery. Front Endocrinol (Lausanne) [Internet] 2020 [cited 2022 Sep 7];11:216. Available from: /pmc/articles/PMC7181885/

358. Yamaguchi Y, Yamamoto K, Sato Y, Inoue S, Morinaga T, Hirano E. Combination of aspartic acid and glutamic acid inhibits tumor cell proliferation. Biomed Res [Internet] 2016 [cited 2022 Sep 7];37(2):153–9. Available from: https://pubmed.ncbi.nlm.nih.gov/27108884/

359. Gregoire FM, Smas CM, Sul HS. Understanding adipocyte differentiation. Physiol Rev [Internet] 1998 [cited 2022 Sep 7];78(3):783–809. Available from: https://pubmed.ncbi.nlm.nih.gov/9674695/

360. Hama K, Fujiwara Y, Hayama T, Ozawa T, Nozawa K, Matsuda K, et al. Very long-chain fatty acids are accumulated in triacylglycerol and nonesterified forms in colorectal cancer tissues. Sci Reports 2021 111 [Internet] 2021 [cited 2022 Sep 7];11(1):1–10. Available from: https://www.nature.com/articles/s41598-021-85603-w

361. Tomin T, Fritz K, Gindlhuber J, Waldherr L, Pucher B, Thallinger GG, et al. Deletion of Adipose Triglyceride Lipase Links Triacylglycerol Accumulation to a More-Aggressive Phenotype in A549 Lung Carcinoma Cells. J Proteome Res [Internet] 2018 [cited 2022 Sep 7];17(4):1415–25. Available from: https://pubmed.ncbi.nlm.nih.gov/29457907/

362. Palomo I, Contreras A, Alarcón LM, Leiva E, Guzmán L, Mujica V, et al. Elevated concentration of asymmetric dimethylarginine (ADMA) in individuals with metabolic syndrome. Nitric oxide Biol Chem [Internet] 2011 [cited 2022 Sep 8];24(4):224–8. Available from: https://pubmed.ncbi.nlm.nih.gov/21419857/

363. Hajer GR, Van Der Graaf Y, Olijhoek JK, Verhaar MC, Visseren FLJ. Levels of homocysteine are increased in metabolic syndrome patients but are not associated with an increased cardiovascular risk, in contrast to patients without the metabolic syndrome. Heart [Internet] 2007 [cited 2022 Sep 8];93(2):216. Available from: /pmc/articles/PMC1861402/

364. Furuhashi M. New insights into purine metabolism in metabolic diseases: Role of xanthine oxidoreductase activity. Am J Physiol - Endocrinol Metab [Internet] 2020 [cited 2022 Sep 8];319(5):E827–34. Available from: https://journals.physiology.org/doi/10.1152/ajpendo.00378.2020

365. Wu LL, Wu JT. Hyperhomocysteinemia is a risk factor for cancer and a new potential tumor marker. Clin Chim Acta [Internet] 2002 [cited 2022 Sep 8];322(1–2):21–8. Available from: https://pubmed.ncbi.nlm.nih.gov/12104077/

366. Park J, Shin Y, Kim TH, Kim DH, Lee A. Plasma metabolites as possible biomarkers for diagnosis of breast cancer. PLoS One [Internet] 2019 [cited 2022 Sep 8];14(12):e0225129. Available from: https://journals.plos.org/plosone/article?id=10.1371/journal.pone.0225129

367. Li H, Zhou Y, Zhao A, Qiu Y, Xie G, Jiang Q, et al. Asymmetric dimethylarginine attenuates serum starvation-induced apoptosis via suppression of the Fas (APO-1/CD95)/JNK (SAPK) pathway. Cell Death Dis 2013 410 [Internet] 2013 [cited 2022 Sep 8];4(10):e830–e830. Available from: https://www.nature.com/articles/cddis2013345

368. Jain M, Nilsson R, Sharma S, Madhusudhan N, Kitami T, Souza AL, et al. Metabolite profiling identifies a key role for glycine in rapid cancer cell proliferation. Science [Internet] 2012 [cited 2022 Sep 8];336(6084):1040–4. Available from: https://pubmed.ncbi.nlm.nih.gov/22628656/

369. Baliou S, Kyriakopoulos AM, Spandidos DA, Zoumpourlis V. Role of taurine, its haloamines and its lncRNA TUG1 in both inflammation and cancer progression. On the road to therapeutics? (Review). Int J Oncol [Internet] 2020 [cited 2022 Sep 8];57(3):631–64. Available from: http://www.spandidos-publications.com/10.3892/ijo.2020.5100/abstract

370. Tao LX, Yang K, Liu XT, Cao K, Zhu HP, Luo YX, et al. Longitudinal Associations between Triglycerides and Metabolic Syndrome Components in a Beijing Adult Population, 2007-2012. Int J Med Sci [Internet] 2016 [cited 2022 Sep 8];13(6):445. Available from: /pmc/articles/PMC4893559/

371. Borena W, Stocks T, Jonsson H, Strohmaier S, Nagel G, Bjørge T, et al. Serum triglycerides and cancer risk in the metabolic syndrome and cancer (Me-Can) collaborative study. Cancer Causes Control [Internet] 2011 [cited 2022 Sep 8];22(2):291–9. Available from: https://link.springer.com/article/10.1007/s10552-010-9697-0

372. Wu TK, Wei CW, Pan YR, Hsu RJ, Wu CY, Yu YL. The uremic toxin p-cresyl sulfate induces proliferation and migration of clear cell renal cell carcinoma via microRNA-21/ HIF-1α axis signals. Sci Reports 2019 91 [Internet] 2019 [cited 2022 Sep 8];9(1):1–10. Available from: https://www.nature.com/articles/s41598-019-39646-9

373. Peng Y Sen, Syu JP, Wang S De, Pan PC, Kung HN. BSA-bounded p-cresyl sulfate potentiates the malignancy of bladder carcinoma by triggering cell migration and EMT through the ROS/Src/FAK signaling pathway. Cell Biol Toxicol [Internet] 2020 [cited 2022 Sep 8];36(4):287–300. Available from: https://link.springer.com/article/10.1007/s10565-019-09509-0

374. Tataranni T, Agriesti F, Pacelli C, Ruggieri V, Laurenzana I, Mazzoccoli C, et al. Dichloroacetate Affects Mitochondrial Function and Stemness-Associated Properties in Pancreatic Cancer Cell Lines. Cells [Internet] 2019 [cited 2023 Jun 9];8(5). Available from: /pmc/articles/PMC6562462/

375. Tian W, Yao Y, Fan G, Zhou Y, Wu M, Xu D, et al. Changes in lipid profiles during and after (neo)adjuvant chemotherapy in women with early-stage breast cancer: A retrospective study. PLoS One [Internet] 2019 [cited 2022 Sep 8];14(8):e0221866. Available from: https://journals.plos.org/plosone/article?id=10.1371/journal.pone.0221866

376. Morad SAF, Cabot MC. Ceramide-orchestrated signalling in cancer cells. Nat Rev Cancer 2012 131 [Internet] 2012 [cited 2022 Sep 8];13(1):51–65. Available from: https://www.nature.com/articles/nrc3398

377. Moro K, Nagahashi M, Gabriel E, Takabe K, Wakai T. Clinical Application of Ceramide in Cancer Treatment. Breast Cancer [Internet] 2019 [cited 2023 Jan 24];26(4):407. Available from: /pmc/articles/PMC7315770/

378. Chen XQ, Wu PW, Liu DH, Yan SJ, Shen XM, Yang LY. Prognostic significance of high triglyceride and apolipoprotein B levels in patients with stage III and high-risk stage II colorectal cancer undergoing curative surgery. Oncol Lett [Internet] 2020 [cited 2022 Sep 8];20(1):705. Available from: /pmc/articles/PMC7285852/

379. Saito R de F, Andrade LN de S, Bustos SO, Chammas R. Phosphatidylcholine-Derived Lipid Mediators: The Crosstalk Between Cancer Cells and Immune Cells. Front Immunol 2022;13:215.

380. Elliott JA, Reynolds J V. Visceral Obesity, Metabolic Syndrome, and Esophageal Adenocarcinoma. Front Oncol 2021;11:692.

381. Rothman KJ. BMI-related errors in the measurement of obesity. Int J Obes (Lond) [Internet] 2008 [cited 2022 Sep 9];32 Suppl 3:S56–9. Available from: https://pubmed.ncbi.nlm.nih.gov/18695655/

382. de Rham C, Ferrari-Lacraz S, Jendly S, Schneiter G, Dayer JM, Villard J. The proinflammatory cytokines IL-2, IL-15 and IL-21 modulate the repertoire of mature human natural killer cell receptors. Arthritis Res Ther [Internet] 2007 [cited 2022 Sep 9];9(6). Available from: https://pubmed.ncbi.nlm.nih.gov/18053164/

383. Jin W, Dong C. IL-17 cytokines in immunity and inflammation. Emerg Microbes Infect [Internet] 2013 [cited 2022 Sep 9];2(9):e60. Available from: /pmc/articles/PMC3820987/

384. Zenewicz LA, Flavell RA. IL-22 and inflammation: Leukin' through a glass onion. Eur J Immunol [Internet] 2008 [cited 2022 Sep 9];38(12):3265–8. Available from: https://onlinelibrary.wiley.com/doi/full/10.1002/eji.200838655

385. Duvallet E, Semerano L, Assier E, Falgarone G, Boissier MC. Interleukin-23: a key cytokine in inflammatory diseases. Ann Med [Internet] 2011 [cited 2022 Sep 9];43(7):503–11. Available from: https://pubmed.ncbi.nlm.nih.gov/21585245/

386. Weber GF, Chousterman BG, He S, Fenn AM, Nairz M, Anzai A, et al. Interleukin-3 amplifies acute inflammation and is a potential therapeutic target in sepsis. Science [Internet] 2015 [cited 2022 Sep 9];347(6227):1260. Available from: /pmc/articles/PMC4376966/

387. El-Wakkad A, Hassan NEM, Sibaii H, El-Zayat SR. Proinflammatory, anti-inflammatory cytokines and adiponkines in students with central obesity. Cytokine [Internet] 2013 [cited 2022 Sep 9];61(2):682–7. Available from: https://pubmed.ncbi.nlm.nih.gov/23306429/

388. Radovic B, Aflaki E, Kratky D. Adipose triglyceride lipase in immune response, inflammation, and atherosclerosis. Biol Chem [Internet] 2012 [cited 2022 Sep 10];393(9):1005. Available from: /pmc/articles/PMC3520003/

389. Howie D, Bokum A Ten, Cobbold SP, Yu Z, Kessler BM, Waldmann H. A novel role for triglyceride metabolism in Foxp3 expression. Front Immunol 2019;10(AUG):1860.

390. Rettig TCD, Verwijmeren L, Dijkstra IM, Boerma D, Van De Garde EMW, Noordzij PG. Postoperative Interleukin-6 Level and Early Detection of Complications After Elective Major Abdominal Surgery. Ann Surg [Internet] 2016 [cited 2022 Sep 9];263(6):1207–12. Available from: https://pubmed.ncbi.nlm.nih.gov/26135695/

391. Belizon A, Balik E, Feingold DL, Bessler M, Arnell TD, Forde KA, et al. Major Abdominal Surgery Increases Plasma Levels of Vascular Endothelial Growth Factor: Open More So Than Minimally Invasive Methods. Ann Surg [Internet] 2006 [cited 2022 Sep 9];244(5):792. Available from: /pmc/articles/PMC1856599/

392. Yang C, Bork U, Schölch S, Kulu Y, Kaderali L, Bolstorff UL, et al. Postoperative course and prognostic value of circulating angiogenic cytokines after pancreatic cancer resection. Oncotarget [Internet] 2017 [cited 2022 Sep 9];8(42):72315. Available from: /pmc/articles/PMC5641132/

393. El-Ghonaimy EA, El-Shinawi M, Ibrahim SA, El-Ghazaly H, Abd-El-Tawab R, Nouh MA, et al. Positive lymph-node breast cancer patients – activation of NF-κB in tumor-associated leukocytes stimulates cytokine secretion that promotes metastasis via C-C chemokine receptor CCR7. FEBS J [Internet] 2015 [cited 2022 Sep 9];282(2):271–82. Available from: https://onlinelibrary.wiley.com/doi/full/10.1111/febs.13124

394. Davern M, Donlon NE, Connell FO, Gaughan C, O' Donovan C, Habash M, et al. Acidosis Significantly Alters Immune Checkpoint Expression Profiles of T Cells. SSRN Electron J [Internet] 2021 [cited 2021 Nov 15];Available from: https://papers.ssrn.com/abstract=3946994

395. Choi SYC, Collins CC, Gout PW, Wang Y. Cancer-generated lactic acid: a regulatory, immunosuppressive metabolite? J Pathol [Internet] 2013 [cited 2022 Sep 10];230(4):350. Available from: /pmc/articles/PMC3757307/

396. Aoki S, Inoue K, Klein S, Halvorsen S, Chen J, Matsui A, et al. Placental growth factor promotes tumour desmoplasia and

treatment resistance in intrahepatic cholangiocarcinoma. Gut [Internet] 2022 [cited 2022 Sep 10];71(1):185–93. Available from: https://pubmed.ncbi.nlm.nih.gov/33431577/

397. Dragoo JL, Shapiro SA, Bradsell H, Frank RM. The essential roles of human adipose tissue: Metabolic, thermoregulatory, cellular, and paracrine effects. J Cartil Jt Preserv 2021;1(3):100023.

398. Khanna D, Khanna S, Khanna P, Kahar P, Patel BM. Obesity: A Chronic Low-Grade Inflammation and Its Markers. Cureus [Internet] 2022 [cited 2023 Jan 31];14(2). Available from: https://pubmed.ncbi.nlm.nih.gov/35386146/

399. Hopkins BD, Goncalves MD, Cantley LC. Obesity and cancer mechanisms: Cancer metabolism [Internet]. J. Clin. Oncol.2016 [cited 2020 Mar 16];34(35):4277–83. Available from: http://www.ncbi.nlm.nih.gov/pubmed/27903152

400. Tvrzicka E, Kremmyda LS, Stankova B, Zak A. Fatty acids as biocompounds: their role in human metabolism, health and disease--a review. Part 1: classification, dietary sources and biological functions. Biomed Pap Med Fac Univ Palacky Olomouc Czech Repub [Internet] 2011 [cited 2023 Mar 16];155(2):117–30. Available from: https://pubmed.ncbi.nlm.nih.gov/21804620/

401. DiNicolantonio JJ, O'Keefe JH. Monounsaturated Fat vs Saturated Fat: Effects on Cardio-Metabolic Health and Obesity. Mo Med [Internet] 2022 [cited 2023 Mar 16];119(1):69. Available from: /pmc/articles/PMC9312452/

402. Vázquez-Mosquera ME, Fernández-Moreno M, Cortés-Pereira E, Relaño S, Dalmao-Fernández A, Ramos-Louro P, et al. Oleate Prevents Palmitate-Induced Mitochondrial Dysfunction in Chondrocytes. Front Physiol 2021;12:811.

403. Sergi D, Luscombe-Marsh N, Naumovski N, Abeywardena M, O'Callaghan N. Palmitic Acid, but Not Lauric Acid, Induces Metabolic Inflammation, Mitochondrial Fragmentation, and a Drop in Mitochondrial Membrane Potential in Human Primary Myotubes. Front Nutr [Internet] 2021 [cited 2023 Jan 29];8:663838. Available from: /pmc/articles/PMC8200524/

404. Yang C, Ko B, Hensley CT, Jiang L, Wasti AT, Kim J, et al. Glutamine Oxidation Maintains the TCA Cycle and Cell Survival during Impaired Mitochondrial Pyruvate Transport. Mol Cell 2014;56(3):414–24.

405. Wang YY, Attané C, Milhas D, Dirat B, Dauvillier S, Guerard A, et al. Mammary adipocytes stimulate breast cancer invasion through metabolic remodeling of tumor cells. JCI insight [Internet] 2017 [cited 2023 Mar 16];2(4). Available from: https://pubmed.ncbi.nlm.nih.gov/28239646/

406. Wu KM, Hsu YM, Ying MC, Tsai FJ, Tsai CH, Chung JG, et al. High-density lipoprotein ameliorates palmitic acid-induced lipotoxicity and oxidative dysfunction in H9c2 cardiomyoblast cells via ROS suppression. Nutr Metab [Internet] 2019 [cited 2023 Mar 16];16(1):1–13. Available from: https://nutritionandmetabolism.biomedcentral.com/articles/10.1186/s12986-019-0356-5

407. Carrière A, Carmona MC, Fernandez Y, Rigoulet M, Wenger RH, Pénicaud L, et al. Mitochondrial reactive oxygen species control the transcription factor CHOP-10/GADD153 and adipocyte differentiation: a mechanism for hypoxia-dependent effect. J Biol Chem [Internet] 2004 [cited 2023 Mar 16];279(39):40462–9. Available from: https://pubmed.ncbi.nlm.nih.gov/15265861/

408. Ciesielska K, Gajewska M. Fatty Acids as Potent Modulators of Autophagy Activity in White Adipose Tissue. Biomolecules [Internet] 2023 [cited 2023 Mar 16];13(2):13. Available from: /pmc/articles/PMC9953325/

409. Bleve A, Durante B, Sica A, Consonni FM. Lipid Metabolism and Cancer Immunotherapy: Immunosuppressive Myeloid Cells at the Crossroad. Int J Mol Sci 2020, Vol 21, Page 5845 [Internet] 2020 [cited 2023 Jan 30];21(16):5845. Available from: https://www.mdpi.com/1422-0067/21/16/5845/htm

410. Karasawa T, Kawashima A, Usui-Kawanishi F, Watanabe S, Kimura H, Kamata R, et al. Saturated Fatty Acids Undergo Intracellular Crystallization and Activate the NLRP3 Inflammasome in Macrophages. Arterioscler Thromb Vasc Biol [Internet] 2018 [cited 2023 Jan 30];38(4):744–56. Available from: https://pubmed.ncbi.nlm.nih.gov/29437575/

411. Cao H, Zhang J, Liu H, Wan L, Zhang H, Huang Q, et al. IL-13/STAT6 signaling plays a critical role in the epithelial-mesenchymal transition of colorectal cancer cells. Oncotarget [Internet] 2016 [cited 2023 Jan 29];7(38):61183–98. Available from: https://www.oncotarget.com/article/11282/text/

412. Duffen J, Zhang M, Masek-Hammerman K, Nunez A, Brennan A, Jones JEC, et al. Modulation of the IL-33/IL-13 Axis in Obesity by IL-13Rα2. J Immunol [Internet] 2018 [cited 2023 Jan 29];200(4):1347–59. Available from: https://pubmed.ncbi.nlm.nih.gov/29305434/

413. Pestel J, Chehimi M, Bonhomme M, Robert M, Vidal H, Eljaafari A. IL-17A contributes to propagation of inflammation but does not impair adipogenesis and/or insulin response, in adipose tissue of obese individuals. Cytokine [Internet] 2020 [cited 2023 Jan 29];126. Available from: https://pubmed.ncbi.nlm.nih.gov/31629101/

414. Mendez-Enriquez E, García-Zepeda EA. The multiple faces of CCL13 in immunity and inflammation [Internet]. Inflammopharmacology2013 [cited 2021 Feb 26];21(6):397–406. Available from: https://pubmed.ncbi.nlm.nih.gov/23846739/

415. Oft M. IL-10: Master Switch from Tumor-Promoting Inflammation to Antitumor Immunity. Cancer Immunol Res [Internet] 2014 [cited 2022 Sep 27];2(3):194–9. Available from: https://aacrjournals.org/cancerimmunolres/article/2/3/194/467083/IL-10-Master-Switch-from-Tumor-Promoting

416. Mendez-Enriquez E, García-Zepeda EA. The multiple faces of CCL13 in immunity and inflammation. Inflammopharmacology [Internet] 2013 [cited 2023 Jan 30];21(6):397–406. Available from: https://pubmed.ncbi.nlm.nih.gov/23846739/

417. Ballak DB, Stienstra R, Tack CJ, Dinarello CA, van Diepen JA. IL-1 family members in the pathogenesis and treatment of metabolic disease: Focus on adipose tissue inflammation and insulin resistance. Cytokine [Internet] 2015 [cited 2023 Jan 30];75(2):280. Available from: /pmc/articles/PMC4553099/

418. Dufour JH, Dziejman M, Liu MT, Leung JH, Lane TE, Luster AD. IFN-gamma-inducible protein 10 (IP-10; CXCL10)-deficient mice reveal a role for IP-10 in effector T cell generation and trafficking. J Immunol [Internet] 2002 [cited 2023 Jan 30];168(7):3195–204. Available from: https://pubmed.ncbi.nlm.nih.gov/11907072/

419. Yang WC, Hwang YS, Chen YY, Liu CL, Shen CN, Hong WH, et al. Interleukin-4 supports the suppressive immune responses elicited by regulatory T cells. Front Immunol 2017;8(NOV):1508.

420. Lichtenegger FS, Mueller K, Otte B, Beck B, Hiddemann W, Schendel DJ, et al. CD86 and IL-12p70 Are Key Players for T Helper 1 Polarization and Natural Killer Cell Activation by Toll-Like Receptor-Induced Dendritic Cells. PLoS One [Internet] 2012 [cited 2022 Sep 26];7(9):e44266. Available from: https://journals.plos.org/plosone/article?id=10.1371/journal.pone.0044266

421. Kolb R, Sutterwala FS, Zhang W. Obesity and cancer: inflammation bridges the two [Internet]. Curr. Opin. Pharmacol.2016 [cited 2020 Mar 19];29:77–89. Available from: http://www.ncbi.nlm.nih.gov/pubmed/27429211

422. Catalán V, Gómez-Ambrosi J, Rodríguez A, Frühbeck G. Adipose tissue immunity and cancer. Front Physiol [Internet] 2013 [cited 2023 Jan 30];4. Available from: https://pubmed.ncbi.nlm.nih.gov/24106481/

423. Nicholas DA, Zhang K, Hung C, Glasgow S, Aruni AW, Unternaehrer J, et al. Palmitic acid is a toll-like receptor 4 ligand that induces human dendritic cell secretion of IL-1β. PLoS One [Internet] 2017 [cited 2023 Jan 30];12(5):e0176793. Available from: https://journals.plos.org/plosone/article?id=10.1371/journal.pone.0176793

424. Sapoznikov A, Kozlovski S, Feigelson SW, Davidzohn N, Wigoda N, Feldmesser E, et al. Dendritic cell ICAM-1 strengthens immune synapses but is dispensable for effector and memory responses. bioRxiv [Internet] 2021 [cited 2023 Jan 29];2021.10.27.466043. Available from: https://www.biorxiv.org/content/10.1101/2021.10.27.466043v1

425. Iwamoto M, Shinohara H, Miyamoto A, Okuzawa M, Mabuchi H, Nohara T, et al. Prognostic value of tumor-infiltrating dendritic cells expressing CD83 in human breast carcinomas. Int J Cancer [Internet] 2003 [cited 2023 Jan 29];104(1):92–7. Available from: https://onlinelibrary.wiley.com/doi/full/10.1002/ijc.10915

426. Dixon KO, Tabaka M, Schramm MA, Xiao S, Tang R, Dionne D, et al. TIM-3 restrains anti-tumour immunity by regulating inflammasome activation. Nat 2021 5957865 [Internet] 2021 [cited 2023 Jan 29];595(7865):101–6. Available from: https://www.nature.com/articles/s41586-021-03626-9

427. Peng Q, Qiu X, Zhang Z, Zhang S, Zhang Y, Liang Y, et al. PD-L1 on dendritic cells attenuates T cell activation and regulates response to immune checkpoint blockade. Nat Commun 2020 111 [Internet] 2020 [cited 2023 Jan 29];11(1):1–8. Available from: https://www.nature.com/articles/s41467-020-18570-x

428. Hou Y, Wei D, Zhang Z, Guo H, Li S, Zhang J, et al. FABP5 controls macrophage alternative activation and allergic asthma by selectively programming long-chain unsaturated fatty acid metabolism. Cell Rep 2022;41(7):111668.

429. Makita N, Hizukuri Y, Yamashiro K, Murakawa M, Hayashi Y. IL-10 enhances the phenotype of M2 macrophages induced by IL-4 and confers the ability to increase eosinophil migration. Int Immunol [Internet] 2015 [cited 2023 Jan 30];27(3):131–41. Available from: https://academic.oup.com/intimm/article/27/3/131/2950818

430. Mosser DM, Edwards JP. Exploring the full spectrum of macrophage activation. Nat Rev Immunol 2008 812 [Internet] 2008 [cited 2023 Jan 30];8(12):958–69. Available from: https://www.nature.com/articles/nri2448

431. Kratochvill F, Neale G, Haverkamp JM, Van de Velde LA, Smith AM, Kawauchi D, et al. TNF counterbalances the emergence of M2 tumor macrophages. Cell Rep [Internet] 2015 [cited 2023 Jan 30];12(11):1902. Available from: /pmc/articles/PMC4581986/

432. Castoldi A, De Souza CN, Saraiva Câmara NO, Moraes-Vieira PM. The Macrophage Switch in Obesity Development. Front Immunol [Internet] 2015 [cited 2023 Jan 30];6(JAN):1. Available from: /pmc/articles/PMC4700258/

433. Poglio S, Galvani S, Bour S, André M, Prunet-Marcassus B, Pénicaud L, et al. Adipose Tissue Sensitivity to Radiation Exposure. Am J Pathol [Internet] 2009 [cited 2023 Feb 5];174(1):44. Available from: /pmc/articles/PMC2631317/

434. Shreder K, Rapp F, Tsoukala I, Rzeznik V, Wabitsch M, Fischer-Posovszky P, et al. Impact of X-ray Exposure on the Proliferation and Differentiation of Human Pre-Adipocytes. Int J Mol Sci [Internet] 2018 [cited 2023 Feb 6];19(9). Available from: /pmc/articles/PMC6163807/

435. Fang Y, Dou R, Huang S, Han L, Fu H, Yang C, et al. LAMC1-mediated preadipocytes differentiation promoted peritoneum pre-metastatic niche formation and gastric cancer metastasis. Int J Biol Sci [Internet] 2022 [cited 2023 Feb 7];18(7):3082. Available from: /pmc/articles/PMC9066104/

436. Shaikh S, Channa NA, Talpur FN, Younis M, Tabassum N. Radiotherapy improves serum fatty acids and lipid profile in breast cancer. Lipids Health Dis [Internet] 2017 [cited 2023 Feb 5];16(1):1–8. Available from: https://lipidworld.biomedcentral.com/articles/10.1186/s12944-017-0481-y

437. Zhou Z, Zhao J, Hu K, Hou X, Sun X, Pan X, et al. Single High-Dose Radiation Enhances Dendritic Cell Homing and T Cell Priming by Promoting Reactive Oxygen Species-Induced Cytoskeletal Reorganization. Int J Radiat Oncol Biol Phys [Internet] 2021 [cited 2023 Feb 6];109(1):95–108. Available from: http://www.redjournal.org/article/S0360301620337408/fulltext

438. Haffar T, Akoumi A, Bousette N. Lipotoxic Palmitate Impairs the Rate of β-Oxidation and Citric Acid Cycle Flux in Rat Neonatal Cardiomyocytes. Cell Physiol Biochem [Internet] 2016 [cited 2023 Feb 6];40(5):969–81. Available from: https://www.karger.com/Article/FullText/453154

439. Eynaudi A, Díaz-Castro F, Bórquez JC, Bravo-Sagua R, Parra V, Troncoso R. Differential Effects of Oleic and Palmitic Acids on Lipid Droplet-Mitochondria Interaction in the Hepatic Cell Line HepG2. Front Nutr 2021;8:901.

440. Pimenta AS, Gaidhu MP, Habib S, So M, Fediuc S, Mirpourian M, et al. Prolonged exposure to palmitate impairs fatty acid oxidation despite activation of AMP-activated protein kinase in skeletal muscle cells. J Cell Physiol [Internet] 2008 [cited 2023 Feb 6];217(2):478–85. Available from: https://pubmed.ncbi.nlm.nih.gov/18561258/

441. Marcucci F, Rumio C. Glycolysis-induced drug resistance in tumors—A response to danger signals? Neoplasia 2021;23(2):234–45.

442. Yuan ZH, Liu T, Wang H, Xue LX, Wang JJ. Fatty Acids Metabolism: The Bridge Between Ferroptosis and Ionizing Radiation. Front Cell Dev Biol 2021;9:1691.

443. Vilalta M, Rafat M, Graves EE. Effects of Radiation on Metastasis and Tumor Cell Migration. Cell Mol Life Sci [Internet] 2016 [cited 2023 Feb 5];73(16):2999. Available from: /pmc/articles/PMC4956569/

444. Antal O, Hackler L, Shen J, Mán I, Hideghéty K, Kitajka K, et al. Combination of unsaturated fatty acids and ionizing radiation on human glioma cells: Cellular, biochemical and gene expression analysis. Lipids Health Dis 2014;13(1).

445. Kim ES, Choi YE, Hwang SJ, Han YH, Park MJ, Bae IH. IL-4, a direct target of miR-340/429, is involved in radiation-induced aggressive tumor behavior in human carcinoma cells. Oncotarget [Internet] 2016 [cited 2023 Feb 5];7(52):86836–56. Available from: https://pubmed.ncbi.nlm.nih.gov/27895317/

446. Deshmane SL, Kremlev S, Amini S, Sawaya BE. Monocyte Chemoattractant Protein-1 (MCP-1): An Overview. J Interf Cytokine Res [Internet] 2009 [cited 2023 Feb 5];29(6):313. Available from: /pmc/articles/PMC2755091/

447. Hashimoto I, Wada J, Hida A, Baba M, Miyatake N, Eguchi J, et al. Elevated serum monocyte chemoattractant protein-4 and chronic inflammation in overweight subjects. Obesity (Silver Spring) [Internet] 2006 [cited 2023 Feb 5];14(5):799–811. Available from: https://pubmed.ncbi.nlm.nih.gov/16855189/

448. Nalla AK, Gogineni VR, Gupta R, Dinh DH, Rao JS. Suppression of uPA and uPAR blocks radiation-induced MCP-1 mediated recruitment of endothelial cells in meningioma. Cell Signal 2011;23(8):1299–310.

449. Yang X, Walton W, Cook DN, Hua X, Tilley S, Haskell CA, et al. The Chemokine, CCL3, and Its Receptor, CCR1, Mediate Thoracic Radiation–Induced Pulmonary Fibrosis. https://doi.org/101165/rcmb2010-0265OC [Internet] 2012 [cited 2023 Feb 5];45(1):127–35. Available from: www.atsjournals.org

450. Ehrenpreis ED, Jani A, Levitsky J, Ahn J, Hong J. A prospective, randomized, double-blind, placebo-controlled trial of retinol palmitate (vitamin A) for symptomatic chronic radiation proctopathy. Dis Colon Rectum [Internet] 2005 [cited 2023 Feb 5];48(1):1–8. Available from: https://pubmed.ncbi.nlm.nih.gov/15690650/

451. Mitra S, Leonard WJ. Biology of IL-2 and its therapeutic modulation: Mechanisms and strategies. J Leukoc Biol [Internet] 2018 [cited 2023 Feb 5];103(4):643–55. Available from: https://onlinelibrary.wiley.com/doi/full/10.1002/JLB.2RI0717-278R

452. Valenzuela J, Schmidt C, Mescher M. The Roles of IL-12 in Providing a Third Signal for Clonal Expansion of Naive CD8 T Cells. J Immunol [Internet] 2002 [cited 2023 Feb 5];169(12):6842–9. Available from: https://journals.aai.org/jimmunol/article/169/12/6842/34843/The-Roles-of-IL-12-in-Providing-a-Third-Signal-for

453. Parameswaran N, Patial S. Tumor Necrosis Factor-α Signaling in Macrophages. Crit Rev Eukaryot Gene Expr [Internet] 2010 [cited 2023 Feb 5];20(2):87. Available from: /pmc/articles/PMC3066460/

454. Farag MA, Gad MZ. Omega-9 fatty acids: potential roles in inflammation and cancer management. J Genet Eng Biotechnol [Internet] 2022 [cited 2023 Feb 5];20(1):48. Available from: /pmc/articles/PMC8927560/

455. Werner E, Wang H, Doetsch PW. Role of Pro-inflammatory Cytokines in Radiation-Induced Genomic Instability in Human Bronchial Epithelial Cells. Radiat Res [Internet] 2015 [cited 2023 Feb 5];184(6):621–9. Available from: https://pubmed.ncbi.nlm.nih.gov/26579942/

456. Gu Q, Wang D, Wang X, Peng R, Liu J, Deng H, et al. Basic fibroblast growth factor inhibits radiation-induced apoptosis of HUVECs. II. The RAS/MAPK pathway and phosphorylation of BAD at serine 112. Radiat Res [Internet] 2004 [cited 2023 Feb 5];161(6):703–11. Available from: https://pubmed.ncbi.nlm.nih.gov/15161349/

457. Park I, Yang H, Park JS, Koh GY, Choi EK. VEGF-Grab Enhances the Efficacy of Radiation Therapy by Blocking VEGF-A and Treatment-Induced PlGF. Int J Radiat Oncol Biol Phys [Internet] 2018 [cited 2023 Feb 5];102(3):609–18. Available from: https://pubmed.ncbi.nlm.nih.gov/30017791/

458. Chen YH, Pan SL, Wang JC, Kuo SH, Cheng JCH, Teng CM. Radiation-induced VEGF-C expression and endothelial cell proliferation in lung cancer. Strahlenther Onkol [Internet] 2014 [cited 2023 Feb 5];190(12):1154–62. Available from: https://pubmed.ncbi.nlm.nih.gov/24989178/

459. Kusmartsev S, Eruslanov E, Kübler H, Tseng T, Sakai Y, Su Z, et al. Oxidative Stress Regulates Expression of VEGFR1 in Myeloid Cells: Link to Tumor-Induced Immune Suppression in Renal Cell Carcinoma. J Immunol [Internet] 2008 [cited 2023 Feb 5];181(1):346–53. Available from: https://journals.aai.org/jimmunol/article/181/1/346/79593/Oxidative-Stress-Regulates-Expression-of-VEGFR1-in

460. Cengiz M, Akbulut S, Atahan IL, Grigsby PW. Acute phase response during radiotherapy. Int J Radiat Oncol Biol Phys [Internet] 2001 [cited 2023 Feb 5];49(4):1093–6. Available from: https://pubmed.ncbi.nlm.nih.gov/11240251/

461. Sproull M, Kramp T, Tandle A, Shankavaram U, Camphausen K. Serum Amyloid A as a Biomarker for Radiation Exposure. Radiat Res [Internet] 2015 [cited 2023 Feb 5];184(1):14–23. Available from: https://pubmed.ncbi.nlm.nih.gov/26114330/

462. Wang CY, Hsieh MJ, Chiu YC, Li SH, Huang HW, Fang FM, et al. Higher serum C-reactive protein concentration and hypoalbuminemia are poor prognostic indicators in patients with esophageal cancer undergoing radiotherapy. Radiother Oncol [Internet] 2009 [cited 2023 Feb 5];92(2):270–5. Available from: https://pubmed.ncbi.nlm.nih.gov/19195729/

463. Zhao J, Li X, Zhao X, Wang J, Xi Q, Hu G. Study on the correlation of serum amyloid A level with overall survival and radiation pneumonitis in non-small cell lung cancer patients receiving thoracic radiotherapy. Precis Radiat Oncol [Internet] 2017 [cited 2023 Feb 5];1(2):46–51. Available from: https://onlinelibrary.wiley.com/doi/full/10.1002/pro6.20

464. Benedicto A, Romayor I, Arteta B. Role of liver ICAM-1 in metastasis. Oncol Lett [Internet] 2017 [cited 2023 Feb 5];14(4):3883. Available from: /pmc/articles/PMC5604125/

465. Zhang D, Bi J, Liang Q, Wang S, Zhang L, Han F, et al. VCAM1 Promotes Tumor Cell Invasion and Metastasis by Inducing EMT and Transendothelial Migration in Colorectal Cancer. Front Oncol [Internet] 2020 [cited 2023 Feb 5];10:1066. Available from: /pmc/articles/PMC7390920/

466. Liu M, Guo S, Stiles JK. The emerging role of CXCL10 in cancer (Review). Oncol Lett [Internet] 2011 [cited 2023 Feb 5];2(4):583. Available from: /pmc/articles/PMC3406435/

467. Mangi MH, Newland AC. Interleukin-3: Promises and Perspectives. Hematology [Internet] 1998 [cited 2023 Feb 5];3(1):55–66. Available from: http://www.ncbi.nlm.nih.gov/pubmed/27416283

468. Isvoranu G, Surcel M, Munteanu AN, Bratu OG, Ionita-Radu F, Neagu MT, et al. Therapeutic potential of interleukin-15 in cancer (Review). Exp Ther Med [Internet] 2021 [cited 2023 Feb 5];22(1). Available from: /pmc/articles/PMC8112152/

469. Tsao CH, Shiau MY, Chuang PH, Chang YH, Hwang J. Interleukin-4 regulates lipid metabolism by inhibiting adipogenesis and promoting lipolysis. J Lipid Res [Internet] 2014 [cited 2023 Feb 5];55(3):385. Available from: /pmc/articles/PMC3934724/

470. Eder K, Baffy N, Falus A, Fulop AK. The major inflammatory mediator interleukin-6 and obesity. Inflamm Res [Internet] 2009 [cited 2023 Feb 5];58(11):727–36. Available from: https://pubmed.ncbi.nlm.nih.gov/19543691/

471. Bae HR, Choi MS, Kim S, Young HA, Gershwin ME, Jeon SM, et al. IFNγ Is a Key Link between Obesity and Th1-Mediated AutoImmune Diseases. Int J Mol Sci [Internet] 2021 [cited 2023 Feb 5];22(1):1–14. Available from: /pmc/articles/PMC7794719/

472. Um JY, Rim HK, Kim SJ, Kim HL, Hong SH. Functional Polymorphism of IL-1 Alpha and Its Potential Role in Obesity in Humans and Mice. PLoS One [Internet] 2011 [cited 2023 Feb 5];6(12):29524. Available from: /pmc/articles/PMC3246492/

473. Nov O, Shapiro H, Ovadia H, Tarnovscki T, Dvir I, Shemesh E, et al. Interleukin-1β Regulates Fat-Liver Crosstalk in Obesity by Auto-Paracrine Modulation of Adipose Tissue Inflammation and Expandability. PLoS One [Internet] 2013 [cited 2023 Feb 5];8(1):e53626. Available from: https://journals.plos.org/plosone/article?id=10.1371/journal.pone.0053626

474. Škopková M, Penesová A, Sell H, Rádiková Ž, Vlček M, Imrich R, et al. Protein Array Reveals Differentially Expressed Proteins in Subcutaneous Adipose Tissue in Obesity. Obesity [Internet] 2007 [cited 2023 Feb 5];15(10):2396–406. Available from: https://onlinelibrary.wiley.com/doi/full/10.1038/oby.2007.285

475. Burke SJ, Karlstad MD, Regal KM, Sparer TE, Lu D, Elks CM, et al. CCL20 is elevated during obesity and differentially regulated by NF-κB subunits in pancreatic β-cells. Biochim Biophys Acta - Gene Regul Mech [Internet] 2015 [cited 2021 Mar 1];1849(6):637–52. Available from: https://pubmed.ncbi.nlm.nih.gov/25882704/

476. De la Fuente López M, Landskron G, Parada D, Dubois-Camacho K, Simian D, Martinez M, et al. The relationship between chemokines CCL2, CCL3, and CCL4 with the tumor microenvironment and tumor-associated macrophage markers in colorectal cancer. Tumour Biol [Internet] 2018 [cited 2023 Feb 5];40(11). Available from: https://pubmed.ncbi.nlm.nih.gov/30419802/

477. Pandey VK, Shankar BS. Radiation-induced augmentation in dendritic cell function is mediated by apoptotic bodies/STAT5/Zbtb46 signaling. https://doi.org/101080/0955300220201767818 [Internet] 2020 [cited 2023 Feb 6];96(8):988–98. Available from: https://www.tandfonline.com/doi/abs/10.1080/09553002.2020.1767818

478. Zhu S, Yang N, Wu J, Wang X, Wang W, Liu YJ, et al. Tumor microenvironment-related dendritic cell deficiency: a target to enhance tumor immunotherapy. Pharmacol Res 2020;159:104980.

479. Han G, Chen G, Shen B, Li Y. Tim-3: An activation marker and activation limiter of innate immune cells. Front Immunol 2013;4(DEC):449.

480. Chiba S, Baghdadi M, Akiba H, Yoshiyama H, Kinoshita I, Dosaka-Akita H, et al. Tumor-infiltrating DCs suppress nucleic acid–mediated innate immune responses through interactions between the receptor TIM-3 and the alarmin HMGB1. Nat Immunol 2012 139 [Internet] 2012 [cited 2023 Feb 6];13(9):832–42. Available from: https://www.nature.com/articles/ni.2376

481. Wild AB, Krzyzak L, Peckert K, Stich L, Kuhnt C, Butterhof A, et al. CD83 orchestrates immunity toward self and non-self in dendritic cells. JCI Insight [Internet] 2019 [cited 2023 Feb 6];4(20). Available from: https://doi.org/10.1172/jci.insight.126246

482. Lim TS, Goh JKH, Mortellaro A, Lim CT, Hämmerling GJ, Ricciardi-Castagnoli P. CD80 and CD86 differentially regulate mechanical interactions of T-cells with antigen-presenting dendritic cells and B-cells. PLoS One [Internet] 2012 [cited 2023 Feb 6];7(9). Available from: https://pubmed.ncbi.nlm.nih.gov/23024807/

483. Brake DK, Smith EOB, Mersmann H, Smith CW, Robker RL. ICAM-1 expression in adipose tissue: Effects of diet-induced obesity in mice. Am J Physiol - Cell Physiol [Internet] 2006 [cited 2023 Feb 6];291(6):1232–9. Available from: https://journals.physiology.org/doi/10.1152/ajpcell.00008.2006

484. Sheng X, Parmentier JH, Tucci J, Pei H, Cortez-Toledo O, Dieli-Conwright CM, et al. Adipocytes Sequester and Metabolize the Chemotherapeutic Daunorubicin. Mol Cancer Res [Internet] 2017 [cited 2021 Aug 11];15(12). Available from: https://pubmed.ncbi.nlm.nih.gov/29117945/

485. Woolthuis CM, Stranahan AW, Park CY, Minhajuddin M, Gasparetto M, Stevens B, et al. Leukemic Stem Cells Evade Chemotherapy by Metabolic Adaptation to an Adipose Tissue Niche. Cell Stem Cell [Internet] 2016 [cited 2023 Mar 2];19(1):23–37. Available from: http://www.cell.com/article/S1934590916301515/fulltext

486. Lehuédé C, Li X, Dauvillier S, Vaysse C, Franchet C, Clement E, et al. Adipocytes promote breast cancer resistance to chemotherapy, a process amplified by obesity: Role of the major vault protein (MVP). Breast Cancer Res [Internet] 2019 [cited 2020 Mar 16];21(1):7. Available from: http://www.ncbi.nlm.nih.gov/pubmed/30654824

487. Elliott JA, Donohoe CL, Reynolds J V. Obesity and increased risk of esophageal adenocarcinoma. Expert Rev Endocrinol Metab [Internet] 2015 [cited 2023 Feb 17];10(5):511–23. Available from: https://pubmed.ncbi.nlm.nih.gov/30298765/

488. Zhang J, Suh Y, Choi YM, Ahn J, Davis ME, Lee K. Differential expression of cyclin G2, cyclin-dependent kinase inhibitor 2C and peripheral myelin protein 22 genes during adipogenesis. Animal [Internet] 2014 [cited 2021 Feb 24];8(5):800–9. Available from: https://pubmed.ncbi.nlm.nih.gov/24739352/

489. Wang SJ, Chao D, Wei W, Nan G, Li JY, Liu FL, et al. CD147 promotes collective invasion through cathepsin B in hepatocellular carcinoma. J Exp Clin Cancer Res [Internet] 2020 [cited 2023 Mar 1];39(1). Available from: https://pubmed.ncbi.nlm.nih.gov/32727598/

490. Goyal S, Amar SK, Dubey D, Pal MK, Singh J, Verma A, et al. Involvement of cathepsin B in mitochondrial apoptosis by p-phenylenediamine under ambient UV radiation. J Hazard Mater [Internet] 2015 [cited 2023 Mar 1];300:415–25. Available from: https://pubmed.ncbi.nlm.nih.gov/26223015/

491. Ali MM, Mirza I, Naquiallah D, Hassan C, Masrur M, Bianco FM, et al. CD147 Levels in Blood and Adipose Tissues Correlate with Vascular Dysfunction in Obese Diabetic Adults. J Cardiovasc Dev Dis [Internet] 2021 [cited 2023 Mar 1];9(1). Available from: https://pubmed.ncbi.nlm.nih.gov/35050217/

492. Shankar A, Kumar S, Iskander A, Varma NRS, Janic B, deCarvalho A, et al. Subcurative radiation significantly increases cell proliferation, invasion,and migration of primary glioblastoma multiforme in vivo. Chin J Cancer [Internet] 2014 [cited 2023 Mar 1];33(3):148. Available from: /pmc/articles/PMC3966215/

493. Koundouros N, Poulogiannis G. Reprogramming of fatty acid metabolism in cancer. Br J Cancer 2019 1221 [Internet] 2019 [cited 2021 Aug 13];122(1):4–22. Available from: https://www.nature.com/articles/s41416-019-0650-z

494. Arner P, Rydén M. Fatty Acids, Obesity and Insulin Resistance. Obes Facts [Internet] 2015 [cited 2023 Mar 1];8(2):147–55. Available from: https://www.karger.com/Article/FullText/381224

495. Liu DS, Hoefnagel SJM, Fisher OM, Krishnadath KK, Montgomery KG, Busuttil RA, et al. Novel metastatic models of esophageal adenocarcinoma derived from FLO-1 cells highlight the importance of E-cadherin in cancer metastasis. Oncotarget [Internet] 2016 [cited 2023 Mar 3];7(50):83342–58. Available from: https://www.oncotarget.com/article/13391/text/

496. Nieman KM, Kenny HA, Penicka C V., Ladanyi A, Buell-Gutbrod R, Zillhardt MR, et al. Adipocytes promote ovarian cancer metastasis and provide energy for rapid tumor growth. Nat Med [Internet] 2011 [cited 2023 Feb 21];17(11):1498–503. Available from: https://pubmed.ncbi.nlm.nih.gov/22037646/

497. Yu L, Chen X, Sun X, Wang L, Chen S. The Glycolytic Switch in Tumors: How Many Players Are Involved? J Cancer [Internet] 2017 [cited 2023 Mar 2];8(17):3430. Available from: /pmc/articles/PMC5687156/

498. Dranka BP, Benavides GA, Diers AR, Giordano S, Zelickson BR, Reily C, et al. Assessing bioenergetic function in response to oxidative stress by metabolic profiling. Free Radic Biol Med [Internet] 2011 [cited 2023 Feb 15];51(9):1621–35. Available from: https://pubmed.ncbi.nlm.nih.gov/21872656/

499. Chen M, Huang J. The expanded role of fatty acid metabolism in cancer: new aspects andtargets. Precis Clin Med [Internet] 2019 [cited 2023 Mar 2];2(3):183. Available from: /pmc/articles/PMC6770278/

500. Chacko BK, Kramer PA, Ravi S, Benavides GA, Mitchell T, Dranka BP, et al. The Bioenergetic Health Index: a new concept in mitochondrial translational research. Clin Sci [Internet] 2014 [cited 2023 Feb 15];127(6):367–73. Available from: /clinsci/article/127/6/367/70836/The-Bioenergetic-Health-Index-a-new-concept-in

501. Shi DY, Xie FZ, Zhai C, Stern JS, Liu Y, Liu SL. The role of cellular oxidative stress in regulating glycolysis energy metabolism in hepatoma cells. Mol Cancer [Internet] 2009 [cited 2023 Mar 2];8:32. Available from: /pmc/articles/PMC2702299/

502. Pascual G, Domínguez D, Elosúa-Bayes M, Beckedorff F, Laudanna C, Bigas C, et al. Dietary palmitic acid promotes a prometastatic memory via Schwann cells. Nat 2021 5997885 [Internet] 2021 [cited 2023 Mar 2];599(7885):485–90. Available from: https://www.nature.com/articles/s41586-021-04075-0

503. Pramanik R, Sheng X, Ichihara B, Heisterkamp N, Mittelman SD. Adipose tissue attracts and protects acute lymphoblastic leukemia cells from chemotherapy. Leuk Res [Internet] 2013 [cited 2023 Feb 28];37(5):503. Available from: /pmc/articles/PMC3622767/

504. Panov A, Schonfeld P, Dikalov S, Hemendinger R, Bonkovsky HL, Brooks BR. The Neuromediator Glutamate, through Specific Substrate Interactions, Enhances Mitochondrial ATP Production and Reactive Oxygen Species Generation in Nonsynaptic Brain Mitochondria. J Biol Chem [Internet] 2009 [cited 2023 Mar 2];284(21):14448. Available from: /pmc/articles/PMC2682893/

505. Zhu L, Zhu X, Wu Y. Effects of Glucose Metabolism, Lipid Metabolism, and Glutamine Metabolism on Tumor Microenvironment and Clinical Implications. Biomolecules [Internet] 2022 [cited 2023 Mar 2];12(4). Available from: /pmc/articles/PMC9028125/

506. Li YJ, Fahrmann JF, Aftabizadeh M, Zhao Q, Tripathi SC, Zhang C, et al. Fatty acid oxidation protects cancer cells from apoptosis by increasing mitochondrial membrane lipids. Cell Rep 2022;39(9):110870.

507. Zhong J, Rajaram N, Brizel DM, Frees AE, Ramanujam N, Batinic-Haberle I, et al. Radiation induces aerobic glycolysis through reactive oxygen species. Radiother Oncol [Internet] 2013 [cited 2023 Feb 14];106(3):390. Available from: /pmc/articles/PMC3770265/

508. Juaristi I, Llorente-Folch I, Satrústegui J, del Arco A. Extracellular ATP and glutamate drive pyruvate production and energy demand to regulate mitochondrial respiration in astrocytes. Glia [Internet] 2019 [cited 2023 Mar 2];67(4):759–74. Available from: https://pubmed.ncbi.nlm.nih.gov/30623988/

509. Colangelo N, de Toledo S, Azzam E. Irradiation of Glioblastoma Cells Increases CD147 Levels in their Extracellular Vesicles: Contribution to Increased MMP9 Activity in the Tumor Microenvironment. Int J Radiat Oncol [Internet] 2017 [cited 2023 Mar 2];99(2):E585. Available from: http://www.redjournal.org/article/S0360301617330626/fulltext

510. Li J, Huang Q, Long X, Zhang J, Huang X, Aa J, et al. CD147 reprograms fatty acid metabolism in hepatocellular carcinoma cells through Akt/mTOR/SREBP1c and P38/PPARα pathways. J Hepatol [Internet] 2015 [cited 2023 Mar 2];63(6):1378–89. Available from: https://pubmed.ncbi.nlm.nih.gov/26282231/

511. Gilles C, Polette M, Mestdagt M, Nawrocki-Raby B, Ruggeri P, Birembaut P, et al. Transactivation of vimentin by beta-catenin in human breast cancer cells. Cancer Res [Internet] 2003 [cited 2023 Mar 2];63(10):2658–64. Available from: https://www.hal.inserm.fr/inserm-00149065

512. Usman S, Waseem NH, Nguyen TKN, Mohsin S, Jamal A, Teh MT, et al. Vimentin Is at the Heart of Epithelial Mesenchymal Transition (EMT) Mediated Metastasis. Cancers (Basel) [Internet] 2021 [cited 2023 Mar 2];13(19):4985. Available from: /pmc/articles/PMC8507690/

513. Bergers G, Fendt SM. The metabolism of cancer cells during metastasis. Nat Rev Cancer [Internet] 2021 [cited 2023 Mar 3];21(3):162. Available from: /pmc/articles/PMC8733955/

514. Bhat AA, Nisar S, Maacha S, Carneiro-Lobo TC, Akhtar S, Siveen KS, et al. Cytokine-chemokine network driven metastasis in esophageal cancer; promising avenue for targeted therapy. Mol Cancer 2020 201 [Internet] 2021 [cited 2023 Mar 3];20(1):1–20. Available from: https://molecular-cancer.biomedcentral.com/articles/10.1186/s12943-020-01294-3

515. Zeng X, Zhu M, Liu X, Chen X, Yuan Y, Li L, et al. Oleic acid ameliorates palmitic acid induced hepatocellular lipotoxicity by inhibition of ER stress and pyroptosis. Nutr Metab [Internet] 2020 [cited 2021 Mar 1];17(1). Available from: https://pubmed.ncbi.nlm.nih.gov/32021639/

516. Bousquenaud M, Fico F, Solinas G, Rüegg C, Santamaria-Martínez A. Obesity promotes the expansion of metastasis-initiating cells in breast cancer. Breast Cancer Res [Internet] 2018 [cited 2023 Mar 3];20(1):1–11. Available from: https://breast-cancer-research.biomedcentral.com/articles/10.1186/s13058-018-1029-4

517. Li J, Zhao S, Zhou X, Zhang T, Zhao L, Miao P, et al. Inhibition of Lipolysis by Mercaptoacetate and Etomoxir Specifically Sensitize Drug-Resistant Lung Adenocarcinoma Cell to Paclitaxel. PLoS One [Internet] 2013 [cited 2023 Mar 3];8(9):e74623. Available from: https://journals.plos.org/plosone/article?id=10.1371/journal.pone.0074623

518. Qu Q, Zeng F, Liu X, Wang QJ, Deng F. Fatty acid oxidation and carnitine palmitoyltransferase I: emerging therapeutic targets in cancer. Cell Death Dis 2016 75 [Internet] 2016 [cited 2023 Mar 3];7(5):e2226–e2226. Available from: https://www.nature.com/articles/cddis2016132

519. Liu Y, Metzinger MN, Lewellen KA, Cripps SN, Carey KD, Harper EI, et al. Obesity contributes to ovarian cancer metastatic success through increased lipogenesis, enhanced vascularity, and decreased infiltration of M1 macrophages. Cancer Res [Internet] 2015 [cited 2023 Mar 3];75(23):5046–57. Available from: https://aacrjournals.org/cancerres/article/75/23/5046/606432/Obesity-Contributes-to-Ovarian-Cancer-Metastatic

520. Ebadi M, Field CJ, Lehner R, Mazurak VC. Chemotherapy diminishes lipid storage capacity of adipose tissue in a preclinical model of colon cancer. Lipids Health Dis [Internet] 2017 [cited 2023 Feb 17];16(1):1–12. Available from: https://lipidworld.biomedcentral.com/articles/10.1186/s12944-017-0638-8

521. Ladanyi A, Mukherjee A, Kenny HA, Johnson A, Mitra AK, Sundaresan S, et al. Adipocyte-induced CD36 expression drives ovarian cancer progression and metastasis. Oncogene 2018 3717 [Internet] 2018 [cited 2023 Mar 20];37(17):2285–301.

Available from: https://www.nature.com/articles/s41388-017-0093-z

522. Wang H, Franco F, Tsui YC, Xie X, Trefny MP, Zappasodi R, et al. CD36-mediated metabolic adaptation supports regulatory T cell survival and function in tumors. Nat Immunol 2020 213 [Internet] 2020 [cited 2023 Mar 20];21(3):298–308. Available from: https://www.nature.com/articles/s41590-019-0589-5

523. Bauerschlag DO, Maass N, Leonhardt P, Verburg FA, Pecks U, Zeppernick F, et al. Fatty acid synthase overexpression: target for therapy and reversal of chemoresistance in ovarian cancer. J Transl Med [Internet] 2015 [cited 2023 Mar 20];13(1). Available from: https://pubmed.ncbi.nlm.nih.gov/25947066/

524. Papaevangelou E, Almeida GS, Box C, deSouza NM, Chung YL. The effect of FASN inhibition on the growth and metabolism of a cisplatin-resistant ovarian carcinoma model. Int J cancer [Internet] 2018 [cited 2023 Mar 20];143(4):992–1002. Available from: https://pubmed.ncbi.nlm.nih.gov/29569717/

525. Wu ZS, Huang SM, Wang YC. Palmitate Enhances the Efficacy of Cisplatin and Doxorubicin against Human Endometrial Carcinoma Cells. Int J Mol Sci [Internet] 2022 [cited 2023 Feb 15];23(1). Available from: /pmc/articles/PMC8744704/

526. Davern M, Donlon NE, Sheppard AS, Majcher KD, Connell FO, Heeran AB, et al. FLOT and CROSS chemotherapy regimens alter the frequency of CD27+ and CD69+ T cells in oesophagogastric adenocarcinomas: implications for combination with immunotherapy. J Cancer Res Clin Oncol [Internet] 2022 [cited 2022 Nov 27];1–22. Available from: https://link.springer.com/article/10.1007/s00432-022-04283-9

527. Sica V, Bravo-San Pedro JM, Stoll G, Kroemer G. Oxidative phosphorylation as a potential therapeutic target for cancer therapy. Int J Cancer [Internet] 2020 [cited 2023 Feb 14];146(1):10–7. Available from: https://onlinelibrary.wiley.com/doi/full/10.1002/ijc.32616

528. Yang H, Villani RM, Wang H, Simpson MJ, Roberts MS, Tang M, et al. The role of cellular reactive oxygen species in cancer chemotherapy. J Exp Clin Cancer Res [Internet] 2018 [cited 2023 Feb 14];37(1). Available from: /pmc/articles/PMC6211502/

529. Andalib S, Varshosaz J, Hassanzadeh F, Sadeghi H. Optimization of LDL targeted nanostructured lipid carriers of 5-FU by a full factorial design. Adv Biomed Res [Internet] 2012 [cited 2023 Feb 14];1(1):45. Available from: /pmc/articles/PMC3544134/

530. Al-Mutairi AA, Alkhatib MH, Gashlan HM. Antitumor activities of Co-loading gemcitabine and oxaliplatin into oleic acid-based solid lipid nanoparticle against non-small cell lung cancer cells. Biointerface Res Appl Chem 2022;12(1):49–60.

531. Baeten CIM, Castermans K, Lammering G, Hillen F, Wouters BG, Hillen HFP, et al. Effects of radiotherapy and chemotherapy on angiogenesis and leukocyte infiltration in rectal cancer. Int J Radiat Oncol Biol Phys [Internet] 2006 [cited 2023 Feb 14];66(4):1219–27. Available from: http://www.redjournal.org/article/S0360301606025740/fulltext

532. Vilalta M, Brune J, Rafat M, Soto L, Graves EE. The role of granulocyte macrophage colony stimulating factor (GM-CSF) in radiation-induced tumor cell migration. Clin Exp Metastasis [Internet] 2018 [cited 2023 Feb 14];35(4):247–54. Available from: https://pubmed.ncbi.nlm.nih.gov/29536224/

533. Multhoff G, Radons J. Radiation, inflammation, and immune responses in cancer. Front. Oncol.2012;2 JUN:58.

534. McKelvey KJ, Hudson AL, Back M, Eade T, Diakos CI. Radiation, inflammation and the immune response in cancer. Mamm Genome [Internet] 2018 [cited 2023 Feb 14];29(11):843. Available from: /pmc/articles/PMC6267675/

535. Baker KJ, Houston A, Brint E. IL-1 family members in cancer; two sides to every story. Front Immunol 2019;10(JUN):1197.

536. Chau K, Xu B, Hennessy A, Makris A. Effect of Placental Growth Factor on Trophoblast-Endothelial Cell Interactions In Vitro. Reprod Sci [Internet] 2020 [cited 2023 Feb 14];27(6):1285–92. Available from: https://pubmed.ncbi.nlm.nih.gov/32016802/

537. Bernatchez PN, Soker S, Sirois MG. Vascular endothelial growth factor effect on endothelial cell proliferation, migration, and platelet-activating factor synthesis is Flk-1- dependent. J Biol Chem [Internet] 1999 [cited 2023 Feb 14];274(43):31047–54. Available from: http://www.jbc.org/article/S0021925819517847/fulltext

538. Cao Y, Linden P, Farnebo J, Cao R, Eriksson A, Kumar V, et al. Vascular endothelial growth factor C induces angiogenesis in vivo. Proc Natl Acad Sci U S A [Internet] 1998 [cited 2023 Feb 14];95(24):14389. Available from: /pmc/articles/PMC24383/

539. Junttila IS. Tuning the cytokine responses: An update on interleukin (IL)-4 and IL-13 receptor complexes. Front Immunol 2018;9(JUN):888.

540. Zijtregtop EAM, van der Strate I, Beishuizen A, Zwaan CM, Scheijde-Vermeulen MA, Brandsma AM, et al. Biology and Clinical Applicability of Plasma Thymus and Activation-Regulated Chemokine (TARC) in Classical Hodgkin Lymphoma. Cancers 2021, Vol 13, Page 884 [Internet] 2021 [cited 2023 Feb 14];13(4):884. Available from: https://www.mdpi.com/2072-6694/13/4/884/htm

541. Hernandez P, Gronke K, Diefenbach A. A catch-22: Interleukin-22 and cancer. Eur J Immunol [Internet] 2018 [cited 2023 Feb 15];48(1):15–31. Available from: https://onlinelibrary.wiley.com/doi/full/10.1002/eji.201747183

542. Wang HW, Joyce JA. Alternative activation of tumor-associated macrophages by IL-4: Priming for protumoral functions. Cell Cycle [Internet] 2010 [cited 2023 Feb 15];9(24):4824. Available from: /pmc/articles/PMC3047808/

543. Fousek K, Horn LA, Palena C. Interleukin-8: a Chemokine at the Intersection of Cancer Plasticity, Angiogenesis, and

Immune Suppression. Pharmacol Ther [Internet] 2021 [cited 2022 Sep 22];219:107692. Available from: /pmc/articles/PMC8344087/

544. Jiang H, Cui J, Chu H, Xu T, Xie M, Jing X, et al. Targeting IL8 as a sequential therapy strategy to overcome chemotherapy resistance in advanced gastric cancer. Cell Death Discov 2022 81 [Internet] 2022 [cited 2023 Feb 15];8(1):1–13. Available from: https://www.nature.com/articles/s41420-022-01033-1

545. Kimura S, Nanbu U, Noguchi H, Harada Y, Kumamoto K, Sasaguri Y, et al. Macrophage CCL22 expression in the tumor microenvironment and implications for survival in patients with squamous cell carcinoma of the tongue. J Oral Pathol Med [Internet] 2019 [cited 2023 Feb 15];48(8):677–85. Available from: https://onlinelibrary.wiley.com/doi/full/10.1111/jop.12885

546. Mailer RKW, Joly AL, Liu S, Elias S, Tegner J, Andersson J. IL-1β promotes Th17 differentiation by inducing alternative splicing of FOXP3. Sci Reports 2015 51 [Internet] 2015 [cited 2023 Feb 15];5(1):1–9. Available from: https://www.nature.com/articles/srep14674

547. Liu X, Sun S, Liu D. IL-17D: A Less Studied Cytokine of IL-17 Family. Int Arch Allergy Immunol [Internet] 2020 [cited 2023 Feb 15];181(8):618–23. Available from: https://www.karger.com/Article/FullText/508255

548. Chen Y, Chauhan SK, Tan X, Dana R. Interleukin-7 and -15 Maintain Pathogenic Memory Th17 Cells in Autoimmunity. J Autoimmun [Internet] 2017 [cited 2023 Feb 15];77:96. Available from: /pmc/articles/PMC5276802/

549. Limagne E, Euvrard R, Thibaudin M, Rébé C, Derangère V, Chevriaux A, et al. Accumulation of MDSC and Th17 Cells in Patients with Metastatic Colorectal Cancer Predicts the Efficacy of a FOLFOX-Bevacizumab Drug Treatment Regimen. Cancer Res [Internet] 2016 [cited 2023 Feb 15];76(18):5241–52. Available from: https://pubmed.ncbi.nlm.nih.gov/27496709/

550. Theobald L, Stroeder R, Melchior P, Iordache II, Tänzer T, Port M, et al. Chemoradiotherapy-induced increase in Th17 cell frequency in cervical cancer patients is associated with therapy resistance and early relapse. Mol Oncol [Internet] 2021 [cited 2023 Feb 15];15(12):3559–77. Available from: https://onlinelibrary.wiley.com/doi/full/10.1002/1878-0261.13095

551. Luotola K. IL-1 Receptor Antagonist (IL-1Ra) Levels and Management of Metabolic Disorders. Nutrients [Internet] 2022 [cited 2023 Feb 15];14(16). Available from: /pmc/articles/PMC9415765/

552. Riedel F, Götte K, Goessler U, Sadick H, Hörmann K. Targeting Chemotherapy-induced VEGF Up-regulation by VEGF Antisense Oligonucleotides in HNSCC Cell Lines. Anticancer Res [Internet] 2004 [cited 2023 Feb 15];24(4):2179–84. Available from: https://ar.iiarjournals.org/content/24/4/2179

553. Doronzo G, Viretto M, Barale C, Russo I, Mattiello L, Anfossi G, et al. Oleic Acid Increases Synthesis and Secretion of VEGF in Rat Vascular Smooth Muscle Cells: Role of Oxidative Stress and Impairment in Obesity. Int J Mol Sci [Internet] 2013 [cited 2023 Feb 15];14(9):18861. Available from: /pmc/articles/PMC3794811/

554. Sultani M, Stringer AM, Bowen JM, Gibson RJ. Anti-inflammatory cytokines: important immunoregulatory factors contributing to chemotherapy-induced gastrointestinal mucositis. Chemother Res Pract [Internet] 2012 [cited 2023 Feb 15];2012:1–11. Available from: https://pubmed.ncbi.nlm.nih.gov/22973511/

555. Heim L, Yang Z, Tausche P, Hohenberger K, Chiriac MT, Koelle J, et al. IL-9 Producing Tumor-Infiltrating Lymphocytes and Treg Subsets Drive Immune Escape of Tumor Cells in Non-Small Cell Lung Cancer. Front Immunol 2022;13:1421.

556. Stott B, Lavender P, Lehmann S, Pennino D, Durham S, Schmidt-Weber CB. Human IL-31 is induced by IL-4 and promotes TH2-driven inflammation. J Allergy Clin Immunol [Internet] 2013 [cited 2023 Feb 15];132(2). Available from: https://pubmed.ncbi.nlm.nih.gov/23694808/

557. Halwani R, Sultana A, Vazquez-Tello A, Jamhawi A, Al-Masri AA, Al-Muhsen S. Th-17 regulatory cytokines IL-21, IL-23, and IL-6 enhance neutrophil production of IL-17 cytokines during asthma. J Asthma [Internet] 2017 [cited 2023 Feb 15];54(9):893–904. Available from: https://pubmed.ncbi.nlm.nih.gov/28635548/

558. Yoshimoto T, Yoshimoto T, Yasuda K, Mizuguchi J, Nakanishi K. IL-27 suppresses Th2 cell development and Th2 cytokines production from polarized Th2 cells: a novel therapeutic way for Th2-mediated allergic inflammation. J Immunol [Internet] 2007 [cited 2023 Feb 15];179(7):4415–23. Available from: https://pubmed.ncbi.nlm.nih.gov/17878337/

559. Liu H, Rohowsky-Kochan C. Interleukin-27-Mediated Suppression of Human Th17 Cells Is Associated with Activation of STAT1 and Suppressor of Cytokine Signaling Protein 1. J Interf Cytokine Res [Internet] 2011 [cited 2023 Feb 15];31(5):459. Available from: /pmc/articles/PMC3083723/

560. Tsavaris N, Kosmas C, Vadiaka M, Kanelopoulos P, Boulamatsis D. Immune changes in patients with advanced breast cancer undergoing chemotherapy with taxanes. Br J Cancer 2002 871 [Internet] 2002 [cited 2023 Feb 15];87(1):21–7. Available from: https://www.nature.com/articles/6600347

561. Brand MD, Nicholls DG. Assessing mitochondrial dysfunction in cells. Biochem J [Internet] 2011 [cited 2023 Feb 15];435(Pt 2):297. Available from: /pmc/articles/PMC3076726/

562. Schneider V, Krieger ML, Bendas G, Jaehde U, Kalayda G V. Contribution of intracellular ATP to cisplatin resistance of tumor cells. J Biol Inorg Chem [Internet] 2013 [cited 2023 Feb 15];18(2):165–74. Available from: https://pubmed.ncbi.nlm.nih.gov/23183891/

563. Baffy G, Derdak Z, Robson SC. Mitochondrial recoupling: a novel therapeutic strategy for cancer? Br J Cancer [Internet] 2011 [cited 2023 Feb 15];105(4):469. Available from: /pmc/articles/PMC3170958/

564. Balogh E, Veale DJ, McGarry T, Orr C, Szekanecz Z, Ng CT, et al. Oxidative stress impairs energy metabolism in primary cells and synovial tissue of patients with rheumatoid arthritis. Arthritis Res Ther [Internet] 2018 [cited 2023 Feb 16];20(1):1–15. Available from: https://arthritis-research.biomedcentral.com/articles/10.1186/s13075-018-1592-1

565. Hill BG, Benavides GA, Lancaster JJR, Ballinger S, Dell'Italia L, Zhang J, et al. Integration of cellular bioenergetics with mitochondrial quality control and autophagy. Biol Chem [Internet] 2012 [cited 2023 Feb 16];393(12):1485. Available from: /pmc/articles/PMC3594552/

566. Boreel DF, Span PN, Heskamp S, Adema GJ, Bussink J. Targeting Oxidative Phosphorylation to Increase the Efficacy of Radio- and Immune-Combination Therapy. Clin Cancer Res [Internet] 2021 [cited 2023 Feb 16];27(11):2970–8. Available from: https://pubmed.ncbi.nlm.nih.gov/33419779/

567. Bakke SS, Moro C, Nikolić N, Hessvik NP, Badin PM, Lauvhaug L, et al. Palmitic acid follows a different metabolic pathway than oleic acid in human skeletal muscle cells; lower lipolysis rate despite an increased level of adipose triglyceride lipase. Biochim Biophys Acta [Internet] 2012 [cited 2023 Feb 16];1821(10):1323–33. Available from: https://pubmed.ncbi.nlm.nih.gov/22796147/

568. Fuhrmann DC, Olesch C, Kurrle N, Schnütgen F, Zukunft S, Fleming I, et al. Chronic Hypoxia Enhances β-Oxidation-Dependent Electron Transport via Electron Transferring Flavoproteins. Cells [Internet] 2019 [cited 2023 Feb 16];8(2). Available from: /pmc/articles/PMC6406996/

569. Ma DY, Clark EA. The role of CD40 and CD40L in Dendritic Cells. Semin Immunol [Internet] 2009 [cited 2023 Feb 16];21(5):265. Available from: /pmc/articles/PMC2749083/

570. Haghayegh Jahromi N, Marchetti L, Moalli F, Duc D, Basso C, Tardent H, et al. Intercellular Adhesion Molecule-1 (ICAM-1) and ICAM-2 Differentially Contribute to Peripheral Activation and CNS Entry of Autoaggressive Th1 and Th17 Cells in Experimental Autoimmune Encephalomyelitis. Front Immunol 2020;10:3056.

571. Jiang X, Zhou T, Xiao Y, Yu J, Dou S, Chen G, et al. Tim-3 promotes tumor-promoting M2 macrophage polarization by binding to STAT1 and suppressing the STAT1-miR-155 signaling axis. Oncoimmunology [Internet] 2016 [cited 2023 Feb 6];5(9). Available from: https://pubmed.ncbi.nlm.nih.gov/27757304/

572. Yan W, Liu X, Ma H, Zhang H, Song X, Gao L, et al. Tim-3 fosters HCC development by enhancing TGF-β-mediated alternative activation of macrophages. Gut [Internet] 2015 [cited 2023 Feb 16];64(10):1593–604. Available from: https://pubmed.ncbi.nlm.nih.gov/25608525/

573. Zhang C, Yang M, Ericsson AC. Function of Macrophages in Disease: Current Understanding on Molecular Mechanisms. Front Immunol 2021;12:635.

574. Alonso-Torre S, Carrillo C, Cavia M del M. Role of oleic acid in immune system; mechanism of action; a review. Nutr Hosp [Internet] 2012 [cited 2023 Feb 16];27(4):978–90. Available from: https://pubmed.ncbi.nlm.nih.gov/23165533/

575. Porcheray F, Viaud S, Rimaniol AC, Léone C, Samah B, Dereuddre-Bosquet N, et al. Macrophage activation switching: an asset for the resolution of inflammation. Clin Exp Immunol [Internet] 2005 [cited 2023 Feb 16];142(3):481. Available from: /pmc/articles/PMC1809537/

576. Lobstein T, Jackson-Leach R, Powis J, Brinsden H, Gray M. World Obesity Atlas 2023. 2023 [cited 2023 Mar 12];Available from: www.johnclarksondesign.co.uk

577. McMurray F, Patten DA, Harper ME. Reactive Oxygen Species and Oxidative Stress in Obesity—Recent Findings and Empirical Approaches. Obesity [Internet] 2016 [cited 2023 Mar 12];24(11):2301–10. Available from: https://onlinelibrary.wiley.com/doi/full/10.1002/oby.21654

578. Yang H, Villani RM, Wang H, Simpson MJ, Roberts MS, Tang M, et al. The role of cellular reactive oxygen species in cancer chemotherapy. J Exp Clin Cancer Res [Internet] 2018 [cited 2023 Mar 12];37(1). Available from: /pmc/articles/PMC6211502/

579. Mittal M, Siddiqui MR, Tran K, Reddy SP, Malik AB. Reactive Oxygen Species in Inflammation and Tissue Injury. Antioxid Redox Signal [Internet] 2014 [cited 2023 Mar 12];20(7):1126. Available from: /pmc/articles/PMC3929010/

580. Zhang J, Lei W, Chen X, Wang S, Qian W. Oxidative stress response induced by chemotherapy in leukemia treatment (Review). Mol Clin Oncol [Internet] 2018 [cited 2023 Mar 12];8(3):391–9. Available from: http://www.spandidos-publications.com/10.3892/mco.2018.1549/abstract

581. Blücher C, Iberl S, Schwagarus N, Müller S, Liebisch G, Höring M, et al. Secreted Factors from Adipose Tissue Reprogram Tumor Lipid Metabolism and Induce Motility by Modulating PPARα/ANGPTL4 and FAK. Mol Cancer Res [Internet] 2020 [cited 2023 Mar 12];18(12):1849–62. Available from: https://pubmed.ncbi.nlm.nih.gov/32859692/

582. Molofsky AB, Nussbaum JC, Liang HE, Dyken SJV, Cheng LE, Mohapatra A, et al. Innate lymphoid type 2 cells sustain visceral adipose tissue eosinophils and alternatively activated macrophages. J Exp Med [Internet] 2013 [cited 2023 Mar 12];210(3):535–49. Available from: https://pubmed.ncbi.nlm.nih.gov/23420878/

583. Lin HY, Tan GQ, Liu Y, Lin SQ. The prognostic value of serum amyloid A in solid tumors: A meta-analysis. Cancer Cell Int [Internet] 2019 [cited 2023 Mar 12];19(1):1–10. Available from: https://cancerci.biomedcentral.com/articles/10.1186/s12935-019-0783-4

584. Gitto SB, Gitto SB, Beardsley JM, Nakkina SP, Oyer JL, Cline KA, et al. Identification of a novel IL-5 signaling pathway in chronic pancreatitis and crosstalk with pancreatic tumor cells. Cell Commun Signal [Internet] 2020 [cited 2023 Mar 12];18(1):1–14. Available from: https://biosignaling.biomedcentral.com/articles/10.1186/s12964-020-00594-x

585. Petrus P, Lecoutre S, Dollet L, Wiel C, Sulen A, Gao H, et al. Glutamine Links Obesity to Inflammation in Human White Adipose Tissue. Cell Metab [Internet] 2020 [cited 2023 Mar 12];31(2):375-390.e11. Available from: https://pubmed.ncbi.nlm.nih.gov/31866443/

586. Nguyen TL, Durán R V. Glutamine metabolism in cancer therapy. Cancer Drug Resist [Internet] 2018 [cited 2023 Mar 12];1(3):126–38. Available from: https://cdrjournal.com/article/view/2787

587. Li X, Zhu H, Sun W, Yang X, Nie Q, Fang X. Role of glutamine and its metabolite ammonia in crosstalk of cancer-associated fibroblasts and cancer cells. Cancer Cell Int 2021 211 [Internet] 2021 [cited 2023 Mar 12];21(1):1–13. Available from: https://cancerci.biomedcentral.com/articles/10.1186/s12935-021-02121-5

588. Klop B, Elte JWF, Cabezas MC. Dyslipidemia in Obesity: Mechanisms and Potential Targets. Nutrients [Internet] 2013 [cited 2023 Mar 12];5(4):1218. Available from: /pmc/articles/PMC3705344/

589. Fahed G, Aoun L, Zerdan MB, Allam S, Zerdan MB, Bouferraa Y, et al. Metabolic Syndrome: Updates on Pathophysiology and Management in 2021. Int J Mol Sci [Internet] 2022 [cited 2023 Mar 12];23(2). Available from: /pmc/articles/PMC8775991/

590. Sheridan M, Ogretmen B. The Role of Ceramide Metabolism and Signaling in the Regulation of Mitophagy and Cancer Therapy. Cancers (Basel) [Internet] 2021 [cited 2023 Mar 12];13(10). Available from: /pmc/articles/PMC8161379/

591. Moro K, Kawaguchi T, Tsuchida J, Gabriel E, Qi Q, Yan L, et al. Ceramide species are elevated in human breast cancer and are associated with less aggressiveness. Oncotarget [Internet] 2018 [cited 2023 Mar 12];9(28):19874–90. Available from: https://www.oncotarget.com/article/24903/text/

592. Carretta MD, Quiroga J, López R, Hidalgo MA, Burgos RA. Participation of Short-Chain Fatty Acids and Their Receptors in Gut Inflammation and Colon Cancer. Front Physiol 2021;12:405.

593. Tucci J, Chen T, Margulis K, Orgel E, Paszkiewicz RL, Cohen MD, et al. Adipocytes Provide Fatty Acids to Acute Lymphoblastic Leukemia Cells. Front Oncol 2021;11:1413.

594. Shen J, Xiao Z, Zhao Q, Li M, Wu X, Zhang L, et al. Anti-cancer therapy with TNFα and IFNγ: A comprehensive review. Cell Prolif [Internet] 2018 [cited 2023 Mar 12];51(4). Available from: /pmc/articles/PMC6528874/

595. Haabeth OAW, Bogen B, Corthay A. A model for cancer-suppressive inflammation. https://doi.org/104161/onci21542 [Internet] 2012 [cited 2023 Mar 12];1(7):1146–55. Available from: https://www.tandfonline.com/doi/abs/10.4161/onci.21542

596. Eun SH, Hong JH, Glimcher LH. IL-2 production in developing Th1 cells is regulated by heterodimerization of RelA and T-bet and requires T-bet serine residue 508. J Exp Med [Internet] 2005 [cited 2023 Mar 12];202(9):1289. Available from: /pmc/articles/PMC2213245/

597. Sullivan KM, Jiang X, Guha P, Lausted C, Carter JA, Hsu C, et al. Blockade of interleukin 10 potentiates antitumour immune function in human colorectal cancer liver metastases. Gut [Internet] 2023 [cited 2023 Mar 12];72(2):325–37. Available from: https://gut.bmj.com/content/72/2/325

598. Song X, Traub B, Shi J, Kornmann M. Possible Roles of Interleukin-4 and -13 and Their Receptors in Gastric and Colon Cancer. Int J Mol Sci 2021, Vol 22, Page 727 [Internet] 2021 [cited 2023 Mar 12];22(2):727. Available from: https://www.mdpi.com/1422-0067/22/2/727/htm

599. Barsoumian HB, Ramapriyan R, Younes AI, Caetano MS, Menon H, Comeaux NI, et al. Low-dose radiation treatment enhances systemic antitumor immune responses by overcoming the inhibitory stroma. J Immunother cancer [Internet] 2020 [cited 2023 Mar 12];8(2). Available from: https://pubmed.ncbi.nlm.nih.gov/33106386/

600. Gonzalez H, Hagerling C, Werb Z. Roles of the immune system in cancer: from tumor initiation to metastatic progression. Genes Dev [Internet] 2018 [cited 2023 Mar 13];32(19–20):1267. Available from: /pmc/articles/PMC6169832/

601. Mortezaee K, Najafi M. Immune system in cancer radiotherapy: Resistance mechanisms and therapy perspectives. Crit Rev Oncol Hematol 2021;157:103180.

602. Tran AP, Ali Al-Radhawi M, Kareva I, Wu J, Waxman DJ, Sontag ED. Delicate Balances in Cancer Chemotherapy: Modeling Immune Recruitment and Emergence of Systemic Drug Resistance. Front Immunol 2020;11:1376.

603. Peng Q, Qiu X, Zhang Z, Zhang S, Zhang Y, Liang Y, et al. PD-L1 on dendritic cells attenuates T cell activation and regulates response to immune checkpoint blockade. Nat Commun 2020 111 [Internet] 2020 [cited 2021 Nov 11];11(1):1–8. Available from: https://www.nature.com/articles/s41467-020-18570-x

604. Kreuzaler P, Panina Y, Segal J, Yuneva M. Adapt and conquer: Metabolic flexibility in cancer growth, invasion and evasion. Mol Metab [Internet] 2020 [cited 2023 Mar 13];33:83. Available from: /pmc/articles/PMC7056924/

605. Gaude E, Frezza C. Tissue-specific and convergent metabolic transformation of cancer correlates with metastatic potential and patient survival. Nat Commun [Internet] 2016 [cited 2023 Mar 13];7. Available from: https://pubmed.ncbi.nlm.nih.gov/27721378/

606. Mims J, Bansal N, Bharadwaj MS, Chen X, Molina AJ, Tsang AW, et al. Energy Metabolism in a Matched Model of Radiation Resistance for Head and Neck Squamous Cell Cancer. Radiat Res [Internet] 2015 [cited 2023 Mar 13];183(3):291. Available from: /pmc/articles/PMC4465128/

607. Nissen JD, Pajecka K, Stridh MH, Skytt DM, Waagepetersen HS. Dysfunctional TCA-Cycle Metabolism in Glutamate

Dehydrogenase Deficient Astrocytes. Glia [Internet] 2015 [cited 2023 Mar 13];63(12):2313–26. Available from: https://pubmed.ncbi.nlm.nih.gov/26221781/

608. Adhikary G, Shrestha S, Naselsky W, Newland JJ, Chen X, Xu W, et al. Mesothelioma cancer cells are glutamine addicted and glutamine restriction reduces YAP1 signaling to attenuate tumor formation. Mol Carcinog [Internet] 2022 [cited 2023 Mar 13];Available from: https://pubmed.ncbi.nlm.nih.gov/36562471/

609. Wise DR, Thompson CB. Glutamine Addiction: A New Therapeutic Target in Cancer. Trends Biochem Sci [Internet] 2010 [cited 2023 Mar 13];35(8):427. Available from: /pmc/articles/PMC2917518/

610. Habanjar O, Diab-Assaf M, Caldefie-Chezet F, Delort L. The Impact of Obesity, Adipose Tissue, and Tumor Microenvironment on Macrophage Polarization and Metastasis. Biol 2022, Vol 11, Page 339 [Internet] 2022 [cited 2023 Mar 13];11(2):339. Available from: https://www.mdpi.com/2079-7737/11/2/339/htm

611. Asadzadeh Z, Mohammadi H, Safarzadeh E, Hemmatzadeh M, Mahdian-shakib A, Jadidi-Niaragh F, et al. The paradox of Th17 cell functions in tumor immunity. Cell Immunol [Internet] 2017 [cited 2023 Mar 13];322:15–25. Available from: https://pubmed.ncbi.nlm.nih.gov/29103586/

612. Farr A, Stolz M, Baumann L, Bago-Horvath Z, Oppolzer E, Pfeiler G, et al. The effect of obesity on pathological complete response and survival in breast cancer patients receiving uncapped doses of neoadjuvant anthracycline-taxane-based chemotherapy. Breast [Internet] 2017 [cited 2023 Mar 13];33:153–8. Available from: https://pubmed.ncbi.nlm.nih.gov/28395233/

613. Omarini C, Palumbo P, Pecchi A, Draisci S, Balduzzi S, Nasso C, et al. Predictive Role Of Body Composition Parameters In Operable Breast Cancer Patients Treated With Neoadjuvant Chemotherapy. Cancer Manag Res [Internet] 2019 [cited 2023 Mar 13];11:9563–9. Available from: https://pubmed.ncbi.nlm.nih.gov/32009814/

614. Wylie B, Macri C, Mintern JD, Waithman J. Dendritic Cells and Cancer: From Biology to Therapeutic Intervention. Cancers (Basel) [Internet] 2019 [cited 2022 Sep 12];11(4). Available from: /pmc/articles/PMC6521027/

615. Tzeng HT, Chyuan IT, Chen WY. Shaping of Innate Immune Response by Fatty Acid Metabolite Palmitate. Cells 2019, Vol 8, Page 1633 [Internet] 2019 [cited 2023 Mar 14];8(12):1633. Available from: https://www.mdpi.com/2073-4409/8/12/1633/htm

616. Genard G, Lucas S, Michiels C. Reprogramming of tumor-associated macrophages with anticancer therapies: Radiotherapy versus chemo- and immunotherapies. Front Immunol 2017;8(JUL):828.